



Journal which deals with research, Innovation and Originality



Table of Content

Topics	Page no
Chief Editor Board	3-4
Message From Associate Editor	5
Research Papers Collection	6-422

CHIEF EDITOR BOARD

- 1. Dr Chandrasekhar Putcha, Outstanding Professor, University Of California, USA**
- 2. Dr Shashi Kumar Gupta, , Professor, New Zealand**
- 3. Dr Kenneth Derucher, Professor and Former Dean, California State University, Chico, USA**
- 4. Dr Azim Houshyar, Professor, Western Michigan University, Kalamazoo, Michigan, USA**
- 5. Dr Sunil Saigal, Distinguished Professor, New Jersey Institute of Technology, Newark, USA**
- 6. Dr Hota GangaRao, Distinguished Professor and Director, Center for Integration of Composites into Infrastructure, West Virginia University, Morgantown, WV, USA**
- 7. Dr Bilal M. Ayyub, professor and Director, Center for Technology and Systems Management, University of Maryland College Park, Maryland, USA**
- 8. Dr Sarâh BENZIANE, University Of Oran, Associate Professor, Algeria**
- 9. Dr Mohamed Syed Fofanah, Head, Department of Industrial Technology & Director of Studies, Njala University, Sierra Leone**
- 10. Dr Radhakrishna Gopala Pillai, Honorary professor, Institute of Medical Sciences, Kirghistan**
- 11. Dr Ajaya Bhattarai, Tribhuwan University, Professor, Nepal**

ASSOCIATE EDITOR IN CHIEF

- 1. Er. Pragyan Bhattarai , Research Engineer and program co-ordinator, Nepal**

ADVISORY EDITORS

- 1. Mr Leela Mani Poudyal, Chief Secretary, Nepal government, Nepal**
- 2. Mr Sukdev Bhattarai Khattri, Secretary, Central Government, Nepal**
- 3. Mr Janak shah, Secretary, Central Government, Nepal**
- 4. Mr Mohodatta Timilsina, Executive Secretary, Central Government, Nepal**
- 5. Dr. Manjusha Kulkarni, Asso. Professor, Pune University, India**
- 6. Er. Ranipet Hafeez Basha (Phd Scholar), Vice President, Basha Research Corporation, Kumamoto, Japan**

Technical Members

- 1. Miss Rekha Ghimire, Research Microbiologist, Nepal section representative, Nepal**
- 2. Er. A.V. A Bharat Kumar, Research Engineer, India section representative and program co-ordinator, India**
- 3. Er. Amir Juma, Research Engineer ,Uganda section representative, program co-ordinator, Uganda**
- 4. Er. Maharshi Bhaswant, Research scholar(University of southern Queensland), Research Biologist, Australia**

IJERGS

Message from Associate Editor In Chief



Let me first of all take this opportunity to wish all our readers a very happy, peaceful and prosperous year ahead.

This is the Forth Issue of the Forth Volume of International Journal of Engineering Research and General Science. A total of 57 research articles are published and I sincerely hope that each one of these provides some significant stimulation to a reasonable segment of our community of readers.

In this issue, we have focused mainly on the Environment and its challenges. We also welcome more research oriented ideas in our upcoming Issues.

Author's response for this issue was really inspiring for us. We received many papers from many countries in this issue but our technical team and editor members accepted very less number of research papers for the publication. We have provided editors feedback for every rejected as well as accepted paper so that authors can work out in the weakness more and we shall accept the paper in near future. We apologize for the inconvenient caused for rejected Authors but I hope our editor's feedback helps you discover more horizons for your research work.

I would like to take this opportunity to thank each and every writer for their contribution and would like to thank entire International Journal of Engineering Research and General Science (IJERGS) technical team and editor member for their hard work for the development of research in the world through IJERGS.

Last, but not the least my special thanks and gratitude needs to go to all our fellow friends and supporters. Your help is greatly appreciated. I hope our reader will find our papers educational and entertaining as well. Our team have done good job however, this issue may possibly have some drawbacks, and therefore, constructive suggestions for further improvement shall be warmly welcomed.

Er. Pragyan Bhattarai,

Associate Editor-in-Chief, P&REC,

International Journal of Engineering Research and General Science

E-mail -Pragyan@ijergs.org

Introducing Robotics into the Nigerian Secondary Schools Curriculum: Likely Impacts, Challenges and Possible Solutions

Samson Damilola FABIYI, Abdulmuizz Ohiare ABDULMALIK, Habeeb Abiodun TIAMIU

Department of Mechatronics Engineering, Federal University of Technology,

Gidan Kwano, Bosso Local Government Area, Minna, Nigeria.

samsonfabi748@gmail.com

Abstract— One of the ways by which the youths of nowadays can be galvanized and empowered to go on and proffer solutions to the existing, emerging and future technology problems is by introducing them to robotics at their early age. The trend in most developed countries is that priority is usually placed on robotics at all levels of education i.e. primary, secondary and tertiary. This is expected considering the numerous areas of application of robots and its effects on economic growth and technological development of such countries. Reverse is the case in Nigeria. One would then wonder why robotics has not been fully and officially incorporated into the Nigeria secondary schools' curriculum. Probably, some of the top officials in government are not really convinced that introducing such would make any meaningful impact as far as the economy and technological advancement are concern. While relying on data obtained from various secondary sources, this study focuses on presenting the likely impacts and challenges of introducing robotics in to the Nigerian secondary schools curriculum and to put possible solutions forward. The results showed that creation of job opportunity, increased interest in engineering and computer science among prospective university candidates, enhanced academic performance, and solution to the problem of "digital divide" are some of the likely impacts while Inadequate budgetary allocation, Inadequate physical infrastructure, and dwindling electrical power supply have been identified as the major challenges which are likely to be encountered if robotics is finally introduced into the Nigerian secondary schools curriculum.

Keywords— robotics, curriculum, secondary, education, Nigeria, impact, challenge, solution.

INTRODUCTION

Motivating the current crop of secondary students to go on and become the problem-solving leaders of tomorrow without given them the right background is tantamount to sending farmers to the farm without given them the required implements. One of the ways by which the youths of nowadays can be galvanized and empowered in other to be able to proffer solutions to the existing, emerging and future technology problems is by introducing them to robotics at their early age.

The trend in most developed countries is that priority is usually placed on robotics at all levels of education i.e. primary, secondary and tertiary. This is expected considering the numerous areas of application of robots and its effects on economic growth and technological development of such countries. Increased labour productivity, total factory productivity; raised annual growth of gross domestic product (GDP); increased operational safety, enhanced surgery performance, reduction in need for care and care home, more help for the elderly and the chronically ill, possibility of long distance monitoring of isolated patients, are some of the effects of robots cum the variety of applications in the military and nuclear power plants. Against the notion that robots contributes to the unemployment rate, they have been proven to create jobs. Robots cannot design, develop and maintain themselves. Humans have to be employed to carry out those tasks [1, 2, 4, 5, 6].

In Nigeria, it so unfortunate and disheartening that robotics has not been given the right attention and the failure of government to have it included in the secondary schools curriculum has undoubtedly limited our technological capacity. Several attempts have been made in the past by individuals, private, and co-operate bodies to render assistance in this regard. However, these have not been enough.

One would then wonder why robotics has not been fully and officially incorporated into the Nigerian secondary schools curriculum. Probably, some of the top officials in government are not really convinced that introducing such would make any meaningful impact as far as the economy and technological advancement are concern. The major objectives of this work, therefore, are to present the likely impacts of introducing robotics into the Nigerian secondary schools curriculum and to consider the challenges that may be encountered if such policy is to be implemented and finally, to present possible solutions to the identified challenges.

Relevant literature have been reviewed and included in this paper in other to further broaden knowledge and provide an in-depth understanding of the study especially for anyone, a novice, who might be interested in taking up the report of this work

LITERATURE REVIEW

Czech playwright, Karl Capek (1921), in his play R.U.R (Rossum's Universal Robots), brought the word robot forward for the first time [16]. George Devol and Joe Engelberger, in the late 50's and early 60's, developed the first industrial modern robots which were then known as the Unimates [15].

While there is no standard definition for robots, several attempts have been made in the past in this regard. According to the Robot Institute of America (1979), robots are reprogrammable, multifunctional manipulators designed to move material, parts, tools, or specialized devices through various programmed motions for the performance of a variety of task [15]. Robots have also been referred to as machines-which can be angular, flat, tubby, spindly, bulbous, may or may not have faces, bodies- designed to execute one or more tasks repeatedly, with speed and precision. [12, 13, 14]. Robots which are capable of doing too dangerous, boring, onerous, or just plain nasty work are the most frequently encountered types especially in the auto, medical, manufacturing, and space industries [12]. Robots, unlike humans, don't get sick; don't violate company rules; don't demand raises; are quicker and easier to refuel and repair; are less prone to be bored by repetitive task; need no rest; are able to work on 7 * 24; can withstand extremely high and low temperature [4, 5, 6].

Robotics- a term coined by Isaac Asimov, a Russian-born American scientist and writer – can be defined as the study and use of robots [15]. Robotics, according to webopedia and wikipedia, is the field of computer science and engineering concerned with design, construction, operation, and application of robots. [16, 17].

Studying robotics, therefore, implies that students must be actively involved in physics, mechanical engineering, electrical engineering, structural engineering, mathematics, computing, and in exceptional cases, biology, medicine, and chemistry in a deeply problem-posing problem-solving environment [12]. Taking Carnegie Mellon Robotics Academy as a case study. Some of the robotics curriculum dedicated to students in middle schools include: Introduction to Programming VEX IQ, VEX Cortex Video Trainer using ROBOTC (Legacy), Introduction to Programming LEGO MINDSTORMS EV3, ROBOTC Graphical Introduction to Programming LEGO MINDSTORMS EV3, Robot Engineering Vol. 1 – Introduction to Mobile Robotics, Robot Engineering Vol. 2 – Guided Research, Robot Science, NXT Video Trainer 2.0, ROBOTC Curriculum of TETRIX and LEGO MINDSTORMS, and Robot Virtual Worlds. These, according to the academy, were created to, “allow students, in junior high schools to go from having no robotics experience, to programming advanced behaviors.” [18]

METHODOLOGY

Data used for the purpose of this study are those obtained from various secondary data sources namely: web information, historical data and information, mass media products, textbooks, journals, magazine articles, news reports, encyclopedia, and progress reports. In other to achieve the objectives of this work, facts and figures obtained from the data sources were used in carrying out extensive analysis with the sole aim of presenting the likely impacts, and challenges of introducing robotics in to the Nigerian secondary schools curriculum and also, to put possible solutions forward. The information so obtained from the afore-mentioned sources has also been useful in compiling, interpreting and structuring of the entire study.

RESULT AND DISCUSSION

IMPACT

The likely impacts, both positive and negative, of introducing robotics into the Nigerian secondary schools curriculum are discussed below:

• CREATION OF JOB OPPORTUNITY

According to a survey conducted by Jobberman, out of the 500 000 graduates being turned out by Nigerian Universities annually, only 57 percent get employed [25]. With the rate of unemployment on the rise, teaching robotics in secondary schools, both junior and senior, is a potential career opportunity to be explored by graduates of Mechatronics Engineering, and in exceptional cases, those of Electrical and Electronics Engineering, Computer Engineering, Mechanical Engineering, and Computer Science. While some of these graduates with high grades have a better chance of either being retained by their various universities or getting employed by the so-called, “big companies”, others could find a safe abode in teaching robotics at secondary schools. Similarly, Introducing robotics into the Nigerian secondary schools' curriculum will definitely results in having more robots around. Since robots cannot design, develop and maintain themselves, humans have to be employed to get those tasks done. Having more robots around, therefore, will in no doubt results in more jobs for experts in robotics.

• INCREASED INTEREST IN ENGINEERING AND COMPUTER SCIENCE AMONG PROSPECTIVE UNIVERSITY CANDIDATES

Global reform movements, according to Mehmet Ayar, Tubitak, Bugrahan Yalvac and Fatih Ugurdag (2013), are aimed at cultivating STEM (Science, Technology, Engineering and Mathematics) education at K-16 levels because of the decreasing numbers

of youth entering the STEM fields and medicine and the lack of student Interest in these fields [19]. Cher C. Hendricks, Meltem Alemdar, Tamra Williams Ogletree (2012), In their study, reported that 87% of students interviewed, after their participation in a robotics competition, said they were more interested in having a job in a STEM or computer field [20]. It has been shown that only 16 percent of students graduating secondary schools are interested in pursuing a career in STEM (Science, Technology, Engineering, and Mathematics). There is a prospect of increasing this number if robotics is introduced into the Nigerian secondary schools curriculum. Engaging secondary school students, both junior and senior, in robotics activities such as recognition and use of various mechanical, electronic and electrical materials is capable of sparking their interest in the field of engineering [19].

Having a close look at the robotics curriculum for high schools discussed under literature review, one would also conclude that students, upon completion of the secondary schools education, must have been acquainted with the rudiments of programming including its basic elements such as functions, file O/I, classes, abstraction, inheritance, etc. graduating secondary schools students - based on the computational, mathematical, and modeling skills they obtained - must have enriched their knowledge and broadened their problem-solving capability, thus making them more creative and innovative. In a nut shell, the number of prospective University candidates, who are capable and willing to pursue their bachelor's degree program in Mechatronics Engineering, Electrical and Electronics Engineering, Computer Engineering, Mechanical Engineering and Computer Science will have been increased significantly.

- **ENHANCED ACADEMIC PERFORMANCE**

Pat Ko of the University of Texas once submitted a proposal to study and analyze the differences in performances of robotics and non-robotics students in various examinations such as SAT. He stated, in his submission, that there is a theoretical connection between CT skills and students performance (one of the identified long term benefits of CT). In other words, there is a likelihood that robotics students will perform better than students who do not have CT experience [21]. Studying robotics, according Mehmet Ayar, Tubitak, Bugrahan Yalvac and Fatih Ugurdag (2013), provides the motivation for students to learn science, mathematics and other subjects to succeed in the nation-wide university entrance exam [19].

In Nigerian Universities and Polytechnics, one of the major challenges being faced by academic staff/lecturers in the Faculty of Engineering is the increasing failure rates of students. Most times, lecturers, in the name of face-saving, often resort to upgrading of results/addition of marks just to push them to or above the pass mark. The poor academic performance of engineering students is indeed not due to a lack of capacity for new students on the part of tertiary institutions but a lack of interested and qualified students. Studying robotics is not only capable of sparking interest of graduating secondary students in Engineering and related fields but also capable of enhancing their academic performances in tertiary institutions as well as in external/ national examinations [20].

- **SOLUTION TO THE PROBLEM OF “DIGITAL DIVIDE”**

Records have shown that students from educationally-less developed states and minority groups are really lagging behind in terms of participation in Engineering, Computer Science and related fields. This problem of ‘digital divide’ has been attributed, by many, to intentional marginalization of these parts of the country by successive governments. This is not true. It has been proven that most students, while in junior secondary schools, tend to develop interest in particular fields. This has a major influence on them when choosing their career paths. Several students with the potential of becoming future technology problem-solvers opted for other fields like business, law, medicine, etc. This is due to lack of exposure to a curriculum that integrates math, science, and technology content and skills. Technology, they say, ‘is no longer the private domain of a self-selected group of nerds.’ Incorporating robotics into the Nigerian secondary schools curriculum will get the students engage in a ‘complex, strategic problem-solving and higher-order thinking’. This will in turn spark a high level of interest in Engineering, Computer Science and related fields among the students, thereby putting an end to the problem of ‘digital divide.’ [22]

- **NEGATIVE IMPACTS**

Introducing robotics into the Nigerian secondary schools’ curriculum will definitely results in having more robots around. One of the fears of having more robots around is the prospect of robots displacing or replacing workers, mostly low-skilled.

- **OTHERS**

Introducing students to robotics at the secondary school level is capable of making them: designers and developers of future intelligent information technology systems (not just users and consumers), productive in employment and higher institutions, etc. [22]. Evidence has shown that introducing secondary schools students to robotics early is capable of increasing their understanding of physics content [23]. All in all, robotics has been identified as a valuable tool for students to develop cognitive, meta-cognitive and social skills necessary in the workplace of the 21st century [24].

CHALLENGE

Having presented the likely impacts, and seeing that the positives outnumbered the negatives, we cannot but discuss the challenges

which are likely to be encountered if robotics is finally introduced into the Nigerian secondary schools curriculum.

Dimitris Alimisis (2013), identified time consuming nature of robotic activities, high cost of equipment needed for such activities, lack of technologies that support the 21st-century learning skills in schools, and the perceptions that robotics is hard, highly gender-biased (only for boys!) as some of the challenges facing robotics education [24].

Marion Usselman, Mike Ryan, Jeffrey .H. rosen, Jayma Koval, Sabrinna Grossman, Nancy Anna Newsome, and Marcela Nicole Moren (2015), in their submission, concluded that time allocated to basic science subjects, in conformity with the physical science standards, is limited, and so robotics couldn't be accommodated within the allotted class time without jeopardizing student learning of required science standards. In other to further buttress this point, they argued that ,”the middle school physical science curriculum is generally tightly packed with required science content, leaving little time for students to really engage in important science practices, let alone learn valuable but tangential content like computer programming or the basics of mechanical engineering construction” [23].

Robotics, having been considered as a branch of educational technology, will not be exempted from the same old problems well known to be facing the latter, some of which are:

1. Inadequate budgetary allocation: Failure of successive governments to make enough funds available for the education sector has resulted into poor quality of service delivery. It is a well-known fact that old facilities in public secondary schools will not be sufficient if robotics is to be fully incorporated into the Nigerian secondary schools.

2. Inadequate physical infrastructure: most public secondary schools in Nigeria lack libraries equipped with scholastic materials and well equipped science laboratories. These are required, according to Dimitris Alimisis (2013), in other to, “foster critical thinking, problem solving, creativity, and teamwork and communication skills since they are architected for rigorous, disciplined, and scripted experiences” [119].

3. Dwindling electrical power supply: In a country where power generation reportedly dropped from 5000 megawatts to below 1600 megawatts early this year [26], without a stand-by alternative power supply, the problem of disruption and interruption during robotic sessions may be inevitable.

POSSIBLE SOLUTION

The measures listed below will go a long way in overcoming the challenges which are likely to be encountered if the government finally decides on incorporating robotics into the Nigerian secondary schools curriculum:

- The ministry of education, in collaboration with relevant agencies, should come up with a robust time-table which will accommodate robotics in secondary schools without jeopardizing students learning of required science standards.
- Government should make enough funds available for public schools. This will be useful in procuring standard robot kits and other logistics which are indispensable for a thorough, mind-blowing robotics activities.
- The problem of epileptic power supply should be tackled head-on. While concrete steps are being taken towards that, the government should make at least a generator/inverter available in all public secondary schools to avoid unnecessary interruption during robotics sessions.
- Well-equipped science laboratories and libraries equipped with scholastic materials should be put in place in all public secondary schools.
- Finally, the government should set-up control mechanisms and do follow-up on every policy effected to ensure effective monitoring and implementation.

FUTURE

Over the next decades, five key aspects of robotics are expected to make major economic impacts and transform societies. They are: drones; artificial assistants; driverless cars; medical procedures, operations; prosthetics and exoskeleton [10]. According to the saying of William Gibson, “the future is already here- It's just not evenly distributed.” Nigeria cannot afford to lag behind in this regard. With this at the back of our mind and considering the prospect of robots displacing or replacing workers (mostly low-skilled), the onus lies on the government to take the big steps now in anticipation of the glorious and exciting new future.

Finally, the data sources used for the purpose of this study are secondary. This paper, therefore, provides the platform for future researchers who may be willing to carry out further studies on similar issues based on data obtained from primary sources.

CONCLUSION

The results showed that creation of job opportunity, increased interest in engineering and computer science among prospective university candidates, enhanced academic performance, and solution to the problem of “digital divide” are some of the likely impacts while Inadequate budgetary allocation, Inadequate physical infrastructure, and dwindling electrical power supply have been identified as the major challenges which are likely to be encountered if robotics is finally introduced into the Nigerian secondary schools curriculum. Hence, possible solutions were put forward. While it is true that robotics has enormous potential to offer in education, perhaps it must be stated that the benefits thereof can only be guaranteed and fully harnessed when the curriculum is combined with an enabling, conducive learning environment and a holistic educational philosophy. The only thing that remains constant in life is change. As the world keep changing in this direction, the government of the day must rise to the occasion in other to actualize the vision 20-2020 i.e. to be among the top twenty industrialized country by the year 2020. Taking such steps will definitely provide us with the platform to taking a rightful place in the committee of developed nations.

REFERENCES:

- [1] Georg Graetz, Guy Michaels. "Estimating the Impact of Robots on Productivity and Employment." Internet: <http://robohub.org/estimating-the-impact-of-robots-on-productivity-and-employment/>, Jul 14, 2015 [May 17, 2016]
- [2] Rachael Stephens. "Robots at Work: The Economic Effects of Workplace Automation." Internet: <http://journalistsresource.org/studies/economics/jobs/robots-at-work-the-economics-effects-of-workplace-automation>, Sept. 22, 2015 [May 17, 2016]
- [3] William H. Davidow, Michael S. Malone. "What Happens to Society When Robots Replace Workers?" Internet: <https://hbr.org/2014/12/what-happens-to-society-when-robots-replace-workers>, Dec. 10, 2014 [May 18, 2016]
- [4] Diana Cabrera and Adriana Paisano. "Robots and Their Effect on Society." Internet: <https://prezi.com/qrwpl1etx3hs/robots-and-their-effect-on-society/>, Oct. 25, 2012 [May 18, 2016]
- [5] M. O. Qureshi, R. S. Syed. (2014, Dec). "The Impact of Robotics on Employment and Motivation of Employees in the Service Sector, with Special Reference to Health Care." *Safety and Health at Work*. [On-line]. 5(4), pp. 198–202. Available: <http://www.sciencedirect.com/science/article/pii/S2093791114000511> [May 18, 2016]
- [6] Song Li. "Robots Have Negative Effects on Society and Sometimes are Even Dangerous - IELTS Essay." Internet: <http://www.essayforum.com/writing/robots-negative-effects-society-sometimes-59158/>, Sep 26, 2014 [May 18, 2016]
- [7] "How Do Robots Impact Society?" Internet: <https://www.reference.com/technology/robots-impact-society-2edd1fe19adaf219>, [May 18, 2016]
- [8] Seegrid. "Impacts of Robotics on Employment, Safety, Quality, Productivity, and Efficiency." Internet: http://www.roboticstomorrow.com/content.php?post_type=1907, Oct. 15, 2016 [May 18, 2016]
- [9] Rachael Stephens. "The Future of Robots in the Workplace: The Impact on Workers." Internet: <http://journalistsresource.org/studies/economics/jobs/robots-in-the-workplace>, August 11, 2015 [May 18, 2016]
- [10] Colin Lewis "5 Areas in Robotics That Will Transform Society and Their Economic Impact." Internet: <https://robotonomics.com/2014/04/23/5-areas-in-robotics-that-will-transform-society-and-their-economic-impact/>, Apr. 23 2014 [May 18, 2016]
- [11] Darrell M. West. "What Happens If Robots Take The Jobs? The Impact of Emerging Technologies on Employment and Public Policy." Internet: <https://robotonomics.com/2014/04/23/5-areas-in-robotics-that-will-transform-society-and-their-economic-impact/>, Oct. 26, 2015 [May 18, 2016]
- [12] "Introduction to Robots." Internet: <http://www.galileo.org/robotics/intro.html>, [May 23, 2016]
- [13] Adrienne LaFrance "What Is a Robot?" Internet: <http://www.theatlantic.com/technology/archive/2016/03/what-is-a-human/473166/>, Mar. 22, 2016 [May 23, 2016]
- [14] Margaret Rouse. "Robot (Insect Robot, Autonomous Robot)." Internet: <http://whatis.techtarget.com/definition/robot-insect-robot-autonomous-robot>, Apr. 2007 [May 23, 2016]
- [15] Kevin Dowling. "What is Robotics?" Internet: <http://www.cs.cmu.edu/~chuck/robotpg/robofaq/1.html>, Aug. 19, 1996 [May 23, 2016]
- [16] Vangie Beal. "Robotics." Internet: <http://www.webopedia.com/TERM/R/robotics.html>, [May 23, 2016]
- [17] Robotics." Internet: <https://en.wikipedia.org/wiki/Robotics>, May 26, 2016 [May 28, 2016]
- [18] "All Middle School Curricula." Internet: <http://education.rec.ri.cmu.edu/roboticscurriculum/middle-school/>, [May 28, 2016]
- [19] Mehmet Ayar, Tubitak, Bugrahan Yalvac and Fatih Ugurdag. "A Robotics Summer Camp for High School Students: Pipelines Activities Promoting Careers in Engineering Fields." Presented at the 120th annual conference and exposition, Atlanta, USA, 2013.
- [20] Cher C. Hendricks, Meltem Alemdar, TamraWilliams Ogletree. "The Impact of Participation in Vex Robotics Competition on middle and high school students' interest in pursuing stem studies and stem-Related careers." *ASEE Annual Conference*, 2012, pp. 25.1312.1 - 25.1312.16
- [21] Pat Ko. "A Longitudinal Study of the Effects of a High School Robotics and Computational Thinking Class on Academic Achievement (WIP)." In *IEEE Frontiers in Education Conference (FIE)*, 2013, pp. 181 – 183
- [22] "Why Should I Do Robotics with My Middle School Students?" Internet: <http://www.ircs.upenn.edu/pennlincs/robotics/introduction.htm>, [Jun. 6, 2016]
- [23] Marion Usselman, Mike Ryan, and Jeffrey H Rosen. "Robotics in the Core Science Classroom: Benefits and Challenges for Curriculum Development and Implementation (RTP, Strand4)." In 122nd annual conference and exposition, Seattle, USA, 2015.
- [24] Dimitris Alimisis. (2013, Mar.) "Educational Robotics: Open Questions and New Challenges." *Themes in Science & Technology Education*. [On-line]. 6(1), 63-71. Available: <http://connection.ebscohost.com/c/articles/90148056/educational-robotics-open-questions-new-challenges>, [Jun. 6, 2016]
- [25] "About Half of the University Graduates In Nigeria Cannot Find Jobs." Internet: <http://qz.com/603967/about-half-of-the-university-graduates-in-nigeria-cannot-find-jobs/>, Jan. 27, 2016 [Jun. 10, 2016]
- [26] S. D. Fabiyi, A. O. Abdulmalik, and H. A. Tiamiu. (2016, May). *International Journal of Science and Research (IJSR)* "Dwindling Electrical Power Supply in Nigeria: Causes and Possible Solution." [On-line]. 5(5), pp. 635-639. Available: <https://www.ijer.net/archive/v5i5/NOV163290.pdf>, [Jun. 3, 2016]

USE OF BIOFUELS TO CONTROL POLLUTION IN AUTOMOBILES

Dr. Subhadra Rajpoot¹ & Dr. Preeti Singh²
Amity University Greater Noida (India)

ABSTRACT: The world is presently suffering with the twin crises of fossil fuel depletion and environmental degradation. With costs of oil and coal rising, and crude imports growing, India is facing a huge energy crisis. Where does India's energy come from, and where does it go? If we are to reduce demand, boost efficiency and design small-scale, decentralized energy options, we must incorporate the consumer in decision-making. The search for alternative fuels to reduce dependence on petroleum and emission of pollutants into the atmosphere has stimulated many scientific studies. The goal is to develop fuels that can be used in existing vehicles without the need for major changes in their engines. A term often used for fuel derived from renewable sources is 'biofuel', which has strong links with the concept of sustainability, whereby the use of natural resources to meet current needs should not compromise the needs of future generations.

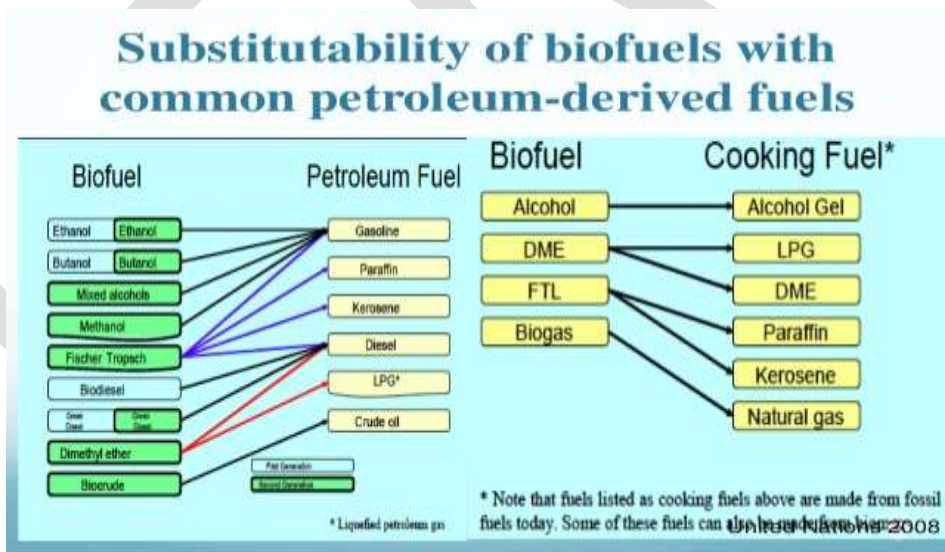
Keywords- Agricultural wastes, Biofuel, Environmental sustainability, Pollution

I. INTRODUCTION

The beginning of the 21st Century marks a change in the composition of transportation fuels, where biofuels, in addition to gasoline and diesel, power our cars. Biofuels are a liquid substitute to gasoline and diesel and are produced from biomass using dispersed production units located in oil-importing countries (e.g., the United States, Brazil, and Europe).¹ Gasoline and diesel are liquid fuels produced from crude oil whose extraction capacity is concentrated in the Organization of the Petroleum Exporting Countries (OPEC).² The biofuels produced from the renewable resources could help to minimize the fossil fuel burning and CO₂ production. Biofuels produced from biomass such as plants or organic waste could help to reduce both the world's dependence on oil and CO₂ production. These biofuels have the potential to cut CO₂ emission because the plants they are made from use CO₂ as they grow. Biofuels and bioproducts produced from plant biomass would mitigate global warming.

II. BIOFUEL

All biofuels and bio-based products come from "biomass", a term that covers all living or recently living biological material which can be used as fuel or for industrial production. The term biofuel is referred to as solid, liquid or gaseous fuels that are predominantly produced from biorenewable or combustible renewable feedstocks. Liquid biofuels are important for the future because they replace petroleum fuels. The biggest difference between biofuels and petroleum feedstocks is oxygen content. Biofuels are non polluting, locally available, accessible, sustainable and are a reliable fuel obtained from renewable sources.



III. RAW MATERIALS

Crop Residues

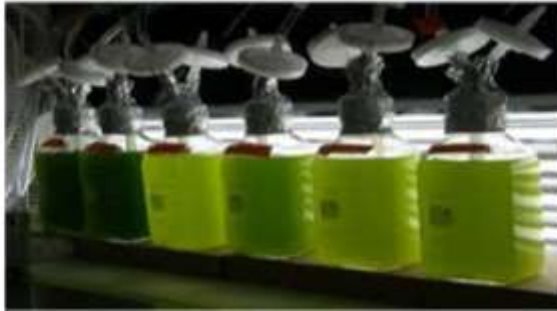
Crops such as corn, wheat, and rice consist not just of the grains we eat or feed to livestock but also of stalks, husks, cobs, and other biomass unsuitable as direct human food. These residues generally account for about half of the total biomass in grown crops. And because they are a by-product of today's primary crops, such residues can be used to produce energy without expanding the amount of land agriculture.

3.2 Wastes from Livestock

Livestock raised in very large confined animal feeding operations (CAFOs) produce nearly unmanageable concentrations of manure, which can be used for bioenergy, but also regularly pollute water supplies in many parts of the country. Fortunately, on the smaller end of the livestock production scale, farmers can use anaerobic digesters to convert manure into biogas while reaping economic and environmental benefit.

IV. TYPES OF BIOFUEL.

Biofuels are classified into three generations



4.1 First-generation biofuels

The most well-known first-generation biofuel is ethanol made by fermenting sugar extracted from sugar cane or sugar beets, or sugar extracted from starch contained in maize kernels or other starch-laden crops. Similar processing, but with different fermentation organisms, can yield another alcohol, butanol. Commercialization efforts for butanol are ongoing [4], while ethanol is already a well-established industry. Global production of first-generation bio-ethanol in 2006 was about 51 billion litres [5], with Brazil (from sugar cane) and the United States (from maize) each contributing about 18 billion litres, or 35 per cent of the total. China and India contributed 11 per cent to global ethanol production in 2006, and production levels were much lower in other countries (Figure 3), with feedstocks that include cane, corn, and several other sugar or starch crops (sugar beets, wheat, potatoes). Many countries are expanding or contemplating expanding their first-generation ethanol production, with Brazil and the United States having by far the largest expansion plans. Ethanol production is expected to more than double between now and 2013 in Brazil [6], and production capacity in the United States will double from the 2006 level once new plants currently under construction are completed.

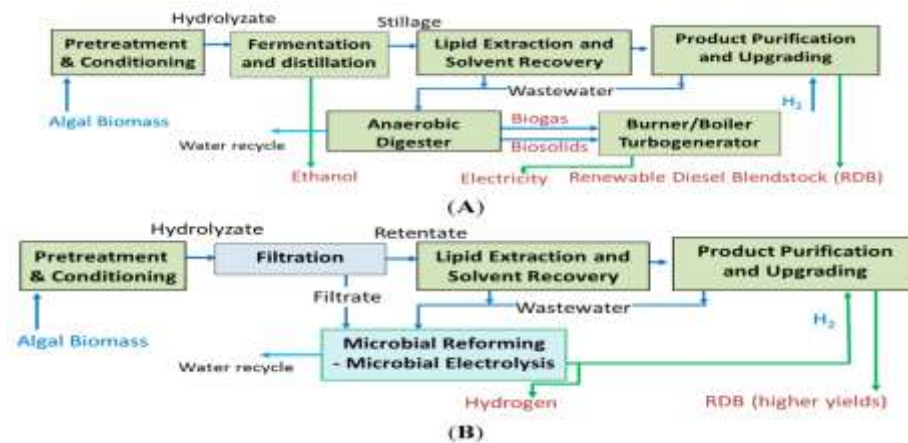
- Biodiesel
- Bioethanol
- Butanol
- Methanol

Table 2. First-generation biofuels

Pros	Cons
• Simple and well-known production methods	• High-cost feedstocks lead to high-cost production (except Brazilian sugar cane ethanol)
• Scalable to smaller production capacities	• Fungibility with existing petroleum-derived fuels
• Experience with commercial production and use in several countries	• Feedstocks compete directly with crops grown for food
• High-cost feedstocks lead to high-cost production (except Brazilian sugar cane ethanol)	• Low land-use efficiency

4.2 Second-generation biofuels

Second-generation biofuels share the feature of being produced from lignocellulosic biomass, enabling the use of lower-cost, non-edible feedstocks, thereby limiting direct food vs. fuel competition. Second-generation biofuels can be further classified in terms of the process used to convert the biomass to fuel: biochemical or thermochemical. Second-generation ethanol or butanol would be made via biochemical processing, while all other second-generation fuels discussed here would be made via thermochemical processing. Second-generation thermochemical biofuels may be less familiar to most readers than second-generation ethanol, because there are no first-generation analogs. On the other hand, many second-generation thermochemical fuels are fuels that are already being made commercially from fossil fuels using processing steps that in some cases are identical to those that would be used for biofuel production (Figure 6).



4.3 Third-generation biofuels

Production of third-generation biofuels (mainly from algae) is still at the research and development stage. The most accepted definition of third-generation biofuels is 'fuels that are produced from algae-derived biomasses. This has a very distinctive growth yield compared with classical lignocellulosic biomass. Algae-based fuels are likely to play an important role in third-generation biofuel production, as they are considered a sustainable feedstock for biofuels and bioproducts from biorefineries.

V. BENEFITS OVERVIEW

Benefits Of Biodiesel Production

Cleaner Environment: Biodiesel is proven to Reduce Dangerous Emissions, Which Contribute to Climate Change: Biodiesel is the only alternative fuel to voluntarily perform EPA Tier I and Tier II testing to quantify emission characteristics and health effects. That study found that B20 (20% biodiesel blended with 80% conventional diesel fuel) reduced total hydrocarbons by up to 30%, Carbon Monoxide up to 20%, and total particulate matter up to 15%. =Pure biodiesel does not contain sulfur and therefore reduces sulfur dioxide exhaust from diesel engines to virtually zero. Biofuels, when blended with conventional fuels, reduce air pollutant emissions such as sulfur, particulates, carbon monoxide and hydrocarbons.

Health Benefits:

Biodiesel is Safer for People to Breathe: Research conducted in the US shows Biodiesel emissions have decreased levels of all target polycyclic aromatic hydrocarbons (PAH) and nitrated PAH compounds, as compared to petroleum diesel exhaust. PAH and nPAH compounds have been identified as potential cancer causing compounds. Targeted PAH compounds were reduced by 75 to 85 percent, with the exception of benzo(a)anthracene, which was reduced by roughly 50 percent. Target nPAH compounds were also reduced dramatically with biodiesel fuel, with 2-nitrofluorene and 1-nitropyrene reduced by 90 percent, and the rest of the nPAH compounds reduced to only trace levels. All of these reductions are due to the fact the Biodiesel fuel contains no aromatic compounds.

National Security:

Biodiesel Reduces our Dependence on Foreign Oil: Biodiesel can play a major role in expanding domestic refining capacity and reducing our reliance on foreign oil. The 500 million gallons of biodiesel produced in the U.S. in 2007 displaced 20 million barrels of petroleum, and increased production and use of biodiesel will further displace foreign oil. In addition, biodiesel is an extremely efficient fuel that creates 5.54 units of energy for every unit of fuel that is required to produce the fuel.

VI. CONCLUSIONS

Biofuels are promoted in many parts of the world and concern of environmental and social problems have grown due to increased production of this fuels. Production of biofuels promises substantial improvement in air quality through reducing emission from burning of the fuel used in vehicle engines. Some of the developing countries have started biofuel production and utilization as transport fuel in local market.

REFERENCES:

- [1] Bender M. Potential conservation of biomass in the production of synthetic organics. Resources conservation and recycling 2000; 30:49–58.
- [2] Demirbas MF. Current technologies for biomass conversion into chemicals and fuels. Energy Sour Part A 2006; 28:1181–8.
- [3] Kamm B, Gruber PR, Kamm M. Biorefinery industrial processes and products. Status and future direction, vols. 1 and 2. Weinheim: Wiley-Verlay GmbH and Co KGaA; 2006.
- [4] Mabee WE, Gregg DJ, Saddler JN. Assessing the emerging biorefinery sector in Canada. Appl Biochem Biotechnol 2005; 121–124:765–78.
- [5] Osamu K, Carl HW. Biomass Handbook. Gordon Breach Science Publisher; 1989.
- [6] Stevens CV, Verhe R. Renewable bioresources scope and modification for nonfood application. England: John Wiley and Sons Ltd.; 2004
- [7] Demiras A, (2007) Gasoline and diesel fuel blends with alcohols, Energy Edu Sci Technol 19:87 – 92

[8] Reijnders L, (2006) Conditions for the sustainability of biomass based fuel use. Energy Policy 34:863 – 876

IJERGS

Energy Efficiency in Analogue and Mixed Signal Integrated Circuit Design

Anish Joseph
anishjoseph01@gmail.com

JyolsnaMary.P
jyolsnamary@gmail.com

Abstract: The Wireless communications field is one of the major successes of the engineering over the past two decades. The progress made in this area has not only produced a huge technological growth, but also a great impact at social and economic level. In fact, the possibility of being connected anywhere at any time has radically changed people character.

The evolution of wireless communications is obviously linked to the power consumption of devices, which also continues increasing due to the growing amount of data and transmission speed required by the new communication standards. This leads to an increasingly gap between power needs and battery capacity. Therefore, energy efficiency of electronics systems has become a crucial factor to maximize the lifetime of the available batteries and one of the most important research topics in integrated circuits design in recent years

Introduction:

The increase in power consumption is less dramatic for the digital domain, since it is partially compensated, as the technology scales-down, by the reduction of the supply voltage and the geometrical dimensions of a single device. The main reason for decreasing the supply voltage in modern CMOS technology is to avoid the possible breakdown of the transistors due to the extremely thin oxide. For a CMOS logic gate, e.g. an inverter, the simplest logic cell, the power consumption can be expressed as:

$$P = C_L \cdot V_{dd}^2 \cdot f \quad (1)$$

where C_L is the load capacitor at the output of the inverter, V_{dd} is the supply voltage and f is the operating frequency. Despite of the ever-increasing working speed, the power consumption in CMOS logic circuits is reduced as the supply voltage and geometry sizes scale down.

The System-On-Chip (SoC) trend is the main cause for the analogue and mixed-signal and digital integrated circuits (ICs) to be fabricated on the same wafer. This fact eventually requires the analogue and mixed-signal ICs to be fabricated in modern CMOS technologies to save cost. However, several challenges are encountered in the scaling-down of the CMOS technologies for analogue designs with not much clear advantages. The threshold voltage is not scaled as aggressively as the supply voltage to avoid leakage current in transistors. As a consequence, the available signal swing is lower and a reduction of the noise of the circuit to maintain the same dynamic range is required. Reducing thermal noise increases the power consumption of analogue and mixed-signal circuitry. Particularly, in discrete time applications, reducing circuit noise means increasing the capacitances which results in higher power consumption in order to maintain the same operation speed. Additionally, as technologies are scaled down, the output resistance of the MOS transistors decreases resulting in lower op-amp gain. In order to increase the gain, it is required to use either cascode transistors or cascade amplifiers, increasing the complexity of the circuits. These solutions worsen the swing problems and increase the power consumption.

The analogue-to-digital (A/D) converter is one of the most important and power consuming building blocks in modern electronics systems.

In portable bio-signals acquisition micro-systems, the power consumption requirements are taken to the extreme. For instance, medical implant devices, such as modern pacemakers, require extremely low power consumption (about 10-40 μ W) in order to operate up to 10 years or more using a small non-rechargeable battery. In wearable electronics for biomedical monitoring applications, extreme miniaturization is required and this will limit the battery size and power draw. Wearable electroencephalography (EEG) is a good example of such a power-limited system. EEG records the voltage between electrodes placed on the scalp and provides a non-invasive interface to the brain.

Another interesting arising application is the Energy Autonomous Sensors (EAS) which will represent a revolution in the use of wireless technologies, such as wireless sensor networks, in the ambient intelligence paradigms. Exploiting this continuously improving energy efficiency and advances in energy harvesting, miniaturized battery-less sensors that do not need to be recharged for their whole operational life are becoming possible nowadays.

1. Power reduction techniques in analogue integrated circuit design.

1.1. Biasing point optimization:

CMOS technology is used in most of the electronic devices because of its high density of integration. Traditional analysis of MOS circuits is often based on the assumption that every transistor is operating in the strong inversion region, although signal amplification can be done in any of the three inversion regions. The better knowledge of the strong inversion models and equations is one of the

main reasons for its use.

Although simple MOS amplifier stages have much higher bandwidths in the strong inversion region, parameters like voltage gain, power dissipation, white noise, and distortion can be optimized by operating in the weak or moderate inversion regions. Most often operation in weak inversion is synonymous to minimum power operation.

There are several advantages that make operating in weak inversion an interesting issue:

1. It is possible to achieve higher gains.
2. Low power consumption can be achieved as the quiescent drain current needed for this level of inversion is quite low.
3. Lower distortion compared to the strong inversion region.
4. Higher output resistance of the devices of the input stage due to the low drain currents of transistors operating in weak inversion region.

But there are also some disadvantages when designing in weak inversion region. The most important is the reduction in circuit bandwidth and therefore in frequency operation although, they can be maximized if some issues are taken into account. In a single transistor, the maximum operating frequency is determined by the gate capacitances, CGS and CGD. In order to maximize the device bandwidth, these capacitors need to be kept as small as possible which is achieved with minimum transistor width and length.

In order to improve MOS modeling techniques, a large amount of research has been done until this moment regarding transistor MOS operation at the three levels of inversion. All this research has been quite useful to define accurate equations for the weak inversion region, as for instance the EKV model.

Many analogue circuits have been designed using weak inversion region, such as operational trans conductance amplifiers, filters, ADCs, etc., all of them performing very low power consumption.

1.2. Digitally assisted techniques:

Recent CMOS technologies open an interesting possibility for ADC design by translating analogue precision problems to the digital domain, where higher frequency signals can be processed at much lower energy cost. The additional complexity of digital processing circuits can be compensated by relaxing the analogue requirements and, as a consequence, lowering the total required energy per conversion.

Digitally assisted techniques have become a major concern in ADC design nowadays. Some traditional A/D conversion architectures (such as Successive-Approximation-Register-based-SAR- and $\Sigma\Delta$ ADCs) can be considered digitally assisted architectures since they make extensive use of CMOS digital logic. On the one hand, oversampling is a widely implemented technique in $\Sigma\Delta$ converters with high energy efficiency. As modern technologies allow a more efficient digital data processing, there are trends to extend these techniques to other Nyquist ADC architectures to decrease the required energy per conversion. On the other hand, there are a great number of approaches based on compensating errors generated in the analogue parts (such as mismatch and offset of the comparators) by means of implementing redundancy-based architectures and digital calibration methods instead of very power-demanding analogue compensation techniques.

In next sections, some of the most interesting trends involving digitally assisted techniques will be explained.

1.2.1 calibration and redundancy:

As it was commented before, the analogue circuits suffer some difficulties due to the MOSFET size reduction. One of the most applied techniques to compensate these errors is to introduce some digital calibration schemes, usually employing redundancy-based ADC architectures.

As an example, a widely employed architecture in wireless communication systems to reach fast operation at very high frequencies is the Flash ADC. Traditionally, these schemes have been characterized by using very power-demanding topologies with multiple gain stages for offset compensation. Actually, there are different design trends, mainly based on "relaxed precision" comparators redundancy combined with digital error compensation of mismatch and offset deviations. A first approach is illustrated in , where a bank of comparators with a factor-four redundancy is implemented with no special care about their offset or mismatch properties, drastically decreasing the consumption in the analogue blocks. In an initial calibration phase, the most suitable comparator for every input range is selected and the rest are powered down, with no contribution to power consumption of the system. Another example is a Flash ADC using process variations to generate the input references from random comparators offsets whose resolution and input signal range are optimized by means of digital calibration.

A great variety of similar approaches combining redundancy and digital error correction methods can be implemented in a similar way. For instance, there are redundancy-based ADC with a current trimming DAC for error compensation to minimize the input-referred offset of the comparators or partially redundant schemes -with only some additional comparators- with background calibration implemented during conversion.

1.2.2. Time

interleaving:

Time-Interleaving (TI) technique is a method based on the concept of running a system with M parallel channels by taking just one sample alternatively from each one. As a consequence, the ADC as a block would operate at an M times higher frequency than each individual channel. This allows reaching higher operation frequencies at no additional cost of analogue power consumption. However, mismatch between channels (usually the most limiting factors are offset and gain mismatch and clock skew errors) will reduce the resolution of the system. It is possible to compensate these errors using digital calibration or post processing.

Where a 6-bit Time- interleaving ADC working at 1.25 GS/s without any off-line calibration, error correction or post processing has been designed. The proposed architecture has been implemented using a two time-interleaved SAR ADCs topology combined

with flash ADC sub-conversion processes, allowing a reduction from 65 to 6 comparators and lowering its power consumption well below typical values for state-of-art flash ADCs without digital calibration techniques. Another example of a Time-interleaving 7-bit SAR ADC working at 2.5 GHz is described on (Alpman et al., 2010). The proposed scheme is based on 16 parallel ADC running at 1.25GS/s with two additional ADC to allow background calibration to compensate offset and mismatch errors. Timing calibration can be done by means of adjusting a programmable delay line, which can be done during the packet header of the communication standard used for data transmission.

1.2.3. Time domain processing.

With the evolution of CMOS fabrication processes, higher bandwidth is available for analogue designers. Therefore, systems that process signals in the time domain can benefit of the improved speeds to achieve larger resolutions. Traditional time-based architectures, such as dual-slope converters, can achieve very high resolution at the cost of large conversion times. Nowadays, as technology scales down, such time-based architectures are not only limited to low speed applications. A good example of achieving high-energy efficiency using time-domain processing and an extensive use of digital logic is the ADC architecture presented in (Yang & Sharpshkar, 2006, 2007). They propose a current-mode ADC that works like a pipelined converter which performs the residue amplification and subtraction in time domain, without the use of conventional amplifiers. The ADC is made of only two matched capacitors, a comparator and a switched reference current source controlled by a digital state machine. Since only a single comparator and one reference current source are used for the entire conversion process, the ADC consumes minimal power and avoids inaccuracies due to gain errors and offsets.

In (Jimenez-Iratorza et al. 2013) an interesting Time-to-Digital converter (TDC) achieving high energy efficiency is presented. It implements a recursive successive approximation algorithm in the time domain to perform the conversion with a low-voltage fully digital circuitry and very low power consumption.

1.3 Analogue circuitry simplification:

In previous sections, the way of successfully translating most of the analogue complexity to the digital domain by applying some techniques has been discussed. Another complementary approach to improve power efficiency could be based on the design of simplified analogue sub-circuits, allowing higher speed operation and power consumption decrease in basic building blocks. These techniques would include not only system level designs strategies but also analogue basic topologies that can be applied to many different architectures. In this way, higher energy efficiency can be obtained also at SoC level.

In the next sections, a review of some of the most interesting approaches for circuitry simplification will be provided.

1.3.1 Switched OP-Amp and OP-Amp sharing.

Op-amps are usually one the most power-consuming basic analogue blocks; therefore, a feasible option to reduce power consumption is to minimize their number in designs. Many switched-capacitor circuits need an active op-amp only during one clock phase, the amplification phase. As a consequence, there are two widely used techniques to reduce the number of active op-amps (Kim et al, 2006); one shares op-amps between successive stages and the other switches them off during the sampling phase. Op-amp sharing is a technique based on using the op-amp for two adjacent stages in successive alternative phases. This technique is widely implemented in pipelined ADCs but can be applied to any op-amp based topology.

Two-stage Class-A switched-op-amp (SO) is the most popular solution for low power switched capacitor (SC) sigma-delta modulators with ultra-low supply voltage conditions. The SO saves about 30%-40% of the total power since its output stage is just turned off at the integrating phase. For instance, an application to implement a 4th order band-pass $\Sigma\Delta$ modulator using switched op-amps is presented in (Kuo & Liu, 2006). While a classic op- amp topology would require four integrators working in two phases, in the proposed architecture the $\Sigma\Delta$ modulator is implemented only with two switched op-amps, drastically reducing the power consumption. To further increase efficiency, class AB output and input stages can be used in the op-amp implementation. In (Wang et al., 2009) by turning off the entire SO together, instead of only the output stage, with its common mode feedback (CMFB) circuit, the power consumption of the SO can be reduced about 50%.

1.3.2. OP-Amp less.

The traditional way of designing analogue circuits relies on high gain op-amps in negative feedback loops. As it was stated before, the op-amp power consumption directly impacts in the overall system. Recently, there is the trend of replacing the op-amps by more power efficient blocks such as comparators, inverters or simple structures based on local feedback. In this section, some of these approaches are described to illustrate this trend.

CBSC (Comparator Based Switched Capacitors) and zero-crossing detector based circuits: The CBSC technique was firstly proposed in (Fiorenza et al., 2006) and is applicable to any traditional op-amp based SC circuit. This technique consists in replacing the op-amp by a comparator and one or more switched current sources. As the author explains, the power reduction relies in the fact that a CBSC circuit senses the virtual ground while in traditional op-amp based SC circuit the virtual ground is forced which is less energy efficient.

Several ADC prototypes have demonstrated the practical application of CBSS and its potential high energy efficiency. In a 10 bits pipelined ADC based in zero- crossing detector fabricated using 65nm CMOS technology is reported. Another pipelined zero-crossing detector based is presented in. It achieves 12 bits of ENOB sampling at 50MS/s with high power efficiency indicated by a FOM of 88fJ/step.

Inverter based $\Sigma\Delta$ Modulator: This technique is another approach in which the op-amp is replaced by a simple inverter, which can be considered as a very simplified amplifier architecture. In the past, inverters had been applied to SC circuits as low-performance amplifiers for micro power consumption (Hosticka, 1979). In spite of the limited performance of inverters compared with op-amps,

inverters attract attention again to be used in deep submicron technologies. This is because of their ability to operate with very low supply voltages. Recent works have demonstrated that inverter-based design techniques can be applicable to high-performance SC circuits in aggressively scaled CMOS technologies.

For example, present a hybrid $\Sigma\Delta$ modulator fabricated in 65nm CMOS technology. It uses a highly digitized architecture with a five bits quantizer and a digital filter in order to reduce the complexity of the feedback DAC. A first order analogue loop filter (implemented using inverters) reduces the analogue parts to the minimum, so the area and power consumption are drastically reduced. In (the inverter behaviour used as an extremely simple amplifier is explained in detail. Three discrete time (DT) $\Delta\Sigma$ modulators of second and third order completely implemented by means of inverters are presented in this work. All of them achieve high dynamic range under low voltage supply conditions with a power consumption that places the best of them in the state-of-the-art nowadays.

Simple analogue cells based in local feedback.: Simple local feedback can lead to substantial enhancement of the performance with low cost in terms of noise, area and power consumption as it is usually implemented by a simple structure.

One good example is the structure called the Flipped Voltage Follower (FVF), a popular building block that relies on the local feedback idea. It was proposed in (Carvajal et al., 2005) to improve the performance of the classical voltage follower by means of local feedback.

A very commonly implemented basic cell in analogue microelectronics is the voltage follower (Fig. 1a). However, the gate-to-source voltage (v_{GS}) of the transistor acting as the follower (M1) depends on the output current, which leads to a high distortion for large output current variations. Some solutions have been proposed to address this problem (Sánchez-Sinencio & Silva-Martínez, 2000), (Barthélemy & Kussener, 2001), (Carvajal et al., 2005). The FVF is the basic cell made up by transistors M1 and M2 and the current source I_B shown in Fig. 1b. The local feedback implemented by transistor M2 keeps constant the current through transistor M1; this decreases the output impedance increasing the linearity of the current copy and in spite of output current variations.

A modified version of the FVF was proposed in (Luján et al., 2013) showing a better performance for large excursions of the input signal up to 10MHz and allowing a reduction in the quiescent power consumption of about 15 times when comparing with the classical solution, for the same linearity performances.

The idea of using local feedback to maintain the linearity requirements, while the power consumption is decreased, can be extended to more complex systems such as ADCs. One example of this is the CT $\Sigma\Delta$ modulator described in the section 2.2 of this chapter. A low power extremely low area CT $\Sigma\Delta$ modulator implementation based on the FVF is explained.

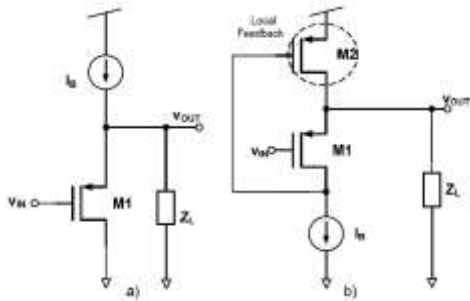


Fig. 1. Voltage followers: a) classical solution and b) FVF

Other op amp less approaches: Another example of a simplified op-amp-less architecture is the ADC array (Draxelmayr, 2004). Using parallelism to exploit the power efficiency of simple structures, a 6-bit ADC working at 600 MS/s based on eight SAR ADCs using a charge redistribution architecture is proposed. A power consumption of only 10 mW is obtained with very simple analogue circuitry (capacitors, switches and a comparator are sufficient) and no need for “precision” analogue blocks, like high gain op-amps In (Van der Plas, 2006) a 4-bit flash scheme with a comparator based simplified structure is proposed to design a high speed low-power ADC. Its structure is reduced to save power by removing all the non-essential blocks: Track & Hold, preamplifiers, reference ladder and bubble error correction. A comparator circuit combining sampling, amplification and reference level generation is used to implement the ADC obtaining a power consumption of only 2.5 mW.

1.4. Efficient use of biasing.

Charge transfer in class-A op-amp circuitry is inherently inefficient; the amplifier is biased with a constant current, while delivering on average only a small fraction of this current to the load. In this section, a more efficient use of biasing is discussed and various approaches adopted to solve this problem are commented

1.4.1 Dynamic and adaptive biasing:

In the last decades, several approaches have been proposed to optimize the efficient use of biasing towards the challenge of minimizing the power consumption-performance ratio. Most of them can be classified according to the concepts of dynamic and adaptive biasing. The term *dynamic biasing* was first coined in (Copeland & Rabaey, 1979), where a method to reduce the power consumption by taking advantage of having several clock phases in a SC integrator is proposed. This method is valid for all those circuits where there is a capacitive feedback between the output and a virtual ground Since then, the concept of dynamic

biasing has been extended, in general, to those approaches in which a block or part of it is connected or disconnected according to the received input power. An example of this technique is proposed in (Ozun et al., 2006) where a parallel combination of trans conductors is used, increasing the power consumption only if very low noise is required.

At the same time, the term of *adaptive biasing* (Degrauwe et al., 1981) has also become popular. It is usually referred to a continuous time change in the biasing according to the input. One of the most important adaptive biasing techniques is the class AB operation. In this technique, the slew rate limitation is tackled by boosting automatically dynamic tail currents for large inputs, keeping a well-controlled low quiescent current (Degrauwe et al., 1981), (Callewaert & Sansen, 1990), (Castello & Gray, 1985), (Tan & Chen, 2007), (Klinke et al., 1989), (Harjani et al., 1999). Several schemes can be found in the literature for class AB operation amplifiers. Most of them require of additional circuitry, which increases both power consumption and active area. Often they also imply additional parasitic capacitances to the internal nodes (Degrauwe et al., 1981), degrading the small signal performance of the circuit which is already poor due to the low quiescent current. In some cases, the stability issues get worse due to the use of positive feedback or structures that are sensitive to variations in process and environmental parameters (Callewaert & Sansen, 1990), (Klinke et al., 1989). Although other contributions consider negative feedback (Harjani et al., 1999), the required additional amplifiers to implement the feedback loops lead to complex designs. Another weakness of the tail current boosting topologies is that usually are not suitable for low voltage applications as in (Castello & Gray, 1985) due to the stacking of gate to source voltages.

Recently, some topologies based in the FVF (López-Martín et al., 2011) or using “Quasi” Floating Gate (QFG) techniques have been proposed (Ramírez-Angulo et al., 2008), while the first one offers simplicity of design and suitability for low-voltage operation simultaneously to high efficiency; the second one also minimizes the additional circuitry required just substituting a normal MOS transistor by a QFG MOS. Class AB operation can be applied to the input, to the output or both. This last option is known as superclass AB operation (López-Martín et al., 2005). The concept of class AB operation is so spread that today we can talk, for instance, about Class AB DACs (Seo et al., 2011), Sample & Holds (Sawigun & Serdjin, 2013) and multipliers (Sawigun & Serdjin, 2009) among others.

1.4.2 Assisted Op-Amp and helper techniques.

Instead of removing op-amps, as it has been explained in section 1.3.2, a less aggressive technique consists in keeping the op-amp but adding helper circuits that increase the energy efficiency by relaxing the requirements for the op-amp gain or bandwidth. For instance, in (Musah et al. 2007) the concept of correlated level shifting (CLS) is introduced. Correlated double sampling (CDS) technique can be used to reduce the error caused by finite open-loop gain, but it limits the maximum speed and its performance is poor near the rails. This makes it unsuitable for low voltage conditions, since the voltage swing is reduced too much. CLS is a SC technique similar to CDS, which also decreases the errors due to finite open-loop gain and allows rail-to-rail operation increasing the “distortion-free” swing. A third clock phase is needed but the settling time is about the same, so it does not have impact on the circuit speed. Open-loop gain requirements can be relaxed for a given resolution, leading to power consumption saving.

2. Applications examples.

In this section, one examples of design which make use of some of the previous power reduction techniques are presented. Then, the design of an efficient op- amp less implementation for CT $\Sigma\Delta$ modulators is described. In the proposed implementation, the op- amp is replaced by the compact local feedback structure explained in previous section.

2.1 Compact op-amp less CT $\Sigma\Delta$ modulator implementation for passive RFID application.

Combining sensors with passive RFID tags opens the way for new applications such as automotive and healthcare. As the passive RFID sensor nodes are intended to be powered by energy scavenging, ultra-low power consumption and robustness against process variations and changes in the supply voltage are essential requirements. In addition, low area occupancy is crucial in order to decrease the fabrication costs.

Low-bandwidth, moderate-resolution ADCs consuming a few microwatts are key elements for the sensor interface. Successive approximation register (SAR) converters are the typical choice for moderate-resolution low-frequency applications with ultra-low power requirements such as passive RFID. This type of converter achieves moderate resolution with very low power consumption and sets the state-of-the art in terms of energy efficiency. However, they consume large active area as the required DAC is normally implemented by a capacitor network. In this work the CT $\Sigma\Delta$ modulator architecture is proposed as an alternative to SAR architecture when the application also requires from very low area occupancy. CT $\Sigma\Delta$ modulators have become very popular over the last years, especially for lower power applications.

Traditionally, the loop filter is implemented either using an active-RC integrator or a gm-C approach. As it has been explained in the section 2 of this chapter, recent trends in low- power ADC design replace the internal op-amps (which usually are the most power consuming building blocks) with simple analogue circuitry. Following this trend, in this work a novel CT $\Sigma\Delta$ modulator implementation based on a local feedback is presented. The feedback provides a virtual ground node for reference subtraction without the need of op- amps or Operational Trans conductance Amplifiers (OTAs). A first-order $\Sigma\Delta$ modulator prototype with low complexity at system level and minimum area occupancy has been designed in order to validate the idea.

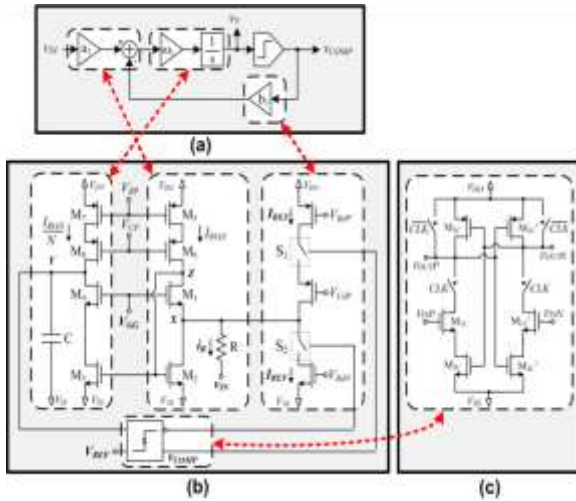


Fig. 2. First-order CT single-bit $\Sigma\Delta$ modulator. (a) Block diagram, (b) Proposed implementation, (c) Comparator schematic.

In Fig .2a the block diagram of a typical first-order CT single-bit $\Sigma\Delta$ modulator is shown. The modulator is made up of a comparator and a CT loop filter, which performs the subtraction and integration, as expressed in equation (1).

$$V_y(s) = (w_1 a_1 v_{in}(s) - b_1 v_{comp}(s)) / s \quad (2)$$

The compact implementation shown in Fig 2.b is proposed, where the input stage, the integrator stage and the feedback DAC have been highlighted.

The input voltage, v_{in} is converted into a current i_R by means of resistor R which connects the input signal to node X . Thanks to the feedback loop built up with transistors $M1$ and $M2$ and current source I_{BIAS} , the equivalent resistance at node X is extremely low.

In order to close the $\Sigma\Delta$ feedback loop the comparator controls two switches, $S1$ and $S2$, so that a reference current I_{REF} is injected or subtracted at node X depending on the comparator output. Therefore, the subtraction between the input signal and the comparator output is performed at node X in current mode. Note that both functions, the input voltage-to-current conversion and the feedback signal subtraction, are carried out by one resistor, two transistors and a current source. Then, the resulting current is copied and integrated in a capacitor. By a proper selection of V_{GG} , so that the quiescent value of the input voltage (V_{in}^Q) is equal to the bias voltage of node X (V_X^Q), the drain current of transistor $M2$ is given by.

$$I_{D,M2} = I_{BIAS} + (V_{in} + V_{in}^Q - V_X^Q) / R \pm I_{REF} / R \\ = I_{BIAS} + V_{in} / R \pm I_{REF} \quad (3)$$

As the input voltage is converted to current by a linear resistor, having a very low impedance at node X is crucial to achieve a good linearity at the input stage. This requirement is achieved thanks to the local feedback that keeps constant the current through transistor $M1$ in spite of output current variations at node X . Neglecting the body effect, the input impedance at node X is given by (Carvajal et al., 2005)

$$r_x = 1 / g_{m1} g_{m2} r_{o1}$$

which, for typical parameter values in the selected technology, is low enough to guarantee the linearity requirements for this application.

The current at the drain of $M2$, $i_{D,M2}$, is copied to node Y by the current mirror implemented with transistors $M3$ and $M4$, where the current I_{BIAS} is removed. The resulting current is injected into capacitor C where the integration is carried out. Finally, the voltage at node Y is given by (in the s-Domain):

$$V_y(s) = V_{in}(s) / R_{cs} \pm I_{REF} / CS \quad (4)$$

Expressions (2) and (4) are equivalent if $a_1 \omega_1 = 1/RC$ and $b_1 \omega_1 V_{COMP} = I_{REF}/C$. Note that no additional circuitry is required to bias the node Y . To reduce power consumption, the current through $M3$ (and $M7$) can be downscaled by modifying the gain of the current mirror. In our implementation a ratio of $N=3$ was chosen.

To save power, the dynamic latch-type comparator show in Fig .2c has been selected to close the modulator loop. Two switches open the latch branches during the reset phase so that the quiescent current consumption is zero.

To verify the proper operation of the proposed implementation, a first-order CT $\Sigma\Delta$ modulator prototype has been fabricated. The modulator digitalizes the signal coming from a MEMS accelerometer, which is a single-ended structure presently available in a $0.35\mu m$ CMOS technology. The ADC will be integrated in the same die with the MEMS accelerometer so it was designed in the same technology and with a single-ended input. The whole system is intended to be powered by an UHF RFID front-end which

provides a 3V nominal supply voltage typical for the selected technology (Vaz et al., 2010). Fig. 8a shows a microphotograph of the fabricated prototype. The total area consumption (without pads) is only 110µm x 125µm for the whole proposed circuit which makes it, to the author’s knowledge, the smallest ΣΔ modulator published for this range of specifications.

To verify the proper operation of the proposed implementation, a first-order CT ΣΔ modulator prototype has been fabricated. The modulator digitalizes the signal coming from a MEMS accelerometer, which is a single-ended structure presently available in a 0.35µm CMOS technology. The ADC will be integrated in the same die with the MEMS accelerometer so it was designed in the same technology and with a single-ended input. The whole system is intended to be powered by an UHF RFID front-end which provides a 3V nominal supply voltage typical for the selected technology (Vaz et al., 2010). Fig. 8a shows a microphotograph of the fabricated prototype. The total area consumption (without pads) is only 110µm x 125µm for the whole proposed circuit which makes it, to the author’s knowledge, the smallest ΣΔ modulator published for this range of specifications.

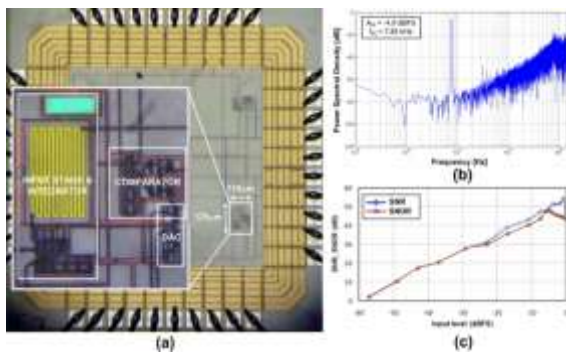


Fig. 3. (a) Circuit microphotograph, (b) Measured output spectrum, (c) SNR/SNDR versus input signal amplitude. Input signal frequency = 7.85 kHz. VDD = 3V.

The designed modulator has also shown to be very robust against supply voltage and bias current variations. The DR remains over 52dB for a supply voltage variation in the range 2.25 to 5 volts even for a 50% decrease of nominal bias current.

The FOM defined by (5) has been used to have an estimation of the energy efficiency achieved by the proposed ΣΔ modulator implementation. The minimum power consumption (4.35µW) was measured for a 2.25V supply voltage, leading to a FOM of 0.267 pJ/step. This value places this work close to the most power efficient CT ΣΔ modulators recently published, despite that it has been implemented in a reasonable old technology.

$$FOM = P / (2^{ENOB} \cdot 2BW) \quad (5)$$

Fig. 4a gives a graphical representation of the state of the art of power efficient ADCs in the same range of bandwidth. The measured performance of the proposed implementation is competitive in terms of energy efficiency compared with the state-of-the-art. The SAR converter (Harpe et al., 2010) sets the state-of-the-art and only a few ΣΔ modulators perform better than the proposed in this work.

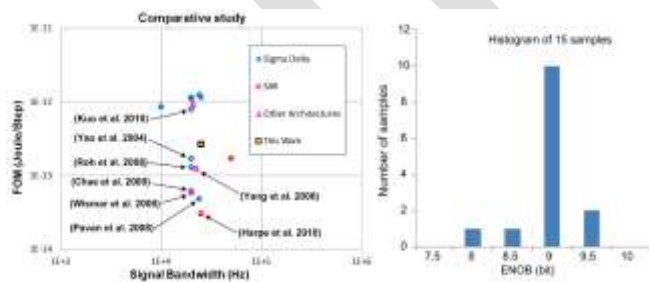


Fig. 4. (a) State of the art of ADCs regarding the selected FOM. (b) ENOB deviation for 15 measured samples (second version of the converter, VDD = 3V, input signal frequency = 7.85 kHz).

Fig. 4b shows a histogram of the ENOB deviation for 15 samples fabricated. Every sample worked properly with an ENOB variation lower than than ±0.5 bits, which is an indication of the robustness of the proposed modulator implementation against the process variation.

A compact implementation for CT ΣΔ modulators based on a local feedback has been presented. In order to validate the idea, a first order CT ΣΔ modulator for a self-powered sensor interface (9-bits of resolution and 25-kHz of signal bandwidth) has been designed in a 0.35µm CMOS technology. Experimental results confirm the idea and show that the proposed implementation leads to an extremely low area and highly power efficient ΣΔ modulator. The measured prototype has also shown to be very robust against process, supply voltage and bias current variations.

3. Conclusions.

In this chapter, the need of minimizing power consumption in electronic devices has been pointed out. For this reason, a review of the most common techniques used by IC designers with this purpose has been done. These techniques have been classified in four categories: biasing point optimization, digitally assisted techniques, analogue circuitry simplification and efficient use of biasing. In order to illustrate the large number of techniques that these categories involve, several references have been proposed through the chapter. Furthermore, one approaches based on the use of some of the reported technique have been described. The design proposes a compact op-amp less CT $\Sigma\Delta$ modulator for passive RFID applications. In order to reduce the power consumption, a local feedback technique is used.

REFERENCES:

- [1].Binkley, D. M.; Hopper, C. E.; Tucker, S. D.; Moss, B. C.; Rochelle, J. M. & Foty, D. P (2003).A CAD methodology for optimizing transistor current and sizing in analog CMOSdesign. *IEEE Transactions on Computer-Aided Design of Integrated Circuits and Systems*, Vol. 22, No. 2, (February 2003), pp. (225–237).
- [2].Borkar, S. (1999). Design challenges of technology scaling. *IEEE Micro*, Vol.19, No.4, Jul-Aug 1999, pp. (23-29).Brooks, L. and Hae-Seung Lee; (2009). A 12b 50MS/s fully differential zero-crossing-based ADCwithout CMFB, *IEEE International Solid-State Circuits Conference - Digest of Technical Papers, ISSCC 2009*, (8-12 Feb. 2009), pp.(166 - 167).
- [3].Callewaert, L.G.A. & Sansen, W.M.C (1990). Class AB CMOS amplifiers with high efficiency, *IEEE Journal of Solid-State Circuits*. Vol. 25, No.3, (June 1990), pp. (684-691). ISSN 0018-9200.
- [4].Wang, H.; Xu, J. and Wu, X. (2009). A high power efficiency Class AB switched-opamp for low voltage low power sigma-delta modulators. *IEEE International Conference of Electron Devices and Solid-State Circuits, EDSSC 2009*. Vol. , No. (25-27 Dec. 2009).
- [5]Wisnar, U.; Wisland, D. & Andreani, P. (2006). A 0.2V 0.44 μ W 20 kHz Analog to Digital SD Modulator with 57 fJ/conversion FoM. *Proceedings of the 32nd European Solid-State Circuits Conference, 2006. ESSCIRC 2006*, (19-21 Sept. 2006).
- [6]Yang, H.Y.; Sarpeshkar, R. (2005). A time- based energy-efficient analog-to-digital converter, *IEEE Journal of Solid-State Circuits*, Vol.40, No.8, (Aug. 2005).
- [7].Yang, H.Y.; Sarpeshkar, R. (2006). A BioInspired Ultra-Energy-Efficient Analog-to-Digital Converter for Biomedical Applications. *IEEE Transactions on Circuits and Systems I:Regular Papers*, Vol.53, No.11, (Nov. 2006).
- [8].Yao, L.; Steyaert, M. & Sansen, W. (2006). *Low-Power Low-Voltage Sigma-Delta Modulators in Nanometer CMOS*. Springer. ISBN-13 978-1-4020-4139-6 (HB), The Netherlands.
- [9].Yeknami, A.F.; Qazi, F.; Dabrowski; J.J. and Alvandpour, A. (2010). *Design of OTAs for Ultra-Low-Power Sigma-Delta ADCs in Medical Applications*. *International Conference on Signals and Electronics Systems ICSES, Poland, September 2010*

Experimental and Analytical Investigation on Partial Replacement of Concrete in the Tension Zone

Soji Soman¹, Anima P²

¹ PG Scholar, Dept of Civil Engineering, Universal Engineering College, Vallivattom, Thrissur, Kerala, India.

² Associate professor, Dept of Civil Engineering, Universal Engineering College, Vallivattom, Thrissur, Kerala, India.

somansoji3@gmail.com

Abstract— A beam is a one dimensional (normally horizontal) flexural member which provides support to the slab and vertical walls. In a normal beam (simply supported) two zones generally arise, i.e. compression zone at top and tension zone at bottom. As concrete is weak in tension, steel is introduced in the tension zone to take the tension, so logically no concrete is required in tension side. But concrete is to be provided on tension side to act as a strain transferring media to steel and may be called as 'sacrificial concrete'. Partial replacement of the concrete below the neutral axis is an idea that can create reduction in weight and savings in materials. In this paper, an experimental and analytical investigation on partial replacement of concrete in the tension zone that is below the neutral axis by creating air voids is discussed. Air voids were created using polyethylene balls and PVC pipes. Beams were cast using different percentage of polyethylene balls and PVC pipes. The results obtained for control specimens, beams with polyethylene balls and for beams with PVC pipes were compared. And analytical study of the same is done using ANSYS.

Keywords— Neutral axis, Polyethylene balls, PVC pipes, Sacrificial concrete, Tension and Compression.

INTRODUCTION

Concrete is the primary structural component that exists in buildings and bridges. In recent days the problem face by the construction industry is acute shortage to raw materials. In case of simply supported reinforced concrete beam; the region below neutral axis is in tension and above neutral axis is in compression. As concrete is weak in taking tension, steel reinforcement is provided in this zone. Concrete below the neutral axis act as a stress transfer medium between the two zones. Therefore the concrete below the neutral axis is known as sacrificial concrete. (The compressive force acts in the top zone at a distance of $0.42 X_u$, X_u is the neutral axis distance from the top of the section.)

Numerous studies are carried out for the investigation of alternate materials that can be used in concrete. Some locally available materials like fly ash, coper slag, rice hush etc. are experimentally evaluated. An alternate method is replacing the zone below the neutral axis with inert weightless substances like polyethylene balls, hollow PVC pipes etc. will not greatly affect the strength, stress geometry and shape characteristics of the beam.

In this paper, studies on partial replacement of concrete below the neutral axis in beams by creating air voids using different percentage of polyethylene balls and PVC pipes are discussed. Experimental results are compared with analytical results obtained using Ansys.

SIGNIFICANCE OF THE WORK

A. Scope of the Work

From the referred previous works, it is understood that in RC beams, less stressed concrete in & below the neutral axis can be replaced by some light-weight materials. Different materials like brick, expanded polystyrene sheet, terracotta, hollow blocks etc. were already studied which shows good results in reducing self-weight. But the ultimate load carrying capacity and first breaking load is very small when compared to control beam. To overcome these drawbacks air voids are created alternatively below the neutral axis by using plastic balls of 3.7cm and PVC pipe of 3.8cm diameter.

B. Objective of the Work

The objective is to reduce the amount of material, weight and cost of the reinforced concrete structures by replacing the concrete below the neutral axis.

C. Methodology

The methodology of the work consists of:

- (1) Selection of concrete grade; M25
- (2) Mix design for M25 grade concrete
- (3) Casting beam specimens of normal RC beams and beams with 4%, 8% & 16% replacement using polyethylene balls and PVC pipes.
- (4) Conducting two point loading test using 50t loading frame.
- (5) Analytical study is done using ANSYS.
- (6) Study on the obtained experimental and analytical results.

MATERIAL TESTS

TABLE I
MATERIAL TEST RESULTS

Test	Material	Equipment Used	Values Obtained
Specific Gravity	Ordinary Portland Cement	Le-Chatelier Flask	3.15
Specific Gravity	Fine Aggregates	Pycnometer	2.7
Specific Gravity	Coarse Aggregates	Vessel	2.94
Workability	M25 Concrete	Slump Cone Apparatus	100mm

MIX DESIGN

TABLE II
M25 MIX PROPORTIONING

Cement (Kg/m^3)	374.30
Fine aggregate (kg/m^3)	751.03
Coarse aggregate (Kg/m^3)	1280.31
Water (li/m^3)	149.72
Water cement ratio	0.40
Mix ratio	1:2.006:3.420

EXPERIMENTAL INVESTIGATION

A. Experimental Procedure

A total of fourteen specimens were cast and tested; two of the specimens are control specimens and the others are specimens with partial replacement of 4%, 8% & 16% below neutral axis. Details of specimens cast are shown in Table III below.

TABLE III
 DETAILS OF SPECIMENS CAST

SL.No:	Number Of Beams	Percentage Of Concrete Replaced	Designation Used	Material Adopted
1	2	0	CS	No Replacement
2	2	4	PB1	Polyethylene Balls
3	2	8	PB2	Polyethylene Balls
4	2	16	PB3	Polyethylene Balls
5	2	4	PP1	PVC Pipes
6	2	8	PP2	PVC Pipes
7	2	16	PP3	PVC Pipes

CS- Control Specimen
 PB- Polyethylene Balls
 PP- PVC Pipe

Dimension of all the specimens are 150mm x 200mm x 1250mm, with an effective span of 990mm. Main reinforcement provided is 3# 12mm diameter bars, 2# 8mm diameter bars are provided as anchor bars and stirrups are provided as 8 mm diameter bars @ 130mm c/c. Two point loading using 50t loading frame was used for testing the specimens.

The depth of neutral axis is calculated by considering M25 grade concrete and Fe 415 steel with an effective cover of 20mm. If the section is designed as a balanced or under-reinforced one, the steel also reaches yield as concrete fails. But in over-reinforced beams, the steel stress at failure will be below its yield strength. Here the section is designed as a balanced section, and neutral axis depth is 90.74mm from the top.

B. Test Procedure

Beams were tested using a 50t loading frame. Dial gauge was used to determine the deflection at the center of the beam. The behaviour of the beams was keenly observed from beginning to failure. The strength of the beam was tested as a two point loading system using a hydraulic jack attached to the loading frame.

The appearance of the first crack, and the development and the propagation of cracks due to increase in the load were also recorded. The loading was continued after the initial crack formation and was stopped when the beam was just on the verge of collapse. The values of load applied and deflection are noted directly and further the plot of load vs deflection is performed which is taken as the output. The load in kN is applied with uniformly increasing the value of the load and the deflection under the different applied loads is noted down. The applied load increased up to the breaking point and the ultimate cracking load was noted.



Fig.1 Experimental setup of beam specimen

EXPERIMENTAL RESULTS

A. Load Carrying Capacity

Ultimate strength of beams under two point loading was confirmed through recording the maximum load indicated by the dial gauge, whereas the cracking load was specified with the development of the first crack on the beam. It was found that there is a high variation in the load carrying capacity of the control specimen and that of beams with partial replacement.

TABLE IV
ULTIMATE LOAD OF ALL SPECIMENS

Beam Specimen	Ultimate Load (kN)
CS	392.40
PB1	445.47
PB2	700.80
PB3	509.68
PP1	471.45
PP2	739.04
PP3	560.65

Table IV shows the ultimate load of all the beam specimens, from the Fig.2 & Fig.3 it is clear that compared to control specimen (CS) the partially replaced specimens i.e. PB1, PB2, PB3, PP1, PP2 & PP3 have higher values. For both, specimens partially replaced using polyethylene balls and PVC pipes it can be clearly seen that PB3 & PP3 there is a decrease in the value. Therefore it can be said that partial replacement upto a range of 8% can be done and beyond that replacement leads to a decrease in the load carrying capacity.

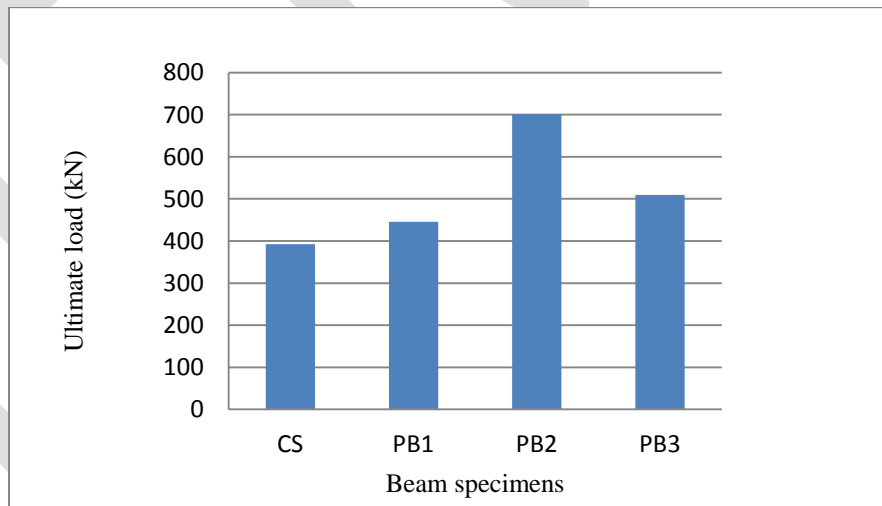


Fig.2 Ultimate load of different percentage of polyethylene balls

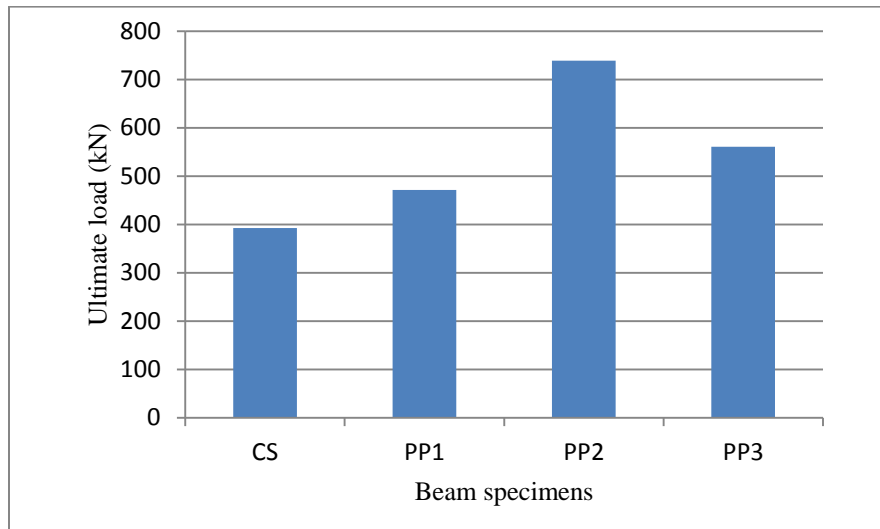


Fig.3 Ultimate load of different percentage of PVC pipes

B. Load Vs Deflection Graph

Due to increase in the load, deflection of the beam starts, upto a certain level the load vs. deflection graph will be linear i.e. load will be directly proportional to deflection. Due to further increase in the load, the load values will not be proportional to deflection, since the deflection values goes on increasing, strength of the material also increases and material loses elasticity undergoing plastic deformation. Hence from the graph we can predict strength of the material by knowing the deflection at the corresponding load values. The load vs deflection curves is shown in Fig. 4&Fig. 5.

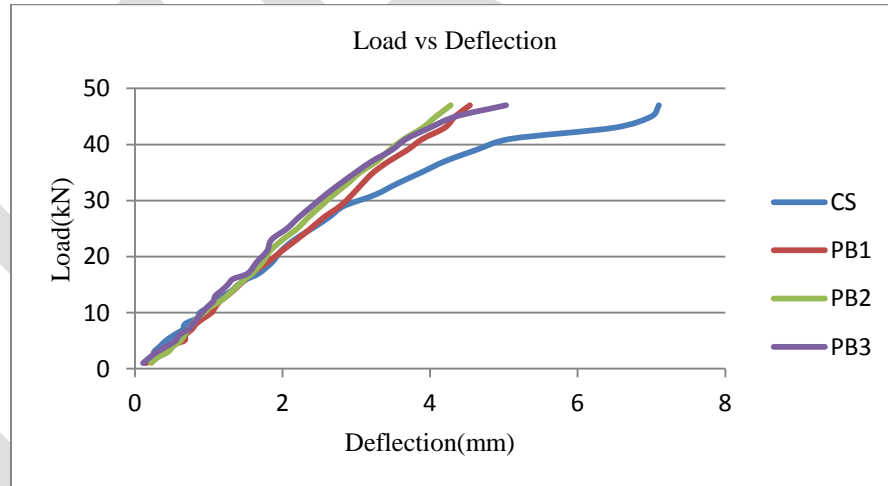


Fig.4 Load vs deflection of beams replaced using polyethylene balls

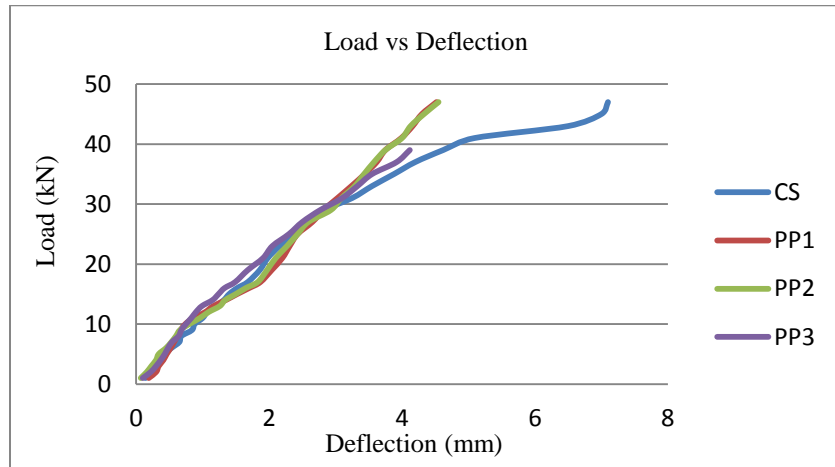


Fig.5 Load vs deflection of beams replaced using PVC pipes

C. Crack Pattern

Mainly shear cracks were developed from the supporting points and widened up as the load increased. At failure, the concrete in the compression region crushed. The cracks continued to widen as the load increased, and failure occurred soon after depicting a typical sudden type of shear failure. The crack pattern of replaced beams is similar to that of control specimen.

ANALYTICAL INVESTIGATION

ANSYS was employed to simulate the flexural and shear behaviour of the beam by finite element method. ANSYS is a general purpose finite element analysis (FEA) software package. FEA is a numerical method of deconstructing a complex system into very small pieces called element. The software implements equations that govern the behaviour of these elements and solves them all. These results can be presented in tabulated or graphical forms. This type of analysis is typically used for the design and optimization of a system far too complex to analyze by hand.

A. Calibration Model

An RCC beam with two point loading case was taken for analysis. Size of reinforced concrete beam-150mm x 200mm; size of loading and support steel plates- 25mm x 150mm, 5mm thick; steel reinforcement details; 3# 10mm diameter at bottom and 2# 8mm diameter bar at the top.

B. Modelling Procedure

1) Element Types and Real constants

TABLE V
 ELEMENT TYPES FOR MODEL

Material types	Element types
Concrete	SOLID 65
Steel reinforcement	LINK180
Steel plates at supports and loading	SOLID 186
PVC pipe	BEAM ELEMENT 186
Polyethylene balls	SOLID 168

TABLE VI
 REAL CONSTANTS FOR ELEMENTS

Real Constant Set	Element Type	Constants	
1	LINK 180	Cross sectional area (m ²)	3.39 x 10 ⁻⁴
		Initial strain	0
2	LINK 180	Cross sectional area (m ²)	1 x 10 ⁻⁴
		Initial strain	0

2) Material Properties

TABLE VII
 MATERIAL PROPERTIES OF ELEMENTS

Material	Young's Modulus	Poisson's Ratio
M25 concrete	25000	0.15
Fe 415 steel	2 x 10 ⁵	0.30
Polyethylene balls	3500	0.34
PVC pipes	3300	0.40

C. Meshing

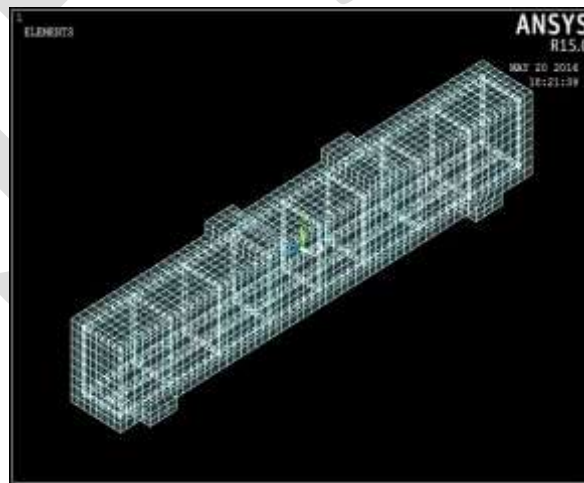


Fig.6 Meshing diagram of CS

D. Loads and Boundary Conditions

Displacement boundary conditions are needed to constrain the model to get a unique solution. The support was modelled in such a way that a roller was created. A single line of nodes on the plate were constrained in the UY and UZ directions.

E. Analysis

The finite element model for this analysis is a simply supported beam under two point loading condition. For the purpose of this model, static analysis type is utilized.

ANALYTICAL RESULTS

A. Load Vs Deflection Graph

Load deflection values were obtained, and using these graphs is plotted as shown in Fig.7& Fig.8.

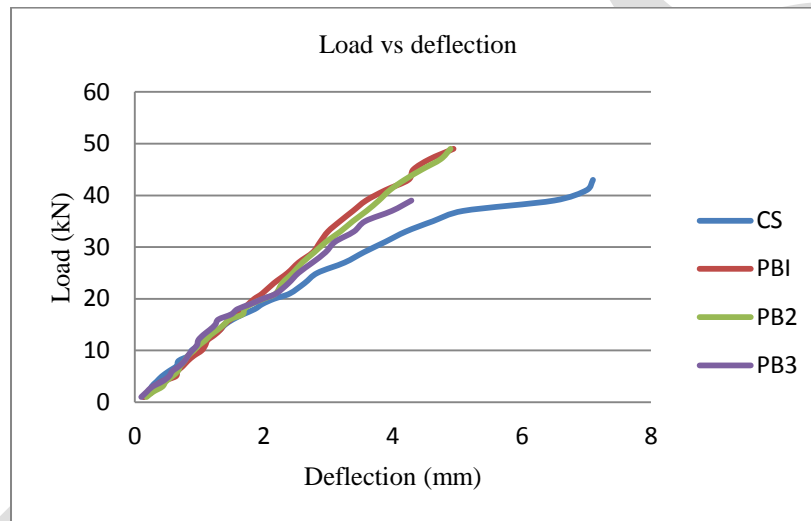


Fig.7 Load vs deflection of beams replaced using polyethylene balls

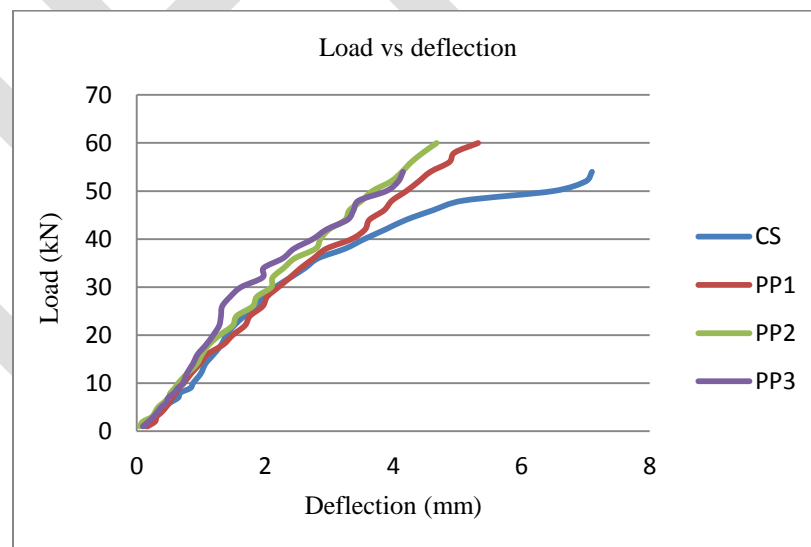


Fig.8 Load vs deflection of beams replaced using PVC pipes

EVALUATION & DISCUSSION

A. Load-deflection relationship

From Fig's 4, 5, 7 & 8, it is found that the load deflection relationship of control beam and that of partially replaced beams, obtained from experimental and analytical evaluation are found to be similar.

B. Concrete Saving

Concrete is one of the most versatile building materials. Material cost is a main component to be considered while construction, mainly this varies from 25 to 75%. Therefore, in order to control the cost, it is necessary to pay maximum attention for controlling the material cost. It should be made sure that the right quantities of materials are consumed with less wastage. This issue can be minimized by avoiding concrete below the neutral axis without bearing significant strength.

C. Labour Reduction

Labours are one of the major resources in construction industries. From the study it is clear that the total volume saving in concrete is directly proportional to the percentage reduction in labour. When the volume of concreting works reduce, the need for labour also get decreased simultaneously, which in turn minimize the production cost.

D. Cost Reduction

In current days the entire field is filled with competition, and it is necessary that a business concern should have utmost efficiency and minimum possible wastages to reduce the cost of production. From the study conducted, we can conclude that by partial replacement below neutral axis in beams, significant amount of concrete can be saved without affecting the strength.

E. Applications

From the results evaluated, it is observed that the reinforced beam with region below the neutral axis replaced with voids can be applied to various fields of constructions such as:

- Raft foundations
- Piers
- Similar other works.

ACKNOWLEDGMENT

My sincere gratitude to my guide, Mrs. Anima P, Associate professor who has believed in me since the beginning and accepted in undertaking my research work. Moreover, she has helped me from start to finish.

I'm thankful to all the teaching and non-teaching staffs of department of Structural Engineering, Universal Engineering College for offering me the opportunity to do this research work and also to Mr. Amal Stephen for his valuable guidance for doing my analytical work.

Finally, deep thanks to God for his unconditional support, and also to my family and friends.

CONCLUSIONS

Behaviour of reinforced concrete beams with region below the neutral axis with voids created using polyethylene balls and PVC pipes is similar to that of control specimen. Presence of voids instead of concrete in the low stressed zone has not caused significant reduction in strength of reinforced concrete beams. It has been observed that the replacement of concrete by voids in reinforced concrete beams does not require any extra labour or time. Economy and reduction of weight in beam depends on the percentage replacement of concrete. Replaced reinforced concrete beams can be used for sustainable and environment friendly construction as it saves concrete which reduces the emission of carbon dioxide during the production of cement. This work can be further investigated by using different diameter PVC pipes and balls. Several other parameters can also be tested like impact resistance, abrasion, fatigue resistance, etc. The work can be extended in other mixes and also by introducing other weightless inert materials.

REFERENCES:

- [1] J. Joy and R. Rajeev, "Effect of Reinforced Concrete Beam with Hollow Neutral Axis", International Journal For Scientific Research And Development, vol .2, issue 10, 2014.
- [2] K.K. Pathak, R. Patel and S. K. Dubey, "Analysis Of Infilled Beams Using Method Of Initial Functions And Comparison With FEM", Engineering Science And Technology, An International Journal, vol. 17, 158- 164, 204.
- [3] B. S. Karthik, Dr. H. Eramma and Madhukaran, "Behaviour of Concrete Grade Variation in Tension and Compression Zones of RCC Beams", International Journal of Advanced Technology In Engineering And Science, vol. 2, issue 07, 2348-7550,2014.
- [4] Dr. G. Hemalatha and W.G Jesudhasan, "Experimental Investigation on Beams Partial Replacement below the Neutral Axis", International Journal of Civil And Structural Engineering Research, 2014
- [5] A. S. Kumar and A. Joy, "Experimental Investigation on Partial Replacement of Concrete below Neutral Axis of Beam", International Journal of Science and Research, vol. 4, issue 8, August 2015.
- [6] S,B,Kandekar, P,D, Dhake and M,R,Wakchaure, "Concrete grade variation in tension and compression zones of RCC beams",IJIRSET, vol 2, issue 8, August 2013.
- [7] R,Patel, Dubey,S,K. and Pathak,K,K, "Brick filled reinforced concrete composite beams",IJET, E- ISSN 0976- 3945, 2012.
- [8] S,Arivalagan and S,Kandasamy, "Flexural behaviour of concrete-filled steel hollow sections beams",JCEM, vol 14, issue 2, 107-114, 2008.
- [9] V,Vanissorn, S,Wahyuni and N,Hamid, "Reinforced concrete beams with lightweight concrete infill", vol 7(27), 2370 -2379, July 2012.
- [10] Vidula ,S,S and M,R,Shiyekar. "Effect of change in grade of concrete on the composite members of a framed structure", International Journal of Engineering Research and Development, vol 2, issue 6, 35-41, August 2012.
- [11] M,Mohammad, M,Z,B,Jumaata, C,Mohamed, A,M,Ali, M,Jameela and S,Akiba., "An experimental investigation on bending stiffness and neutral axis depth variation of over-reinforced high strength concrete beams".pg 2060-2067, 2010.
- [12] L,F,A,Bernardoand.; S,M,R,Lopes, "Neutral axis depth versus flexural ductility in high-strength concrete beams".Pg 452-459, 2004.
- [13] R,Patel, Dubey,S,K. and Pathak,K,K, "Analysis of RC Brick Filled Composite Beams using MIF". Elsevier, 2012.

Retrofitting of Existing Cam Follower Mechanism for Computer Aided Kinematic Analysis

Mohammed Irfan Shamshoddin Pathan¹, S.R. Pawar², M.K.Beldar³

¹Mohammed Irfan Shamshoddin Pathan, Research Scholar, BVDU, COE, Pune

²S.R. Pawar, Assistant Professor, BVDU, COE, Pune

³M.K.Beldar, Assistant Professor, BVDU, COE, Pune

* Corresponding author Contact: +91 9665803857

E-mail address: irfanpathann@rediffmail.com

Abstract- Cam-follower mechanisms are most widely used in various mechanical machineries such as automatic machines, machine tools, IC engines, etc. In this research paper, the complete kinematic analysis is being done to determine the displacement of follower for different rotation angles of cams. The analytical calculations with required experimentations are being done to determine the displacement of follower for different rotation angles of cams. Using potentiometric linear motion sensor and absolute encoder with the required data acquisition system, having Mega 328 Microcontroller is used to find results after integrating with computer for kinematic analysis. The comparisons between real-time and analytical results for follower displacements corresponding to cam rotation angles have been done in MATLAB.

Keywords: Analytical model, Cam-follower, Potentiometric linear motion sensor, Analog Rotary Position Sensor, Tangent Cam, Eccentric Cam, Data Acquisition System, Kinematic analysis

1. Introduction

A cam is a mechanical element used to drive another element, called the follower through a specified motion by direct contact [1]. When the nature of follower motion is specified and the corresponding cam profile is determined, in many cases such cams are difficult and costly to manufacture, since a master cam has first to be made, mostly by hand, and then used as a standard model in the production of other cams of the same shape. From the viewpoint of accuracy of profile and cheapness of manufacture it is much better to form the cam profile of circular arcs and straight lines.

The nature of motion given to the follower may then be determined [2]. Tangent and Circular Cams are generally used in internal combustion engine practice. The aim of this work is to apply analytical and experimental techniques to develop an understanding of the behavior of cam and follower. In this paper, kinematic analysis is carried out for tangent cam and roller follower.

1.1. Kinematic analysis

Kinematic analysis involves the determination of displacement of follower at different cam rotation angles. Equations governing the motion of follower from the literature are used for displacement of followers [3].

1.2. Survey of Computer Aided Kinematic Analysis of cam and follower

1.2.1. Tangent cam with roller follower

In tangent cam, the flanks between the nose and base circles are straight and tangential to both circles. Tangent cam is generally symmetrical about the centre line of cam. A roller follower consists of a cylindrical roller which rolls on the cam surface. The rate of wear is considerably reduced as compared to knife edge follower. Consider a tangent cam having centre of cam at O_1 and that of the nose at O_2 . The straight flank commences from point A and continues till it meets arc of the nose radius at point E [3].

Let r = distance between the cam and nose centers

r_1 = Base circle radius or least radius

r_2 = Nose radius

r_r = Radius of roller

$r = r_1 + \text{lift} - r_2$

θ = angle of cam rotation

β = angle of ascent or rise, $\cos\beta = \frac{r_1 - r_2}{r}$

x = displacement of follower

Case 1

Roller in contact with flank

Consider a tangent cam with roller follower in contact with straight flank. The centre of the roller lies at point C on the pitch curve as shown in fig.1 [3].

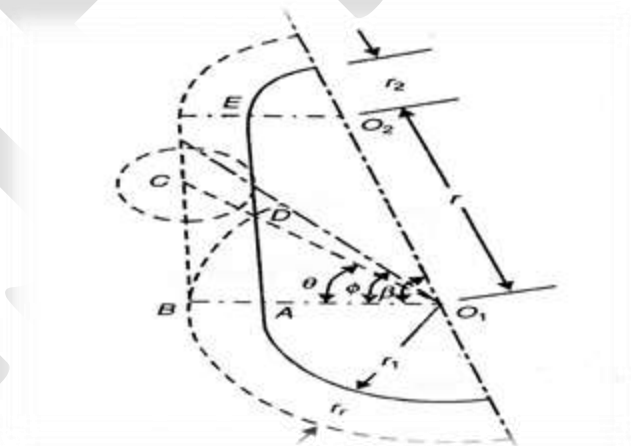


Fig.1. Tangent cam with roller follower in contact with straight flank[3]

Let angle turned by the cam from its original position i.e. beginning of the follower motion is θ° [3]:

$$x = (r_1 + r_r) \left(\frac{1}{\cos\theta} - 1 \right) \text{ where } r_1 = 14.5 \text{ mm and } r_r = 15 \text{ mm for the test cam}$$

Case 2

Roller in contact with circular nose

Consider the case when roller follower is in contact with nose. The centre of the roller lies at point C on the pitch curve of nose as shown in fig. 2[3]:

$$x = r\{\cos(\beta - \theta) + \sqrt{n^2 - \sin^2(\beta - \theta)}\} - (r_1 + r_r) \text{ where } n = \frac{r_2 + r_r}{r}$$

And $r = 14.3 \text{ mm}, r_2 = 10 \text{ mm}$ for the test cam

At the beginning of lift, $\theta = 0^\circ$

$$\tan \theta = \frac{r \sin \beta}{r_1 + r_r} \text{ where } r = 14.3 \text{ mm for the test cam}$$

At this value of θ , straight flank merges into circular nose. $\beta = 72^\circ$

When roller is at the apex of circular nose, $\theta = \beta$ and hence,

$$\phi = \beta - \theta = 0$$

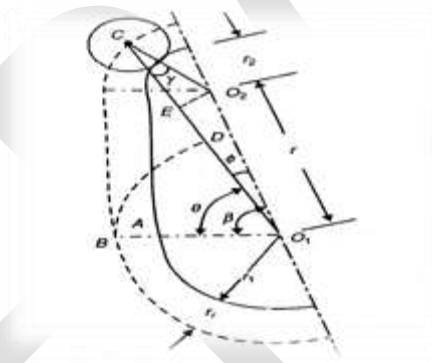
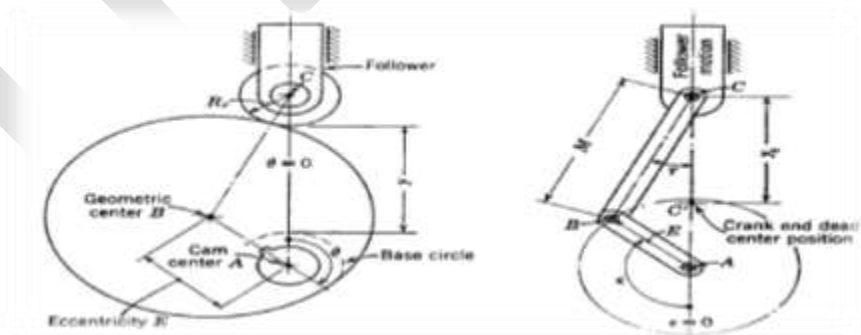


Fig.2. Tangent cams with roller follower in contact with nose of the cam[3]

1.2.2. Eccentric cam with roller follower



(a) Cam and follower

(b) Equivalent mechanism

Fig. 3 Eccentric cam with roller follower [4]

Displacement of follower for eccentric cam is given by $y = E - E \cos \epsilon + M \cos \tau - M$

Where,

M : Equivalent mechanism connecting rod length = 33.65 mm for the test cam

τ : Angle between connecting rod and follower motion = 4.99°

ϵ : Cam rotation angle

2. Existing experimental set up

The machine is a motorized unit consisting of a cam shaft driven by a DC shunt motor. The shaft and double ball bearing are used. A cam can be easily mounted at the end of camshaft. The follower has linear reciprocating motion and the type of the follower can be changed to suit the cam fitted to note the follower displacement for the angle of cam rotation. A spring is used to provide controlling force to the system. Weights on the follower rod can be adjusted as per requirements. The arrangement is provided to vary the speed of cam shaft. The displacement of follower is measured by the dial gauge. The angle of cam rotation is measured by the angular scale fitted to the apparatus.

3. Proposed developments

It is proposed to convert old cam follower set up with computerized one, so that various measurements such as displacement of follower will be recorded in Data Acquisition system.

After rigorous literature survey, it has been found that we can integrate existing set up with potentiometric linear motion sensor and absolute encoder, data acquisition system and thus to computer [5, 14].

New outfits in developed Experimental Set-up



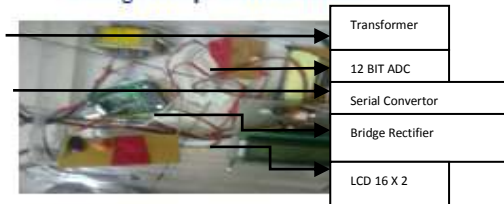
Potentiometric linear motion sensor



Analog Rotary Position sensor



Digital Tachometer



Data acquisition system

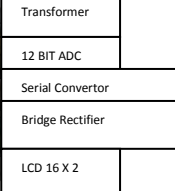


Fig.4. Displacement and angle sensors

New outfits included are:

- Potentiometric linear motion sensor, MTR18B Analog Output, for measuring follower displacement as shown in fig.4
- Analog Contactless Rotary Position Sensor, Series 22A RCBL, for measuring angle of rotation of cam as shown in fig.4.
- Digital advanced Tachometer, MEXTECH DT-2236C, for measuring speed of rotation of cam as shown in fig.4.
- Data acquisition system having Mega 328 Microcontroller for interfacing cam follower with computer as shown in fig.5.
- Computer having MATLAB software for plotting graphs of cam rotation angle versus follower displacement as shown in fig.5.

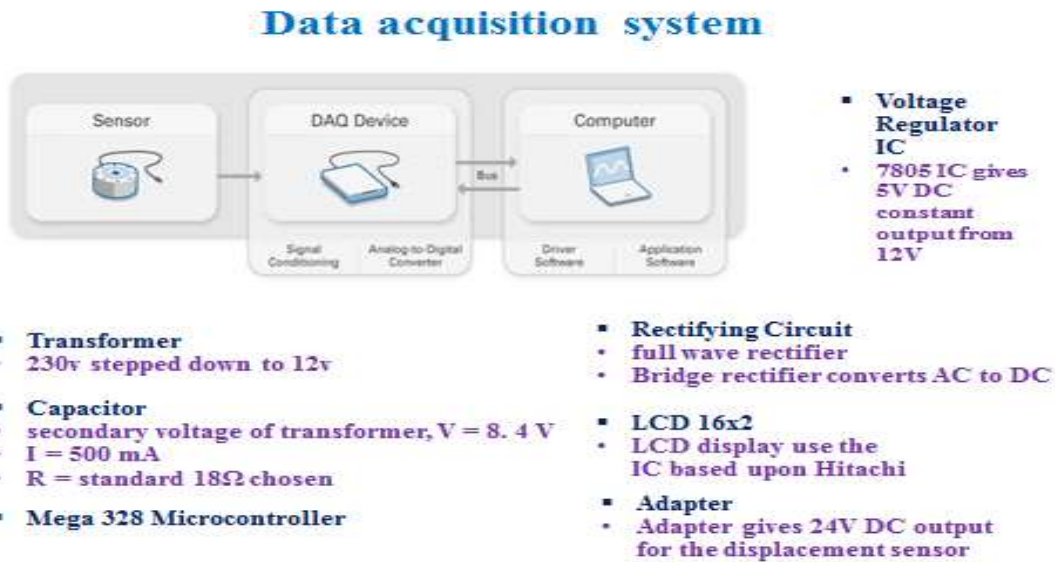


Fig.5. Data acquisition system



Fig.6. Developed Cam follower mechanism

The retrofitted experimental set up is shown in Fig. 6.

4. Results

Analytical and real-time values for follower displacement in mm are shown for cam rotation angle from 0° to 360°, for tangent cam and roller follower at 300 rpm motor speed in table 1.

Table 1. Analytical and Real-Time Results for Tangent Cam and Roller Follower

Sr. no	Angle in Degrees	Displacement in mm (analytical)	Displacement in mm (real-time)	Sr. no	Angle in Degrees	Displacement in mm (analytical)	Displacement in mm (real-time)
1	0	0.00	0.00	20	180	0.00	0.00
2	10	0.46	0.44	21	190	0.00	0.00
3	20	1.89	1.74	22	200	0.00	0.00
4	30	4.31	3.66	23	210	0.00	0.00
5	40	6.52	6.29	24	220	0.00	0.00
6	50	8.23	8.14	25	230	0.00	0.00
7	60	9.34	9.02	26	240	0.00	0.00
8	70	9.79	9.11	27	250	0.00	0.00
9	72	9.83	9.32	28	260	0.00	0.00
10	80	9.60	8.74	29	270	0.00	0.00
11	90	8.75	8.19	30	280	0.00	0.00
12	100	7.27	7.09	31	290	0.00	0.00
13	110	5.24	5.02	32	300	0.00	0.00
14	120	2.79	2.64	33	310	0.00	0.00
15	130	0.90	0.87	34	320	0.00	0.00
16	140	0.07	0.07	35	330	0.00	0.00
17	150	0.00	0.00	36	340	0.00	0.00
18	160	0.00	0.00	37	350	0.00	0.00
19	170	0.00	0.00	38	360	0.00	0.00

In MATLAB, graphs have been plotted for tangent cam by both analytical and real-time ways, as shown in fig.7.

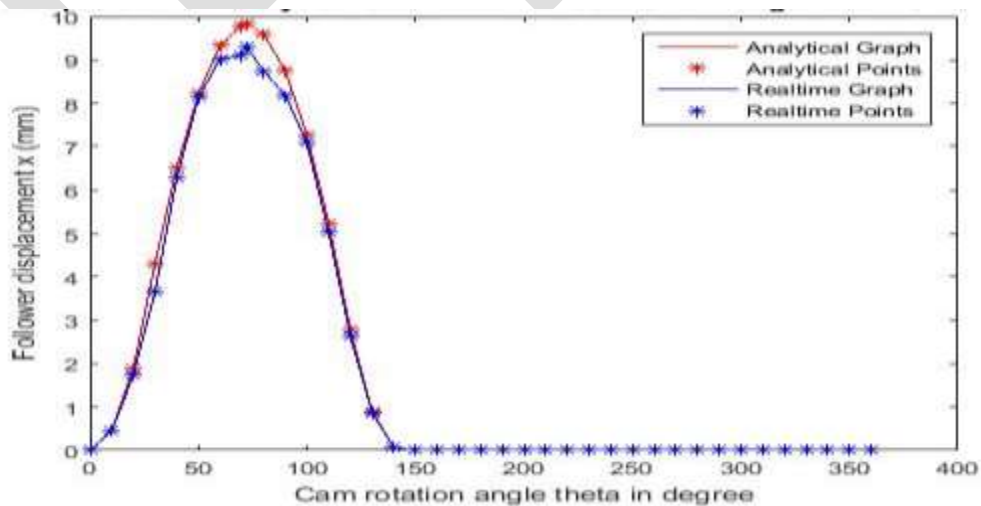


Fig. 7. Comparison of Analytical and Real-time results for Tangent cam

Analytical and real-time values for follower displacement in mm are shown for cam rotation angle from 0° to 360°, for Eccentric cam and roller follower at 300 rpm motor speed in table 2.

Table 2. Analytical and Real-Time Results for Eccentric Cam and Roller Follower

Sr. no	Angle in Degrees	Displacement in mm (analytical)	Displacement in mm (real-time)	Sr. no	Angle in Degrees	Displacement in mm (analytical)	Displacement in mm (real-time)
1	0	0.00	0.00	20	190	11.60	10.77
2	10	0.07	0.07	21	200	11.29	10.44
3	20	0.30	0.27	22	210	10.79	9.77
4	30	0.66	0.66	23	220	10.13	9.51
5	40	1.17	1.10	24	230	9.32	9.24
6	50	1.80	1.71	25	240	8.41	8.41
7	60	2.56	2.36	26	250	7.42	7.09
8	70	3.42	3.26	27	260	6.39	6.21
9	80	4.36	4.30	28	270	5.36	5.03
10	90	5.36	5.07	29	280	4.36	4.30
11	100	6.39	6.15	30	290	3.42	3.33
12	110	7.42	7.35	31	300	2.56	2.48
13	120	8.41	8.34	32	310	1.80	1.60
14	130	9.32	9.02	33	320	1.17	1.17
15	140	10.13	9.62	34	330	0.66	0.66
16	150	10.79	9.67	35	340	0.30	0.30
17	160	11.29	9.71	36	350	0.07	0.07
18	170	11.60	10.29	37	360	0.00	0.00
19	180	11.70	10.81				

In MATLAB, graphs have been plotted for Eccentric cam by both analytical and real-time ways, as shown in fig. 8.

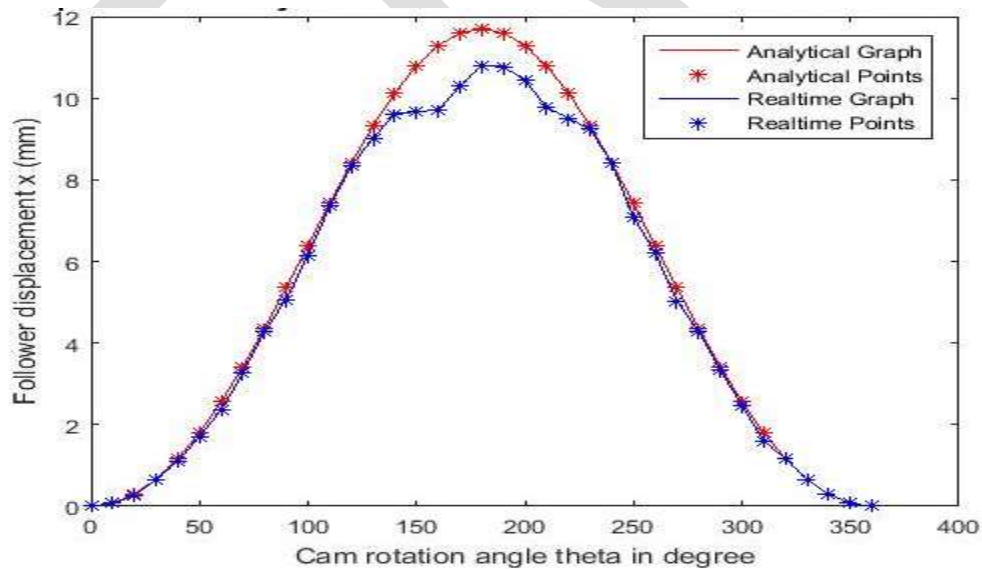


Fig.8. Comparison of Analytical and Real-time results for Eccentric cam

5. Conclusion

Retrofitted Cam Follower Mechanism has been outfitted with new accessories which are Potentiometric linear motion, Analog Contactless Rotary Position Sensor, Digital advanced Tachometer, Data acquisition system and Computer having MATLAB software.

These have facilitated in getting advantages including fast computations, accuracy of final results. Further, we have fabricated suitable fixture for the same, manufacturing of Tangent Cam and Eccentric circle cam as per standards has been done.

During comparisons for Tangent Cam, 3 % deviation (in between analytical and real time) is observed which is not as significant. However for Eccentric Cam, 4 % deviation is noted and that too because of variation in profile of cams (eccentric cam has different profile as compared to tangent cam). And therefore, it can be said that in either case graphs are almost matching. And the reasons behind slight variations (3 % and 4 % deviations) are sudden changes in acceleration which finally induces jerk and thereby inducing vibrations and noises in Cam and Follower Mechanism.

REFERENCES:

1. Joseph Edward Shigley and John Joseph Uicker, Jr., "theory of machines and mechanisms", International Edition MCGRAW-HILL book company.
2. Thomas Bevan, third edition, "the theory of machines", CBS publishers and distributors, Delhi, 1984.
3. C.S. Sharma and Kamlesh Purohit, "Theory of Mechanisms and Machines", PHI Learning Private limited, New Delhi, 2010.
4. Harold A. Rothbart, "CAM DESIGN HANDBOOK", McGRAW-HILL New York Chicago San Francisco Lisbon London Madrid Mexico City Milan New Delhi San Juan Seoul Singapore Sydney Toronto, 2004.
5. M V Ingalkar and C R Patil, "Computer Aided Kinematic Analysis And Simulation of The Cam-Follower Mechanism", International Journal of Mechanical engineering and robotics Research Vol.2, No.2, pp. 164-165, 2013.
6. Carra S, Garziera R and Pellegrini M, "Synthesis of Cams with Negative Radius Follower and Evaluation of the Pressure Angle", Vol. 39, No. 10, pp. 1017-1032, 2004.
7. Mahyuddin A I, Mitha A and Bajaj A K, "On Methods of Evaluation of Parametric Stability and Response of Flexible Cam-Follower Systems", in Proceedings of 21st Biennial ASME Mechanisms Conference on Cams, Gears, Robot and Mechanism Design, DE-Vol. 26, pp. 1-9, 2009.
8. Mills J K, Notash L and Fenton R G, "Optimal Design and Sensitivity Analysis of Flexible Cam Mechanisms", Vol. 28, No. 4, pp. 563-581, 1993.
9. Norton R L, "Cam Design Manufacturing Handbook", Industrial Press Inc., SBN 0831131225, 2002.
10. Rattan S S, "Theory of Machines", Tata McGraw Hill, New York, 2003.
11. Shigley and Joseph Edward, "Theory of Machines and Mechanisms", Tata McGraw Hill, New York, 2003.
12. Valentini P P and Pennestri E, "Design and Simulation of a Variable- Timing Variable-Lift Cam Mechanism", 2009.
13. Yuhua Zhang and Joong-Ho Shin, "A Computational Approach to Profile Generation of Planar Cam Mechanisms", *J. Mech. Des.*, Vol. 126, No. 1, p. 183 (6 pages) doi:10.1115/1.1637652, 2004.
14. Prof. H.D. Desai, Prof. V.K. Patel, "Computer Aided Kinematic and Dynamic Analysis of Cam and Follower", Proceedings of the World Congress on Engineering Vol.2, London, U.K, 2010.

Isolated Word Recognition Using MFCC and Vector Quantization

Manish Kumar Sharma

Department of Electrical Engineering, VJTI Mumbai

Email:-manishkumarsharma0911@gmail.com

Mob. NO. 8380902226

Abstract— Automatic Speech Recognition (ASR) technology is a way to interface with computer. In this paper we describe speech recognition technique using multiple codebooks of MFCC derived features. The proposed algorithm is useful in detecting isolated words of speech. In this algorithm we first create database i.e. codebook by calculating mel frequency cepstral coefficient first and then codeword for each word. Vector quantization method is used to obtain codeword. Different codewords make a codebook. We calculate distance between uttered speech codeword and codewords which are stored in matrix form to detect the particular word. Codebook reduces processing time. The efficiency obtained by MFCC is much more than the other available techniques.

Keywords— MFCC, ASR, Vector quantization, DFT, FFT, Pattern Recognition, Discrete cosine transform.

INTRODUCTION

Recently, there have been a number of successful commercial ASR products. However, still many problems exist in real-world and real-time speech recognition applications. The recognition accuracy of a system is, in most of the cases, very far from that of a human listener, and its performance would degrade drastically with small modification of speech signals or speaking environment [1]. To overcome this problem care must be taken about the signal to noise ratio of speech signal [1] [11].

There are three major types of feature extraction techniques, like, perceptual linear prediction (PLP) Mel frequency cepstrum coefficient (MFCC) and linear predictive coding (LPC). MFCC and PLP are the most commonly used feature extraction techniques in modern ASR systems [2]. In our proposed system we have used MFCC for feature extraction purpose because it gives best results among all the available techniques.

ALGORITHM FOR SPEECH RECOGNITION

In this proposed system we first do the preprocessing on the speech signal and then calculate mel frequency cepstrum coefficient. Using these coefficients we make a codeword for each and every word in our database by using vector quantization method. Different codewords make a codebook. These codewords are stored in the matrix form. Then for speech recognition we calculate Euclidian distance between test sample and with each and every sample which is already stored in the database and that particular stored sample which gives minimum distance will be our output. The same procedure is explained by using figure 1.

A. Data Acquisition

The speech waveform, sampled at 11025 Hz is used as an input to the feature extraction module. Sampling frequency is chosen in such a way that we should have a good quality signal but care should be taken about the size of the speech waveform. Because if we choose higher sampling frequency we may have good quality signal but time taken for processing will increase. The acoustic model of the environment in which we are recording may affect the performance of the system [12].

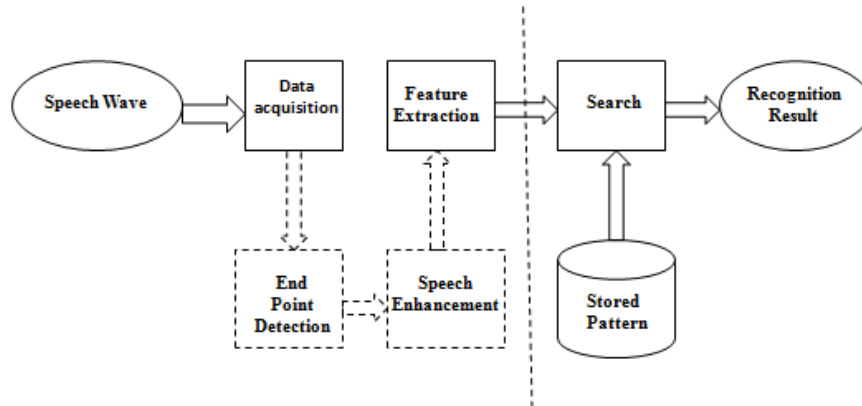


Fig.1. Block diagram for Speech Recognition

B. Endpoints detection

In order to detect an endpoint in the signal, a signal recording has been processed by the Endpoint Detector Algorithm which uses energy and zero crossing rate of signal to detect endpoints [9].

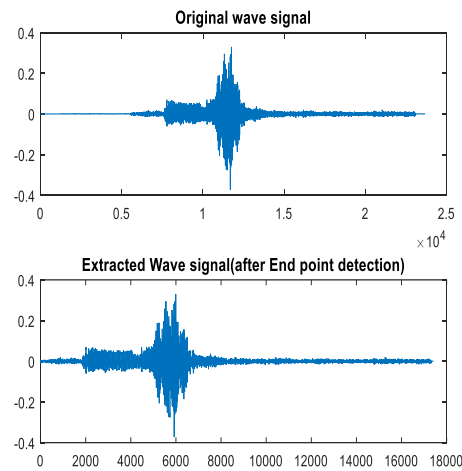


Fig.2. End point detection of signal INDIA

FEATURE EXTRACTION USING MFCC

For feature extraction purpose MFCC is used and its algorithm has following steps:

A. Pre-emphasis

Noise is an unwanted signal and it has a greater effect on the higher modulating frequencies than the lower ones. Hence, to reduce the effect of noise higher frequencies are artificially boosted to increase the signal-to-noise ratio. Pre-emphasis process is used for spectral flattening using a first order finite impulse response (FIR) filter [2]. Equation (1) represents first order FIR filter.

$$H(z) = 1 - \alpha z^{-1}, 0.9 \leq \alpha \leq 1 \quad (1)$$

B. Frame blocking

Speech is a non-stationary signal but for the analysis and feature extraction purpose we always consider short duration frames and we assume that for that short duration signal is stationary. Frame duration should not be too long because it may affect time resolution and frame duration should not be too short because it may affect frequency resolution [2]. In the proposed system frame of length 256 samples is used and frame overlapping length is 128.

C. Windowing

There may be discontinuities at the beginning and end of the frame which are likely to introduce undesirable effects in the frequency response. Hence, to reduce discontinuities each row is multiplied by a window function. A window alters the signal, tapering it to almost zero at the beginning and the end. In the proposed system Hamming window is used as it introduces the least amount of distortion. Our proposed system uses Hamming window of length 256 [5].

$$h(n) = \begin{cases} 0.54 - 0.46 \cos\left(\frac{2\pi n}{N}\right), & 0 \leq n \leq N \\ 0, & \text{otherwise} \end{cases} \quad (2)$$

D. Spectral magnitude of DFT

DFT is used to convert time domain signal into frequency domain signal. Time domain data is converted into frequency domain to obtain the spectral information [5]. By spectral information we mean the energy levels at each and every frequency in the given window. Time domain data is converted to frequency domain by applying Discrete Fourier Transform (DFT) on it.

$$X(k) = \sum_{n=0}^{N-1} x(n) e^{-\frac{j2\pi kn}{N}}, 0 \leq k \leq N-1 \quad (3)$$

For each frame we find its DFT. We have used FFT algorithm to find the DFT of the signal. FFT output is a set of complex numbers i.e. real and imaginary parts. But speech recognition systems deal with real data. Hence, we avoid the use of complex value. Let us assume the real and imaginary parts of $X(k)$ as $\text{Re}(X(k))$ and $\text{Im}(X(k))$, then the magnitude of the speech signal can be obtained by using equation (4).

$$X(k) = \sqrt{(\text{Re}(X(k)))^2 + (\text{Im}(X(k)))^2} \quad (4)$$

E. Mel frequency filter bank

The best thing about the Mel-frequency analysis of speech is that, it is based on human perception experiments. How our ears recognize the speech same is used in Mel frequency analysis and therefore it is proven to be best technology for speech recognition. It

has also been proved that ears of human are more sensitive and have higher resolution to lower frequencies compared to higher frequencies. Therefore, the filter bank is designed in such a way that it emphasizes the low frequency over the high frequency [2].

Also the speech signal does not follow the linear frequency scale used in FFT. Hence, a perceptual scale of pitches equal in distance, namely Mel scale is used for extraction of features. Mel scale frequency is quite similar to the logarithm of the linear frequency, reflecting the human perception. We use log because our ears work in decibels.

$$Mel(f) = 2595 \log_{10}\left(1 + \frac{f}{700}\right) \quad (5)$$

Use of triangular band pass filter is to extract the spectral envelope, which is formed by dominant frequencies present in the speech signal. Therefore, Mel-frequency filters are triangular band pass filters which are non-uniformly spaced on the linear frequency axis but uniformly spaced on the Mel frequency axis and numbers of filters are more in the lower frequency region and less number of filters in the higher frequency region [2].

Below equation (6) denotes the filter bank with M (m = 1, 2, 3...M) filters, where m is the number of triangular filter in the filter bank then Hm(K) will be as below. In the implementation we have used 13 triangular band pass filters and the range of frequency over which we are operating is 133Hz to 2143Hz.

$$H_m(k) = \begin{cases} 0, & \text{for } k < f(m-1) \\ k - \frac{f(m-1)}{f(m)-f(m-1)}, & \text{for } f(m-1) \leq k \leq f(m) \\ f(m+1) - \frac{k}{f(m+1)-f(m)}, & \text{for } f(m) \leq k \leq f(m+1) \\ 0, & \text{for } k > f(m+1) \end{cases} \quad (6)$$

F. Logarithm of filter energies

Human ears smooth the spectrum and use the logarithmic scale approximately. We use equation (7) to compute the log-energy i.e. logarithm of the sum of filtered components for each filter.

$$S(m) = \log_{10}[\sum_{k=0}^{N-1} |X(k)|^2 \cdot H_m(k)], 0 \leq m \leq N \quad (7)$$

G. Discrete cosine transform

The discrete cosine transform (DCT) converts the log power spectrum (Mel frequency domain) into time domains. DCT gathers most of the information of the signal to its lower order coefficients, resulting in significant reduction in computational cost. Equation (8) represents the discrete cosine transform.

$$C(k) = \sum_{m=0}^{M-1} S(m) \cos\left(\frac{\pi k(m+\frac{1}{2})}{M}\right), 0 \leq k \leq K \quad (8)$$

The number of coefficients obtained for each frame is 13 and equal to number of triangular band pass filter. MFCC features will be a matrix and whose rows are equal to number of triangular bandpass filter and columns are equal to number of frames in a word. Number of frames varies for each word so MFCC matrix size will be different for each word.

VECTOR QUANTIZATION

The Vector Quantization (VQ) technique is used for mapping vectors from a large number of vector space to a finite number of regions in that space. We call each region a cluster and can be represented by its centre called a codeword. Accuracy of the system will be defined by inter-cluster variance and intra-cluster variance. For good accuracy inter-cluster variance should be large and intra-cluster variance should be less. The collection of all codeword is called a codebook. After extracting features, the acoustic vectors extracted from input speech of a speaker provide a set of training vectors [4]. The problem of speech recognition belongs to a much broader topic in engineering and scientific research and is called pattern recognition. The goal of pattern recognition is to classify objects of importance into one of a number of classes or categories [3]. The clusters here refer to isolated word.

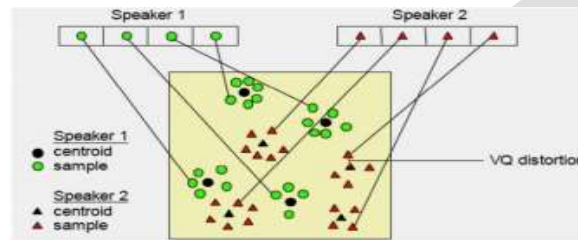


Fig.3. clusters of different codeword

The algorithm which we have used for vector quantization is Lin-Buzo-Gray algorithm. LBG algorithm is like a K-means clustering algorithm which takes a set of input vectors $S = \{x_i \in \mathbb{R}^d | i = 1, 2, \dots, n\}$ as input and generates a representative subset of vectors $C = \{c_j \in \mathbb{R}^d | j = 1, 2, \dots, K\}$ with a user specified $K \ll n$ as output according to the similarity measure. In our implementation we have used $k=16$ and d =number of frames in speech waveform of a word [8].

Vector quantization can give different size of matrix as its output but we have chosen a matrix of 8×16 for each sample as it gives cluster which gives high accuracy. For recognition of test sample we calculate Euclidian distance between test sample and each sample stored in the database. Then we calculated average of the distance of a every cluster and compared all the distances. The minimum distance cluster is output.

RESULTS

In this work five words i.e. Invention, Technology, Science, Teacher and India are used to train and test the system. At first we saved the 10 patterns of these words and then one of the earlier speaker's samples is used to test the system. Test sample used is of word 'Science'. Distance of test sample with word Invention, Technology, Science, Teacher and India is 1.8265, 1.7584, 1.1494, 1.9367 and 1.6327 respectively. The result shows that the distance is minimum for the word science and is equal to 1.1494 hence spoken word is 'Science'. Below figure (4) shows the same result graphically.

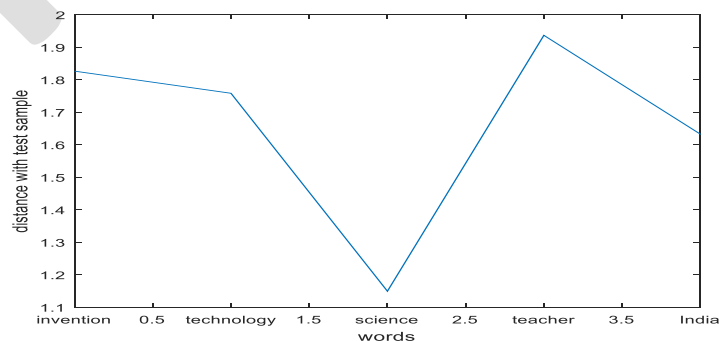


Fig 4. Result showing distance with test sample

ACKNOWLEDGMENT

Authors would like to express their sincere gratitude towards Dr. R N Awale for being a source of help and encouragement to put forth this project. Authors would also like to thank their Institute Veermata Jijabai Technological Institute, Mumbai for providing the necessary facilities for carrying out research work.

CONCLUSION

With MFCC and Vector Quantization, isolated word detection system is generated in MATLAB environment. System is trained by saving templates of five separate words. Results showed that saving ten templates for each word in training phase gives good results compared with five templates but generates delay.

REFERENCES:

- [1] Endpoint Detector Algorithm for Speech Recognition Application E.A. Escoto-Sotelo, E. Escamilla-Hernandez, E. Garcia-Rios, H. M. Perez-Meana Instituto Politecnico Nacional SEPI ESIME Culhuacan
- [2] Yuan Meng, Speech recognition on DSP: Algorithm optimization and performance analysis, The Chinese university of Hong Kong, July 2004, pp. 1-102
- [3] Isolated Word Speech Recognition Using Vector Quantization (VQ) Dipmoy Gupta, Radha Mounima C. Navya Manjunath, Manoj PB Dept. of EC,AMCEC, Bangalore Volume 2, Issue 5, May 2012, pp 164-168
- [4] Vector Quantization in Speech Coding. John Makhoul, Fellow ,IEEE, Salim Roucos, Member IEEE, And Herbert Gish ,Member, IEEE proceedings of the IEEE, Vol 73, No. 11, November 1985 pp. 1552-1586
- [5] An Efficient MFCC Extraction Method in Speech Recognition Wei HAN, Cheong-Fat CHAN, Chiu-Sing CHOY and Kong-Pang PUN Department of Electronic Engineering, The Chinese University of Hong Kong ISCAS 2006 pp. 145-148
- [6] Robust speech recognition using neural networks and hidden markov models Lin Cong, Saf Asghar and Bin Cong Advanced Micro Devices, 3625 Peterson Way, Santa Clara, CA, 95054, USA Dept. of Computer Science, California State University.
- [7] A general approach to natural language conversion Md. Abu Nuser Musud', Md. Muntusir Mamun Joarder', Md. Turiq-UI-Azam
- [8] A Robust Lin-Buzo-Gray Algorithm in Data Vector by Quantization Liu Jing , Wang Quan
- [9] Speech Analysis for Automatic Speech recognition, Norwegian University of Science and Technology by Noelia Alcaraz Meseguer
- [10] MATLAB Based Feature Extraction Using Mel Frequency Cepstrum Coefficients for Automatic Speech Recognition Siddhant C. Joshi, Dr. A.N.Cheeran
- [11] Fundamentals of speech by Lawrence Rabiner and Biing Huang Juang

Wireless Sensor Networks: A Survey

Neetu¹

1. Post-graduation student, Department of Computer Engineering, Punjabi university, Patiala, Punjab, India

Abstract: In recent years Wireless Sensor Network (WSN) has been growing rapidly and provides more services in several areas. Recent advancements in this field of computing, communication and sensing are attracted towards research in WSN. Networks lifetime depends on energy balancing of WSN. Clusters are collection of autonomous servers. The main target of clustering is to improve the scalability and reduce energy consumption. Cluster head absorbs more energy than non-cluster head nodes. Suited option of cluster head grows the network life time and energy efficiency. In this paper, cluster head selection and its techniques has been analysed. It has been observed that Fuzzy based cluster head technique is better than Topology and Coverage area. Because fuzzy logic has the potential to deal with conflicting situations and there are no complex mathematical modelling techniques are required.

Keyword: Wireless Sensor Networks, Clustering and its technique.

1. INTRODUCTION

Wireless sensor networks are sometimes called wireless sensor and actuator networks. These are self-distributed to monitor physical conditions like temperature, sound, pressure, etc. and cooperatively pass their data through the network to a main location. WSN are consisted by large number of homogeneous sensor nodes that have the ability of calculation, perception communication and wireless. Different kinds of sensors are distributed according to its applications. These nodes are sensitive. In these, sensor device is furnishing with non-rechargeable Batteries. Different sensor cluster algorithms are proposed to increase the network life time. The major challenges of WSN are (i) limited energy source (ii) IP address scheme is impossible (iii) Lesser bandwidth and memory. Dynamic topology reduces the network life time. Energy efficiency is one of the big issue in order to increase the life time of sensor networks. Because these are allowed to communicate with the base station and collect the data, and then compress it and transmit the collected data to the base station. Computation burns less energy than communication. We can save this by reducing the number of bits transmitted through computation. The data which consume more energy is facing minimum loss [1]. In other way ZigBee is one of the method that can solve many problems [1]. Each node senses environmental data and transmits it back to the link in the multi hop fashion. Currently, WSN is also advantageous in military applications to examine the goal of intruders and report the army's location to soldiers. In this type of applications, the intruders as well as the soldiers are inherently mobile. Two level network structures are there: the top structure is grid: in bottom number of trees exists. In grid structure it helps to distribute the flow of traffic and deliver them to correct place. Tree structure helps to reduce the energy consumption in data collection. In this, we used data and queries and we kept it into up to date and use it into send info in mobile targets [2]. The most important features of WSN are fault tolerance, scalability, manufacturing costs, hardware, limitations and energy consumption. The advantage of WSN is that it can operate in harsh environment [2].

Cluster head is defining as it collects the data from different network and transmits it to different clusters. Clustering is the best proposed method for (energy and bandwidth) to reduce the traffic load and send the packet to its destination. Cluster network is combination of different network structure and it improves the entire property [1]. Cluster head is the main part of network it combines the coordination, routing and end device to form cluster tree network. In this, some nodes are treated as cluster head and rest work as cluster members. Cluster head consume more energy than cluster members [2].

The rest of this paper is organized as follows: Section 2 discuss the mechanism of cluster head. Section 3 discuss the cluster head and its techniques. Section 4 discuss the strengths and weaknesses of cluster head. Section 5 proposes our conclusions. Section 6 discuss the Reference of Cluster Head Selection.

2. Cluster head and its mechanism

Cluster head is defined as local coordinator for its cluster. Cluster head keep in touch with its member nodes and neighborhood clusters. It performs inter-cluster routing, data forwarding and many other applications [3].

2.1 Gateway Node: It takes the info from neighbours and forward it in between clusters [3].

2.2 Cluster member or ordinary nodes: It is neither a cluster head nor gateway. In fact, it is used to communicate with cluster head and keeps the info update according to corresponding cluster head [3]. We choose the node according to the architecture of cluster tree but the path in which we transmit the data is not ideal, because it transmit the data in large amount and its energy would be exhausted in excess amount and network will be out of whack. There is advancement in performance of network but the problem of its energy consumption is increasing day by day. There are a lot of solutions proposed to overcome the exhaustion of energy. The cluster head combines the data in cluster and send it to the controller. The amounts of cluster head can be decrease by grow up the bottom of cluster. By calculating the energy level, we can determine when we use the new cluster head [1].

The task of topology is to assign functions to each node of network. It decides which node declares itself as a cluster head [6]. In this, node joins to cluster head and becomes a member of cluster head.

3. Cluster Head Selection and its Method

The technology of cluster head was popular, but recently it has been improving their parts like digital electronics, semiconductor manufacturing technology and wireless communication leading to the development of low power, cost, and size with embedded sensing, and communication capabilities. A WSN is composed of hundreds of such sensors. Some nodes called the cluster heads, conserve the energy of the sensor devices that are allowed to communicate with the base station. The data assembled by the sensor node is mailed to the base station situated outside the region of the deployment field [4]. Clustering is the best method to utilize resources like energy and bandwidth. Cluster tree routing is a type of immobile routing. Mainly, there are three types of wireless sensor network knowingly topology, coverage and fuzzy based cluster head. Discussing about topology it must have to bring out, which node is going to be cluster head itself. Also it has to provide the functionality of each node in the network. Traditionally these approaches are assumed as if nodes are either connected or disconnected. Practically there are fully connected wireless links called lossy links. With the help of these lossy links more energy efficient topologies has been produced.

3.1 Topology Based Cluster Head

The term topology control is used mostly by the wireless adhoc and sensor networks research community. It is the collection of diverse members of computer network. The main purpose of topology control in this domain is to save energy, reduce interference between nodes and extend lifetime of the network [5] Topology control has to be executed periodically in order to preserve the desired properties such as connectivity, coverage, density etc. But there are some weak points in topology due to which length of cable is limited. It limits the number of nodes to be connected. The network topology can work efficiently with a few numbers of nodes, if we increase the number of nodes then its efficiency deducted [6]. It performs well in low traffic networks. Central bus is the main part of topology, if there is any defect in central bus then whole network will be destroyed.

3.2 Coverage Based Cluster Head

Instead of using topology, coverage based is better. Sensing coverage is one of the fundamental quality of service (QOS) problem in sensor network in sensing coverage. Coverage in sensor network is a measure of how closely the target area is observed by the sensor nodes. To assure that every point of the whole area to be monitored by at least one sensor node, a predetermined percentage of the monitored area is covered [7]. The sensor network remains connected so that the information collected by the sensor nodes can be relayed back to data sinks or controlled [8]. Different applications require different degree of sensing coverage area. Some applications may only require one node to monitor the location, while other application require significantly higher degree of coverage area [9]. In general, area of the coverage degree can be considered as a measure of the quality of service of wireless sensor network. The higher the area of coverage degree, better the field can be monitored [10]. Along with many benefits there are some disadvantages like minimum coverage breach, barrier coverage problem, bandwidth constraint, fault tolerance [11]. One of the major problem, Sensor networks adversely affects the Quality of service. Lesser movement in sensor networks leads to higher coverage.

3.3 Fuzzy Based Cluster Head

On the other hand, fuzzy logic has the potential to deal with conflicting situations and imprecision in data using heuristic human reasoning without any need of complex mathematical modelling [3].

Topology based	Coverage area	Fuzzy based
<ul style="list-style-type: none"> • Topology control provides tasks to every node of the network. • In this technique, LEACH could work effectively. • Topology control decides which cluster declares itself as a cluster head. 	<ul style="list-style-type: none"> • It scatters the homogenous cluster head, in the network is bear out. • In this LEACH protocol work is based on clustering in which clusters are made randomly in a susceptible and self-organized manner. • It decides where the optimal sensor deployment strategy is connected globally to the network. 	<ul style="list-style-type: none"> • Its task is to find the degree of truthfulness. • Leach protocol is the one of the method to obtain the energy efficiency in the exchanging data between the sensor nodes [4]. • It determines the relative location of every node.

Table1: A comparison of Topology, Coverage and Fuzzy Based cluster heads

4. Advantage & Disadvantage of Cluster Head Selection.

While we send the data collection from cluster node to cluster head then it absorbs more energy. It also affects the coverage area and then transmission becomes lesser. The advantage is it is of low cost and much powerful [12].

5. Conclusion

In this paper we have discussed about Wireless sensor network, cluster head selection and its method. Clustering is backbone of energy efficiency, network scalability and reducing overheads and is a major challenge to select for the same. Researchers have proposed different mechanism for solving selection for cluster head but we are still looking on it and this paper is implied on clustering head importance. From the survey it has been analysed that fuzzy logic is better than coverage and topology. Because in fuzzy no complex mathematical techniques are required and it can also work in violent situations.

REFERENCES:

- [1] "A novel cluster head selection method using energy for ZigBee cluster-tree network". **Qiu, Shu-bo, Yuan Xu, and Xiu-wei Yang**. Automation and Logistics (ICAL), IEEE International Conference on. IEEE, (2011).
- [2] "Energy-efficient Wireless Sensor Networks for Mobile Target Detections"**Chen, G., Cheuh JS, Sun MT, Chiang TC, Jeng AA**. IEEE, (2012) [3] Ahmad Shahrizan Abdul Ghani, Nor Ashidi Mat Isa, "Enhancement of low quality underwater images through integrated global and local contrast correction", Applied Soft Computing Journal, pp. 332-344, August 2015.
- [3] "Fuzzy Logic Implementation of Ant Colony Based Cluster head Selection Algorithm"**Atri, Swati, Dr.Nasib Singh Gill, and Jaideep Atri**. international Journal of Advanced Research in Computer and Communicaton Engineering, (2014).
- [4] "Fuzzy Logic-Based Clustering Approach for Wireless Sensor Networks Using Energy Predication"**Lee, Jin-Shyan. "Senior Member, IEEE, and Wei-Liang**. IEEE Sensors Journal, (2012).
- [5] "Intra-Cluster topology creation in wireless sensor networks"**Jardosh, Sunil, and Prabhat Ranjan**. Third International Conference on. IEEE, (2007).
- [6] "Genetic algorithm based cluster head optimization using topology control for hazardous envirnment using WSN"**Roslin, S.Emalda**. Innovations in Information, Embedded and Communication Systems (ICIIECS), International Conference on IEEE, (2015).
- [7] "CHEFC: cluster head election with full coverage in wireless sensor networks"**Shirmohammadi, Mohammad Mehdi, Mostafa Chhardoli, and Karim Faez**. Communications (MICC), IEEE 9th Malaysia international Conference on IEEE, (2009).
- [8] "Data delivery optimization by efficient cluster head selection of wireless sensor network"**Khan , Asfandyar, Azween B. Abdullah, and Atiq Ur Rahman**. Signal processing & its Applications.CSPA 5th ainternational Colloquium on IEEE, (2009).
- [9] "A distributed and energy efficient algorithm for data collection in sensor networks"**Sharafkandi, Sarah, David HC Du, and Alireza Razavi**. Parallel Processing Workshops (iCPPW), 39th International Conference on. IEEE, (2010).
- [10] "Coverage and Connectivity preserving routing protocol for heterogeneous wireless sensor networks"**Ben Alla, Said, and Abdellah Ezzati**. Next Generation Networks and Services (NGNS), IEEE, (2012).
- [11] "A Clustering algorithm based on energy variance and coverage density in centralized hierarchial wireless sensor networks"**Randriatsiferana, Rivo SA, et al**. AFRICON,2013. IEEE, (2013).
- [12] "A Review of Cluster Head Election in WSN"**Haseeb, Khalid, Kamalrulnizam Abu Bakar, Abdul Hanan Abdullah**. World Applied Sciences Journal, (2013).

PROACTIVE HUMAN BEHAVIOR BASED SAFETY ANALYSIS IN INDUSTRY

ThulasiRajan R¹, Dr. P.V. Arul Kumar²

¹Post Graduate student, Bharat Niketan Engineering College, Theni,

²Associate Professor, Bharat Niketan Engineering College, Theni

Email - thulasimj@gmail.com, Contact No - +91-9944300136

Abstract: Safety is an essential thing which we need to focus in every act and conditions. In day to day life every individual person has to ensure their safety. If not it may lead to any unplanned or unwanted event which will make more severe consequences. To avoid such situations, we need to find the causes of the unsafe incidents. Most of the accidents are happening in industries, because of multi-disciplinary activities are held. In which we can classify the accidents into two major categories. They are unsafe act and unsafe conditions. According to previous strategy, 90% of accidents are happening due to unsafe acts. It's purely rely on Human (Individual) Behaviour. So, in this study the analysis and control measures of Human Behaviour Based Safety are discussed below. For analysing the human behaviour safety, Job safety analysis methodology has been followed. After analysing this, gathered more information which helps to reduce the accidents caused by human behaviour. Risk matrix is used to find out the corrective measures which are appropriate to the hazard. Thus the accidents will be reduce and create the safe work area in Industry.

Keywords: Job Safety Analysis, Risk Assessment, Risk Matrix, Behaviour Based Safety, Dyeing Process, Peer Group Pressure, Safety Culture.

INTRODUCTION

In Industry there are various methods or approaches followed to reduce the accident rates and improve the employee safety. Approximately most of the accidents are caused by unsafe human behaviour. Among that BBS is the one effective method which is implemented to reduce accidents in workplaces. This will help to analysis the dangerous occur in prior to the operation around the workplace. The process is to know about all the possible causes of failures and effects which will harm to persons and equipments. These method shows the idea which to make counter measures for the particular failure. This will help to lead a healthy environment in working area.

IMPORTANCE OF BBS IN AN ORGANIZATION

Behavior safety involves on the behavior of employee within an organization are

- Identifies the behaviour which will harmful and causes injury or accidents.
- Reduces the risk of accidents or injury.
- Collects the data regarding frequency rate of those behaviours.
- Identifies behavior which will reduce and stops injury.
- Feedback and reinforcement to create positive types of behavior in industry.

FACTORS LEADS TO SAFETY

To maintain a good health and safety practice we have to fulfil moral, legal and economic factors.

Moral reason relates to the moral duty that one person has to another. Many people are killed, injured or made sick by their work. This is morally unacceptable and society as a whole demands that people are safe while at work.

The **legal** reason relates to the framework of laws that govern the conduct of businesses and organisations. An employer has a duty to provide a safe plant and equipment, safe systems of work, adequate training and supervision and competent employees.

The **economic** reason relates to the fact that accidents and ill health cost money. When an accident occurs there will be direct and indirect costs as a result of that event. Some of these losses can be insured against many of them will be uninsured.

Management has to provide safe work place, equipment safety, and awareness training programme to ensure employee safety. Here employer's responsibilities to workers, safety indicators, influencing factors of individuals and control measures are discussed below. Good health and safety practice often relies on the perfect behaviour of individuals and people sometimes do not behave in this ideal

way. The solution to a health and safety problem usually requires a worker to carry out their job in a particular way. But people are not robots, they do not behave as they are supposed to all the time.

Workers sometimes make mistakes (they do the wrong thing thinking that it is the right thing to do). Sometimes they deliberately do the wrong thing, knowing that it is wrong, but doing it anyway. The fact that health and safety standards are affected by worker behaviour can be a significant barrier to maintaining good standards in a workplace.

REVIEW OF LITERATURE

Agraz-Boeneker R, Groves W A ^[1] (2007) conducted a study about BBS in oil production. From the examination the information shows the 'number' and 'type' of "safe" and "at risk" behavior observed. Types of incidents -injuries, near miss, fires, spills are obtained by (OW) observation worksheet the (KSP) key safe practices which are classified and examined using an ordinal logistic regression model.

Dawei chen, Hanzhi tian ^[3] (2012) established a study on the safety Index (SI) in construction. It was used to evaluate safety behavior & change trend. The result of the experiment showed that BBS made huge impact on accident prevention and the trial employee safety index was enhanced upto 10% than the base line while the experiment. The BBS approach is implemented in DO IT process. D-Define the target behaviors, O-observe target behavior, I-Intervene to improve behavior, T-Test impact of intervention. Employee's key behavior checklist will be searched under the parameters like -ABC analysis, effect audit, HSE effect, change climate, safety behavior, and decrease accident.

Faridah Ismail ^[4] (2011) carried a case study approach on oil & gas industry by Implementing BBS approach. Four basic steps of BBS are Identification, Observation, Intervention, Review and Monitoring. The preliminary enquiry among safety and health related practitioners will leads to implement the BBS in oil and gas industry effectively. The data collections are done by questionnaire survey, semi- structured interview, and observation. These question survey will help to seek the current implementation of BBS and the barriers. There are five principles which will help to assist the programs. They are-to increase level of risk awareness, feedback communication and bottom-up program approach, minimize paperwork and keep the process simple.

HengLi et al ^[6] (2015) done a study about the Extension of BBS in construction industry. In this proactive construction management system and BBS are merged and implemented in industry. The accident prevention rates are increased by introducing this concept. The proactive approach is enhancing the capacity of on-site workers in detecting sources of key location related dangers and early warnings. The second one is recording the behavior of site workers when they are giving warning signals and observation of unsafe behaviors. PCMS is consists of RTLS-real time location system. VCS-virtual construction simulation.

Kean Eng Koo et al ^[7] (2013) carried a study on engineering students for their self intension & behavior in practicing safety at workshop &lab by using theory of planned behaviour (TPB).Using TpB the research model ,the results of this study has shown that subjective norm, attitude towards safety practices and perceived behavioral control have a significant effect on behavioral intension to practice safety. As a result TpB with the used of safety knowledge has increased the capability of predicting and evaluate young adult students intension and behavior.

LIU Jianhua and SONG xia oyan ^[8] (2014) conducted a study on the Mechanism of BBS management idea & ABC (Activator-behavior-consequence) behavior analysis to reduce accidents & improve safety of coal mine. This research says that to pay attention to behavior observation and measures. A represents the antecedents, belongs to the stimulation factor, appear in behavior, incentive and encourage people to finish some behaviors. B - it's a series action of human can be observed and measured caused by the incentive factor. C-the results, after the behavior .Counter measures like pay attention, positive and negative reinforcement strengthen the staff behavior, feedback are discussed.

Rahmatul Hidayah Salimin, Razidah Ismail ^[2] (2011) evaluated the influence of environment -behavior factors towards safety culture development like internal & external. Internal - safety management system.External-Industry norms, government policies and regulations, economic climate. Interviews among senior management, acknowledged their state of safety culture were contributed by the system established. In internal factors the fundamental basis of effective management is summarized in the simple management circle Model,based on the Plan-Do-Check-Act.

SulastreMatzin and Fariadh Ismail ^[9] (2011) done a study to Identify Employer's behavior safety compliance factor which encourages them. It's an initial study which will lead the establishment of safety indicators for BBS. Ranking value method is used to determine factors compliance in safety improvement. The value for one is "strongly disagree" and to five is for "strongly agree". There are nearly ten variables which are used to improve safety with the help of giving values. The factors are management commitment and followed by organizational commitment, safety communication, safety leadership, effective safety training, safety motivation, safety rules and regulation, safety and health officer and personal protective equipment were ranked in an ascending order of importance.

YUAN xiongiun and WANG kaiquan ^[11] (2012) conducted a study on the Countermeasures for BBS of Small and medium - sized enterprises are discussed. The safety of work places SME's have also become more serious and improved urgently. The procedure for BBS is Identify critical actions, collect action data, provide dual communication and eliminate the hindrance for safety behavior. Some of the measures are enterprise responsible person, establish safety management ideas full participation of employee, motivation. These measures will decrease the accident rates.

Yueng-hsianghuang et al ^[12] (2014) researched about examining employee safety climate perception & supervisory interpretation of safety climate how they similar or different and how they related to important safety outcomes. The results are direct

only if its employee perception of self-reported safety behavior and objective injury is indirect. Here the research says that we should rely on only employee perspectives instead of supervisory interpretation. This will increase to understanding of lone worker context by examining employee safety climate and supervisory interpretations of safety climate.

BEHAVIOUR BASED SAFETY

Safe Place of Work

The employer creates the place of work, which should be reasonably safe and without risk to health. The employer should also provide safe access to and from the workplace.

Safe Plant and Equipment

All the machinery, tools, plant and equipment used on by employees at work should be reasonably safe and without health risk. The greater the risk involved, the greater the care that must be taken.

Safe Systems of Work

There should be recognised procedures for the safe conduct of all work activities. These procedures should cover all foreseeable possibilities. It should cover the routine day to day activities of the organization and non routine occasional or one-off activities as well as any foreseeable emergencies that might arise.

Training, Supervision and Competency of Staff

Employers have a duty to provide appropriate training so that workers are aware of the hazards and risks inherent in their work, the safe systems of work and the emergency procedures. This training can be reinforced by providing information and instruction. They also should supervise workers to ensure that they are carrying out their work with minimal risk to themselves and others. This doesn't mean that supervisors have to stand and watch every worker, they just have to provide adequate levels of supervision. Finally employer should ensure that all workers supervisors and managers are competent.

WORKERS RESPONSIBILITIES AND RIGHTS

- Take reasonable care of their own safety and that of other people who might be affected by the things that they do and the things that they fail to do.
- Comply with safety instructions and procedures.
- Use all safety equipment properly and not tamper with its.
- Report any situation which they believe could be a hazard and which they cannot themselves correct.
- Report any work related accident or ill health.

SAFETY CULTURE

It is defined as the shared attitudes, values, beliefs and behaviours relating to health and safety. Every individual person's behaviour creates culture in organisation.

Positive Culture

In an organisation, majority of the workers think that health and safety is important. Every one works safely because they want to. People who do not share this positive view are in the minority and are likely to come round to the group.

This is because the culture of an organisation tends to be observed by its workers over time. Workers who do not adjust to the group way of thinking may either leave or possibly be dismissed for working unsafely.

Negative Culture

In an organisation, majority of the workers think that health and safety is not important. They are poorly educated and see it as unnecessary or unimportant. Managers do not think about health and safety in their decision making and so let other priorities dictate their actions.

Safety conscious workers are in the minority and are likely to come round to the group way of thinking over time if not they may well leave because they do not like the organisational culture and feel unsafe in the work situation.

Factors that influence Negative impact on health and safety culture in an organisation

- Lack of leadership from management.
- Presence of a blame culture
- Lack of management commitment to safety
- Health and safety receiving lower priority than other business issues.
- Organisational changes (frequent or poorly communicated change)
- High staff turnover rate.
- Lack of resources
- Lack of work consultation
- Interpersonal issues
- External influences (climate resulting in difficult operating conditions)

INDICATORS USED TO ASSESS SAFETY CULTURE

It makes sense to try to assess an organisation's safety culture to see whether it is strong and positive, or if there is room for improvement. But in an organisation it is difficult to assess because there is no one single feature that can be measured.

It is impossible to measure and they are intangible concept. So rather than trying to assess the safety culture directly it is perhaps better to assess it indirectly by looking at the tangible outputs that can be used as indicators.

Accidents

It can be used to work out how many accidents are happening as a rate and compared with Organisation's performance in previous years (indicates whether the rate is increasing or decreasing. decreasing rate might be seen as a positive safety culture) and rate for other organisations that do the same work (an accident rate that is higher than the national average might be seen as indicator of a negative safety culture).

Absenteeism

A high level of worker absenteeism indicates that workers are either not able or not willing. If not able to come means they are suffering ill – health caused. If not willing means they are with holding their labour for some reasons. This is caused by poor workforce morale which in turn can sometimes be linked to poor safety culture.

Sickness Rates

A lot of ill health is caused or made worse by work. It can be used in the same way that accident rate. If the rate increases it shows negative culture.

Staff Turnover

Organisation with positive work culture often feel safe morale is good, training is available. As a result workers stay with their employer for longer, so low staff turnover may indicates a good safety culture while high staff turnover may indicates the opposite.

Compliance with Safety Rules

Formal and informal inspections or audits usually find that there is a high level of compliance, that they influence the positive safety culture. Negative safety culture indicates the reverse, in which workers do not follow the rules either because they do not aware of them or they know but do not want to follow it.

Complaints with Working Conditions

Positive culture organisation may actively encourage complaints, but few serious ones will be made. Negative culture organisation may actively not encourage complaints.

Influence of Peers

When people put into a group, some individuals will have a lot of influences over the group. In this way hierarchy develops. A person wishing to become a member will have to comply with the group norms. This pressure to comply with group norms is “**Peer group pressure**”, which is important factor to take into consideration in thought of behaviour based safety. They way to deal with this problem is usually to tackle the influence people within the group who are the ones responsible. This might be done by training, education, involvement in safety – related projects.

FACTORS INFLUENCING WORKER'S BEHAVIOUR

- The individual – their personal characteristics
- The job – the task that they are carrying out
- The organisation – characteristics of the organisation that they are working for

Organisational Factors

- Safety culture of the organisation
- Policies and procedures – the way that might encourage or discourage safety related behaviour
- Commitment and leadership from management – whether this is visibly demonstrated outside the boardroom
- Levels of supervision – presence or absence of and the competence of supervision.
- Peer group pressure- the extent to which this is allowed to drive unsafe behaviours
- Consultation and worker involvement – the extent to which workers are involved in the management of health and safety issue and in the decision making
- Communication – how effective at using various communication methods to convey health and safety messages and information and how well the organisation then checks understanding of those messages
- Resources – availability of any necessary equipment and allocation of time to provide training in health and safety
- Training – how good the organisation is at identifying health and safety training needs and opportunities and how well it then meets those needs to create well informed, competent staff
- Work patterns – such as shift systems, work at night, extended hours – these can adversely affect workers health and cause fatigue which can lead to poor performance and increase risks

Job Factors

- Task – the characteristics of the work itself in particular the ergonomic requirements. In the absence of ergonomic design workers will find the most comfortable way and it may lead to be not safe
- Workload – amount and rate of work, deadlines and variety of work that individuals have to cope with and the degree to which these are under the direct control of the worker or imposed externally.

- Environment – workplace conditions such as space, lighting, noise, temperature and humidity and the way of that these parameters are controlled so as to minimise their impact on worker performance. They may also start to suffer degradation in physical and mental performance as a result of heat stress.
- Displays and controls – design of these and the way that poorly designed displays and controls can contribute to the likelihood of human errors.
- Procedures – the existence and quality of working procedures. Alack of written procedures or poorly written procedures that are out of date overly complex or impractical can be why workers do not comply. To be effective, procedures should be accurate, concise, use familiar language and they must be do – able.

Individual Factors

Key characteristics of an individual worker's personality that influence their safety related behaviour:

- Attitude – how they think about a particular safety issue.
- Competence – a combination of knowledge, ability, training and experience
- Motivation – the incentives at work.

Attitude

It is a person's point of view or way of looking at something, how they think and feel about it. Changing the attitude is difficult but can be done using various methods. They are:

- Education and Training.
- High impact interventions.
- Enforcement.
- Consultation and involvement in decision making.

Competence

It's a combination of knowledge, experience, training and ability that brings a person to a level where they are able to perform to an acceptable standard and them aware of their own limitations.

Motivation

A person's drive towards a goal. The thing that is making them do what they do is called motivation.

Perception of risk also another important factor for an individual safety behaviour.

CASE STUDY

STUDY AREA

Study was carried out in Talma Garments, Trippur. In this industry many process are carried out, among that dyeing unit area was looked out. The unit area was covered by nearly around 40 to 50 workers and storage area of chemicals which is used for dyeing process.

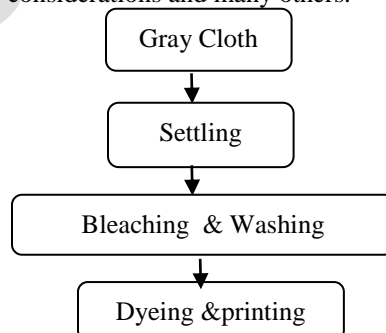
DYEING

Dyeing is the process of adding color to textile products like fibers, yarns, and fabrics. Dyeing is normally done in a special solution containing dyes and particular chemical material. After dyeing, dye molecules have uncut chemical bond with fiber molecules.

DYEING PROCESS

The dyeing process is one of the key factors in the successful trading of textile products. In addition to the design and beautiful color, the consumer usually looks for some basic product characteristics, such as good fixation with respect to light, perspiration and washing both initially and after prolonged use. To ensure these properties, the substances that give color to the fiber must show high affinity, uniform color, resistance to fading, and be economically feasible.

Modern dyeing technology consists of several steps selected according to the nature of the fiber and properties of the dyes and pigments for use in fabrics, such as chemical structure, classification, commercial availability, fixing properties compatible with the target material to be dyed, economic considerations and many others.



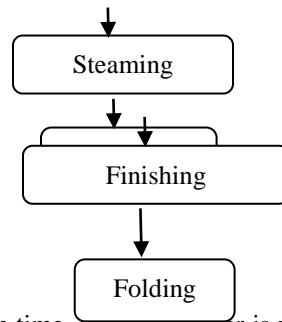


Fig 4.1 Process involved in dyeing

Dyeing methods have not changed much with time. Basically water is used to clean, dye and apply auxiliary chemicals to the fabrics, and also to rinse the treated fibers or fabrics.

Process Involved

- Preparation
- Dyeing
- Finishing

Preparation

In this step the unwanted impurities are removed from the fabrics before dyeing. This can be carried out by cleaning with aqueous alkaline substances and detergents.

Many fabrics are bleached with hydrogen peroxide or chlorine containing compounds in order to remove their natural color, and if the fabric is to be sold white and not dyed, optical brightening agents are added.

Dyeing

Dyeing is the aqueous application of color to the textile substrates, mainly using synthetic organic dyes and frequently at elevated temperatures and pressures in some of the steps.

It is important to point out that there is no dye which dyes all existing fibers and no fiber which can be dyed by all known dyes. During this step, the dyes and chemical aids such as surfactants, acids, alkali/bases, electrolytes, levelling agents, promoting agents, softening agents are applied to the textile to get a uniform depth of color with the color fastness properties suitable for the end use of the fabric.

This process includes diffusion of the dye into the liquid phase followed by adsorption onto the outer surface of the fibers, and finally diffusion and adsorption on the inner surface of the fibers. Depending on the expected end use of the fabrics, different fastness properties may be required.

Different types of dye and chemical additives are used to obtain these properties, which is carried out during the finishing step. Dyeing can also be accomplished by applying pigments (pigments differ from dyes by not showing chemical or physical affinity for the fibers) together with binders (polymers which fix the pigment to the fibers).

Finishing

Here involves treatments with chemical compounds aimed at improving the quality of the fabric. Permanent press treatments, water proofing, softening, stain release and microbial/fungal protection are all examples of fabric treatments applied in the finishing process.

Process Methodology

Dyeing can be carried out as a continuous or batch process. The most appropriate process to use depends on several factors, such as type of material (fiber, yarn, fabric, fabric construction, and garment), generic type of fiber, size of dye batch and quality requirements for the dyed fabric, but batch processes are more commonly used to dye textile materials.

In continuous processing, heat and steam are applied to long rolls of fabric as they pass through a series of concentrated chemical solutions. The fabric retains the greater part of the Eco-Friendly Textile Dyeing and Finishing chemicals while rinsing removes most of the preparation chemicals.

Each time a fabric is passed through a solution, an amount of water equivalent to the weight of the fabric must be used. In batch processing, sometimes called exhaust dyeing, since the dye is gradually transferred from the dye bath to the material being dyed over a relatively long period of time, the dyeing occurs in the presence of dilute chemicals in a closed equipment.

Unlike the continuous process, instead of being passed through various baths in a long series of equipment sections, in the batch process the fabric remains in a single piece of equipment, which is alternately filled with water and then drained, at each step of the process. Each time the fabric is exposed to a separate bath, it uses five to ten times its own weight in water.

Some batch dyeing machines only operate at temperatures up to 100°C. However, the system can be pressurized, allowing for the use of temperatures above 100°C. Cotton, rayon, nylon, wool and some other fibers dye well at temperatures of 100°C or below. Polyester and some other synthetic fibers dye more easily at temperatures above 100°C.

Since the degree of dye fixation depends on the nature of the fiber, it is important to consider this topic. The fibers used in the textile industry can be divided into two main groups denominated **natural fibers** and **synthetic fibers**.

Natural fibers are derived from the environment (plants or animals), such as wool, cotton, flax, silk, jute, hemp and sisal, most of which are based on cellulose and proteins.

On the other hand, **synthetic fibers** are organic polymers, mostly derived from petroleum sources, for example, polyester, polyamide, rayon, acetate and acrylic. The two most important textile fibers are cotton, the largest, and polyester. Cotton has been used for over

7000 years, and consists of mainly cellulose, natural waxes and proteins. The large number of hydroxyl groups on the cellulose provides a great water absorption capacity.

ANALYSIS AND METHODOLOGY

JOB SAFETY ANALYSIS

JSA is a procedure which helps integrate accepted safety and health principles and practices into a particular task or job operation. In this each step of the job is to identify potential hazards and to recommend the safest way to do the job.

STEPS INVOLVED IN JSA

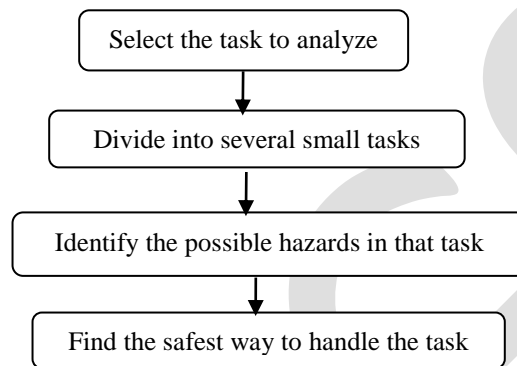


Fig. 5.1 Steps involved in JSA

The legal requirement for risk evaluation or assessment applies to all employers. The process for carrying out a risk assessment can be broken down into a series of steps:

Hazards and Those at Risk

Looking for those things at work that have the potential to cause harm, and identifying workers who may be exposed to the hazards. Using workers' knowledge helps to ensure hazards are spotted and workable solutions implemented. Consultation encourages workers to commit themselves to health and safety procedures and improvements.

A risk assessment should cover all workers regardless of whether they are employed on long- or short-term contracts. Where there are persons employed by another organisation on site, there is a duty on the two employers to cooperate and safeguard the health and safety of workers.

Risk assessment should take account of differences in workers, such as by gender, age, or disability. For example, older employees may learn differently than a younger worker, and also have different concepts of risk due to a lack of experience. Different prevention measures may be required for these worker groups. Work, its organisation and the equipment used should be adapted to the worker, not the other way around. This principle is enshrined in EU legislation.

Workers with disabilities should be considered specifically in the risk assessment process. For example, people with disabilities may be subjected to bullying, which can lead to work-related stress. Consultation with workers with disabilities is vital to ensure a risk assessment is appropriate.

Evaluating and Prioritising Risks

Evaluate how likely it is that the hazard will lead to harm or injury, and how severe that injury is likely to be. Consider what control measures are in place and whether they are sufficient. It is essential that the work to be done to eliminate or prevent risks is prioritised. The focus for cost-effective and sustainable risk management should be on collective protection and preventative measures.

Deciding on Preventive Action

Identifying the appropriate measures to eliminate or control the risks. List the preventive measures needed in order of priority, then take action, involving the workers and their representatives in the process. Targeting the underlying problems is the most cost-effective method of risk management.

Taking Action

Risk assessment is the first step to successful risk management. Put in place the preventive and protective measures through a prioritisation plan (most probably all the problems cannot be resolved immediately) and specify who does what and when, when a task is to be completed, and the means allocated to implement the measures.

Interventions should be agreed with the workforce, either directly or through worker safety representatives. The agreed solutions should be carefully implemented, monitored and evaluated. The information arising from the risk assessment must be shared with the appropriate persons. Action should be supported by appropriate training.

Monitoring and Reviewing

The assessment should be reviewed at regular intervals to ensure it remains up to date. It has to be revised whenever significant changes occur in the organisation or as a result of the findings of an accident or “near miss” investigation.

JSA IN TEXTILE INDUSTRY

In the textile process dyeing unit is an essential one where the chemicals are used in hugely by the persons. More usage of chemicals will harm the individuals health and safety. To avoid that the dyeing unit area has been selected to make an analyze to find out the possible hazards involve in that.

After selecting the task dyeing unit has been divided into smaller tasks to find out exact hazards can occur. This can be classified into three major types. They are preparation, dyeing and finishing.

To make an analyze risk assessment had been carried out in order to find out the hazardous area and tasks. This will help to choose the appropriate safe way to follow the operation and shows the exact hazard to make a corrective action. It shows the individual person error or attitude which leads to an accidents.

After that area has identified the corrective action like monitoring, individual training, motivation schemes will be implement to encourage the workers to do the job safely. This will reduce the accident rates and injury rates in the industry. It will also help to choose the safe work procedure which prevents unsafe acts by an individual.

This way human behaviour based safety can improve the safe work standard in working industry area.

RISK ASSESSMENT AND ANALYSIS

Risk assessment is a process which is a key tool to find out the hazards involved in that particular process/area. Based on this we can easily identify the hazards and can give control measures to reduce the number of accidents.

Areas Taken for Assessment

- Preparation
- Dyeing
- Finishing
- Storage area of chemicals

Risk Matrix

Risk matrix is a universally acceptable method to make an assessment easier by making hazard and its risk into some numerical value.

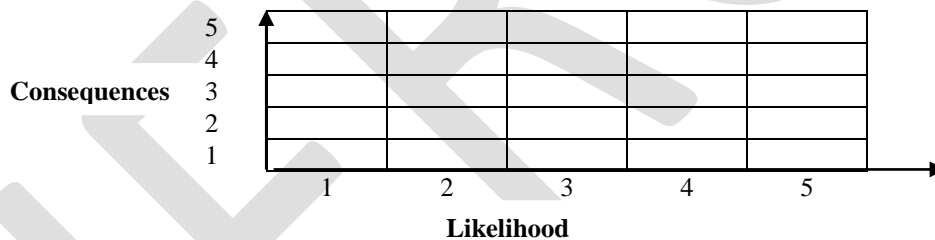


Fig. 5.2 Structure of Risk Matrix

Table 5.1 Showing likelihood of harms and its severity outcomes

Likelihood of harm	Severity of outcomes
1- Extremely unlikely	1-Very minor injury
2- unlikely	2-First aid injury
3 – possible	3-lost time injury
4 - Likely	4-hospital treatment
5 – Very Probable	5 – disabling injury

Data Collected From Industry

Major accident scenario in previous years

Accidents data were collected from the industry for the selected process for the period from 2013 to 2015 which is showing in Table 5.2.

Table 5.2 Accident data from 2013 to 2016

Year	2013	2014	2015
Preparation	2	3	3
Dyeing	4	4	3
Finishing	3	3	4
Chemical storage area	6	5	5
Total no of accidents	17	16	16

The collected data were converted into percentage data and presented in Table 5.3

Table 5.3 Year wise accidents in Percentage

Year	2013	2014	2015
Preparation (%)	11.76	18.75	18.75
Dyeing (%)	23.53	25.00	18.75
Finishing (%)	29.41	25.00	31.25
Chemical storage area (%)	35.29	31.25	31.25

The accident variation percentage in each year with respect to particular area were compared and it's showing in Figure 5.3

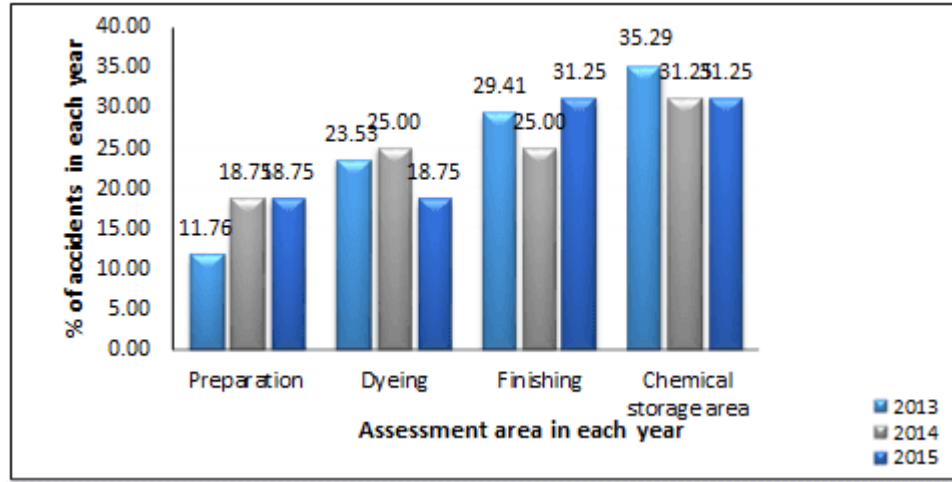


Figure 5.3 Graph between Percentage of Accidents and Assessed Area in Each Year

The present condition in each assessed area in 2016 (till date) and the possible reduced number of accidents by applying safety measures were presented in Table 5.4.

Table 5.4 Collected accident data in 2016 and effect of safety measures

Year	2016 (till date)	Possible Reduced accidents
Preparation	2	1
Dyeing	3	2
Finishing	4	2
Chemical storage area	6	4
Total no of accidents	15	2

The percentage of accidents in 2016 and after applying safety measures the reduced percentage are shown in Table 5.5

Table 5.5 Percentage of Accident Data in 2016 and Effect of Safety Measures

Year	2016 (till date)	Possible Reduced accidents
Preparation (%)	13.33	6.67
Dyeing (%)	20.00	13.33
Finishing (%)	26.67	13.33
Chemical storage area (%)	40.00	26.67

The accident percentage in 2016 (till date) with respect to particular assessed area were compared with reduced percentage of accidents by applying safety measures is showing in Figure 5.4

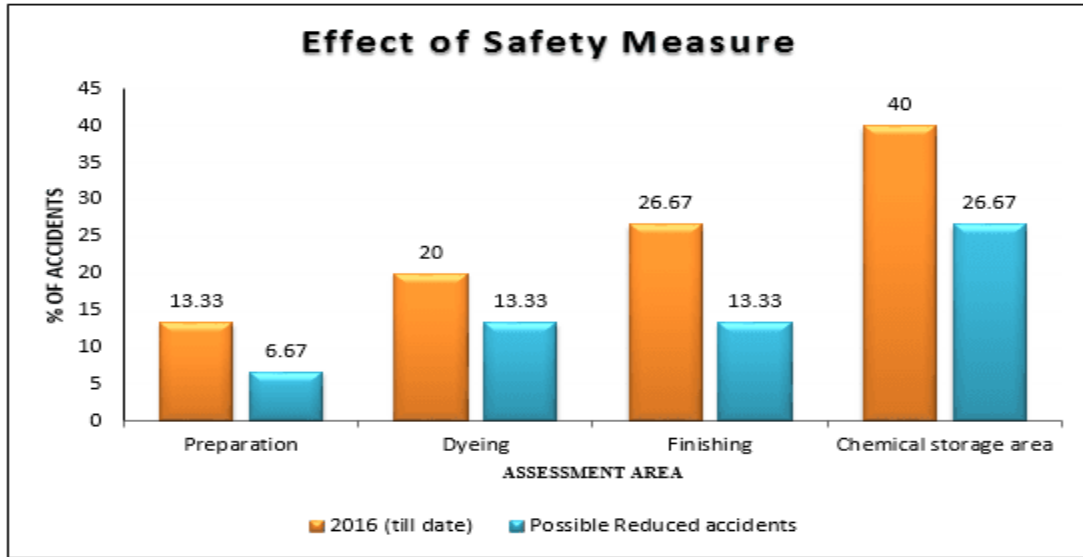


Figure 5.4 Percentage of Accident Data in 2016 and Effect of Safety Measures

By comparing the accidents in each year it showing that in 2013, the maximum number of accidents were occurred. So keeping the maximum value, the percentage of accident in 2013, 2014, 2015, 2016 (till date) and possible reduced accident in each assessed area were carried out and presented in Table 5.6

Table 5.6 percentage of accident in each assessed area

Year	2013	2014	2015	2016 (Till Date)	Possible Reduced accidents
Preparation (%)	11.76	17.65	17.65	11.76	5.88
Dyeing (%)	23.53	23.53	17.65	17.65	11.76
Finishing (%)	29.41	23.53	29.41	23.53	11.76
Chemical storage area (%)	35.29	29.41	29.41	35.29	23.53

The comparison in each assessed area in each period are compared and shown in following Figure 5.5 (a), (b), (c) and (d).

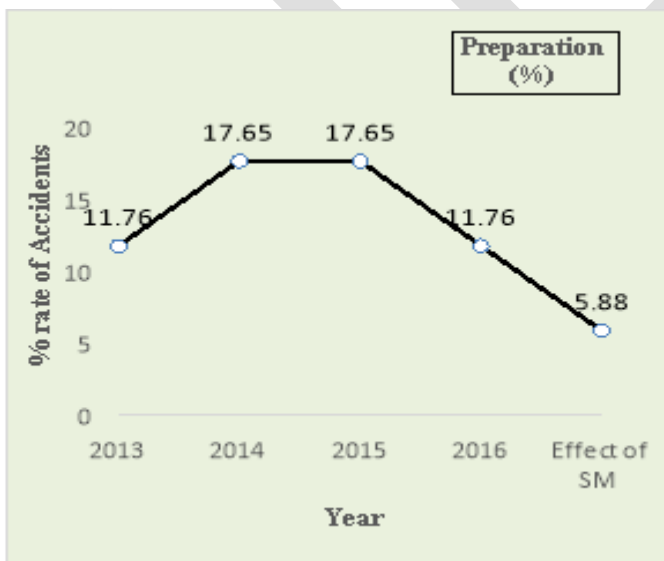


Fig. 5.4 Comparison in Preparation Area between Each Period in Percentage

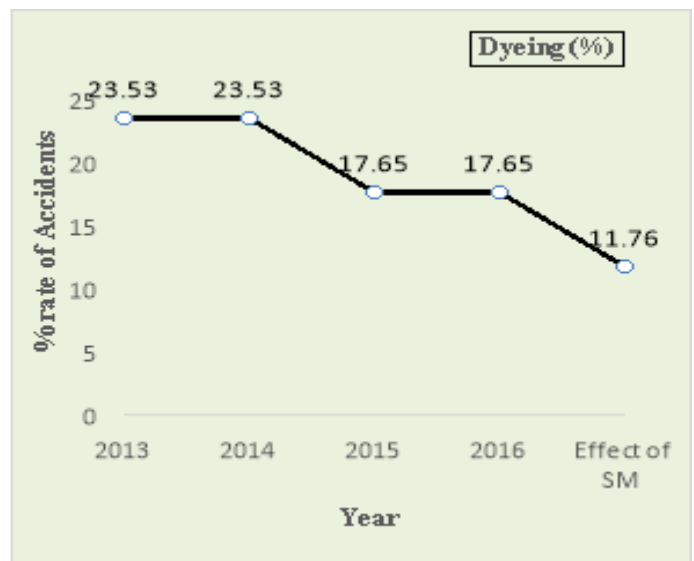


Fig 5.5 Comparison in Dyeing Area between Each Period in Percentage

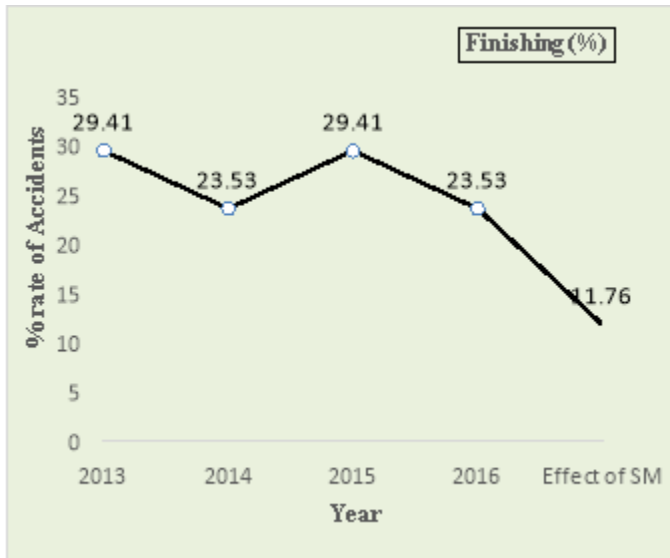


Fig. 5.6 Comparison in Finishing Area between Each Period in Percentage

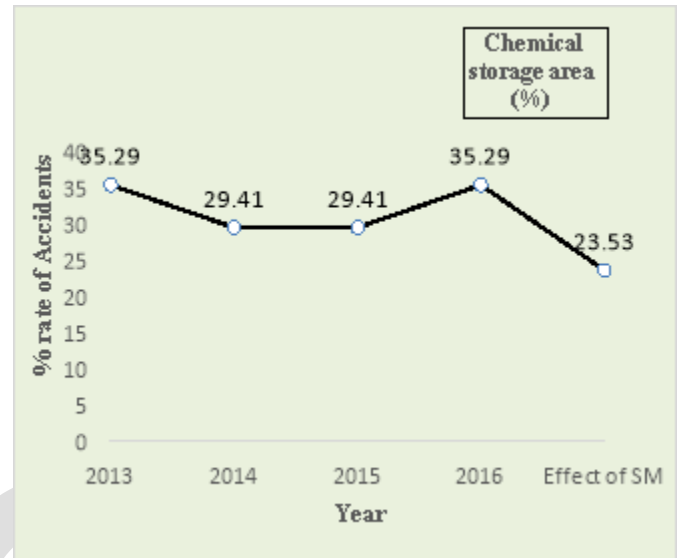


Fig 5.7 Comparison in Chemical Storage Area between Each Period in Percentage

Control Measures for Behaviour Based Safety Culture

- Management commitment and leadership.
- Disciplinary procedures.
- Competent staff.
- Effective communication.
- Co-operation and consultation.
- Training.

Management commitment and leadership

The commitments start from top level of the organisation. The senior managers provide the leadership to inspire and motivate the others. To show the visible commitment they need to involve in such activities like behaving themselves safely in the organisation, involvement in daily day-to-day operations and management's health and safety like safety meetings, taking part in safety audits and tours.

Disciplinary procedures

Sometimes it's necessary to take disciplinary action procedures to ensure the health and safety rules in organisation.

Competent staff

A competent person is a person who has sufficient training, knowledge, experience and other abilities to carry out their work safely and without any risk to health. It will make some responsibilities among them. This has a positive influence on safety culture.

Effective communication

Communication is a process of delivering information from sender to a recipient. To get that effective it should be a correct information and clear with details. This can be achieved by verbal, written and graphic.

Consultation

A positively safety culture can be created only when the organisation appreciate the workers involvement and co-operation with them. If the workers feel they are being consulted then it will make them some responsibilities to them and it leads to follow the safety culture. This can be done by direct consultation or worker representatives.

Training

It is defined as the planned, formal process of acquiring and practising knowledge and skills in relative field. The effect of training has the major influence among the workers to follow the safe behaviour.

Risk Matrix Calculation

$$\text{Risk} = \text{Likelihood} * \text{consequences}$$

According to the data collected and based on the chances of getting harm with the severity it can cause the risk value will be made and it may help to reduce rate of occurrence by making the effective corrective measures.

In this study, the chemical storage area will be the most harmful and so the risk value should be as $4*5=20$.

After implementing the safe BBS culture in the working area the risk value will be reduce as $3*3=9$. Similarly the other area also comes under the risk matrix value and it helps to reduces the effect of accidents and safe working area.

CONCLUSION

In Industry there is always a chance for accidents. This can be occur due to many ways like mechanical fault, human error, improper handling of machines, improper maintenance of the machines and working area.

In those areas can be assessed with the help of risk assessment to find out the hazards involve in it. This will be used as a data to calculate the risk values of each hazard. By make use of risk values, the appropriate corrective measures are taken to control it.

Those corrective measures are all relevant to the human behavior which is more needed to avoid accidents in working area. Thus the human behavior based safety concept is used to control and avoid accidents and leads to safe working places.

REFERENCES:

- [1] Agraz-Boeneker R, Groves W Aand Haight J M , “An Examination of Observations and Incidence Rates for a Behavior Based Safety Program “American Society of Safety Engineers, Volume 4, Number 3, 2007.
- [2] Cheyne A, Tomas J M, Cox S and Oliver A, “Perceptions of safety climate at different employment levels”, International Journal of Work, Health &Organisations, Volume17, Number 1, pages 21–37, 2003.
- [3] Dawei Chen and Hanzhi Tian, “Behavior Based Safety for Accidents Prevention and Positive Study in China Construction Project-International Symposium on safety science and Engineering”, Social behaviour and Science,Volume43, Pages 528-534, 2012.
- [4] Faridah Ismail and Ahmad EzaneeHashim,“Steps for the Behavioral Based Safety:A Case Study Approach”, International Journal of Engineering and Technology, Volume4, Number5, pages 595-597,2012.
- [5] Faridah Ismail, Ahmad EzaneeHashim, Wan Zuriea Wan Ismail, HikmahKamarudin and Zarita Ahmad Baharom (2011) “Behavior Based Approach for Quality and Safety Environment Improvement: Malaysian Experience in the Oil and Gas Industry -International Conference on Environment-Behaviour Studies, North Cyprus”Social behaviour and Science, Volume35, Pages 586-594,December 2011.
- [6] FaridahIsmail,RahmatulHidayahSalimin and Razidah Ismail(2011) “The Organisational Environment-BehaviourFactors’Towards Safety Culture Development - International Conference on Environment-Behaviour Studies, North Cyprus”Social behaviour and Science, Volume35, Pages 611-618,December 2011.
- [7] Kean Engkoo,M.D.AhmadNurulazam, M.Z.SitiRohaida ,Tang Ghee Teo and ZulhisyamSalleh“Examining the Potential of Safety knowledge as Extension construct for Theory of planned Behavior: Explaining Safety practices of Young Adults at Engineering Lab And Workshops -5th World Conference on Educational Sciences”Social behaviour and Science, Volume116, Pages 1513-1518,2013.
- [8] LIU Jianhua and SONG Xiaoyan “Countermeasures of mine safety management based on behavior safety mode - International Symposium on safety science and Engineering”, Social behaviour and Science,Volume 84, Pages 144-150, 2014.
- [9] Sulastre Mat Zin and Faridah Ismail “Employer’s Behavioural Safety Compliance Factors toward Occupational, Safety and Health Improvement in the Construction Industry”Social behaviour and Science,Volume 36, Pages 742-751, 2011.
- [10] Willam R. Holliday and CSP,“Behavior Based Safety-Safety Professional's View”American Society of Safety Engineer, Georgia Chapter, Volume 42, 114-117, 1999.
- [11] YUAN Xiongjun and WANG Kaiquan “Study on Safety management of small and medium-sized enterprises based on BBS”International Journal of Engineering and Technology, Volume 3, Number11, pages 195-197, 2014.
- [12] Yueng-hsiang Huang, Michelle M.Robertson, Jin Lee, Jenn Rineer,LaurenA.Murphy, Angela Garabet and Marvin J.Dainoff (2014) “Supervisory interpretation of Safety climate versus employee safety climate perception:Association with safety behavior and outcomes for lone workers”, Traffic Psychology and Behaviour, Volume 26, Pages 348–360,2014.

CONTRAST ENHANCEMENT BASED IMAGE FORGERY DETECTION

Haritha.T, Jyothirmayi devi

College of engineering Chengannur, 93haritha@gmail.com ,7025870201

Abstract— Contrast enhancement is generally used to adjust the global brightness and contrast of digital images. Malicious users perform contrast enhancement for creating a realistic composite images. Nowadays contrast enhancement is used for checking authenticity and originality of images. In this paper two novel algorithms are proposed in-order to detect manipulated digital images involving contrast enhancement. First, we focus on the detection of contrast enhancement applied to JPEG-compressed images. The histogram peak/gap artifacts incurred as a result of the JPEG compression and pixel value mappings are analyzed theoretically and notable by identifying the zero-height gap fingerprints. Second, for identifying the composite image formed by enforcing contrast alteration on both source regions. This paper propose a method to find which type contrast enhancement is affected to the raw image. Also detect contrast enhancement whether the image is affected by any type of noising, with the help of these results we can train the datasets by using neural network and calculate the accuracy of the method.

Keywords— Contrast enhancement, Image forgery, Neural networks

1. INTRODUCTION

Contrast enhancement is frequently referred to as one of the most important issues in image processing. Currently, image forgeries are widespread on the Internet and other security-related applications such as surveillance and recognition that utilize images are therefore impacted. The event and scene information delivered in images might become no longer believable. In the applications such as law enforcement and news recording, it is also necessary to verify the originality and authenticity of digital images, and make clear the image manipulation history to get more information.

Image enhancement processes consist of a collection of techniques that seek to improve the visual appearance of an image that is better suited for analysis by a human or machine. The term image enhancement also mean as the improvement of an image appearance by increasing dominance of some features or by decreasing ambiguity between different regions of the image. Most of the contrast enhancement methods can be classified into two main categories: intensity-based techniques and feature-based techniques. Forgery is the process of making adapting or imitating objects. Forgery consists of filling in blanks on a document containing a genuine image, or materially altering or erasing an existing image. Instruments of forgery may include bills of exchange, bills of lading, promissory notes, checks, bonds, receipts, orders for money or goods, mortgages, discharges of mortgages, deeds, public records, account books, and certain kinds of tickets or passes for transportation or events. Methods of forgery include handwriting, printing, engraving, and typewriting. The related crime of uttering a forged image occurs when an inauthentic image is intentionally as genuine. Some modern statutes include this crime with forgery.

With the rapid development of digital media editing techniques, digital image manipulation becomes rather convenient and easy. While it benefits to legal image processing, malicious users might use such innocent manipulations to tamper digital photograph images. Currently, image forgeries are widespread on the Internet and other security-related applications such as surveillance and recognition that utilize images are therefore impacted. The event and scene information delivered in images might become no longer believable. In the applications such as law enforcement and news recording, it is also necessary to verify the originality and authenticity of digital images, and make clear the image manipulation history to get more information. To circumvent such a problem, digital forensic techniques have been proposed to blindly verify the integrity and authenticity of digital images.

2. RELATED WORKS

S. Bayram, I. Avcubas, B. Sankur, and N. Memon [2] proposed a technique for the detection of doctoring in digital image. Doctoring includes multiple steps i.e. a sequence of basic image-processing operations such as rotation, scaling, smoothing, contrast shift etc. The methodology used is based on the three categories of statistical features including binary similarity, image quality and wavelet statistics. The three categories of forensic features are as follows:

- 1) Image Quality Measure: These focus on the difference between a doctored image and its original version. The original not being available, it is emulated via the blurred version of the test image.
- 2) Higher Order Wavelet Statistics: These are extracted from the multi-scale decomposition of the image.

3) Binary Similarity Measure: These measures capture the correlation and texture properties between and within the low significance bit planes, which are more likely to be affected by manipulations.

To deal with the detection of doctoring effects, firstly, single tools to detect the basic image-processing operations are developed. Then, these individual weak detectors assembled together to determine the presence of doctoring in an expert fusion scheme.

M. Stamm and K. Liu [3] proposed a blind forensic algorithm for detecting the use of global contrast enhancement operations on digital images. Proposed work is based on the fact that, gray level histogram of the unaltered images exhibit a smooth contour whereas, gray level histogram of contrast enhanced images shows unsmoothness (peak/gap artifacts). A separate algorithm is proposed to identify the use of histogram equalization, a commonly Implemented contrast enhancement operation. The methodology used is as follows. The methodology used is known as global contrast enhancement detection technique. This algorithms works by seeking out the unique artifacts left behind by histogram equalization. However, the paper specifies only about the detection of global enhancement and not about the local enhancement.

M. C. Stamm and K. J. R. Liu [4] proposed different methods not only for the detection of global and local contrast enhancement but also for identifying the use of histogram equalization and for the detection of the global addition of noise to a previously JPEG-compressed image. The methodologies used are as follows.

1) Detecting globally applied contrast enhancement in image

Contrast enhancement operations are viewed as nonlinear pixel mapping which introduce artifacts into an image histogram. Nonlinear mappings are separated into regions where the mapping is locally contractive. The contract mapping maps multiple unique input pixel values to the same output pixel value. Result in the addition of sudden peak to an image histogram.

2) Detecting locally applied contrast enhancement in image

Contrast enhancement operation may be locally applied to disguise visual clues of image tampering. Localized detection of these operations can be used as evidence of cut-and-paste type forgery. The forensic technique is extended into a method to detect such type of cut-and- paste forgery.

3) Detecting Histogram equalization in image

Just like any other contrast enhancement operation, histogram equalization operation introduces sudden peaks and gaps into an image histogram. The techniques are extended into method for detecting histogram equalization in image.

4) Detecting Noise in image

Additive noise may be globally applied to an image not only to cover visual evidence of forgery, but also in an attempt to destroy forensically significant indicators of other tampering operations. Though the detection of these types of operations may not necessarily pertain to malicious tampering, they certainly throw in doubt the authenticity of the image and its content. The technique for detecting noise is able to detect whether the image is in noise or not, such as speckle noise, Gaussian noise etc.

M. Stamm and K. Liu [5] focuses on recovering the possible information about the unmodified version of image and the operations used to modify it, once image alterations have been detected. An iterative method based on probabilistic model is proposed to jointly estimate the contrast enhancement mapping used to alter the image as well as the histogram of the unaltered version of the image. The probabilistic model identifies the histogram entries that are the most likely to occur with the corresponding enhancement artifacts.

G. Cao, Y. Zhao, and R. Ni [6] present a blind method for the detection of gamma correction, a special type of contrast enhancement. The technique used is based on the histogram characteristics that are measured by patterns of the peak gap features. These peak gap features for the gamma correction detection are distinguished by the precomputed histogram of images.

Proposed Contrast Enhancement Detection Algorithm

The proposed contrast enhancement detection algorithm as follows.

1) Get the images normalized gray level histogram $h(x)$.

2) Detect the bin at k as a zero-height gap bin if it satisfies:

$$h(k) = 0$$
$$\min \{h(k-1), h(k+1)\} > \tau$$
$$\sum_{x=k-w_1}^{k+w_1} h(x) > \tau$$

Here, the first sub-equation assures that the current bin is null. To define a gap bin, the second sub-equation keeps two neighboring bins larger than the threshold, as shown in Fig. 1. To exclude the zero-height gap bins which may be incorrectly detected in histogram trail-ends, the average of neighboring $2w_1 + 1$ bins should be larger than, as constrained by the third sub equation. Experiments show that $w_1 = 3$ and 0.001 are appropriate. Note that we focus on the detection of isolated zero-height gap bins but not connected bins, which are rarely present in the middle of histograms.

3) Count the number of detected zero-height gap bins, denoted by N_g . If it is larger than the decision threshold, contrast enhancement is detected, else not. In the proposed system it detects image forgery based on contrast enhancement and also train the images in the database. It is an efficient method to find images is a manipulated one or not. Using neural network it trains and built the database.

3. SYSTEM DESIGN

A novel algorithm is proposed to identify the source-enhanced composite image created by enforcing contrast adjustment on either single or both source regions. The outline of our technique is shown in Fig 1. Since positional distribution of the peak/gap bins incurred by contrast enhancement is unique to the involved pixel value mapping, such positional information could serve as fingerprinting feature for identifying different contrast enhancement manipulations. Consistency between the peak/gap artifacts detected in different regions is checked for discovering composite images.

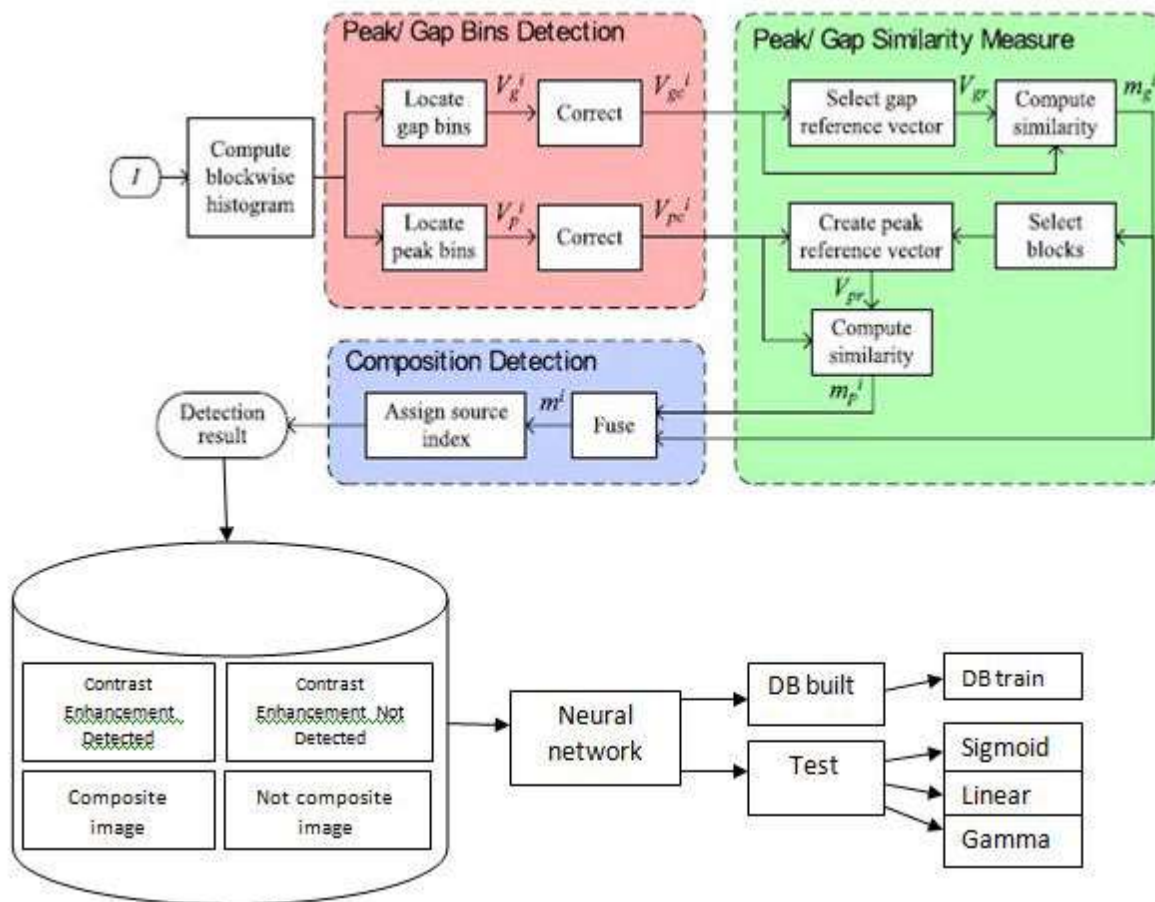


Fig 1: Flowchart of the proposed composite image detection technique.

3.1 Block wise Peak/Gap Bins Location

To locate composition, the test image I is first divided into non overlapping blocks. For the i -th block, peak/gap bins in its gray level histogram are located as follows. Here and below, $i = 1, 2, \dots, N_b$, where N_b is the number of divided blocks.

1) Gap Bins Location: The zero-height gap bins are detected. The position of detected gap bins is labelled as $Vig = [Vig(0), Vig(1), Vig(k), Vig(255)]$, where $Vig(k) = 1$, if the bin at k is a gap; $Vig(k) = 0$, otherwise.

2) Peak Bins Location: Peak bins which behave as impulse noise can be located by median filtering. Specifically, the gap bins are first filled with the average of neighboring bins, then median filtering is applied to the gap-filled histogram. As shown in fig 2, the filtered histogram possesses a smooth contour. Lastly, peak positions are located by thresholding the difference between the gap-filled histogram and its filtered version. The histogram differences for the enhanced and primary example images are shown in Fig. 2(b) and (c), respectively. It can be seen that peak bins are not detected in the primary image. Record the detected peak positions as $Vip = [Vip(0), Vip(1), Vip(k), Vip(255)]$, where $Vip(k) = 1$ refers to a peak. The peak/gap bins which are theoretically computed from contrast enhancement mapping may not appear since the histogram is too narrow to cover such bin positions. To address such a factor, Effective Detection Range (EDR) for the i -th block wise peak/gap position vector, is defined as the set of gray levels around which the histogram bins are not all zeros. In other words, the histogram bins at the gray levels out of EDR are zeros. Because of the narrow histograms incurred by low resolution, EDR of most position vectors actually contains limited gray levels. Specifically, we apply a simple and strict threshold-based binarization to $Cg = \sum Vig / N_b$. The detected co-existing gap positions are recorded as $Vg =$

$[Vg(0), Vg(1), \dots, Vg(k), \dots, Vg(255)]$, where $Vg(k) = 1$, if $Cg(k)$ is larger than the threshold; $Vg(k) = 0$, otherwise. To eliminate the gap bins which might not be caused by contrast enhancement, the corrected gap position vector V_{gc} is generated as

$$V_{gc}^i = V_g^i \odot V_g,$$

where \odot denotes Hadamard product, $k = 0, 1, 2, \dots, 255$. Similarly, the corrected peak position vector V_{ipc} can also be obtained.

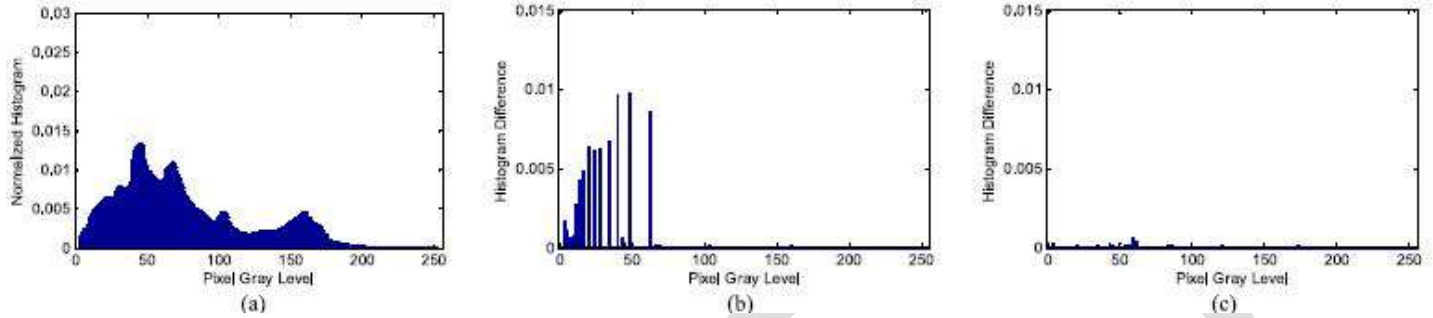


Fig 2: Peak bins location. (a) Filtered gap-filled version of the histogram; histogram difference for the (b) enhanced and (c) unenhanced image.

3.2 Gap Based Similarity Measure

To discriminate two source regions, we should first set a reference position vector for either one. Then each block can be classified by the similarity between its position vector and the reference one. It is reasonable to deem that the blocks with approximate similarity come from the same source image. The reference position vector should not be selected from splicing boundary. Fortunately, the block with the largest number of zero-height gap bins is believed to locate within one source region. In boundary blocks, the interaction between the pixels from different source regions makes the number of zero height bins decrease. As a result, the reference gap position vector for its located source region (marked as $S1$) can be set as $V_{rg} = V^k$ where.

$$k = \arg \max_{i \in \{1, 2, \dots, N_b\}} (\|V_{gc}^i\|).$$

Here, $\| \cdot \|$ denotes 1-norm of a vector. EDR of the reference gap position vector. To measure the overall similarity between the gap position vectors V_{gc}^i and V_{gr} , each gap-involved pair $V_{gc}^i(k)$ and $V_{gr}(k)$ should be investigated firstly. Since the histogram at the gray levels out of EDR does not deliver any effective peak/gap information left by contrast enhancement, the element pairs in the intersection of two EDRs are used to measure the similarity. As shown in Fig. 3, there exist three possible correspondences for a gap-involved pair. They are,

- ① $V_{gr}(k) = 1, V_{gc}^i(k) = 1;$
- ② $V_{gr}(k) = 0, V_{gc}^i(k) = 1;$
- ③ $V_{gr}(k) = 1, V_{gc}^i(k) = 0.$

We can see that the gap-involved pair is matched in the case but mismatched in. The overall similarity between V_{gc}^i and V_{gr} is determined by such three cases frequency. In the intersection between two EDRs, the ratio between the number of matched pairs and that of total gap-involved pairs is defined as the similarity. The pair is completely matched in the case. The more pairs occur as such, the more similar the two gap position distributions are. In the case, the detected gap is not marked in the reference vector. In the case, the gap in the reference vector is absent in the unlabeled histogram.

Both and attribute to the different contrast enhancement mapping applied to the image region out of the reference block. Based on the above analyses, the similarity between V_{gc}^i and V_{gr} denoted by m_g^i , can be defined as the below equation. Here,

$$m_g^i = \frac{\sum_{k \in \Omega_i \cap \Omega_{gr}} V_{gc}^i(k) \cdot V_{gr}(k)}{\sum_{k \in \Omega_i \cap \Omega_{gr}} V_{gc}^i(k) \cdot V_{gr}(k) + \overline{V_{gc}^i(k)} \cdot V_{gr}(k) + V_{gc}^i(k) \cdot \overline{V_{gr}(k)}},$$

When no gap-involved pair is $m^{ig} = 1$. We can see that m^{ig} becomes larger if more gaps co-exist. m^{ig} approaches the maximum 1 if all gaps are matched, and decreases to 0 if all gap-involved pairs behave as . Correspondingly, the possibility that the two blocks undergo the same pixel value mapping ranges from the largest to the smallest.

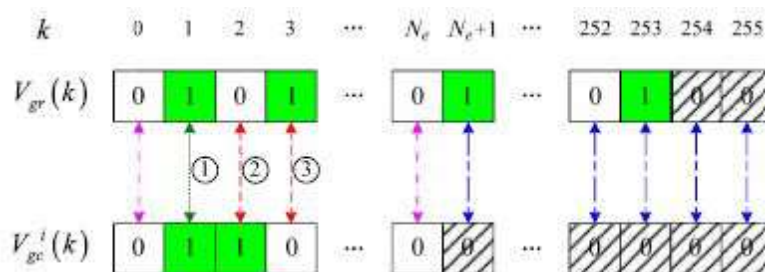


Fig 3: Correspondence between V_{gr} and V^{igc} . Here, EDRs of V_{gr} and V^{igc} respectively. The positions out of EDR are marked by the box with shadow. The gap-involved pair is matched in the case and mismatched in the cases.

3.3 Peak Based Similarity Measure

Since the image block usually owns a narrow histogram, the theoretical gap bins might be unavailable in not a few blocks. Such blocks cannot be assigned to either source region merely based on the gap information. However, the narrow histogram without gap bins might carry with peak bins. As such the peak bins should also be exploited to identify mappings. The reference peak position vector V_{pr} is created by combining the peak position vectors which are more possible from the source region of V_{gr} , namely S_1 . Such creation of V_{pr} is reliable since the collected peak information is relatively accurate. Specifically, we have

$$V_{pr}(k) = \ell \left(\sum_{n \in N_R} V_{pc}^n(k) > 0 \right).$$

Here, $k = 0, 1, 2, \dots, 255$. $\ell(\cdot)$ is the indicator function. $N_R = \{n | m_{ig}^n > t_g\}$ where t_g is the threshold used to candidate block. As defined m^{ig} in (8), the similarity between V^{igc} and V_{pr} marked as m^{ip} , is defined in the same form by replacing the gap variables with the corresponding peak ones. If no peak involved pair exists in EDR intersection, we mark $m^{ip} = -1$ select the candidate blocks.

3.4 Similarity Maps Fusion for Composition Detection

Before fusion, $m^{ig} = -1$ and $m^{ip} = -1$ the block wise similarities are updated by averaging the available neighboring effective measurements. The resulting similarity for the i -th unlabeled block, denoted by m_i , can be generated by fusing the peak/gap based similarities.

$$m^i = (m_g^i + m_p^i) / 2.$$

When $m^{ig} = -1$ or $m^{ip} = -1$: $m_i = \max(m^{ig}, m^{ip})$. when $m_i = -1$ occurs scarcely in both-source-enhanced composite images. If all the blocks in an unsaturated region own $m_i = -1$ while the blocks out of the region have $m_i > t$, the test image can be identified as a single-source-enhanced composite image. Otherwise, each block is classified as: 1) if $m_i > t$, contrast enhancement mapping applied to S_1 is detected; 2) if $m_i < t$, a different contrast enhancement mapping applied to the other source region is detected. Hence, the both-source enhanced composite image is detected if two different mappings are detected in two complementary regions, respectively. The threshold t is experimentally set as 0.2.

Using neural network this project detects which type of contrast enhancement applied to the images. According to contrast variation enhancements are classified into 3 main categories:

- 1) Linear contrast enhancement
- 2) Sigmoid contrast enhancement
- 3) Gamma contrast enhancement.

1) Linear contrast enhancement

Linear contrast stretching (LCS) is an enhancement method performed on an image for locally adjusting each picture element value to improve the visualization of structures in both darkest and lightest portions of the image at the same time. This type referred a contrast stretching, linearly expands the original digital values of the remotely sensed data into a new distribution. By expanding the original input values of the image, the total range of sensitivity of the display device can be utilized. Linear contrast enhancement also makes subtle variations within the data more obvious. These types of enhancements are best applied to remotely sensed images with Gaussian or near-Gaussian histograms, meaning, all the brightness values fall within a narrow range of the histogram and only one mode is apparent.

2) Sigmoid contrast enhancement

Sigmoid contrast enhancement is based on modifying the appearance of an image by controlling the input pixel values via an equation depending on the sigmoid function. This enhancement adjust the shadows and highlights in poor contrast images as well as the signal to noise ratio. The sigmoid function has the characteristics that it is a smooth continuous function, the function outputs within the range 0 to 1, mathematically the function is easy to deal with; it goes up smoothly and kindly.

3) Gamma contrast enhancement

Gamma is an important but seldom understood characteristic of virtually all digital imaging systems. It defines the relationship between a pixel's numerical value and its actual luminance. Without gamma, shades captured by digital cameras wouldn't appear as they did to our eyes (on a standard monitor).

Neural network is a nonlinear mapping system whose structure is loosely based on principles of the real brain. The whole network is build up with simple processing units, structures of those can be seen. The unit is a simplified model of a real neuron. Its parts are the input vector x whose containing information is manipulated by the weighted nodes by weigh vector w . The weight change in each layer is done with steepest descent algorithm. The back-propagation algorithm is carried out in the following steps:

1. Select a training pair from the training set; apply the input vector to the network input.
2. Calculate the output of the network.
3. Calculate the error between the network output and the desired output (the target vector from the training pair)
4. Adjust the weights of the network in a way that minimizes the error.
5. Repeat the steps 1 through 4 for each vector in the training set until the error for the entire set is acceptably low.

ACKNOWLEDGMENT

This project would never have been successful to this point if it weren't for the dedication put in by many minds selflessly. First, I thank GOD, THE ALMIGHTY for showering his abundant blessings upon me for the fulfillment of this project. I express my sincere thanks to my project guide Ms.Jyothirmayi Devi, Assistant Professor in Computer Science Engineering, for guiding me in my work and providing timely advices and valuable suggestions. This humble endeavor wouldn't have become a success without the constant support, inspiration and blessings from my parents.

CONCLUSION

The proposed contrast enhancement based image manipulation methods could work particularly well when contrast enhancement is performed as the last step of manipulation. In the future work, I would try to improve the robustness of such methods against post processing, such as JPEG compression. It is also essential to enhance the security rather than forensics. In this paper we proposed an iterative algorithm to jointly estimate an images unaltered pixel value histogram as well as the contrast enhancement mapping used to modify the image given only a contrast enhanced version of the image. We used a probabilistic model of an images histogram to identify the histogram entries most likely to correspond to contrast enhancement artifacts. We then used this model along with knowledge of how contrast enhancement modifies an images histogram to obtain our unaltered histogram and contrast enhancement mapping estimates. Simulation results indicate that our algorithm is capable of providing accurate estimates even when nonstandard forms of contrast enhancement are applied to an image.

REFERENCES:

- [1] Contrast enhancement-based forensics in digital images Gang Cao, Yao Zhao, Senior Member, IEEE, Rongrong Ni, Member, IEEE, and Xuelong Li, Fellow, IEEE.
- [2] S. Bayram, I. Avcubas, B. Sankur, and N. Memon Image manipulation detection, J.Electron. Imag., vol. 15, no. 4.
- [3] M.stamm and K.Liu, Blind forensics of contrast enhancement in digital images,IEEE Trans. Signal Process., vol. 53, no. 2,pp. 758-767, Feb. 2005.

- [4] C. Stamm and K. J. R. Liu Forensic detection of image manipulation using statistical intrinsic fingerprints ,IEEE Trans. Inf. Forensics Security, vol. 5, no. 3, pp. 492-506,Sep. 2010.
- [5] M. C. Stamm and K. J. R. Liu, Forensic estimation and reconstruction of a contrast enhancement mapping, in Proc. IEEE Int. Conf. Acoust., Speech Signal, Dallas, TX,USA, Mar. 2010, pp. 1698-1701.
- [6] G. Cao, Y. Zhao, and R. Ni, Forensic estimation of gamma correction in digital images, in Proc. 17th IEEE Int. Conf. Image Process., Hong Kong, 2010, pp. 2097-2100.
- [7] A. Swaminathan, M. Wu, and K. J. R. Liu, Digital image forensics via intrinsic fingerprints, IEEE Trans. Inf. Forensics Security, vol. 3, no. 1,pp. 101-117, Mar. 2008.
- [8] H. Cao and A. C. Kot, Manipulation detection on image patches using FusionBoost, IEEE Trans. Inf. Forensics Security, vol. 7, no. 3,pp. 992-1002, Jun. 2012.
- [9] J. Fan, H. Cao, and A. C. Kot Estimating EXIF parameters based on noise features for image manipulation detection, IEEE Trans. Inf. Forensics Security, vol. 8, no. 4, pp. 608-618, Apr. 2013.
- [10] T. Bianchi and A. Piva, Detection of non-aligned double JPEG compression based on integer periodicity maps, IEEE Trans. Inf. Forensics Security, vol. 7, no. 2, pp. 842-848, Apr. 2012.
- [11] G. Cao, Y. Zhao, R. Ni, and A. C. Kot Unsharp masking sharpening detection via overshoot artifacts analysis, IEEE Signal Process. Lett., vol. 18, no. 10, pp. 603-606,Oct. 2011.
- [12] P. Ferrara, T. Bianchiy, A. De Rosaz Reverse engineering of double compressed images in the presence of contrast enhancement, in Proc. IEEE Workshop Multimedia Signal Process., Pula, Croatia, Sep.Oct. 2013, pp. 141-146.

GSM Based Industrial Security and Energy Conservation System

Parthiban NR,
M.Tech Embedded Systems
Bharath university
parthibanr@outlook.com

V.Srinivasan,
M.Tech Embedded Systems
Bharath university
sriniraj99@gmail.com

Abstract: An intelligent control system was developed using simple control methodologies for a H₂- powered fuel cell scooter with the aid of a built-in microprocessor. This system increases the power input to drive a hydrogen fuel cell scooter, particularly during uphill conditions by running both the batteries and the fuel cell source in parallel. This system also improves the energy management of the scooter by recharging the battery using the fuel cell as well as automatic switching to the battery source when the hydrogen fuel cell is running low on hydrogen. This system was tested on a bench set simulating a 254 W hydrogen fuel cell stack equipped on a 200 W scooter. The entire operation was embedded in a PICAXE-18 microcontroller for automatic switching between the batteries and the fuel cell source. It has been shown that an increase in the DC motor efficiency by 6 %. The uphill angle of the scooter has been increased by 19.3 %, which means the scooter would be able to travel in more steeper hills.

Key words: Hydrogen Fuel Cell, Energy Management, Fuel Cell Scooter.

1. INTRODUCTION

Australia, a major producer and user of coal, has the highest per capita greenhouse gas emissions in the industrialized world [1]. The ultimate goal is clear: the introduction of a zero emissions transport fuel that can be made from a wide range of primary energy resources [2, 3]. This goal leads to companies to undertake various strategies to cut down on harmful emissions, one being the introduction of hydrogen as an alternative vehicle fuel. One of the methods is by using a fuel cell. Hydrogen fuel cells are being considered as ideal candidates for future vehicles, due to their high efficiency and near zero emissions [4].

Hydrogen is the most abundant element on the planet, and it is the cleanest burning fuel on the basis of carbons atoms per fuel molecule [5-6]. It anational Journal of Computer Science and Communication Mobile Computing, Vol.4 Issue.10,Nov - 2014, pg. 244-249

As fuel cells today becoming less expensive, plug-in hybrid vehicles are becoming more and more popular today. A PEM fuel cell costs are about \$1100/kW when used with pure oxygen and about \$2200/kW [9-10] when used with air. The costs are projected to be \$650 - \$1150 by 2010 .

The plug-in fuel cell hybrid vehicle relies on any number of combinations of fuel cells, batteries, capacitors and ICEs to power the vehicle [11, 12]. The plug-in aspect of this vehicle allows grid electricity or onboard charging of the batteries, during the night or when the vehicle is stagnant. About half the distance traveled by automobiles each day in the US are within the first 32 km traveled by each vehicle in a day . Renault introduced a commercial plug-in hybrid vehicle in 2003 [13,14].

Fuel cell and batteries can have a powerful combination. The combination of the two can provide better performance and lower cost than batteries alone of fuel cells alone [15].

One of the steps to reduce harmful emissions is to incorporate batteries to hydrogen fuel cells into scooters. Currently, there are over 400,000 motorcycles and scooters registered through out Australia [16]. Thus hydrogen fuel cell scooters are considered the way to go to lower emissions to move Australia to a cleaner environment.

Hydrogen fuel cell scooters are being developed, especially in Taiwan, China as well as India. This is because Numbers of scooters in use are high in Asia, and growth rates are also high. The People's Republic of China, for instance, had 500,000 motorcycles in 1980, and 10 million in 1994 - an annualized growth rate of 24%, faster than the 15-20% of Chinese urban vehicles in general [17]. India had an average annual growth rate of 16% for two-wheeled vehicles from 1981 to 1998 [18].

One of the problems that lie with the fuel cell scooters is that fuel cells encounter insufficient power densities and thus the power generated by fuel cell scooters are not enough for various conditions.

Take the uphill example for urban areas. For a scooter travelling uphill with one or possibly two people can pose a great challenge as well as a threat to the passengers if the power generated by the scooter is insufficient to travel over the uphill hurdle.[19-22]

In this paper, a regenerative energy control system. This system increases the power input to drive a hydrogen fuel cell scooter,

particularly during uphill conditions by running both the batteries and the fuel cell source in parallel to increase the power input to the DC motor. This system also improves the energy management of the scooter by recharging the battery using the fuel cell as well as automatic switching to the battery source when the hydrogen fuel cell is running low on hydrogen. This was tested on a bench set simulating a 254 W hydrogen fuel cell stack equipped on a 200 W scooter. The entire operation was embedded in a PICAXE-18 microcontroller for automatic switching between the batteries and the fuel cell source

2. CONTROL METHODOLOGY

One of the methods is to incorporate rechargeable batteries to the hydrogen fuel cell scooter.

Fuel cell systems designed for applications that require fast start-up, such as back up or emergency power contain rechargeable batteries. This is usually also true for fuel cells applied to transportation, even without reformers. Batteries or super-capacitors are commonly installed in the system to mitigate the insufficient power density problem encountered by the existing fuel cells [19]. This hybrid technology can be seen in many fuel cell scooters today.

This method was incorporated and tested on bench set up simulating a 254 W hydrogen fuel cell stack equipped on a 200 W scooter, which was developed by the HART research team at the University of Tasmania. The current system developed originally runs on a fuel cell source. Once the hydrogen depletes, a flick of a switch will change the main source from the fuel cell to a set of batteries. Note that this two sources work independently.

A main problem faced by the University of Tasmania hydrogen fuel cell scooter is the need for more power especially during uphill conditions.

Thus a proposed new control system for the scooter was introduced. This control system is basically controlled by the micro controller by reading current levels and thus operates the 2 reed relay switches to either switch to modes to recharge the battery or runs the battery in parallel with the fuel cell source to increase the power input to the DC motor. Also, the current detector before the motor controller detects the availability of the hydrogen gas. If the metal hydride tank is running low on hydrogen, the power assist system will automatically switch for continuous running of the scooter, this time by using the rechargeable batteries.

3. EXPERIMENTAL SETUP

The proposed system was simulated on a bench. The three main goals to be demonstrated are:

Developing a power assist system using the battery as a secondary cell to run in parallel with the fuel cell to enable the scooter to ascend steeper slopes.

Developing a charging system that enables the fuel cell to recharge the batteries when the power assist is not needed (when traveling in a flat surface for example). This is to keep the batteries fully charged every time so that when the hydrogen depletes, the batteries can be used as the main power source.

Automatic switching circuit to switch from fuel cell to batteries when hydrogen is running low.

All automatic switching circuit is done using a programmable microprocessor and the switching device used is a normal reed relay. The physical set up block diagram of the bench is shown in Figure

- (1) A DC source of 24 V was used to mimic the fuel cells behavior.
- (2) Two sealed lead acid batteries with each 12V are providing the extra current for the electric DC motor during the power assist operation. Lead acid batteries are chosen due to their high power density, reliability and ability to satisfy widely varying loads [8].
- (3) The throttle, which is adjusted on the scooter handlebar, is used for changing the DC motor speed and consequential scooter speed. The throttle was used to run different speeds from 500 rpm up to the maximum. It is based on the principal of a varying resistor.
- (4) The scooter control system controls the speed, direction and optimizes energy conversion. It gets and regulates the voltage and current signals. The regulated signals goes into the DC motor.
- (5) 24V DC motor is a permanent magnet motor using permanent magnets rather than electromagnetic windings in the stator. It has a relatively high maintenance because of its brushes but also a higher efficiency than other DC motors due to the lack of stator field windings [8]. This is connected to a dynamometer.

(6) The battery charger is constructed using a LM371K voltage regulator. The output voltage is set to 28 V. This is to charge the 24 V batteries, which have a fully charged voltage of 28 V.

(7, 8) Hall effect current sensors are installed to sense the current levels and outputting a voltage level with respect to the current sensed. Two LOHET 650-554 sensors are installed, one is to detect the current drawn by the motor and one is to detect the current provided by the fuel cell source.

(9, 10) The reed relays used are OMRON's G2RL-1-E relays. The 4 modes of switching are:

Normal and charging mode (same as the same relay was used)

Power assist mode

Backup power mode

(11) The dynamometer works in these tests as a consumer or generator, because the power for turning the dynamometer shaft is supplied by the DC motor. It is a universal commutator motor with a necessary field voltage of 8 V DC and an armature voltage of 25 V DC. The dynamometer has two spring balances installed to measure the torque and load.

(12) The consumer load is a variable resistor (max 28.2 • with 4 A) that is connected in the electrical generator output circle.

(13) 8 V DC power source was used for generating the dynamometer field current. The field strength generates the resistance in the dynamometer.

(14) This variable resistor (max 32 • with 3.3 A) regulates the dynamometer field strength.

4. RESULTS

For the power assist system, as loading increases, the motor current reaches a maximum of 12

A. This is to protect the motor from burning as the rated motor current is just 11.5 A. An additional 4 A of current was supplied by the battery on top of the 8 A current from the DC source. At maximum loading, about 12 N, the maximum current for the original system (fuel cell only) is 8 A and the maximum current for the integrated system (fuel cell and battery in parallel) is 12 A. This will certainly increase the power input to the DC motor. The battery will start assisting the fuel cell when the current reaches about 7.5 A, with a maximum provided current of 4 A.

Also, at maximum loading, the efficiency achieved by the original system is 64% and the new system is 70%.

For the charging system, a constant current of 1.5 A at 28 V was supplied to the battery by the charger. The charging rate was calculated to about 11.67 hours to charge the batteries from flat until floating.

International Journal of Computer Science and Communication Mobile Computing, Vol.4 Issue.10,Nov - 2014, pg. 244-249

5. CONCLUSION

This paper presents a study on plug-in hybrids on small-sized urban scooters. This is to improve the system efficiency and battery life with acceptable load capability.

All the system components above were tested to obtain the final results. The final results showed the efficiency before the new system was installed was 64 % and after incorporation, the efficiency is 70%. The current drawn by the DC motor reaches a maximum of 12 A, comparing to just 8 A on the old system. Finally, a battery charging process was incorporated as well as an automatic switching to battery source when the hydrogen runs out.

The final results show that with the incorporation of batteries to fuel cell scooters, the motor efficiency can be increased as well as building a market for future research on urban fuel cell scooters.

REFERENCES:

1. Turton H. 2004 Greenhouse Gas Emissions in Industrialized Countries: Where does Australia Stand? *Discussion Paper No. 48, The Australia Institute, Canberra.*
2. Rifkin J. 2002. *The Hydrogen Economy*; Jeremy P. Tarcher: New York.
3. Wald ML. May 2004 Questions about Hydrogen Economy. *Scientific American.*
4. He X, Leslie A, Cordaway A, Maxwell T, Parten M. 2004 Peripheral System for a Fuel Cell Powered Vehicle. *SAE World Congress, Detroit, MI, SAE Technical Paper Series 2004-01-0240.*
5. He X, Maxwell T, Parten M. 2006 Development of a Hybrid Electric Vehicle with a Hydrogen-Fueled IC Engine, *IEEE Transactions on Vehicular Technology* 55 (6).

6. Stockhausen W, Naitkin R, Kabat D, Reams L, et al. 2004 Ford P2000 Hydrogen Engine Design and Vehicle Development Program. *SAE World Congress, Detroit, MI, SAE Technical Paper Series 2002-01-0240*.
7. Heywood JB. 1995. *Internal Combustion Engine Fundamentals*; McGraw-Hill: New York.
8. Lin B. 1990 Conceptual Design and Modelling of a Fuel Cell Scooter for Urban Asia, *Master's Thesis, Department of Mechanical and Aerospace Engineering, Princeton University*.
9. Energy Technology Fact Sheet. Published by United Nations Environment Program, Division of Technology, Industry, and Economics, <http://www.uneptie.org/energy>, accessed April 1st 2007.
10. John AA, Foulkes FR. 1989. *Fuel Cell Handbook*; Van Nostrand Reinhold; 193-196. The vehicle described was an Austin A-40 developed by Karl Kordesch at Union Carbide and run off compressed hydrogen tanks. It was driven by Kordesch on public roads from 1971-1975
11. Graham N. 2002 Plug-in Hybrid Electric Vehicles Significant Market Potential. See <http://www.arb.ca.gov/msprog/zevprog/2003rule/1202wkshp/graham.pdf>, accessed April 1st 2007.
12. Vyas AD, Ng HK. 1997 Batteries for Electric Drive Vehicles: Evaluation of Future Characteristics and Costs through a Delphi Survey. <http://www.transportationnl.gov/pdfs/TA/103.pdf>, accessed April 1st 2007.

Analysis of Cloud IDEs for Software Development

Ms. Pooja Arora

BCIIT, Delhi.

poojadhanrajani@gmail.com

Dr. Anurag Dixit

Galgotias University, Greater Noida.

anurag.dixit@galgotiasuniversity.edu.in

ABSTRACT: In today world using cloud services has become a convenience for software developers to develop application. An integrated development environment(IDE) facilitates the development of apps in shorter software delivery timelines. A cloud based IDE is an 'next gen' solution and still in the incubation stage because the cloud based private workspace is yet to evolve fully.as of now, there still is not any good java-supporting cloud IDE available. Evaluation of different cloud IDEs is discussed in this paper.

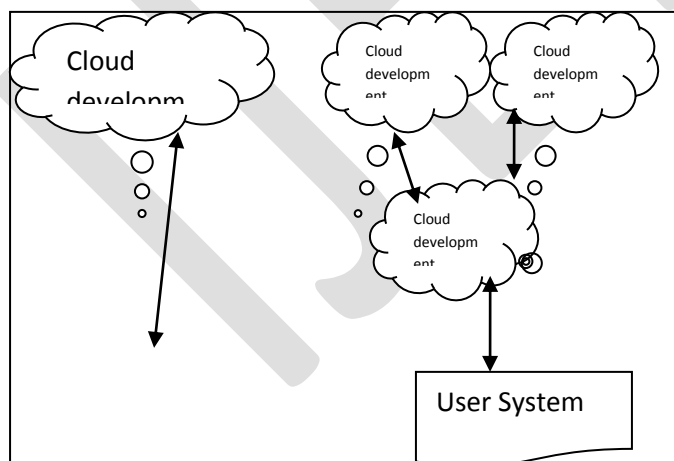
This paper discuss an open source virtual environment for cost effective and better community based collaborative software development. In this paper we analyze a cloud based development facility that can be accessible from anywhere and be used without much interfacing in the local developer system such as software installation, network boundary etc.

Keywords : IDE, Software development, deployment environment, cloud IDE, Virtual Environment, Java, J2EE

1. INTRODUCTION

The development process plays a vital role in developing a software product. The software development process consists of requirement gathering and analysis, designing, coding, testing, deployment and maintenance. The basic requirements for software development are hardware and software tools, a server to deploy and test the application and a coding development environment. Cloud based development brings in a lot of cost savings and efficiency into the process of software development. The cloud provides a deployment environment for developers and the developer do not require building, developing or maintaining this environment but can share it easily from the public environment.

Figure 1.1 Software development and the cloud IDE



An integrated development environment is a software tool that integrates various features required for the development of a software application. The cloud IDE is the latest improvement in this area. The cloud IDE is a virtual development environment. To develop a java application, we use Eclipse or Netbeans as the IDE, which provides an integrated plugin facility to develop java code, auto complete java APIs, has syntax highlighting, apart from the capability to compile, execute, test and analyze static code. In

traditional software development environment, all developers install the IDE in their respective systems, and upload their developed code into a concurrent version system(CVS) or source code management system. Once the code is checked in, it requires the harmony of other developers, which takes more time if the number of developers is high in a project. So there is the fundamental need to provide a software development environment for a large number of developers to work together on a collaborative project, yet achieve a shorter delivery time, a cloud IDE is one of the best solutions to reduce the development process time, as it provides a more convenient and flexible common environment for software developers.

2. THE CLOUD IDE

The basic motive behind the cloud IDE based platform is to create a virtual development environment. It can provide the following features for the software development process :

- a. programmer can develop an application in one or more software technologies such as Java, C++, HTML, JavaScript and so on.
- b. It has an application container to deploy the application on-the-fly.
- c. It offers repository management to store, retrieve and share code between groups of developers.
- d. In addition to these basic features, we need to add security to limit the access to only the selected group of developers. This can be achieved by an authentication system that protects the development environment from public use.

2.1 Standard expectation from a cloud IDE

The following standard expectations from a cloud IDE are :

- It should be lightweight and flexible enough.
- It should be able to highlight syntax.
- It should have the auto completion facility.
- It should have an internal compilations facility.
- It should support remote repository management for source code.
- It should provide minimum debugging facilities.
- It should support cloud deployment.

In addition to this, proficient developers who have worked on various IDEs like Eclipse, JDevelopers, IntelliJ, Visual Studio etc would look for some add-on features like :

- Support for screen design with a visual designer tool.
- API or language help; for example, tooltip for a Java API.
- Static code analysis to follow best practices in coding.
- Coding convention and code formatting or styling; for example, the number of characters in a line, tab, indentation etc.

2.2 Advantages of working in cloud-based IDEs

- Programming workspace is a single and centralized environment in which multiple people can co-build, co-edit and co-debug
- Easy and instant access to codes and libraries through the web
- Enables developers to work on the go without the need to occupy systems with loads of heavy codes and data
- Accessible through all devices and browsers
- Facilitates better collaboration among developers located at different locations
- Reduces duplication of work

3. ANALYSIS OF OPEN SOURCE CLOUD IDES

The popular open source cloud IDEs include Cloud9, codeanywhere, Eclipse Orion, Coderun Studio, Codebox, Codeiad, IDE One and Codenvy-Eclipse Che. In the following section the various features and advantages and disadvantages of these tools based on experience of users are discussed.

3.1 Cloud9

Cloud9 IDE is capable of handling projects from JS, HTML, PHP AND Ruby. it support development in JavaScript, GIT, Selenium, HTML/CSS, XML, XQuery, PHP, Ruby and Node.js. it can be used for web application development. Cloud9 supports repositories like GIT, the distributed revision control tool Mercurial, and Apache subversion. It also facilitates

deployment, which can be done directly from Cloud9 to Joyent and Heroku. Its limitation is that it is not useful for Java application development or J2EE application development/handling.

Advantages: Supports a variety of languages and various repository tools.

Disadvantages: can be used for simple application development but not for large or complex applications.

3.2 Codeanywhere

This is lightweight browser based IDE tool. It supports web application development. It support HTML, CSS, Java Script, PHP, MySQL, and more.

This tool is used to develop and test code from anywhere i.e from mobile device also as it is also available as a mobile application. Codeanywhere is supported in IOS, Android and BlackBerry based mobile devices and tablets.

Advantages : Lightweight and easy to use. Support for mobile devices.

disadvantages: it is more useful for web page development and it doesnot support a variety of programming languages.

3.3 Eclipse Orion

This can be used as a local standalone IDE or an online IDE through a browser. This is the Eclipse version of Orion. It only supports Chrome, FF Safari and IE10. This is more for client side scripting like HTML, JS and CSS. Java syntax highlighting is supported during static code review, and doesn't integrate with the java build and development environment. It has shell features with a very limited command facility.

It doesn't support the private cloud and hence is not suitable for secured application development. This is one of the lightweight cloud IDEs for software development in HTML/CSS and javascript.

Advantages : can be used as a standalone local installation tool or as a cloud IDE. It offers static code analysis. Shell features provides facility for UNIX script development, which is a unique feature many cloud IDEs do not offer.

Disadvantages : it doesn't support the private cloud/secure development, and doesn't support build/compilation of code or online testing.

3.4 Coderun Studio

This is simple and efficient cloud IDE. It support application development in ASP.net, HTML, CSS and JavaScript, Microsoft visual studio. It also facilitates code completion, syntax highlighting, debugging and native compilation. This provides flexibility for community development by providing a unique URL and access to peers for a multi-user development environment.

Advantages : unique URL for multi-user development, in parallel. More suitable for pair/peer programming. Supports Microsoft code development, debugging and native compilation.

Disadvantages : development using latest frameworks or languages like Scala, Ruby, NodeJS, AngularJS is not supported by this tool.

3.5 Codebox

This is an open source IDE with code available. It enables the users to customize the tool and encourages them to share it for community development.

Programmer can download the code from this repository, and build to prepare an IDE in their local desktop. It supports Windows, Chromebox and Mac based operating system. This tool is used to develop local or cloud based application. It facilitates pair programming by providing cloud based IDEs for sophisticated community development in Java, JavaScript, C++, Ruby, Scala, HTML, CSS, NodeJS and UNIX script programming.

It provides auto completion of code, syntax highlighting and supports cross-platform development on the desktop, laptop , tablet and on Chromebook.

This tool provides supports for Scala based program development and deployment to cloud based platforms. It is an open source with licensing under Apache 2.0, and provides command line development for shell programming. It provides supports for Google Docs and database support using MySQL.

Advantages: provide support for variety of repositories, cloud deployment, scala based program development, cross platform support and auto completion of code.

Disadvantages : it does not support PHP application development.

3.6 Codiad

This is simple tool which supports more than 40 programming languages, and provides plugins for integration with other popular IDEs like Eclipse. There is no database required to be installed locally, and no application server or local installation required to run this browser based IDE tool.

Advantages : simple and efficient tool that supports a variety of languages. Application server support for local deployment is available.

Disadvantages : it doesn't support a variety of database types and is not so flexible in pair programming.

3.7 Online java IDE

This IDE has facilities for java/J2EE development. It also supports spring, ojdbc, MySQL, mail APT and Axis frameworks. This IDE is not very user friendly and typing/editing is not too comfortable. The package creation option is not available for modular programming. There is no download and upload facility to synchronize with the local development environment.

Advantages : supports a variety of database drivers and frameworks like Mailx, Axis etc

Disadvantages : Packages and deployment is not available limited to java development only.

3.8 IDE One

This is a very simple online IDE which supports Java. It can be more useful as a unit or stub testing environment- as a quick try. The code development in this tool is done online and there is no 'Save' option. It doesn't have extensive support for real-time application development/deployment.

Advantages : simple tool with real-time application

Disadvantages : lacks user friendliness.

3.9 Codenvy - Eclipse Che

It supports a variety of Java/J2EE frameworks. This IDE provides unlimited open source community development support and user access. Usability is high, being as simple as using a desktop version of Eclipse or the Netbeans IDE. The deployment facility includes a variety of PaaS cloud environments. Integration is seamless and automatic. When user trigger deployment from an IDE, it connects to the PaaS and pushes the build to the deployment zone.

GIT is the default management repository and it has a local as well as remote GIT facility, where users can either keep the source local to Codenvy (like storing in local development machine) or connect to remote GIT to check-in/check-out.

It has JSP AND SPRING support in built, using the project template features. It has features to import external jars and hence JSF or the Struts Framework can be used for code development. Applications with DB support can be simply chosen from the wizard. Archive download of the project to a local system is available. Uploading the existing projects is possible, and so the user can switch between the local environment and the online IDE. Package creation support is also available. Codenvy is bit slow when 'initialising Java tool' and supports non-IE browsers such as Safari, Firefox or Chrome.

It has shell access for UNIX development with basic commands. Build and deploy is integrated in the IDE. It supports deployment to cloud environments

Advantages : has a variety of features and is flexible in development. Supports download of archive code-on-the-fly.

Disadvantages : it doesn't support IE browser. Slows down sometimes when users compile or do a cloud deployment.

4. CONCLUSION

For a developer or a small company that lacks the capability to install an IDE locally for software development or wants to develop a program on-the-fly, the tools described above would be helpful to experiment on, prior to choosing a development

environment. With the adoption of several simple security precautions and an open mindset, any software developer can reap the rewards of Cloud software suites without any real danger.

REFERENCES:

- [1] Chia Hung Kao, Shin Tze Liu , Chun Cheng Lin “Toward a Cloud based Framework for Facilitating Software Development and Testing Tasks” 2014 IEEE/ACM 7th International Conference on Utility and Cloud Computing DOI-978-1-4799-7881-6/14 \$31.00 © 2014 IEEE
- [2] Deepak Puthal*, B. P. S. Sahoo†, Sambit Mishra‡, and Satyabrata Swain, “Cloud Computing Features, Issues and Challenges: A Big Picture” , 2015 International Conference on Computational Intelligence & Networks, DOI 10.1109/CINE.2015.31
- [3] Wei-Tek Tsai, Wenjun Wu, Michael N. Huhns, “Cloud-Based Software Crowdsourcing”, Published by the IEEE Computer Society 1089-7801/14/\$31.00 © 2014 IEEE
- [4] Dave Thomas, “Enabling Application Agility - Software as A Service, Cloud Computing and Dynamic Languages” in Journal of Object Technology, vol. 7 no. 4 May-June 2008, pp. 29-32
- [5] Codeanywhere <https://codeanywhere.net/>
- [6] Cloud9 <https://c9.io>
- [7] Codenvy <https://codenvy.com>
- [8] <http://www.compilerjava.net>
- [9] <https://ideone.com>
- [10] <http://codiad.com>
- [11] <http://codebox.in/>
- [12] <http://coderuncom/studio>
- [13] [G. Fylaktopoulos](#), [G. Goumas](#), [M. Skolarikis](#), [A. Sotiropoulos](#), and [I. Maglogiannis](#) “An overview of platforms for cloud based development” Published online 2016 Jan 16. doi: [10.1186/s40064-016-1688-5](https://doi.org/10.1186/s40064-016-1688-5), Springerplus. 2016; 5: 38

Analysis of Flow Dynamics of an Incompressible Viscous Fluid in a Channel

Deepak Kumar

Assistant Professor, Department of Mechanical Engineering, Amity University Gurgaon, India

E-mail: deepak209476@gmail.com

Contact No: +91-9416627599

Abstract— In this study, the time -independent laminar flow of a viscous, incompressible fluid in two dimensions was analyzed using Navier –Stokes equations with continuity equation as an incompressibility constraint and vorticity – stream function approach. The fluid was allowed to flow in a rectangular channel with uniform incident velocity. The CFD computer code Flex PDE was used to analyze the flow dynamics.

Keywords— Channel flow, Rectangular obstruction, Two- dimensional flow dynamics, Navier- Stokes equations, Vorticity-Stream function, Flex PDE, Reynolds number.

INTRODUCTION

In the channels, many a times it has been observed that the fluid flow is constricted by obstructions of different shapes and sizes affecting the fluid flow dynamics. The understanding of the complexities of the fluid flows arising out of these constrictions is of importance in computational fluid dynamics. Researchers in this field have introduced different types of mathematical methods and techniques to understand the complexities of the fluid flows under different kinds of obstructions.

Roshko [1] investigated the effects of vortex formations and bluff body similarity using dimensional analysis of a wake model. He gave an empirical relation between the universal Strouhal number and the wake Reynolds number (R_e). Using this relation, drag was calculated from the shedding frequency measurements. In his work, different bluff bodies were correlated in a single relation. Greenspan [2] analyzed the numerical study of steady, viscous, incompressible flow in a channel with a step in two dimensions. He showed the variation of streamlines and equi-vorticity at different Reynolds numbers and concluded that as the Reynolds number is increased, the size of the right vortex also increases. Zdravkovich[3]presented a review of flow interference between the two circular cylinders in various arrangements for different separation distances and Reynolds numbers. In side- by- side arrangement to the approaching flow of two circular cylinders interference in drag coefficient was observed for a separation distance smaller than five cylinder diameters. The flow pattern in side- by- side arrangements showed a bi stable nature. He further observed that for a separation distance greater than two, the process of the vortex formation of both cylinders is exactly the same as that of the single cylinder and when the separation distance becomes smaller, the bulk flow between the two cylinders deflected to one side or the other can equally take place. Valencia[4]performed the experimental investigations on the wake interference of a row of normal flat plates consisting of two, three and four plates arranged side- by- side in a uniform flow with Reynolds numbers of about 10^4 . Braza et al.[5]used a second-order finite volume method and analyzed the dynamical characteristics of the pressure and velocity fields of the unsteady, incompressible and laminar wake behind a circular cylinder. Different vortex and physical aspects of the initiation of vortex shedding as well as the interactions of the velocity and the pressure in the wake, outside the wake and near wake were analyzed in their work.

Gera et al. [6] carried out a numerical simulation for a two-dimensional unsteady laminar flow past a square cylinder for the Reynolds number in the range 50-250 and captured the features of flows past a square cylinder in a domain with the use of CFD code. The variation of Strouhal number with Reynolds number was found from this analysis and it was found that up to Reynolds number 50, the flow is steady and between the Reynolds numbers 50 to 55, instability occurred and vortex shedding

appeared and flow became unsteady. Kumaret al.[7]studied the flow past a rotating circular cylinder experimentally in a water tunnel at Reynolds numbers of 200, 300, and 400 and non-dimensional rotation rates α (ratio of surface speed of the cylinder to the free stream velocity) varying from 0 to 5. They presented global view of the wake structure at the three Reynolds numbers and various rotation rates. It was found that for $0 < \alpha < 1.95$, regular periodic vortex shedding was observed with vortex shedding suppression occurring at $\alpha = 1.95$ for all Reynolds numbers. The Reynolds number was observed to influence the wake morphology more strongly near the vortex shedding suppression rotation rate. Lam and Leung [8] investigated the vortices behind a long flat plate inclined at a small angle of attack to a main flow stream. In this study, velocity fields were obtained at three angles of attack $\alpha = 20^\circ, 25^\circ$ and 30° and at a Reynolds number $Re \approx 5,300$. Vikramet al. [9] analyzed the numerical investigation of two-dimensional unsteady flow past two square cylinders with in-line arrangements in a free stream to investigate the influences on the size of the eddy, velocity, frequency of vortex shedding, pressure coefficient and lift coefficient by varying pitch to perimeter ratio of two square cylinders. It was found that the size of the eddy and the monitored velocity in between the square cylinders increased with the increase in the pitch to perimeter ratio. In this investigation, frequency of vortex shedding was found to be same in between the cylinders and in the downstream of the cylinder and the pressure distribution near to the surface of the cylinder was observed to be quite low due to the viscous effects. In this analysis, the upstream cylinder was found to experience higher lift compared to the downstream cylinder.

Domaet al. [10] described the motion of the steady flow of a viscous incompressible fluid passing a rectangular plate and simulated numerically. In this study, the Reynolds number was varied as 0.5, 1, 10, 20, 100, 200 and 300 and the variation of streamlines was studied alongwith the pressure force, velocity magnitude, vorticity magnitude. Gowda and Tulapurkaraz [11] studied the flow through and around a parallel-walled channel with an obstruction (flat plate) placed at the channel inlet. Depending on the position of the obstruction, the flow inside the channel was observed to be in a direction opposite to that outside, stagnant or in the same direction as outside but with reduced magnitude. The parameters that varied were the gap between the obstruction and the entry to the channel, the length of the channel and the Reynolds number. In this study, the maximum value of the reverse flow velocity was found to be about 20 % of that of the flow outside and the maximum forward velocity inside the channel (when it occurred) was observed to be only about 65% of the outside velocity even for very large gaps between the obstruction and the channel entrance. Bhattacharyya and Maiti [12] gave information about the uniform flow past a long cylinder of square cross-section placed parallel to a plane wall. In this study, the maximum gap between the plane walls to the cylinder was taken to be 0.25 times the cylinder height and found that the critical value of the gap height for which vortex shedding was suppressed depended on the Reynolds number which was based on the height of the cylinder and the incident stream at the surface of the cylinder. Kabir et al. [13] studied the numerical simulation of the reverse flow phenomena in a channel with obstruction geometry of triangular, circular, semi-circular and flat plate at the entry. In this study, the simulations were performed for different gap to width ratios and for different Reynolds numbers. The simulation results predicted the occurrence of reverse flow and existence of other flow features such as vortex shedding.

In this study, the influence of the different ratios of the length of the rectangular solid obstruction to the channel width termed as the blockage ratio on the velocity and pressure fields and the stream patterns was investigated numerically using the Navier-Stokes equations along with the continuity equation as a compressibility constraint and the stream and vorticity mathematical formulations for the two-dimensional, steady, laminar flow of incompressible and viscous fluid in a rectangular channel.

GOVERNING MATHEMATICAL FORMULATION

The flow dynamics for incompressible (divergence-free) Newtonian fluid within the flow domain is described by the Navier-Stokes equations (momentum equations- a set of second-order partial differential equations relating first and second derivatives of

fluid velocity) under isothermal and steady state conditions neglecting gravity force in the Laplace formulation in the vector form along with the continuity equation for the conservation of mass as:

$$(\mathbf{U} \cdot \nabla) \mathbf{U} + (\nabla p)/\rho - \nu \nabla^2 \mathbf{U} = 0 \quad (1)$$

$$\nabla \cdot \mathbf{U} = 0 \quad (2)$$

Where the first term in Eq.(1) is the inertia force due to the time-independent convective acceleration associated with the change in velocity vector $\mathbf{U}(x, y)$ over position causing non-linearity. ∇p is the gradient of pressure force $p(x, y)$, ρ is the density of the fluid i.e. water in this analysis, ν is the kinematic viscosity (ratio of the dynamic viscosity μ and the density ρ) of the fluid under consideration. The divergence of velocity vector $\nabla \cdot \mathbf{U}$ representing the continuity equation acts as the incompressibility constraint for the Navier-Stokes equations ensuring the conservation of mass of the fluid under consideration.

In this study, for the two-dimensional flow under above stated assumptions, the Navier-Stokes equations (Eq.1) and the continuity equation (Eq. 2) in the primitive variable formulation in Cartesian coordinate system are written as:

$$\left(u \frac{\partial u}{\partial x} + v \frac{\partial u}{\partial y}\right) = \frac{1}{\rho} \left[-\frac{\partial p}{\partial x}\right] + \nu \left(\frac{\partial^2 u}{\partial x^2} + \frac{\partial^2 u}{\partial y^2}\right) \quad (3)$$

$$\left(u \frac{\partial v}{\partial x} + v \frac{\partial v}{\partial y}\right) = \frac{1}{\rho} \left[-\frac{\partial p}{\partial y}\right] + \nu \left(\frac{\partial^2 v}{\partial x^2} + \frac{\partial^2 v}{\partial y^2}\right) \quad (4)$$

$$\frac{\partial u}{\partial x} + \frac{\partial v}{\partial y} = 0 \quad (5)$$

Where u and v are the components of the velocity vector \mathbf{U} in the directions x (along the channel) and y (across the channel), respectively. Eq.(1) was converted to non-dimensional form by scaling the terms using characteristic (reference) length (L) and characteristic (reference) velocity (U^*). In this analysis, the characteristic length and the characteristic velocity were taken as the channel width and the mean velocity of the flow, respectively. The dimensionless form of Navier-Stokes equations for the two-dimensional flow in the vector form are written as:

$$(\bar{\mathbf{U}} \cdot \bar{\nabla}) \bar{\mathbf{U}} + \bar{\nabla} \bar{p} - \frac{1}{Re} (\bar{\nabla}^2 \bar{\mathbf{U}}) = 0 \quad (6)$$

Where Re is the Reynolds Number (ratio of inertial to viscous forces) and the dimensionless variables are as under:

$$\bar{x} = \frac{x}{L} \quad ; \quad \bar{y} = \frac{y}{L} \quad ; \quad \bar{\mathbf{U}} = \frac{\mathbf{U}}{U^*} \quad ; \quad \bar{p} = \frac{p}{P}$$

$$\frac{\partial}{\partial \bar{x}} = \bar{\nabla} = L \frac{\partial}{\partial x} \quad ; \quad \frac{\partial}{\partial \bar{y}} = \bar{\nabla} = L \frac{\partial}{\partial y}$$

$$\frac{\partial^2}{\partial \bar{x}^2} = \bar{\nabla}^2 = L^2 \frac{\partial^2}{\partial x^2} \quad ; \quad \frac{\partial^2}{\partial \bar{y}^2} = \bar{\nabla}^2 = L^2 \frac{\partial^2}{\partial y^2}$$

Here, the two dimensionless groups in the non-dimensional Navier-Stokes equations are as:

$$\frac{P}{\rho U^{*2}} \text{ And } \frac{\mu}{\rho U^* L}$$

The inverse of the dimensionless group $\left(\frac{\mu}{\rho U^* L}\right)$ is the Reynolds number. For two-dimensional fluid flow, Eqs. (3 and 4) in the non-dimensional form are written as:

$$\bar{u} \frac{\partial \bar{u}}{\partial \bar{x}} + \bar{v} \frac{\partial \bar{u}}{\partial \bar{y}} = -\frac{\partial \bar{p}}{\partial \bar{x}} + \frac{1}{Re} \left(\frac{\partial^2 \bar{u}}{\partial \bar{x}^2} + \frac{\partial^2 \bar{u}}{\partial \bar{y}^2}\right) \quad (7)$$

$$\bar{u} \frac{\partial \bar{v}}{\partial \bar{x}} + \bar{v} \frac{\partial \bar{v}}{\partial \bar{y}} = -\frac{\partial \bar{p}}{\partial \bar{y}} + \frac{1}{Re} \left(\frac{\partial^2 \bar{v}}{\partial \bar{x}^2} + \frac{\partial^2 \bar{v}}{\partial \bar{y}^2}\right) \quad (8)$$

Where $\bar{u} = \frac{u}{U^*}$; $\bar{v} = \frac{v}{U^*}$

The continuity equation (Eq.5) in the non-dimensional form is written as:

$$\frac{U^*}{L} \left[\frac{\partial \bar{u}}{\partial \bar{x}} + \frac{\partial \bar{v}}{\partial \bar{y}} = 0 \right] \text{ or } \frac{\partial \bar{u}}{\partial \bar{x}} + \frac{\partial \bar{v}}{\partial \bar{y}} = 0 \quad (9)$$

The vorticity-stream function formulation was employed in which the derived variables in terms of the vorticity vector ω (curl of the flow velocity vector) is written as:

$$\omega = \nabla \times U \quad (10)$$

The stream vorticity vector for two-dimensional case is written as:

$$\omega = \frac{\partial v}{\partial x} - \frac{\partial u}{\partial y} \quad (11)$$

For developing the streamlines (lines with constant value of stream function) pattern, the stream function was used. The usefulness of the stream function $\psi(x, y)$ lies in the fact that the velocity components in the x and y direction at a given point are given by the partial derivatives of the stream function at that point and also the two-dimensional continuity equation (Eq.5) implies the existence of a function called the stream function $\psi(x, y)$ such that

$$\frac{\partial \psi}{\partial x} = -v \text{ and } \frac{\partial \psi}{\partial y} = u \quad (12)$$

By combining the above definitions with Eqs.(7 and 8), the non-pressure vorticity transport equation for steady state condition is obtained as:

$$u \frac{\partial \omega}{\partial x} + v \frac{\partial \omega}{\partial y} = \frac{1}{Re} \left(\frac{\partial^2 \omega}{\partial x^2} + \frac{\partial^2 \omega}{\partial y^2} \right) \quad (13)$$

The incompressibility constraint is satisfied by expressing the velocity vector in terms of stream function as given in Eq. (12). By coupling the Eq. (12) and the scalar vorticity ($\omega = \nabla \times U$, k ; k being the unit vector in z direction) of Eq. (11), the two-dimensional mathematical formulation for the stream function $\psi(x, y)$ in the elliptic form (Poisson equation) is obtained as:

$$\frac{\partial^2 \psi}{\partial x^2} + \frac{\partial^2 \psi}{\partial y^2} = -\omega \text{ or } \nabla^2 \psi = -\omega \quad (14)$$

The stream function $\psi(x, y)$ was found from the vorticity function (Eq. 14).

PROBLEM DESCRIPTION

In this study, the two-dimensional steady and laminar flow of an incompressible and viscous fluid under isothermal condition normal to a solid flat rectangular obstruction (plate) of a finite length in a fluid bounded by a rectangular channel walls as shown in Fig. A In the present investigation the problem has been computed by applying boundary conditions as follows.

- (a) Inlet – Uniform flow ($U = 1.0, V = 0$)
- (b) Outlet Boundary – ($P = 0$)
- (c) On the surface – No slip condition ($U=V=0.0$)

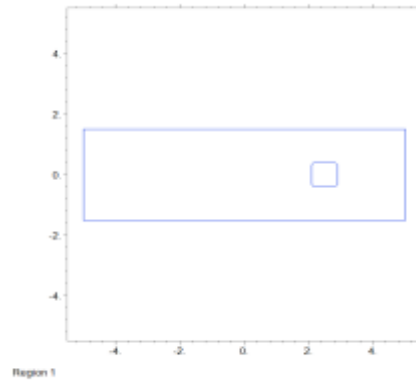


Figure A

NUMERICAL SIMULATION

For simulating the stream line patterns, velocity and pressure distributions in the flow regime under study were simulated using CFD computer code Flex PDE (A flexible solution system for partial differential equations by PDE solutions Inc., www.pdesolutions.com) This code utilizes the finite element numerical solver.

FlexPDE performs the operations necessary to turn a description of a partial differential equations system into a finite element model, solve the system, and present graphical and tabular output of the results. It performs the entire range of functions necessary to solve partial differential equation systems: an editor for preparing scripts, a mesh generator for building finite element meshes, a finite element solver to find solutions, and a graphics system to plot results.

Flex PDE can solve systems of first or second order partial differential equations in one, two or three-dimensional Cartesian geometry, in one-dimensional spherical or cylindrical geometry, or in axi-symmetric two-dimensional geometry. The system may be steady-state or time-dependent. The equations can be linear or nonlinear. (Flex PDE automatically applies a modified Newton-Raphson iteration process in nonlinear systems.) Flex PDE is a fully integrated PDE solver, combining several internal facilities to provide a complete problem solving system.

- **A symbolic equation analyzer** expands defined parameters and equations, performs spatial differentiation, and symbolically applies integration by parts to reduce second order terms to create symbolic Galerkin equations. It then symbolically differentiates these equations to form the Jacobian coupling matrix.
- **A mesh generation facility** constructs a triangular or tetrahedral finite element mesh over a two or three-dimensional problem domain. In two dimensions, an arbitrary domain is filled with an unstructured triangular mesh. In three-dimensional problems, an arbitrary two-dimensional domain is extruded into third dimension and cut by arbitrary dividing surfaces. The resulting three-dimensional figure is filled with an unstructured tetrahedral mesh.
- **A Finite Element numerical method facility** selects an appropriate solution scheme for steady-state, time-dependent or eigen value problems, with separate procedures for linear and nonlinear systems. The finite element basis may be linear, quadratic or cubic.
- **An adaptive mesh refinement procedure** measures the adequacy of the mesh and refines the mesh wherever the error is large. The system iterates the mesh refinement and solution until a user-defined error tolerance is achieved.
- **A dynamic time step control procedure** measures the curvature of the solution in time and adapts the time integration step to maintain accuracy.

RESULTS AND DISCUSSION

In fig 1 velocity in x direction (u) is shown. The pattern of velocity in y direction is shown in figure 2. Figure 3 shows the variation of speed. The flow pattern is shown in figure 4. Figure 5 shows the variation of pressure pattern. The continuity error is shown in figure 6. In figure 7,8 and 9 we have shown with the help of graph how the velocity in x direction is changing.

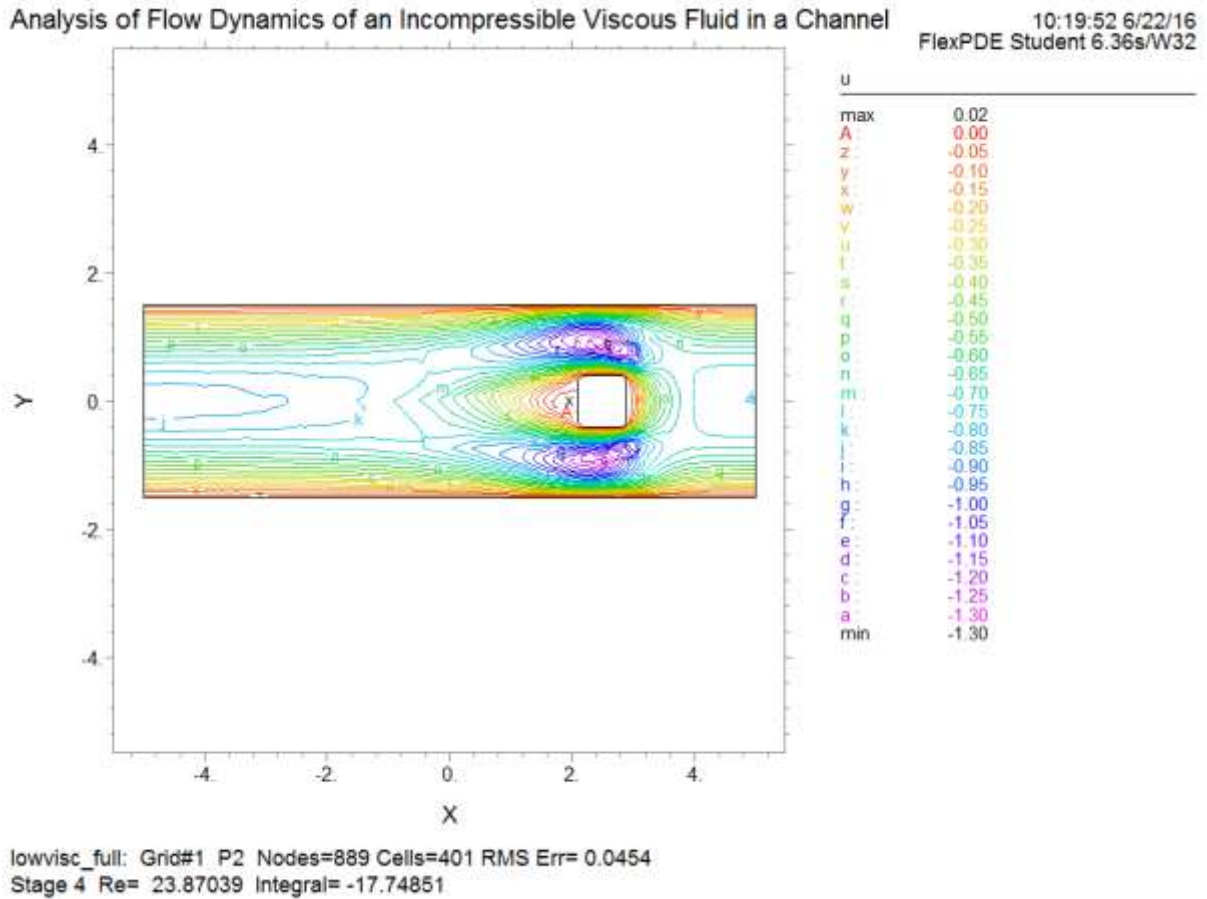


Figure 1

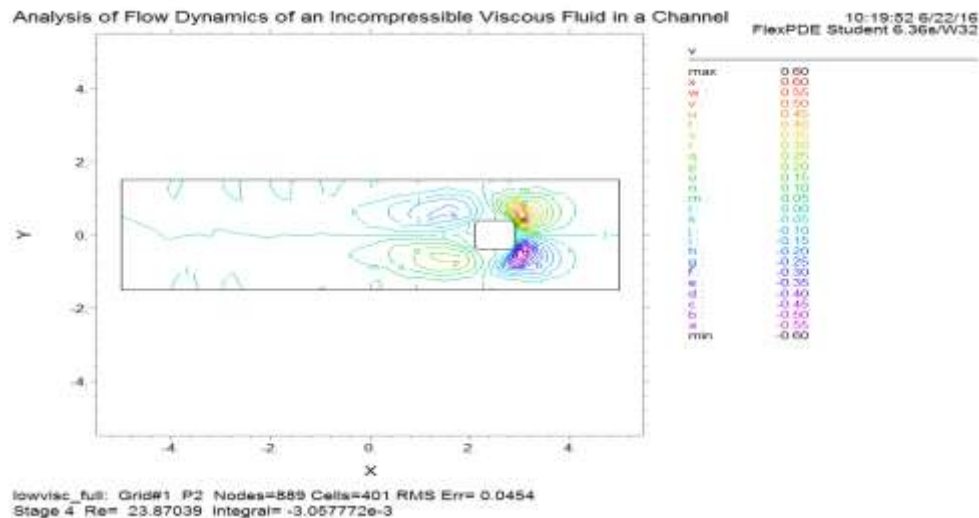


Figure 2

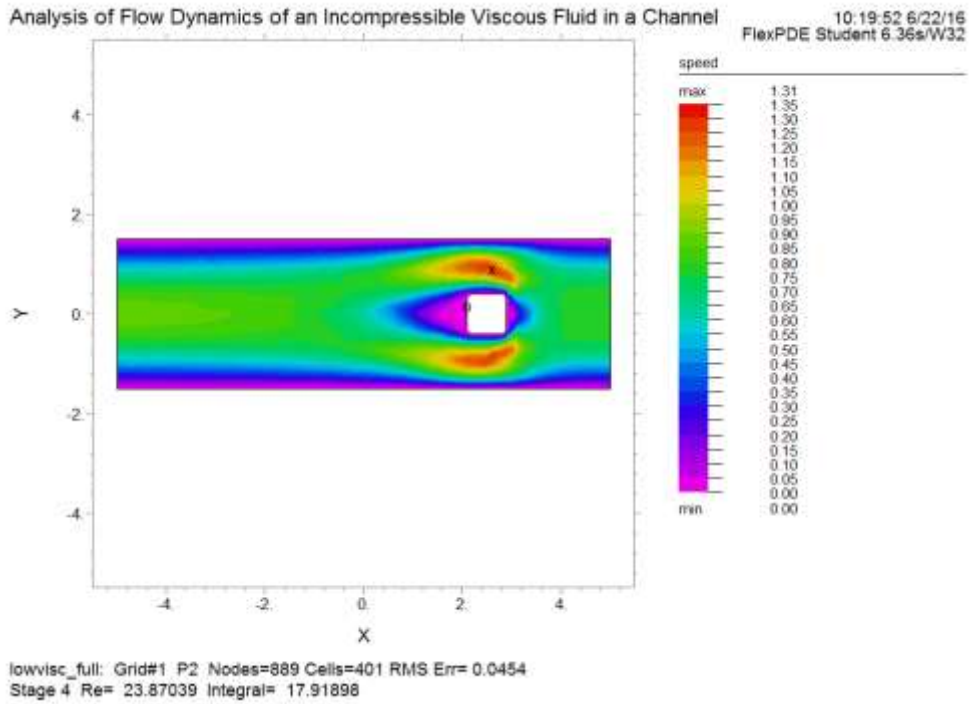


Figure 3

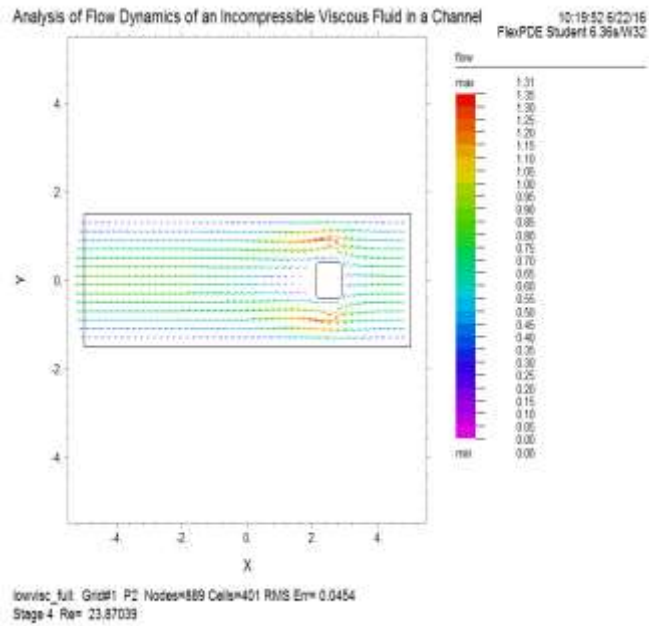


Figure 4

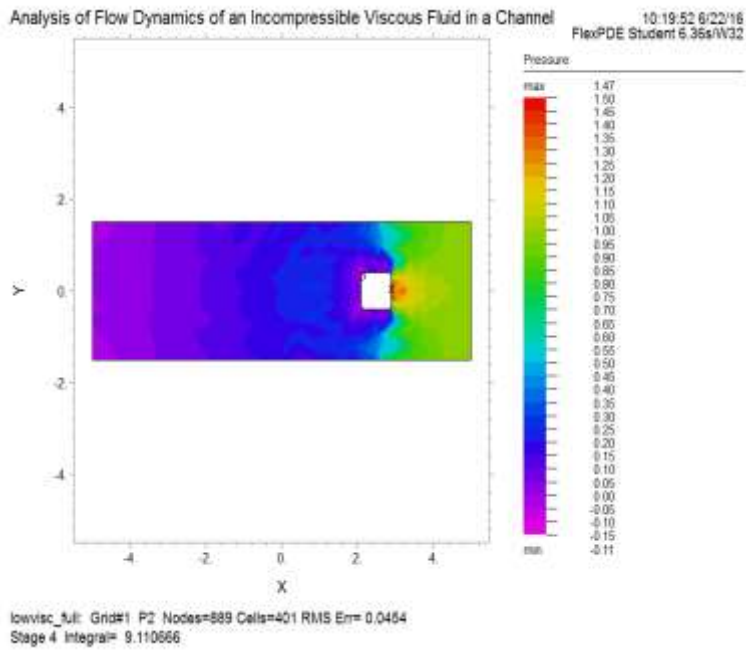


Figure 5

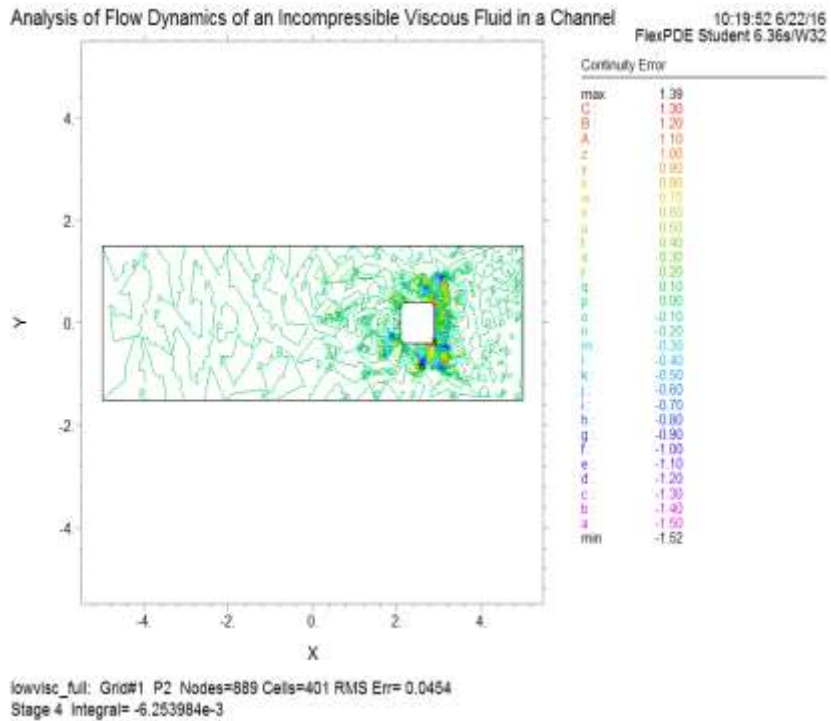


Figure 6

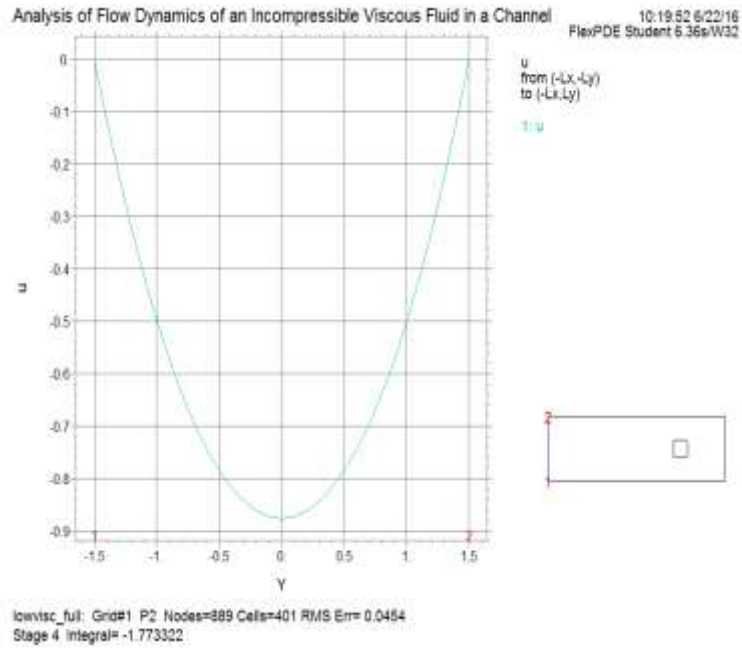


Figure 7

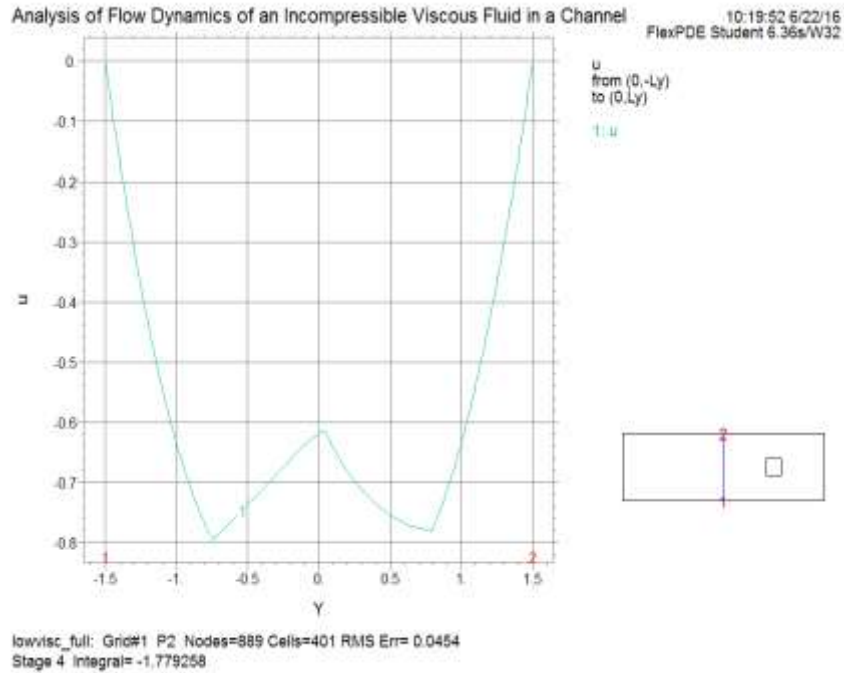


Figure 8

Analysis of Flow Dynamics of an Incompressible Viscous Fluid in a Channel

10:19:52 6/22/16
FlexPDE Student 6.36s/W32

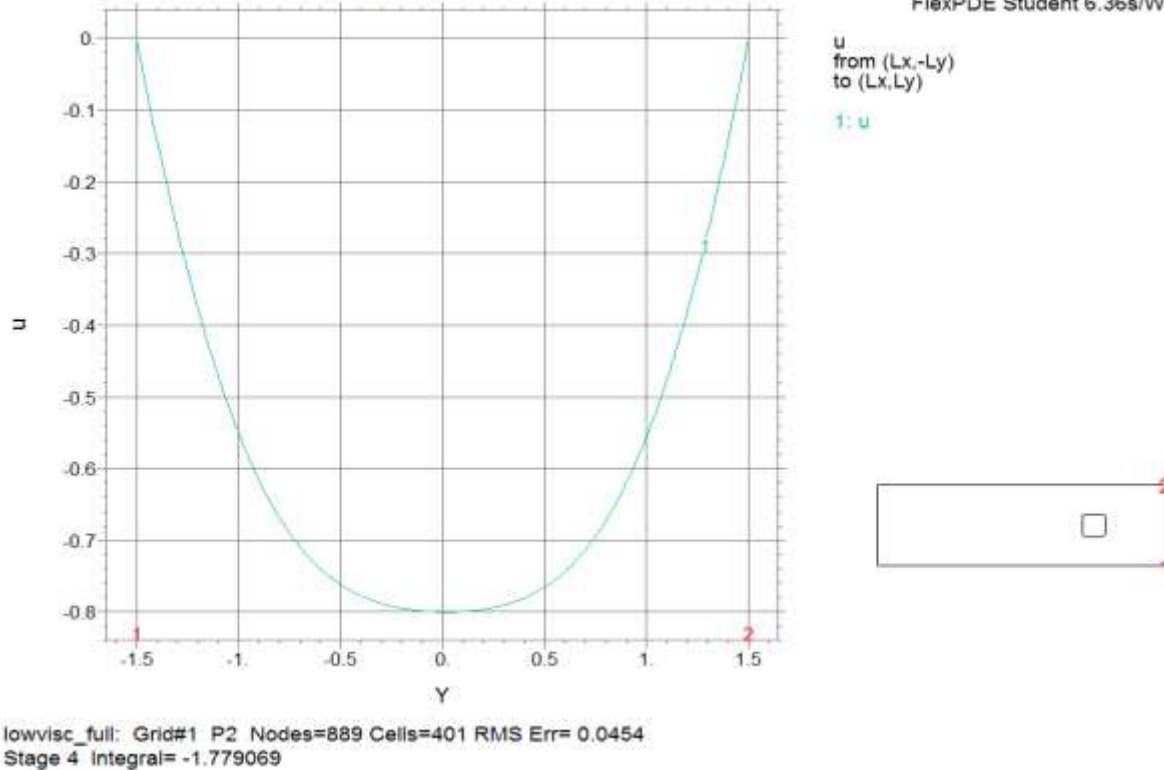


Figure 9

CONCLUSION

The Flex PDE software was used for numerical simulation of fluid dynamics to evaluate the flow characteristics of incompressible viscous fluid i.e. water flowing in rectangular channel as laminar flow and obstructed by a solid rectangular obstruction (flat plate) of variable length using the Navier-Stokes equations alongwith continuity equation as an incompressibility constraint and the vorticity-stream function approach. In this study the variation of velocity in x and y direction is shown. Also the variation of pressure is highlighted. The variation of flow pattern is also shown.

REFERENCES:

- [1] Roshko, A. "On the wake and drag of bluff bodies." *J. Aero. Sci.* 22(2): 124 -132. 1955.
- [2] Greenspan, D. "Numerical studies of steady, viscous, incompressible flow in a channel with a step." *J. Engg. Math.* 3(1): 21-28. 1969.
- [3] Zdravkovich, M.M. "Conceptual overview of laminar and turbulent flows past smooth and rough circular cylinders." *J. Wind Engg. and Industrial Aerodynamics*, 33: 53-62. 1990.
- [4] Valencia, A. "Laminar Flow Past Square Bars Arranged Side By Side In A Plane Channel." *Departamento de Ingeniería Mecánica Universidad de Chile Casilla 2777 Santiago, Chile*
- [5] Braza, M., Chassaing, P. and Haminh, H. "Numerical study and physical analysis of the pressure and velocity fields in the near wake of a circular cylinder." *J. Fluid Mech.* 166: 79-130. 1986.
- [6] Gera, B., Sharma, P.K. and Singh, R.K. "CFD analysis of 2D unsteady flow around a square cylinder", *Intern. J. Appl. Engg. Res.* 1(3): 602-612. 2010.

- [7] Kumar,S.,Cantu,C. and Gonzalez,B. “Flow past a rotating cylinder at Low and high rotation rates.” J. Fluids Engg.133(4): doi.10.1115/1.4003984. 2011.
- [8] Lam,K.M. and Leung, M.Y.H. “Asymmetric vortex shedding flow past an inclined flat plate at high incidence.” Euro. J. Mech. B/Fluids 24: 33–48.2005.
- [9] Vikram, C. K.,Gowda, Y. T. and Ravindra, H.V. “Numerical simulation of two dimensional unsteady flow past two square cylinders.”Intern. J. Tech. & Engg. Sys.2 (3):2011.
- [10] Doma,S.B., El-Sirafy,I.H. and El-Sharif,A.H. “Two-dimensional fluid flow past a rectangular plate with variable initial velocity”.Alexandria J. Math1(2): 36-57.2010.
- [11] Gowda, B.H.L. and Tulapurkaraz, E. G. “Reverse flow in a channel with an obstruction at the entry.” J. Fluid Mech. 204:229-244.1989.
- [12] Bhattacharyya,S.andMaiti,D. K. “Vortex shedding suppression for laminar flow past a square cylinder near a plane wall: a two-dimensional analysis.” ActaMechanica, 184: 15–31.2006.
- [13] Kabir, M.A., Khan, M.M.K. and Rasul, M.G. “Numerical modeling of reverse flow phenomena in a channel with obstruction geometry at the entry.” WSEAS Trans.Fluid Mech. 3(3): 250 – 260.2008.
- [14] Kumar Deepak,Malk R.K.” Modelling of Flow Dynamics of an Incompressible Viscous Fluid in a Channelwith Solid Obstruction of Variable Length”IJERGS.3(1):117-127.2015.

ANALYSIS OF P-DELTA EFFECT ON HIGH RISE BUILDINGS

Pushparaj J. Dhawale [1]

Prof. G. N. Narule [2]

ME Structural Engineer

VPKBIET

Baramati, India

pushparajdhawale@gmail.com

contact no:- +91 7709899696

Abstract— P-delta effect is secondary or second order effect on structure. It is also known as ‘Geometric Nonlinearity effect’. As number of storey increases, P-delta effect becomes more important. If the change in bending moments, shear forces and displacements is more than 10%, P-delta effect should be considered in design. In this study the P-delta effect on high rise building is studied. Linear static analysis (without P-delta effect) and nonlinear static analysis (with P-delta effect) on high rise buildings having different number of storey is carried out. For the analysis G+19, G+24, G+29 (i.e. 20, 25, 30 storey) R.C.C. framed buildings are modeled. Earthquake load is applied on model of structure as per IS-1893(2002) for zone III in SAP2000-12 software. Load combinations for analysis are set as per IS-456(2000). All analysis is carried out in software SAP 2000-12. Bending moment, story displacement with and without P-delta effect is calculated and compared for all models. The results show that it is essential to consider the P-delta effect for 25 storey building. So buildings having height more than or equal to 75m, should be designed considering P-delta effect. Also we can say that up to 25 storey building, it is not necessary to consider P-delta effect in design and first order analysis is sufficient for design.

Keywords: P-delta effect, high-rise building, Static nonlinear analysis, displacements, bending moments, SAP2000-12, second order effect

INTRODUCTION

Engineers today typically use linear elastic static (first order) analysis to determine design forces and moments resulting from loads acting on a structure. First order analysis assumes small deflection behavior; the resulting forces and moments take no account of the additional effect due to the deformation of the structure under load. Second order analysis combines two effects to reach a solution:-

- Large displacement theory; the resulting forces and moments take full account of the effects due to the deformed shape of both the structure and its members.
- “Stress stiffening”; the effect of element axial loads on structure stiffness, tensile loads stiffening an element and compressive loads softening an element.

As the structure becomes more slender and less resistant to deformation, it is necessary to consider 2nd order and to be more specific, P-delta effects arises. As a result, Codes of Practice are referring engineers more and more to the use of 2nd order analysis in order that P-delta and “stress stiffening” effects are accounted for when appropriate in design. This is as true in concrete and timber design as it is in the design of steelwork.

P-DELTA EFFECTS:-

P-Delta is a non-linear effect that occurs in every structure where elements are subject to axial load. P-Delta is actually only one of many second-order effects. There are two P-Delta effects:-

- P-“BIG” delta (P- Δ) - a structure effect
- P-“little” delta (P- δ) - a member effect



Fig.1 P-delta effects

The P-Delta Effect Example:

The P-Delta effect refers specifically to the nonlinear geometric effect of a large tensile or compressive direct stress upon transverse bending and shear behavior. A compressive stress tends to make a structural member more flexible in transverse bending and shear, whereas a tensile stress tends to stiffen the member against transverse deformation.

The basic concepts behind the P-Delta effect are illustrated in the following example.

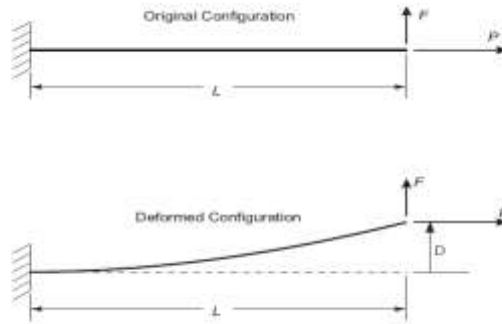


Fig.2 P-delta effect on cantilever beam

If equilibrium is examined in the original configuration (using the undeformed geometry), the moment at the base is $M = FL$. If, instead, equilibrium is considered in the deformed configuration, there is an additional moment caused by the axial force P acting on the transverse tip displacement Δ . The moment no longer varies linearly along the length; the variation depends instead upon the deflected shape. The moment at the base is now $M = FL - P\Delta$. The moment diagrams for various cases are shown in Figure.

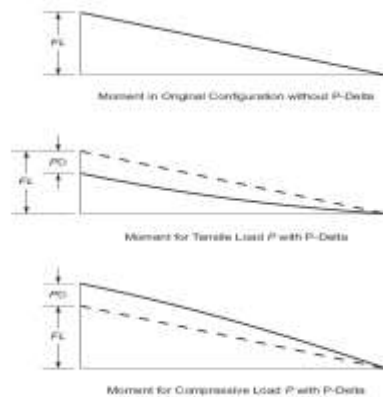


Fig.3 Change in B.M. of cantilever beam due to P-delta effect

The key feature is that a large axial force, acting upon a small transverse deflection, produces a significant moment that affects the behavior of the member or structure.

Consideration of P-delta effect:

As per 'National Building Code, Technical Standard of Building E.030 Earthquake-Resistant Design', clause 4.1.5, page 19: The second order effects (P-delta effect) must be considered when an increase of more than 10% occurs in internal force

AIM AND OBJECTIVE OF STUDY

Scope of this study includes analysis of 20, 25 and 30 storey R.C.C. building with and without considering P-delta effects. Analysis can be done using SAP 2000. Lateral load is Earthquake load for zone III. If the change in the values of deflections, forces, and bending moments considering P-delta effect is not more than 10%, they can be neglected. From this analysis we can decide whether it is necessary to include P-delta effect for the buildings up to 30 stories.

Analysis of High rise buildings in SAP 2000:-

Buildings having same plan but with different number of stories are analyzed in SAP2000 with and without considering P-delta effect and their results are compared.

- 1) 20 storey
- 2) 25 storey
- 3) 30 storey

Plan of building:-

- 1) Residential building, RCC framed structure.
- 2) Storey height is 3m.
- 3) Length of building in X-direction = 18.8m
- 4) Length of building in Y-direction = 30.35m

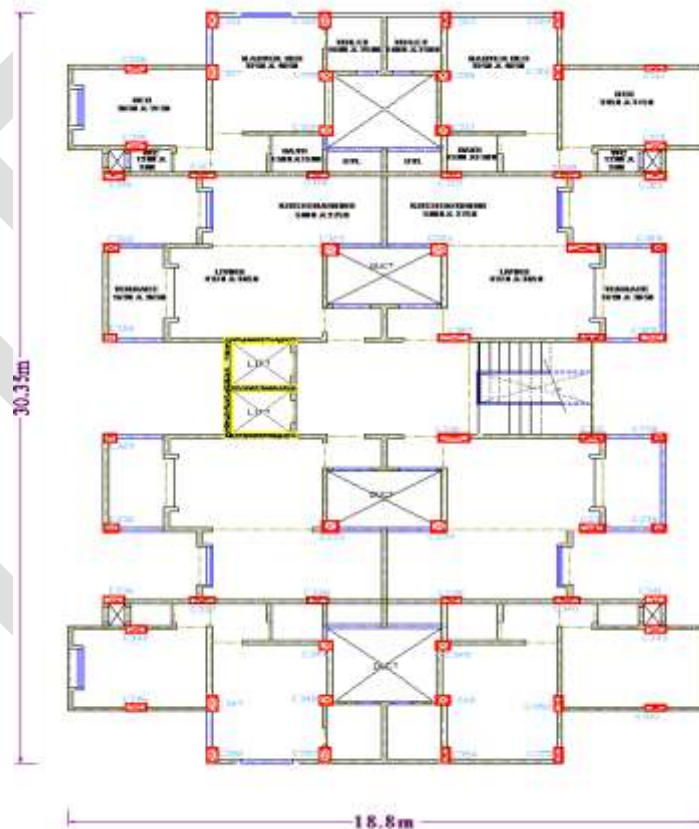


Fig.4:-Typical floor plan of building

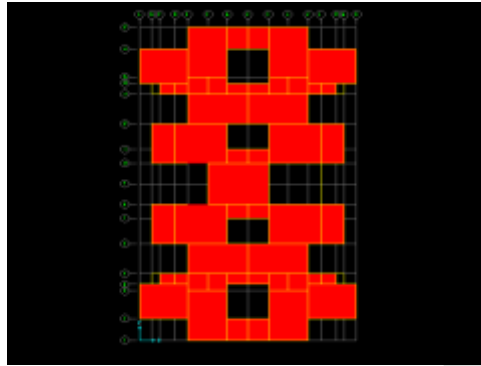


Fig.5 SAP Model (Plan View)

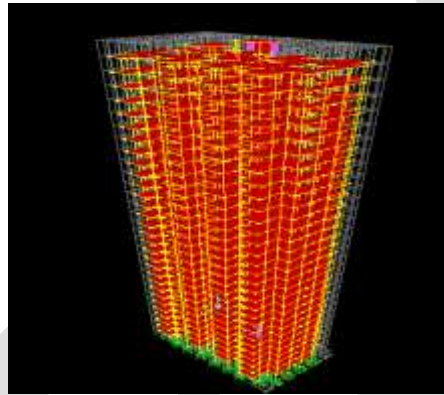


Fig.6:- SAP Model (3D View)

Material properties:-

- 1) **Concrete:** M30
Density: 25 KN/m³
Modulus of Elasticity: 27386 N/mm²
Poissons ratio: 0.2
- 2) **Steel:** Fe500
Density: 7850 Kg/m³
Modulus of Elasticity: 2.1 X 10⁵ N/mm²
Poisson's ratio: 0.3
- 3) **Masonry:** Brick
Density= 20 KN/m³

Section Properties:-

- 1) **Beam:** 230X450, 230X600, 230X750
- 2) **Column:**
230X825, 300X825, 375X900.
- 3) **Slab:** various sections with thickness varying from 150.
- 4) **Shear wall:** with thickness of 200mm.

Loads:-

- 1) **Dead load:**
 - a) Self weight
 - b) Floor finish: 1.25 KN/m²

c) Wall load:

Load = Height x thickness x density of masonry

For 3m height of wall:

For 150mm thick wall, Load = 10 KN/m²

For 1.2m height of wall (Parapet wall):

Load = 5 KN/m²

2) Live load:

i) Floor = 2 KN/m²

ii) Roof = 1.5 KN/m²

3) Earthquake loads: As per IS1893:2002 for Zone III

EQX: Earthquake load in X-direction

EQY: Earthquake load in Y-direction

Zone factor = 0.16

Soil = Type II

Importance factor = 1

Response reduction factor = 3

LOAD CASES:-

As per IS-456(2000) in which both gravity and lateral loads are included.

- 1) 1.2 (DL + LL + EQX)
- 2) 1.2 (DL + LL - EQX)
- 3) 1.2 (DL + LL + EQY)
- 4) 1.2 (DL + LL - EQY)
- 5) 1.5(DL + EQX)
- 6) 1.5(DL - EQX)
- 7) 1.5(DL + EQY)
- 8) 1.5(DL - EQY)
- 9) 0.9DL + 1.5EQX
- 10) 0.9DL - 1.5EQX
- 11) 0.9DL + 1.5EQY
- 12) 0.9DL - 1.5EQY

ANALYSIS RESULTS

1) For 20 storey building:-

Sr. No.	Load Case	B.M. at base (KNm)		
		Without P-delta	With P-delta	% Difference
1)	1.2 (DL + LL + EQX)	-201.82	-206.4	2.27
2)	1.2 (DL + LL - EQX)	159.7	162.46	1.73
3)	1.2 (DL + LL + EQY)	67.75	71.7	5.83
4)	1.2 (DL + LL - EQY)	-65.26	-69.36	6.28
5)	1.5(DL + EQX)	-249.8	-256.15	2.54
6)	1.5(DL - EQX)	202.1	206.2	2.03
7)	1.5(DL + EQY)	84.7	90.3	6.61
8)	1.5(DL - EQY)	-81.5	-87.4	7.24
9)	0.9DL + 1.5EQX	-240.6	-243.87	1.36
10)	0.9DL - 1.5EQX	211.63	214.24	1.23
11)	0.9DL + 1.5EQY	84.07	87.26	3.79
12)	0.9DL - 1.5EQY	-82.2	-85.7	4.26

Table 1: B.M. at joint at base with and without

P-delta effect (20 storey building)

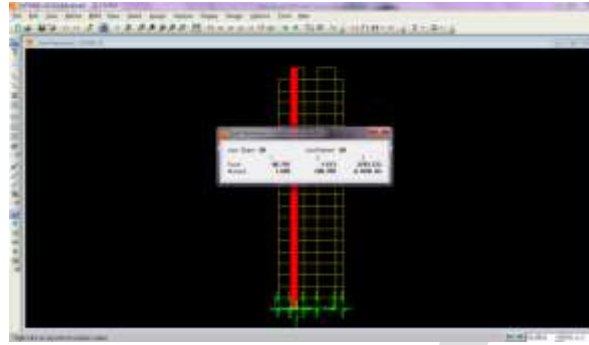


Fig. 8: B.M. at joint 60 due to load case 1 (with P-delta)

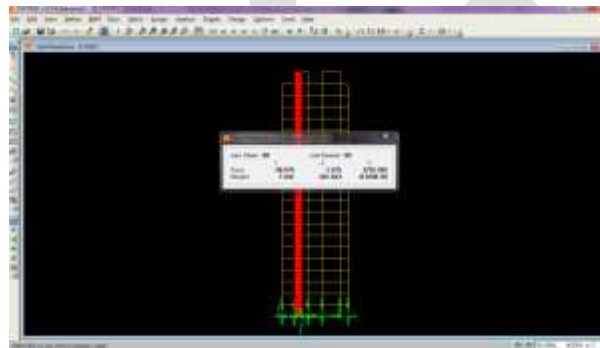


Fig 7.: B.M. at joint 60 due to load case 1 (without P-delta)

Sr. No.	Load Case	Deflection at top(mm)		
		Without P-delta	With P-delta	% Difference
1)	1.2 (DL + LL + EQX)	73.4	76.6	4.36
2)	1.2 (DL + LL - EQX)	-62.9	-64	1.75
3)	1.2 (DL + LL + EQY)	105.3	115.6	9.78
4)	1.2 (DL + LL - EQY)	-103.24	-113.43	9.87
5)	1.5(DL + EQX)	91.5	95.8	4.70
6)	1.5(DL - EQX)	-78.9	-80.6	2.15
7)	1.5(DL + EQY)	131.5	146.3	11.25
8)	1.5(DL - EQY)	-129.17	-143.85	11.36
9)	0.9DL + 1.5EQX	89	91.5	2.81
10)	0.9DL - 1.5EQX	-81.4	-82.5	1.35
11)	0.9DL + 1.5EQY	131.05	139.55	6.49
12)	0.9DL - 1.5EQY	-129.6	-138.06	6.53

Table 2: Deflection at joint at top storey with and without P-delta effect (20 storey building)

Storey no.	Member no.	B.M. (KNm)	Load case No.					
			1	2	3	4	5	6
5	1053	Initial	78.0	-107.9	39.3	-61.2	98.2	-134.2
		With P-delta	82.4	-110.8	46.4	-68.2	104.4	-139.0
		%	5.6	2.6	18.1	11.5	6.2	3.6
10	2323	Initial	66.6	-104.2	25.5	59.8	84.5	-129.1
		With P-delta	70.7	-106.5	30.3	64.8	90.1	-132.4
		%	6.0	2.1	18.9	8.4	6.6	2.6
15	798	Initial	-37.4	83.0	20.4	47.7	-48.1	102.3
		With P-delta	-39.9	83.9	18.9	49.0	-51.6	103.3
		%	6.7	1.2	-7.5	2.8	7.1	1.0
20	3091	Initial	-6.8	32.3	-16.1	-14.1	-7.5	39.2
		With P-delta	-6.3	31.9	-16.8	-13.1	-6.9	38.7
		%	-6.9	-1.3	4.7	-6.9	-7.7	-1.2

Storey no.	Member no.	B.M. (KNm)	Load case No.					
			7	8	9	10	11	12
5	1053	Initial	50.1	-75.6	105.4	-126.9	55.2	-70.5
		With P-delta	60.4	-85.7	109.0	-129.5	61.1	-76.1
		%	20.7	13.5	3.4	2.1	10.7	8.1
10	2323	Initial	33.4	73.1	93.4	-120.2	41.1	65.0
		With P-delta	40.4	80.3	96.7	-122.2	45.3	69.1
		%	20.8	9.8	3.5	1.7	10.2	6.3
15	798	Initial	24.1	57.5	-59.0	91.5	13.2	47.8
		With P-delta	22.1	59.4	-61.0	92.1	12.1	49.0
		%	-8.3	3.3	-3.4	0.7	-8.4	2.4
20	3091	Initial	-18.6	-16.1	-3.4	30.2	-11.6	-9.2
		With P-delta	-19.7	-14.8	-3.9	30.0	-12.3	-8.4
		%	6.1	-8.4	12.6	-0.9	5.5	-8.5

Table 3: B.M. in members with and without P-delta effect (20 storey building) continued

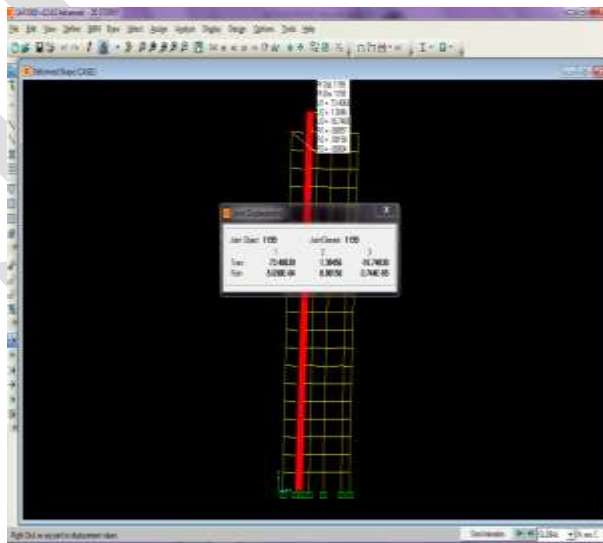


Fig.9: Deflection at joint 1199 due to load case1 (Without P-delta)

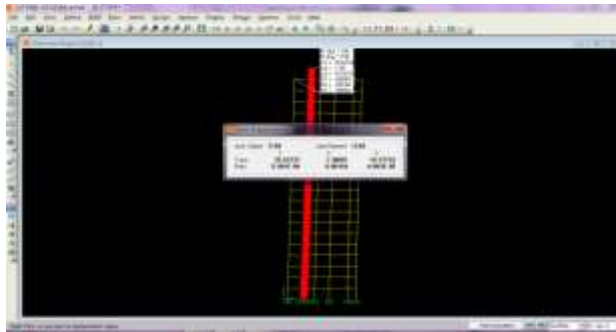


Fig. 10: Deflection at joint 1199 due to load case 1 (with P-delta)

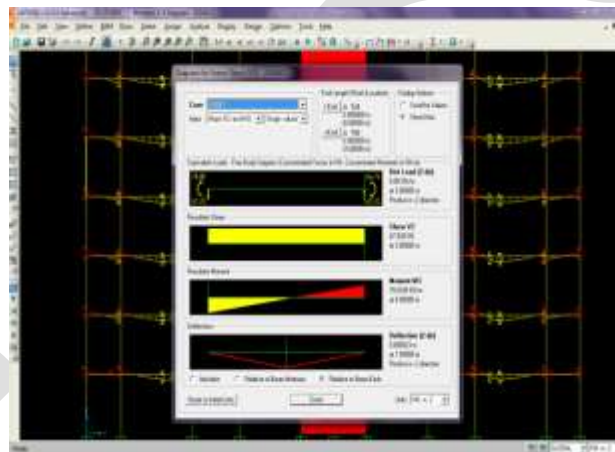


Fig. 11: B.M. of member 1053 due to load case 1 (without P-delta)

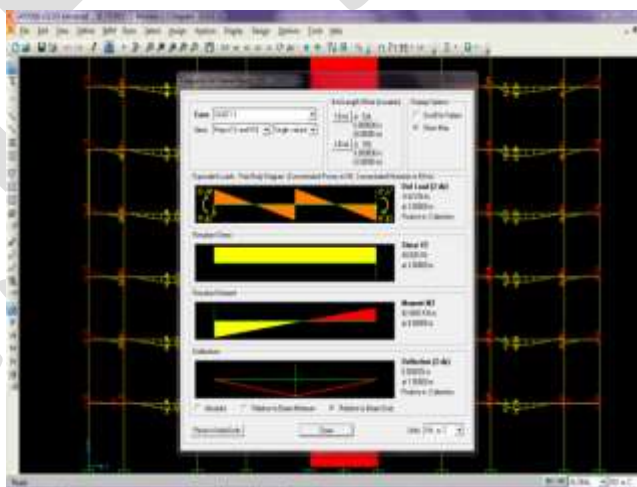


Fig. 12:- B.M. of member 1053 due to load case 1 (with P-delta)

2) For 25 storey building:-

Sr. No.	Load Case	B.M. at bottom (KNm)		
		Without P-delta	With P-delta	% Difference
1)	1.2 (DL + LL + EQX)	-234.4	-240.7	2.69
2)	1.2 (DL + LL - EQX)	183.9	187.52	1.97
3)	1.2 (DL + LL + EQY)	83.79	87.9	4.91
4)	1.2 (DL + LL - EQY)	-80.5	-84.7	5.22
5)	1.5(DL + EQX)	-290.16	-298.9	3.01
6)	1.5(DL - EQX)	232.8	238.17	2.31
7)	1.5(DL + EQY)	104.72	110.58	5.60
8)	1.5(DL - EQY)	-100.64	-106.68	6.00
9)	0.9DL + 1.5EQX	-278.68	-283.64	1.78
10)	0.9DL - 1.5EQX	244.26	247.7	1.41
11)	0.9DL + 1.5EQY	103.9	107.25	3.22
12)	0.9DL - 1.5EQY	-101.45	-105.04	3.54

Table 4: B.M. at base with and without P-delta effect
(25 storey building)

Sr. No.	Load Case	Deflection at top(mm)		
		Without P-delta	With P-delta	% Difference
1)	1.2 (DL + LL + EQX)	93.19	98.8	6.02
2)	1.2 (DL + LL - EQX)	-73.35	-75.05	2.32
3)	1.2 (DL + LL + EQY)	124.65	139.42	11.85
4)	1.2 (DL + LL - EQY)	-122.18	-136.77	11.94
5)	1.5(DL + EQX)	130	138.51	6.55
6)	1.5(DL - EQX)	-106.22	-109.65	3.23
7)	1.5(DL + EQY)	173.18	196.87	13.68
8)	1.5(DL - EQY)	-170.38	-193.86	13.78
9)	0.9DL + 1.5EQX	125.3	130.19	3.90
10)	0.9DL - 1.5EQX	-111	-113.12	1.91
11)	0.9DL + 1.5EQY	172.62	186.07	7.79
12)	0.9DL - 1.5EQY	-170.94	-184.26	7.79

Table 5: Deflection at joint at top storey with and without P-delta effect (25 storey building)

Storey no. Member no.	B.M. (KNm)	Load Case No.					
		1	2	3	4	5	6
5	Initial	82.79	-110.3	38.67	-71.76	101.18	-137.1
1053	With P-delta	88.65	-114.3	43.04	-78.4	112.43	-143
	%	7.08	3.63	10.47	9.25	11.12	4.24
10	Initial	69.51	-111.4	29.56	67.54	88.24	-137.9
2323	With P-delta	75.31	-115.1	39.01	76.16	96.39	-143.3
	%	8.34	3.26	31.97	12.76	9.24	3.87
13	Initial	53.18	-95.24	16.27	-59.92	68.24	-117.9
798	With P-delta	58.09	-97.85	21.14	-64.96	74.81	-121.4
	%	8.82	2.74	29.93	8.41	9.63	2.93
20	Initial	29.65	56.88	12.77	-42.06	-37.97	70.19
3091	With P-delta	32.38	57.27	11.18	-41.2	-41.7	70.91
	%	9.21	0.69	-12.45	2.71	9.82	1.83
23	Initial	-7.61	29.84	-19.72	-16.79	-8.42	36.06
4546	With P-delta	-6.97	29.32	-20.6	-15.58	-7.6	35.42
	%	-8.41	-1.74	4.46	-4.93	-9.74	-1.77

Storey no. Member no.	B.M. (KNm)	Load Case No.					
		7	8	9	10	11	12
5	Initial	49.7	-68.28	110.77	-130.6	57.46	-80.58
1053	With P-delta	58.98	-97.82	115.57	-134	62.76	-88.97
	%	18.67	10.81	4.33	2.67	9.22	10.41
10	Initial	38.8	82.46	98.18	-128	47.42	73.19
2323	With P-delta	52.51	95.03	102.91	-131.2	55.08	80.4
	%	35.34	15.24	4.82	2.52	16.15	9.55
15	Initial	22.43	-72.82	78.18	-107.6	32.5	-62.74
798	With P-delta	29.45	-80.06	81.97	-110.1	36.5	-66.84
	%	31.30	9.94	4.85	2.34	12.31	6.53
20	Initial	15.5	-50.43	-44.42	63.75	10.45	-40.44
3091	With P-delta	12.94	-52.03	-46.55	64.24	11.17	-41.39
	%	-16.52	3.17	4.50	0.77	6.89	2.35
25	Initial	-22.86	-19.15	-1.81	27.49	-14.46	-10.74
4546	With P-delta	-24.18	-17.5	-2.4	27.13	-15.18	-9.77
	%	5.77	-8.62	32.60	-1.31	4.98	-9.03

Table 6: B.M. in members with and without P-delta effect (25 storey building)

3) For 30 storey building:-

Sr. No.	Load Case	B.M. at base (KNm)		
		Without P-delta	With P-delta	% Difference
1)	1.2 (DL + LL + EQX)	-255.84	-264.13	3.24
2)	1.2 (DL + LL - EQX)	204.75	209.59	2.36
3)	1.2 (DL + LL + EQY)	105.19	110.29	4.85
4)	1.2 (DL + LL - EQY)	-101.63	-106.83	5.12
5)	1.5(DL + EQX)	-316.97	-328.49	3.63
6)	1.5(DL - EQX)	258.77	266.05	2.81
7)	1.5(DL + EQY)	131.49	138.78	5.54
8)	1.5(DL - EQY)	-127.04	-134.55	5.91
9)	0.9DL + 1.5EQX	-305.33	-311.86	2.14
10)	0.9DL - 1.5EQX	270.4	275	1.70
11)	0.9DL + 1.5EQY	130.6	134.75	3.18
12)	0.9DL - 1.5EQY	-127.9	-132.37	3.49

Table 7: B.M. at base with and without P-delta effect (30 storey building)

Sr. No.	Load Case	Deflection at top(mm)		
		Without P-delta	With P-delta	% Difference
1)	1.2 (DL + LL + EQX)	131.65	141.01	7.11
2)	1.2 (DL + LL - EQX)	-108.32	-111.87	3.28
3)	1.2 (DL + LL + EQY)	170.72	192.64	12.84
4)	1.2 (DL + LL - EQY)	-167.78	-189.46	12.92
5)	1.5(DL + EQX)	164.2	177.16	7.89
6)	1.5(DL - EQX)	-135.76	-141.28	4.07
7)	1.5(DL + EQY)	213.23	245.06	14.93
8)	1.5(DL - EQY)	-209.9	-241.44	15.03
9)	0.9DL + 1.5EQX	158.51	166	4.73
10)	0.9DL - 1.5EQX	-141.45	-144.85	2.40
11)	0.9DL + 1.5EQY	212.5	230.4	8.42
12)	0.9DL - 1.5EQY	-210.57	-228.29	8.42

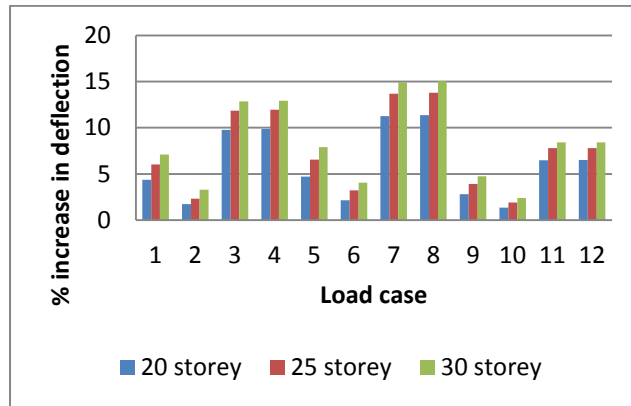
Table 8: Deflection at joint at top storey with and without P-delta effect (30 storey building)

Storey no. Member no.	B.M. (KNm)	Load case No.					
		1	2	3	4	5	6
5	Initial	88.02	-116.6	59.23	-77.13	110.75	-145
5548	With P-delta	95.27	-121.6	44.94	-83.31	121	-152.3
	%	8.24	4.30	14.56	8.01	9.26	5.03
10	Initial	78.87	-119.7	25.43	-77.32	100.03	-148.2
1053	With P-delta	86.28	-124.8	32.5	-84.09	110.5	-155.6
	%	9.40	4.20	27.80	8.76	10.47	4.96
15	Initial	64.74	-112.3	25.66	-74.43	82.65	-138.6
2323	With P-delta	71.55	-116.3	35.42	-84.18	92.24	-144.7
	%	10.92	3.56	38.04	13.10	11.60	4.34
20	Initial	47.74	92.06	12.23	62.92	61.38	113.31
798	With P-delta	53.08	94.61	17.3	68.24	68.82	117.14
	%	11.19	2.77	41.46	8.46	12.12	3.38
25	Initial	-25.72	52.68	3.52	-43.3	-33.1	64.89
3091	With P-delta	-28.83	52.83	4.43	-44.48	-37.35	65.36
	%	12.17	0.32	-19.38	2.73	12.84	0.72
30	Initial	-8.65	28.28	-21.44	-18	-9.69	34.09
4546	With P-delta	-7.85	27.56	-22.35	-16.66	-8.67	33.21
	%	-9.25	-2.55	-4.24	-7.44	-10.53	-2.58

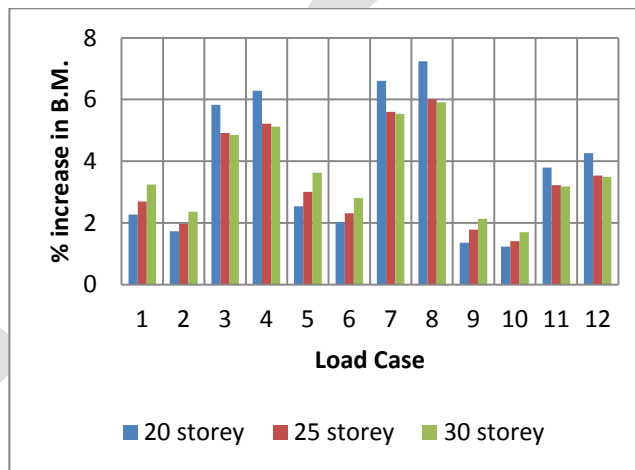
Storey no. Member no.	B.M. (KNm)	Load case No.					
		7	8	9	10	11	12
5	Initial	50.6	-84.8	117.6	-138.1	59.45	-86
5548	With P-delta	58.9	-103.7	123.54	-142.6	64.24	-91.05
	%	16.40	9.39	5.05	3.19	8.00	5.87
10	Initial	34.17	-84.37	109.67	-138.6	46.19	-82.25
1053	With P-delta	44.49	-105.2	115.75	-143	52.04	-88.18
	%	30.20	31.64	5.54	3.18	12.67	7.45
15	Initial	34.4	90.61	93.85	-127.4	45.43	89.1
2323	With P-delta	48.74	104.92	99.19	-131.1	53.16	86.96
	%	41.69	15.79	5.90	3.86	17.40	-2.40
20	Initial	17.74	76.14	71.72	-102.7	29.26	84.35
798	With P-delta	25.11	83.84	76.01	-104.9	33.4	68.89
	%	41.54	10.11	5.98	2.14	14.15	6.74
25	Initial	4.09	-51.7	-39.46	58.33	7.34	-40.66
3091	With P-delta	3.01	-51.34	-41.89	58.89	8.23	-41.64
	%	-26.41	3.17	6.16	0.62	0.42	2.41
30	Initial	-24.84	-20.53	-1.66	25.6	-15.76	-13.46
4546	With P-delta	-26.23	-18.64	-1.07	23.1	-18.5	-10.15
	%	5.56	9.21	-35.54	-1.95	4.70	-9.69

Table 9: B.M. in members with and without P-delta effect (30 storey building) continued

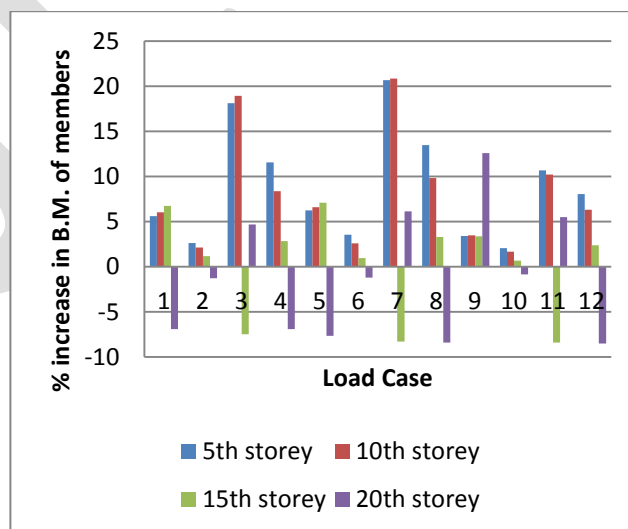
DISCUSSION OF RESULTS



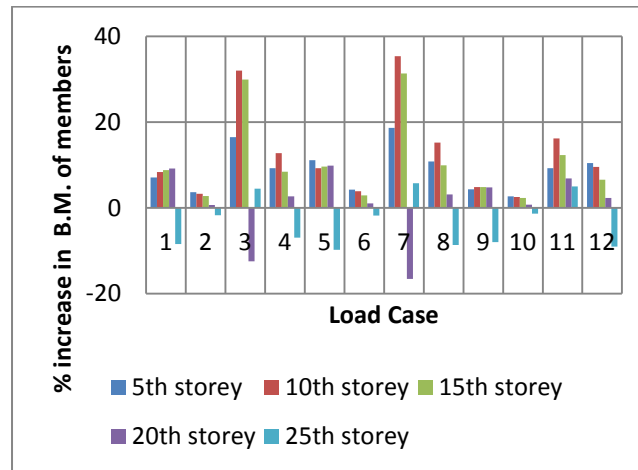
Graph 1: % increase in deflection due to P-delta effect for all load cases



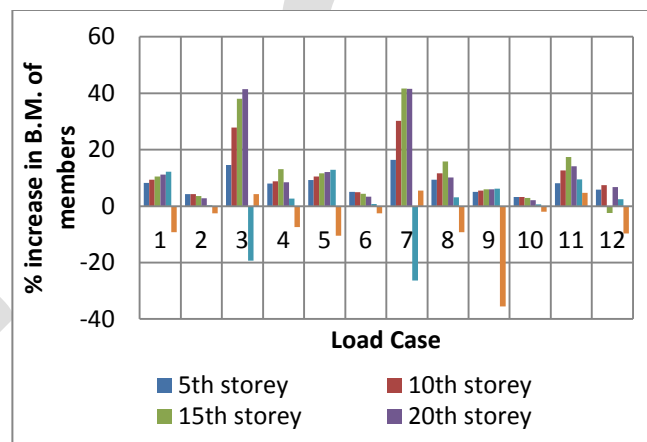
Graph 2: % increase in B.M. at base due to P-delta effect for all load cases



Graph 3: % increase in B.M. of members due to P-delta effect at different storey levels for all load cases (For 20 storey building)



*Graph 4: % increase in B.M. of members due to P-delta effect at different storey levels for all load cases
(For 25 storey building)*



*Graph 5: % increase in B.M. of members due to P-delta effect at different storey levels for all load cases
(For 30 storey building)*

Discussion:

1) For 20 storey building:-

1. Change in B.M. at base is 2-6%.
2. Change in the deflection is 1-11%.
3. Change in the B.M. of beams is less than 10%.
4. Change in the B.M. of columns is up to 20% for some members in some load cases. But it is found that their initial values are very small (i.e. not more than 30KNm). So we can say that practically it is not necessary to consider P-delta effect.
5. Hence for 20 storey building, it is not necessary to consider P-delta effect. So building can be designed by performing 1st order analysis.

2) For 25 storey building:-

1. Change in B.M. at base is 2-4% .
2. Change in the deflection is 2-14%.
3. Change in the B.M. of beams which are parallel to y-direction is up to 15%.
4. Change in B.M. of columns is 8-30%. It is more observed at the exterior columns and their nearby beams. Also it is more observed at intermediate stories.
5. So P-delta effect is observed in some load cases for 25 storey building.
6. So it is necessary to consider P-delta effect while designing a 25 storey building.

3) For 30 storey building:-

1. Change in B.M. at base is 2-4%.

2. Change in the deflection is 3-15%.
3. Change in the B.M. of some beams is up to 15%.
4. Change in B.M. of some columns is 10-35%. It is more observed at the exterior columns and their nearby beams. Also it is more observed at intermediate stories.
5. So it is necessary to consider P-delta effect for designing a 30 storey building.

ACKNOWLEDGMENT

I deem it my proud privilege to express my heartfelt gratitude to Prof. **G. N. Narule**, Professor of the Structural Engineering Department, Vidya Pratishthan's Kamalnayan Bajaj College of Engineering and Technology Baramati, pune. I take this opportunity to express my profound gratitude to them for their invaluable guidance, continuous encouragement, suggestions, and discussions at various stages of work. These words are formal thanks, which cannot express the real depth of feeling and affection that I have towards them.

CONCLUSION

In this study, the three building models with different number of stories are analyzed with and without considering P-delta effect for seismic loads. By studying the results of analysis, following conclusions are drawn.

- As number of storey increases P-delta effect becomes more important.
- P-delta effect is only observed in some of the beams and columns (Exterior columns and their adjacent beams) in some load cases. If these load cases are governing load cases for design of member, then only we can say that it is considerable. This condition is observed in 25 and 30 storey buildings and mostly in 30 storey building.
- So we can say that, at least it is necessary to check the results of analysis with and without considering P-delta effect for the buildings with 25 stories (height = 75m).
- Iterative P-delta analysis method is used. Building is analyzed for 10 numbers of iterations. But it is found that the results are converged after 2 iterations. So there is no change in the results by increasing the number of iterations.
- Also the analysis is performed by considering the seismic loading in other zones in India. Similar results are observed in the form of increase in internal forces.
- So we should perform P-delta analysis for designing a minimum of 25 storey building. And buildings up to 25 stories can be designed by conventional primary analysis or linear analysis.
- This conclusion is valid for regular RCC residential buildings and may not be applicable for commercial, educational or industrial buildings.

REFERENCES:

- [1] Experimental study of P-delta effect in High rise buildings - M.A.A. Mollick
- [2] Effect of P-delta analysis for slender building structures -T.K. Bandyopadhyay, D. Datta Saha, A. Chaudhuri
- [3] Interaction of torsion and P-delta effect in tall buildings - A.S. Moghdam and A. Aziminejad
- [4] Modification to current P-delta implementation to rigid diaphragms- Bulent M. Alemdar
- [5] Comparison of P-delta analysis of plane frames using commercial structural analysis programs and current AISC design specifications by Angela M. Schimizza
- [6] SAP 2000 Analysis reference manual and SAP videos.

A survey on Li-Fi based audio transmission with home / office automation system.

Amit Jaykumar Chinchawade, Prof. K. Sujatha.

Dept. Electronics & Tele-Communication Engineering,

Shree Ramchandra College of engineering Lonikand (Pune), India.

amitchinchawade@yahoo.co.in

Contact Number:- 9970700801.

Abstract— This paper represent the importance of LI-FI Technology in the audio transmission and to monitor and control the house/office appliances and other equipments. Today Wi-Fi is replaced by LI-FI in many applications due the high data transmission rate of LI-FI as compare to Wi-Fi and due to low cost of LI-FI as compared to Wi-Fi technology. It is a visible light communication that uses LED's for audio and data transfer.

Keywords— LED (Light Emitting Diode), Wi-Fi (Wireless Fidelity), Li-Fi (Light Fidelity), VLC (Visible Light Communication), RF (Radio Frequency), DTMF (Dual Tone Multiple Frequency), LDR (Light Dependant Register.)

INTRODUCTION

Today, we have may technology for audio transmission as well as controlling the devices. Which may be wired or wireless. Li-Fi is the most effective technology for data transmission. It is a wireless technology. This uses LED's for data transmission. Li-Fi technology developed by Harald Haas. The technology was demonstrated at the 2012 Consumer Electronics Show in Las Vegas. Sending data through a LED light bulb that varies in intensity faster than the human eye, if the LED is on, you transmit a digital 1, if it's off you transmit a 0. They can be switched on and off very quickly, which gives nice opportunities for transmitted data. The LED intensity is modulated so rapidly that human eye cannot notice, so the output appears constant.

For Audio transmission the Power amplifier and voltage amplifier converts the sound into the digital signals i.e. '0' and '1'.

For home / office automation DTMF Encoder encodes the data form keypad and sends it to LED driver. At the receiver side DTMF Decoder is used to decode the data which encoded by the encoder and turn ON or OFF the devices. Advantage by using the Li-Fi technology is fast and safe audio transmission with fast and safe device switching.

METHODOLOGY

A mice and Audio jack are the inputs to the audio transmission. These audio signals are given to power amplifier and voltage amplifier. Then this signal is given to LED driver to transmit the signal using Li-Fi.

At the input side 4x4 keypad is connected to DTMF Encoder for encode the data for switching the devices. DTMF encoder encodes the data and sends it to power and voltage amplifier. This amplifies the data and sends it to LED driver to transmit the data using Li-Fi.

At receiver side LDR receives the signals which is transmitted by the LED. The audio signal is given to power and audio amplifier. And the output of amplifier is given to speaker.

The another DTMF signal is given to DTMF Decoder. The DTMF decoder decodes the signal which is encoded by the DTMF Encoder and turn ON of OFF the particular device.

HARDWARE UNITS REQUIRED

1. Power supply unit:-

It required two voltages levels +12 V & +5 V.

2. DTMF Encoder:-

Dual Tone Multiple Frequency is used to send multi key strokes with different frequencies. In DTMF each key has a unique frequency by combination of row and column frequency . When any of the key is pressed particular code is transmitted. This code consist of two frequency g which one is higher frequency and second one is lower frequency.

3. Keypad:-

4x4 key matrix is used to select the particular device by pressing the key to ON or OFF the selected device. It sends the frequency to DTMF encoder.

4. Microcontroller:-

The Atmel AT89C51 microcontroller is used to control the overall operation of the MIC, DTMF Encoder and decoder. It is a 8-bit microcontroller. AT89C51 has 4KB of Flash programmable and erasable read only memory (PEROM) and 128 bytes of RAM. In 40 pin AT89C51, there are four ports designated as P1, P2, P3 and P0. All these ports are 8-bit bi-directional ports.

5. LED Drivers:-

This is used to drive the relay where the output is complement of input which is applied to the drive but current will be amplified.

6. Li-Fi transmitter:-

White LED bulb is the Li-Fi transmitter.

7. Li-Fi receiver:-

LDR i.e. Light Dependent Register is the Li-Fi receiver.

8. Speakers:-

Speaker is the electrical device which converts electrical signals into voice signals. Here 4 Ohm speaker required.

9. DTMF Decoder :-

DTMF Decoder is decodes the signal which is encoded by the DTMF Encoder. This identifies the which key is pressed on the keypad by the user for turn ON or OFF the particular device.

10. Relays:-

It is a electromagnetic device. It will used to turn ON or OFF the device which is connected to relay. Here 12v relay is required.

SOFTWARE REQUIREMENT

It requires Keil compiler μ Vision 3.

ADVANTAGES

- 5.1 Use of Li-Fi in this project increases the speed of voice communication and data transmission.
- 5.2 Due to Li-Fi this project becomes very cheap, because it does not required any licence like Wi-Fi.
- 5.3 Due to use of Li-Fi the device switching is very simple.
- 5.4 Due to use of Li-Fi the installation cost is very low, because it uses simple LED.

APPLICATIONS

- 6.1 This project can be used for audio transmission in different Auditoriums, Multiplexes, Homes and offices.
- 6.2 This project can be used for device automations in different areas like Hospitals, Power lines, etc. where Wi-Fi can be restricted.

FUTURE SCOPE

- 7.1 This project can be used in Robotics control.
- 7.2 This project can be used in Heavy machinery controls in varies industries.

ACKNOWLEDGMENT

First of all I would like to thank my parents for their blessing and the trust they have shown for pursuing my M.E. degree. I wish to express my pleasure of acknowledging and thanks towards Prof. K.Sujatha, my Project Guide for providing the technical guidelines and constructive suggestions regarding the line of this work. He encourages me all the times for doing this quality research work in tuned with the target puts before me. I have been very fortunate to have his appreciable guidance during my stay at the department.

I also wish to extend my sincere thanks our concerned teaching staff for their insightful comments and suggestions to improve my performance during my presentations at the department.

In addition, I would also like to thank Dr. A.D.Desai, Principal of SRE'S Shree Ramachandra College of Engineering for providing me necessary resources and support granted throughout my master's fellowship.

I also thank to my friends those have rendered their help during the course of this work.

CONCLUSION

Li-Fi replaces the Wi-Fi. Li-Fi can be used in varies field. Use of Li-Fi in audio transmission and device automation can improves the speed of communication and speed of device automation in varies fields. Li-Fi can be used in varies areas where frequencies can be restricted. The audio transmission and device automation is becomes secured due to use of Li-Fi technology.

REFERENCES:

- [1] World Academy of Science, Engineering and Technology International Journal of Computer, Electrical, Automation, Control and Information Engineering Vol:6, No:8, 2012,titled as Design and Implementation of a Wi Fi Based Home Automation System.
- [2] Md. Kayesar Ahmmed , Anmona Shabnam Pranti. Low Cost Voice Communication Device Design Using Ordinary Laser Torch and LDR Available in Bangladesh,www.lificonsortium.org. International Journal of Electronics and Electrical Engineering Vol. 1, No. 4, December, 2013.
- [3] M.Kavehrad, "Sustainable Energy Efficient Wireless Applications Using Light," IEEE Commun. Mag., vol. 48, no. 12, Dec. 2010, pp. 66-73.

- [4] Dinesh Suresh Bhadane, Monali D. Wani, Sanjeev. A. Shukla, Aniket R. Yeole, Titled A Review on Home Control Automation Using GSM and Bluetooth,]International Journal of Advanced Research in Computer Science and Software Engineering Research Paper. Volume 5, Issue 2, February 2015 ISSN: 2277 128X
- [5] Technologies in Home Automation System: A Survey International Journal on Recent and Innovation Trends in Computing and Communication ISSN: 2321-8169 Volume: 3 Issue: 2 637 – 640
- [6] T.Komine and M.Nakagawa, "Fundamental analysis for visible light communication systems using LED Lights," IEEE Trans. Consumer Electronics, vol. 59, no.1, Feb, 2004.
- [7] IEEE CS year 2005 by Anil Madhav a peddy, David Scott, and Alastair Tse University of Cambridge and Richard Sharp Intel Research Cambridge.
- [8] Y. Tanaka et al., "Indoor Visible Light Data Transmission System Utilizing White LED Lights," IEICE Trans. Commun., vol. E86-B, no. 8, Aug. 2003, pp. 2440–54.
- [9] P. Amirshahi, M. Kavehrad, "Broadband Access over Medium and Low Voltage Power lines and use of White Light Emitting Diodes for Indoor Communications," IEEE Consumer
- [10] In International Journal of Emerging Technology and Advanced Engineering , (ISSN 2250-2459, ISO 9001:2008 Certified Journal, Volume 5, Issue 4, April 2015) titled as A Review: Real-Time Wireless Audio-Video Transmission by Nalini Bagal, Prof. Shivani Pandita.
- [11] International Journal of Electronics and Electrical Engineering Vol. 1, No. 4, December, 2013, Titled Low Cost Voice Communication Device Design Using Ordinary Laser Torch and LDR Available in Bangladesh by Md. Kayesar Ahmmed ,Anmona Shabnam Pranti.
- [12] T.D.C. Little, P. Dib, K. Shah, N. Barraford, and B. Gallagher, "Using LED Lighting for Ubiquitous Indoor Wireless Networking", IEEE International Conference on Wireless & Mobile Computing, 10.1109/WiMob.2008.57.
- [13] International Journal of Advanced Research in Computer Science and Software Engineering Research Paper. Volume 5, Issue 2, February 2015 ISSN: 2277 128X Titled A Review on Home Control Automation Using GSM and Bluetooth by Dinesh Suresh Bhadane, Monali D. Wani, Sanjeev. A. Shukla, Aniket R. Yeole

ANALYSIS OF CRACK INFLUENCE ON AN OPEN FRAME L-STRUCTURE USING FEM

Y.P. Mamatha¹, Sujith Kumar S², Vivek G², Sumanth D R², Vinay N².

¹Assistant Professor, Department of Mechanical Engineering, Vidyavardhaka College of Engineering, Mysuru.

Email: mamathayp@vvce.ac.in

²B.E. Students, Department of Mechanical Engineering, Vidyavardhaka College of Engineering, Mysuru.

Email: sujithskum@gmail.com, vikuuvivek@gmail.com

ABSTRACT: Detection of crack is very important to maintain the safety of the structure. When a crack develops in a structure it leads to changes in its vibration parameters, these affect modal parameters. Based on these changes, it is possible to estimate the crack size and location by measuring the changes in vibration of the structure.

The aim of this project is to carry out modal analysis of In-plane free vibration analysis of two-member open frame with transverse crack. The 3D model of Open frame L-structure is created and analysed with the changes in crack dimensions, crack locations and for with and without concentrated mass (end mass) conditions for both horizontal and vertical members using ANSYS. The results obtained from the vibration analysis of L-frame structure shows that Crack depth is inversely proportional to natural frequency while keeping crack location constant and natural frequency is lower near fixed end region and increases for farther regions.

Keywords- Flexibility, Modal Analysis, Modal Parameters, Mode Shapes, Natural Frequency, Vibration Parameters, ANSYS.

INTRODUCTION

The importance of early detection of cracks is crucial, as it is the most common reason for structural defect. Presence of crack affects the mechanical behaviour of the structure and also reduces the stiffness, the developed crack propagate in size thereby causing failure of the structure in long run. Cracks may develop in a structure due to reduction in fatigue strength, mechanical defects and as a result of improper manufacturing process. Currently research has focused on using modal parameters over other traditional methods. Modal parameters include detection of crack size and location using natural frequency and mode shapes as natural frequencies can easily be obtained and monitored. The main focus of this project is to detect Natural frequency and mode shapes of an open frame L structure using vibrational analysis method for various crack size and location and for with and without mass conditions. The L-frame has vertical and horizontal segment on which the crack is introduced separately, the crack is a transverse crack with uniform width along thickness of frame. The crack introduced causes local flexibility in that region due to strain energy concentration at the tip of the crack, which is a function of crack depth only. So the crack depth is only varied in a particular crack location and results are tabulated.

LITERATURE REVIEW

Structures are usually united to withstand loads with stability, all structures must withstand loads for which they are designed, loads may be dynamic or static loads. When this type of loads are present it leads to fatigue cracks, so the development of cracks lead to many faulty results so the study regarding this has been chosen as area of interest. Many methods and research works have been proposed in order to identify the natural frequency of the structures in which the cracks are developed. The main methods in which the work is done are theoretical, experimental and numerical methods. Theoretically it is usually done by Euler-Bernoulli beam theory, Rayleigh-Ritz theory and Timoshenko beam theory. In experimental method, the crack is induced in the structure, constraints or boundary conditions are applied and using accelerometer equipment the structure is vibrated and the natural frequency is determined.

Numerical methods are done in software packages which help in getting faster results and complex structures can be easily studied. Based on these above mentioned ideas many work has been done in vibration analysis of cantilever beam and other structures, this helps us in understanding their constraints in usage. The vibration analysis of L-frame structure which is used commonly in building structures, trusses is important.

In this work, vibration analysis is carried out in ANSYS WORKBENCH, similar work has been carried out by Y P Mamatha^[1], the analysis is carried out theoretically by using Euler-Bernoulli beam theory introducing crack as rotational spring. A comparison has been made with numerical results and theoretical results, a maximum of 5% error occurs for no mass condition and 20 % for other mass conditions. This proves that numerical and theoretical results are in good agreement. H Alper Ozyigit^[2] carried out the linear vibrations of frames with circular cross-section where one of the frame is straight and another curved. This research work shows how the natural frequency decreases when a point mass is added at the right tip of the curved beam while the straight beam is fixed. Alejandro R. Ratazzi, Diana V. Bambill and Carlos A. Rossitn^[3] have carried out vibration analysis on L-shaped beam theoretically with elastic boundary conditions and a crack in one of the segment which is modelled as rotational spring using Euler-Bernoulli's theorem. P Yamuna, K Sambasivarao^[4] carried out the work on vibration analysis of simply supported beam with varying crack location which shows how the natural frequency varies when crack location varies using ANSYS, they used SOLID 186 tetrahedral 20 node brick element. Dr Luay S Al-Ansari^[5] did experimental and numerical modal analysis for cracked simply supported solid and hollow beams, in his experiment. It shows that the natural frequency decreases when the crack depth increases in solid beams and the natural frequency increases when crack depth increases in hollow beams, he has used SOLID Tetrahedral 10 node 187 elements in mesh in his analysis in ANSYS. Ranjan K. Behera, Anish Pandey, Dayal R. Parhic^[6] performed analysis in-order to find the natural frequency of cantilever beam for inclined cracks.

MODELLING OF L-FRAME STRUCTURE

- **GEOMETRIC MODELLING**

The system consist of two flexible members which are arranged as shown in Fig.1. The L-frame with span of $L_1=0.9\text{m}$ vertically, $L_2=0.6\text{m}$ horizontally and with a cross section of $0.05\text{m} \times 0.03\text{m}$ (h x w) is modelled using SOLID EDGE v19. The angle between two beams is 90° . The transverse crack is introduced by cutting out a portion of the structure according to crack size as specified later.

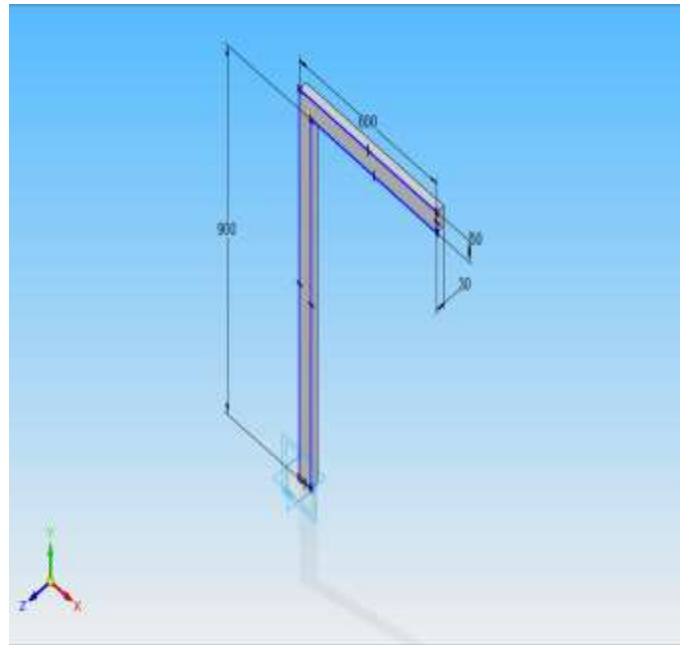


Fig.1. Geometric model of L- frame Developed in SOLID EDGE

• **CRACK MODELLING**

Crack size is introduced as a ratio of a/h where ‘a’ is depth of the crack and ‘h’ is the thickness of the beam. The various crack sizes are in ratios of 0.1, 0.2, 0.3, 0.4, 0.5 and 0.6. Crack location for Vertical segment and horizontal segment is introduced as a ratio of L_c/L_1 and L_c/L_2 where L_c is the crack location, L_1 is the length of the vertical segment and L_2 that of horizontal segment as shown in Fig.2 and Fig.3.

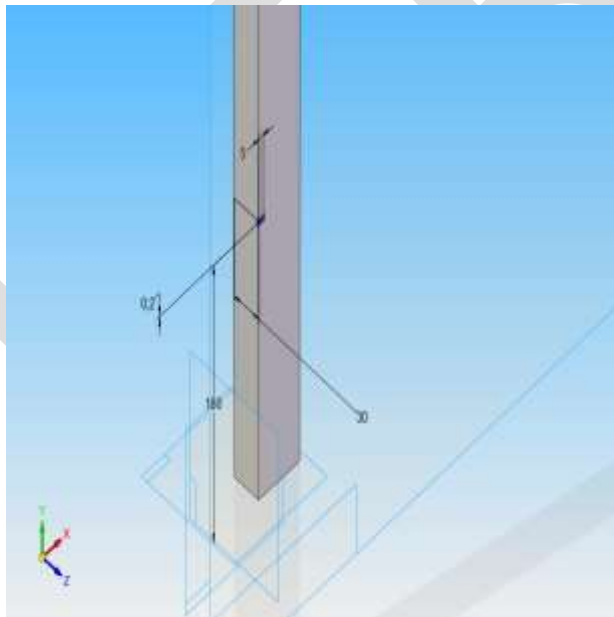


Fig.2.The Crack introduced on the Vertical member of L-frame.

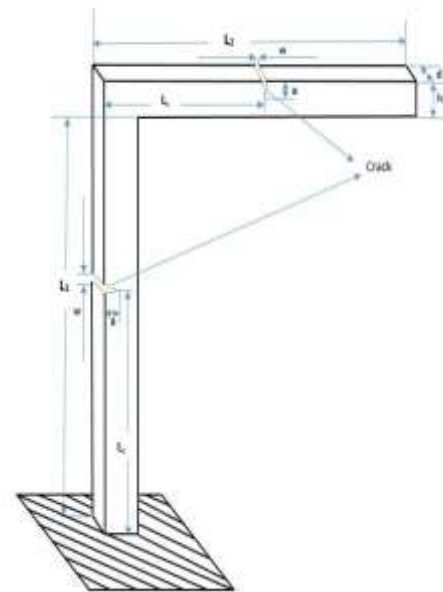


Fig.3. L-frame structure with crack

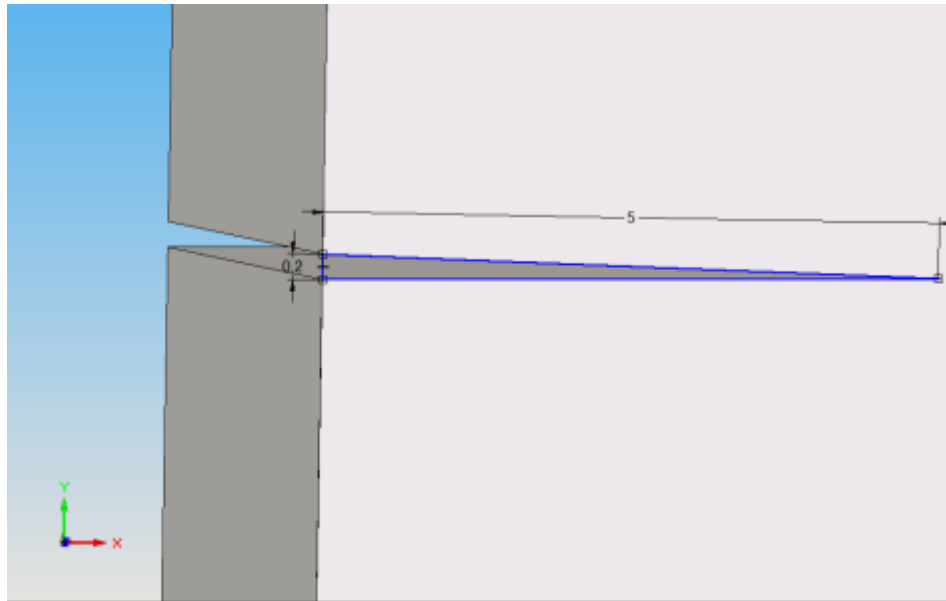


Fig.4. Crack of 5 mm depth and uniform width along thickness on L- frame.

- **FEM-ANALYSIS**

Finite element analysis (FEA) is a computerized method for predicting how a product reacts to real-world forces, vibration, heat, fluid flow, and other physical effects. In this project modal analysis method, which is the study of the dynamic properties of structures under vibration excitation is used. Modal analysis is the field of measuring and analyzing the dynamic response of structures during excitation.

STEPS INVOLVED IN ANSYS WORKBENCH 15

- 1. Selecting analysis type**

Modal analysis

- 2. Material properties**

Material-Aluminum

Young's Modulus (E) = 70Gpa

Density (ρ) = 2600 Kg/m³

Poisson's ratio (ν) = 0.33

- 3. Importing geometry**

The geometry created in SOLID EDGE is imported in .igs format.

- 4. Selecting element type and MESHING**

In this analysis, **Tetrahedral 10 node SOLID 187** mesh element with **3 cycles of refinement** is used because of its quadratic displacement behavior which is more suitable for irregular meshing and to obtain fine mesh. This helps in dividing the solid structure into small elements and meshing the crack location clearly. The SOLID 187 is as shown in Fig.5 it has three degrees of freedom at all the 10 nodes.

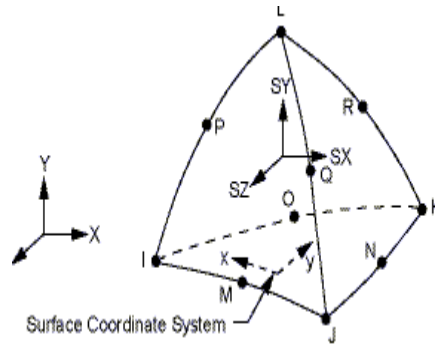


Fig.5. Tetrahedral 10 node SOLID 187 element of meshing

The Fig.6 shows meshing which is done in **ANSYS WORKBENCH 15** using SOLID 187 element for triangular crack on vertical segment.

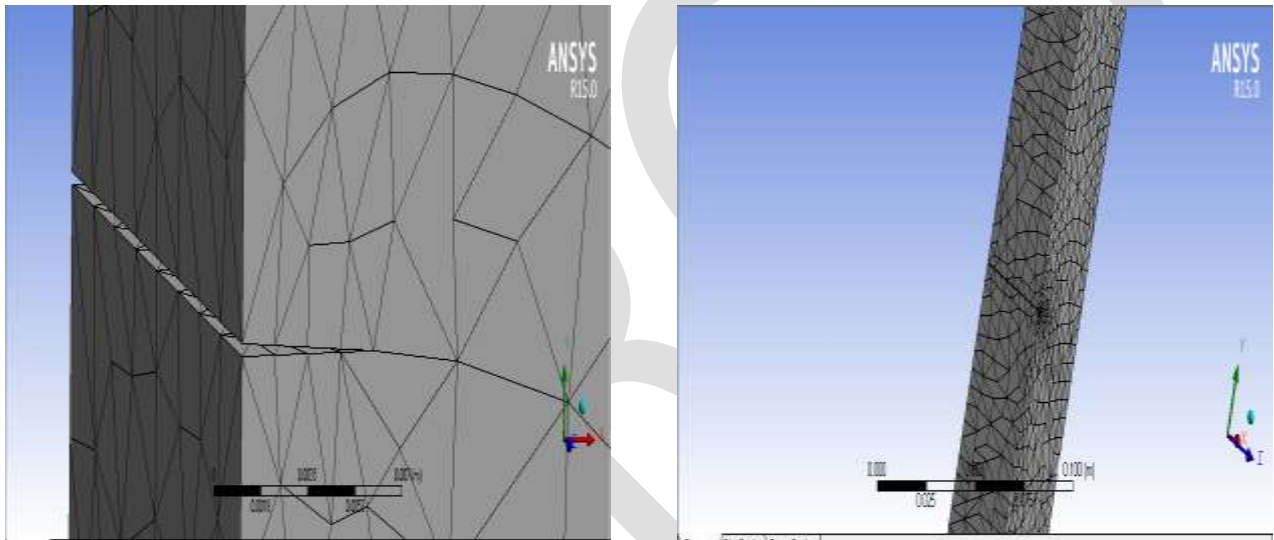


Fig.6. Meshing of the structure at the Crack

5. Applying boundary conditions

Using fixed support option the bottom end of the vertical segment is constrained in all DOF as shown in Fig.7.

6. Adding end mass

Different mass conditions are considered here. The various mass conditions are **No Mass**, **0.4kg** and **0.8kg**, which are applied to the free end face of the horizontal beam individually for corresponding crack size and location to study the changes in modal parameters of the structure by using point mass option as shown in Fig.8.

Fig.7.The Bottom end is fixed using fixed support

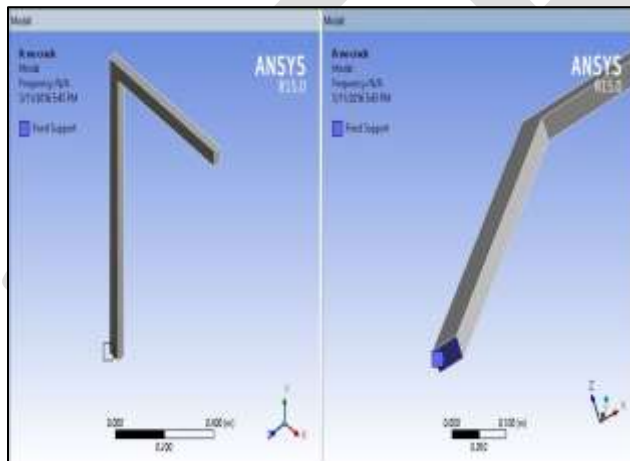
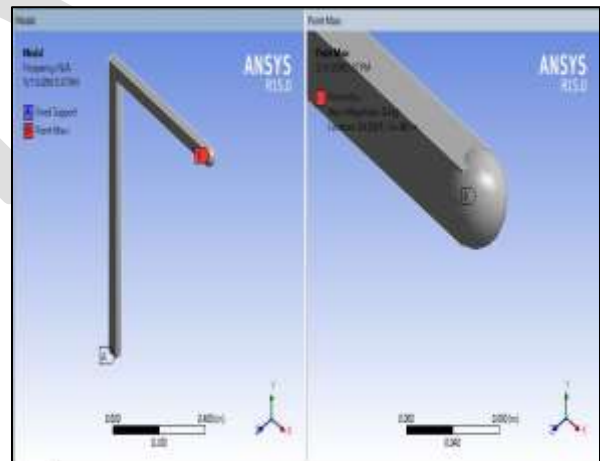


Fig.8.L-frame with 0.4 kg End mass at face of free end



7. Solution

The modal analysis solution is done using **BLOCK LANCZOS** mode extraction method.

8. Results

The modal analysis solution is done for *total deformation* of the structure and *mode shapes* are extracted for in-plane and out-plane vibrations of the structure. The natural frequencies for the first four modes are tabulated for various conditions considered. Natural frequencies for various crack size and location is obtained and the frequency ratio in percentage is calculated using the formula. $\omega_{\text{uncracked}}$ is considered as reference frequency.

FREQUENCY RATIO

$$\% \text{ Diff} = \frac{\omega_{\text{cracked}} - \omega_{\text{uncracked}}}{\omega_{\text{uncracked}}} \times 100$$

TABULAR RESULTS

1 In-Plane Natural Frequencies for Crack on Vertical Segment (L1) without End Mass									
Crack Location (L _c /L ₁)	Crack Size (a/h)	Natural Frequencies (Hz)							
		ω ₁	%Diff	ω ₂	%Diff	ω ₃	%Diff	ω ₄	%Diff
No Crack		23.5498		81.5947		290.8431		596.6108	
0.2	0.1	23.4532	-0.4101	81.5303	-0.0789	290.7937	-0.0170	596.3694	-0.0405
0.2	0.2	23.1443	-1.7218	81.3589	-0.2890	290.6903	-0.0525	595.7983	-0.1362
0.2	0.3	22.6219	-3.9400	81.0679	-0.6456	290.5122	-0.1138	594.6185	-0.3339
0.2	0.4	21.7894	-7.4754	80.6060	-1.2117	290.2142	-0.2162	592.4379	-0.6994
0.2	0.5	20.5901	-12.5680	79.9893	-1.9675	289.8333	-0.3472	588.8811	-1.2956
0.2	0.6	18.7725	-20.2858	79.1347	-3.0149	289.3058	-0.5286	582.6287	-2.3436
0.6	0.1	23.5202	-0.1258	81.5165	-0.0958	290.0258	-0.2810	596.5763	-0.0058
0.6	0.2	23.4288	-0.5138	81.2858	-0.3786	287.5711	-1.1250	596.4448	-0.0278
0.6	0.3	23.2574	-1.2415	80.9064	-0.8436	283.2572	-2.6082	596.2304	-0.0638
0.6	0.4	22.9720	-2.4535	80.2841	-1.6062	276.5983	-4.8977	595.7159	-0.1500
0.6	0.5	22.5240	-4.3558	79.3429	-2.7598	267.3159	-8.0893	594.7421	-0.3132
0.6	0.6	21.7575	-7.6105	77.8736	-4.5605	254.1809	-12.6055	592.7568	-0.6460

2 In-Plane Natural Frequencies for Crack on Vertical Segment (L1) with End Mass=0.4Kg									
Crack Location (L _c /L ₁)	Crack Size (a/h)	Natural Frequencies (Hz)							
		ω ₁	%Diff	ω ₂	%Diff	ω ₃	%Diff	ω ₄	%Diff
No Crack		21.3818		67.8189		278.6443		522.3525	
0.2	0.1	21.2974	-0.3950	67.7572	-0.0909	278.5938	-0.0181	522.2040	-0.0284
0.2	0.2	21.0276	-1.6568	67.5888	-0.3392	278.4487	-0.0702	521.9427	-0.0784
0.2	0.3	20.5701	-3.7965	67.3048	-0.7581	278.2095	-0.1560	521.3538	-0.1912
0.2	0.4	19.8382	-7.2195	66.8577	-1.4173	277.8228	-0.2948	520.2103	-0.4101
0.2	0.5	18.7786	-12.1751	66.2622	-2.2953	277.3051	-0.4806	518.3499	-0.7663
0.2	0.6	17.1615	-19.7382	65.4425	-3.5040	276.5777	-0.7417	515.0334	-1.4012
0.6	0.1	21.3529	-0.1355	67.7679	-0.0752	277.8580	-0.2822	522.2402	-0.0215
0.6	0.2	21.2637	-0.5525	67.6184	-0.2957	275.4961	-1.1298	521.8746	-0.0915
0.6	0.3	21.0968	-1.3329	67.3803	-0.6466	271.3241	-2.6271	521.2789	-0.2055
0.6	0.4	20.8196	-2.6295	66.9868	-1.2269	264.8904	-4.9360	520.1359	-0.4243
0.6	0.5	20.3861	-4.6569	66.3885	-2.1092	255.9089	-8.1593	518.2688	-0.7818
0.6	0.6	19.6492	-8.1035	65.4572	-3.4824	243.1433	-12.7406	515.1115	-1.3862

3 In-Plane Natural Frequencies for Crack on Vertical Segment (L1) with End Mass=0.8Kg									
Crack Location (L _c /L ₁)	Crack Size (a/h)	Natural Frequencies (Hz)							
		ω_1	%Diff	ω_2	%Diff	ω_3	%Diff	ω_4	%Diff
No Crack		19.6933		59.8975		272.0090		497.2525	
0.2	0.1	19.6179	-0.3832	59.8371	-0.1009	271.9566	-0.0192	497.1220	-0.0262
0.2	0.2	19.3770	-1.6062	59.6692	-0.3813	271.7892	-0.0808	496.9305	-0.0648
0.2	0.3	18.9678	-3.6843	59.3869	-0.8525	271.5163	-0.1811	496.4737	-0.1566
0.2	0.4	18.3111	-7.0187	58.9447	-1.5907	271.0797	-0.3416	495.5637	-0.3396
0.2	0.5	17.3567	-11.8653	58.3558	-2.5739	270.4871	-0.5595	494.0935	-0.6353
0.2	0.6	15.8918	-19.3038	57.5475	-3.9235	269.6505	-0.8671	491.4628	-1.1643
0.6	0.1	19.6653	-0.1422	59.8596	-0.0634	271.2413	-0.2822	497.1095	-0.0288
0.6	0.2	19.5793	-0.5792	59.7488	-0.2482	268.9347	-1.1302	496.6534	-0.1205
0.6	0.3	19.4185	-1.3958	59.5775	-0.5343	264.8506	-2.6317	495.9146	-0.2691
0.6	0.4	19.1518	-2.7500	59.2924	-1.0102	258.5532	-4.9468	494.5534	-0.5428
0.6	0.5	18.7359	-4.8618	58.8571	-1.7370	249.7531	-8.1820	492.4014	-0.9756
0.6	0.6	18.0321	-8.4356	58.1815	-2.8649	237.2160	-12.7911	488.9131	-1.6771

4 In-Plane Natural Frequencies for Crack on Horizontal Segment (L2) without End Mass									
Crack Location (L _c /L ₂)	Crack Size (a/h)	Natural Frequencies (Hz)							
		ω_1	%Diff	ω_2	%Diff	ω_3	%Diff	ω_4	%Diff
No Crack		23.5520		81.6253		290.9321		596.6835	
0.2	0.1	23.5482	-0.0161	81.3684	-0.3147	290.2343	-0.2398	596.2835	-0.0670
0.2	0.2	23.5431	-0.0378	80.6708	-1.1694	288.4241	-0.8621	595.3094	-0.2303
0.2	0.3	23.5343	-0.0752	79.4583	-2.6548	285.4237	-1.8934	593.7079	-0.4987
0.2	0.4	23.5191	-0.1397	77.6028	-4.9280	281.1838	-3.3507	591.3899	-0.8872
0.2	0.5	23.4894	-0.2658	74.4321	-8.8125	274.6877	-5.5836	587.8572	-1.4792
0.2	0.6	23.4371	-0.4879	69.8449	-14.4323	266.7055	-8.3272	583.5182	-2.2064
0.6	0.1	23.5495	-0.0106	81.5597	-0.0804	290.6953	-0.0814	594.1593	-0.4230
0.6	0.2	23.5492	-0.0119	81.4983	-0.1556	290.3392	-0.2038	586.5906	-1.6915
0.6	0.3	23.5486	-0.0144	81.3888	-0.2897	289.7054	-0.4216	573.5862	-3.8709
0.6	0.4	23.5473	-0.0200	81.1785	-0.5474	288.5387	-0.8227	552.0742	-7.4762
0.6	0.5	23.5448	-0.0306	80.8319	-0.9720	286.5098	-1.5200	520.1715	-12.8229
0.6	0.6	23.5401	-0.0505	80.2682	-1.6626	282.7255	-2.8208	475.8786	-20.2461

5 In-Plane Natural Frequencies for Crack on Horizontal Segment (L2) with End Mass=0.4Kg									
Crack Location (L _c /L ₂)	Crack Size (a/h)	Natural Frequencies (Hz)							
		ω_1	%Diff	ω_2	%Diff	ω_3	%Diff	ω_4	%Diff
No Crack		21.3818		67.8189		278.6443		522.3525	
0.2	0.1	21.3793	-0.0120	67.6194	-0.2942	278.1201	-0.1881	522.3020	-0.0097
0.2	0.2	21.3712	-0.0499	67.0062	-1.1983	276.5676	-0.7453	522.1258	-0.0434
0.2	0.3	21.3567	-0.1175	65.9442	-2.7643	273.9944	-1.6688	521.8897	-0.0886
0.2	0.4	21.3323	-0.2317	64.3328	-5.1402	270.3803	-2.9658	521.3911	-0.1840
0.2	0.5	21.2850	-0.4530	61.6060	-9.1610	264.8493	-4.9508	520.7043	-0.3155
0.2	0.6	21.2017	-0.8420	57.7211	-14.8892	258.0783	-7.3807	519.7540	-0.4974
0.6	0.1	21.3813	-0.0024	67.7785	-0.0596	278.4274	-0.0779	519.7598	-0.4963
0.6	0.2	21.3803	-0.0073	67.6917	-0.1876	277.8217	-0.2952	511.9532	-1.9909
0.6	0.3	21.3784	-0.0161	67.5383	-0.4138	276.7408	-0.6831	499.0162	-4.4675
0.6	0.4	21.3748	-0.0329	67.2565	-0.8292	274.7807	-1.3866	478.7243	-8.3523

0.6	0.5	21.3684	-0.0631	66.7940	-1.5112	271.3561	-2.6156	463.1178	-11.3400
0.6	0.6	21.3569	-0.1168	66.0313	-2.6359	264.9377	-4.9190	461.4804	-11.6534

6 In- Plane Natural Frequencies for Crack on Horizontal Segment (L2) with End Mass=0.8Kg									
Crack Location (L _c /L ₂)	Crack Size (a/h)	Natural Frequencies (Hz)							
		ω_1	%Diff	ω_2	%Diff	ω_3	%Diff	ω_4	%Diff
No Crack		19.6933		59.8975		272.0090		497.2525	
0.2	0.1	19.6901	-0.0167	59.7178	-0.3000	271.5326	-0.1751	497.2401	-0.0025
0.2	0.2	19.6797	-0.0692	59.1667	-1.2202	270.1242	-0.6929	497.1722	-0.0161
0.2	0.3	19.6611	-0.1636	58.2138	-2.8110	267.7896	-1.5512	497.1307	-0.0245
0.2	0.4	19.6300	-0.3215	56.7745	-5.2140	264.5175	-2.7541	496.8892	-0.0731
0.2	0.5	19.5699	-0.6267	54.3513	-9.2596	259.5082	-4.5957	496.6304	-0.1251
0.2	0.6	19.4645	-1.1623	50.9268	-14.9768	253.3783	-6.8493	496.2097	-0.2097
0.6	0.1	19.6926	-0.0038	59.8567	-0.0682	271.7637	-0.0902	494.7518	-0.5029
0.6	0.2	19.6909	-0.0123	59.7638	-0.2232	271.0561	-0.3503	487.2766	-2.0062
0.6	0.3	19.6879	-0.0274	59.6002	-0.4963	269.7962	-0.8135	474.9910	-4.4769
0.6	0.4	19.6824	-0.0558	59.3040	-0.9909	267.5290	-1.6470	461.0758	-7.2753
0.6	0.5	19.6726	-0.1054	58.8201	-1.7988	263.5961	-3.0929	459.9908	-7.4935
0.6	0.6	19.6553	-0.1934	58.0236	-3.1286	256.3394	-5.7607	458.6754	-7.7581

IN-PLANE MODE SHAPES

The below Fig.9 shows various mode shapes for In-plane free vibration at no mass and no crack condition for the first four modes. By looking at the mode shapes one can say that deformation has occurred in the same plane for all the modes with variation in knee angle.

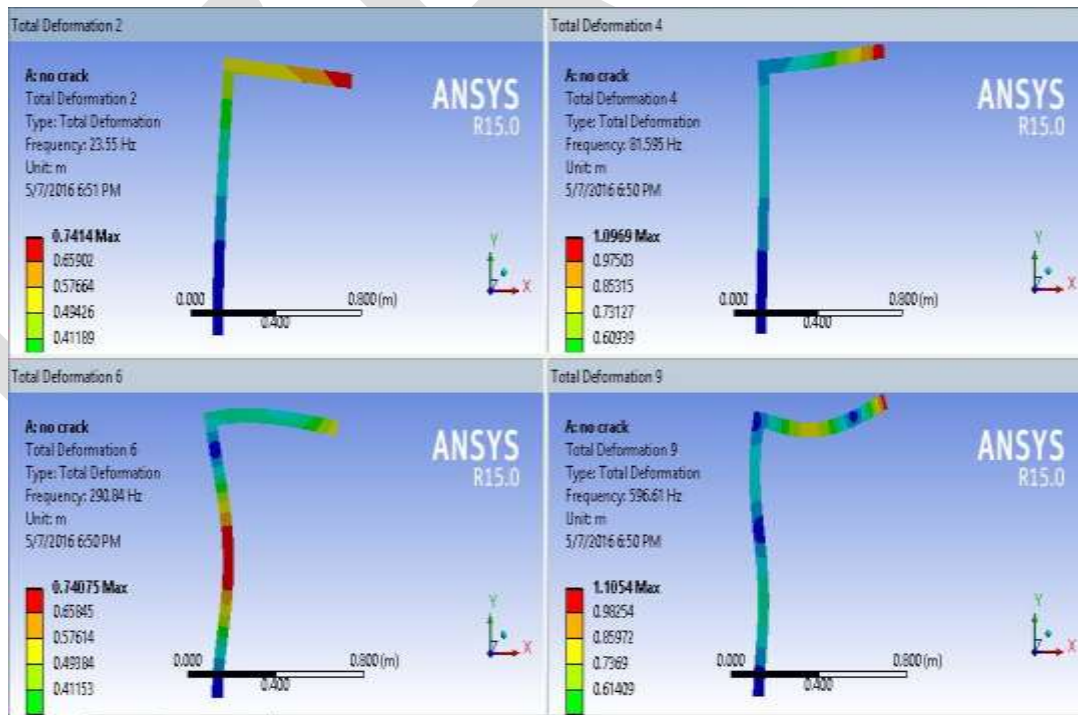


Fig.9. Mode shapes of In-plane vibration

CONCLUSION

In this paper, it can be observed that the crack depth is inversely proportional to natural frequency while keeping crack location constant. When mass is applied on the structure, natural frequency decreases. Natural frequency is lower near fixed end

region and increases for farther regions. From the obtained results it can be stated that natural frequency is affected by mode number. Natural frequency at certain cracked condition tends to increase rather than decreasing because of clapping effect.

REFERENCES:

- [1] Y.P. Mamatha, "In-plane free vibration of two member open frame with transverse crack", M.Tech report, Dept. ME., BMSCE, Bengaluru, Karnataka, IN., Jul. 2008.
- [2] H. Alper Ozyigit, "Linear vibrations of frames carrying a concentrated mass", Mathematical and Computational Applications, Vol. 14, No. 3, pp. 197-206, 2009.
- [3] Alejandro R. Ratazzi, Diana V. Bambill, Carlos A. Rossit, "Free Vibrations of Beam System Structures with Elastic Boundary Conditions and an Internal Elastic Hinge", Hindawi Publishing Corporation, Chinese Journal of Engineering Volume 2013, Article ID 624658.
- [4] P.Yamuna, K.Sambasivarao, "Vibration analysis of beam with varying crack location", International Journal of Engineering Research and General Science Volume 2, Issue 6, October-November, 2014, ISSN: 2091-2730.
- [5] Dr. Luay S. Al-Ansari, "Experimental and Numerical Comparison between the Natural Frequency of Cracked Simply Supported Hollow and Solid Beams", Volume: 3, Issue: 9, Sept 2013, ISSN: 2249-555X.
- [6] Ranjan K. Behera, Anish Pandey, Dayal R. Parhic, "Numerical and Experimental Verification of a Method for Prognosis of Inclined Edge Crack in Cantilever Beam Based on Synthesis of Mode Shapes", 2nd International Conference on Innovations in Automation and Mechatronics Engineering, ICIAME 2014.

NIGHT VISION ASSIST FOR SAFE DRIVING

Bonam Venkata Sumanth¹, Manda SuhasPriyatham², Marthy Siva Sai Krishna³

VASAVI COLLEGE OF ENGINEERING^{1,2}, GITAM UNIVERSITY³

Dept of ECE, venkatasumanth.b95@gmail.com, 9441181709

Abstract— Drivers has to take care of safety measures while driving car. The driver's sight and his vision towards other colors during dark times need more attention. Besides his lack of attention during driving many external parameters usually cause problems to the drivers such as high fog, bad climate/weather, dim street lights usually the one with low intensity etc:-,These things grabs the attention from the engineers to develop night vision systems that helps the driver by improving the visibility on the path during dark times. In general, such a system is developed by using infrared cameras from which the information of objects presenting on the road can be extracted. Then, this system will inform drivers by means of visual, sound sensors or other signals about the obstacles and moving objects appearing in their path. Night Vision Assist focuses on detecting, illuminating and recognizing objects at night. Infrared cameras are adopted to tackle the problem of low visibility at night. Computer vision techniques, such as image enhancement, object detection and recognition etc., are used intensively to analyze videos captured by the infrared cameras. The system can be operated by the driver through a screen and audio notifications are used for informing the driver of the possible dangers if needed by using a microcontroller. We implemented the screen presence for the driver by the image acquisition and its processing using MATLAB.

Keywords— Infrared, CCD, image acquisition, MATLAB, infrared camera, CMOS, microcontroller.

INTRODUCTION

Everybody in this world emits electromagnetic radiation and in particular human body radiates IR signals. Of all the Electromagnetic signals that are existed the human eyes can detect signals whose frequency range is limited with in visible light region. When a light falls on the object the radiation emitted by the object depends on its body type, in all those radiated electromagnetic signals human eye can see signals only that are in visible range. It is well known to everybody that cats can see the things in dark also. Then what makes the things visible to cat eyes in the absence of light? It is IR radiation emitted by the body of the object. Cat eyes can detect even IR signals also. This attention has dragged us to develop night vision assistance for drivers.

DESCRIPTION OF THE SYSTEM

During the dark times the car drivers uses their headlights for vision. As the light from the head light hit the objects and gets back to our eyes. But the visibility range is very less for human eyes. If the number of obstacles is more in the path it is highly difficult and risk for the driver to drive. IR signals have more range than signals in the visible spectrum. So we can use a system where we could use a lens that receives the signals and we can process those signals in such a way that only visible and IR spectrum signals are processed on the screen. Particularly only IR if required. Present day cameras have IR filter in it, so we have to remove it from the circuit. At the head light position we should put together the IR emitter sources also. IR sources are required to detect object movement. Anybody can ask for the requirement of IR sources if the object itself emits IR signals. The IR signals radiated by them are basically less in power .So these IR sources together headlights work in such a way that the IR signals can detect the object movement at the far and near distances and the headlights are used for near action movements. These signals are getting hit by the objects and are received by the camera optical lens. After processing these signals we could use a interface to visualize the surroundings. Interface could be a TV / computer depending upon the requirement.

When the light from the lens fall on the image sensor the light intensity got converted into the number of electrons. These electrons got converted into the voltage and to zeros, ones using analog to digital convertor. These digital signals are processed by the electronic circuits inside the camera. CCD and CMOS are the two main technologies used in making image sensors widely now a day. This is general camera working. In order to make infrared camera we have to take a camera of our own choice and remove the infrared filter inside it as shown in below figures. So the sensor of camera is sensitive to both visible and infrared range signals. In case of only infrared signal input requirement we have to add a band pass filter that stops signals from the visible region band. This produces only the infrared signals on the screen. Here are some pictures of making the infrared camera from the camera of our own choice:



Figure.1 Webcam whose case has been removed.

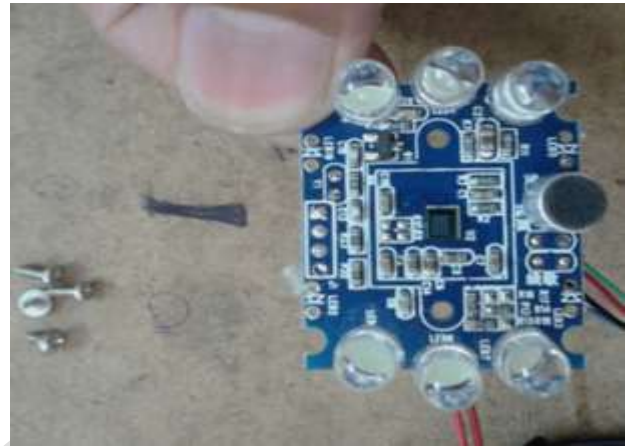


Figure.2 web camera including COMS sensor.



Figure.3 Lens assembly inside camera



Figure.4 Infrared filter from the web camera.

Now, we consider two images that are taken immediately one after other and we will take the difference of the 2 images. From this we can obtain the information regarding the objects that are moving as shown in figure. This difference images are Taken as consideration for grayscale image format. A threshold has to be considered and the grayscale image has to be Created..This can be created by comparing the level of intensities at each point. In case where if the threshold is greater than Intensity value one is generated and in other case zero is generated. These ones are white and zeros are black. These white

Spaces have to be converted into red color as shown in figure below. And that image has to be added to the original image, so that incase of object moving it shows its boundary by red color as shown in figure. The moving objects can be seen under red Colored boundary. Red color is chosen as it can grab human eye attention especially during night times. We can arrange beep sound using sound sensor when ever any object that is far away from the vehicle is moving as a sign of grabbing attention using Microcontrollers.

WORKING PROTOTYPE

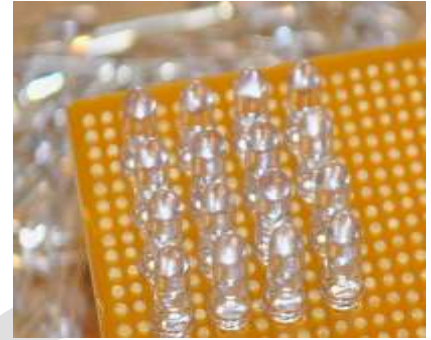


Figure.5 showing the INFRARED radiation source (IR LED's).



Figure.6 Picture 1



Figure.7 Picture 2

Picture 1 and 2 in the above figure 6 and 7 are the original pictures that are required to be processed.



Figure.8



Figure.9

Fig 8 & 9 represent the difference of two consecutive frames in grayscale format



Figure.10



Figure.11

Figure. 10 & 11 are the binary images representing the border of moving object in the frame

OUTPUT

After converting the white shading to red in the above pictures and adding them to the original pictures. We obtain



Figure.10



Figure.11

In the above figures the chairs are stationary so they appear same in both the pictures, but the persons are moving so they appeared with red colored boundary. Thus the moving objects from the near and far range can be seen on the screen.

CONCLUSION

Thus we can see the stationary and moving objects clearly that are present near and far from the car (i.e. to the driver) This system is developed to avoid the fatal incidents caused during the night travelling. This system can be upgraded by using more options to the microcontroller. By disabling the filter that stops both visible and infrared range signals driver can see both near and far objects in the Screen itself. This system will help the drivers who are suffering from long and short sightedness.

REFERENCES:

- [1] Chun-Che Wang, Shih-Shinh Huang , and Li-Chen Fu and Pei-Yung Hsiao “Driver Assistance System for Lane Detection and Vehicle Recognition with Night Vision” IEEE.
- [2] Yun Luo, Jeffrey Remillard, and Dieter Hoetzer “Driver Pedestrian Detection in Near-Infrared Night Vision System” IEEE.
- [3] Rita Kovordanyi, Torbjom Alm, and Kjell Ohlsson “Driver Night-Vision Display Unlit during Uneventful Periods May Improve Traffic Safety” IEEE.
- [4] Cheng Wang, Boliang Wang and Hao Sun “Night vision pedestrian detection using a forwardlooking infrared camera” IEEE.
- [5] Takayuki Tsuji, Hiroshi Hattori, Masahito Watanabe, and Nobuharu Nagaoka ”Development of Night-Vision System” IEEE.
- [6] Siti Zubaidah Binti Rajemi, Rosyati Hamid, Faradila Naim, Nurul Wahidah Arshad “Pedestrian Detection for Automotive Night Vision Using Thermal Camera” IEEE.
- [7] Hyukmin Eum, Jeisung Lee ,Changyong Yoon and Mignon Park “Human Action Recognition for Night Vision Using Temporal Templates with Infrared Thermal Camera” IEEE.

- [8] Karol Piniarski, Pawel Pawlowski, Adam Dbrowski "Pedestrian Detection by Video Processing in Automotive Night Vision System" IEEE.
- [9] "Image Intensification Tube Technology and Evolution". GlobalSecurity.org. Retrieved 2011-03-01
- [10] Jeffrey P. Bialos; Stuart L. Koehl (September 2005). "The NATO Response Force" (PDF). National Defense University. Retrieved 2011-03-01.
- [11] "Seeing in the Dark", Vector, magazine of the Civil Aviation Authority of New Zealand, January/February 2008, pages 10–11.
- [12] Scientists Develop Night Vision Contact Lens - Defensetech.org, 28 March 2014.
- [13] Liew, S. C. "Electromagnetic Waves". Centre for Remote Imaging, Sensing and Processing. Retrieved 2006-10-27.
- [14] Michael Rowan-Robinson (2013). "Night Vision: Exploring the Infrared Universe". p. 23. Cambridge University Press
- [15] "How Night Vision Works". American Technologies Network Corporation. Retrieved 2007-08-12.
- [16] Bryant, Lynn (2007-06-11). "How does thermal imaging work? A closer look at what is behind this remarkable technology". Retrieved 2007-08-12.

IJERGS

Design Single and Multiple Errors Correction Block Codes

Zahraa Raad Mayoof Hajiyat

Faculty of Engineering Technology & Built Environment,

Department of Electrical and Electronic Engineering,

B.Eng (Hons) Communication and Electronic Engineering

UCSI University, Kuala Lumpur, Malaysia

E-mail:glancing@ymail.com

Abstract— Channel coding is a process used in digital communications system to guarantee a transmission is received with minimal or no errors. Some coding methods that employed are achieved by involving additional binary numbers into the transmission. When decoded on the receiving finished, the transmission can be checked for errors that may have happened. Channel coding that apply this method are block codes which called forward error correction (FEC) codes that allow a limited number of errors to be detected and corrected without retransmission. Hamming codes has found a best class of single error correcting codes while Reed–Solomon codes has found a best class of multiple error correcting codes for designing of block codes and it shows how error correction and detection can be accomplished. Beside, using Matlab software to perform single and multiple errors correction design. Also, The BER display for both Hamming codes and Reed-Solomon codes.

Keywords— Communication systems, Errors correction, Channel coding, Block codes, Hamming codes, Reed-Solomon codes, BER display.

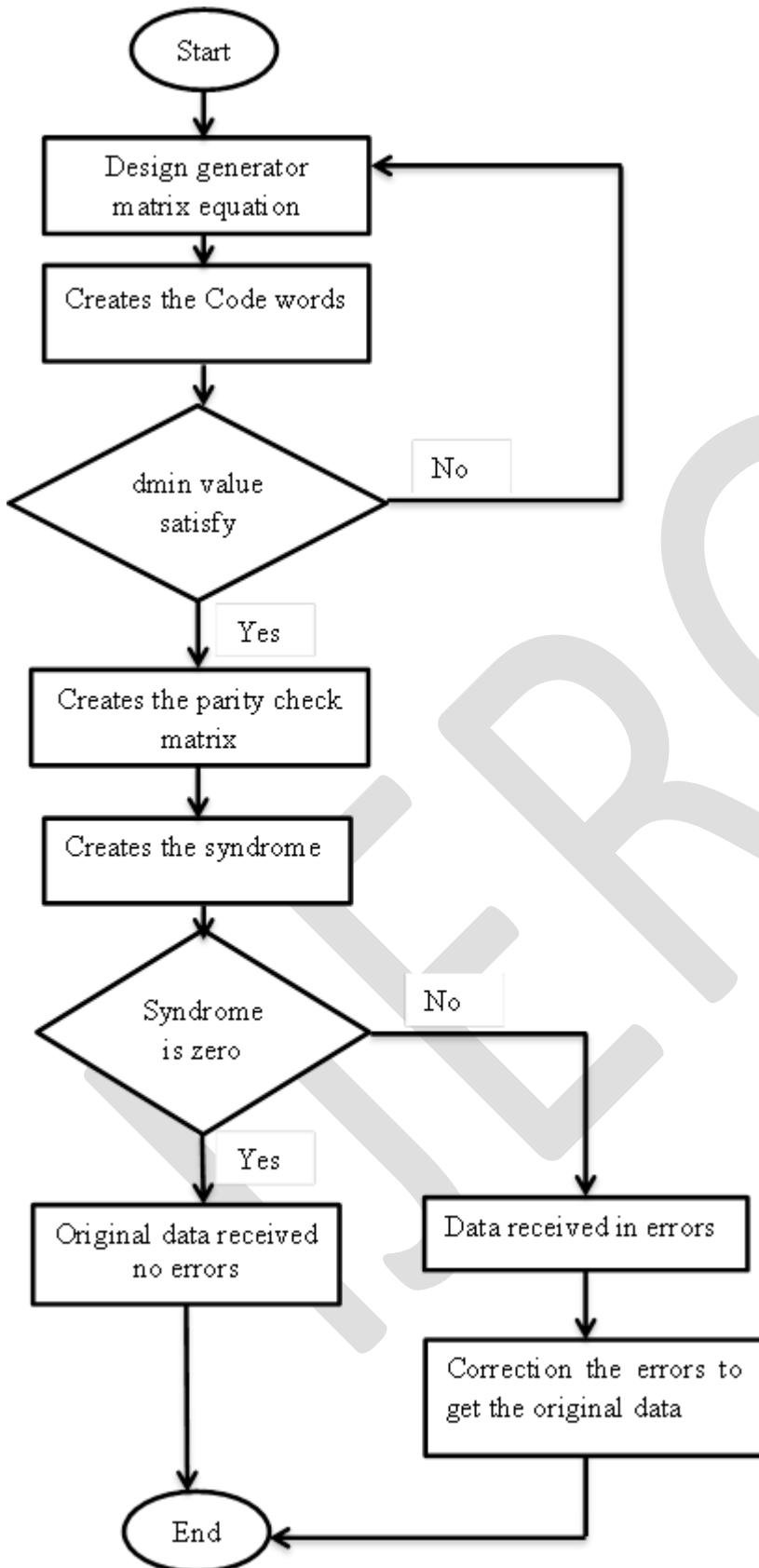
INTRODUCTION

Block code are forward error correction (FEC) codes that allow a limited number of errors to be detected and corrected without retransmission. Thus, block codes can be used to improve the performance of a communications system when increasing the transmitter power is impossible. The block codes have several categories such as Reed- Solomon codes, Hamming codes, Hadamard codes, Expander codes, Golay codes, and Reed–Muller codes. These categories also belong to the class of linear codes, and they are called linear block codes. Mostly, these codes are known as algebraic block codes, or cyclic block codes, because they can be produced using Boolean polynomials. In 1950, Richard Wesley Hamming found a best class of single error correcting codes. The code was used for long distance telephony. Hamming code is an improvement on the parity check method. Hamming is a well-known name in the field of data encoding and decoding. In 1960, Irving Reed and Gus Solomon published a class of error-correcting codes that are now called Reed-Solomon (R-S) codes. These codes have great control and effectiveness, and currently found in many applications from compact disc players to deep-space applications.

METHODOLOGY

The research methodology of design block codes that can correct single and multiple errors such as Hamming codes and Reed-Solomon codes are required to gathering all knowledge, concepts and theories of error detection, error correction, block codes, Hamming codes and Reed-Solomon codes theories. Besides, gathering the theories of block codes principles such as hamming distance, hamming weight, mini hamming distance, linear block codes and symmetric block codes. Furthermore, the generator matrix designs, codewords, parity check matrix and syndrome. When understanding the concepts of block codes, the design will apply these theories with develop the design to able to correct the errors in the transmitting bits messages.

The flow chart for designing block codes such as Hamming codes and Reed-Solomon codes as following:



RESULTS

(11, 4) Hamming code design:

The equation design:

$$C1 = m1 \oplus m2 \oplus m3 \oplus m4$$

$$C2 = m1 \oplus m2 \oplus m3$$

$$C3 = m1 \oplus m3 \oplus m4$$

$$C4 = m1 \oplus m2 \oplus m4$$

$$C5 = m2 \oplus m3 \oplus m4$$

$$C6 = m1 \oplus m4$$

$$C7 = m1 \oplus m3$$

This design of (11, 4) hamming code is for $d_{min} = 5$ using Matlab software.

```
Command Window
>> g=[1 1 1 1 0 1 1;1 1 0 1 1 0 0;1 1 1 0 1 0 1;1 0 1 1 1 1 0]

g =

     1     1     1     1     0     1     1
     1     1     0     1     1     0     0
     1     1     1     0     1     0     1
     1     0     1     1     1     1     0

>> generator=[g,eye(4)]

generator =

     1     1     1     1     0     1     1     1     0     0     0
     1     1     0     1     1     0     0     0     1     0     0
     1     1     1     0     1     0     1     0     0     1     0
     1     0     1     1     1     1     0     0     0     0     1
```

```
>> m=[0000000;00100010;01000101;01100111;0001001;0101011;1001101;1110111]

m =

     0     0     0     0     0
     0     0     0     1
     0     0     1     0
     0     0     1     1
     0     1     0     0
     0     1     0     1
     0     1     1     0
     0     1     1     1
     1     0     0     0
     1     0     0     1
     1     0     1     0
     1     0     1     1
     1     1     0     0
     1     1     0     1
     1     1     1     0
     1     1     1     1
```

```
>> codeword=m*generator

codeword =

    0  0  0  0  0  0  0  0  0  0  0
    1  0  1  1  1  1  0  0  0  0  1
    1  1  1  0  1  0  1  0  0  1  0
    2  1  2  1  2  1  1  0  0  1  1
    1  1  0  1  1  0  0  0  1  0  0
    2  1  1  2  2  1  0  0  1  0  1
    2  2  1  1  2  0  1  0  1  1  0
    3  2  2  2  3  1  1  0  1  1  1
    1  1  1  1  0  1  1  1  0  0  0
    2  1  2  2  1  2  1  1  0  0  1
    2  2  2  1  1  1  2  1  0  1  0
    3  2  3  2  2  2  2  1  0  1  1
    2  2  1  2  1  1  1  1  1  0  0
    3  2  2  3  2  2  1  1  1  0  1
    3  3  2  2  2  1  2  1  1  1  0
    4  3  3  3  3  2  2  1  1  1  1
```

```
>> p=g'

p =

    1  1  1  1
    1  1  1  0
    1  0  1  1
    1  1  0  1
    0  1  1  1
    1  0  0  1
    1  0  1  0

>> paritycheck=[eye(7),p]

paritycheck =

    1  0  0  0  0  0  0  1  1  1  1
    0  1  0  0  0  0  0  1  1  1  0
    0  0  1  0  0  0  0  1  0  1  1
    0  0  0  1  0  0  0  1  1  0  1
    0  0  0  0  1  0  0  0  1  1  1
    0  0  0  0  0  1  0  0  1  0  1
    0  0  0  0  0  0  1  0  1  0  1
```

```
>> error=eye(11)

error =

    1  0  0  0  0  0  0  0  0  0  0
    0  1  0  0  0  0  0  0  0  0  0
    0  0  1  0  0  0  0  0  0  0  0
    0  0  0  1  0  0  0  0  0  0  0
    0  0  0  0  1  0  0  0  0  0  0
    0  0  0  0  0  1  0  0  0  0  0
    0  0  0  0  0  0  1  0  0  0  0
    0  0  0  0  0  0  0  1  0  0  0
    0  0  0  0  0  0  0  0  1  0  0
    0  0  0  0  0  0  0  0  0  1  0
    0  0  0  0  0  0  0  0  0  0  1
```

```
>> H=paritycheck'

H =

    1  0  0  0  0  0  0
    0  1  0  0  0  0  0
    0  0  1  0  0  0  0
    0  0  0  1  0  0  0
    0  0  0  0  1  0  0
    0  0  0  0  0  1  0
    0  0  0  0  0  0  1
    1  1  1  1  0  1  1
    1  1  0  1  1  0  0
    1  1  1  0  1  0  1
    1  0  1  1  1  1  0
```

```
>> syndrome=error*H

syndrome =

    1  0  0  0  0  0  0
    0  1  0  0  0  0  0
    0  0  1  0  0  0  0
    0  0  0  1  0  0  0
    0  0  0  0  1  0  0
    0  0  0  0  0  1  0
    0  0  0  0  0  0  1
    1  1  1  1  0  1  1
    1  1  0  1  1  0  0
    1  1  1  0  1  0  1
    1  0  1  1  1  1  0
```

```
>> r=[1 1 1 0 1 0 1 0 0 1 0] % no error
r=
1 1 1 0 1 0 1 0 0 1 0
>> syndrome=r*H
syndrome =
2 2 2 0 2 0 2
```

```
>> r=[1 1 1 0 1 0 1 0 1 1 0] % one error
r=
1 1 1 0 1 0 1 0 1 1 0
>> syndrome=r*H
syndrome =
3 3 2 1 3 0 2
>> original=r+[0 0 0 0 0 0 0 0 0 1 0 0]
original =
1 1 1 0 1 0 1 0 2 1 0
```

```
>> r=[1 1 1 1 1 1 0 0 0 1 1] % two error
r=
1 1 1 1 1 1 0 0 0 1 1
>> syndrome=r*H
syndrome =
3 2 3 2 3 2 1
>> original=r+[0 0 0 0 0 0 0 0 0 0 1 0]
original =
1 1 1 1 1 1 0 0 0 2 1
```

The (7, 3) Reed-Solomon code design:

The generator polynomial:

$$g(x) = (x - \alpha)(x - \alpha^2)(x - \alpha^3)(x - \alpha^4)$$

$$g(x) = (x^2 - (\alpha + \alpha^2)x + (\alpha \cdot \alpha^2))(x^2 - (\alpha^3 + \alpha^4)x + (\alpha^3 \cdot \alpha^4))$$

$$g(x) = (x^2 - \alpha^4x + \alpha^3)(x^2 - \alpha^6x + \alpha^7)$$

$$g(x) = (x^2 - \alpha^4x + \alpha^3)(x^2 - \alpha^6x + \alpha^0)$$

$$g(x) = x^4 - (\alpha^4 + \alpha^6)x^3 + (\alpha^3 + \alpha^{10} + \alpha^0)x^2 - (\alpha^4 + \alpha^9)x + \alpha^3$$

$$g(x) = x^4 - \alpha^3x^3 + \alpha^0x^2 - \alpha^1x + \alpha^3$$

$$g(x) = \alpha^3 + \alpha^1x + \alpha^0x^2 + \alpha^3x^3 + x^4$$

Adopt the three message bits $010 \rightarrow \alpha^1$, $110 \rightarrow \alpha^3$, $111 \rightarrow \alpha^5$.

So, the message bits sequence is

$$: \alpha^1 + \alpha^3x + \alpha^5x^2 = x^4(\alpha^1 + \alpha^3x + \alpha^5x^2) = \alpha^1x^4 + \alpha^3x^5 + \alpha^5x^6$$

$$\begin{array}{r}
 \alpha^5 x^2 + \alpha^0 x + \alpha^4 \\
 \hline
 \alpha^3 + \alpha^1 x + \alpha^0 x^2 \\
 + \alpha^3 x^3 + x^4 \\
 \hline
 \alpha^5 x^6 + \alpha^3 x^5 + \alpha^1 x^4 \\
 \hline
 \alpha^5 x^6 + \alpha^1 x^5 + \alpha^5 x^4 + \alpha^6 x^3 + \alpha^1 x^2 \\
 \hline
 \alpha^0 x^5 + \alpha^6 x^4 + \alpha^6 x^3 + \alpha^1 x^2 \\
 \hline
 \alpha^0 x^5 + \alpha^3 x^4 + \alpha^0 x^3 + \alpha^1 x^2 + \alpha^3 x \\
 \hline
 \alpha^4 x^4 + \alpha^2 x^3 + \alpha^3 x \\
 \hline
 \alpha^4 x^4 + \alpha^0 x^3 + \alpha^4 x^2 + \alpha^5 x + \alpha^0 \\
 \hline
 \alpha^6 x^3 + \alpha^4 x^2 + \alpha^2 x + \alpha^0
 \end{array}$$

The codeword polynomial is:

$$U(X) = \alpha^0 + \alpha^2 x + \alpha^4 x^2 + \alpha^6 x^3 + \alpha^1 x^4 + \alpha^3 x^5 + \alpha^5 x^6$$

$$U(X) = (100) + (001)x + (011)x^2 + (101)x^3 + (010)x^4 + (110)x^5 + (111)x^6$$

Through transmission, this codeword becomes ruined so that assumes two symbols are received in error.

$$e(X) = 0 + 0x + 0x^2 + \alpha^2 x^3 + \alpha^5 x^4 + 0x^5 + 0x^6$$

$$e(X) = (000) + (000)x + (000)x^2 + (001)x^3 + (111)x^4 + (000)x^5 + (000)x^6$$

The received codeword with errors:

$$U(X) = (100) + (001)x + (011)x^2 + (101)x^3 + (010)x^4 + (110)x^5 + (111)x^6$$

$$e(X) = (000) + (000)x + (000)x^2 + (001)x^3 + (111)x^4 + (000)x^5 + (000)x^6$$

$$\begin{array}{l}
 r(x) = (100) + (001)x + (011)x^2 + (100)x^3 + (101)x^4 + (110)x^5 + (111)x^6 \\
 r(x) = \alpha^0 + \alpha^2 x + \alpha^4 x^2 + \alpha^0 x^3 + \alpha^6 x^4 + \alpha^3 x^5 + \alpha^5 x^6
 \end{array}$$

Checking the syndrome values of received codeword:

$$s_1 = e(\alpha^1)$$

$$s_2 = e(\alpha^2)$$

$$s_1 = \alpha^2(\alpha^1)^3 + \alpha^5(\alpha^1)^4$$

$$s_2 = \alpha^2(\alpha^2)^3 + \alpha^5(\alpha^2)^4$$

$$s_1 = \alpha^5 + \alpha^9$$

$$s_2 = \alpha^8 + \alpha^{13}$$

$$s_1 = \alpha^5 + \alpha^2$$

$$s_2 = \alpha^1 + \alpha^6$$

$$s_1 = \alpha^3$$

$$s_2 = \alpha^5$$

$$s_3 = e(\alpha^3)$$

$$s_4 = e(\alpha^3)$$

$$s_3 = \alpha^2(\alpha^3)^3 + \alpha^5(\alpha^3)^4$$

$$s_4 = \alpha^2(\alpha^4)^3 + \alpha^5(\alpha^4)^4$$

$$s_3 = \alpha^{11} + \alpha^{17}$$

$$s_4 = \alpha^{14} + \alpha^{21}$$

$$s_3 = \alpha^4 + \alpha^3$$

$$s_4 = \alpha^0 + \alpha^0$$

$$s_3 = \alpha^6$$

$$s_4 = 0$$

The syndrome $s \neq 0$.

The correction errors of received codeword:

$$r(x) = (100) + (001)x + (011)x^2 + (100)x^3 + (101)x^4 + (110)x^5 + (111)x^6$$

+

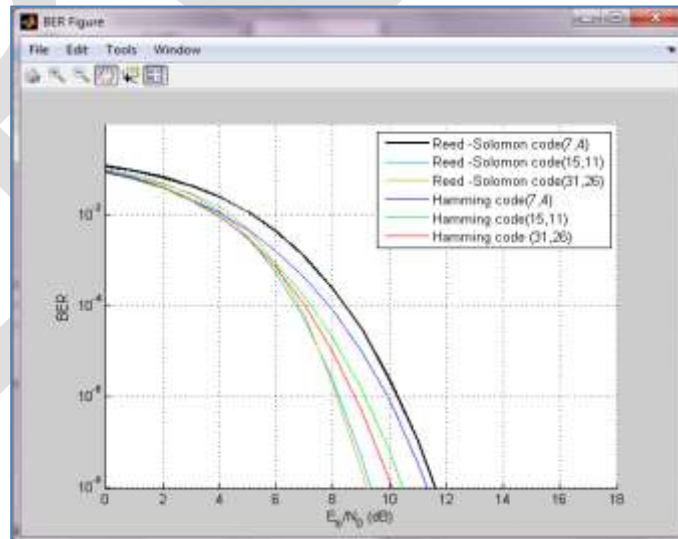
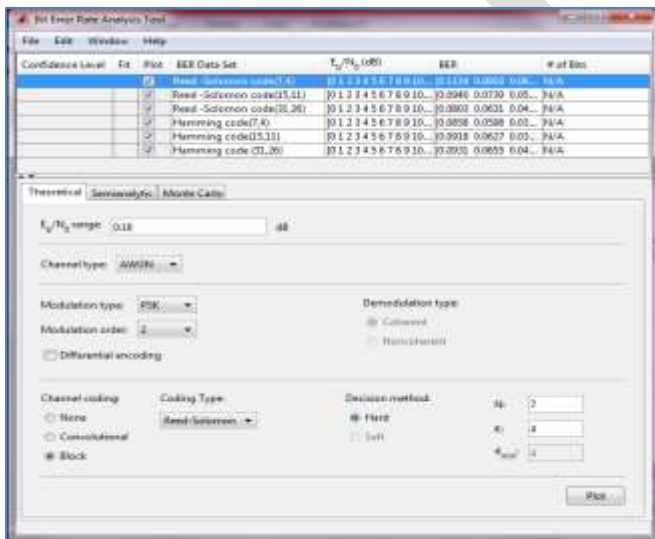
$$e(X) = (000) + (000)x + (000)x^2 + (001)x^3 + (111)x^4 + (000)x^5 + (000)x^6$$

$$U(X) = \frac{(100) + (001)x + (011)x^2 + (101)x^3 + (010)x^4 + (110)x^5 + (111)x^6}{\alpha^0 + \alpha^2x + \alpha^4x^2 + \alpha^6x^3 + \alpha^1x^4 + \alpha^3x^5 + \alpha^5x^6}$$

$$U(X) = \alpha^0 + \alpha^2x + \alpha^4x^2 + \alpha^6x^3 + \alpha^1x^4 + \alpha^3x^5 + \alpha^5x^6$$

The BER display for Both Hamming codes and Reed –Solomon codes:

The plot results of BER of Hamming codes and Reed-Solomon codes as following:



CONCLUSION

In conclusion, the coding theory was introduced for the detection and correction of error in data. Hamming introduced a coding system for the error detection as well as correction of that error at the receiver side. In this procedure, Hamming added some extra bits to the data bits for error detection as well as correction of that error. Also, Reed-Solomon codes methods generally apply same procedure for detection and correction with using the algorithm of Finite field. Currently, interleaving method used to increase the performance of block codes such as Reed-Solomon codes and Hamming codes for detection and correction the errors. Also, the lower probability of bit error rate or BER when the input data is ruined by noise is preferred for receiver side for most of application. As results, the Reed-Solomon code is achieved lower BER compared to Hamming code for same (n, k) block code. In the end, Hamming codes and Reed-Solomon code is a famous designation in the field of data encoding and decoding in the communication systems.

REFERENCES:

- [1] Gallager, R.G., *Information theory and reliable communication*. Vol. 2. 1968: Springer.
- [2] Wicker, S.B., *Error control systems for digital communication and storage*. Vol. 1. 1995: Prentice hall Englewood Cliffs.
- [3] Rappaport, T.S., *Wireless communications: principles and practice*. Vol. 2. 1996: prentice hall PTR New Jersey.
- [4] Stallings, W., *Data and computer communications*. 2007: Pearson/Prentice Hall.
- [5] Costello, D. and S. Lin, *Error control coding*. New Jersey, 2004.
- [6] Reed, I.S. and X. Chen, *Error-control coding for data networks*. Vol. 508. 2012: Springer Science & Business Media.
- [7] Tarokh, V., H. Jafarkhani, and A.R. Calderbank, *Space-time block codes from orthogonal designs*. Information Theory, IEEE Transactions on, 1999. 45(5): p. 1456-1467.
- [8] Vanstone, S.A. and P.C. Van Oorschot, *An introduction to error correcting codes with applications*. Vol. 71. 2013: Springer Science & Business Media.
- [9] Sklar, B., *Digital communications: Fundamentals and Applications*, ed. S. Edition. 2001: Prentice Hall
- [10] Furutani, K., et al., *A built-in Hamming code ECC circuit for DRAMs*. Solid-State Circuits, IEEE Journal of, 1989. 24(1): p. 50-56.
- [11] Peterson, W.W. and E.J. Weldon, *Error-correcting codes*. 1972: MIT press.
- [12] Reed, I.S. and G. Solomon, *Polynomial codes over certain finite fields*. Journal of the society for industrial and applied mathematics, 1960. 8(2): p. 300-304.

Underwater Image Enhancement Using Discrete Wavelet Transform & Singular Value Decomposition

G. S. Singadkar

Department of Electronics & Telecommunication Engineering

Maharashtra Institute of Technology, Aurangabad

Abstract— Underwater image enhancement is one of the challenging tasks in the field of marine species. While dealing to work in the marine class, the researchers face some problems related to the underwater images. As the depth of water increases, the problems related to clear image capturing becomes more. The problems vary according to the type of water, amount of light, depth of water, the distance between camera and object, etc. This paper deals with the underwater image enhancement by working on the resolution and contrast factors to preserve the information of an original image. The proposed system uses Discrete Wavelet Transform (DWT), Interpolation and Singular Value Decomposition (SVD) method to enhance the quality of underwater images.

Keywords— underwater, enhancement, contrast, resolution, DWT, Histogram Equalization, Interpolation, SVD.

INTRODUCTION

Earth is an aquatic planet wherein water occupies 70% of the surface. Nowadays, the area of research has increased its interest in the marine class. But to work on the aquatic objects, it is imperative to get the clear images of the underwater object. As the air interface deals with the environmental and camera problems like dust particles, natural light, reflection, focus and distance, underwater images are also facing the same challenges. The quality of the underwater image depends on the density of water, depth of water, distance between camera and object, artificial light, water particles, etc.

Most occurring problems in the underwater image is light scattering effect and color change effect [1]. If the water is clear or limpid, the image quality and visibility is good. As the depth of water increases, the water becomes denser due to sand, planktons and minerals. Due to increased density, the camera light gets reflected and deflected by particles for sometimes before reaching towards the camera and some part of camera light get absorbed by the particles. This scattering effect results in reduced visibility of image with low contrast. Secondly, the color change effect depends on the wavelength of light travel in the water. The color with the highest wavelength goes the very short distance in water. Fig 1 shows the light penetration pattern in the clear water. Blue color has the shortest wavelength, so it travels very long in the deep water. That's why the blue color is more in underwater images [5]. As the degree of attenuation varies for different wavelengths, the color change effect occurs.

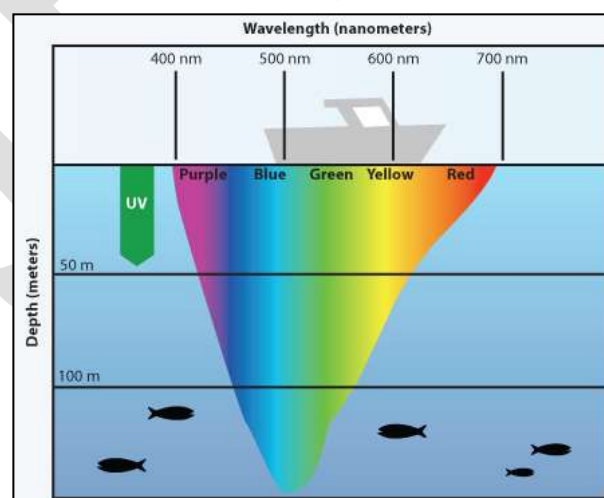


Fig. 1 Light Penetration in Clear water

The scattering effect and color change effect combined results in reduced visibility in underwater images. It affects the resolution and contrast attribute to degrade the quality of the image. Image enhancement is one of the pre-processing methods which improves the quality of an image by increasing the perception of information in it. This task is achieved by suppressing the undesired distortions like light scattering and color change effect to enhance image features relevant for further processing and analysis work.

LITERATURE SURVEY

Image enhancement is the lowest level pre-processing step to improve the quality or information of the image. This pre-processing method can be applied to the color image, grayscale image, underwater image, satellite image, etc. The papers here describe how underwater images get distorted, causes of underwater image distortion and methods or techniques to recover distorted image.

Underwater images can be improved using image enhancement techniques like Histogram Equalization, Dark-channel prior method, Wavelength Compensation & image dehazing (WCID). Histogram equalization increases the contrast of the distorted image, but it is not able to compensate light scattering problem. Dark channel prior method corrects the distorted image affected by light scattering or light attenuation. But this method is not useful when the object is similar to the background light. WCID overcomes all the problems related to light scattering and color change effect. The parameter like the distance between camera & object, artificial light source, underwater depth and image depth range calculations help to enhance the distorted image information with highest PSNR ration of 76.5044 [1]. Filtering is also a process to remove the noisy elements from an image. The edges of the degraded underwater image can be preserved using edge-preserving filters. The speckle reduction by anisotropic filter improves the image quality, suppresses the noise, preserves the edges in an image, enhances and smoothen the image. Homomorphic filtering is used to correct non-uniform illumination and to enhance contrasts in the image. Wavelet filter is also used to suppress the noise, i.e., the Gaussian noise which is naturally present in the camera images and another type of instrument images [2].

Some researchers proposed Unsupervised Colour Correction Method (UCM) and Contrast Limited Adaptive Histogram Equalization (CLAHE) technique for underwater image enhancement. Unsupervised Colour Correction Method (UCM) is based on color balancing and contrast correction of RGB and HSI color model. It balances the colors in the image, removes the color cast and improves the illumination with an increase in actual color [3]. Contrast Limited Adaptive Histogram Equalization (CLAHE) method works on RGB and HSV color models and both results are combined using Euclidean norm. The proposed system significantly improves the visual quality of underwater images by enhancing contrast as well as reducing noise and artifacts [4].

PROPOSED METHODOLOGY

The underwater images commonly suffer due to light scattering and color change effect. These effects degrade the contrast and resolution of the underwater image. The proposed system works on these blurred images using certain image processing operations like Histogram Equalization, Discrete Wavelet Transform (DWT), Singular Value Decomposition (SVD) and Inverse Discrete Wavelet Transform (IDWT) to enhance its quality. Fig. 2 shows the flow diagram of proposed underwater image enhancement technique.

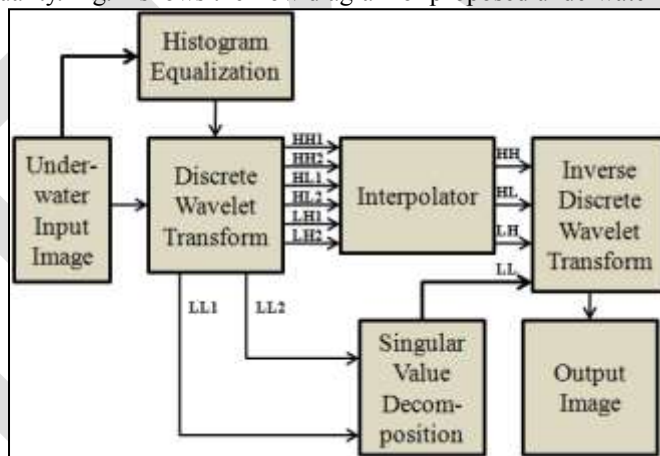


Fig. 2 Flow diagram of Underwater Image Enhancement

Image acquisition is the first step in every digital image processing flow. It collects the input images over which the work should be done. The proposed system is working on the underwater images to enhance the image information. The collected image quality degrades due to the light scattering and color change effect in the water. It mostly affects on the contrast and resolution of the image. Firstly, the system improves the contrast of the captured input image by using histogram equalization technique. Equalization process evenly distributes the gray levels in an image by reassigning the brightness values of pixels. It provides more visually pleasing results across wider range of images.

The original input image and equalized input image is then transformed using Discrete Wavelet Transform (DWT). It decomposes input image $f(i, j)$ in terms of a set of shifted and dilated wavelet functions $\{\psi^{0^0}, \psi^{90^0}, \psi^{\pm 45^0}\}$ and scaling function $\phi(x, y)$

$$f(x, y) = \sum_{k \in \mathbb{Z}^2} S_{j_0, k} \phi_{j_0, k}(x, y) + \sum_{b \in \theta} \sum_{j \geq j_0} \sum_{k \in \mathbb{Z}^2} w_{j, k}^b \psi_{j, k}^b(x, y)$$

Where,

$$\phi_{j_0, k}(x, y) = 2^{j_0} \phi(2^{j_0}(x, y) - k)$$

$$\psi_{j,k}^b(x,y) = 2^j \psi^b(2^j(x,y) - k)$$

And $b \in \{0^\circ, 90^\circ, \pm 45^\circ\}$. The $0^\circ, 90^\circ$ and $\pm 45^\circ$ denotes the sub-bands of the wavelet decomposition. After the decomposition of the input image we get low pass and high pass sub-bands namely HH, HL, LH, LL. High frequency sub-bands (HH, HL and LH) represent detail wavelet coefficients which contain edge information that is used for increasing resolution. Low frequency sub-band (LL) represents coarse coefficient which contains illumination information of image used to enhance contrast.

High-frequency sub-bands are used for resolution setting. Thus to increase the resolution of image, interpolation technique is applied to respective bands of both input and equalized input image. Interpolation technique increases the image information based on the known samples. As the sampling factor increases, the quality of image improves. Here the respective HH, HL, LH bands of input and equalized input images are interpolated as shown in Fig. 2.

Singular Value Decomposition is an image compression technique which stores the useful features of the image. It refactors or decomposes the image into three matrices [6]. As LL band contains the illumination information of the image, this band is applied to SVD, which produces an SVD matrix 'G'.

$$G = U_G \sum_G V_G^T$$

Where, U_G and V_G are orthogonal matrices known as hanger and aligner respectively.

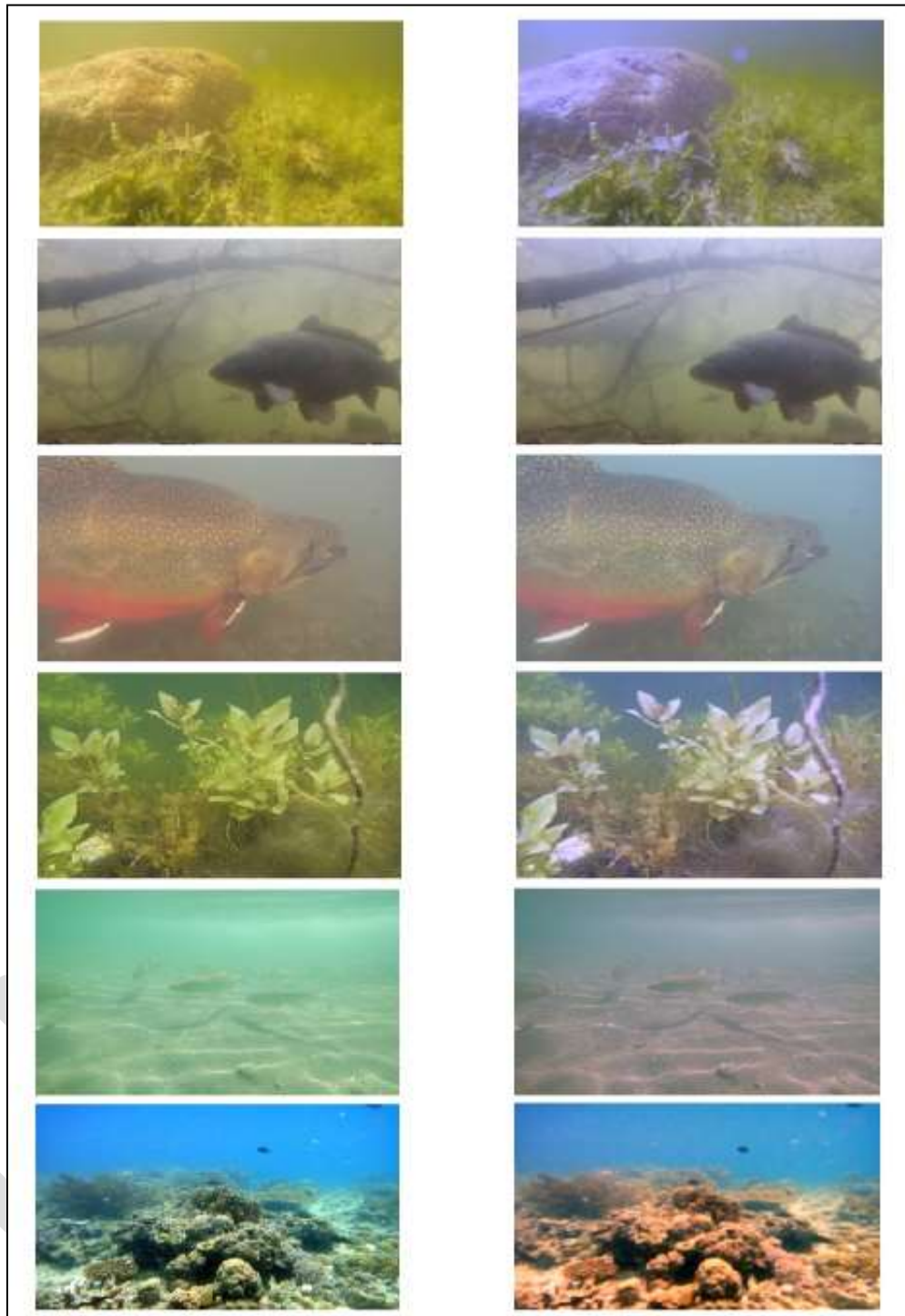
At the end, all these interpolated and SVD produced sub-bands are combined and inversed using Inverse Discrete Wavelet Transform (IDWT). Thus, finally we get the high resolution and contrast output image of the blurred and low-quality input image.

RESULTS & DISCUSSION

The proposed image enhancement system is applied on the blurred or low-quality underwater images. Fig. 3 shows some collected underwater images over which the work is carried out. The images are stored in JPEG format and are enhanced using image processing techniques through MATLAB.



Fig. 3 Original Input Images



Input Images

Output Images

Fig. 4 Final Enhanced Images

Performance of the proposed system is examined using different image quality measures.

1. Peak Signal to Noise Ratio (PSNR): To check the quality of the enhanced image, PSNR is used

$$PSNR = 10 \log_{10} \frac{255^2}{\frac{1}{M \times N} \sum_{i=1}^M \sum_{j=1}^N [f(i, j) - f'(i, j)]^2}$$

Where, $f(i, j)$ represent pixel value of the original image at location (i, j) and $f'(i, j)$ is the pixel value of enhanced image.

2. Mean: Mean is the average of the pixel intensity in an image which is required for finding out the standard deviation.

$$M = \frac{\sum \sum f(i, j)}{m \times n}$$

Where $f(i, j)$ is the pixel value of image of size $m \times n$

3. Standard Deviation: Standard deviation is obtained from the mean value of an image. Standard deviation gives the deviation of the image pixel from its mean value.

$$S = \sqrt{\frac{\sum (X - M)^2}{N - 1}}$$

Table 1 Results of Proposed System

Image	PSNR (dB)	Mean	Standard Deviation	Process Time (sec)
Image1	42.38	131.36	38.66	2.85
Image2	52.70	138.66	40.17	2.90
Image3	51.02	140.28	21.98	2.80
Image4	44.52	135.01	34.31	2.91
Image5	47.81	141.41	15.93	2.84
Image6	46.22	128.50	60.35	2.87

To improve the quality of image, these parameters should be high with less processing time (Table 1). Fig. 4 shows an enhanced version of input images.

CONCLUSION

From the results, it is cleared that the proposed system gives properly enhanced underwater image output with less processing time. The higher value of observed parameters shows that the quality of the image is up to the mark regarding contrast and resolution. And lower processing time proves that the system is faster with the process time below 3 seconds.

REFERENCES:

- [1] Bhanudas Sandbhor. G. U. Kharat, "A Review on Underwater Image Enhancement Techniques", International Journal of Advanced Research in Computer Science and Software Engineering, Vol. 5, Issue 5, May 2015.
- [2] Aanchal Garg, Nirvair Neeru, "Enhancement of Underwater Images: A Review", International Journal of Computer Science and Information Technologies, Vol. 5(4), 2014.
- [3] Kashif Iqbal, Michael Odetayo, Anne James, Rosaline Abdul Salam, Abdullah Zawawi Hj Talib, "Enhancing the Low Quality Images Using Unsupervised Colour Correction Method", 978-1-4244-6588-0/10/\$25.00 ©2010 IEEE.
- [4] MuhummadSuzuri Hitam, Wan Nural Jawahir Hj Wan Yussof, Ezmahamrul Afreen Awalludin, Zainuddin Bachok, "Mixture Contrast Limited Adaptive Histogram Equalization for Underwater Image Enhancement", 978-1-4673-5285-7/13/\$31.00 ©2013 IEEE.
- [5] Pooja Sahu, Neelesh Gupta, Neetu Sharma, "A Survey on Underwater Image Enhancement Techniques", International Journal of Computer Applications, Vol. 87 - No. 13, February 2014.
- [6] Lijie Cao, "Singular Value Decomposition Applied To Digital Image Processing", Division of Computing Studies Arizona State University Polytechnic Campus Mesa, Arizona 85212.
- [7] K. Lebart, C. Smith, E. Trucco, and D. M. Lane, "Automatic indexing of underwater survey video: algorithm and benchmarking method," IEEE J. Ocean. Eng., vol. 28, no. 4, pp. 673–686, Oct. 2003.
- [8] K. Iqbal, R. Abdul Salam, A. Osman, and A. Zawawi Talib, "Underwater image enhancement using an integrated color model," Int. J. Comput. Sci., vol. 34, no. 2, pp. 2–12, 2007.

- [9] C. I. Prabhakar and P. Kumar PU, "An Image Based Technique For Enhancement Of Underwater Images," International Journal of Machine Intelligence, vol. 3, pp. 217-224, 2011.
- [10] A. T. Celebi and S. Erturk, "Visual enhancement of underwater images using Empirical Mode Decomposition and wavelet denoising," in Signal Processing and Communications Applications Conference (SIU), 2012-20th, 2012, pp. 1-4.
- [11] Demirel Hasan, and Gholamreza Anbarjafari, "Image resolution enhancement by using discrete and stationary wavelet decomposition," Image Processing, IEEE Transactions on 20.5 (2011): 1458-1460.
- [12] Dianyuan Han, "Comparison of commonly used image interpolation methods," in Proceedings of 2nd International Conference on Computer Science and Electronics Engineering, 2013.

IJERGS

Review on Effect of Mindfulness Meditation on Brain through EEG Signals

Seema S. Kute¹, Sonali B. Kulkarni²
Department of Master of Computer Applications¹,
Marathwada Institute of Technology, Aurangabad[MH], India.
seemak0518@yahoo.in¹, sonalibkul@gmail.com²

Abstract - Science begun to expose the many sakes of meditation using enlightened tools like neuro-imaging, functional magnetic resonance imaging, brain mapping technology, electroencephalography, thus allowing scientists an unrivalled ability to measure the effects of meditation on the brain and brainwave constitutions. Within the past few decades, there has been a lot much of temptation in the study of mindfulness as psychological states and as a form of clinical approaches. In today's fast life and hectic schedule arises lot much physiological, psychological problems on human body, meditation is one of the best solution in physiological, negative psychological problems, attention. Numerous researchers already conduct the many research study on meditation the outcome of meditation on stress relief and disease improvement. In this review we see the mindfulness meditation plays an important role in the mental health and mindfulness meditation theory and also effects of mindfulness meditation, Transcendental Meditation, Zen Meditation, Samatha-vipassana, Yoga, Sahaji yoga, Sudarshan Kriya , Raj Yoga on Neuroimaging studies, behavioral studies, and structural imaging studies. The effect of meditation on human brain and body using EEG signals. To get the awareness into the nature of EEG during meditation.

Keywords - Introduction, Meditation, EEG, Literature Review.

INTRODUCTION

The mind is the primary source of human joy and misery, and is central to the understanding of the natural world as a whole this premise begins from the Buddhism.[1] A lot of constructive changes have been reported to happen in the brain and the other parts of the human body for those practicing meditation. Practicing meditation is no hassling task that helps bringing in structural and functional modifications in the human organs including the heart and brain with recurrent practice over a prolonged period. Meditation is practiced all across the world and diverse countries have given different names for the meditation that they practice. A case study has revealed a considerable, constructive behavioral modification of the human entity that practice meditation, thereby reducing the number of visits to the physicians by a great extent and the individual concerned is found to save \$200 on the clinician's visit with effective practicing of meditation.[2] Also, another study has concluded the reduced use of medical care by Meditators in comparison to those who don't practice meditation.[3]

MEDITATION

"In meditation, a person learns to focus his attention and suspend the stream of thoughts that normally occupy the mind. This practice is believed to result in a state of greater physical relaxation, mental calmness, and psychological balance. Practicing meditation can change how a person relates to the flow of emotions and thoughts in the mind."[4]

TYPES OF MEDITATION

Mindfulness meditation practice to approach our experience in new ways moment by moment non-judgmental awareness of body sensations, thoughts and emotions. Raj Yoga is concerned with focusing the mind and using its power to control the body. There should be a relationship between the mind and body in order to be disciplined.[5] Transcendental meditation(TM) fits somewhat within the concentrative forms, because practice centers on the repetition of a mantra, but the method places a primary emphasis on absence of concentrative effort and the development of a witnessing, thought-free "transcendental awareness." VM requires becoming aware of all of one's senses and acknowledging any negative feelings, pain, or blockages in order to achieve equanimity. Equanimity is defined as not interfering with the flow of the senses at any level, including the level of preconscious processing [6].

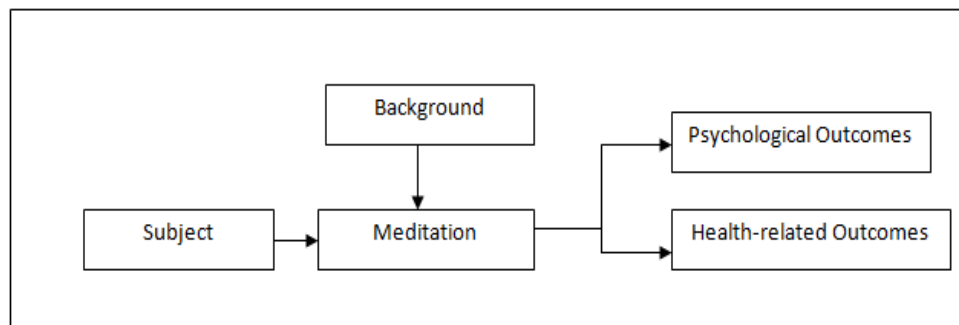


Fig. 1 Meditation



Fig. 2 Mindfulness Meditation[7]

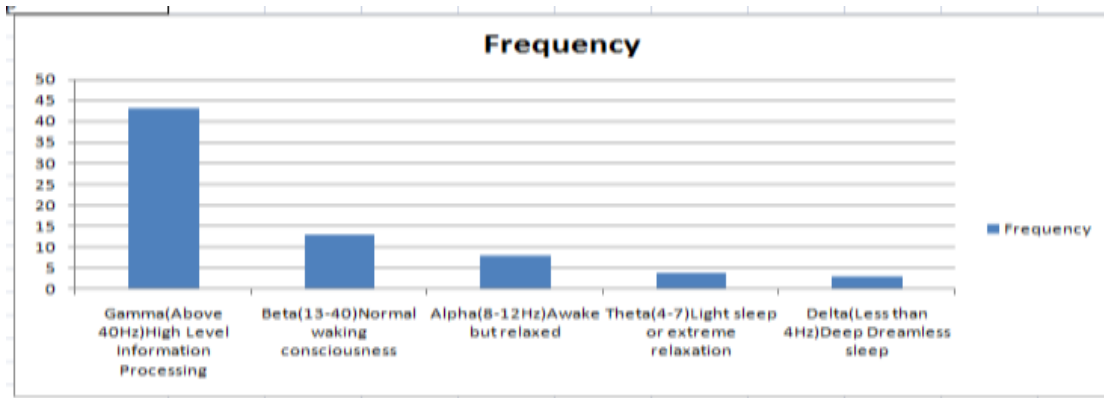
EEG

Many current behavioral, electroencephalographic, and neuroimaging studies have revealed the importance of investigating meditation states to achieve an increased understanding of cognitive and affective neural plasticity, attention, and self-awareness as well as to evaluate their possible clinical implications. The function of electroencephalography is to detect and amplify the bioelectric potential of the brain by electrodes placed on the surface of the scalp. EEG has several strong points as a tool for exploring brain activity. The EEG measures brainwaves of different frequencies within the brain. In relation with the EEG signals, a lot of work has been done to find the significant changes between the signals and the mental states by using different advanced signal processing techniques. EEG studies have utilized these methods to portray the brainwave changes that occur in meditation. [8]

MEDITATION AND BRAIN WAVES EFFECT ON BRAIN

- **Beta Waves (14-24Hz):** Beta Brainwave correspond to the typical “busy mind experience”. The beta frequency range is characterized by a chaotic, fragmented, unbalanced thinking typical of left brain dominance, commonly referred to as the monkey mind.
- **Alpha Waves (8-13Hz):** In the alpha waves the balanced brainwave activity occurs. The more alpha waves that a person is able to produce in ordinary states of consciousness, the easier it is for them to access deeper meditative states.
- **Theta Waves (4-7.5Hz):** In the theta waves balanced brainwave activity increases. The theta state corresponds to the experience of visionary, creative and intuitive levels of experience. It is characterized by inner images and visions that correlate with increased theta activity.
- **Delta Waves (0.5-4Hz):** The delta brings a level of balance that corresponds to the beyond the mind experience at the subtest levels of meditative awareness possible. This is the range in which meditators experience what is termed unified consciousness.[9]

The brainwaves having different frequencies within our brain can be classified as shown in the following graph (with its respective frequency band and the mental state.



LITERATURE REVIEW

In this review paper review various meditation types and the methods used and observes the remarks of these meditation types.

TABLE 1. MEDITATION LITERATURE REVIEW

Sr. No	Author	Year	Meditation Type	Method	Remark	Reference ID
1	Anand B.K. Chhina G.S. Singh B.	1961	Rajyoga Meditation	EEG	No alpha suppression in response to variety stimuli of two yogis	[10]
2	The Venerable Mahasi Sayadaw	1965	Buddhist Satipatthana Meditation	Samatha & vipassana meditation practice	The Stages of Purification performs insight progress	[11]
3	Kasamatsu A, Hirai, T.	1969	Zen Meditation	EEG	Zen meditation could help treat attention deficit and hyperactivity disorder, obsessive-compulsive disorder, anxiety disorder, major depression and other disorders marked by distracting thoughts.	[12]
4	Brown, Daniel P.; Engler, Jack	1980	Mindfulness Meditation	of contemporary indigenous Buddhist meditation practice	The classical subjective reports of meditation stages are more than religious belief systems.	[13]
5	Jon Kobat-zinn	1982	Mindfulness Meditation	Stress Reduction and Relaxation Program	This work does not prove that the meditation practice is directly responsible for stress reduction and relaxation changes.	[14]
6	Shapiro DH Jr.	1982	TM	Long-term and short term meditaors group	A family of techniques which have in common a conscious attempt to focus attention in a non analytical way and an attempt not to dwell on discursive, ruminating thought	[15]

7	Cranson R. Goddard P.H. Orme –Johnson D.	1990	TM	P300	Latency reduced in long term meditation	[16]
8	Lou HC, Kjaer TW, FribergL, Wildschiodtz G, Holm S, Nowak M.	1999	Yoga, Yognidra	H20 PET technique	The (H2)150 PET method may measure CBF distribution in the meditative state as well as during the resting state of normal consciousness, and that characteristic patterns of neural activity support each state.	[10]
9	Elizabeth R. Valentine Philip L.G. Sweet	1999	Mindfulness Meditation	Wilkin's Counting	Improvements in performance on a task of sustained attention for both concentrative and mindfulness meditators in comparison with controls, with greater improvements being associated with longer durations of practice.	[17]
10	Harald Walach , Nina Buchheld , Valentin Buttenmullerc Norman Kleinknecht , Stefan Schmidt	2001	Mindfulness (Vipassana)	FMI(Freiburg Mindfulness Inventory)	The FMI is a useful, valid and reliable questionnaire for measuring mindfulness.	[18]
11	Fabio Ferrarelli Richard Smith Daniela Dentico Brady A. Riedner Corinna Zennig Ruth M. Benca Antoine Lutz Richard J. Davidson Giulio Tononi	2003	Mindfulness Meditation	hdEEG	EEG gamma activity during sleep represents a sensitive measure of the long lasting, plastic effects of meditative training on brain function.	[19]
12	<ul style="list-style-type: none"> • L. I. Aftanas • S. A. Golosh eikin 	2003	Sahaja Yoga Meditation	High Resolution EEG	The θ and α activities in narrow frequency bands reflect the activity of multifunctional neuronal networks selectively associated with processes of cognitive and affective activity.	[20]
13	Baer RA, Smith GT, Allen KB.	2004	Mindfulness Meditation	THE KENTUCKY INVENTORY OF MINDFULNESS SKILLS	Mindfulness skills are differentially related to aspects of personality and mental health, including neuroticism, psychological symptoms, emotional intelligence, alexithymia, experiential avoidance, dissociation, and absorption.	[21]
14	Wiveka Ramel Philippe R. Goldin, Paula E. Carmona John R. McQuaid	2004	Mindfulness Meditation	MBSR	MM practice primarily leads to decreases in ruminative thinking, even after controlling for reductions in affective symptoms and dysfunctional beliefs.	[22]

15	B. Rael Cahn John Polich	2006	Mindfulness and Concentration meditation	EEG ERP fMRI	Meditation state and trait shows considerable discrepancy among results, a fact most likely related to the lack of standardized designs for assessing meditation effects across studies.	[23]
16	Neela Iyer A.Prabhu Britto Vladimir Petrov Velikov Justin Chernow Elizabeth Maier Dr. A.Nagappan Dr.M.Rangasamy Dr. N. Malmurugan Dhyanyogi Omdasji Maharaj	2008	Yoga	EEG	The Divine Sound is expected to be very safe for human physiological systems and may be used as a good meditative guidance, even for a whole day continuously.	[24]
17	Eberth J. Sedlmeier P.	2012	Mindfulness	MBSR	MBSR seems to have its most powerful effect on attaining higher psychological well-being, whereas pure mindfulness meditation studies reported the largest effects on variables associated with the concept of mindfulness.	[25]
18	G. Madhavi Kanakadurga	2012	Yogic Meditation	Quasi Experimental Design	Significant improvement in the attention regulation of the students after meditation practice.	[26]
19	Yugandhara Meshram, Prajakta Fulpatil	2012	Sudarshan Kriya	EEG	Wavelet Transform proves out to be the best method for the time-frequency analysis of EEG signals as it gives the required frequency information along with the time instance at which it occurs.	[27]
20	Peter Sedlmeier, Juliane Eberth, Marcus Schwarz, Doreen Zimmermann, Frederik Haarig, Sonia Jaeger, and Sonja Kunze	2012	TM, Zen Meditation	Meta-analysis		[28]
21	David W. Orme- Johnson Vernon A. Barnes	2013	TM	CMA(Compre hensive Meta- Analysis	TM Practice is more effective than treatment as usual and most alternative treatments with greatest effects observed in individuals with high anxiety.	[29]
22	Oldrich Vysata	2014	Samatha –	EEG	Increased FD during	[30]

	Martin Schatz Jakub Kopal Jan Burian Ales Prochazka Kuchynka Jiri Jakub Hort Martin Valis		vipassana		meditation can be interpreted as an increase in self-similarity of EEG signals during self organisation of hierarchical structure oscillators in the brain.	
23	Mane Satish Ra, Deokar Rekha Rb, Kambale Shubhangi R	2014	Yoga	Experimental group with high and low stress	The high stress affects students' performance negatively. Yoga gives good effects on stress reduction that.	[31]
24	Florian Kurth, AllanMacKenzieGraham, Arthur W. Toga, and Eileen Luders	2015	Mindfulness	MRI, VBM(Voxel-Based Morphometry	The positive correlation between meditation practice years and asymmetry near the posterior intraparietal sulcus may suggest that meditation is accompanied by changes in attention processing.	[32]
25	Aviva Berkovich-Ohana, Joseph Glicksohn, Abraham Goldstein	2015	Mindfulness	EEG	Studying the Default Mode Network using EEG Functional connectivity as well as the importance of studying meditation in relation to it.	[33]

CONCLUSION

In the present review we studied all type of meditation gives the positive effects physically and mentally, It can reduce stress, improve concentration level, attention level and give the positive energy. Mindfulness meditation is not the new concept in most of the clinical problems in both physical and psychological problems mindfulness meditation gives the very effective positive results. Using EEG data we can observe the brain states improvement due to the mindfulness meditation and avoid the mental, behavioral and structural problems. Meditation can improve the functional connectivity also.

REFERENCES:

- [1] Wallace, B.A. "The Buddhist tradition of Samatha: Methods for refining and examining consciousness" Journal of Consciousness Studies, 6, 175-187, 1999.
- [2] J. Achterberg, Mind body interventions, meditation, in B. Berman (Ed.), *Alternative medicine, expanding medical horizons* (Washington DC: Office of Alternative Medicine, National Institute of Health, 1992).
- [3] E. McSherry, Medical economics, in D. Wedding (Ed.), 463-484, *Medicine and behaviour*, (St Louis: Mosby and Co, 1990).
- [4] [Onlineavailable] <http://nccam.nih.gov/health/meditation/>, accessed Feb, 2006.
- [5] [Onlineavailable] http://freemeditations.com/raja_yoga.html
- [6] Young, Shinzen "Purpose and method of Vipassana meditation" Humanistic Psychologist, 22, 53-61, 1994.
- [7] Yi-Yuan Tang, Britta K. Hölzel and Michael I. Posner "The neuroscience of mindfulness meditation", nature reviews neuroscience, Macmillan Publishers Limited. Volume 16, 215, April 2015.
- [8] Shih-Feng Wang, Yu-Hao Lee, Yung-Jong Shiah, Ming-Shing Young, "Time-Frequency Analysis of EEGs Recorded during Meditation," Robot, Vision and Signal Processing (RVSP), First International Conference on , vol., no., pp.73,76, 21-23, November 2011.
- [9] [Onlineavailable] <https://synchronicity.org/free-infographics/meditation-and-its-effects-on-brainwaves>.
- [10] Lou HC, Kjaer TW, Friberg L, Wildschiodtz G., Holm S, Nowak M.A. "150-H2O PET study of meditation and the resting state of normal consciousness" Hum Brain Map,98-105,1999.
- [11] The Venerable Mahasi Sayadaw "The Progress of Insight (Visuddhiñāna-katha)"1965.
- [12] Kasamatsu A. & Hirai T. "An electroencephalographic study of Zen meditation(zazen)" Psychologia,12.225, 2015.

- [13] Brown, Daniel P. Engler, Jack “The stages of mindfulness meditation: A validation study” *Journal of Transpersonal Psychology*, 12, 143-192, 1980.
- [14] Kabat-Zinn, J. “An outpatient program in behavioral medicine for chronic pain patients based on the practice of mindfulness meditation: Theoretical Considerations and preliminary results” *General Hospital Psychiatry*, 4, 33-47, 1982.
- [15] Shapiro DH Jr.” Overview: clinical and physiological comparison of meditation with other self-control strategies”. *Am J Psychiatry*. 139(3):267-274, 1982.
- [16] Cranson,R.,Goddard, P.H., & Orme-Johnson, D. “P300 under conditions of temporal uncertainty and filter attenuation: Reduced latency in long-term practitioners of TM” *Psychophysiology*,27,S23,1990.
- [17] Elizabeth R. Valentine, Philip L.G. Sweet, ”Meditation and attention: a comparison of the effects of concentrative and mindfulness meditation on sustained attention”, *Mental Health, Religion & culture*, Volume 2, November 1, 1999.
- [18] Buchheld, N., Grossman, P., & Walach, H. “Measuring mindfulness in insight meditation(Vipassana) and meditationbased psychotherapy: The development of the Freiburg Mindfulness Inventory(FMI)” *Journal of Meditation and Meditation Research*,1, 11-34,2001.
- [19] Fabio Ferrarelli, Richard Smith, Daniela Dentico, Brady A. Riedner, Corinna Zennig, Ruth M. Benca Antoine Lutz, Richard J. Davidson, Giulio Tononi ”Experienced Mindfulness Meditators Exhibit Higher Parietal-Occipital EEG Gamma Activity during NREM Sleep” Open access *PLOS* Vol.8, Issue 8, August 2013.
- [20] Aftanas,L.I., Goloshekin, S.A.”Changes in cortical activity in altered states of consciousness: the study of meditation by high-resolution EEG.Human” *Physiology*,28,2,143-151, 2003.
- [21] Baer, R.A., Smith, G. T., & Allen, K.B.”Assessment of mindfulness by self report: The Kentucky Inventory of Mindfulness Skills” *Assessment*, 11, 191-206, 2004.
- [22] Wiveka Ramel, Philippe R. Goldin, Paula E. Carmona,and John R. McQuaid ” The Effects of Mindfulness Meditation on Cognitive Processes and Affect in Patients With Past Depression” *Cognitive Therapy and Research*, Vol. 28, No. 4, , pp. 433–455, August 2004 2.
- [23] B.Rael Cahn, John Polich ”Meditation States and Traits: EEG, ERP and Neuroimaging Studies” *Psychological Bulletin*, Vol.132, No.2, 180-211, 2006.
- [24] Neela Iyer, A.Prabhu Britto, R.Satyasundari, D.Saraswady, A.Nagappan, N.Malmurugan and Dhyanyogi Omdasji Maharaj,” Low Decibel Power Infrasound in Divine Sound Meditation”, ISSN: 0974 – 3987 *IJBST*, 1(1):1-9,2008.
- [25] Eberth, J., & Sedlmeier,P. “The effect of mindfulness meditation: A meta-analysis. *Mindfulness*” ,3, 174-189, 2012.
- [26] G. Madhavi Kanakdurga, Dr. D. Vasanta Kumari,”Attention Regulation of Mediators and non-mediators of class IX”, *Indian Journal of Applied Research*, vol 1,Issue 5, February 2012.
- [27] Yugandhara Meshram, Prajakta Fulpatil,” Review Paper on Electroencephalographic Evaluation of Sudarshan Kriya”, *International Journal of Science and Research (IJSR)* ISSN (Online): 2319-7064,2012.
- [28] Peter Sedlmeier, Juliane Eberth, Marcus Schwarz, Doreen Zimmermann, Frederik Haerig, Sonia Jaeger, and Sonja Kunze” The Psychological Effects of Meditation: A Meta-Analysis”, *Psychological Bulletin*, Vol. 138, No. 6, 1139–1171, 2012.
- [29] David W. Orme-Johnson Vernon A. Barnes ,”Effects of the Transcendental Meditation Technique on Trait Anxiety: A Meta-Analysis of Randomized Controlled Trials”, *The journal of alternative and Complementary Medicine*, vol 19, 2013.
- [30] Oldrich Vysata, Martin Schatz, Jakub Kopal, Jan Burian, Ales Prochazka,Kuchynka Jir, Jakub Hort, Martin Valis “Non-Linear EEG Measures in Meditation”, *J. Biomedical Science and Engineering*,7, 731-738, 2014.
- [31] Mane Satish Ra, Deokar Rekha Rb, Kambale Shubhangi Rc,” Management of Stress through Yoga Practice in Academic Performance of College Students”, *Online International Interdisciplinary Research Journal*, {Bi-Monthly}, ISSN 2249-9598, Volume-IV, Issue-II, March-April 2014.
- [32] Florian Kurth, Allan MacKenzie-Graham, Arthur W. Toga, and Eileen Luders, “Shifting brain asymmetry: the link between meditation and structural lateralization”, *Soc Cogn Affect Neurosci* (2015) 10 (1): 55-61. doi: 10.1093/scan/nsu029 First published online: March 17, 2014 .
- [33] Aviva Berkovich-Ohana, Joseph Glicksohn, and Abraham Goldstein, “Studying the default mode and its mindfulness-induced changes using EEG functional connectivity”, *a Soc Cogn Affect Neurosci* (2014) 9 (10): 1616-1624. doi: 10.1093/scan/nst153 First published online: November 4, 2013.

An Effective Algorithms for Optimization of Process Planning and Scheduling: A Review

H.R. Deepika¹, B. Yogesha², H.V. Ramakrishna²

¹Department of Industrial & Production Engineering, Malnad College of Engineering, Hassan, Visvesvaraya Technological University, Belagavi, India.

²Department of Mechanical Engineering, Malnad College of Engineering, Hassan, Visvesvaraya Technological University, Belagavi, India.

Email: deepikahrip@gmail.com

Abstract— The main objective of this paper is to present an effective algorithms to address the manufacturing problems. This paper provides the information about how various authors, researchers, scientists have implemented algorithms in various manufacturing system. This study involves a rigorous review of recent works carried out using different types of algorithms in optimizing the process planning and scheduling. The outcome of this study will help in the manufacturing sector to determine the best algorithm that is best suited for their optimization problems.

Keywords— Algorithm, Process Planning, Scheduling, optimization.

1. INTRODUCTION

Reducing the time from start to delivery by eliminating the source of waste in the work flow is one of the basic concepts. A manufacturing function that can be employed to handle such tasks is manufacturing process planning (MPP). This work focuses on a study of an optimization approach that can be used to address issues that are critical in providing an optimal match of activities and resources in a multi resource manufacturing line that produces multiple parts with reconfigurable flows. Such issues include: process selection, process sequencing and part load scheduling, i.e. the order of processing multiple parts [1]. All these factors caused the manufacturing industry to become highly competitive and new market entries from low wage countries have put pressure on management to make changes in their operating business [2]. One way by which manufacturing plants adapt to those environmental dynamics is the engagement in manufacturing process innovation [3].

Traditionally, process planning and scheduling for parts were carried out in a sequential way, where scheduling was done after process plans had been generated. Considering the fact that the two functions are usually complementary, it is necessary to integrate them more tightly so that performance of a manufacturing system can be improved greatly [4]. Process planning for prismatic parts is a very complex and difficult process. For a prismatic part with complex structures and numerous features, process planning involves selecting machining operations for every feature and sequencing them considering precedence constraints, choosing available manufacturing resources, determining setup plans, and machining parameters, and so forth. In Computer-aided process planning systems, these activities can be carried out simultaneously to achieve an optimal plan, thus the manufacturing efficiency could be largely increased or the production cost could be decreased. So, process planning problem is well known as a combinatorial optimization problem with constraints. With the advance of computer technology, some artificial intelligence (AI) techniques are used to solve combinatorial optimization problem. For example, some bioinspired algorithms are applied in complex decision-making process of solve combinatorial optimization problem [5, 6].

Optimization, in general, is a process of finding the best feasible solution to a problem. An optimization problem can be viewed as a task, the goal of which is to configure a set of given parameters to reach an optimal solution of the given problem and, simultaneously, meet the predefined criteria. The global optimization [7, 8] is a process where such solution is required with the condition that no better solution exists. Solutions are termed bad and good in terms of an objective to which they are optimized. The field of optimization has grown rapidly in recent decades.

2. REVIEW ON PROCESS PLANNING AND SCHEDULING

In General, the manufacturing process is planned in a static manner, whether it is prepared by human or with computer assistance. However, due to the dynamic fluctuation of customer demands in the market, manufacturing enterprises are facing difficulties in rapidly responding to Market changes. Thus, it might be useful if the process plan could be dynamically modified to consider the current state of the manufacturing system so as to study the manufacturing performance in unpredictable situation. For the purpose of increasing the responsiveness of manufacturing systems to handle unstable market changes, the integration of Process planning and production scheduling concept has been introduced [9]. Process planning and production planning are the links between product development and production. However, there is no single definition of these terms and they differ between type of production as well as organization. This work considers only metal cutting using CNC technology. The overall concept of process planning can be divided into many different sub-levels, where one such categorization is made according to the constraints that restricts the possible selections during process planning [10].

Production scheduling is the activities performed in manufacturing companies to manage and control the execution of the production process. Scheduling has to consider operations sequences, machine load and availability of machines. This means that scheduling is based on predetermined process planning. Process planning determines the manufacturing process routing and acts as a bridge between product design and manufacturing. That is, it is a process of allocating resources and operations for manufacturing of products. Process planning and production scheduling activities in a job shop are closely related to each other, but typically they have been handled independently. Process planning has been done without considering the current capacity of the shop in terms of effective use of resources. Also, scheduling has been performed without regard to the opportunities that alternative process plans can provide for acceleration of production flows. In scheduling, an alternative process plan enables the allocation of operations to other machines with flexibility of, thus reducing the possibility of the collision between a job and a machine [11]. when the level uncertainty and randomness in the system increases. A general rule is that as the uncertainty increases, the value of scheduling decreases [12]. Trying to predict and optimize the behavior of a complex system with many uncertainties and high level of randomness is in most cases a waste of time and resources. On the other hand, for more stable systems, putting more effort into scheduling often can improve performance and the use of advanced optimizing methods might in these cases be appropriate. How scheduling is performed also depends on the management of the company and the organization around the scheduling function. Some companies may not have an explicit scheduling method; it is just something that is done implicitly by for instance the workers or shop floor management, while others have very strict approaches that are decided upon by the management. How the schedule is used can also differ between companies and also between different users in the same company. Besides the obvious use on the shop floor other potential uses are to determine system capacity for a higher level production planning system, where the generated schedule is used to determine the feasibility of the production plan or by the sales department to determine if an order with a given lead time should be accepted [13].

3. DIFFERENCE BETWEEN PROCESS PLANNING AND SCHEDULING

The difference between planning and scheduling is a somewhat blurred area and the definition to some degree varies between different sources in the literature. The general idea is that planning is done at a higher, aggregated level over longer time periods and that scheduling involves more details and is done over shorter time periods. As the MPC activities proceed from planning to scheduling each step adds more details and brings the initial demands closer to being executed on the shop floor. Planning uses expected demands and forecasts and therefore always contains some level of uncertainty. As the plans evolve through the planning and scheduling process and details are added, that uncertainty is gradually removed.

Process planning and scheduling used to link product design and manufacturing are two of the most important functions in a manufacturing system. A process plan specifies what manufacturing resources and technical operations/routes are needed to produce a product (a job). The outcome of process planning includes the identification of machines, tools and fixtures suitable for a job, and the arrangement of operations and processes for the job. Typically, a job may have one or more alternative process plans. With the process plans of jobs as input, a scheduling task is to schedule the operations of all the jobs on machines while precedence relationships in the process plans are satisfied [14]. Although there is a close relationship between process planning and scheduling, the integration of them is still a challenge in both research and applications. Process planning and scheduling are two key techniques of the development of distributed and collaborative manufacturing [15]. Although process planning can enhance productivity of manufacturing systems and scheduling can optimise process series, some researches showed that the separated process planning and scheduling systems could not improve the productivity of manufacturing system largely [16, 17].

Traditionally, the integration and interactions of process planning and scheduling are through an iterative and empirical fashion. The process planning system first generates a reasonable process plan for each part. Crucial processes in the system include determining suitable manufacturing resources (machines and tools), selecting set-up plans and sequencing machining operations of the part. The scheduling system then specifies the schedule of manufacturing resources on each operation (job) of the parts according to the

importance of jobs, availability of resources and time constraints. It is usually difficult to produce a satisfactory result in a single iteration of the execution of the two systems. For the process planning system, the decision of selecting machines and tools is usually made based on objectives to achieve the minimal manufacturing cost and ensure the good manufacturability of a part [18].

4. REVIEW ON EFFECTIVE ALGORITHMS

Genetic Algorithm (GA) is effective and robust method for solving many optimization problems. However, it may take more runs (iterations) and time to get optimal solution. The execution time to find the optimal solution also depends upon the niching-technique applied to evolving population. The information about how various authors, researchers, scientists have implemented GA on GPGPU (General purpose Graphics Processing Units) with and without parallelism. Many problems have been solved on GPGPU using GA. GA is easy to parallelize because of its SIMD nature and therefore can be implemented well on GPGPU. Thus, speedup can definitely be achieved if bottleneck in GAs are identified and implemented effectively on GPGPU [19].

Conflict avoidance (CA) plays a crucial role in guaranteeing the airspace safety. To minimize the risk of premature convergence being faced by current approaches and obtain higher quality solutions, an effective strategic framework based on a memetic algorithm (MA), which can markedly improve search capability via a combination of population-based global search and local improvements made by individuals. In addition, a specially designed local search operator and an adaptive local search frequency strategy are proposed to improve the solution quality. Furthermore, a fast GA is presented as the global optimization method. Empirical studies using real traffic data of the Chinese air route network and daily flight plans show that our approach outperformed the existing approaches including the GA based approach and the cooperative coevolution based approach as well as some well-known memetic algorithm based approaches [20].

The continuous growth of air traffic has led to acute airspace congestion and severe delays, which threatens operation safety and cause enormous economic loss. Flight assignment is an economical and effective strategic plan to reduce the flight delay and airspace congestion by reasonably regulating the air traffic flow of China. However, it is a large-scale combinatorial optimization problem which is difficult to solve. In order to improve the quality of solutions, an effective multi-objective parallel evolution algorithm (MPEA) framework with dynamic migration interval strategy is presented [21].

A competitive memetic algorithm (CMA) is proposed to solve the multi-objective distributed permutation flow shop scheduling problem (MODPFSP) with the makespan and total tardiness criteria. Two populations corresponding to two different objectives are employed in the CMA. Some objective-specific operators are designed for each population, and a special interaction mechanism between two populations is designed. Moreover, a competition mechanism is proposed to adaptively adjust the selection rates of the operators, and some knowledge-based local search operators are developed to enhance the exploitation ability of the CMA [22].

An optimization algorithm is a procedure which is executed iteratively by comparing various solutions till the optimum or satisfactory solution is found. Accepting the best solution after comparing a few design solutions is the indirect way of achieving optimization in many industrial design activities. There is no way of guaranteeing an optimal solution with this simplistic approach. Optimization algorithms on the contrary, begin with one or more design solutions supplied by the user and then iteratively check new design solutions, relative search spaces in order to achieve the true optimum solution [23].

The study involves a rigorous assessment of catalogues of recent works carried out using different types of evolutionary algorithms in optimizing the scarce water resources in the semi-arid regions with particular reference to irrigation water management. The behavior and outcome of these techniques under different application types are discussed explicitly. Issues that need to be addressed with respect to the performances of these techniques during different iteration processes are also discussed. The study covers different application areas which include irrigation water allocation and scheduling, irrigation planning with special focus on crop planning and pattern; reservoir operations and irrigation water distribution network. Arid and semi-arid regions experience low annual rainfall and therefore it is imperative to optimize the available water resources for agricultural purposes via irrigation so as to promote food security. The outcome of this study will help stakeholders in the irrigation sector to determine the best evolutionary algorithm that is best suited for their optimization problems [24].

5. CONCLUSIONS

The focus is brought on problems related to the design, organization, and management of the manufacturing system. From the recent published literature, the author has identified the following types of problems as the most addressed: production planning and scheduling of the manufacturing system.

REFERENCES:

- [1]. N. Ismail, F. Musharavati, A S M Hamouda, A R Ramli. Manufacturing process planning optimisation in reconfigurable multiple parts flow lines. *Journal of Achievements in Materials and Manufacturing Engineering*, 31, 2, 2008.
- [2]. Idris F, Rejab R, Ahmad A. Relationships between Investments in Advanced Manufacturing Technology (AMT) and Performances: Some Empirical Evidences. *European Journal of Economics, Finance and Administrative Sciences*, Issue 13, 67-78, 2008.
- [3]. Lee Jung Young, Swink Morgan, Pandejpong, Temyos. The Roles of Worker Expertise, Information Sharing Quality, and Psychological Safety in Manufacturing Process Innovation: An Intellectual Capital Perspective. *Production and Operations Management*, Vol. 20, No. 4, 556-570, 2011.
- [4]. Xinyu Li, Liang Gao, Chaoyong Zhang and Xinyu Shao. A review on Integrated Process Planning and Scheduling. *International Journal of Manufacturing Research*, Vol. 5, No. 2, 2010.
- [5]. J V'ancza and A M'arkus. Genetic algorithms in process planning. *Computers in Industry*, vol. 17, no. 2-3, pp. 181-194, 1991. M.Dorigo, V. Maniezzo, and A. Colomi, "Ant system: optimization by a colony of cooperating agents," *IEEE Transactions on Systems, Man, and Cybernetics B: Cybernetics*, vol. 26, no. 1, pp. 29-41, 1996.
- [6]. P R Srivastava, A Varshney, P Nama, X Yang. Software test effort estimation: a model based on cuckoo search. *International Journal of Bio-Inspired Computation*, vol. 4, no. 5, pp. 278-285, 2012.
- [7]. Leo Liberti and Nelson Maculan. *Global Optimization: From Theory to Implementation*, Springer, ISBN-13: 978-0387282602, 2006.
- [8]. Thomas Weise, *Global Optimization Algorithms - Theory and Application*, 3rd edition, 2011.
- [9]. E Raj Kumar, K Annamalai. Nature Inspired Algorithm For Computer Aided Process Planning. *International Journal of Engineering Research and Applications*. Vol. 2, Issue 5, pp.481-484, 2012.
- [10]. Wiendahl H P. Changeable Manufacturing - Classification, Design and Operation. *Annals of the CIRP*, 56(2): p. 783-809, 2007.
- [11]. Hyung rim choi, byung joo park. Integration of Process Planning and Job Shop Scheduling Using Genetic Algorithm . *Proceedings of the 6th WSEAS International Conference on Simulation, Modelling and Optimization*, Lisbon, Portugal, September 22-24, 2006.
- [12]. Marriott and Stuckey. *Programming with Constraints: An Introduction*. MIT Press. 1998.
- [13]. Kempf Uzoy and Smith Gary. Evaluation and comparison of production schedules. *Computers in industry*. 42, pp 203 - 220, 2000.
- [14]. Sugimura N, Shrestha R, Tanimizu Y and Iwamura K. A study on integrated process planning and scheduling system for holonic manufacturing', *Process Planning and Scheduling for Distributed Manufacturing*, Springer, London, pp.311-334, 2006.
- [15]. Wang L and Shen W. DPP: An agent based approach for distributed process planning. *Journal of Intelligent Manufacturing*, Vol. 14, pp.429-439, 2003.
- [16]. Shobrys D and White D. Planning, scheduling and control systems: Why can they not work together. *Computers and Chemical Engineering*, Vol. 24, pp.163-173, 2000.
- [17]. Saygin C and Kilic S. Integrating flexible process plans with scheduling in flexible manufacturing systems. *International Journal of Advanced Manufacturing Technology*, Vol. 15, pp.268-280, 1999.
- [18]. W D Li and C A McMahon. A Simulated Annealing-based Optimization Approach for Integrated Process Planning and Scheduling. *International Journal of Computer Integrated Manufacturing*, Taylor & Francis, 20 (01), pp.80-95, 2006.
- [19]. A J Umbarkar, M S Joshi and N M Rothe. Genetic algorithm on general purpose graphics processing unit: Parallelism review. *ICTACT journal on soft computing*, vol. 03, Issue. 2, 2013.
- [20]. Guan Xiangmin, Zhang Xuejun, Han Dong, Zhu Yanbo, Lv Ji, Su Jing. A strategic flight conflict avoidance approach based on a memetic algorithm. *Chinese Journal of Aeronautics*, 27(1): 93-101, 2014.
- [21]. Zhang Xuejun, Guan Xiangmin, Zhu Yanbo, Lei Jiaying. Strategic flight assignment approach based on multi-objective parallel evolution algorithm with dynamic migration interval. *Chinese Journal of Aeronautics*, 28(2): 556-563, 2015.
- [22]. Jin Deng, Ling Wang A competitive memetic algorithm for multi-objective distributed permutation flow shop scheduling problem *Swarm and Evolutionary Computation (Article In Press)*.
- [23]. Lin D K J and W Tu. Dual response surface optimization. *Journal of Quality Technology*, Vol. 27, No.1, pp. 34-39, 1995.
- [24]. Akinola Ikudayisi, Josiah Adeyemo. Irrigation water optimization using evolutionary algorithms. *Environmental Economics*, Volume 6, Issue 1, 2015.

Process Intensification of Colemanite Leaching Using Sulfuric Acid in a Batch Reactor

Ademola S. OLUFEMI^{1*}, Mayowa A. AZEEZ², and Oluwafemi O. OLAYEBI³

¹Department of Chemical/Petroleum Engineering, Niger Delta University, Wilberforce Island, Bayelsa State, Nigeria.

²Department of Chemistry, State University of Ekiti, Ado-Ekiti, Ekiti State, Nigeria.

³Department of Chemical Engineering, Federal University of Petroleum Resources, Effurun, Delta State, Nigeria.

E-mails: ¹olufemi.stanford@gmail.com, ²mayowa.azeez@eksu.edu.ng, ³olayebi.oluwafemi@fupre.edu.ng

Abstract— This contribution investigated methods of intensifying the leaching of colemanite using sulphuric acid for the improvement of boric acid recovery. Boric acid is one of the most commonly used boron compounds produced by dissolving colemanite ($2\text{CaO}\cdot 3\text{B}_2\text{O}_3\cdot 5\text{H}_2\text{O}$) in aqueous sulfuric acid which results in the formation of gypsum ($\text{CaSO}_4\cdot 2\text{H}_2\text{O}$) as a by-product and must be separated from the main product. The dissolution of colemanite gives the amount of boric acid formed; the purity and crystallization of boric acid are affected by filtration of gypsum. In this study, and the factors that were examined in this study were stirrer agitation speed, particle size, reaction temperature on the dissolution of colemanite in the reaction of boric acid production. Colemanite having the same elemental chemical composition and particle size, sulfuric acid and distilled water were used as reactants for the boric acid production reaction in this study. The crushing of the colemanites were one in a jaw crusher, ground in a hammer mill and then sieved. The biggest diameter of the colemanite minerals was $150\ \mu\text{m}$ and the experiments were performed at different particle sizes of colemanite (0-150, 0-250 and 250-1000 μm), temperatures (70- 90 °C) and stirring speed (350-500 rpm). The results obtained, showed that increasing the acid concentration results in a significant increase boric acid recovery. The highest recovery was obtained at 85 °C temperature. Increasing the mixing speed from 350 rpm to 500 rpm increased the recovery by 5.5%. Thus, the increase in agitating speed from 350 to 500 rpm resulted in a significant increase in boric acid recovery. Thus, it was concluded that agitation have a significant effect on boric acid recovery above 500 rpm. The batch process proved to be better than the semi-batch process in terms of the amount of boric acid recovered.

Keywords— Colemanite, Boric acid, Sulfuric acid, Batch Reactor, Temperature, Stirring rate, and Particle size.

INTRODUCTION

Boron minerals can be used in some industrial area as crude minerals. In general, their applications after refining and end-products are wider than crude ones. Boron minerals, borates and compounds have a very wide range of applications. With escalating depletion of boron mineral reserve, boron minerals including Tincal [$\text{Na}_2\text{B}_4\text{O}_7\cdot 10\text{H}_2\text{O}$], Kernite [$\text{Na}_2\text{B}_4\text{O}_7\cdot 4\text{H}_2\text{O}$], Ulexite [$\text{NaCaB}_5\text{O}_9\cdot 8\text{H}_2\text{O}$], Probertite [$\text{NaCaB}_5\text{O}_9\cdot 5\text{H}_2\text{O}$], Colemanite [$\text{Ca}_2\text{B}_6\text{O}_{11}\cdot 5\text{H}_2\text{O}$], Pandermite [$\text{Ca}_4\text{B}_{10}\text{O}_{19}\cdot 7\text{H}_2\text{O}$], Boracite [$\text{Mg}_3\text{B}_7\text{O}_{13}\text{Cl}$], Szaibelyite [$\text{MgBO}_2(\text{OH})$], Sassolite [H_3BO_3], and Hydroboracite [$\text{CaMgB}_6\text{O}_{11}\cdot \text{H}_2\text{O}$] are becoming an important source of boric acid (Özbayoğlu et al.,1992).

Colemanite is used as the raw material in the boric acid production. It is one of the most important boron minerals in the world. More than 200 boron minerals have been known but relatively few of them have commercial significance (Roskill, 2002). Colemanite, like other borates, is a complex mineral that is found in desert borax deposits and Tertiary clays in old lake beds. Colemanite is a secondary mineral, meaning that it occurs after the original deposition of other minerals. The mineral borax is directly deposited in regions from the evaporation of water due to run off from nearby mountain ranges. The runoff is rich in the element boron and is highly concentrated by evaporation in the arid climate. Ground water flowing through the borax sediments is believed to react with the borax and form other minerals such as ulexite. It is believed that colemanite may have formed from ulexite. Colemanite is found in geodes within the borax sediment. It's exact means of formation are still not well understood (Amethyst Galleries, 1997). The picture of colemanite mineral is given in Figure 1.1. The basic structure of colemanite contains endless chains of interlocking $\text{BO}_2(\text{OH})$ triangles and $\text{BO}_3(\text{OH})$ tetrahedrons with calcium, water molecules and extra hydroxides interspersed between the chains (Chuck Brown, 2000).



Figure 1: Picture of colemanite mineral

Colemanite [$\text{Ca}_2\text{B}_6\text{O}_{11} \cdot 5\text{H}_2\text{O}$] is frequently leached by using sulphuric acid, though there are various leaching agents (also called lixivants). Leaching can be done by different liquids: acids, bases, water and chelating agents.

However, since acidic medium are advantageous for the dissolution of metals, acids are commonly used for the leaching of heavy metals. Sulphuric acid is the most common leaching agent because of its chemical properties and also its relatively low cost (Napo et al., 2011).

The rate of leaching depends on the parameters used such as temperature, time, pH, particle size, concentration of lixiviant, slurry density and agitation speed (Gupta and Mukherjee, 1990).

Boric acid can be viewed as a hydrate of boric oxide and exists both as a trihydrate, orthoboric acid ($\text{B}_2\text{O}_3 \cdot 3\text{H}_2\text{O}$ or H_3BO_3), and as a monohydrate, metaboric acid ($\text{B}_2\text{O}_3 \cdot \text{H}_2\text{O}$ or HBO_2). Only the more stable orthoboric acid form is of commercial importance and is usually referred to simply as boric acid. The terms "pyroboric acid" and "tetraboric acid" are sometimes encountered in the literature, but these acids do not actually exist as solid-phase compounds (Ullmann, 2002). Boric acid is white granule or powder. Its density is 1.435 g/cm^3 . It melts at $171 \text{ }^\circ\text{C}$. Solubility in water at $20 \text{ }^\circ\text{C}$ is $4.7 \text{ g boric acid/ g solution}$ (Patnaik, 2002).

Boric acid is used to make variety of glasses comprising fiber glass, heat resistant borosilicate glass and sealing glasses and also used to make porcelain. Major use of boric acid is to prepare a number of boron containing compounds which include inorganic borate salts, boron halides, borate esters, fluoroborates and many boron alloys. The usage of boric acid are: antiseptic, eye washes and ointments; a preservative in natural products; to protect wood against insect damage; in washing citrus fruits; as a catalyst in hydrocarbon oxidation; as a flame retardant in cellulose insulation; in nickel electroplating baths; and as a buffer in ammonia analysis of wastewaters by acid titration (Patnaik, 2002).

Heterogeneous solid-liquid reactions leading to crystallization of the product are widely used in production of many industrial chemicals. Some examples for solid-liquid reaction crystallizations are listed in Table 1.

Table 1: Some examples of solid-liquid reaction crystallizations (Bechtloff et al., 2001)

Reaction System
Calcium citrate + Sulfuric acid \rightarrow Citric acid + Calcium sulfate
Oxalic acid + Borax \rightarrow Sodium oxalate + Boric acid
Borax + Propionic acid \rightarrow Sodium propionate + Boric acid
Colemanite + Sulfuric acid \rightarrow Boric acid + Gypsum
Sodium sulfide + Benzylchloride \rightarrow Benzylsulfide + Sodiumchloride

Different type of behavior of reacting solid particles can be seen. Only a solid phase reaction can occur on the surface of the particles if the solid reactant is insoluble in the reaction medium. The shrinking core model developed by Yagi and Kunii (1955, 1961) explains this type of behavior of reacting solid particles. According to this model, the reaction occurs first at the outer skin of the particles. Then, the zone of the reaction moves toward the center of the solid particle leaving behind a solid product layer called as ash (Levenspiel, 1999).

If the solid has a slight or a high solubility, a liquid phase reaction may dominate the process. So, the dissolution of solid reactant and the crystallization of the product happen simultaneously. When the fluid becomes supersaturated, the solid product precipitates. However, the solid product may cover solid reactant. It may lead to a reduced reaction rate or incomplete conversion of solid reactant. (Bechtloff et al., 2001). Table 2 shows the studies on dissolution of colemanite in various mediums, the reaction of colemanite with sulfuric acid is heterogeneous solid-liquid reaction leading to crystallization of the product.

Table 2. Studies on dissolution of colemanite in various mediums

Researchers	Medium	Parameters	Results(Empirical formulas)
Kocakerim and Alkan (1987)	Water saturated with SO ₂	Particle size (250-1700 μm) Temperature (11-40 °C) Stirring rate (200-1000 min ⁻¹)	$1 - (1 - X)^{1/3} = \frac{bk_s C_g M_B}{\rho_B R} t$
Kum and coworkers (1993)	Ammonium chloride solutions	Calcination temperature(300-460 °C) Solution concentration(1-3 mol L ⁻¹) Reaction temperature (25-65 °C) Pre-hydration	$(1 - X)^{-1} - 1 = k [NH_4Cl]^{3/4} t$
Özmetin and coworkers (1996)	Aqueous CH ₃ COOH solutions	Particle size (0.137- 0.081 mm) Solid-to-liquid ratio (5-35 g mL ⁻¹) Temperature (10.6- 50 °C)	$-\ln(1 - X) = 56664(D)^{-1.42} (S/L)^{-0.27} \exp(-6193.0/T)t$
Gürbüz and coworkers (1998)	Boric acid solutions	Boric acid concentration (0-20 % wt)	Solubility (1.7- 19.6 g kg solution ⁻¹)
Temur and coworkers (2000)	H ₃ PO ₄ solutions	Particle size (250-1400 μm) Acid concentration (1.43-19.52 wt %) Solid-to-liquid ratio (0.02-0.08 g mL ⁻¹) Stirring rate (300-600 min ⁻¹) Reaction temperature (2.5 -35 °C)	$1 - (1 - X)^{1/3} = (5.87 \times 10^9)(D)^{-0.744} (S/L)^{-0.453} (C)^{0.328} \exp^{-53.91/RT} t$
Küçük and coworkers (2000)	Water saturated with SO ₂	Particle size (0.150- 1400 mm) Solid-to-liquid ratio (0.02-0.06 g mL ⁻¹) Stirring rate (300-500 min ⁻¹) Reaction temperature(18-40 °C)	$1 - (1 - X)^{1/3} = (3.423 \times 10^4)(D)^{-0.7} (S/L)^{-0.65} \exp^{-4754/T} t$

Tunc and Kocakerim (1998) investigated the dissolution of colemanite in aqueous sulfuric acid. The parameters were temperature (10-60 °C), particle size of colemanite (0.3625-1.5 mm), solid-to-liquid ratio (0.01-0.175 g mL⁻¹), acid concentration (0.25-2 mol L⁻¹) and stirring rate (20.93-62.80 s⁻¹). It was found that temperature and stirring rate had positive effect on the rate. Conversion rate increased with the acid concentration up to 1 mol L⁻¹ and decreased with the concentrations above 1 mol L⁻¹. The rate of dissolution reaction was expressed in equation (1).

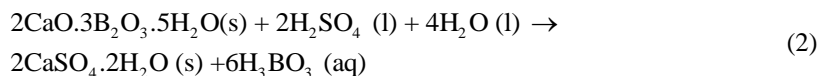
$$-\ln(1 - x) = 82.52(D)^{-0.821} (SR)^{0.426} (S/L)^{-0.383} e^{-3465/T} t \quad (1)$$

where X is the fractional conversion, D is the particle size of colemanite in mm, SR is the stirring rate in s⁻¹, S/L is the solid-to-liquid ratio g mL⁻¹ and t is the time in min.

Kalafatoğlu and coworkers (2000) stated that if in the reaction of colemanite and sulfuric acid the concentration of sulfuric acid was more, besides the colemanite, some other impurities also dissolved. So, in this study, the most suitable concentration for sulfuric acid was searched and it was shown that if the acid concentration was hold around 5 %, the dissolution of clay and the other impurities was

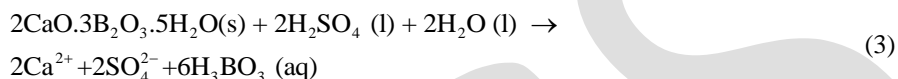
less. Dissolution kinetics of colemanite in sulfuric acid in the absence and presence of ultrasound was studied by Okur and coworkers (2002). An Avrami-type equation was used successfully to explain kinetic data. Activation energy was 30 kJ/mol in both situations. Ultrasound affected the pre-exponential factor in rate constant.

Boric acid is produced from colemanite ($\text{Ca}_2\text{B}_6\text{O}_{11} \cdot 5\text{H}_2\text{O}$) ore by reaction with sulfuric acid. The overall reaction in the reactor is given as below;



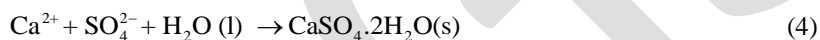
This overall reaction consists of two consecutive reactions, dissolution of colemanite and formation of gypsum. In the first reaction boric acid produced and this reaction is a very fast reaction.

Boric Acid Production Reaction:



In the second step, gypsum crystals are formed and stay in the reaction mixture to grow up to a size large enough to be filtered out of the solution.

Gypsum Crystallization Reaction:



MATERIALS AND METHOD

Materials used

Experiments were conducted using two different reactors; a batch reactor and a leaching cell, colemanite, sulfuric acid, a mechanical stirrer, a heating jacket, a pH meter, a thermocouple, a temperature control unit and a vacuum pump, and distilled water.

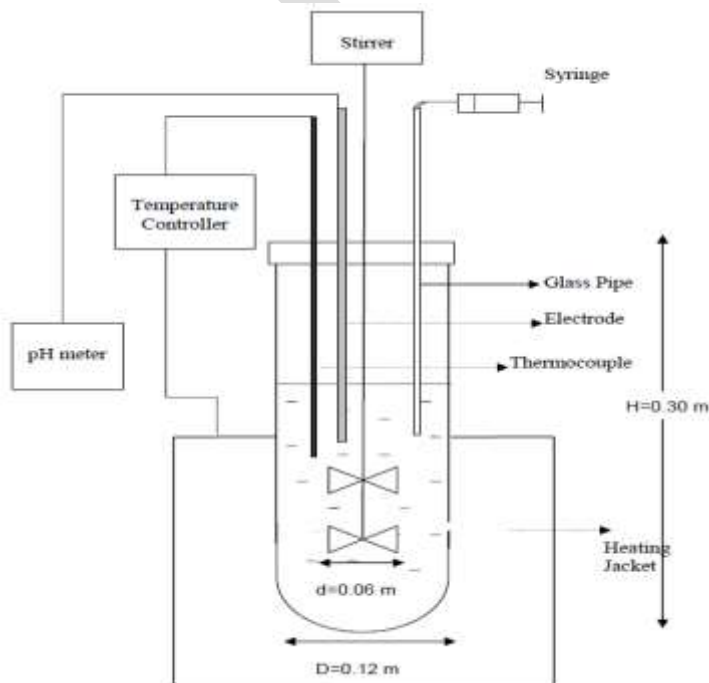


Figure 2: The schematic representation of the batch reactor set-up without filtration Unit

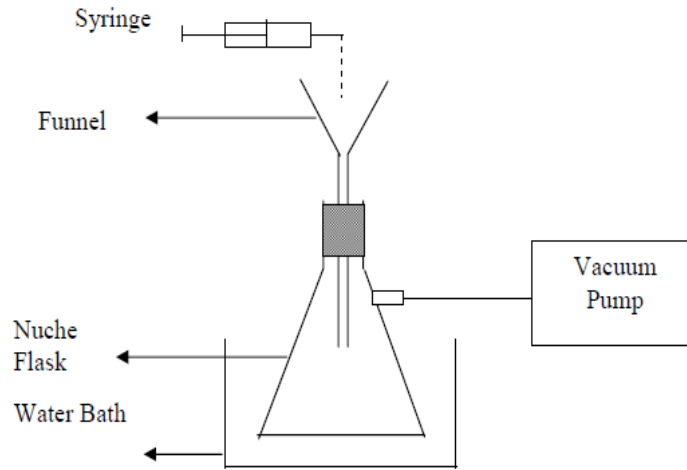


Figure 3: Schematic representation of filtration unit

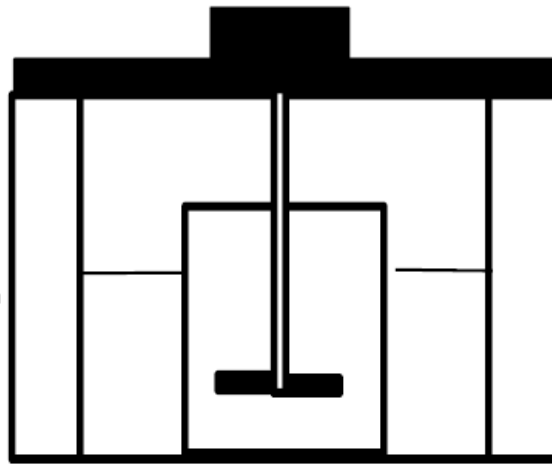


Figure 4: Leaching cell equipment

Method used

The CaO and B₂O₃ contents of the colemanite had to be known to calculate the amount of colemanite added to the reactors according to the CaO/SO₄²⁻ ratio chosen and the conversion of colemanite to boric acid, respectively. Colemanite analysis was done using X-ray Fluorescence (XRF) in Niger Delta University, Chemical Engineering Department. The chemical analysis of colemanite used in the experiments showed that the ore contained between 43.57-43.87 % of colemanite and the remaining percentage is constituted by other oxides as outlined in Table 3.

TABLE 3: XRF COLEMANITE (%) ELEMENTAL COMPOSITION

Component (%)	Colemanite 0-250 μm	Colemanite 250-1000 μm
B ₂ O ₃	43.57	43.87
CaO	30.90	28.61
Na ₂ O	0.22	0.79
MgO	0.79	0.45
Al ₂ O ₃	0.22	0.17
SiO ₂	0.60	0.21
SO ₃	0.14	0.50
Fe ₂ O ₃	0.17	0.31

As ₂ O ₃	0.00	0.03
SrO	0.56	0.64
TiO ₂	0.20	0.056
K ₂ O	0.08	0.059
BaO	0.005	0.015
Li	0.045	*
Others	22.50	17.46

Firstly, a given amount of distilled water was put into the reactor. The mechanical stirrer was started to operate at desired stirring rate. Then sulfuric acid was added slowly into the reactor. An initial sulfate concentration of 0.623 M in solution was used for all experiments. The temperature control unit was adjusted to reaction temperature and kept constant. Certain amount of colemanite was fed into the reactor at once. This time was considered as the starting time of the reaction. The electrode was placed in the reactor to measure the pH of the slurry. The samples were withdrawn by 50 ml syringe attached to a glass pipe. Then, samples were filtered immediately by using vacuum pump connected to 250 ml nuche flask. A funnel was placed on top of flask. Blue band filter paper was put on the funnel. In order to prevent the boric acid solution to crystallize, the flask was placed into hot water. Solid particles and liquid were collected on filter paper and flask, respectively.

The liquid portion was taken from the flask by the help of micropipettes and analyzed for boric acid and calcium ion concentration. The filtrates were analyzed for change of crystal structure of gypsum with respect to time.

RESULTS

In the experiments, particles smaller than 250 µm and greater than 250 µm were used to investigate the effect of particle size on dissolution of colemanite ore, gypsum formation and particle size distribution of gypsum crystals.

Table 4. The screen analysis of Colemanite 0-250 µm

Mesh No	Dpi, µm	Mass Fraction by Weight	Avg. Dpi, µm	Cum. Mass Fraction
60	250	0.280	-	0.720
100	150	0.370	200	0.350
140	106	0.170	128	0.180
170	90	0.075	98	0.105
270	53	0.063	45	0.042
Pan	-	0.042	27	0.000

Table 5. The screen analysis of Colemanite 250-1000 µm

Mesh No	Dpi, µm	Mass Fraction by Weight	Avg. Dpi, µm	Cum. Mass Fraction
25	710	0.193	-	0.807
35	500	0.305	605	0.502
45	355	0.312	428	0.19
60	250	0.176	303	0.014
Pan	-	0.014	125	0.000

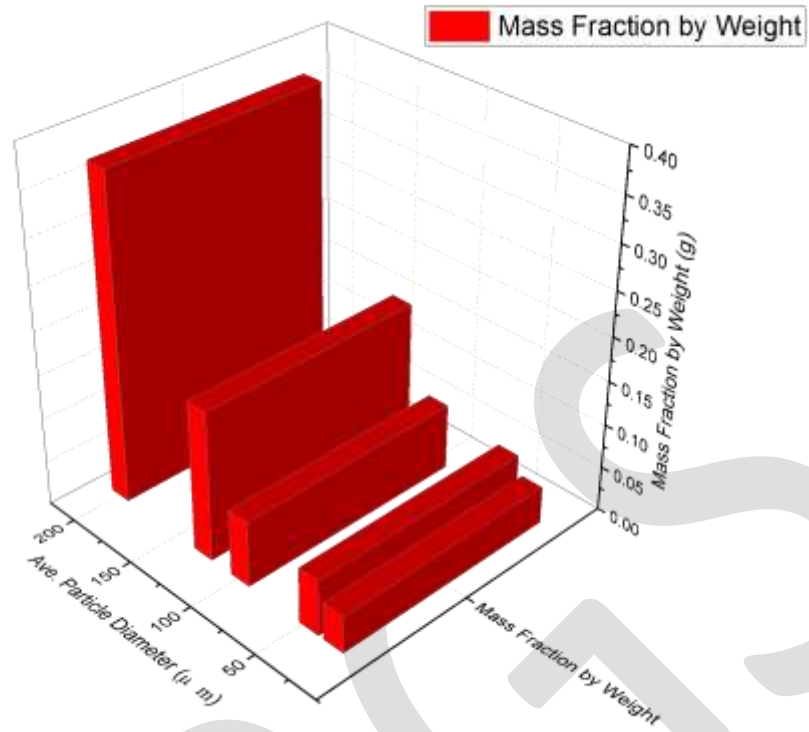


Figure 5: Differential particle size distribution of Colemanite 0-250 μm

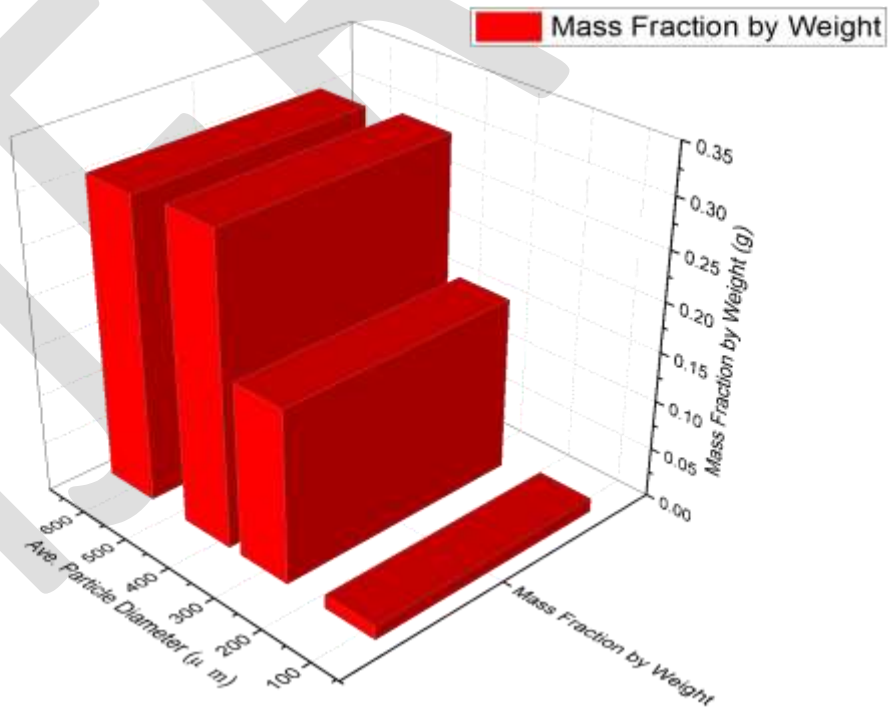


Figure 6: Differential particle size distribution of Colemanite 250-1000 μm

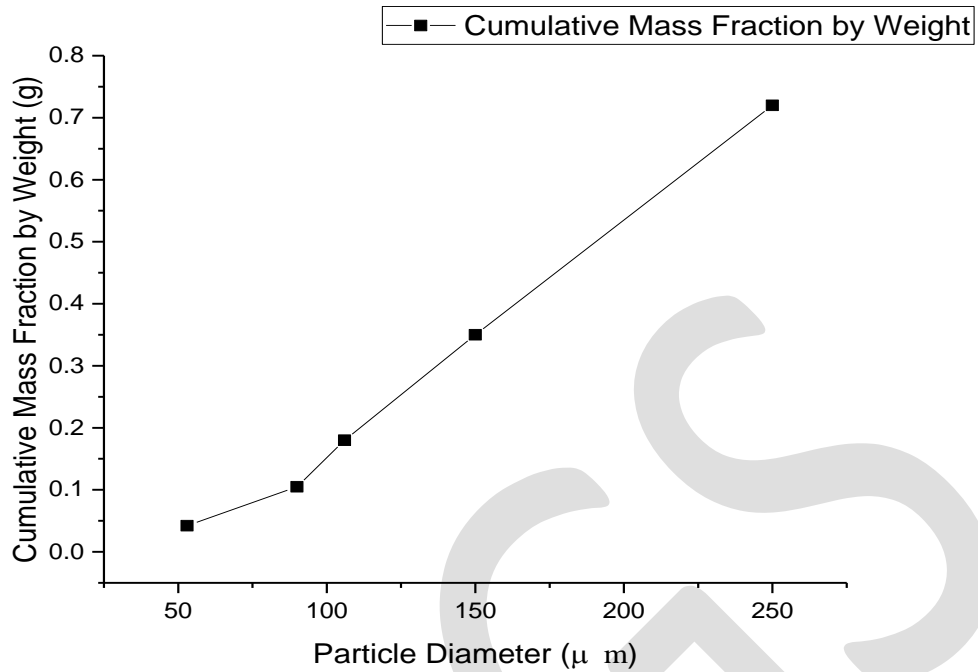


Figure 7: Cumulative particle size distribution curve for Colemanite 0-250 μ m

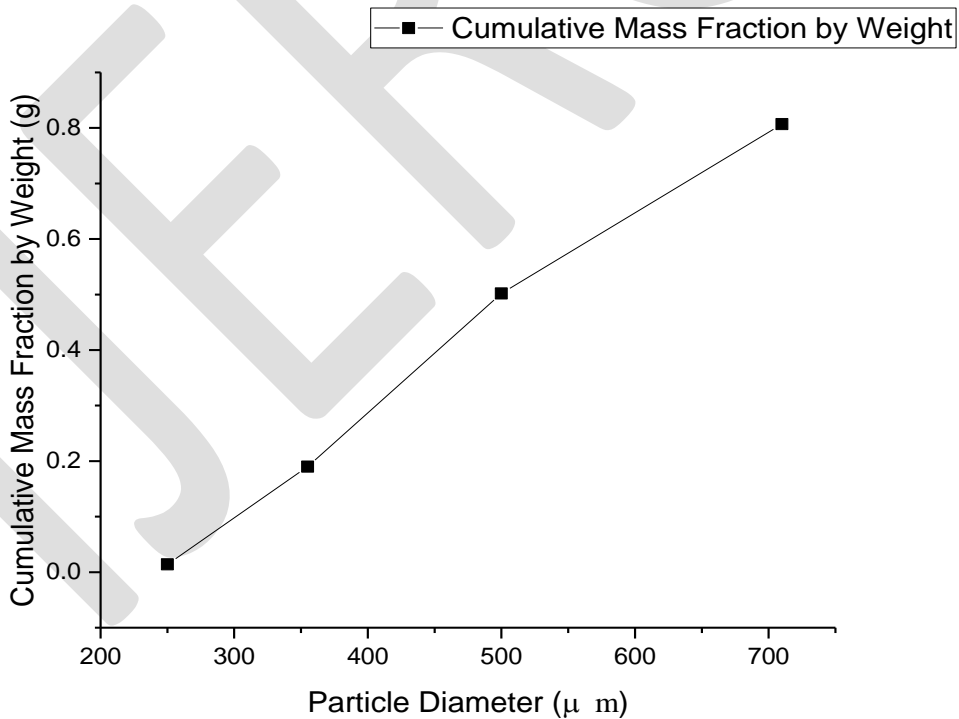


Figure 8: Cumulative particle size distribution curve for Colemanite 250-1000 μ m

Originally, sieve analysis was performed to separate the particles larger than 250 μ m. The 60 mesh sieve (corresponding to 250 μ m) was used for this drive, and was seen that nearly 35 percent of the colemanite was left on this sieve. In other words, nearly 35 percent

of the colemanite particles were larger than 250 μm . The screen analyses of the colemanite lesser and larger than 250 μm are given in Table 4 and Table 5, respectively. In these tables, the mass fractions of the colemanite on each sieve and the cumulative mass fractions of the colemanite under that sieve were represented. The particle diameter is the maximum diameter of the particles that could pass the former sieve. The average particle diameter stands for the arithmetic mean of the minimum and maximum diameter of the particles on that sieve. Figures 5 and 6 present the differential particle size distribution of the colemanite particles smaller and greater than 250 μm , respectively. The mass fractions of the colemanite particles on each sieve according to their average particle diameters were illustrated. Figures 7 and Figure 8 show the cumulative particle size distribution of the colemanite particles smaller and greater than 250 μm , respectively. For each particle diameter, cumulative mass fraction of the colemanite smaller than that diameter was represented. When the particle size distribution of the colemanite mineral was examined, it was seen that most of the particles had had average particle size between 2.5 and 10 cm. Therefore, the colemanite was crushed in the jaw crusher, then grinded in a hammer mill.

The Effect of Particle Size of Colemanite

The experiments were performed at 80 $^{\circ}\text{C}$ and 85 $^{\circ}\text{C}$ at 500 rpm stirring rate. Colemanite minerals smaller than 250 μm and 160 μm were used in the first group. The initial $\text{CaO}/\text{SO}_4^{2-}$ molar ratio was 0.95. In the second group of the experiments, particles smaller and greater than the 250 μm were used. The initial $\text{CaO}/\text{SO}_4^{2-}$ molar ratio was 1.0.

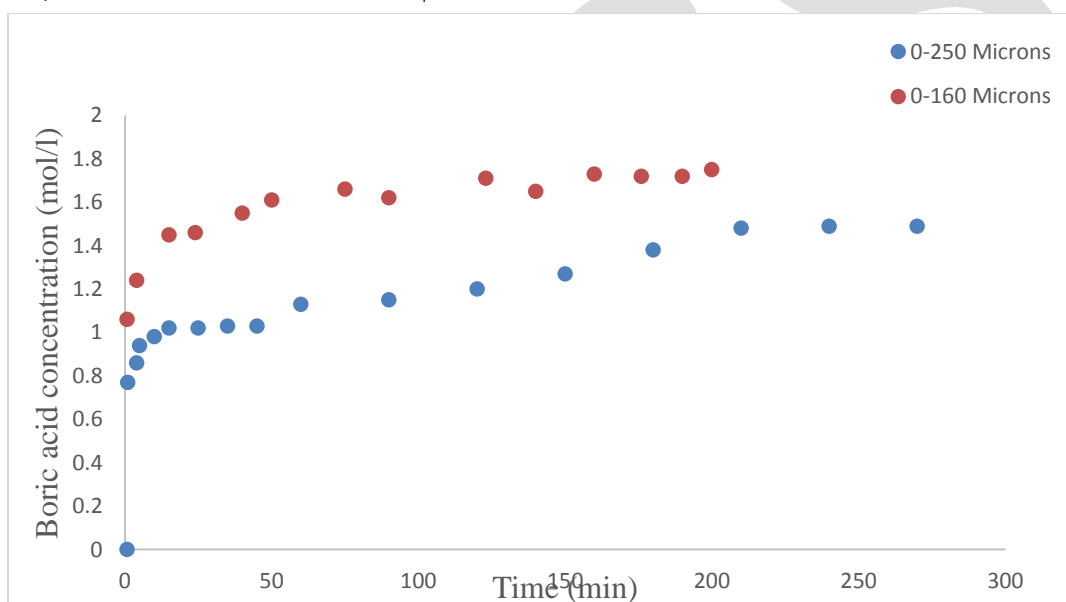


Figure 9: Variation of boric acid concentration in liquid with respect to time of particle size 0-160 and 0-250 microns at 80 $^{\circ}\text{C}$

In the first group, the effect of particle size on dissolution of colemanite and formation of gypsum reactions were analyzed. Figure 9 shows that, the change of the boric acid concentration in the liquid phase with respect to time is slower for colemanite particles smaller than 250 μm . Also, a slightly inclined plateau is observed between 15 and 50 minutes only for these particles. Obviously, the colemanite particle size affects the dissolution reaction rate.

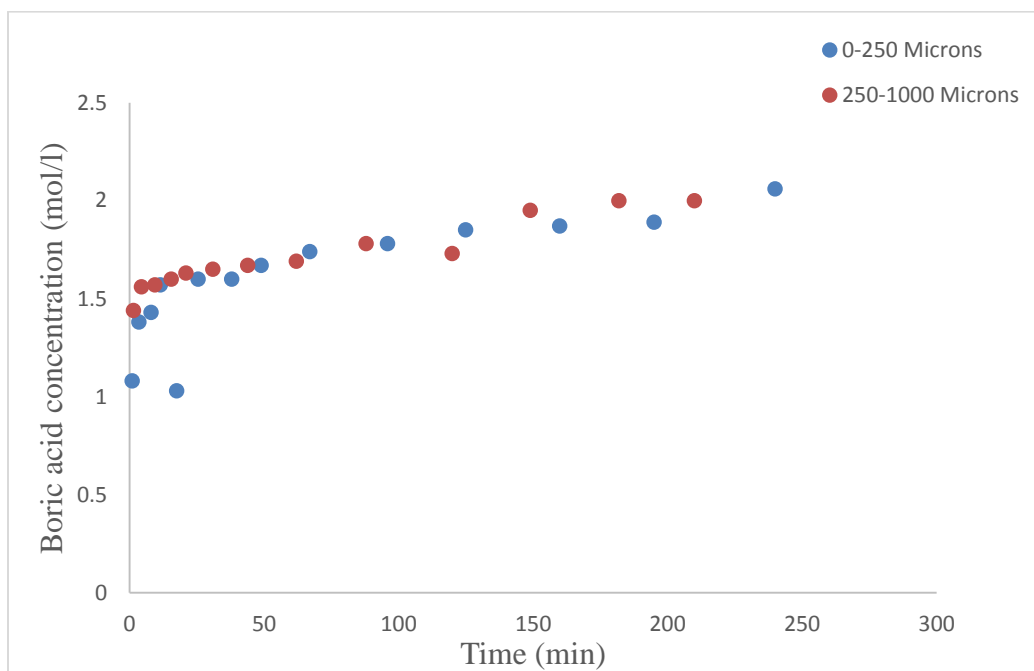


Figure 10: Variation of boric acid concentration in liquid with respect to time of particle size 0-250 and 250-1000 microns at 85 °C

Figure 10 illustrates the change in boric acid concentration in the liquid phase versus time at 85 °C, 500 revolution per minute (rpm) and initial $\text{CaO}/\text{SO}_4^{2-}$ molar ratio of 1.00 for particle sizes greater than 250 μm of colemanite. The reaction mixture was stirred by using two propellers. As seen from the figure, the variation of boric acid concentration shows same trends for both particle sizes. In other words, insignificant effect of particle size of colemanite is observed if the experiments are performed with stirrer having two propeller. It means that stirrer type affects the dissolution.

The saturation concentration of calcium ion is the same for both experiments. Because, the saturation concentration is depend on temperature. In these experiments, the temperature was kept constant at 85° C.

Effect of particle size of colemanite on dissolution reactions becomes negligible if the stirrer used has two propellers. This showed that the stirrer type used is a critical parameter for boric acid production.

The Effect of Stirring Rate

Three experiments were performed at the initial $\text{CaO}/\text{SO}_4^{2-}$ molar ratio of 1.00 and at 85 °C. The effect of stirring rate on dissolution of colemanite reaction were analyzed at 350, 400 and 500 stirring rates. During the experiments, variation of the boric acid concentration with respect to time were determined at different stirring rate is shown in Figure 11. As seen from the figure, the boric acid concentration at certain time increases with increasing stirring rate. This means that the dissolution of colemanite reaction is limited by the rate of diffusion of sulfate ions through the surface of the solid colemanite particles. The increasing stirring rate increases the mass transfer of H^+ ions in solution through colemanite particles so the boric acid concentration increases with increasing stirring rate. The maximum boric acid concentration is obtained as 2.06 mol L^{-1} at 500 rpm stirring rate.

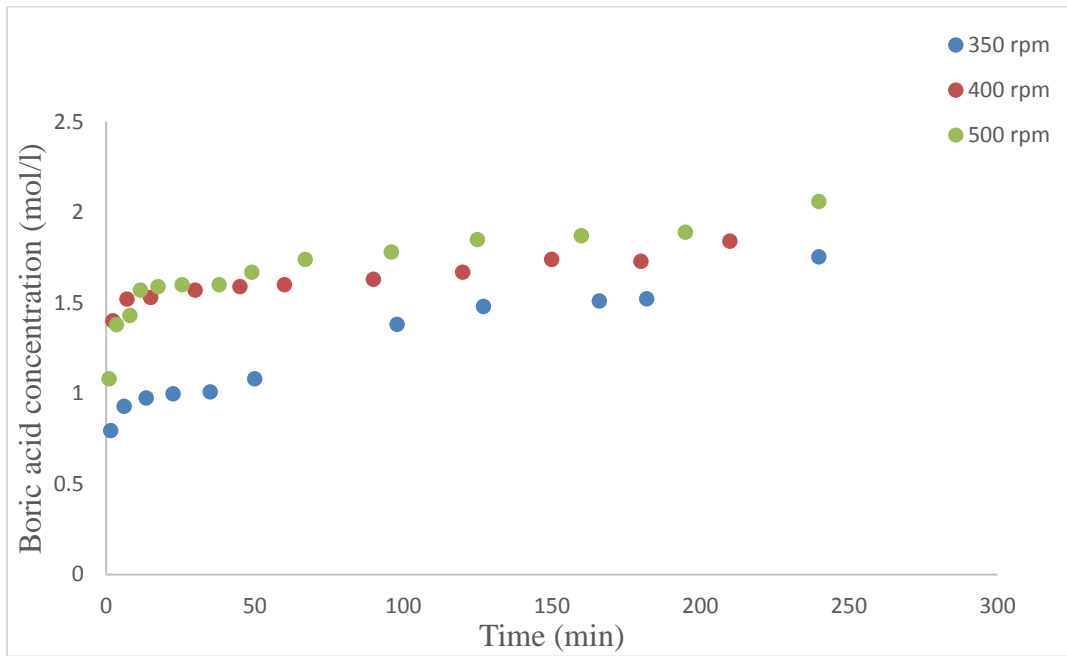


Figure 11: Variation of boric acid concentration in liquid with respect to time of different stirring rate at 85 °C

The Effect of Temperature

Two different types of colemanite were used. Experiments were performed at 70, 80, 85 °C for the particle size of colemanite greater than 250. Three experiments were performed at the initial $\text{CaO}/\text{SO}_4^{2-}$ molar ratio of 1.00. In these experiments, stirring rate was kept constant at 400 rpm. During the experiments, variation of the boric acid concentration with respect to time were determined as shown in Figure 12. From the figure, the boric acid concentration at certain time increases with increasing temperature. Temperature affects the dissolution rate of colemanite. In this range of temperature, the dissolution rate increases with increasing temperature. This means that the rate of boric acid production depends on the reaction temperature.

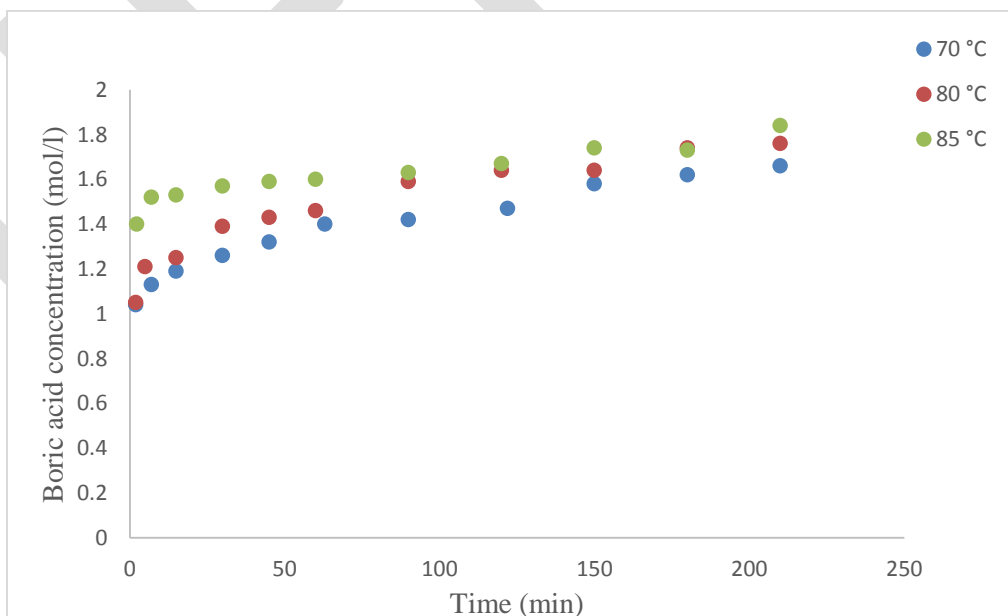


Figure 12: Variation of boric acid concentration in liquid with respect to time of different temperatures at 400 rpm.

CONCLUSION

In this study it is aimed to examine the effects of particle size of colemanite, stirring rate and reaction temperature in the reaction of colemanite in boric acid production.

Boric acid concentration increases and reaches an asymptotic value as the colemanite dissolves. From the material balance calculation, it is observed that nearly 90 % of the colemanite dissolves during first few minutes in the experiments performed with colemanite particle size of greater than 250 μm . So, the dissolution of colemanite is a fast reaction and the rate equation cannot be found from the obtained data. Also, it was seen that, the colemanite dissolution rate increases with decreasing particle size of colemanite (0-150 μm , 0-250 μm , 250-1000 μm) because of increasing surface area, increasing stirring rate (350-500 rpm) due to increasing the mass transfer of H^+ ions in solution through colemanite particles and increasing temperature up to 85 $^{\circ}\text{C}$. The dissolution rate of colemanite was faster at 85 C. Therefore, the optimum temperature for the production of boric acid should be between 80 and 85 $^{\circ}\text{C}$.

REFERENCES:

- 1) Özbayoğlu G. and Poslu K., "Mining and Processing of Borates in Turkey", Mineral Processing and Extractive Metallurgy Review, Vol. 9, pp. 245-254, 1992
- 2) Chuck Brown,"Minerals-n-More", 2000
[URL:http://www.minerals-n-more.com/Colemanite_Info.html](http://www.minerals-n-more.com/Colemanite_Info.html)
- 3) Roskill, "The Economics of Boron", 10th Ed., pp.11-20, 2002
- 4) Amethyst Galleries, 1997
[URL: http://mineral.galleries.com/minerals/carbonat/colemani/colemani.htm](http://mineral.galleries.com/minerals/carbonat/colemani/colemani.htm)
- 5) Napo D., Ntuli F., Muzenda E., and Mollagee M., "Process Intensification of Zinc Oxide Leaching Process Using Sulphuric Acid" *Proceedings of the World Congress on Engineering and Computer Science*, 2011 Vol II WCECS 2011, October 19-21, 2011, San Francisco, USA
- 6) Bechtloff B., Jüsten P., Ulrich J., "The Kinetics of Heterogenous Solid-liquid Reaction Crystallizations-An Overview and Examples", *Chemie Ingenieur Technik*, Vol.73, pp.453-460, 2001
- 7) Gupta C. K. and Mukherjee T.K., "*Hydrometallurgy in extraction processes*", CRC Press, 1990, vo. 2, pp.39-78.
- 8) Ullmann, "Ullmann's Encyclopedia of Industrial Chemistry", 6th Ed., USA, 2002
- 9) Patnaik P., "Handbook of Inorganic Chemicals", Mc. Graw-hill Handbooks, New York, pp. 119-120, 2002
- 10) Levenspiel O., "Chemical Reaction Engineering", 3rd Ed., pp.566-585, 1999
- 11) Tunç M. and Kocakerim M.M., "Kolemanitin H₂SO₄ Çözeltisinde Çözünme Kinetiği", UKMK 3, Erzurum, 2-4 Eylül, pp. 1235-1240, 1998
- 12) Kalafatoğlu İ.E., Örs N. and Özdemir S.S, "Hisarcık Kolemanitinin Sülfürik Asitle Çözünme Davranışı", UKMK 4, İstanbul, 4-7 Eylül, 2000
- 13) Okur H., Tekin T., Ozer A.K., Bayramoğlu M., "Effect of Ultrasound on Dissolution of Colemanite in H₂SO₄", *Hydrometallurgy*, Vol. 67 pp. 79-86, 2002

A UWB Antenna with Band-Notched Characteristics for Wireless Applications

Siddharth Saxena¹, Sudhakar Shastri²

VIT University¹, VIT University², India

Siddharth.saxena2014@vit.ac.in¹, Sudhakar.shastri2014@vit.ac.in²

Abstract— A compact ultrawideband (UWB) antenna having band-notched characteristics is presented. The Microstrip feed antenna consists of a square slot patch and a vertical coupling strip. As the coupling strip is placed nearly at the center of the patch a significant rejection characteristics of the antenna with wide operating band that operates from 2.9 to 12.9 GHz is obtained. Furthermore, relatively good omnidirectional radiation pattern constant gain and transmission responses are obtained in the operating band.

Keywords— ultrawideband (UWB), bandnotched, vertical coupling strip, returnloss, bandwidth, radiation pattern, gain.

INTRODUCTION

ULTRAWIDEBAND (UWB) technology has received an impulsion and attracted industrial attention in the wireless world over a decade. In 2002 the Federal Communication Commission allocated the bandwidth of 7.5 GHz (3.1–10.6 GHz) for commercial applications [1]. The reveal of an extremely wide spectrum of 3.1–10.6 GHz for commercial use has initiated a lot of interest in the research and development of UWB technology especially for short-range wireless communications. Particular attention is given to the planar UWB antennas due to their merits such as small size, high data rate, small emission power, easy manufacture, and low cost. However, over the UWB operating band, there are some other existing narrowband communication systems, such as wireless standards like IEEE802.11a and HIPERLAN2 which create possible electromagnetic interference to the UWB applications. To overcome this problem, many significant band-notched techniques have been suggested in UWB antennas, including etching L-shaped slot [3], U-shaped slot [4], V-shaped slot [5], T-shaped slot [6], C-shaped slot [7], S-shaped slot [8], using a defected ground structure (DGS) [9] or by adding a split ring resonator (SRR) in the antenna structure, the unwanted frequencies can be rejected and performance of the antenna can be improved.

In this letter, a simple monopole antenna is investigated and a vertical coupling strip is employed to overcome the rejection frequency band for UWB operation and the rejection of (IEEE802.11a) and HIPERLAN band has been done by etching a U-shaped slot in the feed line. Proposed UWB antenna possess design specifications of $15(L) \times 15(W) \times 1.6(H)$ mm³. Calculated results show bandwidth of near about 10GHz i.e. from (2.9-12.9GHz). Moreover omnidirectional radiation pattern has been obtained and discussed in later section. Calculated results show bandwidth of near about 10GHz i.e. from (2.9-12.9GHz). Moreover omnidirectional radiation pattern has been obtained and discussed in later section.

ANTENNA DESIGN

Fig1.a represents the geometry of proposed UWB band notched antenna. fabrication is done on a low cost FR-4 substrate having thickness 1.6mm and relative dielectric constant of 4.4 and loss tangent $\tan \delta = 0.002$. The radiation patch is feed by a 50 ohm Microstrip line. Width of Microstrip line is 3.4mm, and antenna is designed using a square slot patch with a vertical coupling strip. The optimal dimension of the antenna is as follows: $L_1=35$ mm, $L_2=30$ mm, $L_3=15$ mm, $L_4=14$ mm, $L_5=3.4$ mm, $L_6=13.3$ mm, $L_7=8.3$ mm, $L_8=7.9$ mm, $L_9=0.2$ mm. Moreover, the overall dimensions of the patch are 15×15 mm² and dimension of the ground plane is taken merely as length of 12mm and width of 30mm

A spacing of about 1mm is given between patch and ground plane in order to achieve good impedance matching characteristics. As coupling strip is placed at center of the Patch having a space of 0.2mm from the patch in order to generate resonance for stop band operation and hence for this strip a center frequency f_r is calculated as

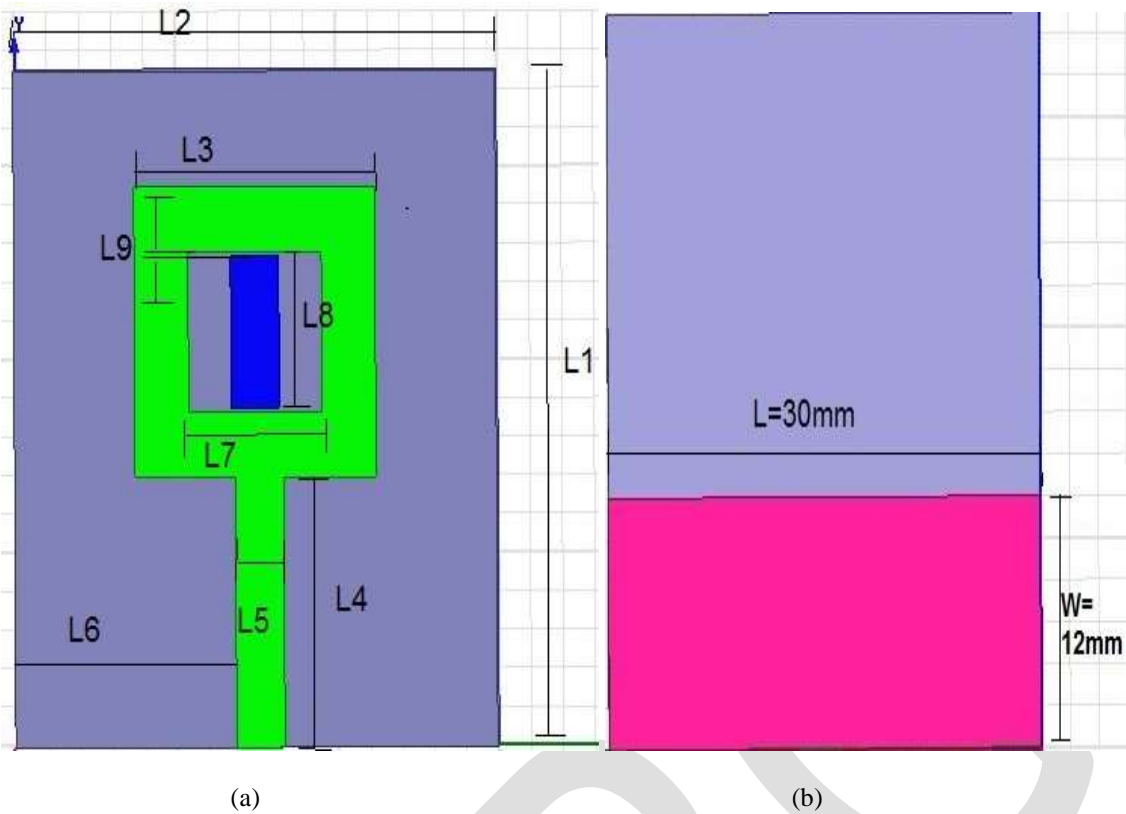


Fig.1. Geometry of the proposed UWB antenna (a)top view and (b) back view

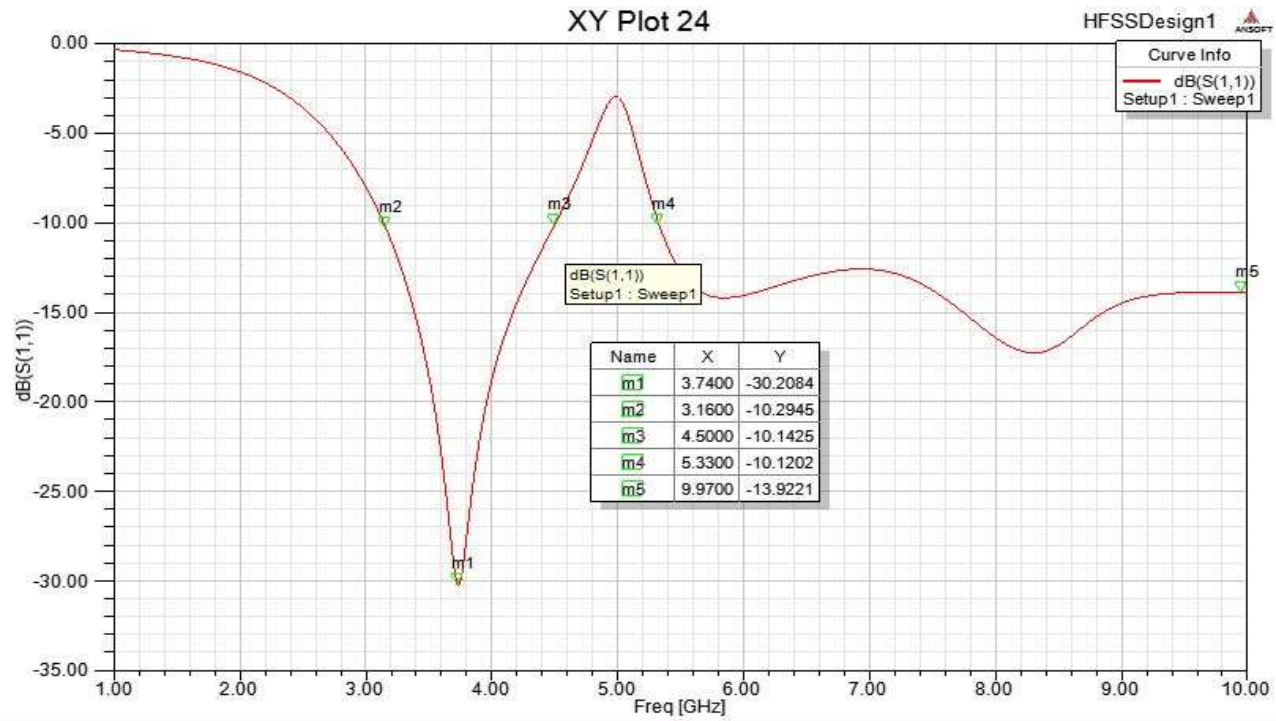
Patch having a space of 0.2mm from the patch in order to generate resonance for stop band operation and hence for this strip a center frequency f_r is calculated as

$$f_r = \frac{c}{(L7 - 2L9) \cdot 4 \cdot \sqrt{\frac{\epsilon_r + 1}{2}}}$$

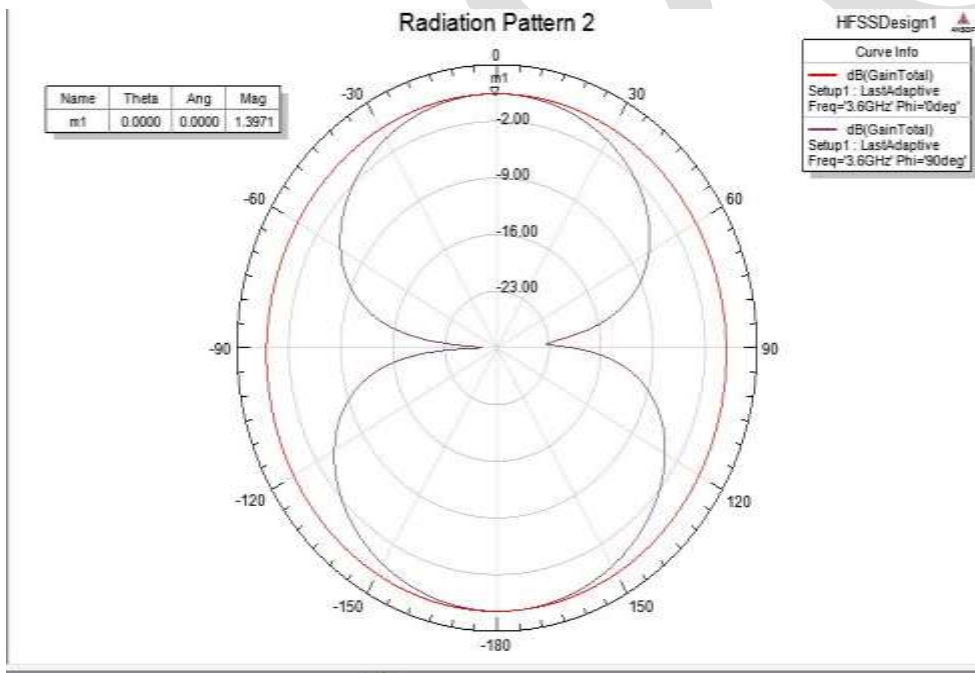
Where, c is speed of light, ϵ_r is dielectric constant.

SIMULATED RESULTS

Fig.2.a shows the simulated results of the designed antenna, return loss is found to be -30dB at 3.6 GHz and measured bandwidth is found to be from 3.16 to 9.97GHz, rejecting 4.5-5.33GHz which is causing frequency interference and Fig.2.b shows radiation patterns of the UWB patch antenna. In this case it has been found to be 1.39dB.



(a)



(b)

Fig.2. (a) Return loss of the UWB patch antenna having notch between 4.5-5.33GHz and
 (b) Radiation patterns of the UWB antenna.

MODIFIED ANTENNA STRUCTURE

In fig. 3 U-shaped slot has been etched in feed line of 0.2mm width so that current length is increased and therefore extra impedance is obtained resulting in a notch and rejecting the centered frequency of about 4.6 to 6.6 GHz i.e. rejecting (IEEE 802.11a) standards [11] and gain is found to be 1.36dB as shown in fig4.a.and 4.b. respectively.

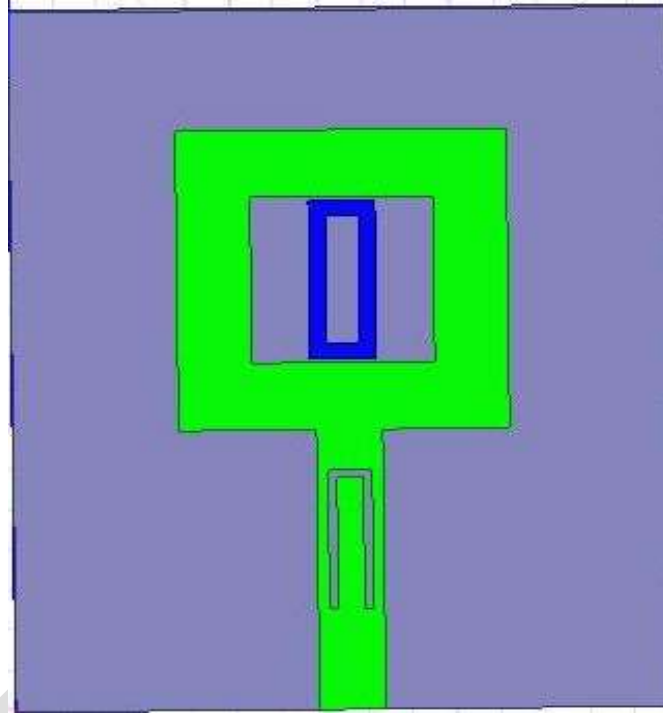


Fig.3. Geometry of the UWB patch antenna having a U-shape slot in the feed line.

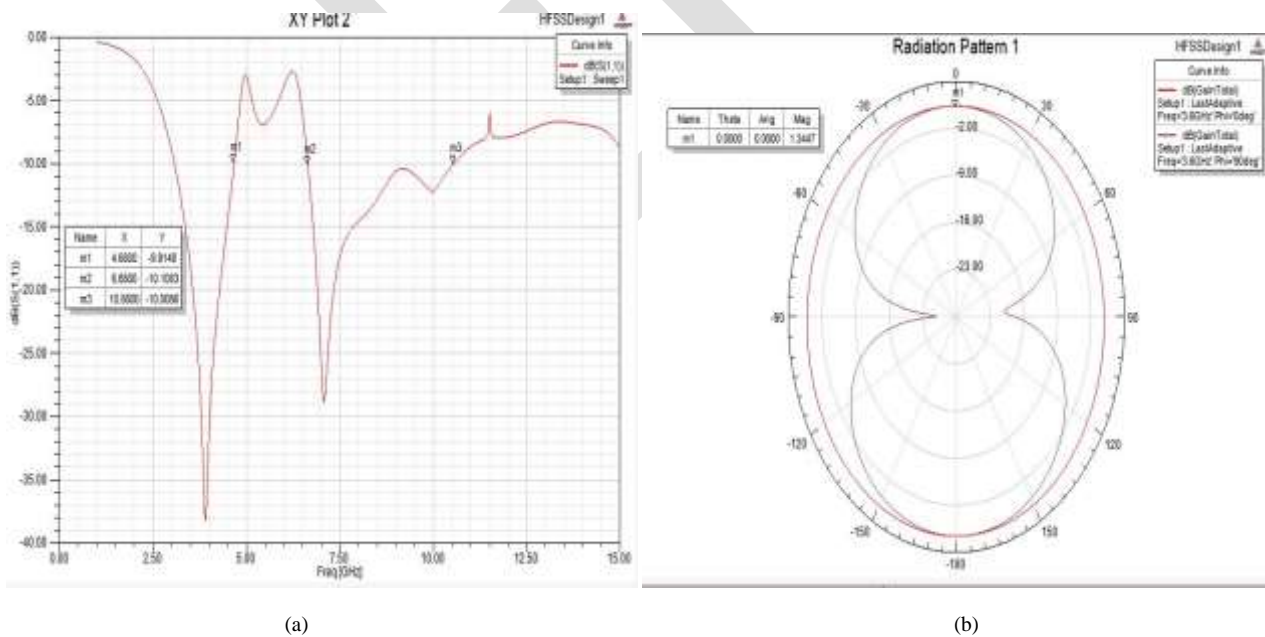


Fig. 4 (a) shows simulated s-parameter having a notch between 4.6-6.6GHz.
(b) shows radiation pattern with variation in gain.

FINAL ANTENNA DESIGN

Fig.5. represents the geometry of proposed UWB band notched antenna. All the design parameters are same and antenna is fed by a 50Ω Microstrip line. [12] A coupling strip is inserted into another coupling strip and patch is cut at an angle of 45° so that current length increases and results in wider impedance bandwidth.

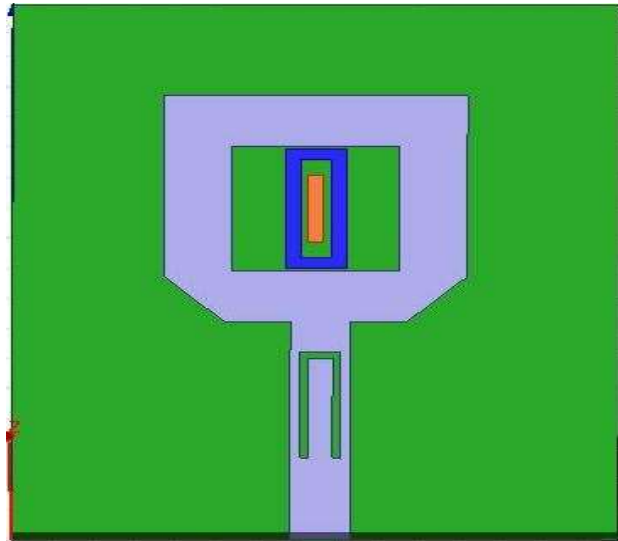
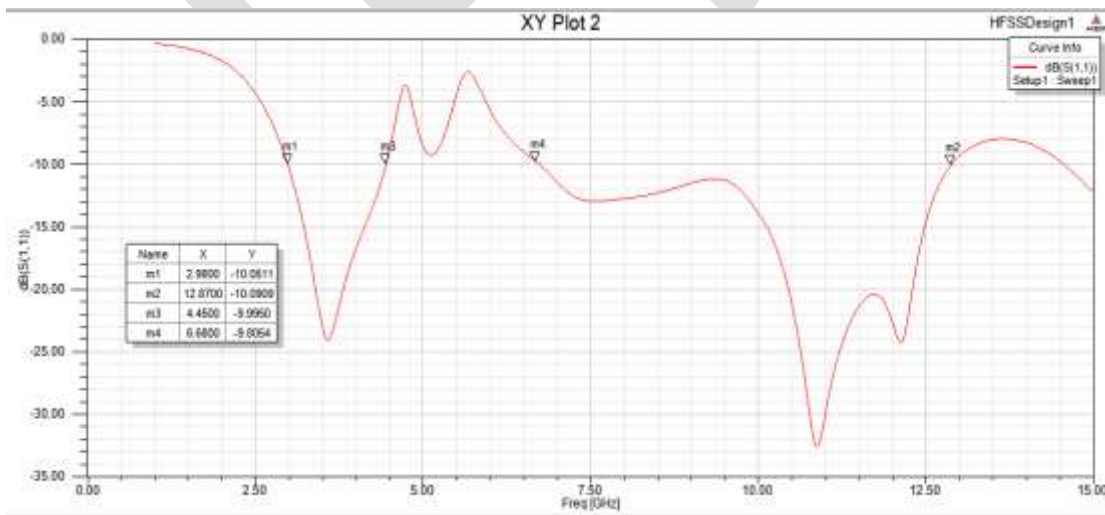


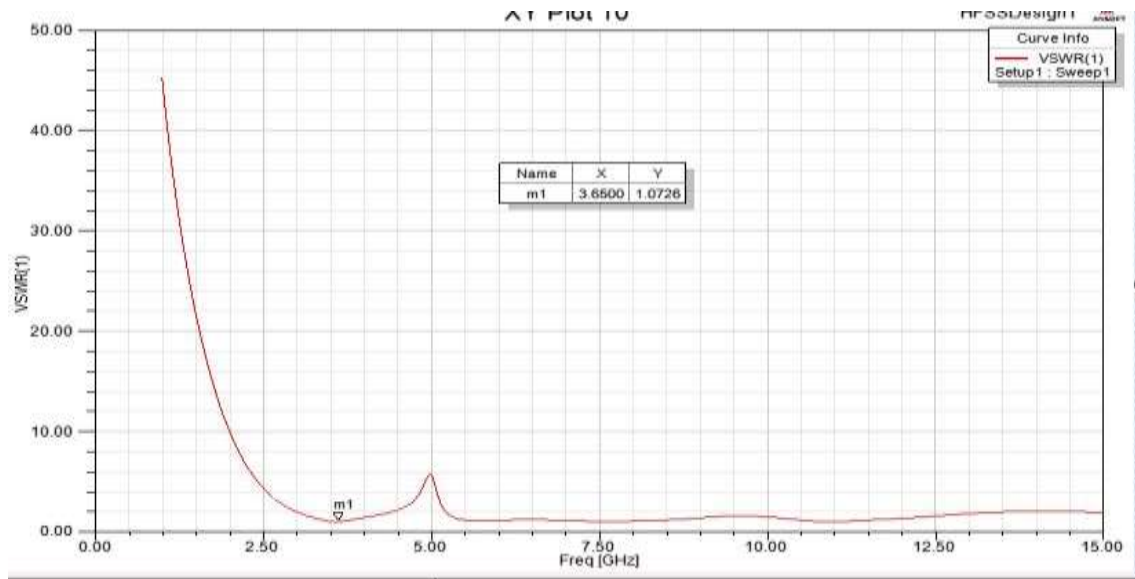
Fig.5. Geometry of the proposed UWB antenna.

SIMULATED RESULTS

The UWB patch antenna is designed with the aid of HFSS 2013 software tool and simulation results are obtained by taking suitable dimensions of antenna, so that it gives better performance and radiation. Measured S -parameter curve can be shown in fig.6.a. It has been observed that simulated impedance bandwidth is 2.9 to 12.9GHz rejecting frequency band from 4.4to 6.6 GHz so that effect due to interference can be avoided.



(a)



(b)

Fig.6. (a) Measured and simulated return loss of the proposed antenna and
 (b) VSWR variation of the patch antenna.

Fig.7 represents radiation pattern of the UWB patch antenna with a gain of 1.36dB. Variation in gain is in accordance with variation in bandwidth. Radiation patterns are prevailed by changing theta (θ) and phi (ϕ) angles. Since, only theta values are varied and phi is remained constant to zero it shows variation in gain with respect to theta. As we define the gain as the ratio of radiation intensity of antenna in particular direction to radiation intensity of isotropic antenna and radiation intensity is directly associated to phi and theta values. Hence gain varies in accordance with respect to theta and phi values [13]. Fig.8 shows the simulated surface current distribution of the antenna at notched frequency.

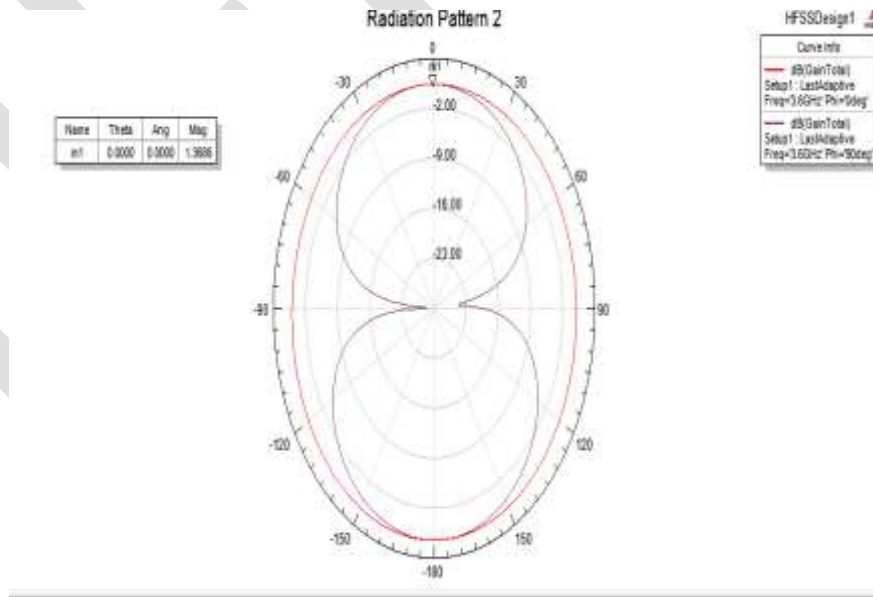


Fig.7. Radiation pattern with gain variation in UWB patch antenna

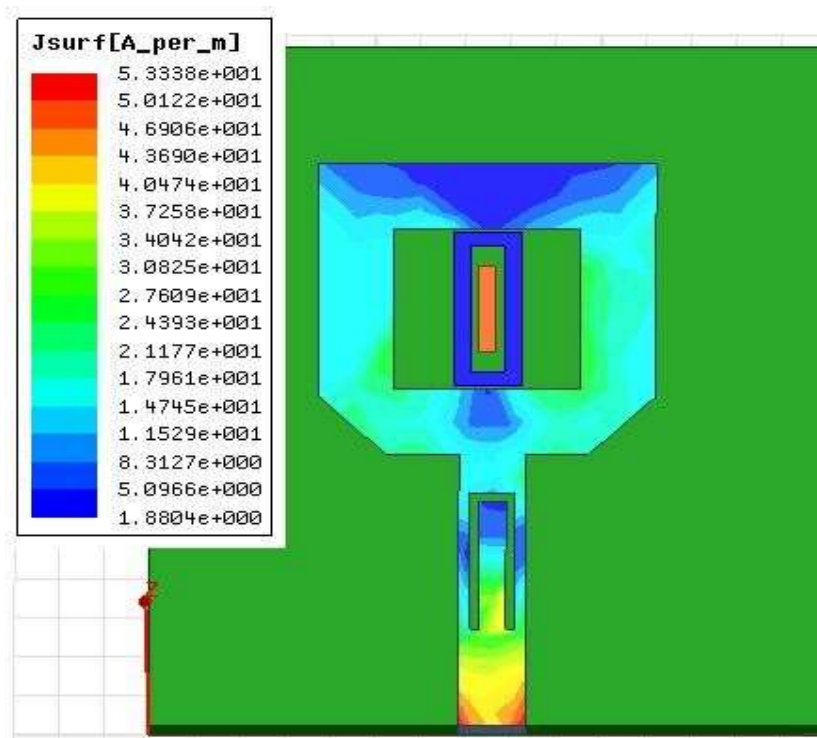


Fig 8. Simulated current distribution at center rejected frequency of 5.2 GHz for the designed antenna.

CONCLUSION

A compact band notched UWB antenna is effectively realized by inserting a U-shaped slot in the feed line and etching a coupling strip in the patch. Moreover a 45° cut has been made in patch in order to obtain wider impedance bandwidth from 2.9 to 12.9GHz. Interferences from (IEEE802.11a) standards and HIPERLAN1 and HIPERLAN2 are addressed well. VSWR is obtained as 1.07(<2). Furthermore good omnidirectional radiation pattern and good impedance matching has been obtained. Thus this is well suitable for UWB applications..

REFERENCES:

- [1] Federal Communication Commission, Washington, DC, USA, "Revision of part 15 of the Commissions' rule regarding ultra- wideband transmission systems FCC 02-48," First Report and Order, Feb. 2002.
- [2] Hsien-Wen Liu, Chia-Hao Ku, Te-Shun Wang, and Chang-Fa Yang, "Compact Monopole Antenna with Band-Notched Characteristic for UWB Applications" *IEEE Antennas and Wireless Propagation Letters*, vol.9,2010
- [3] R. Zaker, C. Ghobadi, and J. Nourinia, "Bandwidth enhancement of novel compact single and dual band-notched printed monopole antenna with a pair of L-shaped slots," *IEEE Trans. Antennas Propag.*, vol. 57, no. 12, pp. 3978-3983, Dec. 2009.
- [4] F. Fan, Z. Yan, T. Zhang, and Y. Song, "Ultra-wideband planar monopole antenna with dual stopbands," *Microw. Opt. Technol. Lett.*, vol. 52, no. 1, pp. 138-141, 2010.
- [5] Y. Kim and D.-H. Kwon, "CPW-fed planar ultra wideband antenna having a frequency band notch function," *Electron. Lett.*, vol. 40, no. 7, pp. 403-404, 2004.
- [6] M. Ojaroudi, C. Ghobadi, and J. Nourinia, "Small square monopole antenna with inverted T-shaped notch in the ground plane for UWB application," *IEEE Antennas Wireless Propag. Lett.*, vol. 8, pp. 728-731, 2009.
- [7] Q.-X. Chu and Y.-Y. Yang, "A compact ultrawideband antenna with 3.4/5.5 GHz dual band-notched characteristics," *IEEE Trans. Antenna Propag.*, vol. 56, no. 12, pp. 3637-3644, Dec. 2008.
- [8] S.-W. Qu, J.-L. Li, and Q. Xue, "A band-notched ultrawideband printed monopole antenna," *IEEE Antennas Wireless Propag. Lett.*, vol. 5, pp.495-498, 2006.
- [9] W. T. Li, X. W. Shi, and Y. Q. Hei, "Novel planar UWB monopole antenna with triple band-notched characteristics," *IEEE Antennas Wireless Propag. Lett.*, vol. 8, pp. 1094-1098, 2009.

- [10] D. Upadhyay, R.P.Dwivedi, "Antenna miniaturization techniques for wireless applications", *Eleventh International Conference on Wireless and Optical Communications Networks*.
- [11] H.-J. Zhou, B.-H. Sun, Q.-Z. Liu, and J.-Y. Deng, "Implementation and investigation of U-shaped aperture UWB antenna with dual band- notched characteristics," *Electron. Lett.*, vol. 44, no. 24, pp. 1387–1388, Nov. 2008.
- [12] J.-W. Jang and H.-Y. Hwang, "An improved band-rejection UWB antenna with resonant patches and a slot," *IEEE Antennas Wireless Propag. Lett.*, vol. 8, pp. 299–302, 2009.
- [13] T. Dissanayake and K. P. Esselle, "Prediction of the notch frequency of slot loaded printed UWB antennas," *IEEE Trans. Antennas Propag.*, vol. 55, no. 11, pp. 3320–3325, Nov. 2007.

IJERGS

Survey on Abandoned Object Detection System

Priyanka V. Saste, Prof.Megha P.kharche.
sastepriya22@gmail.com, meghakharche87@gmail.com

Abstract— In recent years due to various kind of social activities such as theft, bomb attack and other terrorist attack preventive security measures at public places has gained lot of importance. Abandoned Object detection is most crucial task in visual surveillance system. Many Public or open areas are facilitated with cameras at the multiple angles to monitor the security of that area for keeping citizens safe. This is known as the surveillance system. In this paper a new algorithm is proposed for object tracking in video, which is based on image segmentation. With the image segmentation all objects in video can be detected whether they are moving or not by using segmentation results of successive frames. This approach definitely provides security and detects the moving object in a real time video sequence and live video streaming.

Keywords— video surveillance, left baggage detection, background subtraction.

INTRODUCTION

Recent years have seen there are rise in terrorist attacks on crowded public places such as train stations and subways, airports, market, nightclubs, shopping malls, etc. Many surveillance tools have been employed in the fight against terror. Although video surveillance systems have been in operation for the past two decades, the analysis of the CCTV footage has not often put in risk so, its out of the hands of human operators [1]. Recent studies have brought into fore the limits of human effectiveness in analyzing and processing crowded scenes, particularly in the video surveillance systems consisting of multiple cameras. The advent of smart cameras with higher processing capabilities has now made it possible to the design systems which can possibly detect suspicious behaviours and abandoned objects.

Nowadays, terrorists come to public places such as railway stations, airports, bus stations and leave the luggage bomb for explosive attacks. It is very challenging to watch over the public places with crowds by security guards and identify the abandoned objects that have been left by a terrorist. Public places are being investigated with cameras but modern technologies cannot fully prevent the such attacks[2]. To prevent luggage bomb attacks, a fully automatic efficient and effective intelligent surveillance system is required. The intelligent surveillance system can detect stationary object which is alone in the public place and produce an alarm or message to alert the guards for removing such type of abandoned object. Security of public places is a considerably burning issue. Though the CCTV have installed at the laces but the footage is only used after incident had taken a place. Those CCTV cams can be used to prevent such incidents from happening. Hence we are proposing a best way in this project. We are processing the live feed of the CCTV cam with the image processing[2]. If a person is dropping off some bag or any such suspicious thing and leaving then it running away, the camera will catch this activity. And if such a bag is untouched for some time span decided by analyzer after it will give notification to authority[3]. Minimum the time span probability stays 50-50, but as time span increases the robability of that thing are being abandon or hazardous increases. Hence the incident can be avoided in that case.

LITURATURE SURVEY

Kevin Smith, Pedro Quelhas, and Daniel Gatica-Perez[1], authors presented a temporal consistency model is combining a back-tracing algorithm for abandoned object detection. The temporal consistency model is described by a very simple FSM. It exploits the temporal transition pattern generated by short- and long-term background models, which can accurately identify static foreground objects. Their back-tracing algorithm iteratively tracks the luggage owner by using spatial-temporal windows to efficiently verify left-luggage events.

Fatih Porikli, Yuri Ivanov and Tetsuji Haga[2], author presented a robust method that uses dual foregrounds to find abandoned items, stopped objects, and illegally parked vehicles in static camera setups. At every frame, autor adapt the dual background models using Bayesian update, and aggregate evidence obtained from dual foregrounds to achieve temporal consistency. This method does not depend on object initialization and tracking of every single object, hence its performance is not upper bounded to these error prone tasks that is usually fail for crowded scenes. It accurately outlines the boundary of items even if they are fully occluded. Since it will executes pixelwise operations, it can be implemented on parallel processors.

Rajesh Kumar Tripathi, Anand Singh Jalal[3], authors proposed a framework for abandoned object detection in real-time from surveillance video. Author utilized running average method for background modeling which is more suitable for real-time surveillance

video. Proposed contour features are more sensitive to the changes, to distinguish the static objects and moving objects. An edge based object recognition method applied to classify human and non-human static objects either it is full or partial visible. Experimental results demonstrate that proposed approach detect abandoned object even in bad illumination, crowd scene, occlusion and effective to detect object of different size. False detection has been handled through the generated score.

A.Singh, S. Sawan, M. Hanmandlu[4],author presented an abandoned object detection system based on a dual background segmentation scheme. The background segmentation is adaptive in the nature and based on the Approximate Median Model. It consists of two types of the reference backgrounds, Current and Buffered background, each with the different time interval. Blob analysis is done on the segmented background and a dynamic tracking algorithm is devised for tracking the blobs even under the occlusion. Detection results show that the system is robust to variations in lighting conditions and the number of people are in the scene. In addition, the system is simple and computationally less intensive as it avoid the use of expensive filters while achieving better detection results.

YingLi Tian, Rogerio Schmidt Feris, Haowei Liu, Arun Hampapur, and Ming-Ting Sun[5],authors presented a new framework to robustly and efficiently detect the abandoned and removed objects in complex environments for real-time video surveillance. The mixture of Gaussians background subtraction method is employed to detect both background and static foregrounds by using the same Gaussian mixture model. Then static foregrounds were classified into abandoned or removed objects by segmenting and comparing the surrounding area of the background model and the foreground image. Method can handle occlusions in the complex environments with crowds. Furthermore, in order to reduce false alarms, author have employed tracking information in to a small temporal window to provide an additional cue to filter out the impact of spurious and noisy trajectories for abandoned object detection.

Q. Fan, P. Gabbur, and S. Pankanti[6],In this paper authors proposed a novel approach to the abandoned object detection using the framework of relative attributes. Specifically, they design three physically interpretable attributes (staticness, foregroundness and abandonment) to characterize different kinds of alerts raised by various objects in the scene. They learn ranking functions for each of the attributes to rank order the alerts based on their strengths on the corresponding attributes. The attributes are used as input to an alert prioritization method which performs a ranking using alert importance.

H.-H. Liao, J.-Y. Chang, and L.-G. Chen[7],authors have proposed a novel approach to left-luggage detection in surveillance video. Through the use of foreground-mask sampling, authors are able to emulate the human vision capability of limiting and focusing on solely the object of interest to them, while filtering out all of other irrelevant, interfering agents. They are therefore able to apply tracking in a selective, more localized manner. Authors have also proposed an improved implementation of the Hough Transform for detecting the human upper-body contour from the video frames. And they have incorporated a probabilistic framework and employed the MAP principle in their modeling of the luggage-abandonment event and subsequent reasoning.

Kahlil Muchtar, Chih-Yang Lin, Li-Wei Kang , and Chia-Hung Yeh[8],authors proposed an automatic system for abandoned object detection. The main contribution of the method is to provide a comprehensive solution, which can identify the status of an object, abandoned, removed,or partially occluded. He employ the combination of background modeling based on mixture of Gaussians (GMM) and Markov Random Field (MRF) [8]. Furthermore, he employ a cast-shadow approach to enhance the shape of abandoned object. By combining these two approaches the abandoned object detection can perform well and obtain accurate results. The Gaussian Mixture Model (GMM) was proposed by Grimson and Stauffer [8]. The authors presented pixel-based method to the model each pixel (regarded as background) into a mixture of Gaussians. In addition, each Gaussian has its own weight to represent its portion of the data accounted for from corresponding distribution.

ABANDONED OBJECT DETECTION

In [1] Kevin Smith, Pedro Quelhas, and Daniel Gatica-Perez ,proposed a temporal dual-rate foreground integration method for static-foreground estimation for singlecamera video images. Their approach involves constructing both short- and long-term background models learned from an input surveillance video on-line. Subsequently, they introduce a simple pixel-based finite-state machine (PFSM) model that uses temporal transition information to identify the static foreground based on the sequence pattern of each object pixel. Because the proposed approach involves using temporal transition information, they can reduce the influence of imperfect foreground extractions in the double-background models, thereby improving the accuracy of the constructed static foreground inference. An owner-tracking procedure is also employed in their method to semantically verify the abandoned object event. Contributions of the proposed method over previous methods are summarized as follows. 1) They introduce a dual-rate background modeling framework with temporal consistency. It performs considerably better than the single-image-based double background models . 2) They develop a simple spatial-temporal tracking method for back-tracing verification. Compared to the frame-by-frame

tracking approaches such as the KF- or UKF employed in [1], our approach is superior in handling temporary occlusions and is still highly efficient to implement.

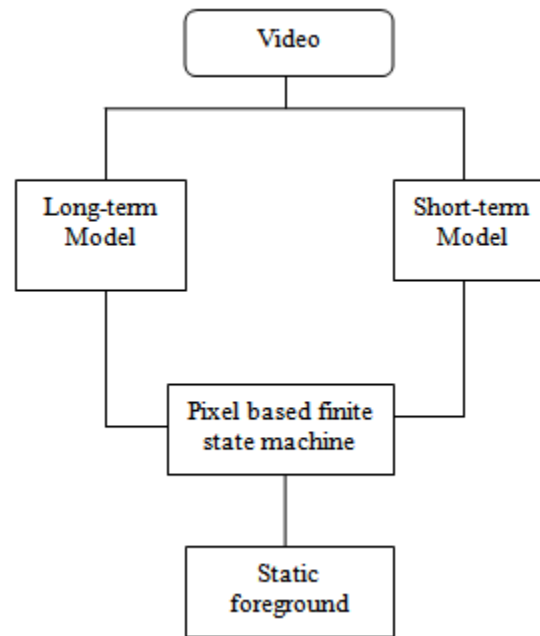


Figure 1. Flowchart of Static Foreground Detection[1]

Figure 1 shows an overview of the integrated background modeling method proposed in this study. First, they describe the long- and short-term models built in their approach for static foreground detection. A small learning rate updates the background model at a faster speed. The model that learns at this small rate is called the short-term background model. By contrast, a large learning rate yields the model that is updated at a slower speed. Similarly, the model that learns at this rate is referred to as the long-term background model. Instead of recognizing the status of each pixel based on only a single frame, they use temporal transition information to identify the stationary objects based on the sequential pattern of each pixel. A pixel is associated with only one state at a time. Based on long- and short-term background models, the state of pixel i can be changed from one state at time t to another state at time $t + 1$. Accordingly, they construct a simple FSM model to describe the behavior of each pixel. Authors detect the static foreground by identifying a specific pattern of transitions.

In [3] Rajesh Kumar Tripathi, Anand Singh Jalal, proposed framework consists of three main steps as shown in Figure.1. First, foreground object is detected in two consecutive frames using the running average method. Then contours are drawn for each object into both frames. In second step, contour features are applied to detect the stationary objects from both consecutive frames. In third step, detected static objects are classified into human or nonhuman objects by using edge based object recognition method. The proposed approach is able to recognize object even it is partially visible. The edge based object recognition process includes the template generation of detected static objects and then matches it with predefined human edge template to generate a score to decide whether the static object is human or non-human objects. It also generates the partial matching score if object is partial visible due to shadow, partial occlusion or other reasons.

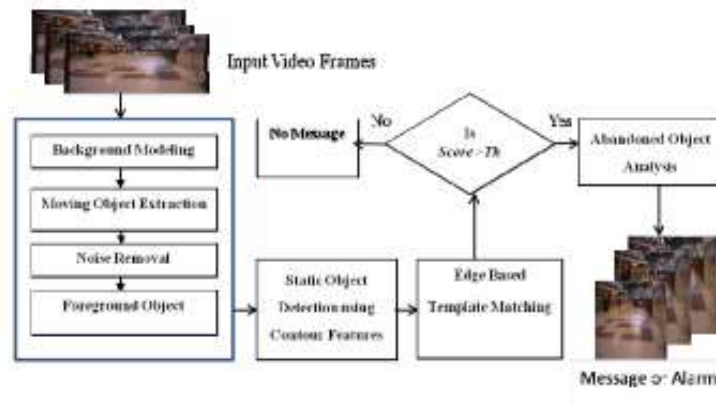


Figure 2. Framework for abandoned object detection[3]

Author have proposed a framework for abandoned object detection in real-time from surveillance video. They have utilized running average method for background modeling which is more suitable for real-time surveillance video. Proposed contour features are more sensitive to the changes, to distinguish the static objects and moving objects. An edge based object recognition method applied to classify human and non-human static objects either it is full or partial visible.

In [4] A.Singh, S. Sawan, M. Hanmandlu, presented an abandoned object detection system based on the simplistic and intuitive mathematical model which works efficiently at QVGA resolution which is the industry standard for most of CCTV cameras. The proposed system consists of a novel selfadaptive dual background subtraction technique is based on the Approximate Median model framework. Algorithms for tracking abandoned objects with or without occlusion are also included.

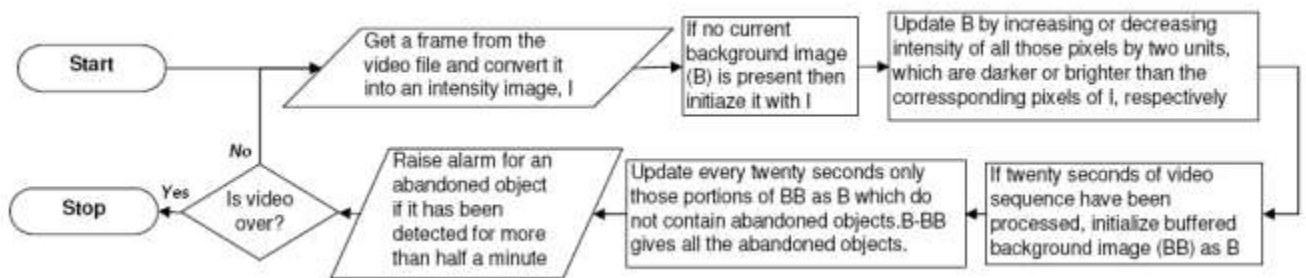


Figure 3: Flowchart of abandoned object detection system[4]

The overall system is modular in the nature and consists of four disparate blocks with each block acting as a discrete processing unit making it easy to modify any block, provided the input and output data types remain compatible with the connecting blocks. The 4 blocks are: Data extraction and conversion unit; Background subtraction module; Still object tracking and occlusion detection block and Alarm raising .display of result unit A live video stream is initially segmented into individual images from which the region of interest is extracted and converted to 3D intensity matrices (height * width * intensity value of each pixel). These matrices are then fed as input to the Background Subtraction module.

In [5] YingLi Tian, Rogerio Schmidt Feris, Haowei Liu, Arun Hampapur, and Ming-Ting Sun, proposed a novel solution to detect abandoned and removed objects. Compared to their previous work, there are four major extensions that are merit being highlighted:

- 1) The previous work did not keep a history of the background objects on scene. The extended method is provide more accurate results to classify static regions into abandoned and removed objects;
- 2) The previous work was not able to the distinguish stationary human from nonhuman objects. In this paper, they integrate human detection in near-field, mid-field, and far-field scenarios into the framework;
- 3) The previous work did not use any tracking information. In order to lessen the false positives in complex videos, we employ the tracking trajectories as the complementary information;
- 4) They add more quantitative experimental results in complex city scenarios and demonstrate the efficiency and robustness of the

proposed work. In addition, the mathematical framework behind the technique are described in this paper. Figure 4 shows their system diagram. The system includes four main components: 1) BGS and static-region detection; 2) object type detection (abandoned or removed); 3) abandoned/removed object alert detection; and 4) integration with human detection and tracking information for abandoned and removed object alert detection.

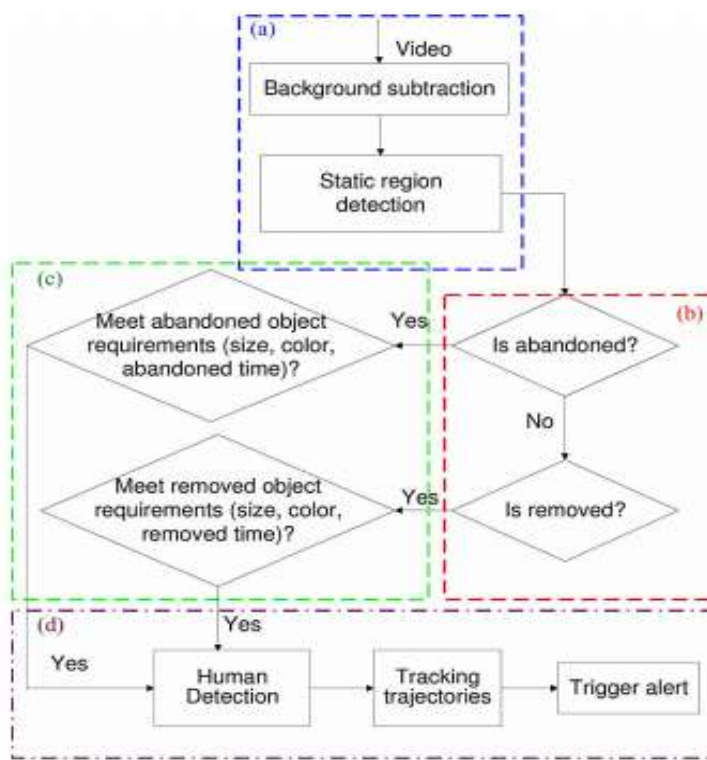


Figure 4. System Architecture[5]

In [9], E. Auvinet, E. Grossmann, C. Rougier, M. Dahmane, and J. Meunier, presented an algorithm to detect abandoned luggage in the real world public environment. This is a typical challenge of nowadays surveillance systems. They present a planar homography constraint to the resolve occlusions and detect the locations of people on the ground plane corresponding to their feet. Their video surveillance process is described in Figure 5.

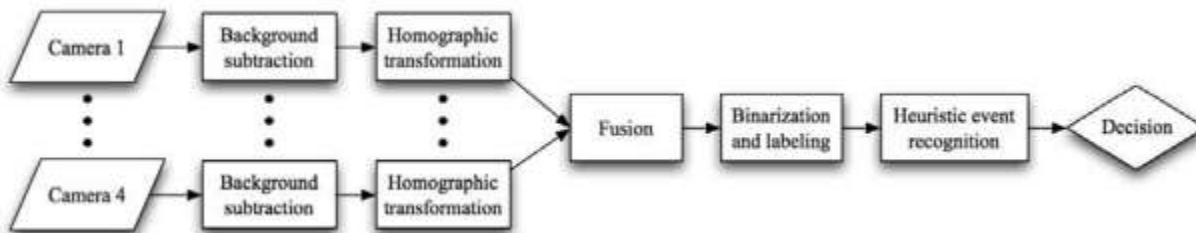


Figure 5. video surveillance process[9]

First, they perform a background subtraction in the image plane of each camera. Then, a homographic transformation is performed to merge information from all cameras in the scene floor homographic image. Finally, they work in the homographic image to track people using a heuristic method to detect suspect events. Their main contribution is to present results obtained by a simple modular system. Its principal merit is that it has a few parameters, most of them being easily identified physical quantities.

Table 1. Abandoned Object detection Methods/Technique.

Authors	Methods	Description
Kevin Lin, Shen-Chi Chen,[1]	Dual Background Subtraction, PFSM	Dual subtraction is used to identify current and background image. Then a Pixel based finite state machine method is applied to that image and the static object can be detected.
F. Porikli, Y. Ivanov, and T. Haga,[2]	Dual Foreground, Bayesian Update	Each pixel as layers of 3D multivariate Gaussians. Each layer corresponds to a different appearance of the pixel. Using Bayesian approach, they are not estimating the mean and variance of the layer, but the probability distributions of mean and variance.
Rajesh Kumar Tripathi, Anand Singh Jalal[3]	Contour feature, Edge based object recognition	<p>Extract two consecutive binary foreground frames and find the contours of both the frames. The area and length of a contour from both frames are calculated and then, area ratio, length ratio and center position of the contour is calculated to determine static object into the frame.</p> <p>Identification of human and non-human static objects is performed by using edge-based object recognition, which is robust in similarity measure when the object is partially visible due to the occlusion. Edge-based object recognition algorithm uses edge information of an object into a human edge based template.</p>
A. Singh, S. Sawan, M. Hanmandlu[4]	Dual background segmentation, Blob detection	Technique requires two reference background images, namely, 'Current Background' and 'Buffered Background'. This technique of storing two backgrounds can be considered as a dual background method. The blob analysis takes as an input a binary image, applies an algorithm and returns various properties of the detected blobs like bounding box, area, centroid position etc.
Y. Tian, R. S. Feris, H. Liu,[5]	Background subtraction with Gaussian Mixture Model	The mixture of Gaussians BGS method is employed to detect both background and static foregrounds by using the same Gaussian mixture model. Then, the static foregrounds were classified into abandoned or removed objects by segmenting and comparing the surrounding areas of the background model and the foreground image.

CONCLUSION

This paper explored related research efforts that focused on Abandoned Object Detection System. We have presented various methods such as background subtraction, dual background segmentation, mixture of Gaussians (GMM), contour search, blob detection etc that used to detect Suspicious/Abandoned object in different environment. Methods are categorized such as Short term and Long term, background subtraction.

REFERENCES:

- [1] Kevin Lin, Shen-Chi Chen, Chu-Song Chen, Daw-Tung Lin, and Yi-Ping Hung, Senior Member, IEEE, "Abandoned Object Detection via Temporal Consistency Modeling and Back-Tracing Verification for Visual Surveillance", *Ieee Transactions On Information Forensics And Security*, Vol. 10, No. 7, July 2015.
- [2] F. Porikli, Y. Ivanov, and T. Haga, "Robust abandoned object detection using dual foregrounds", *EURASIP J. Adv. Signal Process.*, vol. 2008, Jan. 2008, Art. ID 30.
- [3] Rajesh Kumar Tripathi, Anand Singh Jalal, "A Framework for Abandoned Object Detection from Video Surveillance", Dept. of Computer Engineering & Applications GLA University, Mathura Mathura, India.
- [4] A. Singh, S. Sawan, M. Hanmandlu, "An abandoned object detection system based on dual background segmentation", Department of Electrical Engineering I.I.T. Delhi Delhi, India, 2009 Advanced Video and Signal Based Surveillance.
- [5] Y. Tian, R. S. Feris, H. Liu, A. Hampapur, and M.-T. Sun, "Robust detection of abandoned and removed objects in complex surveillance videos," *IEEE Trans. Syst., Man, Cybern. C, Appl. Rev.*, vol. 41, no. 5, pp. 565–576, Sep. 2011.
- [6] Q. Fan, P. Gabbur, and S. Pankanti, "Relative attributes for largescale abandoned object detection," in *Proc. IEEE ICCV*, Dec. 2013, pp. 2736–2743.
- [7] H.-H. Liao, J.-Y. Chang, and L.-G. Chen, "A localized approach to abandoned luggage detection with foreground-mask sampling", in *Proc. IEEE 5th Int. Conf. AVSS*, Sep. 2008, pp. 132–139
- [8] Kahlil Muchtar, Chih-Yang Lin, Li-Wei Kang, and Chia-Hung Yeh, "Abandoned Object Detection in Complicated Environments" Department of Electrical Engineering, National Sun Yat-sen University, Kaohsiung, Taiwan, R.O.C. E-mail: mr.k.stt@gmail.com Tel: +886-7-5252000.
- [9] E. Auvinet, E. Grossmann, C. Rougier, M. Dahmane, and J. Meunier, "Left-luggage detection using homographies and simple heuristics," in *Proc. 9th IEEE Int. Workshop PETS*, 2006, pp. 51–58.

Review on Performance Enhancement of Plastic Injection Molding using Conformal Cooling Channels

Deepika Singh Singraur¹, Dr. Bhushan Patil²

¹Assistant Professor, Production Engineering Department

Fr. Conceicao Rodrigues College of Engineering, Bandra, Mumbai

deepika.singraur@gmail.com

²Professor, Production Engineering Department

Fr. Conceicao Rodrigues College of Engineering, Bandra, Mumbai

Abstract— In injection molding the cooling design is very important as it affects the part quality and the cycle time. The cooling can be achieved by conventional drilling method but it is limited to the complexities of the shape. Thus conformal cooling channels are used to reduce the cycle time for cooling and to control the volume shrinkage to attain dimensional stability. Advanced rapid tooling technologies and rapid prototyping technologies have proved to be helpful for making conformal cooling channels. This paper presents a literature review of various types of cooling channels in injection molding so as to get uniform cooling and reduction in cycle time.

Keywords— Plastics, Injection molding, conformal cooling, cooling channels, cycle time, temperature distribution, simulation

INTRODUCTION

Injection molding is a very common plastic processing method to convert raw plastics to an object of practical use. It is a common manufacturing process to make consumer products, engineering parts, medical devices etc. About 80% of cycle time is taken up by cooling phase. The cooling system must be able to remove the heat at the required rate so that the plastic part can be ejected without distortion. At the same time, the cooling of the part should be kept as uniform and balanced as possible so that undesired defects such as shrink marks, differential shrinkage, internal thermal residual stresses and warpage can be reduced.

In cooling design, design variables typically include the size, location and lay out of cooling channels and the thermal properties, temperature and flow rate of the coolant. The analysis of heat transfer within the mold and part plays a crucial role in optimum cooling system design. Among the number of stages involved in injection molding of plastics, cooling stage is a very important as it affects the productivity and mold quality. A careful control of surface temperatures, and heat transfer rates, to increase production are vital. Many manufacturing processes like injection molding, extrusion, blow molding and die casting can be benefitted by implementing the methods of increased and balanced heat transfer within the tooling. In injection molding the heat transfer is generally carried out using straight cooling channels drilled into the mold. It is difficult to position these cooling channels close to the surface of the cavity in such a way it provides optimal cooling. Thus conformal cooling channels are the better alternatives for this. Due to the rapid advancements in Additive Manufacturing it is easy to produce complex conformal cooling channels with the techniques like 3D printing, Direct Metal Laser Sintering (DMLS), Selective Laser Melting (SLM). With the reduction in cycle time, significant cost saving can be achieved.

LITERATURE REVIEW

Eric Dimla [1] investigated the temperature profile along the mold cavity wall to improve cooling system design to determine optimum and efficient design. The Virtual models were made from Solidworks and Moldflow for straight and conformal cooling channels.

Hsu, F, H, et al. [2] considered two different models with normal and conformal cooling design. Results showed that conformal cooling was effective reducing cooling time and product displacement. Using CFD analysis showed the coolant flow behavior showing cooling channel efficiency.

Wang Yu, et al. [3] designed the conformal cooling circuit on the basis of the relationship formulated between conformal cooling and geometry shape of cooling circuit. The cooling design formulation is done with the help of heat transfer model, approximation of cooling depth, spacing of cooling channels and estimation of number of Voronoi sites. The cooling performance is demonstrated on case studies of helmet and cell phone.

Marques Sabrina, et al. [4] proposed parallel circuit and serial circuit conformal cooling. They also have presented a case study on performance of three cooling designs using CAE simulation (Moldflow V10). Conformal cooling channel in series channel proved to be the best choice for the case investigated.

Qiao H. [5] developed an optimization methodology for computer aided cooling design system in injection molding. They have developed a perturbation approach using boundary element method to perform design sensitivity analysis.

Au K. M. and K. M. Yu. [6] proposed a novel scaffold cooling for more uniform cooling channel. The CAE and CFD analysis indicated that this technique offers more uniform thermal distribution with minor in-cavity residual stresses occurrence.

Wu Tong, et al. [7] has proposed a framework for optimization of additive manufacturing of plastic injection molds. They have investigated numerical thermal FEA modeling, thermal mechanical topology optimization in macroscale and material optimization. Conducted advanced numerical simulation of a die with conformal cooling. ANSYS work bench was used for predicting cycle time and other parameters. They have developed a 2D thermo-mechanical topology optimization algorithm.

Wang Yu et al. [8] developed an approach to generate spiral and conformal cooling channels with high curved surfaces. In the comparison it is indicated that spiral cooling channels made using algorithm and BDM analysis based deposition algorithm is easier to fabricate using copper duct bending.

Brooks Hadley and Kevin Brigden [9] introduced a concept of conformal cooling layers filled with self supporting repeatable unit cells that form lattice throughout the cooling channel. They also designed a methodology to create conformal cooling layers. They have conducted a virtual case study to compare three different cooling systems for a rectangular enclosure. The simulations were done using Solidworks Plastic Advanced 2014.

J. C Ferreira and A. Mateus. [10] proposed a new approach to integrate advanced processing technologies such as Rapid Prototyping (RP) and Rapid Tooling (RT).

Au K. M., et al. [11] proposed a new methodology for automatic preliminary cooling using visibility based cooling generation. They have developed an analogy between mould surface and cooling channel based on visibility from each other. A 3D shell model was used and melt flow analysis was done.

Kunnayut Eiamsa et al. [12] A mold is created by conformal bubbler cooling tunnels by metal deposition process.. The mold core is developed in SolidWorks software keeping injection pressure, mold temperature and clamping force the maximum displacement occurred at midpoint between edge of the mold core and web. The CAD MOLD core was converted to an STL file format. The mold core is formed in hybrid machine through deposition process. Number of simulations related to mold cooling have been introduced.

Khurram Altaf et al. [13] fabricated the conformal cooling channels in aluminum filled epoxy mould using rapid prototyping and rapid tooling techniques. They have two moulds with part cavity, one circular and other profiled. Experimental analysis showed reduced cycle time for PCCC moulds.

A. B. M. Saifullah and S. H. Masood [14] have studied the optimum design for conformal cooling channels using finite element analysis and thermal heat transfer analysis. They have optimized cooling time by ANSYS thermal analysis software.

Omar A Mohamed et al. [15] have done a simulation study of different types cooling channels. The channel was designed using Pro/Engineer Wildfire 5. The IGES CAD model was imported to Autodesk Moldflow Insight (AMI) simulation software for analysis using dual domain meshing. Molding Window has been used for the analysis.

Hong-Seok Park and Xuan-Phuong Dang [16] proposed the use of cooling channel with array of baffles, the performance of heat exchanger in the injection mold can be improved. They have also presented a new algorithm for calculating various parameters that are significant in cooling.

Ping Hu et al. [17] investigated several models of cooling channel designs considering the evaluation indicators as maximum temperature, temperature uniformity, pressure drop between inlet and outlet and maximum velocity in channels. They have defined a figure of merit (FoM). The physical model comprised solid region and liquid region. They have created a CAD model using CATIA. The multi-indicator comprehension evaluation method, it was concluded that serpentine conformal cooling channel has best cooling performance.

D. E. Dimla [18] generated a virtual model of cooling system using Model Master in I-DEAS and used mold flow software to find the best position for the runner. They have conducted a finite element analysis using MPA as a tool material. Simulation results helped in optimization and prediction of best location for channels.

Neculai Ivascu and Cătălin Fetecau [19] proposed a new cooling system that uses a metallic mold with thin walls, to increase heat absorption. They have calculated total amount of heat carried into the mold. Through their work they have found that reduction in wall thickness, reduction in cycling time and reduction in clamp tonnage reduces the cost.

Q Niu et al. [20] developed an intelligent cooling channels design system including automatic layout of cooling system, interface checking, automatic assembly of accessories by interactive interfaces. System was developed using Unigraphics NX CAD/CAM platform. Results were analyzed this using genetic algorithm.

A. B. M. Saifullah et al. [21] presented a comparison between square section conformal cooling channel (SSCCC) and convectional straight cooling channels (CSCC) and simulated using Moldflow Plastic Insight (MPI) software. SSCCC was proven to be better with less cooling time and better temperature distribution.

Emanuel Sachs et al. [22] have compared the mold surface temperature during injection cycle of a 3D printed mold with conformal cooling channels and mold machined with conventional straight channels. They have demonstrated that inserts with conformal cooling channels exhibit more uniform surface temperature than straight channels.

Velia García Loera et al. [23] have done a significant work in setting the process variables in thermoplastic injection molding operation. They were first to do a practical case study based on the application of Data Envelopment Analysis (DEA).

Z. Nooraizedfiza et al. [24] evaluated the performance of cooling channels compared to straight drilled cooling channels in order to minimize warpage on thin shallow parts. The results of simulation were analyzed by using Taguchi method and Analysis of Variance.

C. I. Li et al. [25] developed a framework for layout design for the cooling system. They also have devised a search tree to represent the design process. By conducting the experimental analysis they have verified their layout design.

A. B. M. Saifullah and S. H. Masood [26] designed the CAD model of core and cavities for conformal cooling using Pro/Mold design and Pro-Engineer software. The part chosen was plastic canister made by polypropylene thermoplastic. The thermal analysis was done using ANSYS. The results have indicated that 35 % reduction in total cycle time can be obtained.

B. Duleva and F. Greskovic [27] have described the capabilities and performance of conformal cooling and its manufacturing by Direct Metal Laser Sintering (DMLS).

K. Poornima and M. N. M. Ansari [28] have compared the straight drilling cooling channel (SDCC) with conformal cooling channels. This was done by analyzing multi-cavity rectangular plate for inappropriate draft angles and nominal wall thickness. Designing of rectangular plate was done using Pro-E Wildfire 5 and imported to Autodesk Moldflow for analysis. Spiral cooling channel needed the least cooling time.

Alban Agazzi et al. [29] presented a new approach for determination of cooling system of a 3D industrial part. They have done this formulating the control problem for optimal fluid temperature distribution along cooling surface and then by doing thermal analysis for the location of isotherms in quasi-stationary thermal zones.

Shayfull Zamree Abd Rahim et al. [30] presented a new design of milled grooved square shape conformal cooling channels. They have examined the warpage and cooling time for the molded parts. When simulated using Autodesk Moldflow Insight 2013 and compared with conventional straight drilled cooling channels, the conformal cooling channels were better.

Z. Shayfull et al. [31] presented milled grooved square shape conformal cooling channels gives better cooling than circular or other types of cooling channels. They investigated the case study on front panel housing by simulating on Autodesk Mold Flow Insight.

Melissa Hall and Mark Krystofik [32] discussed about the driving forces of conformal cooling channels. They have also discussed the design limitations for these channels. They have identified four factors that define the feasibility region for length and diameter of cooling channels, coolant pressure and temperature variations, ability to remove support material and actual part geometry.

Juan M. Jauregui-Becker et al. [33] developed a software engineering tool for automating the design of cooling system for injection molding. A comparison of results obtained from the proposed software tool and by applying best practice tool engineering design approach was done. These methods were applied to the mould design of two thin-walled products, namely a rectangular flat box and a cylindrical container with a flat base. The CAD model was developed using SolidWorks API and the algorithm for cooling generation was developed using C#.

CONCLUSION

The above study showed that conformal cooling channels are the most suitable cooling system for plastic injection molding as compared to conventional cooling channels. Better cooling properties are obtained due to low volume shrinkage and lower time to reach ejection temperature which led to reduction in cycle time, less energy consumption. Virtual 3D CAD models for determining optimum and efficient design and effectiveness can be analyzed using simulation software's. With optimum cooling pattern a reduction in cost is achieved.

REFERENCES:

- [1] Dimla, Eric. "DESIGN CONSIDERATIONS OF CONFORMAL COOLING CHANNELS IN INJECTION MOULDING TOOLS DESIGN: AN OVERVIEW." *Journal of Thermal Engineering* 1, no. 7 (2015).
- [2] Hsu, F. H., Kf Wang, C. T. Huang, and RYb Chang. "Investigation on conformal cooling system design in injection molding." *Advances in Production Engineering & Management* 8, no. 2 (2013): 107.
- [3] Wang, Yu, Kai-Min Yu, Charlie CL Wang, and Yunbo Zhang. "Automatic design of conformal cooling circuits for rapid tooling." *Computer-Aided Design* 43, no. 8 (2011): 1001-1010.
- [4] Marques, Sabrina, Adriano Fagali de Souza, Jackson Miranda, and Ihar Yadroitsau. "Design of conformal cooling for plastic injection moulding by heat transfer simulation." *Polímeros* 25, no. 6 (2015): 564-574.
- [5] Qiao, H. "A systematic computer-aided approach to cooling system optimal design in plastic injection molding." *International Journal of Mechanical Sciences* 48, no. 4 (2006): 430-439.
- [6] Au, K. M., and K. M. Yu. "A scaffolding architecture for conformal cooling design in rapid plastic injection moulding." *The International Journal of Advanced Manufacturing Technology* 34, no. 5-6 (2007): 496-515.
- [7] Wu, Tong, Suchana A. Jahan, Praveen Kumar, Andres Tovar, Hazim El-Mounayri, Yi Zhang, Jing Zhang, Doug Acheson, Kim Brand, and Razi Nalim. "A Framework for Optimizing the Design of Injection Molds with Conformal Cooling for Additive Manufacturing." *Procedia Manufacturing* 1 (2015): 404-415.
- [8] Wang, Yu, Kai-Min Yu, and Charlie CL Wang. "Spiral and conformal cooling in plastic injection molding." *Computer-Aided Design* 63 (2015): 1-11.
- [9] Brooks, Hadley, and Kevin Brigden. "Design of conformal cooling layers with self-supporting lattices for additively manufactured tooling." *Additive Manufacturing* 11 (2016): 16-22.
- [10] Ferreira, J. C., and A. Mateus. "Studies of rapid soft tooling with conformal cooling channels for plastic injection moulding." *Journal of Materials Processing Technology* 142, no. 2 (2003): 508-516.
- [11] Au, K. M., K. M. Yu, and W. K. Chiu. "Visibility-based conformal cooling channel generation for rapid tooling." *Computer-Aided Design* 43, no. 4 (2011): 356-373.
- [12] Eiamsa-ard, Kunyut, and Kittinat Wannissorn. "Conformal bubbler cooling for molds by metal deposition process." *Computer-Aided Design* 69 (2015): 126-133.
- [13] Altaf, Khurram, Ahmad Majdi Abdul Rani, and Vijay R. Raghavan. "Prototype production and experimental analysis for circular and profiled conformal cooling channels in aluminium filled epoxy injection mould tools." *Rapid Prototyping Journal* 19, no. 4 (2013): 220-229.

- [14] Saifullah, A. B. M., and S. H. Masood. "Finite element thermal analysis of conformal cooling channels in injection moulding." In *5th Australasian Congress on Applied Mechanics (ACAM 2007)*, vol. 1, pp. 337-341. Engineers Australia, 2007.
- [15] Mohamed, Omar A., S. H. Masood, and Abul Saifullah. "A Simulation Study of Conformal cooling channels in plastic injection molding." *International Journal of Engineering Research*, Volume 2: 344-348.
- [16] Park, Hong-Seok, and Xuan-Phuong Dang. "Optimization of conformal cooling channels with array of baffles for plastic injection mold." *International Journal of Precision Engineering and Manufacturing* 11, no. 6 (2010): 879-890.
- [17] Hu, Ping, Bin He, and Liang Ying. "Numerical investigation on cooling performance of hot stamping tool with various channel designs." *Applied Thermal Engineering* 96 (2016): 338-351.
- [18] Dimla, D. E., M. Camilotto, and F. Miani. "Design and optimisation of conformal cooling channels in injection moulding tools." *Journal of Materials Processing Technology* 164 (2005): 1294-1300.
- [19] Ivascu, Neculai, and Cătălin Fetecau. "Dynamic Temperature Control In Injection Molding With New Conformal Heating/Cooling System." (2010): 1221-4566.
- [20] Niu, Q., X. H. Zhou, and W. Liu. "Research and Development of Intelligent Cooling Channels Design System." *Research and Development* 1 (2014): 11809.
- [21] Saifullah, A. B. M., S. H. Masood, and Igor Sbarski. "New cooling channel design for injection moulding." In *Proceedings of the World Congress on Engineering*, vol. 1. 2009.
- [22] Sachs, Emanuel, Edward Wylonis, Samuel Allen, Michael Cima, and Honglin Guo. "Production of injection molding tooling with conformal cooling channels using the three dimensional printing process." *Polymer Engineering & Science* 40, no. 5 (2000): 1232-1247.
- [23] Loera, Velia García, José M. Castro, Jesús Mireles Diaz, Óscar L. Chacón Mondragón, and Mauricio Cabrera-Ríos. "Setting the Processing Parameters in Injection Molding Through Multiple-Criteria Optimization: A Case Study." *IEEE Transactions on Systems, Man, and Cybernetics, Part C* 38, no. 5 (2008): 710-715.
- [24] Z. Shayfull, Z. Nooraizedfiza, S. A. Adam, S.M. Nasir and M. A. Fairuz " Analysis of Thin Shallow Parts in Three-Plate Molds with Straight Drilled and Conformal Cooling Channels", Australian journal of Basic and Applied Sciences, 7(5): 187-195, ISSN 1991-8178 (2013).
- [25] Li, C. L., C. G. Li, and A. C. K. Mok. "Automatic layout design of plastic injection mould cooling system" *Computer-Aided Design* 37, no. 7 (2005): 645-662.
- [26] Saifullah, A. B. M., and S. H. Masood. "Cycle time reduction in injection moulding with conformal cooling channels" In *Proceedings of the International Conference on Mechanical Engineering, Dhaka, Bangladesh: [sn].* 2007.
- [27] B. Duleva and F. Greskovic. "Conformal Cooling for Plastic Injection Molding", ISSN 1338-0761.
- [28] Poornima, K., and M. N. M. Ansari. "Cooling Channel Design for Multi-Cavity Plastic Injection Moulds", Volume 2 Issue 5, ISSN: 2319-7064 (2013).
- [29] Agazzi, Alban, Vincent Sobotka, Ronan LeGoff, and Yvon Jarny. "Optimal cooling design in injection moulding process—A new approach based on morphological surfaces." *Applied Thermal Engineering* 52, no. 1 (2013): 170-178.
- [30] Rahim, Shayfull Zamree Abd, S. Sharif, Azlan Mohd Zain, S. M. Nasir, and R. Mohd Saad. "Improving the quality and productivity of molded parts with a new design of conformal cooling channels for the injection molding process." *Advances in Polymer Technology* 35, no. 1 (2016).
- [31] Shayfull, Z., S. Sharif, Azlan Mohd Zain, R. Mohd Saad, and M. A. Fairuz. "Milled groove square shape conformal cooling channels in injection molding process." *Materials and Manufacturing Processes* 28, no. 8 (2013): 884-891.
- [32] Melissa Hall and Mark Krystofik "White Paper on Conformal Cooling", <https://www.rit.edu/gis/public/Conformal%20Cooling%20White%20Paper-1.pdf> (2005).
- [33] Jauregui-Becker, Juan M., Guido Tosello, Fred JAM Van Houten, and Hans N. Hansen. "Performance evaluation of a software engineering tool for automated design of cooling systems in injection moulding." *Procedia CIRP* 7 (2013): 270-275.

Experimental Study on Structural Beams Using Waste Foundry Sand and Phosphogypsum

Archana Sukumaran¹, Amritha E.K²

¹ PG Scholar, Dept of Civil Engineering, Universal Engineering College, Vallivattom, Thrissur, Kerala, India.

² Associate professor, Dept of Civil Engineering, Universal Engineering College, Vallivattom, Thrissur, Kerala, India.

archanasukumaran47@gmail.com

Abstract— This experimental research was conducted to study the effect of waste foundry sand and phosphogypsum on structural beams. Phosphogypsum is a byproduct of phosphate based fertilizers. Foundry sand (FS) is a by-product from the metal alloys casting industry with high silica content. This project is relevant as cost of the building material is increasing and availability of the material is decreasing, which leads to many environmental issues. M25 mix concrete was used in the study. The fine aggregate was replaced by foundry sand and cement with phosphogypsum in different proportions. Quarry sand was replaced at 10, 20, 30, 40 and 50% by foundry sand while cement replaced at 4, 6, 8, 10 and 12% with phosphogypsum. The strength properties of the mixes were compared with that of conventional concrete mix. Strength tests such as compressive strength, split tensile strength and flexural strength tests were conducted. The results say that the maximum strength was obtained at an optimum replacement of 30% foundry sand and 10% Phosphogypsum. The beam test results showed good characteristics with respect to the load deflection curves. The replaced material mixes are strong enough as well as economical.

Keywords— Phosphogypsum, Foundry sand, Quarry sand, optimum replacement, silica content, load deflection characteristics.

INTRODUCTION

Construction is a continuous process involved in rising new structures, demolishing old ones and fulfillment of the needs of mankind providing shelter, developing industrial areas and providing a basic foundation for all advancements. For construction there are a wide variety of materials being used especially due to the fast advancing techniques and inventions in this field. Yet the material that meets the standards and which is being termed a “conventional material” is concrete. The reason behind such a terminology must be due to the easy availability of materials, low cost, ease of use, strength characteristics and durability to withstand adverse conditions. In this era of advancement in almost every field, countries worldwide are developing at a steady and speedy rate to secure titles of being a “developed country”. A few problems occurring due to construction is pollution as a result of cement manufacture and lack of resources.

Foundry sand is high-quality silica sand that is used to form molds for ferrous and nonferrous metal castings. They can stand close to the concept of green concrete as it is compatible with the environment. Foundry sand is reused routinely and as the process goes on the particles eventually become too fine for the molding process and finally is discarded as spent foundry sand (SFS) or used foundry sand (UFS). In the long run, this disposal results in millions of tonnes of UFS as landfill. Based on researches done in the past few decades, FS has been utilized in highway applications, but the amount re-utilized was still negligible. For this reason, there is a need to utilize FS in other ways become very imperative. Recently, research has been carried out on the utilization of FS in concrete and concrete related products.

Phosphogypsum contributes in replacing cement partially in order to reduce the problems caused due to cement manufacture. Phosphogypsum is the gypsum formed as a byproduct of phosphate based fertilizer industries. It is produced as solid chemical hazardous waste or byproduct in industries, by wet or dry processes by action of sulphuric acid on phosphate rocks. It is slightly

radioactive and hence the disposal of it in form of landfills is a threat to the surroundings and hence effective ways of disposal should be found out in order to make sure that it is safely disposed off without causing any threat to the environment

SIGNIFICANCE OF THE WORK

A. Scope of the Work

Based on the research works already done, it is seen that replacement of constituents of concrete is effective keeping in view the strength aspects as well as economy. Different replacement materials have been studied so far in order to reduce the use of cement and fine aggregate. The increasing pollution as well as lack of resources has lead researchers to find alternate materials to replace the constituents in conventional concrete. To reduce the consumption of river sand, used foundry sand is being used and cement is being replaced with phosphogypsum.

B. Objective of the Work

The objective is replace cement with phosphogypsum and fine aggregate with foundry sand respectively in order to reduce their consumption as well as keep it economical.

C. Methodology

The methodology of the work consists of: (1) Selection of concrete grade;
M25

(2) Mix design for M25 grade concrete

(3) Casting specimens to find the optimum replacement- 0, 4, 6, 8, 10 and 12% for phosphogypsum and 0, 10, 20, 30, 40 and 50% for foundry sand

(4) Workability, compressive strength, splitting tensile strength and flexural strength tests of concrete were conducted. (5) Optimum percentage of both phosphogypsum and foundry sand was determined.

(6) based on the optimum percentage obtained, RC beams were cast to test strength aspects of the material and study load deflection characteristics.

MATERIAL TESTS

TABLE I
 MATERIAL TEST RESULTS

Test	Material	Equipment	Values
Specific Gravity	Ordinary Portland	Le-Chatelier	3.15
Specific Gravity	Fine Aggregates	Pycnometer	2.7
Specific Gravity	Coarse Aggregates	Vessel	2.94
Workability	M25 Concrete	Slump Cone	100mm

TABLE II
 PHOSPHOGYPSUM PROPERTIES

Property	Results
Fineness	16%
Specific gravity	2.72

Table III

FOUNDRY SAND PROPERTIES

Property	Results
Specific gravity	2.7

MIX DESIGN

TABLE IV
 MIX PROPORTIONS

Cement (Kg/m ³)	374.30
Fine aggregate (kg/m ³)	751.03
Coarse aggregate (Kg/m ³)	1280.31
Water (l/m ³)	149.72
Water cement ratio	0.40
Mix ratio	1:2.006:3.420

TABLE V
 VARIOUS MIXES

Mix	Phosphogypsum (%)	WFS (%)
CM	0	0
P4	4	0
P6	6	0
P8	8	0
P10	10	0
P12	12	0
F10	0	10
F20	0	20
F30	0	30
F40	0	40
F50	0	50
P10F30	10	30



Fig.1 Cast specimens

EXPERIMENTAL INVESTIGATION

A. Experimental Procedure

A total of 188 specimens were cast and tested. Details of specimens cast are shown in Table VI. Five ratios each were selected to replace cement and fine aggregate. CM denotes the control specimen. P denotes Phosphogypsum mix ratios. For example F10 denotes a mix with 10% foundry sand. Based on the optimum percentages, 8 RCC beams were cast.

B. Compressive strength

For compressive strength test, cube specimens of dimensions 150 x 150 x 150 mm were cast for M25 grade of concrete. These were then covered using plastic and later on after 24 hours they were un moulded and kept for curing in curing tanks

C. Split tensile strength

For Split tensile strength test, cylinder specimens of dimension 150 mm diameter and 300 mm length were cast. The specimens were demoulded after 24 hours of casting and were transferred to curing tank wherein they were allowed to cure for 28 days.

D. Flexural strength

For flexural strength test beam specimens of dimension 100x100x500 mm were cast. Flexural strength specimens were tested under two point loading as per I.S. 516-1959, over an effective span of 400 mm on Flexural testing machine. Load and corresponding deflections were noted up to failure.

TABLE
VI

www.ijergs.org

DETAILS OF SPECIMENS CAST

Sl. No.	Specimen	Size (mm)	Nos36.
1	Cubes	150 x 150 x 150	72
2	Cylinders	300 x 150 ϕ	36
3	Cubes	100 x 100 x 100	36
4	Prisms	100 x 100 x 500	36
5	RC beams	150 x 200 x 1250	8

Dimension of all the specimens are 150mm x 200mm x 1250mm, with an effective span of 990mm. Main reinforcement provided is 3# 12mm diameter bars, 2# 8mm diameter bars are provided as anchor bars and stirrups are provided as 8 mm diameter bars @ 130mm c/c. Two point loading using 50t loading frame was used for testing the specimens. Thus a total of 12 mixes including control mix were cast, cured and tested for.

E. Beam Test Procedure

Beams were tested using a 50t loading frame. Dial gauge was used to determine the deflection at the center of the beam. The behaviour of the beams was keenly observed from beginning to failure. The strength of the beam was tested as a two point loading system using a hydraulic jack attached to the loading frame.

The appearance of the first crack, and the development and the propagation of cracks due to increase in the load were also recorded. The loading was continued after the initial crack formation and was stopped when the beam was just on the verge of collapse. The values of load applied and deflection are noted directly and further the plot of load vs deflection is performed which is taken as the output. The load in kN is applied with uniformly increasing the value of the load and the deflection under the different applied loads is noted down. The applied load increased up to the breaking point and the ultimate cracking load was noted. The reinforcement details are provided below



Fig.2 Experimental setup of beam specimen

TABLE VII

REINFORCEMENT DETAILS

Specimen	Longitudinal Reinforcement	Stirrups	FS (%)	PG (%)
RB	3# 12 mm ϕ bars	8 mm dia @ 130mm c/c	0	0
FSB30	3# 12 mm ϕ bars	8 mm dia @ 130mm c/c	30	0
PFB10	3# 12 mm ϕ bars	8 mm dia @ 130mm c/c	0	10
P10F30	3# 12 mm ϕ bars	8 mm dia @ 130mm c/c	30	10

EXPERIMENTAL RESULTS

A. Workability

Workability of all mixes were found out. The workability of the mix reduced on adding the materials. The harshness of foundry added mixture must be due to presence of very fine particles in it. The mix was seen to have a compaction factor of 0.89.

B. Compressive strength on concrete cubes

Fig. 4 shows the 7 day and 28 day compressive strength. It is observed from the graph that there was a gradual increase in compressive strength of concrete on the addition of foundry sand. This increase was seen till 30% beyond which it dropped. Fig 5 shows the variation of compressive strength with increase in phosphogypsum replacements by 0, 4, 6, 8, 10 and 12%. The plot shows a gradual increase in compressive strength values of concrete. The increase is till 10% beyond which it decreases.

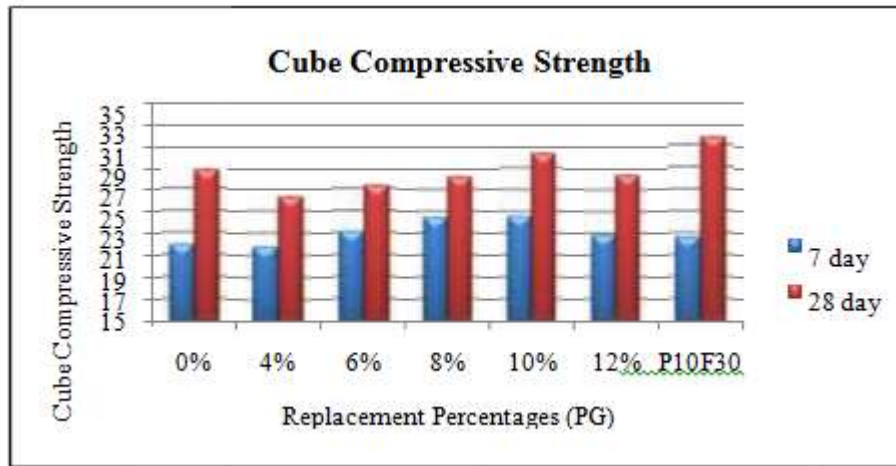


Fig 3. Variation in compressive strength for various mixes of Phosphogypsum

Fig 4. Variation in compressive strength for various mixes of foundry sand

C. Split tensile strength

Split tensile strength for Phosphogypsum incorporated concrete showed a similar trend of increase till 10%. Same is the case for foundry sand where it is seen to be increasing up to 30% replacement. Further replacement shows a decreasing trend. Fig 5 and 6 shows the variation of split tensile strength in case of Phosphogypsum and foundry sand respectively.

D. Flexural strength

Flexural strength increased in both mixes of phosphogypsum and foundry sand. The trend is similar to that of split tensile strength. The plots are given in figures 7 and 8

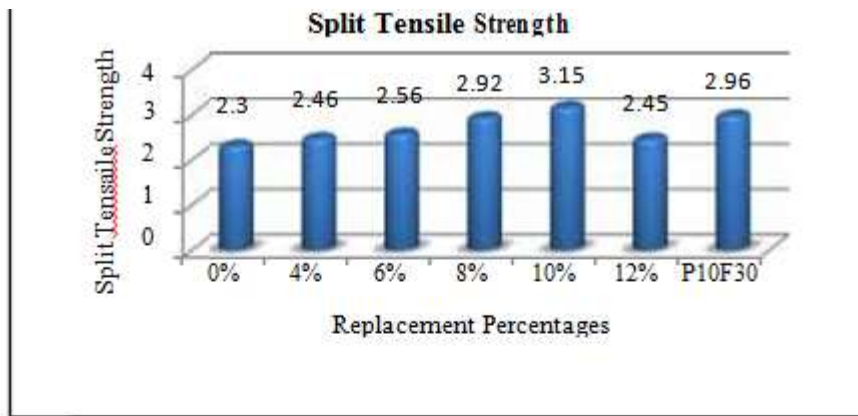


Fig 5. Variation in Split tensile strength for various mixes of Phosphogypsum

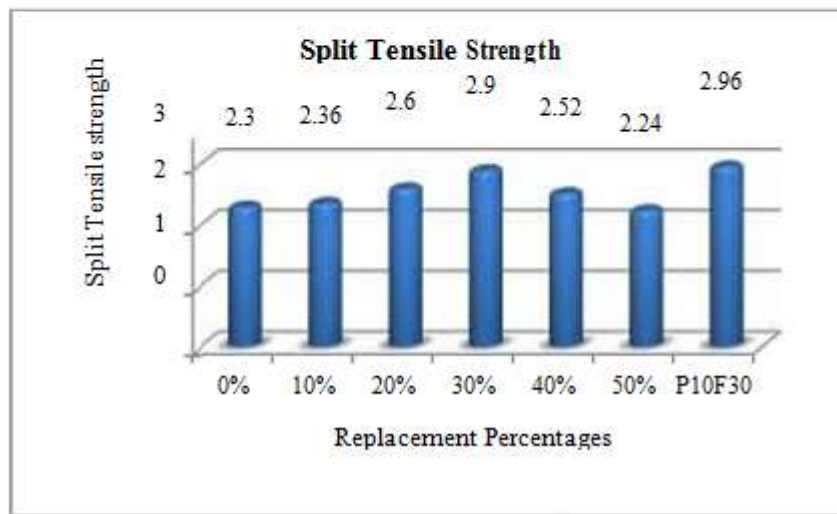


Fig 6. Variation in Split tensile strength for various mixes of Foundry sand

One important factor that leads to an increase in strength upon using waste foundry sand is the particle size. They contain very fine particles, hence making the mix less porous and denser.

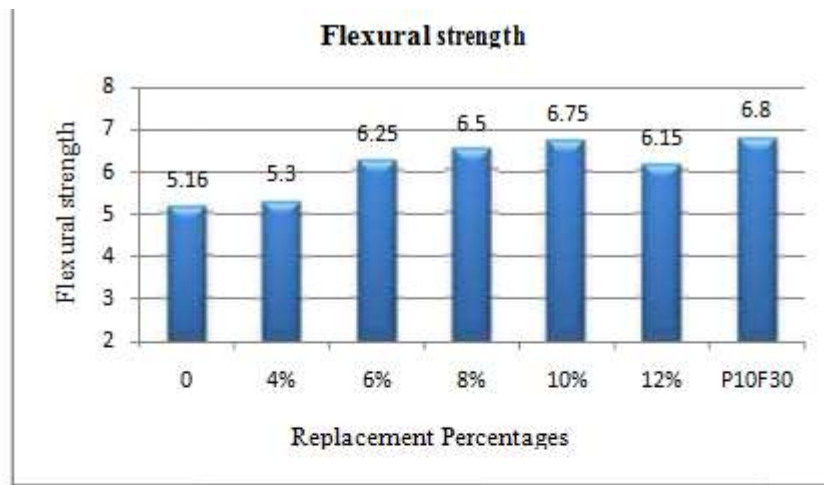


Fig.7. Variation in Flexural strength for various mixes of Phosphogypsum

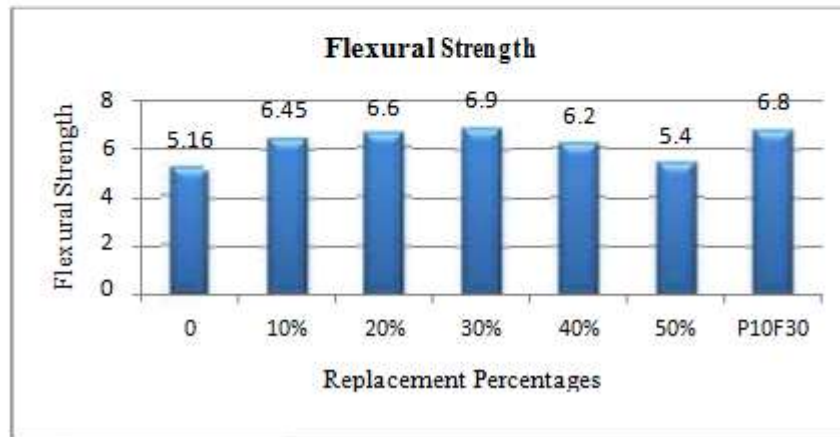


Fig.8. Variation in Flexural strength for various mixes of Foundry sand

The mixes with 10% phosphogypsum and 30% foundry sand were found to have higher strength based on the compressive strength results, flexural strength results and split tensile strength results. Thus the optimum of both materials was found. This found optimum of both obtained were then combined to obtain mixes of good strength. The compressive strength obtained for the combination of both were 31.69 MPa. The split tensile strength obtained was 3.45 MPa and flexural strength 7.25 MPa. From these results it is obvious that the combination of both proves to be successful.

E. Beam Test Results

I. Load Carrying Capacity

Ultimate strength of beams under two point loading was confirmed through recording the maximum load indicated by the dial gauge, whereas the cracking load was specified with the development of the first crack on the beam. Table IX shows the ultimate load of all the beam specimens For both, specimens partially replaced using polyethylene balls and PVC pipes it can be clearly seen that PB3 & PP3 there is a decrease in the value. Mainly shear cracks were developed from the supporting points and widened up as the load increased. At failure, the concrete in the compression region crushed. The crack patterns for different specimens are shown in Fig 5.11 to Fig 5.14 below. At the load approaching the failure load, shear cracks were developed diagonally. The cracks continued to widen as the load increased, and failure occurred soon after depicting a typical sudden type of shear failure. The crack pattern of replaced beams is similar to that of control beam.

TABLE
IX

ULTIMATE LOAD OF ALL SPECIMENS

Beam Specimen	Ultimate Load (kN)
RB	152.44
PB10	175.39
FB30	158.64
P10F30	164.91

II. Load Vs Deflection Graph

Due to increase in the load, deflection of the beam starts, upto a certain level the load vs. deflection graph will be linear i.e. load will be directly proportional to deflection. Due to further increase in the load, the load values will not be proportional to deflection, since the deflection values goes on increasing, strength of the material also increases and material loses elasticity undergoing plastic deformation. Hence from the graph we can predict strength of the material by knowing the deflection at the corresponding load values. The load vs deflection curves is shown in Fig. 10.

III. CrackPattern

Mainly shear cracks were developed from the supporting points and widened up as the load increased. At failure, the concrete in the compression region crushed. The cracks continued to widen as the load increased, and failure occurred soon after depicting a typical sudden type of shear failure. The crack pattern of replaced beams is similar to that of control specimen.



Fig 9. Crack pattern for control specimen

VII. EVALUATION AND DISCUSSION

The experimental study based on replacement of conventional concrete materials has proven to be a successful one in terms of strength as well as economy. Waste foundry sand is being discarded in tonnes and hence its availability is in plenty. An optimum of

30% replacement of fine aggregate makes it suitable for replacing based on strength parameters.

Phosphogypsum which is being discarded in plenty as landfill is a nuisance to public and hence this has proven an effective way to keep a check on it.

The advantages regarding this concrete

are: A. Better strength

The strength properties of the concrete show better results than the conventional concrete. The replacement of both fine aggregate and cement has not reduced the strength in any way. This is the most important criteria kept in mind while conducting replacement experiments.

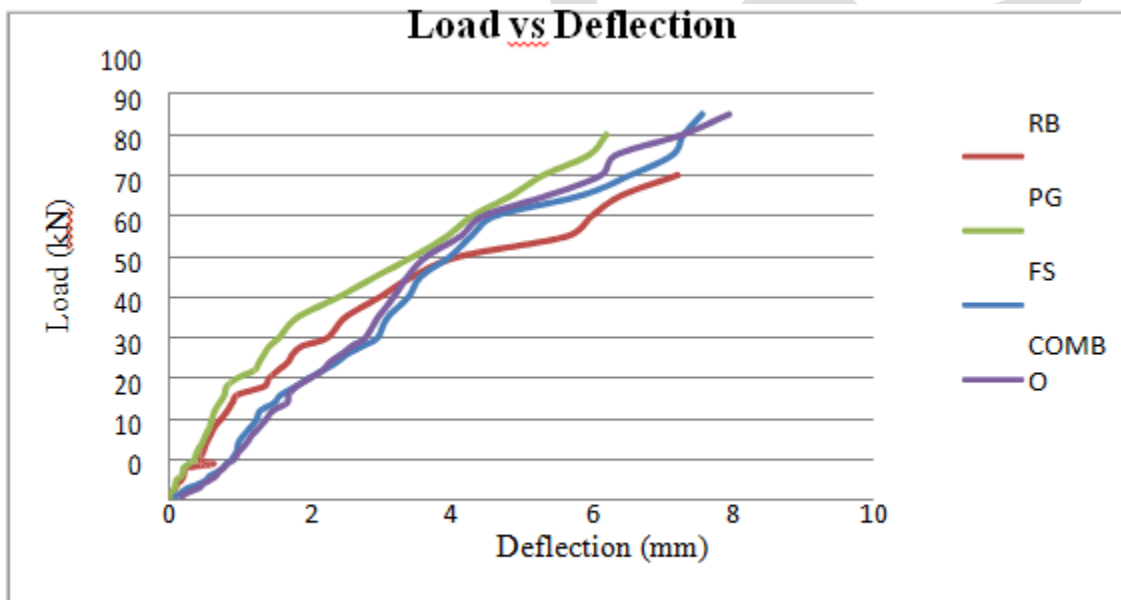


Fig.10 Load Vs Deflection Of Beams

B. Economical

The experiment has proven to be a low cost one without expenses higher than conventional concrete. This is due to the fact that both the materials used in this experiment are available as landfills and hence free of cost. Further with replacement of cement and fine aggregate, the cost further cuts down. Current days the entire field is filled with competition, and it is necessary that a business concern should have utmost efficiency and minimum possible wastages to reduce the cost of production. From the study conducted, we can conclude that usage of these two discarded materials phosphogypsum and foundry sand can be cost efficient than the conventional materials.

ACKNOWLEDGMENT

My sincere gratitude to my guide, Mrs. Amritha E. K, Assistant Professor who has believed in me since the beginning and accepted in undertaking my research work. Moreover, she has helped me from start to finish.

I'm thankful to all the teaching and non-teaching staffs of department of Structural Engineering, Universal Engineering College for offering me the opportunity to do this research work.

Finally, deep thanks to God for his unconditional support, and also to my family and friends who have helped me in the successful completion.

CONCLUSIONS

The research work conducted on partial replacement of cement and fine aggregate with phosphogypsum and waste foundry sand respectively shows that it not only reduces the cost of construction, but also keeps the strength parameters intact. The optimum percentage of phosphogypsum to replace cement partially is 10%. The optimum percentage of waste foundry sand to replace fine aggregate partially is 30%. The workability of the mix on adding foundry sand reduces. This is due to the presence of very fine particles making the mix very harsh to work upon. The strength gain for mixes containing foundry sand is due to the very fine particles which result in a denser mix, hence stronger concrete. The experiment is very economical and materials are easily available. The RC beam load deflection gives satisfactory results in terms of strength. The load deflection curve values showed the beam with combination mix to yield under load greater than that of reference beam.

REFERENCES:

- [1] Y. Aggarwal and R. Siddique, "Microstructure And Properties Of Concrete Using Bottom Ash And Waste Foundry Sand As Partial Replacement Of Fine Aggregates", *Construction and Building Materials*, Vol-54, 2014.
- [2] D. R. Amitkumar, P. Arti and I. K. Alefiya, "Foundry Sand: Utilisation As A Partial Replacement Of Fine Aggregate For Establishing Sustainable Concrete", *International Journal Of Engineering Sciences & Research Technology*, Vol-4, Issue-1, 2015.
- [3] S. S. Bhadauria and B. T. Rajesh, "Utilisation Of Phosphogypsum In Cement Mortar And Concrete", 31st Conference On Our World In Concrete & Structures, 2006.
- [4] D. R. Bhimani, J. Pitroda and J. J. Bhavsar, "Used Foundry Sand: Opportunities For development Of Eco-Friendly Low Cost Concrete", *International Journal of Advanced Engineering Technology*, Vol-4, Issue-1, 2013
- [5] D. R. Bhimani, J. Pitroda and J. J. Bhavsar, "Innovative Ideas for Manufacturing of the Green Concrete by Utilizing the Used Foundry Sand and Pozzocrete", *International Journal of Emerging Science and Engineering*, Volume-1, Issue-6, 2013.
- [6] S. Dhinakaran, and R. S. Shanthi, "Experimental Investigation on Concrete with Phosphogypsum", *International Journal on Emerging Researches in Engineering Science and Technology*, Volume-2, Issue-3. 2015.

- [7] N. Ghafoori and W. F. Chang, "Investigation Of Phosphate Mining Waste For Construction Materials", Journal of Materials in Civil Engineering, Vol. 5, No- 2. 1993.
- [8] H. K. Khater and S. R Zedane, "Geopolymerization of Industrial By-Products and Study of their Stability upon Firing Treatment", International Journal of Engineering and Technology, Vol-2, No. 2, 2012.
- [9] J. M. Khatib and B. A. Herki, "Capillarity of Concrete Incorporating Waste Foundry Sand", Journal of Engineering Research and Applications, Vol. 1, 2012.
- [10] R. N Kraus, T. R Naik, B. W. Ramme and R. Kumar, "Use of foundry silica-dust in manufacturing economical self-consolidating concrete", Construction and Building Materials, Vol-23, 2009.
- [11] K. Lineesh, D. Sivakumar and S. J. Sundaram, "Comparative Study on Partial Replacement of Fine Aggregate by Glass Powder and Foundry Sand", International Journal of Advanced Information Science and Technology, Vol.32, No.32,2014.
- [12] A. B. Mahesh, and S. A. Satone, "An Experimental Investigation Of Partial Replacement Of Cement By Various Percentage Of Phosphogypsum In Cement Concrete", International Journal of Engineering Research and Applications, Vol.2, Issue 4, 2012.

IMPLEMENTATION OF PERTURB AND OBSERVE MPPT ON PV SYSTEM USING BUCK-BOOST CONVERTERS

Srinivas.Sampathirao 1, B.Gayatri²

1P.G.Student, Dept. of EEE, Srisivani institute of technology, Chilakapalem, Andhrapradesh

2 AssistanProfessor, Dept. of EEE, Srisivani institute of technology, Chilakapalem, Andhrapradesh

ABSTRACT : The Maximum Power Point Tracking (MPPT) is a technique used in power electronic circuits to extract maximum energy from the Photovoltaic (PV) Systems. In the recent decades, photovoltaic power generation has become more important due its many benefits such as needs a few maintenance and environment advantages and fuel free. However, there are two major barriers for the use of PV systems, low energy conversion efficiency and high initial cost. One of the method to improve the energy efficiency is to work PV system always at its maximum power point. So far, many researches are conducted and many papers were published and suggested different methods for extracting maximum power point. This paper presents in details implementation of Perturb and Observe MPPT using buck ,boost and buck-boost Converters. Some results such as current, voltage and output power for each various combination have been recorded. The simulation has been accomplished in software of MATLAB Math works.

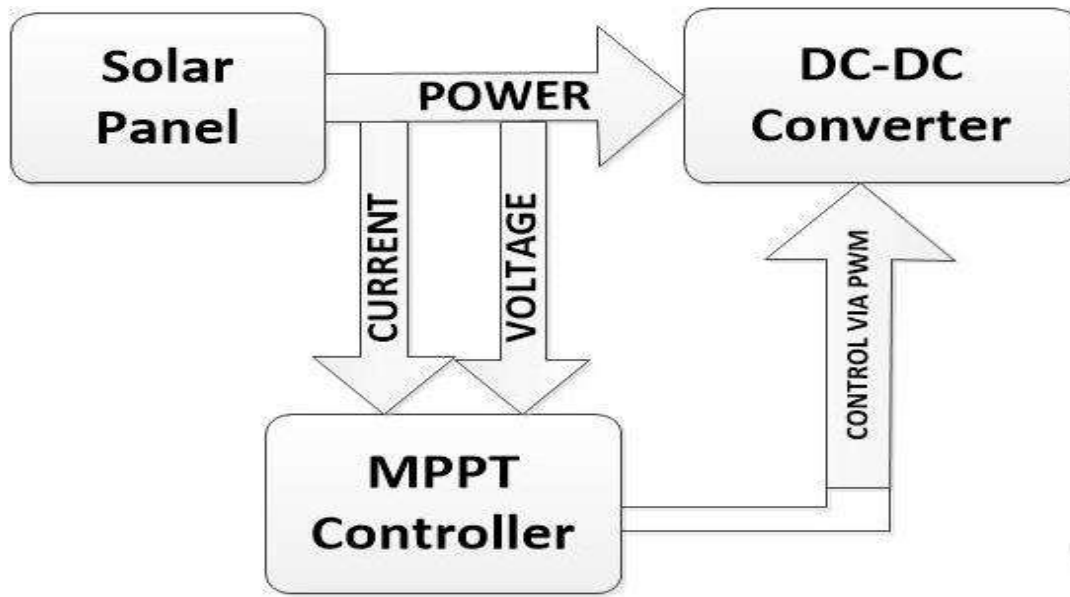
INDEX TERMS: Maximum Power Point Tracking, Perturb and Observe, DC-DC Converters, Photovoltaic System

INTRODUCTION

The usage of modern efficient photovoltaic solar cells (PVSCs) has featured as an masterminding alternative of energy conservation, renewable power and demand-side management. Due to their initial high expensive, PVSCs have not yet been an exactly a tempting alternative for electrical usage who are able to purchase less expensive electrical energy from the utility grid. However ,they have been used widely for air conditioning in remote , water pumping and isolated or remote areas where utility power is not available or is high costly to transport. Although PVSC prices have decreased considerably during the last years due to new developments in the film technology and manufacturing process . The harnessing of solar energy using PV modules comes with its own problems that arise from the change in insulation conditions. Those changes in insulation conditions strongly influence the efficiency and output power of the PV modules. A great deal of research has been accomplished to improve the efficiency of the photovoltaic system. Several methods to track the maximum power point of a PV module have been suggested to solve the problem of efficiency and products using these methods have been made and now commercially available for consumers

As the market is now flooded with species of these MPPT that are intentional to improve the efficiency of PV modules under different isolation conditions it is not known how many of these can actually provide on their promise under a diversity of field conditions. This research then seems at how a different kind of converter affects the output power of the module and also achieve if the MPPT that are said to be highly efficient and do track the true maximum power point under the different conditions. A maximum power point tracker is used for obtaining the maximum power from the solar PV module and conversion to the load. A non isolated DC-DC converter (step up/ step down) offers the purpose of conversion maximum power to the load. A DC-DC converter acts as an interface between the load and the module. By varying the ratio of duty cycle the impedance of load as it appears by the source is varied and matched at the peak power point with the source so as to conversion the maximum power .

Therefore maximum power point tracker methods are required to maintain the PV array' s working at its MPP. Many MPPT methods have been suggested in the literature ; example are the Perturb and Observe (P&O) methods, Incremental Conductance (IC) methods and constant voltage methods.. etc. In this paper the most popular of MPPT technique (Perturb and Observe (P&O) method, Buck and Buck- Boost DC-DC converters will involve in Implementation study figure 1. Some results such as current, voltage and output power for each various combination have been discussed. The MPPT technique will be implemented, by using Matlab tool Simulink, considering the variant of circuit combination.



2. Photovoltaic Cell

Photovoltaic generators are neither fixed current sources nor voltage sources but can be approximated as current generators with dependant voltage sources. During darkness, the solar cell is not an active device. It produces neither a current nor a voltage. A solar panel cell essential is a p-n semiconductor junction. When exposed to the light, a current is generated (DC current). The generated current change linearly with the solar irradiance. Figure 2 show the equivalent electrical circuit of an ideal solar cell.

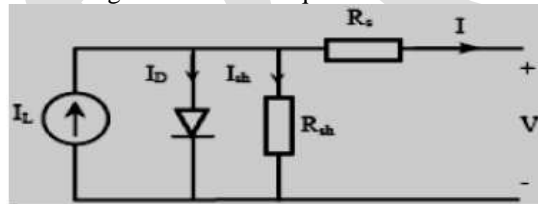


Figure 2. Equivalent circuit of a solar cell

The I-V characteristics of the solar cell circuit can be sets by the following equations . The current through diode is given by:

$$I_D = I_O [\exp (q (V + I R_S) / K T) - 1] \quad (1)$$

While, the solar cell output current:

$$I = I_L - I_D - I_{sh} \quad (2)$$

$$I = I_L - I_O [\exp (q (V + I R_S) / K T) - 1] - (V + I R_S) / R_{sh} \quad (3)$$

Where

I : Solar cell current (A)

IL : Light generated current (A)

IO : Diode saturation current (A)

q : Electron charge (1.6×10^{-19} C)

K : Boltzman constant (1.38×10^{-23} J/K)

T : Cell temperature in Kelvin (K)

V : solar cell output voltage (V)

Rs: Solar cell series resistance (Ω)

Rsh: Solar cell shunt resistance (Ω)

Electrical Characteristics	Ranges
Maximum Power (P_{max})	350
Voltage at P_{max} (V_{mp})	34.5V
Current at P_{max} (I_{mp})	7.25A
Open-circuit voltage (V_{oc})	44.1V
Short-circuit current (I_{sc})	8.65A
Temperature coefficient of I_{sc}	$0.065 \pm 0.015 \% / ^\circ C$
Temperature coefficient of V_{oc}	$-160 \pm 20 mV / ^\circ C$
Temperature coefficient of power	$-0.5 \pm 0.05 \% / ^\circ C$
NOCT	$47 \pm 2 ^\circ C$

3. DC-DC Converter Analysis

3.1 Buck Converter

A buck converter or voltage regulator is also called a step down regulator since the output voltage is lower than the input voltage. In a simple example of a buck converter, a diode is connected in parallel with the input voltage source, a capacitor, and the load, which represents output voltage. A switch is connected between the input voltage source and the diode and an inductor is connected between the diode and the capacitor, shown in Figure 3

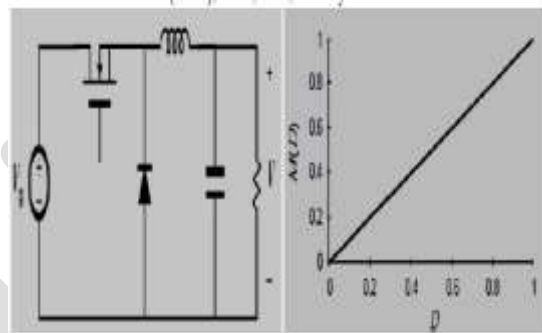
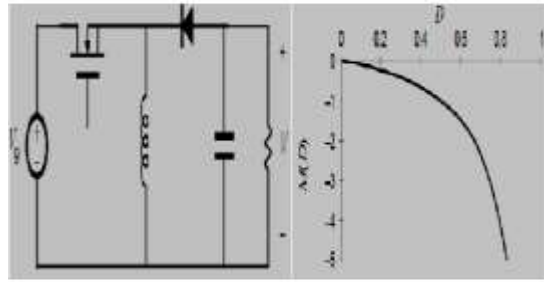


Figure 3. Basic buck converter and its dc conversion ratios $M(D)$

3.2 Buck-Boost Converter

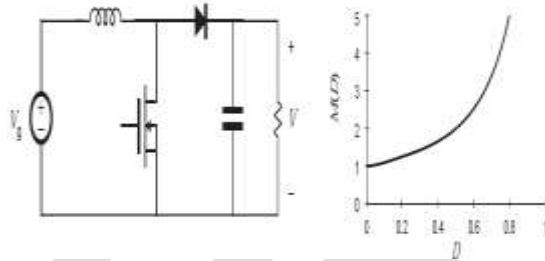
The last and most important type of switching regulator is the buck-boost converter. In this converter, the buck and boost topologies covered earlier are combined into one. A buck-boost converter is also built using the same components used in the converters covered before. The inductor in this case is placed in parallel with the input voltage and the load capacitor. The switch or transistor is placed between the input and the inductor, while the diode is placed between the inductor and the load capacitor in a reverse direction, shown in Figure 4. The buck-Boost converter provides an output voltage that may be less than or greater than the input voltage



BOOST CONVERTER:

3.3. Working Theory:

A boost converter or a voltage stepped up converter is a DC-DC converter with yield voltage enhanced contrasted with enter. It is sort of exchanged mode power supplied or SMPS that holds at any rate a diode and a transistor and in any event a vitality putting away component like capacitor, inductor, or the two together. Channels developed utilizing capacitors which in some cases are utilized within synthesis with inductors have been added to converter yield to lessen yield voltage swell



4. Problem Overview

The MPPT method consider is to automatically find the current I_{MPP} or voltage V_{MPP} at which a PV array should work to extract the maximum output power P_{MPP} under a given temperature and irradiance. Most of MPPT methods respond to variations in both irradiance and temperature, but some are precisely more useful if temperature is approximately constant. Most MPPT methods would automatically respond to various in the array due to aging, though some are open-loop and would require periodic fine tuning. In our context, module will typically be connected to a power converter that can vary the current coming from the PV array to the load

5. MPPT Control Algorithm

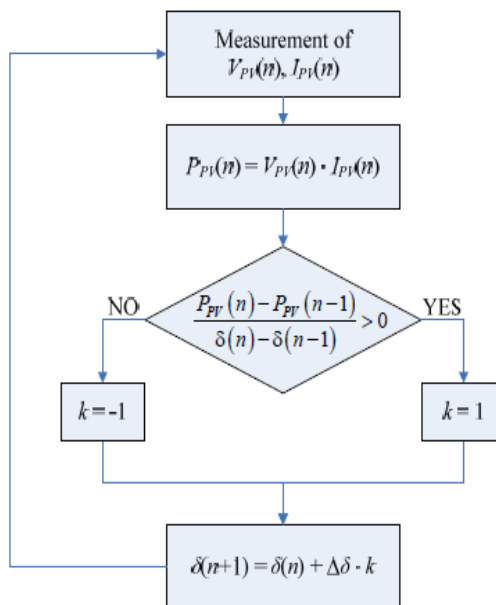
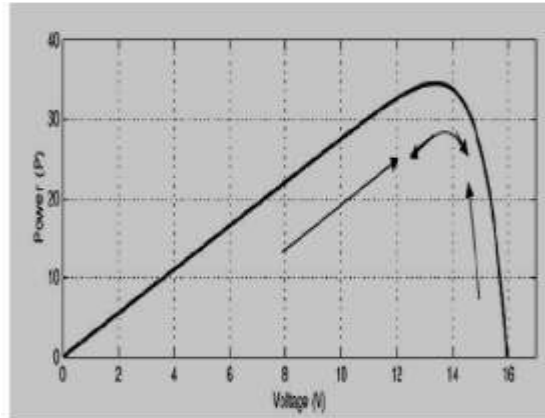
The MPPT algorithm operates based on the truth that the derivative of the output power (P) with respect to the panel voltage (V) is equal to zero at the maximum power point. In the literature, various MPP algorithms are available in order to improve the performance of photovoltaic system by effectively tracking the MPP. However, most widely used MPPT algorithms are considered here, they are:

- Perturb and Observe (P&O)
- Incremental Conductance (In Cond)
- Constant Voltage Method.

5.1 Perturb and Observe (P&O)

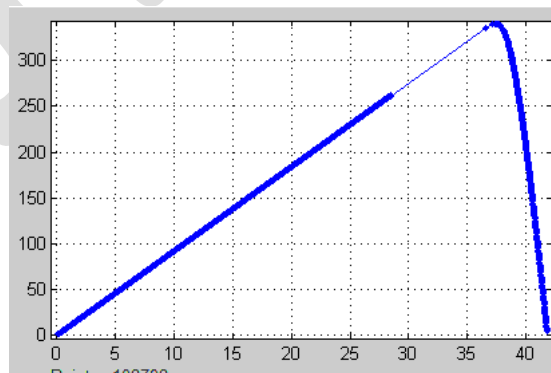
The most commonly used MPPT algorithm is P&O method. This algorithm uses simple feedback arrangement and little measured parameters. In this approach, the module voltage is periodically given a perturbation and the corresponding output power is compared with that at the previous perturbing cycle [17]. In this algorithm a slight perturbation is introduce to the system. This perturbation causes the power of the solar module varies. If the power increases due to the perturbation then the perturbation is continued in the same direction. After the peak power is reached the power at the MPP is zero and next instant decreases and hence after that the perturbation reverses as shown in Figures 5(a) and 5(b).When the stable condition is arrived the algorithm oscillates around the peak power point. In order to maintain the power variation small the perturbation size is remain very small. The technique is advanced in such a style that it sets a reference voltage of the module corresponding to the peak voltage of the module. A PI controller then acts to transfer the operating point of the module to that particular voltage level. It is observed some power loss due to this perturbation also

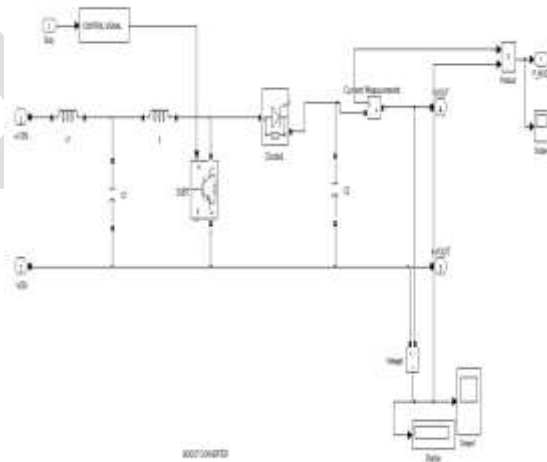
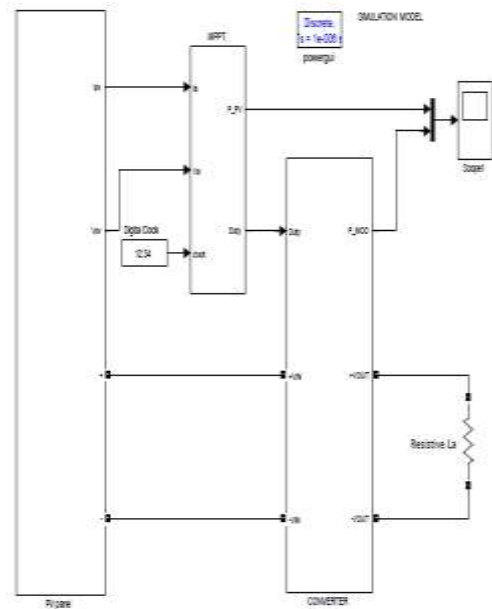
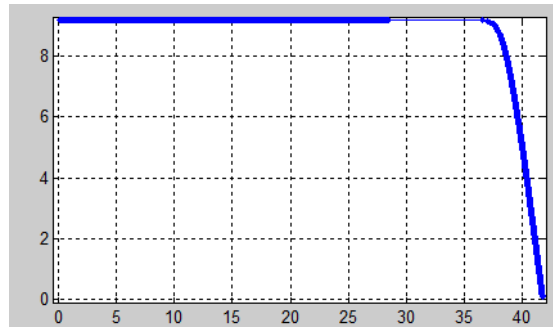
the fails to track the maximum power under fast changing atmospheric conditions. But remain this technique is very popular and simple [7].

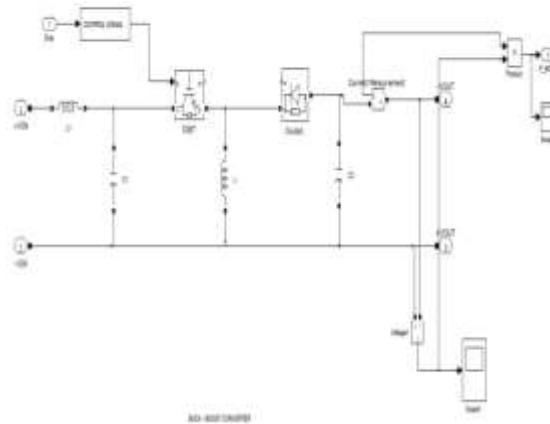
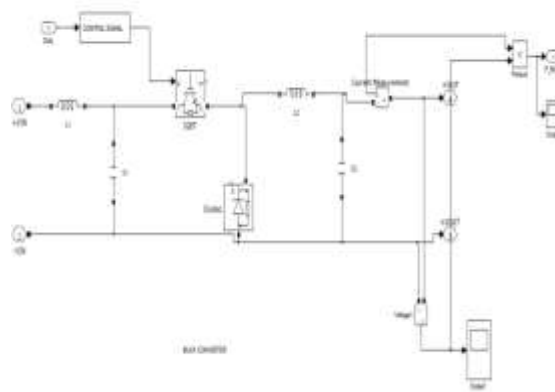


MATLAB-SIMULINK Environment

The model shown in Figure represents a block diagram of a PV array connected to a resistive load through a dc/dc (buck or buck boost) converter with MPPT controller







Results and Simulation

The models shown in the above figures were simulated using MATLAB® / SIMULINK® Simulation and results for buck, boost and buck-boost converters have been recorded to make sure that comparison of the circuit can be obtained accurately. The voltage, current and output power is the main points of comparison to take into account. The complexity and simplicity of the circuit have been set based on the literature. Hardware required, convergence speed and range of effectiveness.

Buck-Boost Converter Simulation With Perturb and Observe Controller

The simulation result at constant temperature ($T=50$ degree) with changes in the insolation ($S=1000$ to 850 w/m²)

It can be seen from Figure that the outputs of the PV panels and buck –boost converter clearly changes due to the change of the insolation as that variation of the converter affects the output of the PV panel the results below including current, voltage and power:

AT $1000\text{w}/\text{m}^2$

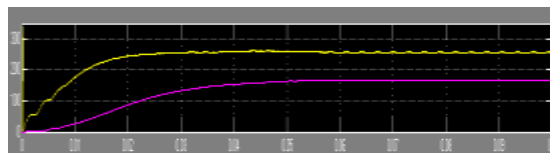
At $T=50$ degree and $S=1000\text{w}/\text{m}^2$

$I= 9.20$ Ampere, $V=27.298$ volt and $P=250$ watt

output of the buck- boost converter with P&O algorithm that results below including current, voltage and power

At $T=50$ degree and $S=1000\text{w}/\text{m}^2$

$I=-4.087$ Ampere, $V=-40.87$ volt and $P=280\text{w}$



AT $850\text{w}/\text{m}^2$

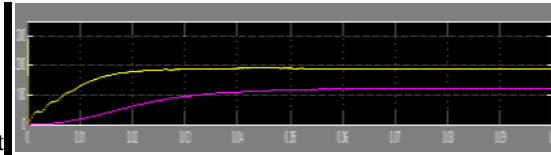
From the Figure , the results below current, voltage, power of pv panel

At $T=50$ degree and $S=850\text{w}/\text{m}^2$

$I=7.82$ Ampere, $V=24.15$ volt and $P= 180$ watt,

the results below current, voltage, power of the buck- boost converter with P&O algorithm

At T=50 degree and S=850 w/ m²



I=-3.471Ampere,V=-34.71voltandP=120watt

7.1 Buck Converter Simulation With Perturb and Observe Controller

The simulation result at constant temperature (T=50 degree) with changes in the insolation (S=1000 to 850 w/m²).

AT 1000w/ m²

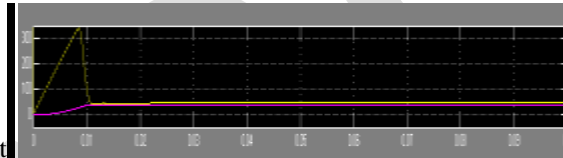
Output current, voltage and power of PV panel

At T=50 degree and S=1000 w/ m²

I= 1.88 Ampere, V=41.1 volt and P=49 watt

Output current, voltage and power of buck converter with P&O algorithm

At T=50 degree and S=1000 w/ m²



I=1.93Ampere,V=19.73voltP=47watt

AT 850 w/ m²

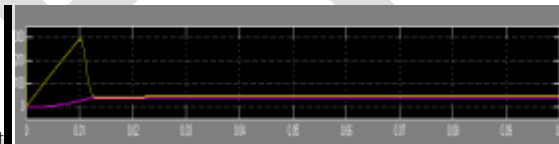
The results below including current, voltage and power pv panel

At T=50 degree and S=850 w/ m²

I=1.076 Ampere, V=41.37 volt and P= 48 watt

Output current, voltage and power of buck converter with P&O algorithm

At T=50 degree and S=850 w/ m²



I=1.93Ampere,V=19.5voltP=46watt

Boost Converter Simulation With Perturb and Observe Controller

The simulation result at constant temperature (T=50 degree) with changes in the isolation (S=1000 to 850 w/m²). AT 1000w/ m²

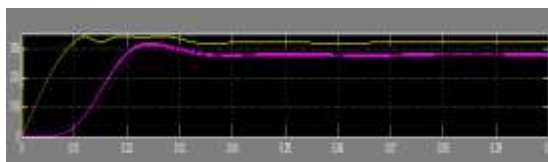
output current, voltage and power of PV panel

At T=50 degree and S=1000 w/ m²

I= 8.4 Ampere, V=38.1 volt and P=320 watt

Output current, voltage and power of boost converter with P&O algorithm

At T=50 degree and S=1000 w/ m²



I=3.767Ampere,V=75.33voltandP=280watt

AT 850 w/ m²

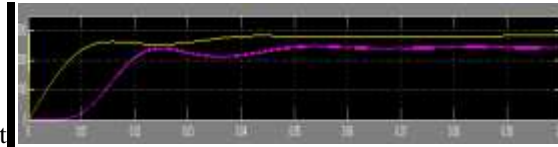
The results below including current, voltage and power pv panel

At T=50 degree and S=850 w/ m²

I=7.85 Ampere, V=36.25 volt and P= 280 watt

The Output current, voltage and power of boost converter with P&O algorithm

At T=50 degree and S=850 w/ m²



I=3.508Ampere, V=70.17volt and P=250watt

At T=50 degree and S=1000w/ m²

CONVERTER	I_{in}	V_{in}	P_{in}	I_{out}	V_{out}	P_{out}
BUCK	1.088A	41.4V	49W	1.943A	39.43V	47W
BOOST	8.404A	38.38V	320W	3.767A	5.33V	280W
BUCK-BOOST	9.20A	27.92V	250W	-4.087A	-40.87V	170W

At T=50 degree and S=850 w/ m²

CONVERTER	I_{in}	V_{in}	P_{in}	I_{out}	V_{out}	P_{out}
BUCK	1.076A	41.37V	48W	1.937A	38.5V	47W
BOOST	7.821A	36.25V	280W	3.508A	70.17V	250W
BUCK-BOOST	7.82A	24.15V	180W	-3.471	-34.71V	120W

Table1

From Tables 1&2, once the converters transfer the electrical power from the solar panel to the load and the controller start function, output value of the solar panel do not provide same input voltage value to controller (V_{in}). This is because the controller function that varies the value of duty cycle will change the input value that sense by the controller. The input voltages of this controller show a different each other. Input voltage of Buck that connected with P&O is 41.4 V(41.37V at 850 w/ m²) while input voltage of buck-boost that connected with P&O is 27.92V (24.15V at 850 w/ m²). while input voltage of boost that connected with P&O is 38.38V (36.25V at 850 w/ m²). The output value behaves as Buck, boost and buck-boost converters behave. The buck voltage will drop from 41.4V to 19.73V (41.37V to 19.5V at 850 w/ m²), while the buck-boost voltage drop from 27.92V to -40.87V (24.15V to -34.71V at 850 w/ m²). while the boost voltage rise from V to 38.38V to 75.33V (36.25V to -70.17V at 850 w/ m²).

This system show that perturb and observe controller will work better with boost controller than buck-boost and buck converter .

CONCLUSION: P&O MPPT method is implemented with MATLAB-SIMULINK for simulation. Through simulation it is observed that the system completes the maximum power point tracking successfully despite of fluctuations. When the external environment changes suddenly the system can track the maximum power point quickly. Boost , buck and buck-boost converters have succeeded to track the MPP but, boost converter is much effective because There is a small loss of power from the solar panel side to the boost converter output side compared with other converters

REFERENCES:

- [1] A.P.Yadav, S. Thirumaliah and G. Harith. "Comparison of MPPT Algorithms for DC-DC Converters Based PV Systems" International Journal of Advanced Research in Electrical, Electronics and Instrumentation Engineering Vol. 1, Issue 1, July 2012.
- [2] Y.-H.Chang and C.-Y. Chang, "A Maximum Power Point Tracking of PV System by Scaling Fuzzy Control," presented at International Multi Conference of Engineers and Computer Scientists, HongKong, 2010.
- [3] S.Mekhilef, "Performance of grid connected inverter with maximum power point tracker and power factor control," International Journal of Power Electronics, vol.1, pp. 49-62.
- [4] M.E.Ahmad and S.Mekhilef, "Design and Implementation of a Multi Level Three-Phase Inverter with Less Switches and Low Output Voltage Distortion," Journal of Power Electronics, vol. 9, pp. 594-604, 2009.
- [5] H.N.Zainudin and S. Mekhilef, "Comparison Study of Maximum Power Point Tracker Techniques for PV Systems" Proceedings of the 14th International Middle East Power Systems ConferenceMEPCON'10), Cairo University, Egypt, December 19-21, 2010.
- [6] R.Faranda and S. Leva, "Energy Comparison of MPPT techniques for PV Systems," WSEASTransaction on Power Systems, vol. 3, pp. 446-455.

- [7] Vikrant A. Chaudhari, "Automatic Peak Power Tracker for Solar PV Modules Using DspaceSoftware," in Maulana Azad National Institute of Technology. Master Thesis of Technology inEnergy. Bhopal: Deemed University, 2005.
- [8] T.P.Nguyen, "Solar Panel Maximum Power Point Tracker," Ph. D. Thesis in Department of ComputerScience & Electrical Engineering: University of Queensland, 2001.
- Emerging Trends in Electrical, Electronics & Instrumentation Engineering: An international Journal(EEIEJ), Vol. 1, No1, February 201444
- [9] S.Balakrishna, N. A. Thanoe, G. Rajamohan, A. S. Kenneth and C. J. Ling, "The Study and Evaluation of Maximum Power Point Tracking Systems," International Conference on Energy andEnvironment 2006 (ICEE 2006), pp. 17-22, 2006.
- [10] C.S.Lee, "A Residential DC Distribution System with Photovoltaic Array Integration," Degree of Honors Baccalaureate of Science in Electrical and Electronics Engineering, Oregon State University,University Honors College 2008.
- [11] T.Esram and P. L.Chapman, "Comparison of Photovoltaic Array Maximum Power Point TrackingTechniques," IEEE Transactions on Energy Conversion, Vol. 22, No. 2, 2007.
- [12] E.I.O. Rivera, "Maximum Power Point Tracking using the Optimal Duty Ratio for DC-DC Converters and Load Matching in Photovoltaic Applications," Twenty Third Annual IEEE Applied Power Electronics Conference and Exposition, APEC 2008, pp. 987-991, 2008.
- [13] D.Peftsis, G. Adamidis, P. Bakas and A. Balouktsis, "Photovoltaic System MPPT Tracker Implementation using DSP engine and buck–boost DC-DC converter", 13th Power Electronics andMotion Control Conference, 2008

One-pot Synthesis of Chalcone Derivatives By Using Anhydrous AlCl_3 as Condensing Agents

Shalini Jaiswal* and Smirti Diwedi

Department of Chemistry, AMITY UNIVERSITY ,

Greater Noida Campus, India

Email*: shalinijaiswal@gmail.com

09953217151

ABSTRACT: Chalcones are α,β -unsaturated keto group containing compound. Chalcones are 1, 3-diphenyl-2-propene-1-one, consist of two aromatic rings linked by a three carbon α,β -unsaturated carbonyl system.

Heterocyclic compounds having nitrogen and sulphur in their skeleton are the most fascinated compound by scientists due to their diverse biological activities. Imidazoles have occupied a unique position in heterocyclic chemistry, and its derivatives have attracted considerable interests in recent years for their versatile properties in chemistry and pharmacology

Different methods are available for the preparation of chalcones²⁻⁴. The most convenient method is the Claisen-Schmidt condensation of aryl methyl ketone with aromatic aldehyde in presence of aqueous solution of sodium hydroxide⁵ at room temperature. Chalcones are used to synthesize several derivatives like cyanopyridines, pyrazolines isoxazoles and pyrimidines having different heterocyclic ring systems.⁶⁻⁹

The synthesized compounds were evaluated for antimicrobial and antifungal activity by disc diffusion method. The antifungal activity was evaluated against *A. niger*, *A. flavus* (fungal strains) using nystatin as the standard drugs. The antibacterial activity was evaluated *E. coli* and *S. aureus* using ciprofloxacin as the standard drugs. activity.

KEY WORDS: Chalcone, Claisen-Schmidt condensation, solvent-free synthesis, Antibacterial activity

INTRODUCTION

Diseases caused by pathogenic bacteria still attract significant attention from medicinal chemists and biologists because of growing antibacterial resistance.

Chalcones are α,β -unsaturated ketone containing compound. Chalcones are 1, 3-diphenyl-2-propene-1-one, consist of two aromatic rings linked by a three carbon α,β -unsaturated carbonyl system.

Chalcones are used to synthesize several derivatives like cyanopyridines, pyrazolines isoxazoles and pyrimidines having different heterocyclic ring systems.¹⁻⁴

Different methods are available for the preparation of chalcones⁵⁻⁷. The most convenient method is the Claisen-Schmidt condensation of arylmethylketone with aromatic aldehyde in presence of aqueous solution of sodium hydroxide⁸ at room temperature.

The synthesized compounds were evaluated for antimicrobial and antifungal activity by disc diffusion method. The antibacterial and antifungal activity was evaluated against *A. niger*, *A. flavus* (fungal strains), *E. coli* and *P. aeruginosa* (Gram negative bacteria), *S. aureus* and *S. pyogenes* (Gram positive bacteria) using Nystatin (for fungi) and ciprofloxacin (for bacteria) as the standard drugs.

The chalcones are associated with different biological activities like insecticidal⁹, anticancer¹⁰, anti-inflammatory¹¹, bactericidal¹², fungicidal¹³, antiviral¹⁴, antitumor¹⁵, antimalarial¹⁶ and antiulcer¹⁷. Literature shows that lieochalcone and oxygenated chalcone has strong antileishmanial activity^{18, 19}. It is reported that chalcones exhibited potent activity against human malarial parasite²⁰.

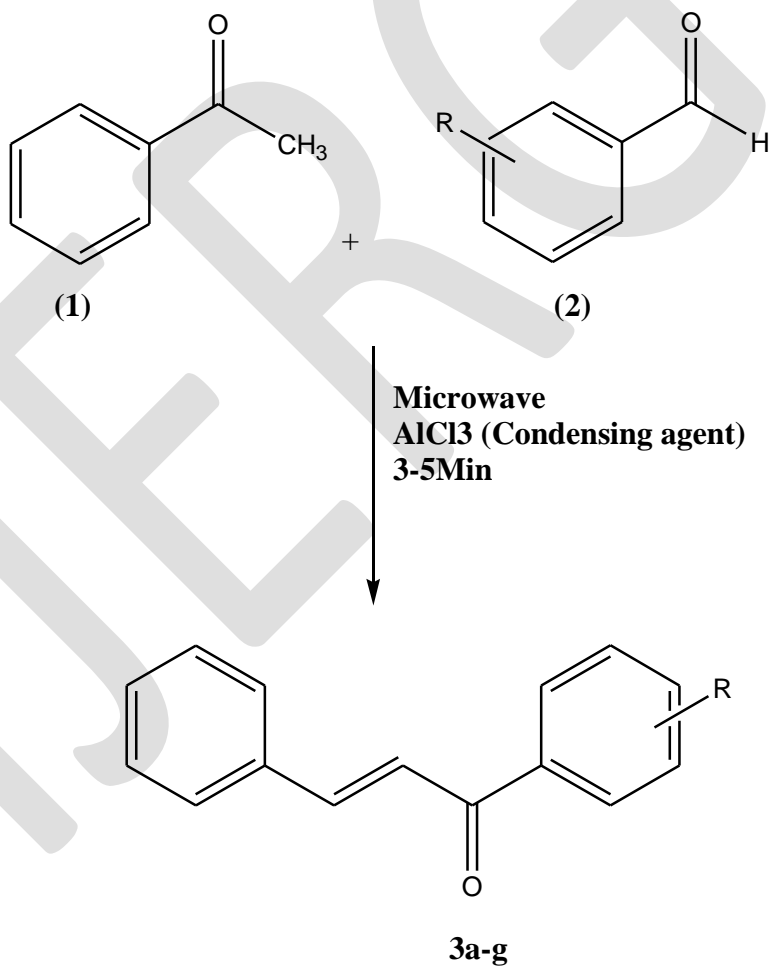
Chalcones are well known intermediates of various heterocyclic compounds. The compounds with the backbone of chalcones have been reported to possess various biological activities such as antimicrobial, anti-inflammatory, analgesic, anti ulcerative, antimalarial, anticancer, antiviral, Antioxidant, Anti tubercular, anti hyperglycemic, activities. The presence of a reactive keto-ethylenic group in chalcones is responsible for their antimicrobial activity.

Chalcones and their derivatives also used as artificial sweeteners^{21, 22}, scintillator²³, polymerization catalyst²⁴, fluorescent whitening agent²⁵.

EXPERIMENTAL SECTION

Melting points were determined by open glass capillary method and are uncorrected. All chemicals used were reagent grade and were used as received. A Laboratory Microwave Oven (Model BP 310/50) operating at 2450 MHz and power output of 600 W was used for all the experiments. The completion of reactions was monitored by TLC (Merk silica gel). IR spectra were recorded on a Shimadzu FTIR-420 spectrophotometer. ¹H NMR and ¹³C NMR spectra were recorded at 400°C on a Bruker AVANCE DPX (400 MHz) FT spectrometer in CDCl₃ using TMS as an internal reference (chemical shift in δ , ppm). Mass spectra were recorded on JEOL SX-303 (FAB) mass spectrophotometer at 70ev.

Scheme-I



GENERAL METHODS AND MATERIALS:

Thermal Method for synthesis of Chalcone (3a-i)

A mixture of substituted aromatic aldehyde (0.01 mol) and acetophenones (0.01 mol) was stirred (at specific time mention in table-2) along with absolute alcohol (40 ml) and then an aqueous solution of NaOH (15 ml) was added to complete the reaction. The mixture was kept overnight at room temperature and next day it was poured into crushed ice/ice chilled water and dil. HCl is used for the acidification. The Chalcone derivative precipitates out as solid. Progress of the reaction was monitored by TLC (Hexane: Ethyl Acetate, 6:1 v/v). The product was extracted with ethanol (3x50 mL). The extract was evaporated under reduced pressure to obtain the final product which was recrystallised from ethanol to get analytically pure compounds (3a-i)

Microwave irradiation for synthesis of Chalcone (3 a-i)

A mixture of substituted aromatic aldehyde (0.01 mol) and acetophenones (0.01 mol) along with condensing agent AlCl₃ were taken in 20 ml beaker and subjected to microwave irradiation at 200-300 W for 1 min. The reaction mixture was then thoroughly mixed outside the microwave oven and again irradiated for another few min in oven. This irradiation-mixing cycle was repeated for the total irradiation time **Table I**. The mixture was kept overnight at room temperature and next day it was poured into crushed ice/ice chilled water and dil. HCl is used for the acidification

After completion of the reaction as indicated by TLC (Hexane: Ethyl Acetate, 6:1 v/v) the product was extracted with ethanol (3x8 mL). The final product was recrystallised from ethanol to obtain analytically pure compounds (3a-i).

Melting point and Yield of Compound 3_{a-g}

Comp ound	R	Time		Yield (%)		M. P. (°C)
		MWI (min)	Stirring at temperature 50°C(hour)	MWI	Thermal	
3a	H	3	8	78	35	58
3b	4-Cl	2	7	85	32	160
3c	4-HO	2	7	88	33	150
3d	4-MeO	2	8	85	34	105
3e	2-NO ₂	3	7	89	33	147
3f	3-MeO, 4-HO	3	7	85	35	145
3g	2-NH ₂	2	7	85	36	90

Table 2: Physical and spectral data of compounds 3_{a-g}

Compd.	Mol.Formulla	1 H-NMR (Cde1 ₃ , Δ, Ppm)	Elemental Analysis	MS (EI, M/Z (M ⁺))
--------	--------------	---	--------------------	-----------------------------------

3a	C ₁₃ H ₁₀ O	7.14-7.30 (m,5H,ArH),7.56-7.90 (s,2H,-CH=CH-),7.45- 7.80(m,5H,ArH)	C:86.51,H:5.81,O:7.68	208
3b	C ₁₅ H ₁₁ OCl	7.14-7.30 (m,5H,ArH),7.56-7.90 (s,2H,-CH=CH-),7.45- 7.75(m,5H,ArH)	C:74.23,H:4.57,Cl:14.61,O : 6.59	242
3c	C ₁₅ H ₁₂ O ₂	7.14-7.30 (m,5H,ArH),7.56-7.90 (s,2H,-CH=CH-) ,5.00(s,1H,OH),6.92- 7.64(m,4H,ArH)	C:80.34,H:5.39, O:14.27	224
3d	C ₁₆ H ₁₄ O	7.14-7.30 (m,5H,ArH),7.56-7.90 (s,2H,-CH=CH-) ,2.53(s,1H,CH ₃),6.92- 7.55(m,4H,ArH)	C:86.45, H:6.35,O:7.20	222
3e	C ₁₅ H ₁₁ NO ₂	7.14-7.30 (m,5H,ArH),7.56-7.90 (s,2H,-CH=CH-) ,2.53(s,1H,CH ₃),8.07- 8.38(m,4H,ArH)	C:71.14,H:4.38,N:5.53, O:18.95	253
3f	C ₁₆ H ₁₄ O ₃	7.14-7.30 (m,5H,ArH),7.56-7.90 (s,2H,-CH=CH-) ,3.73(s,3H,CH ₃),5.00(s,1H ,OH),6.81-7.20(m,4H,ArH)	C:75.57,H:5.55,O:18.88	254
3g	C ₁₅ H ₁₃ NO ₃	7.14-7.30 (m,5H,ArH),7.56-7.90 (s,2H,-CH=CH-) ,3.73(s,2H,NH ₂),6.65-7.56 (m,4H,ArH)	C:80.69,H:5.87,N:6.27; O:7.17	223

ANTIMICROBIAL ACTIVITY

The synthesized)compounds **3a-g** was evaluated for antibacterial and antifungal activity by disc diffusion method. The presence of α , β -unsaturated carbonyl system of chalcone makes it biologically active. The antifungal activity was evaluated against *A. niger*, *A. flavus* (fungal strains) using nystatin as the standard drugs. The antibacterial activity was evaluated *E. coli* and *S.aureus* using ciprofloxacin as the standard drugs. The results of antibacterial and antifungal activities studies are given in **Table-3**.

Table 3: Antibacterial and Antifungal Activities of compounds 3_{a-g}

Compd.	Antibacterial		Antifungal	
	<i>S. aureus</i>	<i>E. coli</i>	<i>A. niger</i>	<i>A. Flavus</i>
3a	8	9	6	7
3b	14	15	12	13
3c	13	13	11	12
3d	12	12	10	10
3e	14	13	11	12

3f	12	13	11	13
3g	13	14	12	12
Ciprofloxacin	16	16	-	-
Nystatin	-	-	13	14

The results show that majority of the synthesized compounds showed varying degrees of activity against bacteria and fungi. The 3b and 3g showed antibacterial and antifungal excellent activity against *S. aureus* and *E. coli*. Whereas the compounds 3c, 3d, 3e, 3f have shown good to moderate activity against *S. aureus* and *E. coli* at concentration 500 µg/ml.

RESULTS & DISCUSSION

Claisen-Schmidt condensation of acetophenone with aromatic aldehyde by using $AlCl_3$ as condensing agent under solvent-free gave regioselective Chalcone derivatives **3a-g**. The Structure of **3a-g** was supported by 1H NMR and elemental spectral analysis. The reactions were also carried out using a water bath at the same temperature. It was found that MW method has improved the yields significantly. MW enhancement of yields and reduction in reaction time can be rationalized on the basis of the formation of dipolar activated complex and greater stabilization of the more dipolar activated complex by dipole-dipole interaction with electric field of the microwaves as compared to the less polar adduct which may reduce the activation energy resulting in the rate enhancement.

The synthesized compounds **3a-g** was evaluated for antibacterial and antifungal activity by disc diffusion method. The results show that majority of the synthesized compounds showed varying degrees of activity against bacteria and fungi.

ACKNOWLEDGEMENT

The authors would like to express their gratitude and thanks to Department of Chemistry, Amity University Greater Noida for necessary facilities to carry out this research work and RSIC, CDRI Lucknow for spectral analysis.

REFERENCES:

1. M. A. El.Hashah; M. El-Kady; M. A. Saiyed and A. A. Elawwy, Egypt. J. Chem., **27**, 715 (1985).
2. L. S. Crawley and W. J. Fanshawe, J. Heterocyclic chem., **14**, 531 (1977).
3. E. C. Taylor and R. W. Morrison, J. Org. Chem., **32**, 2379 (1967).
4. P. S. Utale, P. B. Raghuvanshi and A. G. Doshi, Asian J. Chem., **10**, 597 (1998).
5. H. Rupe and D. Wasserzug, J. Chem. Ber., **34**, 3527 (1901).
6. S. A. Hermes, Chem. Ber., **70**, 96422h (1969).
7. D. S. Breslow and C. R. Houser, Chem. Ber., **62**, 2385 (1940).
8. K. Kazauki, K. Hitayama, S. Yokomori and T. Soki, Chem. Abstr., **85**, 591(1976).
9. M. Larsen, H. Kromann, A. Kharazmi and S. F. Nielsen, Bioorg. Med. Chem. Lett., **15**, 4858 (2005)
10. G. Zongru, H. Rui, F. Z. Shenquang and G. Shuminshu, Chem. Abstr., **125**, 10376r (1996)
11. H. Serre, J. Rey and J. P. Tarayre, Chem. Abstr., **91**, 9494a (1979)
12. S. F. Nielsen, T. Boson, M. Larsen and H. Kromann, Bioorg. Med. Chem. Lett., **12**, 3047 (2004)
13. A. K. Padersen and G. A. Fitz, J. Pharm. Sci., **74**, 188 (1985)
14. D. Binder, C. R. Noe, W. Holzer and B. Rosenwirth, Arch. Pharm., **318**, 48 (1985)
15. Y. Satomi, Ind. J. Cancer, **120**, 208071 (1994)
16. A. Vall, B. Vall, D. Cartier and J. Schrevel, Euro. J. Med. Chem. (in press) 2005.
17. Tashio pharmaceutical Ltd., Chem. Abstr., **101**, 54722j (1984)
18. C. M. Christesen, S. B. Blom and L. Fich, Antimicrobial agents and chemotherapy, **37**, 2550 (1993)
19. M. Chen, S. B. Christensen and T. G. Theander, Antimicrobial agents and chemotherapy, **38**, 139 (1994)
20. C. M. Christensen, S. B. Zhai and M. H. Theander, J. Of Infectious Diseases, **176**, 1327 (1997).
21. R. M. Horowitz and B. Gentili, U. S. Patent, **3**, 890, 298 (1975), Chem. Abstr., **83**, 147706g, (1975)
22. G. P. Rizzi and J. S. Neely, German Patent, **2**, 148, 332 (1972); Chem. Abstr., **11**, 86777h (1972)

23. M. Delcarmen, G. Barrio, J. R. Barrio, G. Walker, A. Noveli and N. J. Leonard, J. Am. Chem. Soc, **95**, 4891 (1973)
24. Mitsubishi Petrochemical Co. Ltd., British Patent **1**, 128, 090 (1968); Chem. Abstr., **69**, 97342y (1968)
25. G. Hayakawa and T. Inoue, Japanese Patent 7, **107**, 386 (1971); Chem. Abstr., **74**, 14332y (1971)

IJERGS

Strength Characteristics Analysis of Concrete Reinforced With Lathe Machine Scrap

Zeeshan Nissar Qureshi¹, Yawar Mushtaq Raina², Syed Mohd Asgar Ruffaie³

^{1, 2, 3}Junior Engineer Public Works (R& B) Department, Government of Jammu and Kashmir

²Corresponding Author, Email:yawarraina35@gmail.com

Abstract— The aim of the paper was to study the feasibility of using lathe machine scrap in concrete by checking the compressive strength, splitting tensile strength, flexural strength and load deflection characteristics. All these parameters were found out by varying proportions of lathe machine by 0%, 1 %, 1.5% and 2% by weight in M20 concrete. Thus finding out optimum percentage of lathe machine scrap in concrete up to which its mechanical properties like compressive strength, splitting tensile strength, flexural strength can be increased. All the tests were conducted by following the guidelines set by Indian Standard. The compressive strength was found out to be 25.5N/mm², 26.8N/mm², 28.4N/mm² and 23.33N/mm² for 0%, 1 %, 1.5% and 2% lathe machine scrap reinforcement respectively. The splitting tensile strength was 2.85N/mm², 3.04N/mm², 3.37N/mm² and 2.94N/mm², where as flexural strength were 4.33N/mm², 5N/mm², 5.66N/mm² and 4.83N/mm² for 0%, 1 %, 1.5% and 2% lathe machine scrap reinforcement respectively. The strength properties of concrete were increasing by adding lathe machine scrap up to 1.5 % by weight in concrete after this slight reduction in strength properties of concrete was noticed. The compressive, split tensile and flexure strengths were increasing by 11.37 %, 18% and 30 % for optimum percentage of lathe machine scrap which was found to be 1.5%. The load carrying capacity of beam at same percentage of lathe machine scrap was found to be 5.66kN and deflection which was also maximum among all percentages was 7mm. Lathe machine scrap was found to be strong and environmental friendly material which can improve structural strength of concrete, decrease steel reinforcements besides, reducing width of cracks when used as reinforced material in concrete.

Keywords— Lathe Machine Scrap, Compressive Strength, Split Tensile Strength, Flexural Strength, Concrete, workability, deflection, Fiber reinforcement,

1. INTRODUCTION

Concrete is considered as the backbone of a modern day structures. Without this it is not possible to build a structure which is strong, durable and capable enough to resist earthquake shocks and other loads like dead load, imposed loads, snow load etc. To resist different types of vibrations a concrete structure has superiority over other structures made up of different materials [1] Concoction of Water, fine and coarse aggregates along with cement after amalgamating them collectively into a solid stone is described as concrete [2][3]. Once these elements are assorted jointly they outline a liquefied mass, being fresh and impressionable, it can be sorted into any yearned form. Properties like strength, density, chemical and thermal resistance in unsullied and solid state are managed by consequent materials through which concrete is formed [4]. Since these ingredients vary in quantity, the properties do not remain same. In order to make sure that freshly obtained concrete is workable and after hardening is capable enough to withstand the weather conditions and the loads the constituents should be correctly mixed [5].

Being strong in compression and weak in tension, concrete is required to be reinforced by materials having higher tensile strength [2][3][6]. To overcome the weakness various researches by using different materials in concrete have been carried out all over the world; one of them has been Fiber reinforced concrete (FRC) which has been very common in the researches carried out in last two decades [7][6][8][9][10][11][12][13][14]. Researchers are also trying to develop high performance concretes by making use of fibers and admixtures in concrete with different proportions [15][16][17][18]. Incorporation of fiber in concrete have found to improve various properties such as cracking resistance, impact, wear resistance, ductility and fatigue resistance besides several other strength properties [19][20][21][22][23]. Besides building structures, concrete pavement is a key part of highway pavement due to increase in ride superiority, minimum maintenance, and extended design life [24] With the use of recycled materials the cost and energy consumption associated with concrete pavements can be lowered down with more effective construction methods [25][26].

In civil engineering applications most commonly used fibers and waste material includes glass, carbon, cellulose, aramid, steel etc [7]. In many developing countries like India there is a need to look over resource conservation, reducing material cost and using waste products paying much attention towards process of recycling of waste materials. This process of recycling of materials from industrial wastes helps to protect natural resources or environmental profits and results in economy [27]. By using various recycled wastes in concrete it has been found that compressive, flexural, tensile strength and other mechanical properties as well as energy absorption have increased [28][29][30]. The flexural properties of concrete reinforced with glass fibers are found to be more than plain concrete [31]. Use of plastic reinforced fiber in concrete can increase the overall strength of concrete and other mechanical properties [9] Besides plastic incarceration of concrete by fiber reinforced polymer tubes can considerably boost the ductility, strength and energy absorption capacity of concrete [32][16][17]. The shear, bending and serviceability properties of concrete improves when RCC beam is reinforced with textile besides this the crack width also reduces [33] Concrete reinforced with cellulose have shown that width of

crack is less as compared to plain concrete beside having less width of crack, cellulose reinforced concrete was found to 40 percent tougher than the unreinforced concrete [34]. Fiber like aramid has been found to improve strength of concrete in an analogous way as that of steel [35]. As far as waste of steel fiber is concerned research done by [36] found that addition of more than 0.5% of the waste wires and steel fibers resulted in considerably higher split tensile strength by about 28 than plain concrete. Beside steel fibers carbon fiber is also being off late as a fiber material in concrete. Carbon fiber reinforced concrete has been found to have piezoelectric activities and can sense large range of loading with soaring compassion beside this it is also scrutinize dynamic loading [37]. By adding 3% of carbon and steel fibers by volume in concrete an increase of 12.1% of original tensile strength have been found [38]. A galvanized iron wire when used in concrete enhances the splitting tensile strength and flexural strength up to 72.65% and 41% [39]. Steel and Polypropylene fiber reinforced concrete of M30 grade results in improvement by 18 % in compressive strength for 28 days [40]. [41] made comparative studies on steel fiber reinforced concrete under flexural and deflection and observed that flexural strength increases from 13% to 48 % by utilization of steel fibers .by using 1% steel fibers flexural strength increase from 13.35% to 23.35%. With 2% steel fibers strength increases from 18% to 32%.and by using 3% steel fiber flexural strength increase from 20.80% to 48.35 %. Use of Steel Chords (a byproduct of tire recycling process) reinforced concrete is 18 % more ductile than the plain when 2 % steel chords by volume of concrete are used in it [42]. Recycled aggregate's use in concrete is found to have increase the split tensile strength and besides being workable for a structural use [43]. [44] Conducted tests on C30 and C50 concretes and obtained results which showed improvement in shear strength of concrete reinforced with steel fiber by 2.15 times for C30 and 2.46 times for C 50 than the plain concrete. The shear strength of pre-stressed concrete I beams also increases by using steel fibers in concrete [45].

With increase in population and industrial activities, the quantity of waste fibers generated from various metal industries will obviously increase. These types of industrial waste fibers can effectively be used for making high- strength low cost FRC after exploring their suitability. To overcome wasteful steel fiber, lathe scrap is used as recycle steel fiber which exhibits the property of steel fiber in fiber reinforced concrete.

In this paper an experimental investigation was carried out to study the feasibility of using scrap obtained from lathe machine in concrete by checking the workability, compressive strength, splitting tensile strength, flexural strength and load deflection characteristics of M20 concrete and thus optimizing the fiber proportions. The outcome of this paper shall be useful for many workshop and industries generating scrap from lathe machine. Ultimately the environment and economy of country will be benefited.

2. MATERIALS

The materials used in the study were cement, fine aggregates (sand), coarse aggregate, Water Lathe machine scrap and Steel fiber. Tests on these materials were conducted as per Indian Standard (IS) guidelines to determine different properties which are explained as follows

a. Cement

Portland Pozzolana Cement (Ambuja cement) shown in figure 1(a) was used in experimental investigation work. Portland Pozzolana Cement was preferred over ordinary Portland cement because it makes concrete more impermeable and denser. Ambuja cement satisfies nearly all the requirements recommended by Indian standard code [46]. Some important physical Properties of cement includes Standard Consistency, Initial and final setting time and Specific Gravity. All these properties were determined by IS guidelines [47]. Table 1 shows some important physical properties of cement.

Table 1: Some Physical properties of cement

S.No	Description	Values obtained	Requirements as per IS-1489, 1991
1	Standard consistency (using vicat apparatus)	28%	-
2	Initial setting time, min	50	>30min
3	Final setting time, min	7 hours 3min	<10hrs
4	Specific gravity	3.0	3.0-3.15

b. Fine Aggregates (Course sand)

Locally available Sand confirming to zone IV was used in the experiment work. As per [48] sieve analysis of the fine aggregates was carried out in the laboratory. The material whose particles are of size as are retained on IS sieve no 480(4.75mm) is termed as coarse sand [48] Fineness modulus of sand was found to be as 2.91. It was found out by carrying sieve analysis [48]. Specific gravity determined by pycnometer method [49] found to be 2.6.

c. Coarse Aggregates

Tests were carried out on locally available crushed coarse aggregates of 20mm in size and angular in shape. The fineness modulus was found to be 6.3 and specific gravity of coarse aggregate was 2.64. Both the properties were determined by sieve analysis [48] and [49] respectively.

d. Water

According to IS code [50], the pH value of water should not be less than 6. Water used for experimental work was portable.

e. Lathe machine scrap

Scrap from lathe machine is produced from different manufacturing processes which are carried out by lathe machine. Scrap which is a waste can be used as a reinforcing material in concrete to enhance the various properties of concrete

All the materials except water are shown in figure 1.



Fig 1: Cement, Course Sand, Course Aggregate and Lathe machine scrap from left to right respectively

The lathe scrap which was used for cost sensitivity analysis was tested in production laboratory with the help of universal testing machines (UTM). The universal testing machine in production engineering lab consists of computer attached to it. The properties of Scrap and steel fiber both were displayed on screen. Some of the important properties which were determined include breaking strength, breaking load, elongation and modulus of elasticity. Table 2 shows some important properties of lathe machine scrap.

Table 2: Properties of Lathe Machine Scrap

S. No	Property	Lathe machine Scrap (LMS)
1	Type	Turned and deformed
2	Length	40-60 mm
3	Diameter	0.4-0.8 mm
4	Aspect ratio	70-100
4	Tensile strength	0.02-0.08N/mm ²
5	Young's modulus	0.04-0.06N/mm ²

3. EXPERIMENTAL PROGRAM

The properties of Unreinforced and Lathe machine scrap reinforced concrete (LMSRC) which includes Workability, Compressive Strength, Tensile Strength, Flexural Strength, deflection were all determined by following the Indian Standard guidelines. The Mix design of Concrete was also done by following the Indian Standard guidelines.

a. Workability

Slump test was conducted to check the workability of unreinforced concrete and the concrete reinforced with lathe machine scrap at percentages 1 %, 1.5% and 2 % by weight. Test was conducted by following the specifications recommended by Indian Standard [51]

b. Compressive strength

A total of 12 specimens' cubes of concrete were casted having size of 150x150x150mm for different proportions (0%, 1%, 1.5%, 2%) by weight of Lathe machine scrap and 3 cubes were used for taking average value. Figure 2(a) shows the Cube Moulds. UTM was used for determining compressive strength. [52] was followed while determination of compressive strength was done.

c. Tensile Strength

12 cylinders specimens were casted for different percentages of lathe machine steel scrap of size 150mm dia. and 300mm in height. Figure 2 (b) shows the cylindrical mould. Split tensile test confirming to Indian Standard code [53] was used. The tensile strength of concrete cylinders reinforced with 0%, 1%, 1.5%, 2% of Lathe machine scrap by weight in concrete was determined.

d. Flexural Strength

In flexural strength test of beam, the specimen of size 100x100x500mm was placed over three point loading arrangements and stress produced during breakage of specimen was determined. This breakage stress is known as Modulus of rupture or the flexural strength. The test was done by following Standard set by [54]. The flexural strength of beams reinforced with lathe machine scrap 0%, 1%, 1.5%, 2% by weight of concrete was determined. Figure 2 (c) shows the beam mould



Figure 2 (a) Cube Moulds



Figure 2 (b) Cylindrical Moulds



Figure 2(c) Beam Moulds

e. Deflection

Deflection was measured by dial gauges with stand having magnetic base. The least count of the gauge was 0.01mm. The deflection and corresponding maximum load carrying capacity of the beam specimen for different proportions (0%, 1%, 1.5%, 2%) by weight of Lathe machine scrap in concrete were determined and load deflection curve has also been plotted.

f. Mix design and Mixing of Concrete

M-20 concrete mix was used with coarse aggregates of size 10mm. Mix design was carried out as per Indian Standard IS guidelines [55]. After mix design it was found that the final Mix proportions were 1:1.88:2.86 (Cement: Fine aggregates: Course Aggregates), W/C ratio was 0.52. Electrically operated concrete mixer was used for mixing of concrete. Proper care was taken for prevention of formation of concrete balls.

e. Batching

Weight batching was used in our experimental program as it is considered to be superior than volume batching [2][3][4].

4. RESULTS AND DISCUSSION

The results which were obtained after carrying out tests on different properties of both unreinforced and reinforced Lathe machine scrap concrete (LMSRC) are presented and discussed in this section.

a. Workability

Workability of concrete is defined as the capability to work alongside concrete. Concrete is said to be workable if it can be taken care of without isolation and loss of uniformity [55]. Slump Value was obtained to check the workability of concrete. The slump value of M20 concrete grade having mix of 1:1.88:2.86 (Cement: Fine aggregates: Course Aggregates), W/C ratio was 0.52 and having no lathe machine scrap in it was found to be 30 mm. When the same mix of concrete was added by 1 % of lathe machine scrap by weight, the slump value decreased to 22mm. For 1.5 % and 2 % lathe machine scrap by weight in the same mix slump values were found out to be 16mm and 10mm respectively. With increase in percentage content of Lathe machine scrap, the slump value decreases. The less is the slump value, more workable is the concrete [18][56][57]. Thus addition of lathe machine steel scrap in concrete was found to be beneficial to make it more workable.

b. Compressive strength, split tensile strength and flexural strength of plain and lathe machine scrap reinforced concrete

The compressive, split tensile and flexural strength were all determined by using M20 mix of 1:1.88:2.86 (Cement: Fine aggregates: Course Aggregates), W/C ratio 0.52. The percentage of lathe machine scrap for each parameter was kept at 0 %, 1 %, 1.5 % and 2 percent by weight of concrete. Compressive strength is the ability of a material to bear up loads having tendency to decrease size of material [58]. A total of 12 cube moulds of concrete were tested to determine the load at which failure will occur. The compressive strength of both plain and LMSRC were determined corresponding to average of failure loads of three specimens at different percentages of Lathe machine scrap. It was observed that addition of lathe machine scrap in concrete increases the compressive strength of concrete. For 0%, 1% and 1.5% lathe machine scrap content by weight in concrete the compressive strength obtained was 25.5N/mm², 26.8N/mm² and 28.4N/mm² respectively, however at 2% scrap content by weight the compressive strength decreases and was found to be 23.33N/mm². The addition of Lathe machine scrap in concrete the Compressive strength of concrete increases by about 11.37% for 1.5 % scrap as compare to conventional concrete. Thus the optimum percentage for lathe machine scrap in M20 concrete up to which Compressive strength can be increased is 1.5 % by weight and corresponding compressive strength was 28.4 N/mm².

Tensile strength is the ability of a material to bear up loads in tension [59]. A total of 12 cylinders specimens of size 15mm diameter and 300mm height were casted for different percentages of lathe steel scrap. The compression load was applied diametrically and along the length of cylinder until the failure of the cylinder along vertical diameter occurs. The split strength of both plain and LMSRC were determined corresponding to average of failure loads of three specimens at different percentages of LMS. It was observed that addition of lathe machine scrap in concrete increases the tensile strength of concrete cylinder. For 0%, 1% and 1.5% lathe machine scrap content by weight in concrete the tensile strength obtained was 2.85N/mm², 3.04N/mm² and 3.37N/mm² respectively, however at 2% scrap content by weight the tensile strength decreases and was found to be 2.94N/mm². The addition of Lathe machine scrap in concrete increases the tensile strength of concrete cylinder by about 18% for 1.5 % scrap as compare to conventional concrete cylinder. Thus the optimum percentage for lathe machine scrap in M20 concrete up to which tensile strength can be increased was found to be 1.5 % by weight in concrete cylinder and corresponding compressive strength is 3.37 N/mm².

Flexural strength or modulus of rupture is mechanical property of brittle material at which it defies bending under load [60]. A total of 12 beam specimens of the specimen of size 100x100x500mm were placed over three point loading arrangements for different percentages of lathe machine scrap to determine the load at which failure will occur. The flexural strength of both plain and LMSRC were determined corresponding to average of failure loads of three specimens at different percentages of LMS. It was observed that addition of lathe machine scrap in concrete increases the flexural strength of concrete beam. For 0%, 1% and 1.5% lathe machine scrap content by weight in concrete the flexural strength obtained was 4.33N/mm², 5N/mm² and 5.66N/mm² respectively, however at 2% scrap content by weight the tensile strength decreases and was found to be 4.83N/mm². The addition of Lathe machine scrap in concrete increases the flexural strength of concrete beam by about 30% for 1.5 % scrap as compare to conventional concrete beam. Thus the optimum percentage for lathe machine steel scrap in M20 concrete up to which flexural strength can be increased is 1.5 % by weight and corresponding compressive strength is 5.66 N/mm². Figure 3 shows the compressive, split tensile and flexural strength at different percentages of lathe machine scrap by weight in concrete.

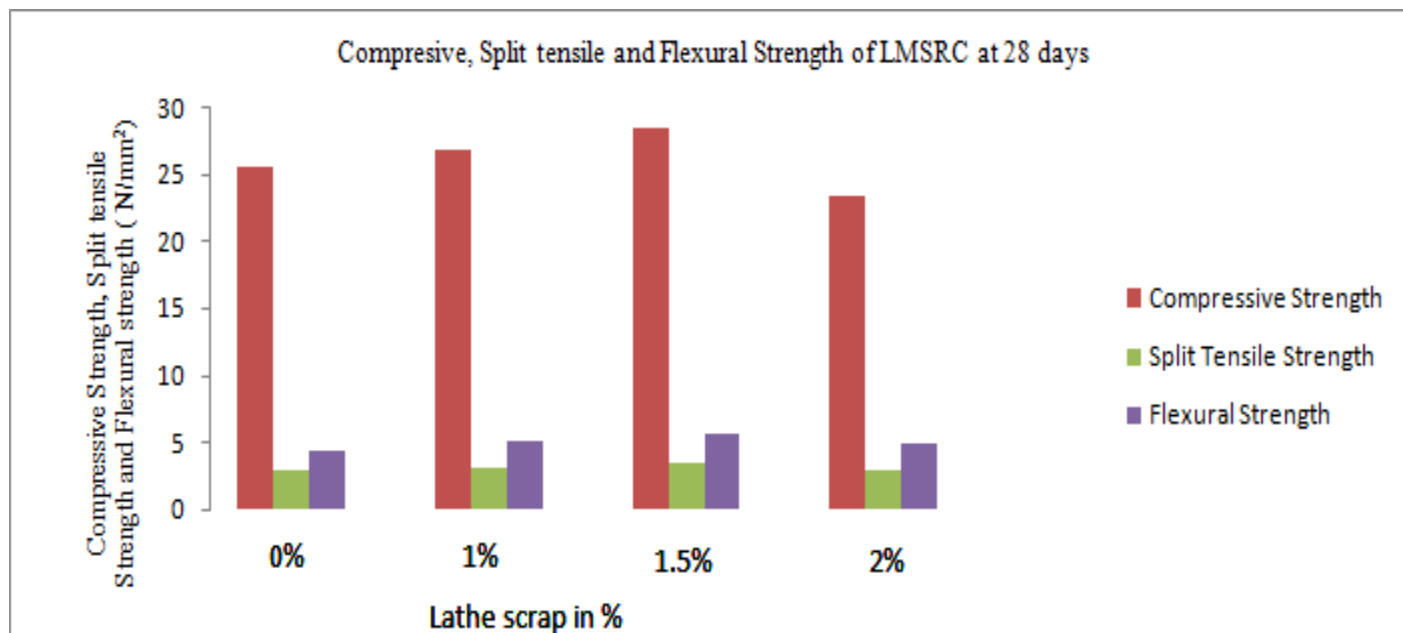


Fig 3: Compressive, Split tensile and flexural strength of concrete at different percentages of Lathe Machine Scrap

c. Load deflection Characteristics

The load deflection characteristics of the beam specimens were studied because it helps us to know how much load a structure or material can bear and how much deformation it is undergoing corresponding to that load, besides this it also enables us to know how much deflection a beam can undergo. For that the load deflection curve was plotted. The load-deflection curve for conventional beam without any Lathe machine scrap has shown maximum deflection of 6mm at failure and maximum load carrying capacity of 4.33kN. Concrete beam reinforced with 1 % LMS by weight showed maximum deflection of 6mm at failure and maximum load carrying capacity of 5kN. Beams with 1.5% and 2% LMS reinforcement by weight showed maximum deflection of 7mm and 6mm at failure respectively where as maximum load carrying capacity of 5.66kN and 4.83kN was noticed at 1.5% and 2% LMS reinforcement by weight in concrete respectively. The detailed load deflection curve and the comparison between the load carrying capacity and deflection of the beam specimen of both unreinforced and reinforced concrete with lathe machine scrap is shown in figure 9. It was clearly observed that the load carrying capacity of 1.5% lathe machine scrap content beam is maximum compared to other beams. It has also been observed that deflection is maximum in case of 1.5% Scrap. Hence beam with 1.5% lathe machine scrap content was found to be more ductile than other beams.

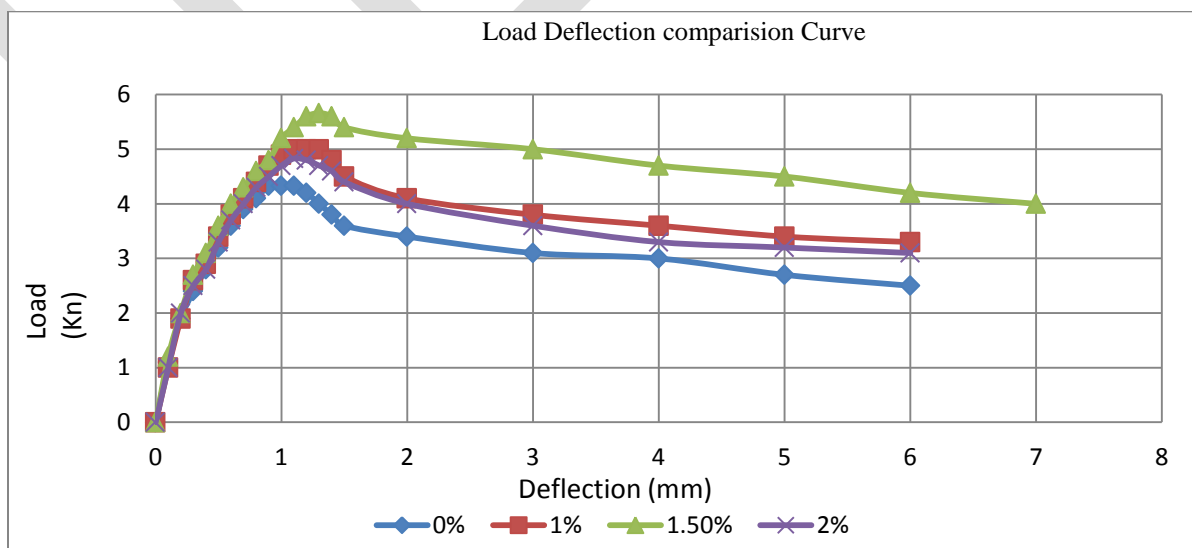


Figure 4: Comparison Load-deflection curve for beams with varying percentages of scrap

5. CONCLUSION

The slump value, compressive, split tensile and flexure strengths of M20 concrete grade were obtained at varying percentages of lathe machine scrap by weight in concrete. Slump Value decreased from 30mm to 10mm for concrete with no reinforcement and concrete with 2 % LMSR. The compressive strength was found out to be 25.5N/mm², 26.8N/mm², 28.4N/mm² and 23.33N/mm² for 0%, 1 %, 1.5% and 2% lathe machine scrap reinforcement respectively. The splitting tensile strength was 2.85N/mm², 3.04N/mm², 3.37N/mm² and 2.94N/mm², where as flexural strength were 4.33N/mm², 5N/mm², 5.66N/mm² and 4.83N/mm² for 0%, 1 %, 1.5% and 2% lathe machine scrap reinforcement respectively. It was observed that strength properties of concrete are increased by adding lathe machine scrap up to 1.5 % and it was found to be the optimum percentage for compressive, split tensile and flexure strengths after this percentage there was reduction in strength of concrete slightly. Deflection of the beam was also found to be maximum in case of 1.5 % lathe machine scrap i.e 7mm and load bearing capacity of the beam was 5.66kN. All in all it is concluded that lathe machine scrap is a strong and environmental friendly material which can improve structural strength of concrete, lessen steel reinforcements besides reducing width of cracks when used as reinforcement in concrete. It can also be used in future also in various concrete works, which includes determining shear strength parameters, durability properties.

REFERENCES:

- [1] Alam, P., Ahmad, K., Afsar, S. S., Akhtar, N., & Raina, Y. M. (2015). Study of Vibrations Produced on Five Different Types of Flyovers in Delhi, India. *International Journal of Structural Engineering*, 6(4), 318-331.
- [2] Neville, A. M. and Brooks, J.J. (1990). *Concrete Technology* (2nd ed.). Harlow, UK: Longman Scientific & Technical.
- [3] Nagesh, M. (2012). *Concrete Technology*. Ramanagara, India: Government Engineering College.
- [4] Owens, G. (2009). *Fultons concrete technology* (9th ed.). Midrand: Cement & Concrete Institute.
- [5] Custódio, J. (2015). Structural Adhesives. In *Materials for Construction and Civil Engineering* (pp. 717-771). Springer International Publishing
- [6] Hensher, D. A. (2016). *Fiber-reinforced-plastic (FRP) reinforcement for concrete structures: properties and applications* (Vol. 42). Elsevier
- [7] Zollo, R. F. (1997). Fiber-reinforced concrete: an overview after 30 years of development. *Cement and Concrete Composites*, 19(2), 107-122
- [8] L'hermite, R. (1977). Use of bonding techniques for reinforcing concrete and masonry structures. *Materials and Structures*, 10(2), 85-89.
- [9] Varastehpour, H., & Hamelin, P. (1997). Strengthening of concrete beams using fiber-reinforced plastics. *Materials and Structures*, 30(3), 160-166
- [10] Qi, C., Weiss, J., & Olek, J. (2003). Characterization of plastic shrinkage cracking in fiber reinforced concrete using image analysis and a modified Weibull function. *Materials and Structures*, 36(6), 386-395
- [11] Lee, M. K., & Barr, B. I. G. (2004). A four-exponential model to describe the behaviour of fibre reinforced concrete. *Materials and structures*, 37(7), 464-471
- [12] Michels, J., Barros, J., Costa, I., Sena-Cruz, J., Czaderski, C., Giacomini, G. & Zile, E. (2016). Prestressed FRP Systems. In *Design Procedures for the Use of Composites in Strengthening of Reinforced Concrete Structures* (pp. 263-301). Springer Netherlands
- [13] Su, Y., Li, J., Wu, C., Wu, P., & Li, Z. X. (2016). Influences of nano-particles on dynamic strength of ultra-high performance concrete. *Composites Part B: Engineering*, 91, 595-609
- [14] Fiorelli, J., Rempe, N., Molina, J. C., & Dias, A. A. (2015). Natural Fiber-Reinforced Polymer for Structural Application. In *Agricultural Biomass Based Potential Materials* (pp. 35-49). Springer International Publishing.
- [15] Afroughsabet, V., Biolzi, L., & Ozbakkaloglu, T. (2016). High-performance fiber-reinforced concrete: a review. *Journal of Materials Science*, 51(14), 6517-6551
- [16] Preti, M., & Meda, A. (2015). RC structural wall with unbonded tendons strengthened with high-performance fiber-reinforced concrete. *Materials and Structures*, 48(1-2), 249-260.
- [17] Caverzan, A., Colombo, M., di Prisco, M., & Rivolta, B. (2015). High performance steel fibre reinforced concrete: residual behaviour at high temperature. *Materials and Structures*, 48(10), 3317-3329.
- [18] Yew, M. K., Mahmud, H. B., Shafiqh, P., Ang, B. C., & Yew, M. C. (2016). Effects of polypropylene twisted bundle fibers on the mechanical properties of high-strength oil palm shell lightweight concrete. *Materials and Structures*, 49(4), 1221-1233.
- [19] Carpinteri, A., Cadamuro, E., & Ventura, G. (2015). Fiber-reinforced concrete in flexure: a cohesive/overlapping crack model application. *Materials and Structures*, 48(1-2), 235-247
- [20] Zhao, G., di Prisco, M., & Vandewalle, L. (2015). Experimental investigation on uniaxial tensile creep behavior of cracked steel fiber reinforced concrete. *Materials and Structures*, 48(10), 3173-3185.
- [21] Tanyildizi, H., & Şahin, M. (2016). Taguchi optimization approach for the polypropylene fiber reinforced concrete strengthening with polymer after high temperature. *Structural and Multidisciplinary Optimization*, 1-6.
- [22] Daviau-Desnoyers, D., Charron, J. P., Massicotte, B., Rossi, P., & Tailhan, J. L. (2016). Characterization of macrocrack propagation under sustained loading in steel fibre reinforced concrete. *Materials and Structures*, 49(3), 969-982.

- [23] Shajil, N., Srinivasan, S. M., & Santhanam, M. (2016). An experimental study on self-centering and ductility of pseudo-elastic shape memory alloy (PESMA) fiber reinforced beam and beam-column joint specimens. *Materials and Structures*, 49(3), 783-793
- [24] Shahin, M. Y. (2005). *Pavement management for airports, roads, and parking lots (Vol. 501)*. New York: Springer
- [25] Wu, H. C., Lim, Y. M., & Li, V. C. (1996). Application of recycled tyre cord in concrete for shrinkage crack control. *Journal of materials science letters*, 15(20), 1828-1831
- [26] Correia, J. R., De Brito, J., & Pereira, A. S. (2006). Effects on concrete durability of using recycled ceramic aggregates. *Materials and Structures*, 39(2), 169-177
- [27] Hossain, M. U., Poon, C. S., Lo, I. M., & Cheng, J. C. (2016). Evaluation of environmental friendliness of concrete paving eco-blocks using LCA approach. *The International Journal of Life Cycle Assessment*, 21(1), 70-84.
- [28] Wang, Y., Zureick, A. H., Cho, B. S., & Scott, D. E. (1994). Properties of fibre reinforced concrete using recycled fibres from carpet industrial waste. *Journal of materials science*, 29(16), 4191-4199.
- [29] De Brito, J., & Saikia, N. (2013). *Use of Industrial Waste as Aggregate: Properties of Concrete in Recycled Aggregate in Concrete* (pp. 115-228). Springer London
- [30] Pedro, D., de Brito, J., & Evangelista, L. (2015). Performance of concrete made with aggregates recycled from precasting industry waste: influence of the crushing process. *Materials and Structures*, 48(12), 3965-3978
- [31] Benmokrane, B., Chaallal, O., & Masmoudi, R. (1995). Glass fibre reinforced plastic (GFRP) rebars for concrete structures. *Construction and Building Materials*, 9(6), 353-364
- [32] Saafi, M., Toutanji, H., & Li, Z. (1999). Behavior of concrete columns confined with fiber reinforced polymer tubes. *ACI materials journal*, 96(4), 500-509.
- [33] Brückner, A., Ortlepp, R., & Curbach, M. (2006). Textile reinforced concrete for strengthening in bending and shear. *Materials and structures*, 39(8), 741-748
- [34] Soroushian, P., & Ravanbakhsh, S. (1998). Control of plastic shrinkage cracking with specialty cellulose fibers. *Materials Journal*, 95(4), 429-435
- [35] Nanni, A. (1992). Properties of aramid-fiber reinforced concrete and SIFCON. *Journal of materials in civil engineering*, 4(1), 1-15.
- [36] Agheee, K., Yazdi, M.A., & Tasadaridis, K.D (2014). Investigation into the Mechanical Properties of Structural Lightweight Concrete Reinforced with Waste Steel Wires. *Magazine of Concrete research*, 66(1), 1-9
- [37] Sun, M., Liu, Q., Li, Z., & Hu, Y. (2000). A study of piezoelectric properties of carbon fiber reinforced concrete and plain cement paste during dynamic loading. *Cement and Concrete Research*, 30(10), 1593-1595.
- [38] Mello, E., Ribellato, C., & Mohamedelhassan, E. (2014). Improving Concrete Properties with Fibers Addition. *World Academy of Science, Engineering and Technology, International Journal of Civil, Environmental, Structural, Construction and Architectural Engineering*, 8(3), 249-254.
- [39] Aravindan, S, Arunkumar, C.D. (2013), Experimental studies on fibre reinforced concrete from industrial waste, *Middle east journal of scientific research* 18 (12), 1738-1744
- [40] Tamil Selvi, M and Thandavamoorthy, T.S., (2013) " Studies on the Properties of Steel and Polypropylene Fibre Reinforced Concrete without any Admixture", *International Journal of Engineering and Innovative Technology* 3(1)
- [41] Shende, A. M. (2011). Comparative Study on Steel Fibre Reinforced Concrete Under Flexural and Deflection. *International Journal of Advanced Engineering Sciences and Technologies (IJAEST)*, 6(1), 116-120.
- [42] Bdour, A., N., Al-Khalayleh, Y., A. (2010), Innovative Application of Scrap tire Steel Cords in Concrete Mixes *Jordan Journal of Civil Engineering*, 4(1), 55-61
- [43] McNeil, K., & Kang, T. H. K. (2013). Recycled concrete aggregates: A review. *International Journal of Concrete Structures and Materials*, 7(1), 61-69
- [44] Marar, K., Eren, Ö., & Roughani, H. (2016). The influence of amount and aspect ratio of fibers on shear behaviour of steel fiber reinforced concrete. *KSCE Journal of Civil Engineering*, 1-7.
- [45] Tadepalli, P. R., Dhonde, H. B., Mo, Y. L., & Hsu, T. T. (2015). Shear strength of prestressed steel fiber concrete I-beams. *International Journal of Concrete Structures and Materials*, 9(3), 267-281.
- [46] Standard, I. (1991). IS-1489., 1991. "Portland-Pozzolana cement-Specification", Bureau of Indian Standards, Manak Bhawan, 9.
- [47] Standard, I. (1988). IS-4031-1988. "Methods Of Physical Tests For. Hydraulic Cement", Bureau of Indian Standards, Manak Bhawan, 9.
- [48] Standard, I. (1970). IS-383-1970. "Specification for Coarse and Fine Aggregates From Natural Sources For Concrete.", Bureau of Indian Standards, Manak Bhawan, 9.
- [49] Standard, I. (1980). IS-2720-1980. "Methods of Test for Soils. Part III Determination. of Speciflc Gravity.", Bureau Of Indian Standards, Manak Bhawan, 9.
- [50] Standard, I. (2000). IS-456. 2000. Plain and Reinforced Concrete-Code of Practice", Bureau of Indian Standards, Manak Bhawan, 9.
- [51] Standard, I. (1974). (IS 7320-1974). Specification for concrete slump test apparatus", Bureau of Indian Standards, Manak Bhawan, 9
- [52] Standard, I. (1959). IS-516. 1959. Method of Tests for Strength of Concrete", Bureau of Indian Standards, Manak Bhawan, 9.

- [53] Standard, I. (1970). (IS 5816-1970). Method of Tests for Tensile Strength of Concrete”, Bureau of Indian Standards, Manak Bhawan, 9.
- [54] Standard, I. (2009). (IS 10262-2009). Indian Standard Concrete Mix Proportioning-Guidelines”, Bureau of Indian Standards, Manak Bhawan, 9
- [55] Tattersall, G. H. (2003). Workability and quality control of concrete. CRC Press
- [56] De Larrard, F., Ferraris, C. F., & Sedran, T. (1998). Fresh concrete: a Herschel-Bulkley material. *Materials and Structures*, 31(7), 494-498.
- [57] Wallevik, J. E. (2006). Relationship between the Bingham parameters and slump. *Cement and Concrete Research*, 36(7), 1214-1221.
- [58] Carreira, D. J., & Chu, K. H. (1985). Stress-strain relationship for plain concrete in compression. In *Journal Proceedings* 82(6), 797-804.
- [59] McHenry, D., & Karni, J. (1958). Strength of concrete under combined tensile and compressive stress. In *Journal Proceedings* 54(4), 829-839.
- [60] Mangat, P. S., & Elgarf, M. S. (1999). Flexural strength of concrete beams with corroding reinforcement. *Structural Journal*, 96(1), 149-158

PROGRESSIVE COLLAPSE STUDY ON REGULAR STEEL SPACE FRAMES SUBJECTED TO SEISMIC LOADING

V.Lakshmi Prasanna, PG student, ANAMACHARAYA INSTITUTE OF TEHNOLOGY AND SCIENCES,KADAPA.

G.BHAGYAMMA, ASSISTANT PROFESSOR, ANAMACHARYA INSTITUTE OF TECHNOLOGY AND SCIENCES.

Dr.P.SRI CHANDANA,PROFESSOR AND HOD DEPARTMENT OF CIVIL ENGINEERING. ANAMACHARYA INSTITUTE OF TECHNOLOGY AND SCIENCES.

Abstract: Progressive collapse refers to a phenomenon in which local damage in a primary structural element leads to total or partial structural system failure. When investigating the progressive collapse of structures, nonlinear dynamic procedures lead to more accurate results than static procedures. However, nonlinear dynamic procedures are very complicated and the evaluation or validation of the results can become very time consuming. Therefore, it is better to use simpler methods. In this study, a simplified analysis procedure for the progressive collapse analysis of steel structures is presented using the load displacement and capacity curve for steel space framed structure using STAAD Pro.

KEYWORDS:PUSHOVER,PROGRESSIVECOLLAPSE,BASESHEAR,CAPACITYCURVE,ZONES,

DISPLACEMENT

Introduction:

A simple computer-based push-over analysis is a technique for performance-based design of building frameworks is Push-over analysis attains much importance in the past decades due to its simplicity and the effectiveness of the results. The present study develops a push-over analysis for steel frame designed according to IS-800 (2007) and ductility behaviour of each frame.

Suitable capacity parameters and their acceptable values, as well as suitable methods for demands prediction will depend on the performance level to be evaluated. In light of these facts, it is imperative to seismically evaluate the existing building with the Present day knowledge to avoid the major destruction in the future earthquakes. The Buildings found to be seismically deficient should be retrofitted or strengthened.

Pushover Methodology:

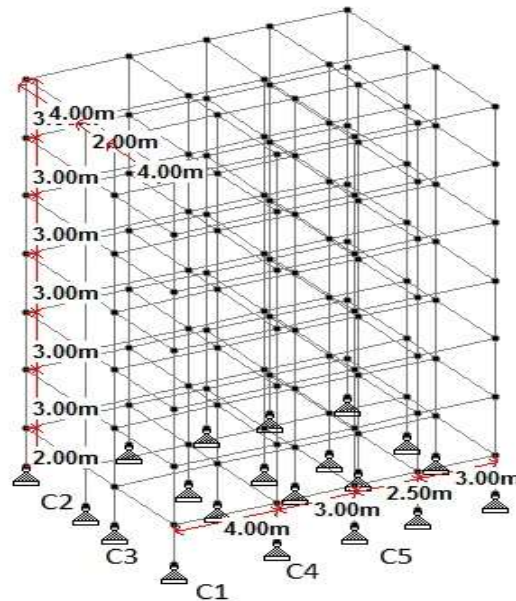
A pushover analysis is performed by subjecting a structure to a monotonically increasing pattern of lateral loads, representing the inertial forces which would be experienced by the structure when subjected to ground shaking. Under incrementally increasing loads various structural elements may yield sequentially. Consequently, at each event, the structure experiences a loss in stiffness. Using a pushover analysis, a characteristic non-linear force displacement relationship can be determined.

Structural modelling:

The study in this thesis is based on nonlinear analysis of steel frames on different configurations of frames are selected such as

REGULAR FRAMED STRUCTURE:

case-(1): Regular G+5 frame ,**case-(2):** progressive collapse load case by removing a column (C1) at assumed corner joint, **case-(3):** progressive collapse load case by removing a column (C2) at assumed exterior edge joint in Z direction, **case-(4):** progressive collapse load case by removing a column (C3) at assumed exterior edge joint in Z direction, **case-(5):** progressive collapse load case by removing a column (C4) at assumed exterior edge joint in X direction, **case-(6):** progressive collapse load case by removing a column (C5) at assumed exterior edge joint in X direction.



Isometric View of RF modelled in STAAD.Pro

Results and Discussions:

SEISMIC ZONE	BASE SHEAR (KN)					
	(RF)	(RFC-1)	(RFC-2)	(RFC-3)	(RFC-4)	(RFC-5)
Seismic zone	BASE SHEAR	BASE SHEAR	BASE SHEAR	BASE SHEAR	BASE SHEAR	BASE SHEAR
	(kN)	(kN)	(kN)	(kN)	(kN)	(kN)
SEISMIC ZONE II	1434.1	110.94	107.855	114.018	111.699	113.45
SEISMIC ZONE III	1434	114.832	111.208	111.208	110.343	111.19
SEISMIC ZONE IV	1436	111.54	113.076	113.076	119.992	113.43
SEISMIC ZONE V	1436.8	121.337	116.705	116.705	117.13	117.65

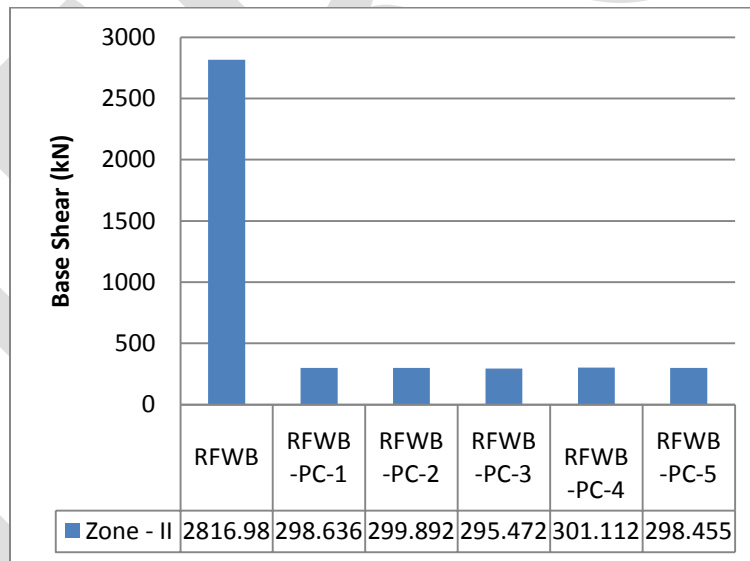
SEISMIC ZONE	REGULAR FRAMED structure DISPALCEMENT (mm) FOR					
	(RF)	(RFC	(RFC	(RFC-	(RFC	(RFC

		-1)	-2)	3)	-4)	-5)
Seismic zone	DISP LAC EMENT	DISP LAC EMENT	DISP LAC EMENT	DISPLACEMENT	DISP LAC EMENT	DISP LAC EMENT
	(mm)	(mm)	(mm)	(mm)	(mm)	(mm)
SEISMIC ZONE II	50.026	5.07	5.009	5.429	5.099	5.176
SEISMIC ZONE I	50.024	5.249	5.165	5.12	5.037	5.073
SEISMIC ZONE IV	50.057	5.099	5.525	5.206	5.478	5.175
SEISMIC ZONE V	50.05	5.547	5.42	5.373	5.347	5.368

REGULAR FRAMED STRUCTURE:

Comparison between base shears and displacements from the capacity curves obtained from the pushover analysis at Seismic zone II:

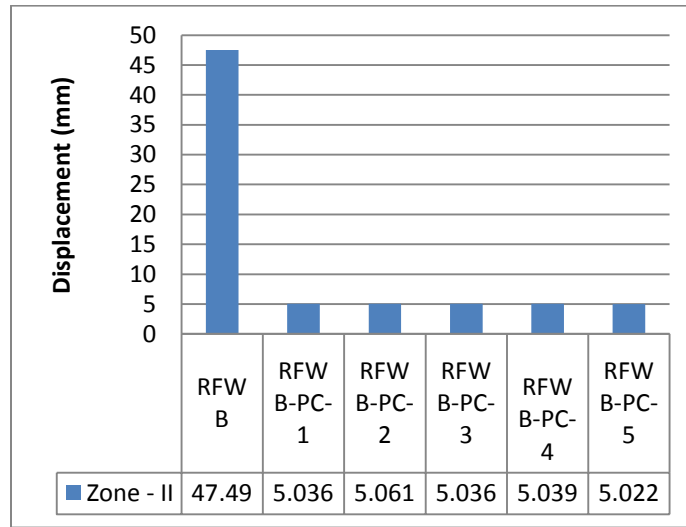
BASE SHEAR:



Comparison of Base shear at Seismic zone-II

It was observed that base shear capacity of RFWB-PC-1, RFWB-PC-2, RFWB-PC-3, RFWB-PC-4, and RFWB-PC-5 was decreased by 89%, 89.35%, 89.47%, 89.5% and 89.4 % when compared to RFWB.

DISPLACEMENT:

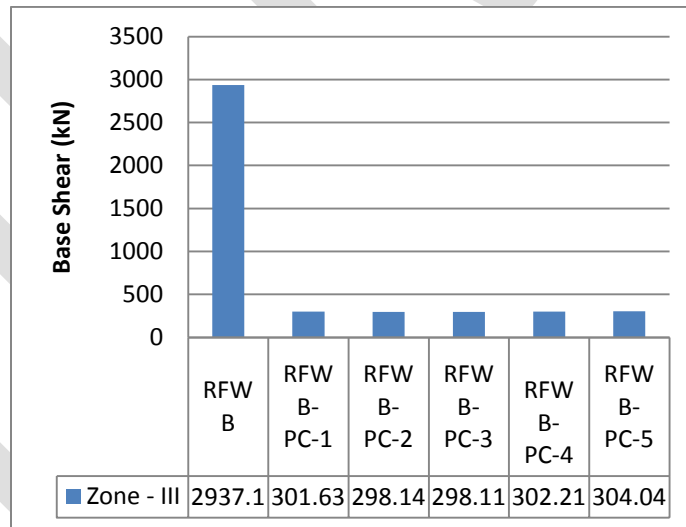


Comparison of displacements at Seismic zone-II

It was observed that displacement resistance of RFWB-PC-1, RFWB-PC-2, RFWB-PC-3, RFWB-PC-4, and RFWB-PC-5 was decreased by 89.3%, 89.3%, 89.39%, 89.38% and 89.38 % when compared to RFWB.

Comparison between base shears and displacements from the capacity curves obtained from the pushover analysis at Seismic zone III:

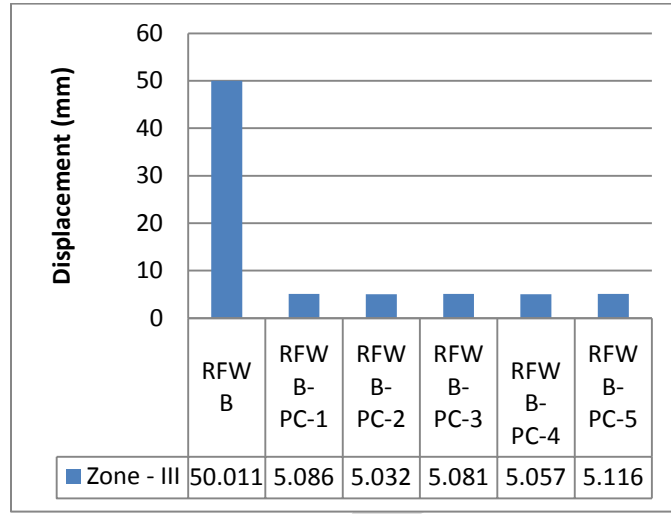
BASE SHEAR:



Comparison of Base shear at Seismic zone-III

It was observed that base shear capacity of RFWB-PC-1, RFWB-PC-2, RFWB-PC-3, RFWB-PC-4, and RFWB-PC-5 was decreased by 89.7%, 89.8%, 89.8%, 89.7% and 89.6 % when compared to RFWB.

DISPLACEMENT:

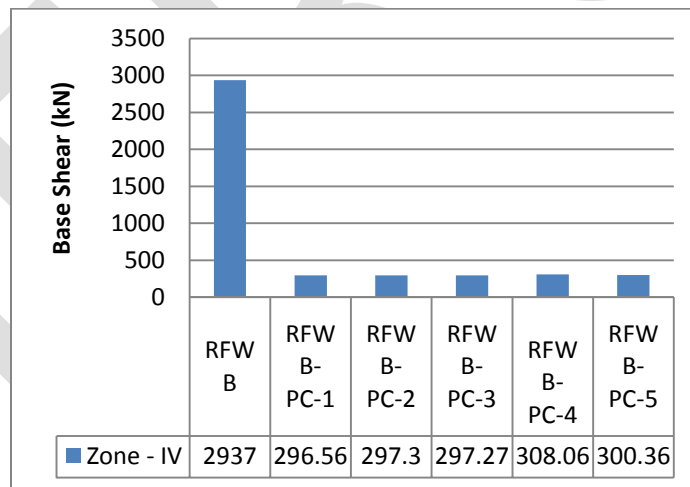


Comparison of displacements at Seismic zone-III

It was observed that displacement resistance of RFWB-PC-1, RFWB-PC-2, RFWB-PC-3, RFWB-PC-4, and RFWB-PC-5 was decreased by 89.8%, 89.9%, 89.8%, 89.88% and 89.7 % when compared to RFWB.

Comparison between base shears and displacements from the capacity curves obtained from the pushover analysis at Seismic zone IV:

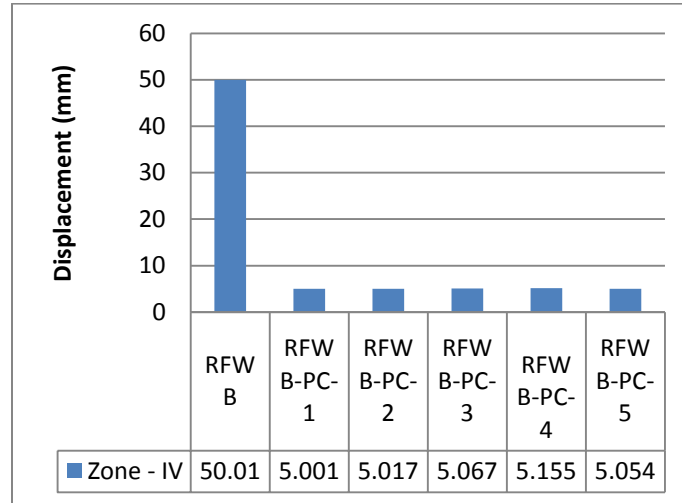
BASE SHEAR:



Comparison of Base shear at Seismic zone-IV

It was observed that base shear capacity of RFWB-PC-1, RFWB-PC-2, RFWB-PC-3, RFWB-PC-4, and RFWB-PC-5 was decreased by 89.9%, 89.9%, 89.8%, 89.5% and 89.7 % when compared to RFWB.

DISPLACEMENT:

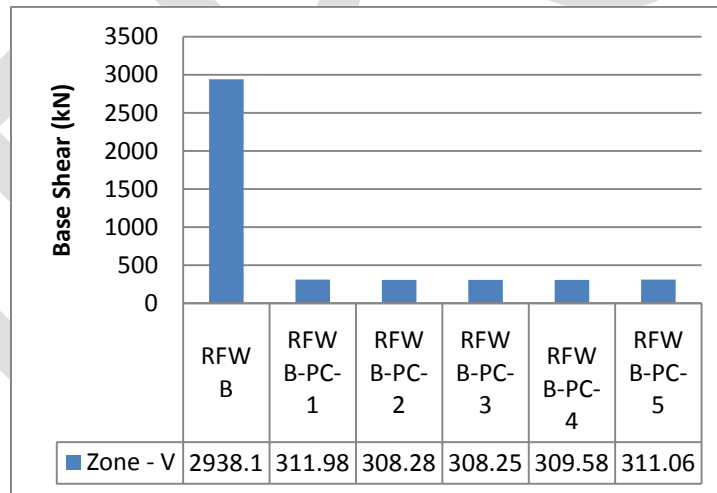


Comparison of displacement at Seismic zone-IV

It was observed that displacement resistance of RFWB-PC-1, RFWB-PC-2, RFWB-PC-3, RFWB-PC-4, and RFWB-PC-5 was decreased by 90%, 90%, 89.8%, 89.69% and 89.89 % when compared to RFWB.

Comparison between base shears and displacements from the capacity curves obtained from the pushover analysis at Seismic zone V:

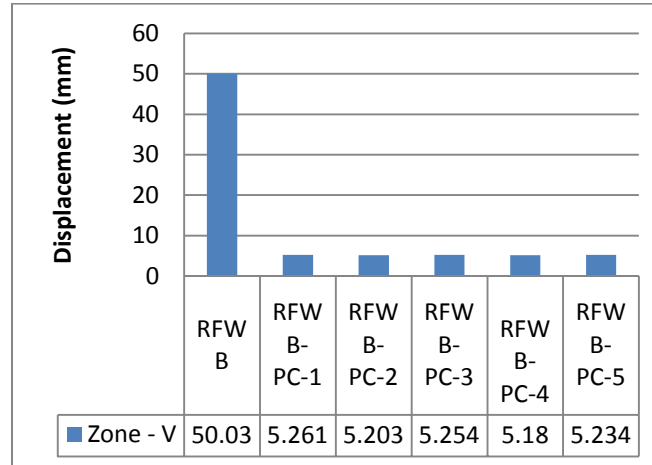
BASE SHEAR:



Comparison of base shear at Seismic zone-V

From the fig. 4.31, it was observed that base shear capacity of RFWB-PC-1, RFWB-PC-2, RFWB-PC-3, RFWB-PC-4, and RFWB-PC-5 was decreased by 89.4%, 89.5%, 89.5%, 89.4% and 89.41 % when compared to RFWB.

DISPLACEMENT:



Comparison of displacement at Seismic zone-V

It was observed that displacement resistance of RFWB-PC-1, RFWB-PC-2, RFWB-PC-3, RFWB-PC-4, and RFWB-PC-5 was decreased by 89.48%, 89.48%, 89.49%, 89.64% and 89.53 % when compared to RFWB.

Conclusion:

1. The maximum base shear and maximum displacement capacity of the Space frame with considering progressive collapse case is reduced by 92.4% and 90.093% when compared to Regular space frame in Seismic zone II
2. The maximum base shear and maximum displacement capacity of the Space frame with considering progressive collapse case is reduced by 92.3% and 89.9% when compared to Regular space frame in Seismic zone III
3. The maximum base shear and maximum displacement capacity of the Space frame with considering progressive collapse case is reduced by 92.2% and 89.8% when compared to Regular space frame in Seismic zone IV
4. The maximum base shear and maximum displacement capacity of the Space frame with considering progressive collapse case is reduced by 91.9% and 89.27% when compared to Regular space frame in Seismic zone V
5. In all the progressive collapse load cases the percentage change in reduction of base shear and displacements is very minute in the same Seismic zone.

REFERENCES:

1. A. Vijay and K.Vijayakumar (2013), Performance of Steel Frame by Pushover Analysis for Solid and Hollow Sections”, International Journal of Engineering Research and Development, Vol. 8, Issue 7 (September 2013), PP. 05-12
2. Ashutosh Bagchi (2009) “performance of a 20- story steel moment resisting steel frame building”, designed for western part of Canada.
3. F. Hejazi, S. Jilani, J. Noorzaei, C. Y. Chieng, M. S. Jaafa A, and A. Abang Ali (2011) „Effect of Soft Story on Structural Response of High Rise Buildings”, IOP Conf. Series: Materials Science and Engineering.
4. Gaurav Joshi (2013), ‘Seismic Performance of Soft Storey Composite Column’, International Journal of Scientific & Engineering Research, Vol. 4, Issue 1, January-2013 ISSN 2229-5518.
5. Hiten L. Kheni, and Anuj K. Chandiwala (2014), „Seismic Response of RC Building with Soft Stories”, International Journal of Engineering Trends and Technology (IJETT), and Vol. 10 Number 12 - Apr 2014.

6. IS:1893(Part1)–(2002), „Indian Standard Code of Practice for Criteria for Earthquake resistant Design of Structures“, Bureau of Indian Standard, New Delhi.
7. Nelson lam N. Raut and Swati D. Ambadkar (2013), „Pushover analysis of multistoried building“, Global Journal of Researches in Engineering, Vol. 13 Issue 4 Version 1.0
8. P.B.Lamb, and R.S. Londhe (2012), „Seismic Behavior of Soft First Storey“, IOSR Journal of Mechanical and Civil Engineering, ISSN: 2278-1684 Vol. 4, Issue 5 (Nov. - Dec. 2012)
9. Padmakar Maddala (2013), „Pushover analysis of steel frames „Department of Civil Engineering National Institute Of Technology Rourkela, Orissa (Unpublished).
10. Rahiman G. Khan and M. R. Vyawahare (2013),Push Over Analysis of Tall Building with Soft Stories at Different Levels“, International Journal of Engineering Research, Vol. 3, Issue 4, July, pp.176-185.
11. Rakshith Gowda K.R and Bhavani Shankar (2014),Seismic Analysis Comparison of Regular and Vertically Irregular RC Building with Soft Storey at Different Level“, International Journal of Emerging Technologies and Engineering, Vol. 1, ISSN 2348– 8050.
12. SuchitaHirde and Ganga Tepugade (2014), Seismic Performance of Multistorey Building with Soft Storey at Different Level with RC Shear Wall“, International Journal of Current Engineering and Technology, Vol.4, No.3

HOME AUTOMATION SYSTEM

Prof.Fr. John Rose S.J
Information Technology Dept.
Xavier Institute of Engineering
Mumbai

Sophiya Kunjumon
Information Technology
Xavier Institute of Engineering
Mumbai
Phone: 9619909318

Kenneth Pinto
Electronics and Telecommunication
Xavier Institute of Engineering
Mumbai

Abstract— In the Home Automation Project, a smart home solution is provided to create a wireless interface to communicate with electrical appliances in the home environment. Electrical and Electronic appliances are controlled by means of a website hosted using an Arduino microcontroller and Ethernet Shield. This creates a uniform interface which can be accessed locally or remotely using smart phones, laptops or any internet web browser capable devices. An HTML5, AJAX, JavaScript and CSS3 based website is utilized for this project. Pyroelectric Infrared (PIR) sensors are calibrated according to the dimensions. If the presence of humans is detected, based on preset conditions, certain electrical appliances will switch ON or OFF. If not, all non-essential electronics (lights, fans, ACs) will switch OFF automatically after a buffer period. Also, Infrared (IR) signal frequencies from remotes belonging to TVs and ACs will be mapped and recreated using an IR LED transmitter which will be interfaced with an Arduino and be used to control the corresponding devices based on commands received from the control website. The Arduino used will be connected to the mains using a power relay.

Keywords— Home Automation, PIR, Power Relay, Arduino, LED, Ethernet Shield.

INTRODUCTION

Home automation, or the idea of smart homes, is the controlling and monitoring of home appliances in a unified system. These include lighting, heating, and even home electronics. Home automation is closely related to (industrial) building automation where lighting, climate control (HVAC: Heating, Ventilation, and Air Conditioning), and security systems are integrated for central and/or automated control. Building automation often focuses on the automation of large commercial buildings. In contrast, home automation focuses more on comfort and entertainment, but both HVAC and security can be (and often are) part of a smart home. Introduction Home automation, or the idea of smart homes, is the controlling and monitoring of home appliances in a unified system. These include lighting, heating, and even home electronics. Home automation is closely related to (industrial) building automation where lighting, climate control (HVAC: Heating, Ventilation, and Air Conditioning), and security systems are integrated for central and/or automated control. Building automation often focuses on the automation of large commercial buildings. In contrast, home automation focuses more on comfort and entertainment, but both HVAC and security can be (and often are) part of a smart home.

Proposed System:

Interface:

The Home Automation system will be controlled using a web site hosted on the internet using Arduino, a Wi-Fi Shield and its libraries. Users can securely login over the internet to control different appliances like Lights, Fans, TVs and Air Conditioners. There are two sections of code involved:

1. The Arduino sketch
2. The .html Webpage

The Arduino sketch sets up the network and handles the communications. It involves setting up the website, receiving commands over the internet and executing the respective commands. The sketch also calls a .html webpage stored on the SD card and communicates this one line at a time over the internet, acting as a web server. Users can login remotely on this web server and using the UI provided, control the appliances.

Use of IR transmitter: An IR remote works by turning the LED on and off in a particular pattern. However, to prevent interference from IR sources such as sunlight or lights, the LED is not turned on steadily, but is turned on and off at a modulation frequency (typically 36, 38, or 40KHz). The time when a modulated signal is being sent will be called a mark, and when the LED is off will be called a space. Each key on the remote has a particular code (typically 12 to 32 bits) associated with it, and broadcasts this code when the key is pressed. If the key is held down, the remote usually repeatedly broadcasts the key code. For an NEC remote, a special repeat code is sent as the key is held down, rather than repeatedly sending the code. For Philips RC5 or RC6 remotes, a bit in the code is toggled each time a key is pressed; the receiver uses this toggle bit to determine when a key is pressed down a second time. On the receiving end, the IR detector demodulates this signal, and outputs a logic-level signal indicating if it is receiving a signal or not. The IR detector will work best when its frequency matches the sender's frequency, but in practice it doesn't matter a whole lot.

Transmitter section



Receiver Section



Block Diagram of Infrared Remote Control Switch

Implemented Output:

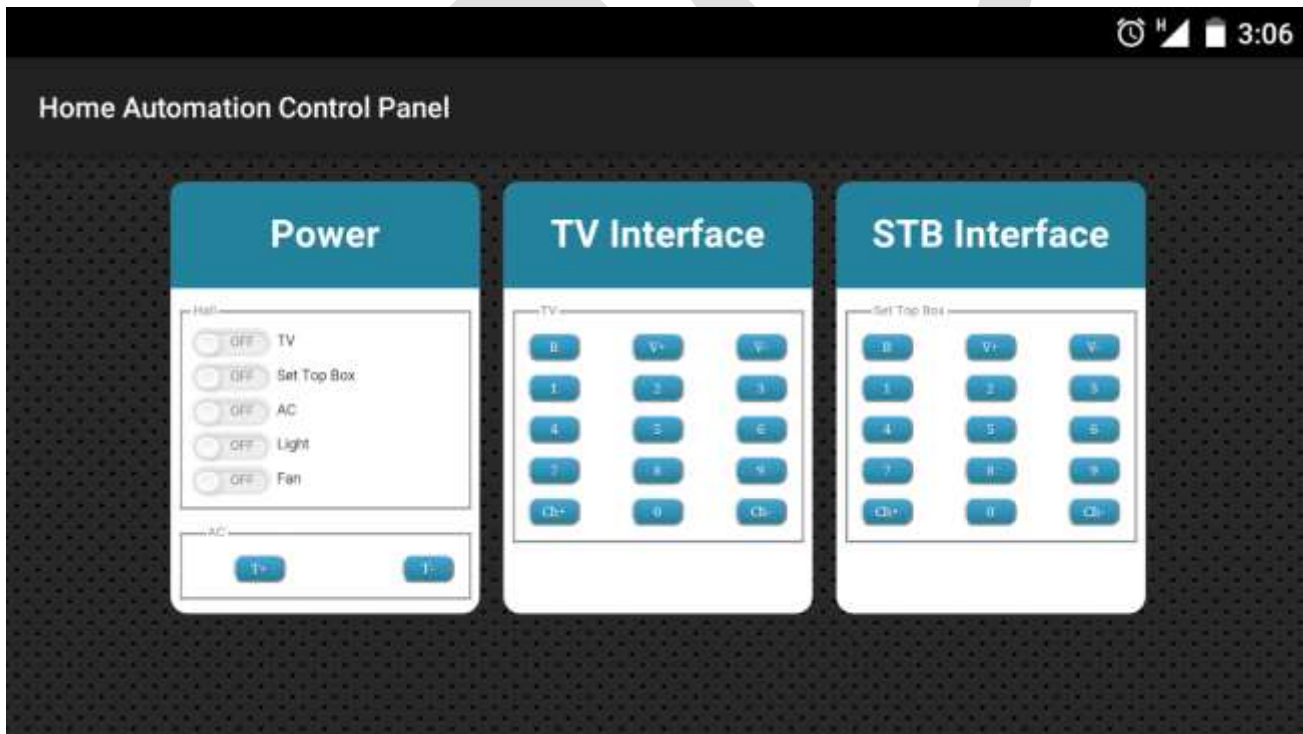


FIG 3. OUTPUT OF THE SYSTEM.

ACKNOWLEDGMENT

Our project “Home Automation System” is a challenging and demanding project. We would like to extend our special thanks to our internal project guide, **Prof. Fr. John Rose S.J** for taking interest in our project and guiding and correcting various documents with utmost care and attention to detail. We also thank our academic circles for their valuable input and help, particularly the head of the IT department in our college, **Prof. Chhaya Narvekar**. We would like to express our sincere gratitude to the principal,

Dr. Y. D. Venkatesh, for maintaining an environment of academic rigor along with providing us the required infrastructure for our project research and development. We would like to express our appreciation to the non-teaching staff as well. In writing this report, we have drawn on a vast amount of literature, and we owe an intellectual debt to numerous authors who have provided the same. The cooperation and feedback of friends and family members is also worth mentioning, and we are deeply grateful to them.

CONCLUSION

It is evident from this project work that home automation system can be cheaply made from low-cost locally available components and be used to control multiple appliances ranging from the television to the air conditioning system and even the entire house lighting system. And better still, the components required are so small and few that they can be packaged into a small container. The designed home automation system was tested a number of times and certified to control home appliances used like the lights, fans and the television. This home automation system can also be implemented over Bluetooth, Infrared and WAP connectivity without much change to the design and yet still be able to control a variety of home appliances. Hence, this system is scalable and flexible.

REFERENCES:

- [1] RENATO JORGE CALEIRA NUNES "HOME AUTOMATION - A STEP TOWARDS BETTER ENERGY MANAGEMENT"
- [2] Poul Ejnar Rovsing, Peter Gorm Larsen, Thomas Skjideberg Toftegaard and Daniel Lux "A Reality Check on Home Automation Technologies"
- [3] Jaeseok Yun and Sang-Shin Lee "Human Movement Detection and Identification Using Pyroelectric Infrared Sensors"
- [4] Dr. Subhi R. M. Zeebaree, Hajar M. Yasin "Arduino Based Remote Controlling for Home: Power Saving, Security and Protection"
- [5] Bader M. O. Al-thobaiti, Iman I. M. Abosolaiman, Mahdi H. M. Alzahrani, Sami H. A. Almalki, Mohamed S. Soliman "Design and Implementation of a Reliable Wireless Real-Time Home Automation System Based on Arduino Uno Single-Board Microcontroller" [Journal]
- [6] Anon, (2016). [online] Available at: <http://www.righto.com/2009/11/controlling-your-stereo-over-web-with.html> [Accessed 20 Jan. 2016].
- [7] Anon, (2016). [online] Available at: <https://learn.adafruit.com/using-an-infrared-library/sending-ir-codes> [Accessed 25 Feb. 2016]

Analysis of Self supporting Steel Stacks with Variable Geometrical Configuration under the seismic loading for different shapes

Babita Devi^[1], Shashi Shekhar Singh^[2],

MVN University, Palwal, Haryana ^{[1][2]}

babita.devi@mvn.edu.in, +919050646524^[1]

Abstract— The present study deals with seismic behavior in zone IV for the different shapes of steel stacks with variable heights of 30m, 40m, and 50m. This work is carried out with sole objective to find which shape of steel stack is more stable under the seismic loading condition in terms of fundamental frequency and maximum deflection. The Seismic analysis is done by using the ‘Staad Pro Vi8 ss5’ software on the different shapes with some assumptions as per IS 6533:1989(part-1&II).

Keywords— Steel stacks, Seismic analysis, Maximum deflection, Fundamental frequency, Response spectrum.

INTRODUCTION

Stacks or chimney are very important industrial structures for emitting harmful gases to a higher elevation in atmosphere such that the gases do not contaminate nearby atmosphere. Failure of steel stacks is prime issue in most of industries. The cause behind the failure is analyzed by the seismic analysis of stacks. Total 9 stacks with different shape (simple circular, flare base and tapered) with Variable heights (30, 40,50m) were proposed for Seismic analysis as mentioned in Table-1. The analysis is done by using Staad Pro Vi8 ss5.

ANALYSIS OF STEEL STACKS:

Seismic effects include the effect of dynamic force exerted on steel stacks during earthquake. In the current work Response spectrum method is used to analyze the selected stacks.

A. *Geometry for flare base and tapered steel stacks:*

Basic geometry of steel stacks is governed by top diameter (D_t), base diameter (D_b) and effective height (H_e). Following IS code are used for the analysis of steel stacks.

- IS 6533 (part-1):1989, “Indian standard code of practice for design and construction of steel chimney –code of practice-Mechanical aspects.”
- IS 6533 (part-2):1989, “Indian standard code of practice for design and construction of steel chimney –code of practice-Structural aspects.”
- IS 1893(part-4):2005 for the Seismic analysis.

Minimum top diameter of unlined chimney should be one twentieth of effective Height of chimney/stacks and minimum outside diameter at base should be equal to 1.6 times the top diameter of stack. (As per IS 6533(part2):1989(reaffirmed in 2003) cl.7.2.4 (b) &(c).

Table: 1 Geometry of Flare base and tapered steel stacks (Effective height H_e only for Flare base)

Total Height of stack (Meters) (H)	Effective Height (H_e) ($2/3 \times H$) (meter)	Top Diameter (constant) ($H/30$) (m)	Varying top to bottom diameters ratio (D_b/D_t) ratio (m)
			1.6
H	H_e	D_t	D_b
30	20	1	1.6
40	26.67	1.33	2.128
50	33.34	1.66	2.656

PROBLEM -STATEMENT

Analyze the behavior of self-supporting circular; flare base, Tapered steel stacks with variable geometric configurations for the seismic response as per Indian standard code of practice.

A. Details of selected stacks:

- Type: self-supported unlined industrial circular steel stacks with constant shell thickness as IS 6533 Part-1.
- Total 9 steel stacks (3 stacks of different heights, shapes and each stack with variable diameters)
- Selected heights of steel stacks are 30m, 40m, 50m.
- Top diameter for each stack is taken as minimum $h/30$ as per provision in IS 6533:1989.
- Variation in base diameter for each stack for fixed value of top diameter will be in following incremental ratio (ratio D_b/D_t) : 1.6
- Base condition : Rigid support at base
- Thickness of stack shell=16mm (constant for all stacks)
- Material : Stainless steel
- Location of stack :Agra
- Seismic zone :zone IV ...(IS 1893:2005)
- Materials for steel stack are conforming to IS2062:2006.

RESULTS:

Seismic analysis results are tabulated in terms of Fundamental frequency and maximum deflection in table-2(for SCSC), Table-3(for FBSC), Table-4(TSC) and Table-5(maximum deflection). Fig-1, Fig-2 and Fig-3 shows the seismic behaviour, graphical representation of fundamental frequency and maximum deflections in SCSC, FBSC, TSC respectively which are as follows:

A. Seismic response for circular steel stacks:

The fundamental time period increase with increment in height of steel stack. The frequency for the simple circular steel stacks decrease with the increment in height for the seismic loading as mentioned in the table-2.

Table: 2 Seismic response for simple circular steel stack (SCSC)

Height (m)	Top Diameter (m)	Bottom Diameter (m)	Modes	Fundamental Time Period (T) sec	Fundamental Frequency (f) (cycle/sec)
30	1	1	1	0.44844	2.230
40	1	1		0.79461	1.258
50	1	1		1.26307	0.792

B. Seismic response for flare base steel stacks:

The fundamental time period increase with increment in height of steel stack. The frequency for the flare base steel stacks decrease with the increment in height for the seismic loading as mentioned in the table-3.

Table: 3 Seismic response of Flare base steel stacks (FBSC)

Height (m)	Top Diameter (m)	Bottom Diameter (m)	Modes	Fundamental Time Period (T) sec	Fundamental Frequency (f) (cycle/sec)
30	1.00	1.600	1	0.33214	3.011
40	1.33	2.128		0.43840	2.281
50	1.66	2.656		0.55652	1.797

C. Seismic response for Tapered steel stacks:

The fundamental time period increase with increment in height of steel stack. The frequency for the tapered steel stacks decrease with the increment in height for the seismic loading as mentioned in the table-4.

Table: 4 Seismic response of Tapered steel stacks (TSC)

Height (m)	Top Diameter (m)	Bottom Diameter (m)	Modes	Fundamental Time Period (T) sec	Fundamental Frequency (f) (cycle/sec)
30	1	1.6	1	0.267	3.747
40	1.33	2.128		0.357	2.803
50	1.66	2.656		0.447	2.238

D. Fundamental frequency due to Seismic response:

The fundamental frequency decreases with the increment in height of steel stack for all shapes. Fundamental frequency is more in tapered shape steel stacks as compare to simple circular and flare base steel stack for the 1st mode.

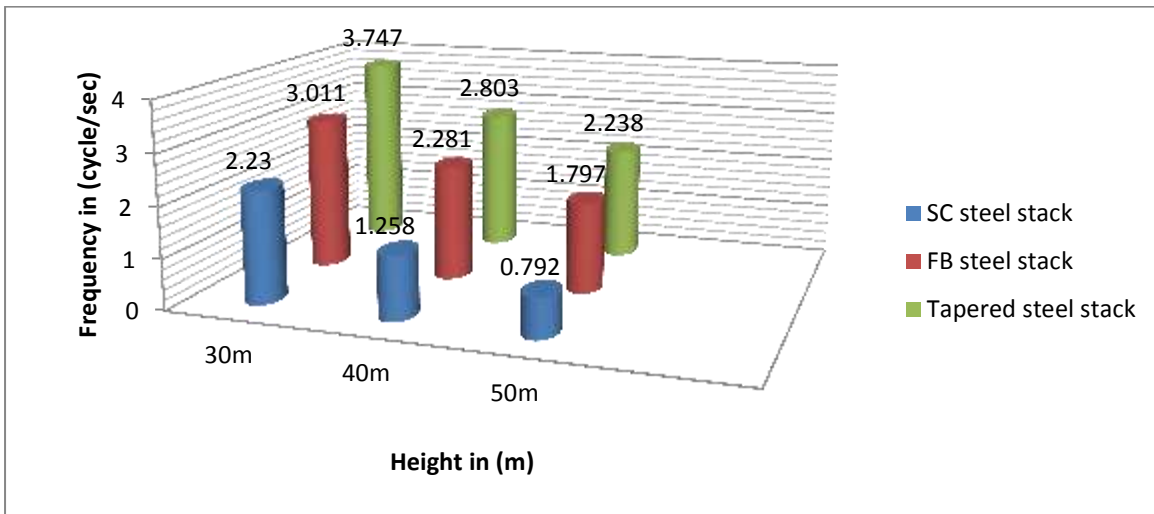


Fig-1 Fundamental frequencies in different shapes of steel stacks with variable heights

E. Max. Deflection due to Seismic response:

Maximum deflection increases with the increment in height of steel stack for all shapes. Tapered steel stacks are having less deflection as compare with simple circular and flare base stacks as per table-5 and Fig-2.

Table 5 Maximum Deflection (mm) Due to Seismic Response of steel stacks

Height	Simple circular steel stacks in (mm)	Flare base steel stacks in (mm)	Tapered steel stacks in (mm)
30m	3.394	2.168	1.415
40m	8.009	3.609	2.606
50m	12.729	5.963	4.086

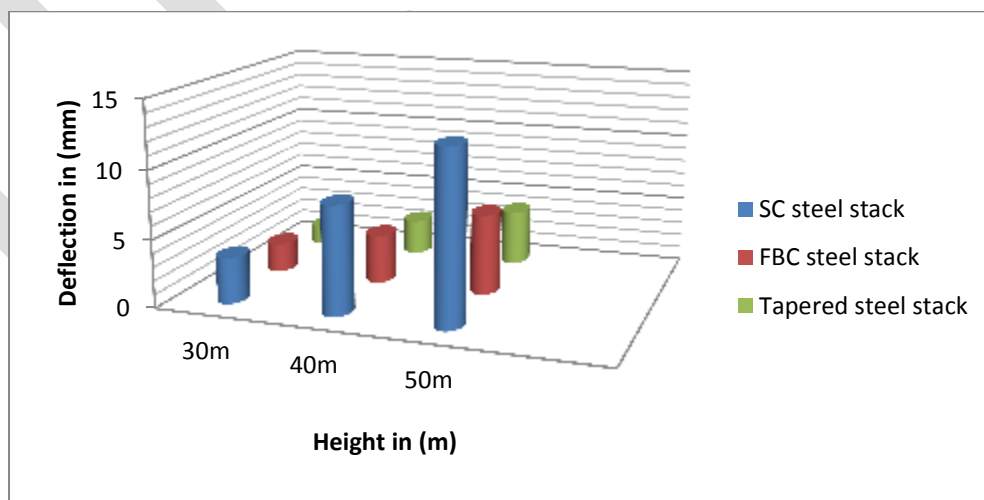


Fig-2 Maximum Deflection due to Seismic response with variable Heights (Different shapes) for 1st mode

CONCLUSION:

Following conclusions are obtained from all above graphical representations:

1. Fundamental frequency in tapered shape steel stacks(30,40,50m) is (40.49,55.12,64.61%) less than as compare with simple circular steel stacks of (30,40,50m).and (19.64,18.62,19.71%) less than as compare to flare base steel stacks of 30,40,50m.
2. Maximum deflection in Simple circular shape steel stacks(30,40,50m) is (58.31,67.46,67.90%) more than as compare with tapered steel stacks of (30,40,50m).and (34.73,27.79,31.48%) more in flare base steel stacks as compare with tapered steel stacks of 30,40,550m.
3. Tapered shape of steel stack is more stable under the seismic loading condition.

REFERENCES:

1. **IS 6533 Part-1; 1989**, “*Design and construction of steel chimney*”, Bureau of Indian Standards, New Delhi (2002).
2. **IS 6533 Part-2; 1989**, “*Design and construction of steel chimney*”, Bureau of Indian Standards, New Delhi (2005).
3. **G. Murali et al., (2012)**, “*Response of Mild Steel chimney Under Wind Loads*”, International Journal of Engineering Research and Applications, 2(2), pp. 490-498.
4. **Harshal deshpane, (2015)**, “*Correlation of Geometry and Dynamic Response of Self-Supported short Circular Steel stacks*”, Saraswati collage of Engineering, kharghar.
5. **J.kawecki and J.A. Zuranski (2007)**, “*Cross wind vibration of steel chimneys-A new case history*”, Journal of wind Engineering and industrial Aerodynamics.95.1166-194.

Study of Design Parameter Variations in Simple Grounded Active Inductor

Lakshmi V Nair, Prameela B

M.tech Student, ASIET kalady, vnair.025@gmail.com, 9847540039

Abstract— This paper presents a fundamental active inductor topology named Simple Grounded Active Inductor (SGAI) for analyzing variations in Q factor and inductance. Design parameters like aspect ratios and biasing of the transistors are varied and the Q factor and inductance variations are measured at 2.4GHz. The SGAI structure is simulated using Cadence Virtuoso spectre using 180nm technology and a supply voltage of 3.3 V. For a biasing current of 500 μ A and aspect ratio of 5 μ m/0.18 μ m, the Q factor is 2.45, inductance is 2.5nH, and the self resonating frequency is 23.47GHz at 2.4GHz. The designed SGAI circuit consumes a power of 3.3mW.

Keywords— SGAI, SRF, Q factor, SCAI, Regulated Cascode, CMOS, RFIC

INTRODUCTION

In order to make Moore's law pronouncing in radio frequency integrated circuits (RFIC), the RF components can no more be passive in nature. RFIC normally work between 300MHz to 30GHz. High Q factor inductor is a major parameter that determines the reliability and efficiency of CMOS RF blocks. Usually inductors are realized on chip as spiral inductors. But they consume a higher area and also has a limited Q factor due to various losses. The inductance and q factor of spiral inductors is determined by design parameters like total length, width, thickness of wire, number of loops, conductivity of the metal etc. Even though passive inductors are simpler to design, they possess a low Q factors in the range of 5 for bulk CMOS and 20 for SOI at GHz frequencies [1].

As the RFIC performance is mainly determined by the tank circuit, a reliable inductor design is inevitable. Active inductors are a promising solution in this scenario. They offer many advantages over their passive counter parts like small chip area, tunable inductance, high Q factor etc [2]. Even though there are several active inductor topologies in the literature most of them are based on gyrator-C configuration [3]. An ideal gyrator is a linear two port network that neither stores nor dissipates energy.

BASIC ACTIVE INDUCTORS

Usually active inductors are build on gyrator type configuration where two transistors are connected in a back to back fashion [5]. The topology utilizes the parasitic capacitance of the transistors in order to make the overall circuit to behave inductive. Simple Grounded Active Inductor (SGAI) is the fundamental topology that uses two transistors to mimic the inductive behavior [10]. However the Q factor that can be achieved is limited and for improving the same, Simple Cascoded Active Inductors (SCAI) can be used. Problem with SCAI is the reduction in the frequency range of the operation. To alleviate that drawback, regulated cascode active inductors [6] are there which provide a better performance compared to SGAI in terms of Q factor and SCAI in terms of frequency range.

A. Theory of operation of SGAI

Input voltage V_{in} is applied to the gate of M_1 which converts the voltage into a current that charges C_{gs2} . The voltage across C_{gs2} is then translated into current by M_1 that maintain I_2 as a constant [5]. Initially, $I_{d2}=I_2$. Increasing I_{in} causes voltage across C_{gs1} to increase. This increases I_{d1} and since I_1 is a constant current source, charges from C_{gs2} is extracted out to meet the increased current demand of M_1 . Reduction in gate voltage along with increase in source voltage of M_2 reduces I_{d2} . Now to hold KCL, the increase in input current is utilized by I_2 to remain constant. In this manner SGAI resist the changes in current thereby mimicking inductive behavior.

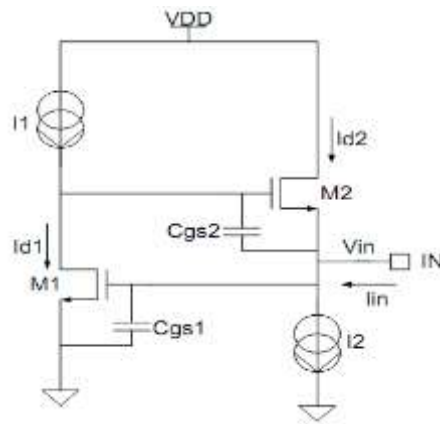


Fig1: Circuit Schematic of SGAI illustrating parasitic capacitances.

B. Figure of merits of inductors

Frequency range

A gyrator-C based active inductor exhibits inductive characteristics over a specific frequency range [8]. Lowest frequency bound is determined by the zero (ω_z) and upper bound by the pole (ω_o) of impedance transfer function. Gyrator-C network will be resistive when $\omega < \omega_z$, inductive when $\omega_z < \omega < \omega_o$ and capacitive when $\omega > \omega_o$. ω_o is also referred to as Self Resonating Frequency (SRF) [4] where the magnitude of impedance is at its peak.

Q factor

The Quality factor or Q factor is a performance indicator that indicates the energy losses within a resonant element. It is dimensionless frequency dependent parameter and can be defined as the ratio of inductive reactance to resistance.

Inductance Tunability

Inductance value can be tuned by varying the transconductance and biasing currents [11]. Since aspect ratio of inductor cannot be tuned once it is fabricated, it is done with biasing currents. So active inductors are beneficial in reconfigurable systems [1].

Chip Area

Active inductors being implemented with active devices, reduces the chip area to a greater extent when compared with their passive versions.

Linearity

Linearity defines the ability of active inductor to sustain a constant inductance and Q factor over a wide input power range [1]. Square law relationship followed by gate source voltage and drain current is the reason for nonlinearity in active inductors [11].

Noise

Active inductors exhibit a higher noise level compared to their passive counterparts [1]. The dominant contributors of noise are thermal noise in the transistor channel and flicker noise due to dangling bonds near the surface [12].

C. Design considerations in SGAI

When the transconductors used for the synthesis of AI has finite input and output impedance, there will be parasitic capacitive (parallel capacitance C_p) and resistive effects (parallel resistance R_p & series resistance R_s) which make the structure lossy. Fig2 below shows the equivalent structure of AI with parasitic effects. Applying KCL at nodes 1 and 2 gives

$$\text{Node1} \Rightarrow (sC_1 + G_{o1})V_1 - g_{m1}V_2 = 0 \quad (1)$$

$$\text{Node2} \Rightarrow -I_{in} + (sC_2 + G_{o2})V_2 - g_{m2}(-V_1) = 0 \quad (2)$$

Admittance looking into node 2 is given by

$$Y = \frac{I_{in}}{V_2} = sC_2 + G_{o2} + \frac{1}{s\left(\frac{C_1}{g_{m1}g_{m2}}\right) + \frac{G_{o1}}{g_{m1}g_{m2}}} \quad (3)$$

Above equation can be represented by an equivalent RLC network (Fig2) with following parameters.

$$R_p = \frac{1}{G_{o2}} \quad (4)$$

$$C_p = C_2 \quad (5)$$

$$R_s = \frac{G_{o1}}{g_{m1}g_{m2}} \quad (6)$$

$$L = \frac{C_1}{G_{m1}G_{m2}} \quad (7)$$

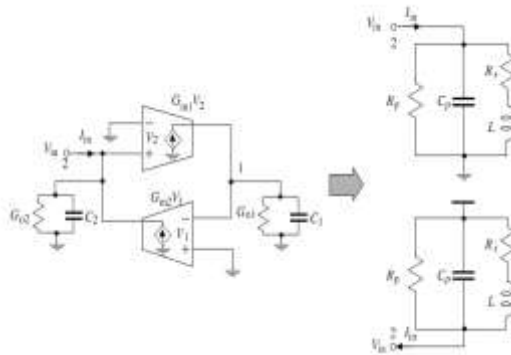


Fig2: Lossy single-ended gyrator-C active inductors. C_1 and G_{o1} , C_2 and G_{o2} denote the total capacitance and conductance at nodes 1 and 2, respectively.

Theoretical equations relating figure of merits and design parameters of active inductors are [7][9]:

$$L = \frac{cgs2}{(gm1gm2)} \quad (8)$$

$$Q = \sqrt{\frac{gm2cgs1}{gm1cgs2}} \quad (9)$$

$$Q = \frac{\text{im}\{Z\}}{\text{re}\{Z\}} \quad (10)$$

$$Q = \frac{\omega L}{R_s} \quad (11)$$

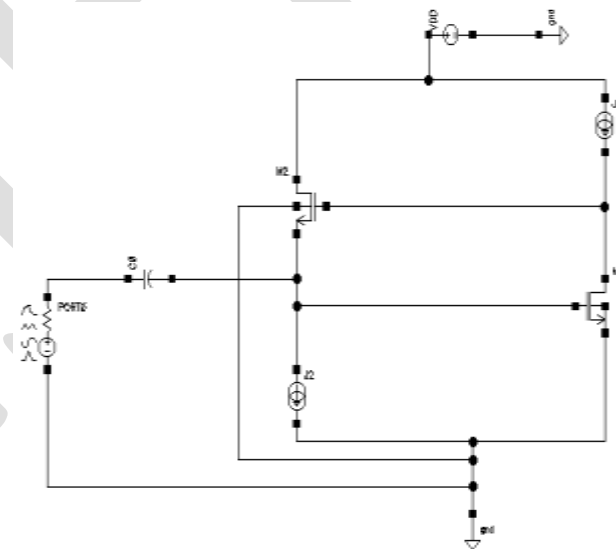
$$R_s = \frac{G_{o1}}{g_{m1}g_{m2}} \quad (12)$$

DESIGN METHODOLOGY

In this section, we discuss the design considerations and simulation results of SGAI. As many of the wireless communication techniques are operating in 2.4GHz, it is kept as the frequency of concern and L & Q factor are measured and optimized for 2.4GHz. For this frequency Q factor and inductance are measured by varying aspect ratios and biasing and dependency pattern in theoretical and practical cases are compared. For measuring SRF the design parameters are set meeting the following criteria.

TABLE I SGAI DESIGN REQUIREMENTS

Technology	180nm
V _{DD}	3.3V
Frequency	2.4GHz
Q factor	2-3
Inductance	2-3nH



.Fig3: Experimental setup of SGAI

A. Varying the aspect ratios

To understand the variations in Q factor and inductance with respect to aspect ratios, biasing currents J_1 and J_2 are arbitrarily fixed and aspect ratios of both transistors are varied in equal fashion.

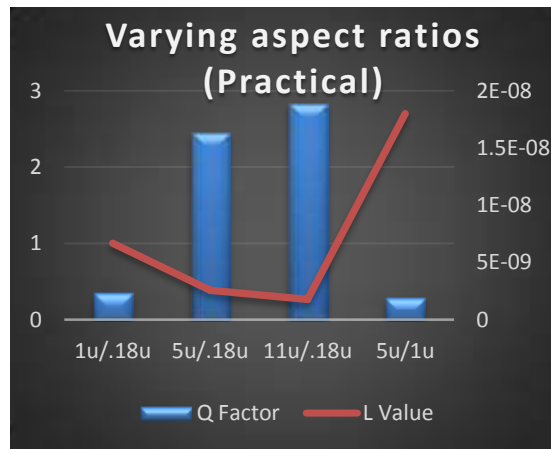


Fig4: Q factor & L for varying aspect ratios- practical case

From the above figure, it can be concluded that increasing the aspect ratios of transistors increases the Q factor and reduces the inductance. As width of M_1 & M_2 increases for a fixed length, g_{m1} and g_{m2} increases. Since L is inversely proportional to both g_{m1} and g_{m2} (eq.8), increasing width reduces L. Increase in g_{m1} and g_{m2} reduces effective series resistance R_s due to inverse proportionality (eq.12). Q factor which is inversely related to R_s thus increases for increasing width (eq.11). From the two graphs that have been plotted it is found that both L and Q factor follows the same pattern theoretically and practically. Variations in the values of theoretical and practical cases are due to the frequency of operation. Theoretical values are measured under its dc operating point and practical values are measured under the required operating conditions. So it can be concluded that both Q factor and L of the SGAI follows the basic relationships as defined in theory and practical values are used for verifying the design.

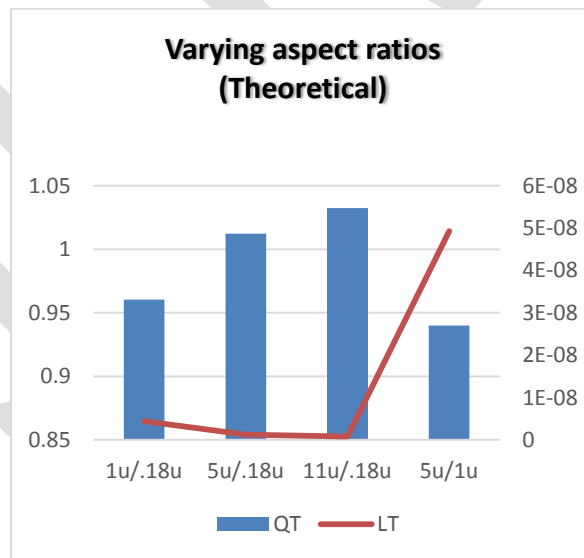


Fig5: Q factor & L for varying aspect ratios- theoretical case

B. Varying biasing currents

Increase in J_2 increase transconductance of M_1 thereby improving Q factor and reducing L. As J_1 is the bias for M_2 , increase in J_1 increases transconductance of M_2 and since there is no change in aspect ratio of the transistor, c_{gs2} remains almost constant. Also g_{m2} and c_{gs1} are almost constants. Thus increasing J_1 enhances Q factor and degrades L.

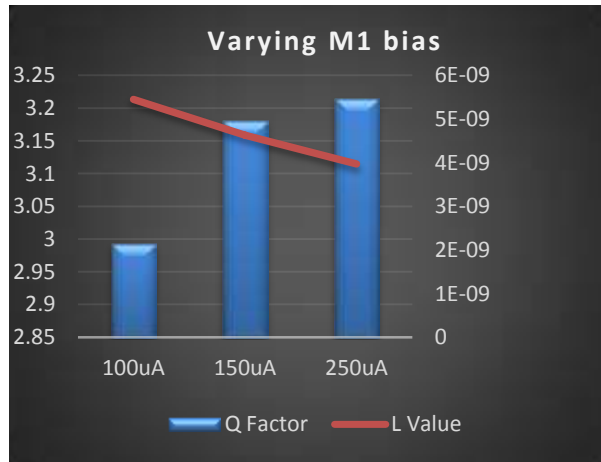


Fig6: Q factor & L for varying M_1 bias

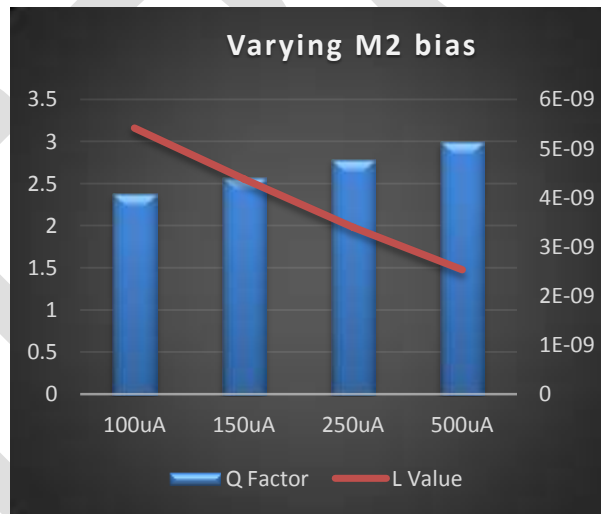


Fig7: Q factor & L for varying M_2 bias

C. Frequency range and power consumption

From the analysis carried out, parameters are fixed for obtaining an inductance of 2.5nH and Q factor in the range 2-3 for analyzing the frequency range and power consumption. . Between ω_z & ω_0 $\text{ph}\{Z\}$ is greater than 0° denoting an overall inductive nature. At SRF $\text{mag}\{Z\}$ is at its peak, $\text{ph}\{Z\}$ is zero (crossing from positive (inductive) to negative (capacitive)) and $\text{im}\{Z\}$ becomes zero thereby making Q factor to be zero. The circuit draws a current of 1.003mA from power supply thereby consuming a power of 3.3mW.

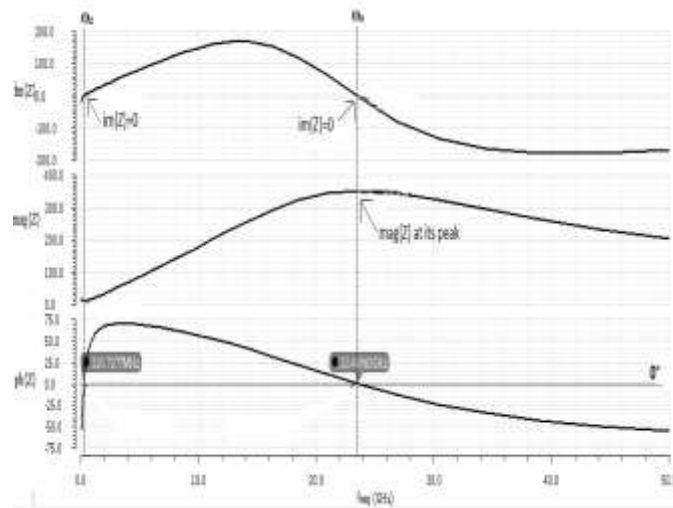


Fig8: Inductive frequency range of SGAI

TABLEII SGAI PERFORMANCE SUMMARY

Technology	180nm
V _{DD}	3.3V
Frequency	2.4GHz
Q factor	2.45
L	2.5nH
ω_z	310.73MHz
ω_o	23.47GHz
Power	3.3mW

CONCLUSION

Through transistor level simulation, we have verified relationship between the design parameters and figure of merits of a basic active inductor topology named Simple Grounded Active Inductor both theoretically and practically. The structure is then optimized for an inductance of 2.5nH and Q factor of 2.45 for analyzing its inductive frequency range and power consumption. The analysis has shown a SRF of 23.47GHz which is around ten times the required frequency of operation.

REFERENCES:

- [1] [Robert F.](#), [Cathelin P.](#), [Diet A.](#), [Villegas M.](#), “A highly linear and tunable feed forward current source active inductor in 65nm CMOS technology for mobile applications” in *Wireless and Microwave Technology Conference, 2011.*
- [2] Chun-Lee Ler, Abu Khari Bin Aain, and Albert Victor Kordesch, “CMOS Active Inductor Linearity Improvement Using Feed-Forward Current Source Technique” in *IEEE Transactions on Microwave Theory and Techniques*, August 2009.
- [3] Murli U Nair, Yuanjin Zheng, Yong Lian, “An Active Inductor based Low-Power UWB LNA” in *IEEE International Conference*, September 2007.
- [4] [Zito D.](#), [Pepe D.](#), [Fonte A.](#), “High Frequency CMOS Active Inductor Design Methodology and Noise Analysis” in *IEEE Transactions on Very large Scale Integration Systems*, July 2014.
- [5] U Yodprasit and J Ngarmnil, “Q-Enhancing Technique for RF CMOS Active Inductor” in *IEEE International Symposium on Circuits and Systems*, May 2000.
- [6] William Bucossi and James P Becker, “Practical Considerations In The Use of CMOS Active Inductors” in *IEEE Topical Meeting on Silicon Monolithic Integrated circuits in RF Systems*, 2008.
- [7] Gao Zhiqiang, Xu Honglin, Zhang Zhongzhao, Lan Jinbao, “Design Consideration of Multi-band RF CMOS Filter Based on Active Inductors” in *IEEE Journal of Solid-State Circuits*, 2010.
- [8] Guochi Huang, Byung-Sung Kim, “Programmable Active Inductor Based Quadrature VCO Design” in *Proceedings of Asia-Pacific Microwave Conference 2007*
- [9] Hsieh-Hung Hsieh, Yu-Te Liao, Liang-Hung Lu, “A Compact Quadrature Hybrid MMIC Using CMOS Active Inductors” In *IEEE Transactions on Microwave Theory and Techniques*, vol. 55, NO. 6, June 2007
- [10] Sang-Ki Eun , Choon Sik Cho, Jae W. Lee, Jaeheung Kim, “A Low Power VCO Using Active Inductor For Low Phase Noise and Wide Tuning Range” in *Proceedings of the 39th European Microwave Conference*
- [11] Vincenzo Stornelli, Giorgio Leuzzi, Leonardo Pantoli, Stefano Del Re, “High Dynamic Range Bandpass Filters Design Based on Active Inductor” in *Proceedings of the 6th European Microwave Integrated Circuits Conference*
- [12] Mohsen Moezzi, M. Sharif Bakhtiar, “Wideband LNA Using Active Inductor With Multiple Feed-Forward Noise Reduction Paths” in *IEEE Transactions on Microwave Theory and Techniques*, vol. 60, NO. 4, April 2012

Causes of Variation Orders on Public Building Projects in Addis Ababa

Andualem Endris Yadeta¹

¹*School of Civil and Environmental Engineering, Addis Ababa Institute of Technology, Addis Ababa University, Addis Ababa, Ethiopia.*

P.O Box: 57381, Addis Ababa, Ethiopia

andu0117@yahoo.com

Abstract: Variation is inevitable in construction projects due to the complex nature of the construction industry. It is common in all types of construction projects and it determines the time limits and anticipated budget of the projects. Variation order is observed as one of the most frequently occurring issues in construction projects in Ethiopia. Like other regions of the country, construction projects in Addis Ababa are exposed to variation orders. These variations are known to impact various aspects of the projects. The study investigates the various causes of variation orders on public building projects in Addis Ababa. To achieve the study objectives, through a comprehensive study of literatures review 38 common causes of variation orders were identified. A desk study, interview and questionnaire survey were carried out to identify the causes of variation orders. The desk study conducted on five selected public building projects and the causes of variation orders were identified. Interviews were made with selected experienced public building project participants for expert opinion. The questionnaire responses were analyzed using the relative index method. A triangulation method on the desk study, survey and the literatures was done to improve the validity of the findings from the study. The results indicated that design changes, incomplete contract documents, impediment in prompt decision making process, inadequate working drawing details, and change in specifications were the main causes of variation orders on public building projects. The study concluded based on the findings of the research and recommendations were forwarded to minimize the occurrence of variation on public building projects in Addis Ababa.

Key words: Variation order, cause, public projects, Addis Ababa

1. INTRODUCTION

The construction industry in Ethiopia has been on fast growing mode which plays an instrumental role in the country development. Addis Ababa in the last ten years experienced a huge volume of work in the field of constructions. Large and complex government buildings have been built, attracting domestic contractors and construction companies from all over the world. This situation coupled with inexperienced consultants and the client has led to inadequate design resulting in many changes to plans, specifications, and contract terms which resulted in variation orders. Variations and conflicts in construction projects, at work, and even in our daily lives are very common (Arain and Pheng, 2006). Variation orders have an impact on overall project performance (Ruben, 2008). This is because variations can cause substantial adjustment to the contract duration, total direct and indirect cost, or both. In most cities of the country like Addis Ababa where new infrastructure and buildings are being built, the occurrence of variation orders on public projects seems usual. Due to general background of the problem in the construction industry and the specific problem within the public buildings, there is a cause for a study to investigate the impact of variation orders on public building projects in Addis Ababa.

2. LITERATURE REVIEW

There is no single definition of what constitutes a variation. The term 'variation' as described and/or defined by various standard forms of contract differs from one to another but in principle the definition and/or meaning is more or less similar. Usually, any standard form of building contract will contain a definition of a variation in terms of specific actions and activities. The building contract dictionary defined variations as alterations, additions or omissions in work, materials, working hours, work space, etc. As defined in PPA (2006) conditions of contract, "variation" is an instruction given by the engineer, which varies the works. According to FIDIC (1999) conditions of contract, "variation" means any change to the works, which is instructed or approved as a variation. Various authors had identified different causes of variation orders in construction projects both on the private and public projects. Contractual clauses relating to variation allows parties involved in the contract to freely initiate variation orders within the ambit of the scope of the work without alteration of the original contract (Ruben, 2008). But variation orders are common in construction projects, and improved understanding would require identifying their causes. The works of many researchers show that that variation has come to stay as part of the construction projects and it cut across various stakeholders. According to Sunday (2010), the main causes of variation orders on construction projects are inadequate working drawing details, design discrepancies, conflicts between contract documents, the change of plans or scope by owner, impediment in prompt decision making process, inadequate project objectives, and replacement of materials or procedures, differing site conditions, shortage of skilled manpower, contractor's desired profitability and contractor's financial difficulties. As Mohammad *et al.* (2010) identified, change of plan by the owner, substitution of materials by the owner, change in design by the consultant, errors and omissions in design, and owner's financial problems are the main causes of variation orders. Ming *et al.* (2004) noted that at a more detailed level, the causes of construction project variation are usually

generated from either design or construction activities. The design generated causes include design changes, design errors, omissions and operational improvements. Construction driven causes are often linked to the unsatisfactory site conditions that hinder good workmanship, material handling and plant operation. Ssegawa *et al.* (2002) investigated the opinion of project parties regarding the frequency of occurrence, causes, and originators of variation orders. The study found that additions and omissions are the most common cause of variations in projects, which represented about 45.7% of all variation orders in building projects. As Ruben (2008) found out, the most frequent causes of variation orders were change of schedule, specifications and design and errors in design and inadequate working drawing details. Lots of studies are conducted to identify the causes of variation orders (Mohammad *et al.*, 2010; Arain and Pheng, 2006; Sunday, 2010; Ssegawa *et al.* (2002); Ruben, 2008; Thomas and Napolitan, 1994; Fisk, 1997). The main causes of variation orders from the literatures are:

- Change of plans or scope
- Change of schedule
- Change in specifications
- Change in design
- Errors and omissions in design
- Inadequate working drawing details
- Non-compliant design with government regulations
- Impediment in prompt decision making process
- Unforeseen problems
- Replacement of materials or procedures
- Inadequate shop drawing details
- Lack of judgment and experience
- Financial problems
- Inadequate scope of work for one or more parties to the contract
- Design complexity
- Lack of communication
- Defective workmanship
- Design discrepancies
- Inadequate project objectives
- Long lead procurement
- Lack of coordination
- Fast track construction
- Ambiguous design details
- Unavailability of skills
- Weather conditions
- Lack of strategic planning
- Lack of knowledge of available materials and equipment
- Lack of involvement in design of one or more parties to the contract
- Non-compliant design with owner's requirement
- Health and safety considerations
- Lack of a specialized construction management
- Obstinate nature of one or more of the parties to the contract
- Differing site conditions
- Poor procurement process
- Conflicts between contract documents
- Value engineering
- Change in economic conditions
- Honest wrong beliefs of one or more parties to the contract
- Lack of required data
- Unavailability of equipment
- Unfamiliarity with or unawareness of local conditions
- Socio-cultural factors
- Change in government regulations
- Speculation on desired profitability
- Technology change

3. Research Methodology

Due to the nature of data to be collected from the relevant parties for the study, a purposive sampling method was adopted to select the population for the study. A combination of qualitative and quantitative approaches was used in the study. A desk study, interview and questionnaire survey were carried out to identify the causes of variation orders on public building projects. A triangulation method on the desk study, survey and the literatures was done to improve the validity of the findings from the study. The desk study conducted on five selected public building projects and the causes of variation orders were identified. Interviews were made with selected experienced public building project participants for expert opinion. The questionnaire responses were analyzed using the relative index method. Qualitatively, the study focused to obtain the perceptions of public building construction stakeholders relative to the causes of variation orders. The variables that identified from the literatures were quantitatively measured to determine the most frequent causes of variation orders on public building projects.

The questionnaire was designed to gather data from professionals that were involved in public building projects in Addis Ababa. The respondents were asked to rate the questions on Likert's scale of five ordinal measures as shown in **Figure 3.1** below.

The ranking of the responses was by using Likert's scale of five ordinal measures which arranged in ascending order from 1 to 5. It included a total of 38 required responses.

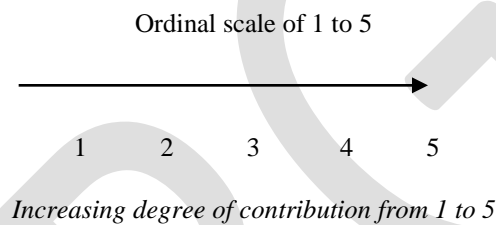


Figure 3.1: Five ordinal measures by Likert Scale

The main approach used to analyze the data was by using the Relative Index (RI) technique. The responses were analyzed using the Microsoft Excel software package. The analysis included ranking the factors in terms of degree of effecting. In the computation of the relative index the following formula was used;

$$RI = \frac{(5n_5 + 4n_4 + 3n_3 + 2n_2 + n_1)}{5(n_5 + n_4 + n_3 + n_2 + n_1)}$$

Where:

RI: Relative Index

*n*₅, *n*₄, *n*₃, ... : number of responding indices.

The Spearman (rho) rank correlation coefficient is used for measuring the differences in ranking between two groups of respondents scoring for various factors (i.e. clients versus consultants, clients versus contractors, and consultants versus contractors). The Spearman (rho) rank correlation coefficient for any two groups of ranking is given by the following formula:

$$Rho (\rho_{cal}) = \frac{1 - 6 \times (\sum d_i^2)}{N \times (N^2 - 1)}$$

Where:

- $Rho (\rho_{cal})$: Spearman's rank correlation coefficient;
- d_i : the difference in ranking between each pair of factors; and
- N : number of factors (variables).

The value of the Spearman (rho) rank correlation coefficient varies between -1 and +1. A correlation coefficient of +1 implies perfect positive correlation, 0 implies no correlation and -1 implies perfect negative correlation.

4. Result Analysis and Discussion

This part of the paper analyses the data collected using questionnaires, desk study and interviews. The collected data from the questionnaires were tabulated and analyzed according to their ranking on Relative Index (RI). Interviews from selected respondents are presented, together with observations from desk study. The objective of this chapter is to identify the highest ranked factors for discussion and to find correlation with findings from the interviews and desk study.

Result Analysis

Desk Study Result

During the study period, there were a total of thirty-eight (38) public building projects which were under execution in Addis Ababa and twenty-eight (28) project samples are taken for the study. From this number five (5) completed projects in which variation orders (VO) approved were selected for desk study in order to fully understand the causes and impacts of variation orders and to determine what recommendations or strategies could be taken to minimize variation orders on public building projects. These projects were 100% completed and selected as a representative to the occurrences of variation orders of each of the public building projects. The list of selected projects is as shown in **Table 4.1**.

Table 4.1: List of selected public building projects

Project Code	Project Name	Contract Amount (Birr)	V.O (Birr)	Percent of V.O (%)
Project A	Sport Commission	51,931,227.89	8,284,485.09	15.95
Project B	Education Bureau	60,343,438.45	4,091,699.06	6.78
Project C	Police Commission	99,444,398.79	8,152,255.70	8.20
Project D	Credit & Savings Institution	36,914,578.87	7,234,368.3	19.60
Project E	Fire and Emergency Service	58,076,253.18	5,150,610.80	8.87

(Source: Addis Ababa Housing Development & Construction Bureau (2012))

The desk study findings showed fourteen (14) causes of variation orders. Due to the repetition, it was further syntheses to eight (8) from the most to the least repetitive causes of variation orders to be used in questionnaire for the verification and validation process to evaluate their degree of important. But all the eight causes were already the domain of the variables which identified from the literatures review. Below is the document study finding of summary of causes of variation orders from the five projects contract documents:

- Design changes
- Incomplete contract documents
- Incomplete working drawings
- Errors in design by the consultant
- Design modification
- Non-compliant design with owner's requirement
- Lack of communication between the parties
- Lack of decision making process by the client

Interview Result

These interviews were made between selected construction industry practitioners who are currently involved in public building projects focusing on their perceptions on variations orders. In total three interviews were conducted, namely with a senior project supervision and follow up team leader (A) from the clients' group, a senior contract administrator (B) from the consultants', and a senior project manager (C) from the contractors' group. The interview aimed at discovering the causes of variation orders on public building projects. From the interview, sixteen (16) causes of variation orders were found. These variables were merged and checked if they were out of the literatures in order to include them in the questionnaire. But more of them with the same meaning were the domain of the variables identified from the literatures. The findings from the interview revealed that incomplete contract document, design changes, change in specifications, errors in design, unforeseen conditions, design complexity, lack of communication and coordination between the parties, lack of experience and of judgment were the causes which contribute to the occurrence of variation orders.

Questionnaire Survey Result

The respondents were grouped into three major groups namely client, consultant and contractor. The returns from the three groups are tabulated in **Table 4.2** below which shows an average response rate. Out of 45 targeted responses, only 32 (71%) of them completed and returned the questionnaire. Thirty one questionnaires from 9 clients, 4 consultants and 19 contractors were received.

Table 4.2: Questionnaire return rate

Group	Number of Questionnaires distributed	Number of Questionnaires Returned	Response Rate (%)
Client	12	9	75
Consultant	5	4	80
Contractor	28	19	68
Total	45	32	71

Among the nine responses received from clients, seven (78%) of them were construction supervisors and follow-up engineers while two (22%) were contract administrators.

Among the four responses received from consultants, three (75%) of them were resident engineers and one (25%) was contract administrator. And among the nineteen responses received from contractors, eight (42%) of them were project managers, eight (42%) of them were office engineers, three (16%) were quantity surveyors. **Figure 4.1** below shows the composition of respondents by their position in their organization.

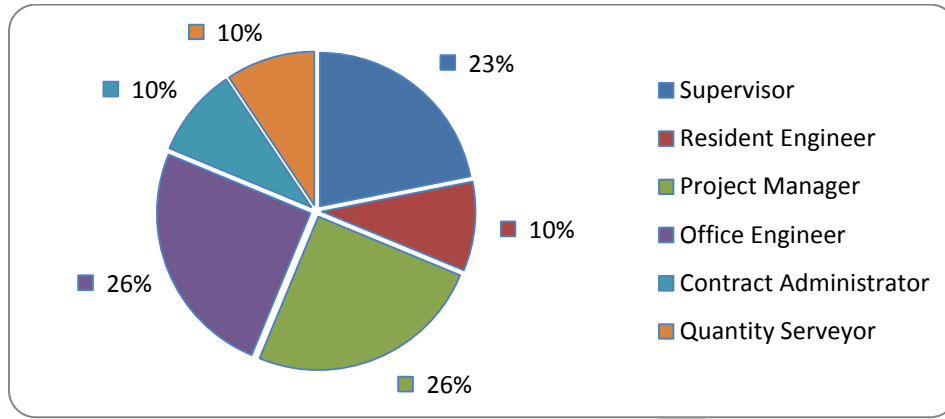


Figure 4.1: Position of respondents

All the respondents have different levels of work experience in building projects. It was observed that the majority of the respondents from the clients have between five to ten years of experience. Majority of the respondents from the consultants have also between five to ten years of experience. And about one half of the respondents from the contractors have less than five years of experience.

From the forty five (45) causes of variation identified from the literatures, only thirty-eight (38) mutually exclusive causes of variation orders on building projects were used in questionnaire survey. A ranking system using the Relative Index (RI) method was calculated to find the most significant factor for each section. The value of RI ranges from 0.2 to 1. The value 0.2 represents the lowest strength and the value 1 representing the maximum strength. A correlation test is also done between different groups of respondents.

Table 4.3: Summary of correlation test on the ranking of causes of variation orders

Respondents	$Rho(r_{cal}) = 1 - \frac{6x(\sum d_i^2)}{N x (N^2 - 1)}$	Relation of the respondents
Client Vs Consultant	0.999	strong
Consultant Vs Contractor	1.000	strong
Client Vs Contractor	1.000	strong

From the correlation table above, it can be concluded that there is a strong correlation between the attitudes of the respondents in all the three groups. This means that most of the respondents have the same perception about the causes of variation orders.

From the questionnaires survey result, it was possible to rank the causes of variation orders combining the responses of all respondents as shown in **Table: 4.4** below. The most raked causes of variation orders by all respondents were impediment in prompt decision making process, change in design by the consultant, and inadequate working drawing details dominate with the same value (RI=0.669). Change in specifications and poor procurement process came next with equal value (RI=0.663). Errors and omissions in design, lack of communication and unforeseen problems followed with the same value (RI=0.656) and then design discrepancies and contractor's desired profitability (RI=0.650). Change in government regulations (RI=0.456) and health and safety considerations (RI=0.425) were the least ranked causes of variation orders.

Table 4.4: Frequency of causes of variation orders

Causes of Variation Orders	Overall RI	Ranking
Impediment in prompt decision making process	0.669	1
Change in design by the consultant	0.669	2
Inadequate working drawing details	0.669	3
Change in specifications	0.663	4
Poor procurement process	0.663	5
Errors and omissions in design	0.656	6
Lack of communication	0.656	7
Unforeseen problems	0.656	8
Design discrepancies	0.650	9
Contractor's desired profitability	0.650	10
Lack of contractor's involvement in design	0.644	11
Change of plans or scope	0.638	12
Change of schedule	0.631	13
Lack of strategic planning	0.631	14
Contractor's lack of required data	0.613	15
Consultant's lack of judgment and experience	0.606	16
Conflicts between contract documents	0.600	17
Lack of consultant's knowledge of available materials	0.600	18
Consultant's lack of required data	0.594	19
Lack of coordination	0.588	20
Lack of a specialized construction manager	0.588	21
Differing site conditions	0.581	22
Unfamiliarity with local conditions	0.581	23
Non-compliant design with owner's requirement	0.575	24
Unavailability of skills	0.569	25

Defective workmanship	0.569	26
Change in economic conditions	0.569	27
Design complexity	0.563	28
Honest wrong beliefs of contractor	0.563	29
Technology change	0.519	30
Non-compliant design with government regulations	0.513	31
Weather conditions	0.506	32
Inadequate project objectives	0.494	33
Honest wrong beliefs of consultant	0.469	34
Fast track construction	0.469	35
Socio-cultural factors	0.469	36
Change in government regulations	0.456	37
Health and safety considerations	0.425	38

Discussion

From the questionnaires, the desk study and interview, the common causes of variation orders on public building projects were design changes and incomplete contract documents, which resulted from numerous additional works.

The first major cause of variation orders was change in design by the consultant. This could also be caused due to the client change of mind. Design change is indeed one of the most causes of variation orders and this fact is supported by the interviewees and the observations in the desk study. This similarly confirms with the literature review that design change was one of the major causes of variation orders. Incomplete contract document was the second major cause of variation orders. This occurs due to the client or the consultant work before tendering and it increases the project cost or schedule. Contract documents of most public projects done by the clients and it could be difficult to prepare a complete document because they are busy of work. The third major cause of variation order was impediment in prompt decision making process, which is due to lack of judgment by the client or the consultant. There is no doubt that lack of decisions delay the project and causes the contractors to re-design the requirements, reschedule their works and material procurement which would have an adverse impact on the project. Inadequate working drawing details was the fourth major cause of variation order which is the out-come of the consultant. A well detailed working drawing is believed to decrease variation orders. Most professionals argue that a detailed working drawing should be prepared before the tender stage.

The fifth major cause of variation order was change in specifications which confirms with the literature review and the interview. In a design stage, it could be a failure to change the specification due to change of mind of the client or the consultant which results in variation orders. Consequently change in specifications can be the major cause.

5. CONCLUSION AND RECOMMENDATIONS

The desk study of the five projects confirmed that the most frequent causes of variation orders on public building projects was design changes. According to the interview made between three selected construction practitioners involved in public building projects they pointed out that the main cause of variation orders was design changes. From the questionnaire responses, it was concluded that impediment in prompt decision making process, change in design by the consultant, inadequate working drawing details, change in specifications, and poor procurement process were the most important causes of variation orders on public building

projects. From the findings of the desk study, interview and questionnaire, change in design, incomplete contract documents, impediment in prompt decision making process, inadequate working drawing details, and change in specifications were the major causes of variation orders on public building projects in Addis Ababa.

The recommendations of this study are as follows:

- The client should allow sufficient time to prepare an elaborately detailed project brief.
- Variations can be minimized if consultants produce a complete design.
- Direct communication among the project team is a key to minimize variations due to communication gap during design and execution phase.
- Consultants should give sufficient time for planning and design phase, this will assist in minimizing variation orders due design changes at construction stage.
- A detailed design would be able to exert control to unnecessary interference from consultants or other external influences.
- The consultants should prepare completed contract document before the tendering stage.
- Contractors should identify and inform the varied item of work to the client before the activity starts to reduce variations. Because the client will have sufficient time to check the varied item in different perspectives to give work order at minimum variations.
- There should be improvement in decision making process on the part of the client during project execution stage.
- The results of this research should help construction practitioners, policy makers and researchers in the field of construction management.

REFERENCES:

- [1] Al-Hammad, M. and Assaf, S.A. (1992) Design-Construction interface problems in Saudi Arabia, *Journal of Building Research and Information*, vol.20, no.1, pp. 60-63.
- [2] Arain, F.M. & Pheng, L.S. 2006, 'Developers' views of potential causes of variation orders for institutional buildings in Singapore', *Architectural Science Review*, vol. 49, no. 1, pp 59-74
- [3] FIDIC (1999) General Conditions of Contract for Construction
- [4] Fisk, E.R. (1997), *Construction Project Administration*, 5th ed., Prentice-Hall, Upper Saddle River, NJ.
- [5] Ming, S., Martin, S., & Chimay, A. 2004, 'Managing Changes in Construction Projects', Industrial Report, University of the West of England, Bristol, pp 7-10
- [6] Mohammad, N., Che Ani, A., Rakmat, R., & Yusof, M. 2010, 'Investigation on the Causes of Variation Orders in the Construction of Building Project- A Study in the State of Selangor, Malaysia', *Journal of Building Performance*, Kebangsan University, Selangor Malaysia
- [7] PPA (2006) General Conditions of Contract for Procurement of Works
- [8] Ruben, N. 2008, "An analysis of the impact of variation orders on project performance", Cape Peninsula University of Technology, *Theses & Dissertations*, Paper 33
- [9] Ruben, N. and Haupt, C. 2008, 'Uncovering the origins of variation orders', *Proceedings of the 5th Post Graduate Conference on Construction Industry Development*, Bloemfontein, South Africa, 88-96
- [10] Ssegawa, K., Mfolwe, M., Makuke, B. & Kutua, B. 2002, 'Construction Variations: A Scourge or a Necessity?', *Conference Proceedings*, Cape Town, South Africa, pp 87-96
- [11] Sunday, O. 2010, 'Impact of Variation Orders on Public Construction Projects', *Conference Proceedings*, Leeds, UK, 101-110
- [12] Thomas, R. and Napolitan, L. 1995, 'Quantitative effects of construction changes on labor productivity', *Journal of Construction Engineering and Management*, vol. 121, no.3, pp 292-294

Flux-Limiter Schemes for the Convective Acceleration

Laila Mouakkir , Mohamed Loukili , Soumia Mordane
Polymer Physics and Critical Phenomena Laboratory, Sciences Faculty
Ben M'sik, P.O Box 7955, university Hassan II, Casablanca Morocco

Abstract- A 3D numerical model MECCA (Model of Estuarine and Coastal Circulation Assessment) to simulate coastal flow coupled with some physical processes (sediment transport) is available at our laboratory. This model uses the finites differences method to discretize a set of the governing equations (3D shallow water equations). The Upwind scheme was chosen to approximate the advective terms. This scheme is characterised by a large numerical diffusion especially in the vicinity of discontinuities regions. To eliminate this unrealistic effect, in this paper we introduce some limiters schemes initially used for gas dynamics such : Minmod, Superbee, MC and Van Leer. Our prupose is the use this kind of schemes to aproximate the all advective terms (hydrodynamic and scalar transport equation (S.T.E)). Throught the numerical tests, in this study we conclude that for the coupled model and in order to reduce the numerical diffusion, it's necessary to use the limiters schemes for all terms advective. However, for the Saint-Venant equations with a regular initial and boundaries condition, it's suggested also to use the limiters schemes at most to give the true physical effect (turbulence effect) of the viscosity coefficient, because generally this physical coefficient became a calibration parameter in the ocean modelling.

Keywords--- Flux-limiter, numerical diffusion, High resolution schemes, Total variation diminishing Schemes.

1. Introduction

This study investigates several flux-limiter schemes, that have been chosen because they satisfy many of the requirements of a good advection scheme, they are Total Variation Diminishing (TVD), mass conservative and less diffusive than the simpler schemes. It is well known that the scalar transport is the combination of different physical processes: (i) advection, by the statistical mean of velocity in which all scalar quantities are transported in the direction of the flow without deforming their initial distribution, (ii) diffusion, due to turbulent velocity fluctuation where scalar shape may be smoothed. The numerical approximation of the advective process in the oceanographic and meteorological modelling requires important choices and compromises to be made when flow simulations are carried out. One example of these compromises is the numerical treatment of the advective terms in the transport equation. These compromises are necessary, to minimize both artificial numerical diffusion and dispersion. The resulting numerical diffusion may severely damp the flow, producing exaggerated inaccurate results, whereas the artificial numerical dispersion may introduce non-physical oscillations called wiggles.

Traditionally the large scale oceanography and meteorology models use the upwind and central difference scheme to solve the advective terms present in the flow equation and passive scalar equations, for example the Princeton Ocean Model (POM) [1] and the Model of Estuarine and Coastal Circulation Assessment (MECCA) [2]. However, these schemes give rise to numerical instability or exaggerated numerical diffusion.

This present work relates to an improvement of the space discretization of the three-dimensional equations of model MECCA [3], [4], this model use the Upwind scheme to approximate the advective terms, This scheme is characterized by a large numerical diffusion especially in the vicinity of discontinuities regions. To eliminate this unrealistic effect, in this paper we introduce some limiters schemes initially used for gas dynamics such: Minmod, Superbee, MC and Van Leer. Smaoui and al. [5], [6] have implemented the limiters schemes patterns to identify fresh water /salt water generated by the flow in Somme estuary in the Eastern Channel (Northern of France) . In this paper and to the difference of previous work [5], [6], we implement the flux-limiters schemes to approach the convective terms of the equations of momentum and transport scalar. The question which thus arises and which justifies this work is the following: "With the fluxl imiters schemes in the equations of the momentum, what one limits of advantage the numerical diffusion attached to the numerical solution of the equation of concentration ?" To answer to this question, we carried out two numerical tests covering some applications in geophysics flows. These tests have been devoted to solve numerically the equation of Burger coupled with the scalar transport equation. Let us note that we chose the equation of Burger to represent the hydrodynamics, because under certain initial conditions and in extreme cases, this equation offers an exact solution. Consequently, we will be able to quantify the errors due to the numerical approximations. This work is organized in the following way : The second section briefly describes model MECCA. To illustrate the principle of operation of the flux-limiter methods, we present in the third section the discretization of a convective equation 1D by this kind of method. The fourth and the fifth section will relate to the results and simulation undertaken in this work. Finally, we finish by a conclusion in which we summarize the whole of the got results.

2. Brief description of the MECCA model

The MECCA model (Model of Estuarine and Coastal Circulation Assessment), initially developed by Hess [2], uses finite-difference approximations to solve the discretized 3D equations governing conservation of momentum, mass, heat and salt on a beta plane, subject to the hydrostatic and Boussinesq approximations. It is able to simulate time-varying water currents, salinities and temperatures in shallow-water domains at time scales ranging from a few minutes to several months, and space scales stretching from a few kilometres to a few hundred kilometres. The mode is designed to simulate circulation driven by tides, wind, water density

gradients as well as atmospheric pressure gradients. The MECCA model was applied successfully to simulate a tidal flow and the sediment transport at English Channel [4], Chesapeake Bay [2], and the Mediterranean Sea [3].

3. Transport equations and their discretization

Let us start by solving the transport equation that describes the purely advective concentration C in a flow field. This equation is described by:

$$\frac{\partial C}{\partial t} + \nabla \cdot (\vec{V}C) = 0 \quad (1)$$

where \vec{V} is the velocity vector. For simplicity we illustrate the methods under study by considering the one dimensional scalar advection equation:

$$\frac{\partial C}{\partial t} + \frac{\partial uC}{\partial x} = 0 \quad (2)$$

The flux of the concentration C is denoted by F , the regular grid spacing by Δx , and the time step by Δt . Hence discretization of Eq. (2) is obtained in the flux form on a staggered grid by integration over the finite volume $\Omega_i = [x_{i-1/2}, x_{i+1/2}]$ and can be expressed explicitly in time as:

$$C_i^{n+1} = C_i^n - \frac{\Delta t}{\Delta x} \left[(uC)_{i+1/2}^n - (uC)_{i-1/2}^n \right] \quad (3)$$

Where n is the time level $t_n = n\Delta t$, $C_i = C(x_i, t_n)$ and $F_{i+1/2}^n, F_{i-1/2}^n$ are the C fluxes (called also numerical fluxes) through the right and left boundaries of the grid cell respectively. The accuracy of finite volume discretization is mainly related to the computation of the cell-face fluxes. Many methods have been proposed [7-8] for example, the piecewise polynomial interpolation suggested by van Leer [9]. The basic idea of this so-called k -interpolation is that linear and quadratic approximations of the solution on each cell lead respectively to second and third order space discretizations [10]. The second order schemes have been successful in eliminating the numerical diffusion, but they give rise to non-physical oscillations near regions of large gradients. In the next section we shall present a method to obtain higher order schemes without oscillations.

3.1. Flux-limiter methods

The most straightforward approximation to $C_{i+1/2}^n$ is certainly $C_{i+1/2}^n = 0.5(C_{i+1} + C_i)$. This expression gives an approximation of the partial derivative $\frac{\partial uC}{\partial t}$ by central differences. Unfortunately, this method leads to the appearance of spurious oscillations in the numerical solution. A free-oscillations solution is provided, by the use of the upstream approach (also called upwind scheme),

$$\left(F_{i+1/2}^n \right)_{Up} = \begin{cases} u_{i+1/2}^n C_i^n & \text{if } u_{i+1/2}^n \geq 0, \\ u_{i+1/2}^n C_{i+1}^n & \text{if } u_{i+1/2}^n < 0 \end{cases} \quad (4)$$

which can be written by a single formula :

$$\left(F_{i+1/2}^n \right)_{Up} = \frac{1}{2} \left[\left(u_{i+1/2}^n + |u_{i+1/2}^n| \right) C_i^n + \left(u_{i+1/2}^n - |u_{i+1/2}^n| \right) C_{i+1}^n \right] \quad (5)$$

This amounts to replacing $\left(\frac{\partial uC}{\partial t} \right)$ by the so called upwind differences, which avoids non-physical oscillations, but is unfortunately affected by excessive numerical diffusion. One strategy to avoid non-physical oscillations and excessive numerical diffusion is the hybrid method which uses the second order numerical flux in smooth regions and limits the solution in vicinity of discontinuities by

using the monotonic upwind method in these regions. This procedure is carried out by introducing a slope-limiter (also called flux-limiter) based on the local gradient of the solution (4). We write the interface value $C_{i+1/2}^n$ as the sum of the diffusive first order upwind term and an "anti-diffusive" one. The higher order anti-diffusive part is multiplied by the flux limiter, which depends locally on the nature of the solution by means of the non-linear function $\theta_{i+1/2}$. This function is expressed by the slopes ratio at the neighborhood of the interfaces in the upwind direction (4).

$$\theta_{i+1/2} = \begin{cases} \frac{C_i^n - C_{i-1}^n}{C_{i+1}^n - C_i^n} = \theta_{i+1/2}^+ & \text{if } u_{i+1/2}^n \geq 0, \\ \frac{C_{i+2}^n - C_{i+1}^n}{C_{i+1}^n - C_i^n} = \theta_{i+1/2}^- & \text{if } u_{i+1/2}^n < 0 \end{cases} \quad (6)$$

Introduction of this new parameter namely (θ) and the limiter function ϕ , leads to the flux limiter version of the hybrid scheme as :

$$C_{i+1/2}^n = \begin{cases} C_i^n + \frac{1}{2}(C_{i+1}^n - C_i^n)\phi(\theta_{i+1/2}^+) & \text{si } u_{i+1/2}^n \geq 0 \\ C_{i+1}^n - \frac{1}{2}(C_{i+1}^n - C_i^n)\phi(\theta_{i+1/2}^-) & \text{sinon} \end{cases} \quad (7)$$

The interface value $C_{i-1/2}^n$ is obtained from $C_{i+1/2}^n$ by substituting the indice i by $i-1$. Note that expression (6) is the inverse of the definition used in [12], but the same expression can be obtained if the limiter function ϕ is symmetric, i.e.

$$\phi(\theta) = \theta\phi\left(\frac{1}{\theta}\right) \quad (8)$$

From Eq. (7), one can see that if $\phi = 0$ once again we find the upwind scheme, and if $\phi = 1$ the scheme is reduced to the centred one. The limiting procedure must be carried out under some constraints to ensure stability of the scheme. A well-known criterion, as proposed by Gastell and Lau [11], is the so-called convection boundless criterion (CBC). In this paper, the flux-limiter must be built to satisfy the total variation diminishing (TVD) concept due to [12], following [13].

3.2. Total variation diminishing concepts

The theory of the TVD concept and slope limiter was introduced by Harten [12], as the criterion to combine accuracy and monotonicity properties of the higher order schemes used to solve the scalar conservation equation. With this concept, during the time evolution no new under- or overshoots could be created. We recall the main results from this concept. The total variation of the discrete solution is defined as:

$$TV(C^n) = \sum_{i=-\infty}^{i=+\infty} |C_i^n - C_{i-1}^n| \quad (9)$$

A scheme is said to satisfy the TVD constraints if

$$TV(C^{n+1}) \leq TV(C^n) \quad (10)$$

For our purposes, we assume that the scheme Eq. (3) can be written in an incremental form:

$$C_i^{n+1} = C_i^n - A_{i-1/2}^n(C_i^n - C_{i-1}^n) + B_{i+1/2}^n(C_{i+1}^n - C_i^n) \quad (11)$$

With

$$A_{i-1/2}^n = A(C_{i-2}^n, C_{i-1}^n, C_i^n, C_{i+1}^n) \quad \text{and} \quad B_{i+1/2}^n = B(C_{i-1}^n, C_i^n, C_{i+1}^n, C_{i+2}^n) \quad (12)$$

The discrete solution C_i^n called monotonic if for each i

$$\min(C_{i-1}^n, C_{i+1}^n) \leq C_i^n \leq \max(C_{i-1}^n, C_{i+1}^n) \quad (13)$$

Scheme Eq. (11) is called monotonicity preserving if C_{i+1}^n remains monotonic when C_i^n is monotonic. Hence, no new minima or maxima are created when time evolves. The following theorem due to [12] gives a sufficient condition to ensure monotonicity preservation of the numerical scheme.

Theorem 1. Total Variation Diminishing scheme is monotonicity preserving

The main interest of the incremental form Eq. (11) for scheme Eq. (3) is that sufficient conditions can be derived in order to achieve the TVD property of the family of approximate solutions. In this way Harten [15] proves the following lemma.

Lemma 1.

If $A_{i+1/2} \geq 0$, $B_{i+1/2} \geq 0$ and $A_{i+1/2} + B_{i+1/2} \leq 1$ then the scheme Eq.(11) is TVD In order to satisfy the TVD condition, the Harten’s lemma implies that the flux-limiter must satisfy certain constraints. For example with an uniform positive velocity u , and the symmetric property of the limiter i (i.e. $(F_{i+1/2})_{U_p} = uC_i^n$), the substitution of (7) in (3) gives :

$$C_i^{n+1} = C_i^n - u \frac{\Delta t}{\Delta x} \left[1 + \frac{1}{2} \frac{\phi(\theta_{i+1/2}^+)}{\theta_{i+1/2}^+} - \frac{1}{2} \phi(\theta_{i+1/2}^+) \right] (C_i^n - C_{i-1}^n) \tag{14}$$

This is a scheme of the incremental form (11) with

$$A_{i-1/2}^n = \frac{\Delta t}{\Delta x} \left[1 + \frac{1}{2} \frac{\phi(\theta_{i+1/2})}{\theta_{i+1/2}} - \frac{1}{2} \phi(\theta_{i+1/2}) \right] \text{ and } B_{i+1/2}^n = 0 \tag{15}$$

applying the Harten’s lemma, the scheme is TVD if

$$\left| \frac{\phi(r)}{r} - (s) \right| \leq 2 \tag{16}$$

Sweby [13] also specifies that $\phi(r) > 0$ and that $\phi(r) = 0$ for $r \leq 0$. Under these additional restrictions the condition (16) becomes

$$0 < \frac{\phi(r)}{r} \leq 2 \quad \text{et} \quad 0 \leq \phi(r) \leq 2 \tag{17}$$

The region defined by (17) is shown in Fig. 1 along with the limiter corresponding to the centred differences. Since this scheme is known to produce spurious wiggles in the solution with strongly varying gradients, it is not surprising that this scheme is not uniformly within the TVD region. Among the proposals, which have been discussed in Refs. [14, 12] the following limiter functions used in this study satisfy these constraints [14] including the following :

- Limiter Minmod : $\phi(\theta) = \max(0, \min(1, \theta))$

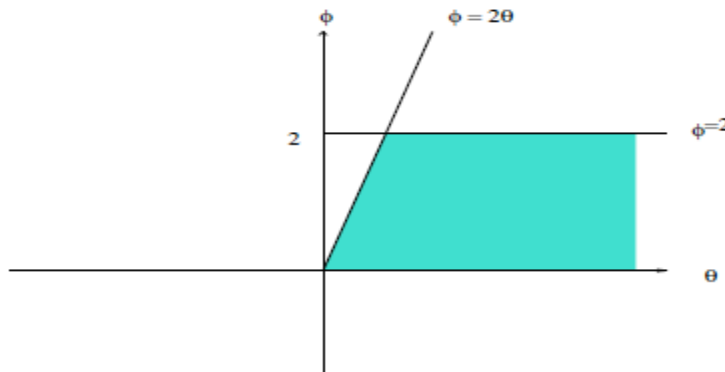


Fig. 1 – Total Variation Diminishing region for pure convection.

- Limiter Superbee : $\phi(\theta) = \max(0, \min(1, 2\theta), \min(2, \theta))$

- Limiter de Van Leer : $\phi(\theta) = (\theta + |\theta|)/(1 + |\theta|)$

- Limiteur MC : $\phi(\theta) = \max[0, \min((1 + \theta)/2, 2\theta)]$

The Minmod and Superbee limiters have been introduced by Roe in [15] and [16]. The Van Leer limiter was introduced in [17] and the MC limiter was also introduced by Van Leer in a later paper [18]. Note that it is easy to verify that the limiter functions proposed above are symmetric.

3.2.1 Two-dimensional case

The generalization of the numerical schemes to the multi-dimensional case is not always an easy task in the numerical computation. For example, in the 2D case the Lax-Wendroff scheme introduces the cross derivative terms. These terms must be included in spatial discretization if the second order approximation in time is desired. Besides accuracy problems of the schemes, sometimes also the mathematical properties are not carried over directly from one dimension to two dimensions. For example Spekreijse [19] shows that for explicit schemes, a 2D monotonic scheme is not necessarily TVD. However, numerical experiments [19] have shown that 2D schemes using the splitting technics (1D second order accurate TVD scheme in each direction perpendicular to the cell face) give accurate results, with no oscillations. In this section we present the 2D algorithm to solve the two-dimensional purely advective scalar equation given by

$$\frac{\partial C}{\partial t} + \frac{\partial uC}{\partial x} + \frac{\partial vC}{\partial y} = 0 \quad (18)$$

Where u and v are the velocity components in x - and y -directions respectively. Discretization of Eq. (18) in the incremental form gives :

$$C_{i,j}^{n+1} = C_{i,j}^n - \alpha_{i-1/2,j}^n (C_{i,j}^n - C_{i-1,j}^n) + \beta_{i+1/2,j}^n (C_{i+1,j}^n - C_{i,j}^n) - \lambda_{i,j-1/2}^n (C_{i,j}^n - C_{i,j-1}^n) + \mu_{i,j+1/2}^n (C_{i,j+1}^n - C_{i,j}^n) \quad (19)$$

With

$$\alpha_{i-1/2,j}^n = \alpha(C_{i-2,j}^n, C_{i-1,j}^n, C_{i,j}^n, C_{i+1,j}^n) \quad , \quad \beta_{i+1/2,j}^n = \alpha(C_{i-1,j}^n, C_{i,j}^n, C_{i+1,j}^n, C_{i+2,j}^n) \\ \lambda_{i,j-1/2}^n = \lambda(C_{i,j-2}^n, C_{i,j-1}^n, C_{i,j}^n, C_{i,j+1}^n) \quad , \quad \mu_{i,j+1/2}^n = \mu(C_{i,j-1}^n, C_{i,j}^n, C_{i,j+1}^n, C_{i,j+2}^n) \quad (20)$$

In Ref. [19], a class of explicit schemes in two dimensions is considered, a new definition of monotonicity is also introduced.

Definition 1. Scheme Eq. (19) is called monotonic if

$$\alpha_{i-1/2,j}^n \geq 0 \quad , \quad \beta_{i+1/2,j}^n \geq 0 \quad , \quad \lambda_{i,j-1/2}^n \geq 0 \quad , \quad \mu_{i,j+1/2}^n \geq 0 \quad (21)$$

As mentioned above and for description simplicity, we use in this paper the 2D extension of fluxlimiting schemes as splitting mode in each one-dimensional direction. Application of this to (18) with the cell-centred finite volume discretization gives the semi-discrete equation :

$$\frac{dC_i}{dt} |\Delta x \Delta y = -[uC]_{i-1/2}^{i+1/2} - [vC]_{j-1/2}^{j+1/2} \quad (22)$$

In the one-dimensional case, we give the complete expressions of the interface values $C_{i+1/2,j}^n, C_{i,j+1/2}^n$ for an arbitrary velocity field :

$$C_{i+1/2,j}^n = \begin{cases} C_{i,j}^n + \frac{1}{2}(C_{i+1,j}^n - C_{i,j}^n)\phi(\theta_{i+1/2,j}^+) & \text{si } u_{i+1/2,j}^n \geq 0 \\ C_{i+1,j}^n - \frac{1}{2}(C_{i+1,j}^n - C_{i,j}^n)\phi(\theta_{i+1/2,j}^-) & \text{sinon} \end{cases} \quad (23)$$

$$C_{i,j+1/2}^n = \begin{cases} C_{i,j}^n + \frac{1}{2}(C_{i,j+1}^n - C_{i,j}^n)\phi(\theta_{i,j+1/2}^+) & \text{si } v_{i,j+1/2}^n \geq 0 \\ C_{i,j+1}^n - \frac{1}{2}(C_{i,j+1}^n - C_{i,j}^n)\phi(\theta_{i,j+1/2}^-) & \text{sinon} \end{cases} \quad (24)$$

With

$$\theta_{i+1/2,j}^+ = \frac{C_{i,j}^n - C_{i-1,j}^n}{C_{i+1,j}^n - C_{i,j}^n}, \quad \theta_{i+1/2,j}^- = \frac{C_{i+2,j}^n - C_{i+1,j}^n}{C_{i+1,j}^n - C_{i,j}^n}$$

$$\theta_{i,j+1/2}^+ = \frac{C_{i,j}^n - C_{i,j-1}^n}{C_{i,j+1}^n - C_{i,j}^n}, \quad \theta_{i,j+1/2}^- = \frac{C_{i,j+2}^n - C_{i,j+1}^n}{C_{i,j+1}^n - C_{i,j}^n}$$

Note that if the limiter function ϕ satisfies the conditions (17), then the scheme given by Eq. (23) and (24) is monotonic. This is a direct consequence of Theorem 1 and Definition 1.

4. Results and discussion

For to test the performance of the numerical schemes, we realize some numerical tests. In these tests, we consider the Burgers equation with a transport equation scalar. To achieve the objective of this paper, we carry out a first series of tests which we discretize the Burger equation with the Upwind scheme and the transport equation with all other schemes. The second series will use the Superbee limiter to the equation Burger and other schemes for the transport equation.

4.1. Test 1 : Coupling Burger/Transport

This test solves the monodimensional convection of a discontinuous profile of a concentration transported by a velocity field calculated by the Burger equation on the domain $[-L, L]$ or L is an arbitrary coefficient in R :

$$\begin{cases} \frac{\partial u}{\partial t} + \frac{\partial(u^2/2)}{\partial x} = 0 & \text{for } x \in [-L, L[\\ \frac{\partial c}{\partial t} + \frac{\partial uc}{\partial x} = 0 & \text{for } x \in [-L, L[\\ c(x, 0) = c_0(x) \text{ et } u(x, 0) = u_0(x) \\ \left(\frac{\partial c}{\partial x}\right)_{x=L} = 0 \text{ et } \left(\frac{\partial u}{\partial x}\right)_{x=L} = 0 \end{cases} \quad (25)$$

Where the initial conditions u_0 and c_0 are taken with discontinuities:

$$c(x, 0) = c_o(x) = \begin{cases} 1 & \text{si } a \leq x \leq b \\ 0 & \text{sinon} \end{cases} \quad (26)$$

with a and b are parameters to choose in $[-L, L]$.

$$u(x, 0) = u_o(x) = \begin{cases} 0, & \text{si } x \in [-L, 0] \\ 1, & \text{sinon} \end{cases} \quad (27)$$

In fact, it is this model that will allow us to answer the question that arises. for this, we have split this application into two numerical test. In the first, one approach the convective acceleration by the Upwind scheme, while in the second it is discretized by the best performing slope limiter (Superbee) [6]. For both tests, the transport equation will be tested by all schemes used in this work. We recall that for this test, we comment only the results of the transport equation.

• Test 1.1 (Burger : Upwind/ transport : all schemes)

The results of this simulation are presented in figures 2 et 3 where the curves are plotted in simple line. The examination of table (I) shows a perfect conservation of the mass from all schemes ($R_{mas} = \left| \frac{\sum_{i=1}^{N_x} u_{i,num}}{\sum_{i=1}^{N_x} u_{i,initial}} \right| = 1$) In figure (2.a), the upwind scheme shows an

excessive spreading out of the profil of the concentration and a loss of de 42% of the maximum value of the solution. We report the non-monotonic character of the schemes centred and Second upwind which appears by the violation of the extremums of the solution $C_{min} \leq 0, C_{max} \geq 1$ (figure 2.b, figure 3.c). As for slope limiters, we observe the superiority of Superbee limiter on other limiters (Table 1). All figures (3.d, 3.e, 3.f, 3.g) shows that the limiter Minmod diffuse more than the other limiters, but much less than the Upwind scheme. Also, we note the Superbee limiter keeps the best shape of the concentration profile (Conservation the mass). Finally, we note that the MC limiter is located in performance between the limiter Van Leer and Superbee limiter.

• **Test 1.2 (Burger :Superbee / transport :all schemes)**

The results of this simulation are presented in Figures 2 and 3 where the curves are shown by a solid line.

This is certainly the key test of this study, these results will help answer the question that was asked at the beginning. It allows to assess the contribution of the approximation of the acceleration convective by a high-order scheme on the coupling in transport equation.

The comparison figures (2.a) for Upwind scheme shows a spread of the solution less important in "test 1.2" than "test 1.1". Note also that the loss of the maximum value of the solution is less than in "test 1.2" that "test 1.1", this report is also also observed for all other limiters. Figures (2b) and (3c) show a contrary to other schemes a degradation in the performance which results in an amplification of the parasitic oscillations. Table (II) shows that the approximation of convective acceleration by the Superbee limiter reduced advantage of numerical diffusion generated by the discretization of the convective term in the transport equation. This reduction is quantified by a gain to the maximum of the solution compared to the results of " test 1.1". And given the percentage gain for different schemes.

- 10.29% for centred scheme.
- 09.43% for Mimnod limiter.
- 09.06% for Upwind scheme.
- 08.97% for Van Leer limiter.
- 07.68% for M.C. limiter
- 06.98% for Superbee limiter.

We note that the Superbee limiter has the lowest rate of gain over other schemes. This report is not surprising, since this is the limiter is most powerful that the others and therefore any improvement will have a lesser effect on this limiter (in other essential term of the improvement is already in the definition itself of the limiter). Finally, the comparison for example of the figures (3.e) makes it possible to deduce that the limitation from the accelaration convective also allowed a significant improvement in the conservation of the form. This remark also applies to all schemes except the centred and Second Upwind schemes.

Schemes	Rmass	Cmin	Cmax
Upwind	0.9998	0	0.5892
centred	1.0000	-0.2803	1.3060
Second Upwind	1.0000	-0.2803	1.3060
Minmod	1.0000	0	0.8360
Superbee	1.0000	0	0.9337
Van Leer	0.9999	0	0.9076
MC	0.9999	0	0.9273

Tab. I – Comparing the convection schemes for simulation of a concentration equation with Upwind Scheme for the velocity. $\Delta t = 1$, $\Delta x = 1$, at $t = 25$

Schemes	Rmass	Cmin	Cmax
Upwind	0.9998	0	0.6426
centred	1.0000	-0.3391	1.4404
Second Upwind	1.0000	-0.3391	1.4404
Minmod	1.0000	0	0.9149
Superbee	1.0000	0	0.9989
Van Leer	0.9999	0	0.9891
MC	1	0	0.9986

Tab. II – Comparing the convection schemes for simulation of a concentration equation with Superbee scheme for the velocity. $\Delta t = 1$, $\Delta x = 1$, at $t = 25$

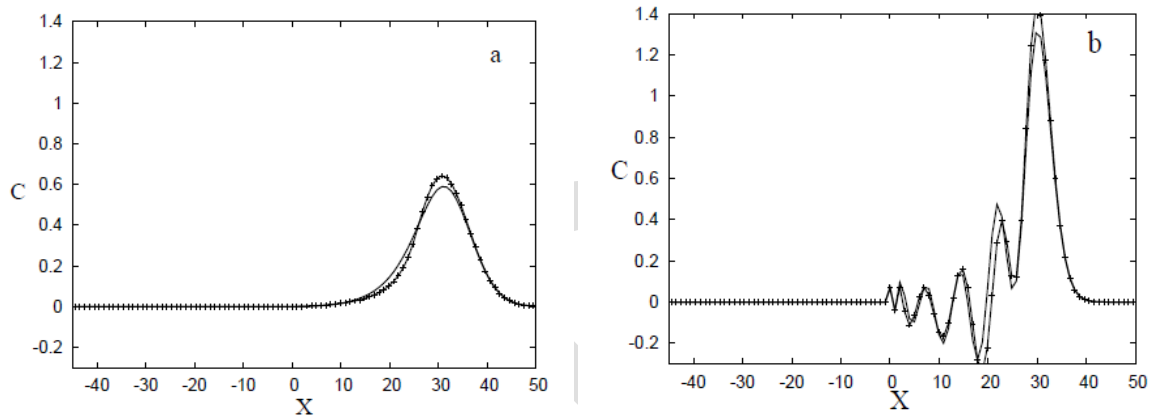
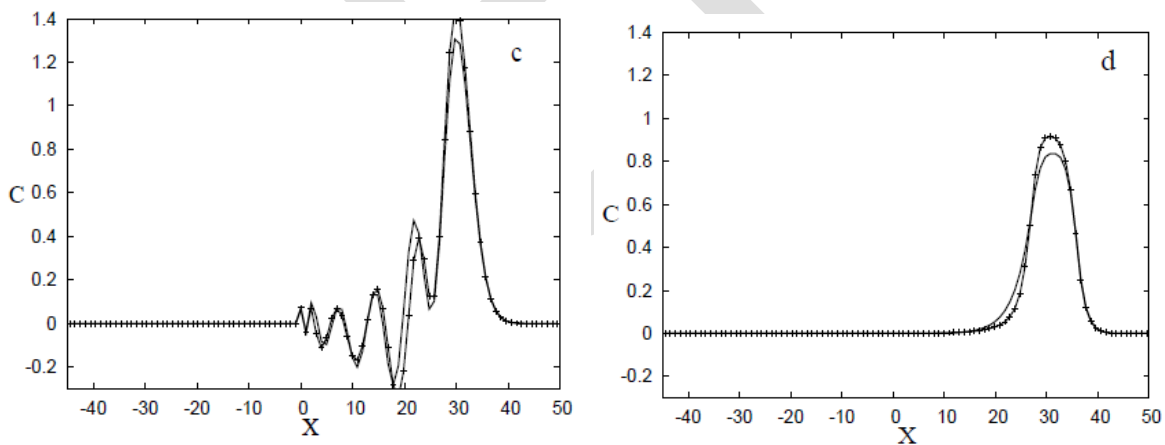


Fig. 2 – The concentration profile C obtained with a scheme : a) Upwind ; b)centred. solid line : Burger approached by Superbee, discontinuous line :Burger approached by Upwind



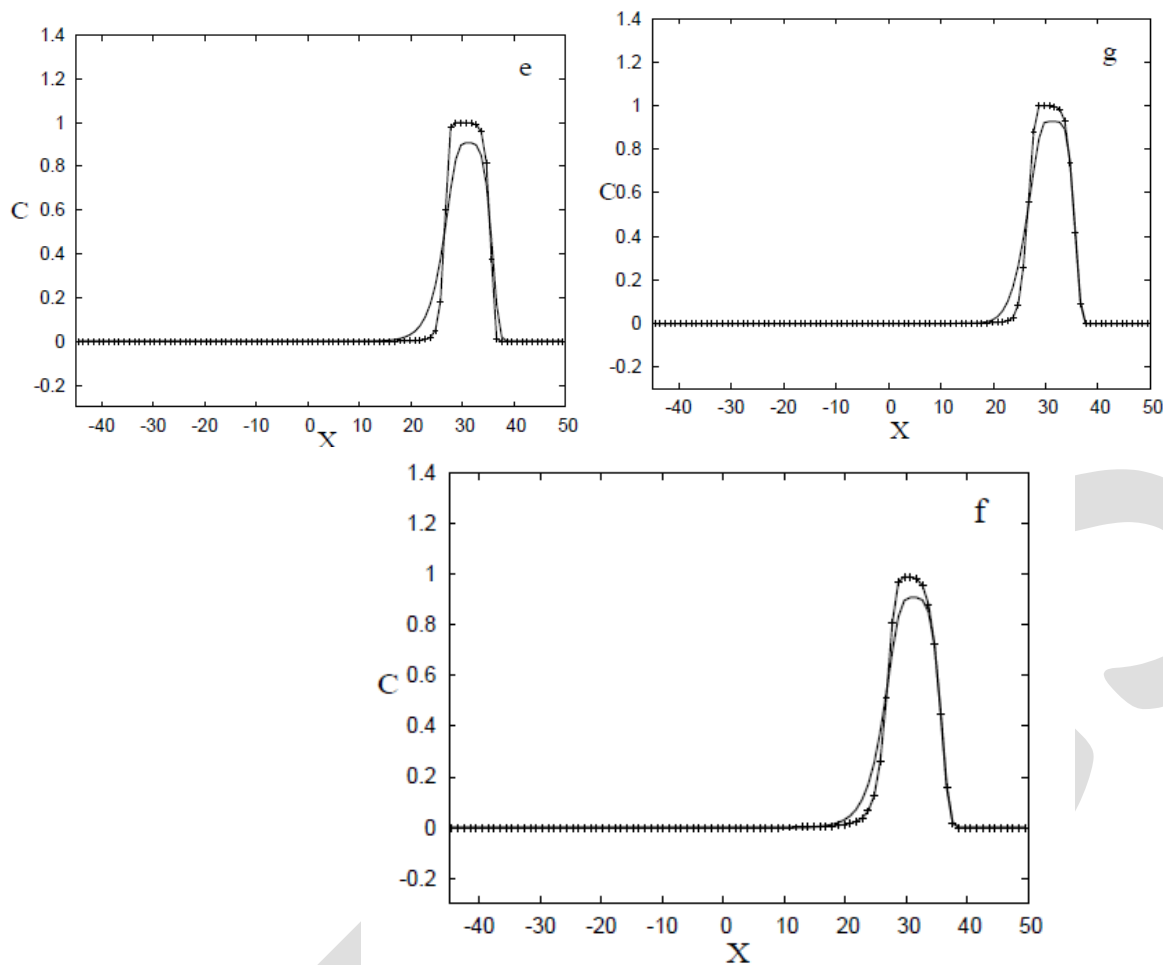


Fig. 3 – The concentration profile C obtained with a scheme : c)Second Upwind d)Minmod ; e)Superbee ; f)VanLeer ; g)M.C. solid line Burger approached by Superbee, discontinuous line : Burger approached by Upwind

5. Conclusion

A series of slope limiter schemes was introduced and tested for monodimensional case. These schemes can be an alternative to advection schemes commonly used in ocean modeling. The Upwind and centred schemes were compared to four limiters slope (Minmod, Superbee Van Leer, MC) admitting the TVD property. These limiters Capable of reducing the numerical diffusion and limit the dispersion introduced by the terms of third order due to truncation errors. The schemes of order two in space are preferred oceanographers probably for the simplicity of their implementation and the absence of the numerical diffusion. However, these schemes are too dispersive, but this handicap can be absorbed by increasing the value of the coefficient of horizontal viscosity. This technique has also the disadvantage of returning this coefficient (resulting from the physical processes of turbulence) like a numerical parameter of chock. The tests presented in this study show that the slope limiters a total variation diminishing (TVD) can be implemented successfully in ocean modeling. In what we concerns, the slope limiters and in particular the Superbee limiter has considerably improves the characteristics of solution concentration when this one is coupled with the Burger equation. The tests undertaken here revealed that for a coupled problem, the numerical diffusion introduced in hydrodynamics is struck directly on the solution concentration (comparison test1.1 and test1.2).

REFERENCES:

- [1] A. Blumberg, G. Mellor, A description of a three-dimensional coastal ocean circulation model, in: Three-dimensional coastal ocean models, Coastal and Estuarine Sciences, vol. 4, American Geophysical Union Washington, 1987, pp. 116.
- [2] Hess, K,W. 1986 : Numerical model of circulation in Chesapeake bay and the continental shelf, N.O.A.A Technical Memorandum, AISC6, U.S Dpt of commerce, pp 47
- [3] Berthet .C, 1996 : Ecoulements et transports littoraux tridimensionnels : application numériques. Thèse de doctorat de l'Université Joseph Fourier- Genoble 1

- [4] Smaoui.H 1996 : Modélisation numérique tridimensionnelle de l'hydrodynamique et des transports sédimentaires en Manche Orientale et dans le sud de la Mer du Nord, thèse de doctorat de l'U.S.T.L. Lille, France
- [5] Smaoui.H, Ouahssine.A, 1999 : Flux-limiter schemes for oceanic tracers : application to the English Channel tidal model ; Computer methods in applied mechanics and engineering. 179(1999)307-325
- [6] Smaoui. H and Radi.B 2001: Comparative study of different advective schemes : Application to the MECCA model. J. Env. Fluid. Mech. Vol 1 (4), pp 361-381.
- [7] J. Fromm, A method for reducing dispersion in convective difference schemes, J. Comput. Phys. 3 (1969) 176189. [8] D. Bradley, M. Missaghi, S.B. Chin, A Taylor series approach to numerical accuracy and a third-order scheme for strong convective flow, Compt. Meth. Appl. Mech. Eng. 69 (1988) 133151.
- [9] B. Van Leer, Upwind-difference methods for aerodynamics problems governed by the Euler equations, Lectures in Appl. Math. 22 (1985) 327336.
- [10] M. Zijlema, P. Wesseling, Higher order flux-limiting methods for steady-state multidimensional convection-dominated flow, Delft University Report (1995) 95131.
- [11] P.H. Gastell, A.K.C. Lau, Curvature-compensate convective transport : SMART, a new boundedness-preserving transport algorithm, Int. J. Num. Meth. Fluids 8 (1988) 617641.
- [12] Harten.A 1983 : Higt resolution schemes for hyperbolic conservation laws, J.Comput.Phys. Vol 49 pp. 357-393.
- [13] Sweby.P.K 1984 : Higt resolution schemes using flux limiters for hyperbolic conservation laws, SIAM J.Num.Anal. Vol 21 N5.pp. 995-1011
- [14] R. Leveque, High-resolution conservative algorithms for advection in incompressible ow, SIAM J. Num. Anal. 33 (1996) 627 665.
- [15] Roe.B : Some contribution to the modeling of discontinous flows, Lect. Notes Apple. Math. 22 (1985) 163-193.
- [16] B. Roe, D. Sidilkover, Optimum positive linear schemes for advection in two and three dimensions, SIAM J. Num. Anal. 29 (1992) 15421568.
- [17] B. Van Leer, Towards the ULTIMATE conservation difference scheme. II. Monotonicity and conservation combined in a second order scheme, J. Comput. Phys. 14 (1974) 361-370.
- [18] B. Van Leer, Towards the ULTIMATE conservation difference scheme. IV. A new approach to numerical convection, J. Comput Phys. 23 (1977) 276299.
- [19] Spekrijse.S.P : Multigrid Solution of the Steady Euler Equations. PhD thesis, Centrum voor Wiskunde en Informatica, Amsterdam, Nov. 1987.

Analysis of Cloud IDEs for Software Development

Ms. Pooja Arora

BCIIT, Delhi.

poojadhanrajani@gmail.com

Dr. Anurag Dixit

Galgotias University, Greater Noida.

anurag.dixit@galgotiasuniversity.edu.in

ABSTRACT- In today world using cloud services has become a convenience for software developers to develop application. An integrated development environment(IDE) facilitates the development of apps in shorter software delivery timelines. A cloud based IDE is an 'next gen' solution and still in the incubation stage because the cloud based private workspace is yet to evolve fully.as of now, there still is not any good java-supporting cloud IDE available. Evaluation of different cloud IDEs is discussed in this paper.

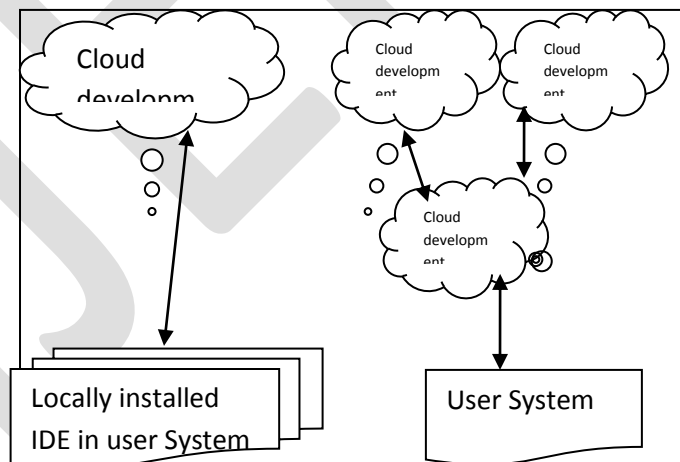
This paper discuss an open source virtual environment for cost effective and better community based collaborative software development. In this paper we analyze a cloud based development facility that can be accessible from anywhere and be used without much interfacing in the local developer system such as software installation, network boundary etc.

Keywords : IDE, Software development, deployment environment, cloud IDE, Virtual Environment, Java, J2EE

1. INTRODUCTION

The development process plays a vital role in developing a software product. The software development process consists of requirement gathering and analysis, designing, coding, testing, deployment and maintenance. The basic requirements for software development are hardware and software tools, a server to deploy and test the application and a coding development environment. Cloud based development brings in a lot of cost savings and efficiency into the process of software development. The cloud provides a deployment environment for developers and the developer do not require building, developing or maintaining this environment but can share it easily from the public environment.

Figure 1.1 Software development and the cloud IDE



An integrated development environment is a software tool that integrates various features required for the development of a software application. The cloud IDE is the latest improvement in this area. The cloud IDE is a virtual development environment. To develop a java application, we use Eclipse or Netbeans as the IDE, which provides an integrated plugin facility to develop java code, auto complete java APIs, has syntax highlighting, apart from the capability to compile, execute, test and analyze static code. In traditional software development environment, all developers install the IDE in their respective systems, and upload their developed code into a concurrent version system(CVS) or source code management system. Once the code is checked in, it requires the harmony

of other developers, which takes more time if the number of developers is high in a project. So there is the fundamental need to provide a software development environment for a large number of developers to work together on a collaborative project, yet achieve a shorter delivery time, a cloud IDE is one of the best solutions to reduce the development process time, as it provides a more convenient and flexible common environment for software developers.

2. THE CLOUD IDE

The basic motive behind the cloud IDE based platform is to create a virtual development environment. It can provide the following features for the software development process :

- e. programmer can develop an application in one or more software technologies such as Java, C++, HTML, JavaScript and so on.
- f. It has an application container to deploy the application on-the-fly.
- g. It offers repository management to store, retrieve and share code between groups of developers.
- h. In addition to these basic features, we need to add security to limit the access to only the selected group of developers. This can be achieved by an authentication system that protects the development environment from public use.

2.1 Standard expectation from a cloud IDE

The following standard expectations from a cloud IDE are :

- It should be lightweight and flexible enough.
- It should be able to highlight syntax.
- It should have the auto completion facility.
- It should have an internal compilations facility.
- It should support remote repository management for source code.
- It should provide minimum debugging facilities.
- It should support cloud deployment.

In addition to this, proficient developers who have worked on various IDEs like Eclipse, JDevelopers, IntelliJ, Visual Studio etc would look for some add-on features like :

- Support for screen design with a visual designer tool.
- API or language help; for example, tooltip for a Java API.
- Static code analysis to follow best practices in coding.
- Coding convention and code formatting or styling; for example, the number of characters in a line, tab, indentation etc.

2.2 Advantages of working in cloud-based IDEs

- Programming workspace is a single and centralized environment in which multiple people can co-build, co-edit and co-debug
- Easy and instant access to codes and libraries through the web
- Enables developers to work on the go without the need to occupy systems with loads of heavy codes and data
- Accessible through all devices and browsers
- Facilitates better collaboration among developers located at different locations
- Reduces duplication of work

3. ANALYSIS OF OPEN SOURCE CLOUD IDES

The popular open source cloud IDEs include Cloud9, codeanywhere, Eclipse Orion, Coderun Studio, Codebox, Codeiad, IDE One and Codenvy-Eclipse Che. In the following section the various features and advantages and disadvantages of these tools based on experience of users are discussed.

3.10 Cloud9

Cloud9 IDE is capable of handling projects from JS, HTML, PHP AND Ruby. it support development in JavaScript, GIT, Selenium, HTML/CSS, XML, XQuery, PHP, Ruby and Node.js. it can be used for web application development. Cloud9 supports repositories like GIT, the distributed revision control tool Mercurial, and Apache subversion. It also facilitates deployment, which can be done directly from Cloud9 to Joyent and Heroku. Its limitation is that it is not useful for Java application development or J2EE application development/handling.

Advantages: Supports a variety of languages and various repository tools.

Disadvantages: can be used for simple application development but not for large or complex applications.

3.11 Codeanywhere

This is lightweight browser based IDE tool. It supports web application development. It support HTML, CSS, Java Script, PHP, MySQL, and more.

This tool is used to develop and test code from anywhere i.e from mobile device also as it is also available as a mobile application. Codeanywhere is supported in IOS, Android and BlackBerry based mobile devices and tablets.

Advantages : Lightweight and easy to use. Support for mobile devices.

disadvantages: it is more useful for web page development and it doesnot support a variety of programming languages.

3.12 Eclipse Orion

This can be used as a local standalone IDE or an online IDE through a browser. This is the Eclipse version of Orion. It only supports Chrome, FF Safari and IE10. This is more for client side scripting like HTML, JS and CSS. Java syntax highlighting is supported during static code review, and doesn't integrate with the java build and development environment. It has shell features with a very limited command facility.

It doesn't support the private cloud and hence is not suitable for secured application development. This is one of the lightweight cloud IDEs for software development in HTML/CSS and javascript.

Advantages : can be used as a standalone local installation tool or as a cloud IDE. It offers static code analysis. Shell features provides facility for UNIX script development, which is a unique feature many cloud IDEs do not offer.

Disadvantages : it doesn't support the private cloud/secure development, and doesn't support build/compilation of code or online testing.

3.13 Coderun Studio

This is simple and efficient cloud IDE. It support application development in ASP.net, HTML, CSS and JavaScript, Microsoft visual studio. It also facilitates code completion, syntax highlighting, debugging and native compilation. This provides flexibility for community development by providing a unique URL and access to peers for a multi-user development environment.

Advantages : unique URL for multi-user development, in parallel. More suitable for pair/peer programming. Supports Microsoft code development, debugging and native compilation.

Disadvantages : development using latest frameworks or languages like Scala, Ruby, NodeJS, AngularJS is not supported by this tool.

3.14 Codebox

This is an open source IDE with code available. It enables the users to customize the tool and encourages them to share it for community development.

Programmer can download the code from this repository, and build to prepare an IDE in their local desktop. It supports Windows, Chromebox and Mac based operating system. This tool is used to develop local or cloud based application. It facilitates pair programming by providing cloud based IDEs for sophisticated community development in Java, JavaScript, C++, Ruby, Scala, HTML, CSS, NodeJS and UNIX script programming.

It provides auto completion of code, syntax highlighting and supports cross-platform development on the desktop, laptop, tablet and on Chromebook.

This tool provides supports for Scala based program development and deployment to cloud based platforms. It is an open source with licensing under Apache 2.0, and provides command line development for shell programming. It provides supports for Google Docs and database support using MySQL.

Advantages: provide support for variety of repositories, cloud deployment, scala based program development, cross platform support and auto completion of code.

Disadvantages : it does not support PHP application development.

3.15 Codiad

This is simple tool which supports more than 40 programming languages, and provides plugins for integration with other popular IDEs like Eclipse. There is no database required to be installed locally, and no application server or local installation required to run this browser based IDE tool.

Advantages : simple and efficient tool that supports a variety of languages. Application server support for local deployment is available.

Disadvantages : it doesn't support a variety of database types and is not so flexible in pair programming.

3.16 Online java IDE

This IDE has facilities for java/J2EE development. It also supports spring, ojdbc, MySQL, mail APT and Axis frameworks. This IDE is not very user friendly and typing/editing is not too comfortable. The package creation option is not available for modular programming. There is no download and upload facility to synchronize with the local development environment.

Advantages : supports a variety of database drivers and frameworks like Mailx, Axis etc

Disadvantages : Packages and deployment is not available limited to java development only.

3.17 IDE One

This is a very simple online IDE which supports Java. It can be more useful as a unit or stub testing environment- as a quick try. The code development in this tool is done online and there is no 'Save' option. It doesn't have extensive support for real-time application development/deployment.

Advantages : simple tool with real-time application

Disadvantages : lacks user friendliness.

3.18 Codenvy - Eclipse Che

It supports a variety of Java/J2EE frameworks. This IDE provides unlimited open source community development support and user access. Usability is high, being as simple as using a desktop version of Eclipse or the Netbeans IDE. The deployment facility includes a variety of PaaS cloud environments. Integration is seamless and automatic. When user trigger deployment from an IDE, it connects to the PaaS and pushes the build to the deployment zone.

GIT is the default management repository and it has a local as well as remote GIT facility, where users can either keep the source local to Codenvy (like storing in local development machine) or connect to remote GIT to check-in/check-out.

It has JSP AND SPRING support in built, using the project template features. It has features to import external jars and hence JSF or the Struts Framework can be used for code development. Applications with DB support can be simply chosen from the wizard. Archive download of the project to a local system is available. Uploading the existing projects is possible, and so the user can switch between the local environment and the online IDE. Package creation support is also available. Codenvy is bit slow when 'initialising Java tool' and supports non-IE browsers such as Safari, Firefox or Chrome.

It has shell access for UNIX development with basic commands. Build and deploy is integrated in the IDE. It supports deployment to cloud environments

Advantages : has a variety of features and is flexible in development. Supports download of archive code-on-the-fly.

Disadvantages : it doesn't support IE browser. Slows down sometimes when users compile or do a cloud deployment.

4. CONCLUSION

For a developer or a small company that lacks the capability to install an IDE locally for software development or wants to develop a program on-the-fly, the tools described above would be helpful to experiment on, prior to choosing a development environment. With the adoption of several simple security precautions and an open mindset, any software developer can reap the rewards of Cloud software suites without any real danger.

REFERENCES:

- [1] Chia Hung Kao, Shin Tze Liu , Chun Cheng Lin “Toward a Cloud based Framework for Facilitating Software Development and Testing Tasks” 2014 IEEE/ACM 7th International Conference on Utility and Cloud Computing DOI-978-1-4799-7881-6/14 \$31.00 © 2014 IEEE
- [2] Deepak Puthal*, B. P. S. Sahoo†, Sambit Mishra‡, and Satyabrata Swain, “Cloud Computing Features, Issues and Challenges: A Big Picture” , 2015 International Conference on Computational Intelligence & Networks, DOI 10.1109/CINE.2015.31
- [3] Wei-Tek Tsai, Wenjun Wu, Michael N. Huhns, “Cloud-Based Software Crowdsourcing”, Published by the IEEE Computer Society 1089-7801/14/\$31.00 © 2014 IEEE
- [4] Dave Thomas, “Enabling Application Agility - Software as A Service, Cloud Computing and Dynamic Languages” in Journal of Object Technology, vol. 7 no. 4 May-June 2008, pp. 29-32
- [5] Codeanywhere <https://codeanywhere.net/>
- [6] Cloud9 <https://c9.io>
- [7] Codenvy <https://codenvy.com>
- [8] <http://www.compilerjava.net>
- [9] <https://ideone.com>
- [10] <http://codiad.com>
- [11] <http://codebox.in/>
- [12] <http://coderuncom/studio>
- [13] [G. Fylaktopoulos](#), [G. Goumas](#), [M. Skolarikis](#), [A. Sotiropoulos](#), and [I. Maglogiannis](#) “An overview of platforms for cloud based development” Published online 2016 Jan 16. doi: [10.1186/s40064-016-1688-5](https://doi.org/10.1186/s40064-016-1688-5), Springerplus. 2016; 5: 38

Vibration Analysis Of Double Roller Autofeeder Ginning Machine Seed Channel By Global Stiffness Matrices : Vibration Measurement & Its Effects

Sachin W Gajghate (Author)

Research Student (M-Tech , CAD/CAM)
Vidarbha Institute of Technology, RTM Nagpur University
Uti , Umred Road, Nagpur (MH),India
sachin_gajghate@yahoo.co.in

Vaibhav H Bankar (Guide)

Assistant Professor & HOD (M-Tech , CAD/CAM)
Vidarbha Institute of Technology, RTM Nagpur University
Uti ,Umred Road, Nagpur (MH),India
vhbankar@gmail.com

Abstract— Noise is sound that is not wanted by the perceiver, because it is unpleasant, loud, or interferes with hearing. This results in the subjective discretion between sound and noise, where any sound may be considered noise depending on the perceiver. By extension, in experimental sciences, "noise" refers to any random fluctuations of data that makes more difficult the perception of an expected signal. Specifically, acoustic noise is any sound in the acoustic domain, either deliberate (music, speech, etc.) or unintended. In contrast, noise in electronics may not be audible to the human ear and often requires instruments for detection. Environmental is the accumulation of all noise present in a specified environment. The principal sources of environmental noise are surface motor vehicles, aircraft, trains and industrial sources. These noise sources expose millions of people to noise pollution that creates not only annoyance, but also significant health consequences such as elevated incidence of hearing loss and cardiovascular disease. There are a variety of mitigation strategies and controls available to reduce sound levels including source intensity reduction, land use planning strategies, noise barriers and sound baffles, time of day use regimens, vehicle operational controls and architectural acoustics design measures.

Keywords: stiffness matrix, global matrix, displacement matrix, quadratic equations material, measurement, seed channel parameters ginning machine, noise, vibration, ginning machine spares, operation

INTRODUCTION

Ginning machine is manufacturing in India and most of the economically low pay group people & working for their survivals .the operator continue with the dirty exposure and noisy condition ,they are also felt sick due to the environmental hazardous condition .out of these problem one major problem which is mostly and continuous exposure of ginning machine seed channel vibration ,it causes directly or indirectly affecting the normal working interest of machine operator .to control this machine vibration which may either during manufacturing or generated due to continuous operation of ginning machine over the period of time .we must understood the effect vibration on operator and machine performance as well .this is very important to find out the areas where the machine vibration may generated during design , manufacturing or during assembling of spares .once find out , selection of specific procedure to minimize it or make some changes in design textiles constitute an important component of India's economy. Ginning is the first and most important mechanical process by which seed cotton is separated into lint (fibre) and seed and machine used for this separation is called as gin. There are mainly two types of gins (i) roller gins- most commonly used in India, Egypt, Uganda, Tanzania etc. and (ii) saw gins- extensively used in countries like USA, China, Australia, Uzbekistan etc. Ginning machine which are used in Indian formats are Knife Roller Gin / Roller Gin, Saw Gin, Macarthy Gin ,Three Types Of Macarthy Gins :Single acting Macarthy Gin. , Macarthy Gin Double roller Macarthy Gin / Double Roller autofeeder Gin

Part s included in Ginning machine

Ginning machine consist of following parts

- ☐ Beater shaft,
- ☐ Auto feeder
- ☐ Roller assembly,
- ☐ Gear mesh, hopper,
- ☐ Gin stand,
- ☐ Power supply,
- ☐ Transmission system,

- ☐ Seed channels,
- ☐ Balance weight etc.



Seed channel

Seed channel exit path to the seeds, design and placement of this is very important

Following due care must be taken while design and ease to assembling

- ☐ Material selection
- ☐ Material mechanical and metallurgical properties
- ☐ Material strength
- ☐ Operating environment
- ☐ Design feasibility
- ☐ Assembly joining processes
- ☐ Vibration analysis
- ☐ Operator occupational health

MATERIAL SELECTION

MECHANICAL PROPERTIES

Details	301	304/304L	316/316L	310S	430	409
Density (gm/cm ³)	7.9	7.9	8.0	7.9	7.7	7.7
Modules of Elasticity (kg/mm ²)	19700	19700	19700	20300	20300	20300
Specific Heat Capacity Cal/gm ^o C	0.12	0.12	0.12	0.12	0.11	0.11
Thermal conductivity (Cal/cm ² /Sec ^o C/cm at 100 ^o c	0.039	0.039	0.037	0.033	0.0625	0.0595
Specific Electrical Resistance (u.cm3)	72	72	74	80	60	57
Coefficient of thermal expansion (%x10 ⁻⁶ , 0-520 ^o C)	19.8	18.4	16.0	16.9	11.34	11.52
Melting Range (°C)	1400-1420	1400-1455	1370-1400	1400-1455	1430-1510	1430-1510

THICKNESS RANGES

Thick (mm)	300 series (Density: 8g/cc)	400 series (Density: 7.7 g/cc)
0.30	2.40	2.31
0.40	3.20	3.08
0.50	4.00	3.85
0.63	4.00	3.85
0.70	5.04	4.85
0.80	5.60	5.39
0.90	6.4	6.16
1.00	8.00	7.70
1.25	10.00	9.63

Material reference: Steel Authority of India Ltd, Cold rolled stainless steel: grade 300 series

DESIGN ASSUMPTIONS

- ☐ Material must follows Hooks law
- ☐ Homogeneous material

- ☐ Uniform material thickness i.e. for 1.2 mm THK
- ☐ Thickness deviation +/- 0.08mm/meter
- ☐ No external load is applied
- ☐ Self weight is taken into considerations
- ☐ Material density is 7860gm/cc (*cold rolled SS*)

Abbreviations and Acronyms

All dimensions are in MM, force applied or self weight, F (N), material density in Kg/mm³ stiffness in N/mm frequency in Hz

Units

Young’s modulus (E) =210Gpa, Density (rho) =7860gm/cc Material thickness =1.2mm, Area =mm² Volume =mm³

Length=mm , deflection (u) =µm

Equations

Global Stiffness matrix, K^G

$$K^G = \sum K^1 + K^2 + K^3 + \dots + K^N$$

Stiffness matrix (*section 1*), K =

$$k1 = \frac{EA1}{L1} \begin{bmatrix} 1 & -1 \\ -1 & 1 \end{bmatrix} \begin{matrix} u1 \\ u2 \end{matrix}$$

Global force matrix, (F^G) = ∑ External Force, F + ∑ Body Self Weight, W

$$(F^G) = \sum F^1 + F^2 + F^3 + \dots + K^N + \sum W^1 + W^2 + W^3 + \dots + W^N$$

Self weight W (N)

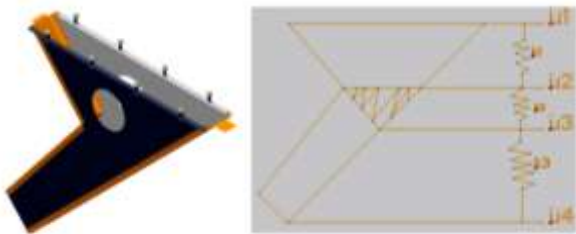
$$W1 = \frac{\rho \times A1 \times L1}{\square} \begin{pmatrix} 0.5 \\ 0.5 \end{pmatrix}$$

Final equation

$$(F^G) = (K^G) (U)$$

CALCULATION

Seed Channel assembly & stiffness Matrix



Expanded view of Seed Channel assembly

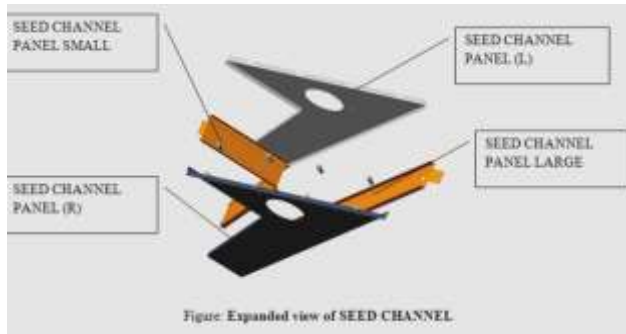


Figure: Expanded view of SEED CHANNEL

Part name	Volume (mm ³)	Density (kg/m ³)	Mass (kg)	E (kg/m ²)
Seed channel panel (L)	223464.09	7850 x10 ⁻⁹	1.75	2.11 x10 ⁴
Seed channel panel (R)	223464.09	7850 x10 ⁻⁹	1.75	2.11 x10 ⁴
Panel large	306720	7850 x10 ⁻⁹	2.40	2.11 x10 ⁴
Panel small	191700	7850 x10 ⁻⁹	1.50	2.11 x10 ⁴
inspection door (L)	$\pi \times 75^2 \times t$ 21195	7850 x10 ⁻⁹	0.16	2.11 x10 ⁴
inspection door (R)	$\pi \times 75^2 \times t$ 21195	7850 x10 ⁻⁹	0.16	2.11 x10 ⁴
SEED CHANNEL ASSEMBLY MASS= 7.72 KGs				

1.2.1 CALCULATION FOR K1

a= 800 MM b= 314.4MM

(a+b)/2 = 242.8 MM

AREA = (242.8 X105) - (240.4X102.6)

A=25494-24665.04

A=828.96 mm²

$$K1 = \frac{EA}{L} \begin{pmatrix} 1 & -1 \\ -1 & 1 \end{pmatrix}$$
$$= 828.96 \times (2.1 \times 10^4) / 260 \begin{pmatrix} 1 & -1 \\ -1 & 1 \end{pmatrix}$$
$$K1 = 10^3 \times \begin{pmatrix} 66.95 & -66.95 \\ -66.95 & 66.95 \end{pmatrix}$$

1.2.2 CALCULATION FOR K2

$$A_2 = 314.4 \text{ MM } B_2 = 157.21 \text{ MM}$$

$$(A_2 + B_2) / 2 = 78.6 \text{ MM}$$

$$\text{AREA} = (78.6 \times 105) - (76.2 \times 102.6)$$

$$A = 8253 - 8001 \text{ A} = 252 \text{ mm}^2$$

$$K2 = \frac{EA}{L} \begin{pmatrix} 1 & -1 \\ -1 & 1 \end{pmatrix}$$
$$= 252 \times (2.1 \times 10^4) / 168.33 \begin{pmatrix} 1 & -1 \\ -1 & 1 \end{pmatrix}$$
$$= 10^3 \times \begin{pmatrix} 31.43 & -31.43 \\ -31.43 & 31.43 \end{pmatrix}$$

1.2.3 CALCULATION FOR K3

$$A_3 = 195 \text{ MM, } B_3 = 105 \text{ MM}$$

$$(A_3 + B_3) / 2 = 45 \text{ MM}$$

$$\text{AREA} = (45 \times 105) - (42.6 \times 102.6)$$

$$A = 4725 - 4473$$

$$A = 252 \text{ mm}^2$$

$$K3 = \frac{EA}{L} \begin{pmatrix} 1 & -1 \\ -1 & 1 \end{pmatrix}$$
$$= 252 \times (2.1 \times 10^4) / 550 \begin{pmatrix} 1 & -1 \\ -1 & 1 \end{pmatrix}$$
$$= 10^3 \times \begin{pmatrix} 9.62 & -9.62 \\ -9.62 & 9.62 \end{pmatrix}$$

1.2.4 Force Matrices

Note: no external force is applied; only self weight of each should be taken into consideration

$$F = 0$$

Self weight

Section	Density (kg/mm ³)	Area	Length (mm)	Self weight (kg)
Section A	7850×10^{-9}	828.96	260	1.70/2
Section B	7850×10^{-9}	252	168.33	0.33/2
Section C	7850×10^{-9}	252	377.8	0.74/2

1.2.5 Force + [self weight] = [kg]. [u]

$$\begin{pmatrix} 66.95 & -66.95 & 0 & 0 \\ -66.95 & 98.38 & -31.43 & 0 \\ 0 & -31.43 & 41 & -9.62 \\ 0 & 0 & -9.62 & 9.62 \end{pmatrix} \times \begin{pmatrix} U1 \\ U2 \\ U3 \\ U4 \end{pmatrix} = \begin{pmatrix} 0.85 \\ 1.015 \\ 0.165 \\ 0 \end{pmatrix}$$

At fixed point, displacement is zero

$$\begin{pmatrix} 66.95 & -66.95 & 0 & 0 \\ -66.95 & 98.38 & -31.43 & 0 \\ 0 & -31.43 & 41 & -9.62 \\ 0 & 0 & -9.62 & 9.62 \end{pmatrix} \times \begin{pmatrix} U1 \\ U2 \\ U3 \\ U4 \end{pmatrix} = \begin{pmatrix} 0.85 \\ 1.015 \\ 0.165 \\ 0 \end{pmatrix}$$

1.2.5.1 Quadratic Equations after boundary conditions

$$\begin{aligned} 98.38 u_2 - 31.43 u_3 &= 1.015 \\ -31.43 u_2 + 41 u_3 - 9.62 u_4 &= 0.165 \\ -9.62 u_3 + 9.62 u_4 &= 0 \end{aligned}$$

1.3 Displacement

$$U_2 = 0.01890 \text{ MM} = 18.90 \mu\text{M}$$

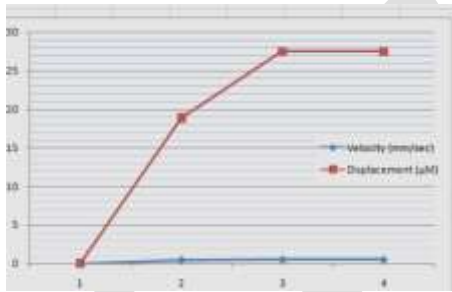
$$U3 = 0.02427 \text{ MM} = 24.27 \mu\text{M}$$

$$U4 = 0.02427 \text{ MM} = 24.27 \mu\text{M}$$

1.4 Frequency & velocity

Frequency = $1/6.28 \sqrt{g/u}$

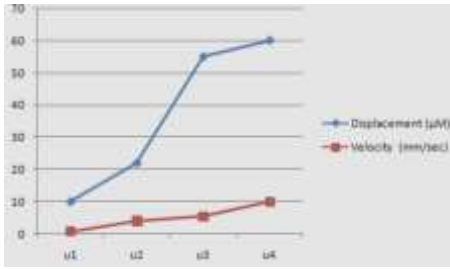
position	Frequency (Hz)	Angular velocity (rad/sec)	Velocity (mm/sec)	Displacement (μM)
U1	0	0	0	0
U2	3.62	21.8	0.41202	18.90
U3	3.20	20.1	0.48782	27.47
U4	3.20	20.1	0.48782	27.47



1.5 ON SITE READINGS

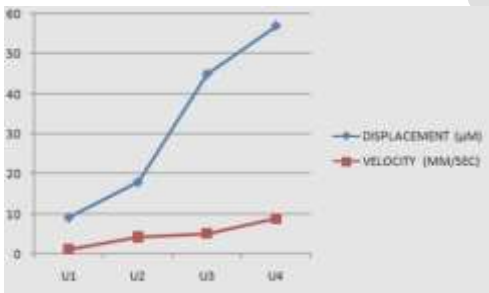
1.5.1 SEED CHANNEL READINGS WITHOUT LOADING OF GINNING MACHINE

position	Displacement (μM)	Velocity (mm/sec)
u1	10	0.8
u2	22	4
u3	55	5.5
u4	60	10



1.5.2 SEED CHANNEL READINGS WITH LOADING OF GINNING MACHINE

POSITION	DISPLACEMENT (µM)	VELOCITY (MM/SEC)
U1	9.2	1.2
U2	18	4.2
U3	45	5.1
U4	57	8.8

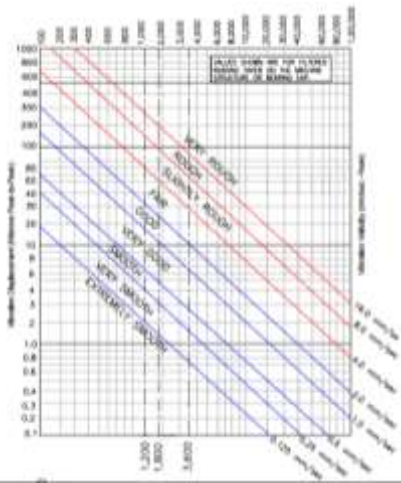


NOTE: Measuring Instrument-IRD306 PORTABLE ANALOG VIBRATION METER

1.6 Severity Chart

Instrumental Intensity	Acceleration (g)	Velocity (cm/s)	Perceived Shaking	Potential Damage
I	< 0.0017	< 0.1	Not Felt	None
II-III	0.0017 - 0.014	0.1 - 1.1	Weak	None
IV	0.014 - 0.039	1.1 - 3.4	Light	None
V	0.039 - 0.092	3.4 - 8.1	Moderate	Very light
VI	0.092 - 0.18	8.1 - 16	Strong	Light
VII	0.18 - 0.34	16 - 31	Very Strong	Moderate
VIII	0.34 - 0.65	31 - 60	Severe	Moderate to Heavy
IX	0.65 - 1.24	60 - 116	Violent	Heavy
X+	> 1.24	> 116	Extreme	Very Heavy

1.7 GENERAL MACHINERY VIBRATION SEVERITY CHART (METRIX)



Working Environment





RESULT & CONCLUSION

Remarkable advancement has taken place in the ginning technologies in during and post TMC era in India. It has kept the momentum of modernization of cotton ginning & pressing sector of India. Increased productivity of ginning machines, reduction of manpower and electrical power, reduction in contamination and improved cotton quality are benefits of these developments which resulted in increased export of cotton from India. Further, the developments taken in the cotton ginning & pressing technologies in India have made India a net exporter of these technologies, machinery and turnkey projects to various countries. Roller ginning technology would be a viable alternative for ginning the cotton produced in

Bangladesh.

The effects of whole-body vibration are usually greatest at the lower end of the range, from 0.5 to 100 Hz. For hand-transmitted vibration, frequencies as high as 1,000 Hz or more may have detrimental effects. Frequencies below about 0.5 Hz can cause motion sickness. The transmissibility of the body is highly dependent on vibration frequency, vibration axis and body posture. Vertical vibration on a seat causes vibration in several axes at the head; for vertical head motion, the transmissibility tends to be greatest in the approximate range of 3 to 10 Hz. The broader frequency range associated with whole-body vibration (between 0.5 and 100 Hz) compared to that for natural motion (between 2 and 8 Hz for voluntary movements, and below 4 Hz for locomotion) is a further difference that helps to explain reactions of the neuromuscular control mechanisms at very low and at high frequencies. Electromyography data suggest that an increased spinal load can occur due to reduced muscular stabilization of the spine at frequencies from 6.5 to 8 Hz and during the initial phase of a sudden upward displacement. In spite of weak EMG activity caused by whole-body vibration, back muscle fatigue during vibration exposure can exceed that observed in normal sitting postures without whole-body vibration. Tendon reflexes may be diminished or disappear temporarily during exposure to sinusoidal whole-body vibration at frequencies above 10 Hz. Minor changes of postural control after exposure to whole-body vibration are quite variable, and their mechanisms and practical significance are not certain. Experiments with short-term and prolonged combined exposures to noise and whole-body vibration, seem to suggest that vibration has a minor synergistic effect on hearing. As a tendency, high intensities of whole-body vibration at 4 or 5 Hz were associated with higher additional temporary threshold shifts (TTS)

REFERENCES:

1. Patil, P.G. and Padole, P.M. 2003. Double Roller cotton ginning machine, its drawback and possible modification. Proceedings of 11th National Conference on Machines and Mechanisms (NaCOMM-2003), IIT, Delhi, pp 745-749.
2. Patil, P. G., Arude, V. G., Anap, G. R. 2006. Design and development of cylinder type cotton pre-cleaner. Journal of Agricultural Mechanisation in Asia, Africa and Latin America (AMA), 37(3), 46-51.

10. Sharma, M. K., 2014. Advances in Cotton Ginning Technology in India during 2010-2013.
6. Book of papers, National Seminar on "Advances in Cotton Ginning and Testing Technology" organised by Indian Fibre Society (IFS) and CIRCOT, Mumbai.
7. Anthony, W.S. and O.L. McCaskill. 1978. Low-noise versus standard brush cylinders for gin machinery. Transactions of the
8. ASAE 21(6):1045-1050.
9. Anthony, W.S. R.A. Wesley and O.L. McCaskill. 1978. Noise levels of cotton ginning systems. Transactions of the ASAE
10. 21(2):574-580.
11. Laird, Weldon, and Joe D. Anderson. 1977. Better doffing: less noise. The Cotton Ginners' Journal and Yearbook. 45(1):30-
12. 37.
13. Miller, R.K. 1976. Handbook of Industrial Noise Management. Atlanta, GA: The Fairmont Press.
14. <http://www.sengpielaudio.com/calculator-soundlevel.htm>

IJERGS

AN EXPERIMENTAL INVESTIGATION ON USE OF MULTI-WALLED CARBON NANOTUBES TO IMPROVE THE PERFORMANCE OF AN OILFIELD APPLICABLE WATER-BASED DRILLING FLUID

Shadfar Davoodi¹, Ahmad Ramazani S.A², Khalil Shahbazi³, Sajad Mardaninia⁴

¹ Sharif University of Technology, Chemical and Petroleum Engineering Department, Kish International Campus, Iran

davoodi_shadfar@kish.sharif.edu

² Sharif University of Technology, Chemical and Petroleum Engineering Department, Tehran, Iran

ramazani@sharif.edu

³ Petroleum University of Technology, Ahwaz, Iran

Shahbazi@put.ac.ir

⁴ Islamic Azad University, faculty of engineering, Omidiyeh, Iran

sajad.mardaninia@yahoo.com

Abstract— Multi-walled carbon nanotubes (MWCNTs) is one of the novel nanomaterials in the industry. In this research, the MWCNTs was added to an industrial water based drilling fluid as a substitution for polyanionic cellulose (PAC-LV) to reduce the fluid loss volume under LP-LT well condition. The effects of different concentrations of MWCNTs addition on the rheological and filtration properties and filter cake characteristics was investigated. The achieved results of this work proved that the fluid loss volume of the water based drilling fluid is decreased about 46.5% in the presence of 1.75 gr MWCNTs. In addition, the mud cake characteristics and rheological properties such plastic viscosity, yield point and gel strength of nanofluids with different concentrations of MWCNTs were better than the based fluid which had PAC-LV in its formulation. The successful use of MWCNTs showed that this nano materials can replace in water-based drilling fluid instead of PAC-LV to improve the drilling fluid performance.

Keywords — Filtrate Volume ,Filter Cake Thickness, Fluid Loss Volume, Rheological Properties, Water base Drilling Fluid, Multi-Walled Carbon Nano Tubes.

1-Introduction

The success of drilling oil and gas wells are highly relying on the drilling mud utilized during drilling and completion operations, therefore, design and formulate a suitable drilling fluid which has good rheology and filtration properties is an important key to a successful drilling operation (A.R Ismail, Tan. C Seong, N. A. Buang, & Sulaiman, 2014; Hareland, Wu, Lei, Husein, & Zakaria, 2012). Filtration loss (fluid loss) is a measure of the relative amount of fluid invaded (filtrate) through permeable formations when the drilling fluid is exposed to a pressure differential (Nmegbu, 2014). Filtration control is so important during a well drilling to minimize the expenditures of the drilling fluids and also decrease the formation damage which is a challenge that happens because of the invasion of the mud filtrate into the permeable formation. Most of the drilling fluids have solid particles such as clays, barite and etc. which these solid particles can migrate by filtrate invasion into the formation and bridge in the formation pores entrance which it can damage the formation. Overly, filtrate invasion into reservoir formation can reduce the productivity of the well by closing the exit flow paths of the hydrocarbon and collapsing the formation pores (A.R Ismail, Tan. C Seong, N. A. Buang, & Sulaiman, 2014). many different additives usually have been used to control and minimize the filtration loss volume such as starch, lignosulfonates, bentonite and some polymers (Krueger, 1963). Nanotechnology comes to the interest of oil and gas industry as a candidate that offer the solution for the above challenges due to its special character (A.R Ismail, Tan. C Seong, N. A. Buang, & Sulaiman, 2014). Carbon nanotubes (CNTs) are graphitic carbon hollow nanometer size tubes of graphitic carbon. A carbon nanotube can be supposed as a graphene sheet rolled in the form of a seamless cylinder. CNTs can be separated into two main types: the first type is single-walled carbon nanotubes (SWCNTs) and another type is multi-walled carbon nanotubes (MWCNTs). A single-walled carbon nanotube can be depicted as a single graphene sheet rolled into a tube, whereas, the multi-walled nanotubes can be depicted as a number of concentric SWCNTs which different diameters (Ahmad et al., 2013). A variety of nano materials has been used in recent research on drilling fluids to improve the rheological properties and minimize the fluid loss volume of the drilling fluids. Abdul Razak Ismail et al, investigated the effects of nano metal oxides such aluminum oxide, copper oxide and titanium oxide on the performance

of a water-based drilling fluid. The rheological and filtration characteristics of each mud samples with different nano metal oxides were evaluated by HP-HT filter press and rotational viscometer. They proved that use of nanoparticles into water base drilling fluid at HPHT condition have better results since the fluid loss and the filter cake thickness was reduced. For example, the addition of 1 gr titanium oxide in the water-based drilling fluid resulted more than 50% reduction in filtration loss and the mud cake thickness reduced to about 30%. This is due to the large surface area to volume ratio of nanoparticles to build structural barriers to the pore spaces to block and seal the porous media (A.R Ismail, Tan. C Seong, N. A. Buang, & Sulaiman, 2014). Adel M. Salem Ragab et al, showed in their work that the nanoparticles of silicon oxide (SiO₂) can be utilized in the drilling fluid to improve its filtration properties and reduce the fluid loss volume. Their results proved that silica nanoparticles can be more effective to reduce the filtrate volume than conventional fluid loss control additive such PAC-LV and PAC-HT (Ragab & Noah, 2014). The objective of this work is that use the MWCNTs as a substitution for low viscosity polyanionic cellulose (PAC-LV) to minimize the fluid loss volume in a field applicable water based drilling fluid which is being used for drilling a well at the low-pressure low-temperature condition in one of the Iranian oilfields. Additionally , the use of nanoparticles may successfully improve the rheological properties of the drilling fluid because of the specific properties of nanomaterials. The successful using of MWCNTs can convince that this nano-Materials is applicable in the industrial drilling fluid for using in the oilfield drilling operations to reduce and minimize the formation damage which may happen due to the fluid loss through the reservoir formation.

2-Materials and Methods

2-1- Testing Equipment

The equipment which was used in this work comprises Hamilton beach mixer, digital pH meter, mud balance, Fann viscometer, API LT-LP filter press, measuring cylindrical tube, vernier caliper.

2-2- Materials

The materials which were utilized in the formulation and their function to prepare the mud samples are presented in table 1.

Table 1- The materials and their function	
<i>Component</i>	<i>Function</i>
<i>Water</i>	<i>The continuous phase of drilling mud sample</i>
<i>Caustic soda</i>	<i>pH modifier additive</i>
<i>Soda ash</i>	<i>pH modifier additive</i>
<i>Sodium chloride</i>	<i>shale inhibitor and d weighting agent</i>
<i>Potassium chloride</i>	<i>Used as shale inhibitor additive</i>
<i>Polyanionic cellulose (PAC)</i>	<i>Used as a fluid loss control additive</i>
<i>Limestone</i>	<i>weighting agent</i>
<i>Starch HT</i>	<i>viscosifire and fluid loss control additive</i>
<i>XC polymer</i>	<i>viscosifire additive</i>
<i>Multi-walled Carbon Nanotubes</i>	<i>fluid loss control additive</i>

2.3 Multi-Walled Carbon Nanotubes Characterization

Multi-walled carbon nanotubes are one of the novel nanomaterials in the industry. The specification of the MWCNTs which was used in the experiments is presented in table 2. Scanning Electron Microscopy (SEM) image of MWCNTs which was used in the experiments is shown figure 1.

<i>Criteria</i>	<i>Details</i>
<i>Product name</i>	<i>Multi-walled carbon nanotubes</i>
<i>Purity</i>	<i>95 wt% (carbon nanotubes)</i>
<i>Outside diameter</i>	<i>20-30 nm</i>
<i>Inside diameter</i>	<i>5-10 nm</i>
<i>Length</i>	<i>10-30 um</i>
<i>Color</i>	<i>Black</i>
<i>True density</i>	<i>2.1 g/cc</i>

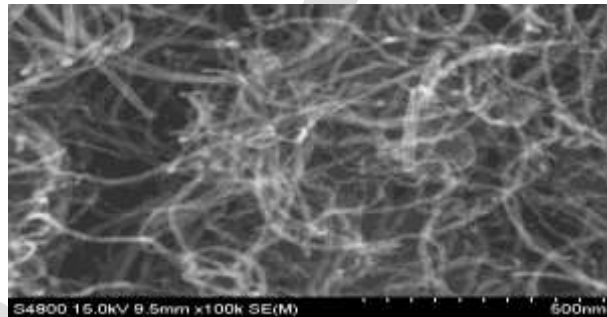


Figure 1- SEM imaging of MWCNT

2-4 Mud Sample Preparation

A field applicable mud formulation which has being used to drill a well in one of the Iranian oilfields was selected and four mud sample were designed and formulated which the mud formulations are presented in table 3. From table 3, It can be noticed that there were no multi-walled carbon nanotube (MWCNTs) in the base mud sample but the other samples, MWCNT with different concentration was subtracting in the mud formulation as fluid loss control agent instead of the PAC-LV to examine the performance of nano additive as filtration control additive in compared to PAC-L.

Component	Base Mud	Mud 1	Mud 2	Mud 3
-----------	----------	-------	-------	-------

<i>Water (bbl)</i>	350	350	350	350
<i>Caustic soda (lb/bbl)</i>	0.5	0.5	0.5	0.5
<i>Soda ash (lb/bbl)</i>	0.5	0.5	0.5	0.5
<i>Sodium chloride (lb/bbl)</i>	90.8	100	100	100
<i>Potassium chloride (lb/bbl)</i>	20	15	15	15
<i>Polyanionic cellulose (lb/bbl)</i>	1.75	–	–	–
<i>Limestone (lb/bbl)</i>	60	30	30	30
<i>Starch HT (lb/bbl)</i>	8.9	8.9	8.9	8.9
<i>XC polymer (lb/bbl)</i>	0.6	0.6	0.6	0.6
<i>MWCNT (wt. %)</i>	–	1	3	5

3- Results and discussions

3-1 Effect of MWCNTs Concentration on the density and pH value of drilling fluid

The nanofluid samples and the base mud have the same value of pH which is about 9.5 .According to that nanoparticles have low density and the amount of used nanoparticles to formulate the samples is small so the density of the nanofluid samples and the base mud is equal and the density of the mud sample is 10.5 pound per gallon.

3-2 Effects of MWCNTs Concentration on the drilling fluid Rheology

The rheological performance of drilling fluid can be defined in three characteristics of the fluid which are plastic viscosity (PV), yield point (YP) and gel strength. Plastic viscosity is the Fluid resistance to flow which is due to mechanical friction between the solid phase and liquid phase of drilling fluid .the another component of the fluid resistance to flow in Bingham plastic model is yield point which is due to electrochemical forces between the particles under the conditions of flowing. These electrochemical forces are the result of charges positioned on the surface the particles which are dispersed in the fluid phase. The strength of attractive force (gelation) in the satirical conditions is defined as fluid gel strength (Wahid, Yusof, & Hanafi, 2015). The rheological properties of the mud samples were measured by a rotational viscometer and the comparison of plastic viscosity and yield point for the samples which were obtained from two different speeds (300 and 600) of rotational viscometer dial reading based on Bingham Plastic Model are presented in figure 2.

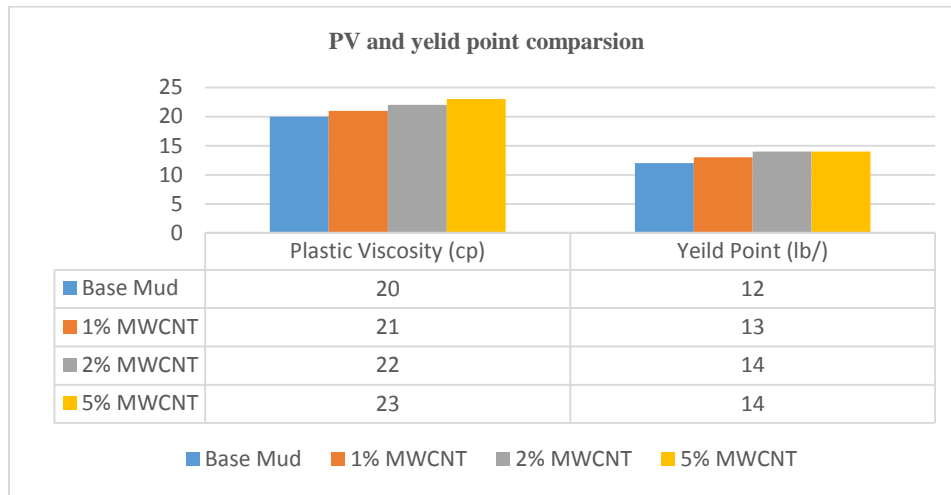


Figure 2- The comparison of plastic viscosity and yield point

Nano Materials have more surface area per volume than other materials such micro and macro sized Materials. The nanoparticles surface area can serve as places for bonding with functional groups can affect chain entanglement and therefore can create a wide range of properties in the matrix. Therefore, the base fluid and the nanoparticles may be created a bond with each other directly or through certain intermediate chemical linkages to make better the plastic viscosity of water based drilling fluid (Quintero, Cardenas, & Clark, 2014) . The results in figure 2 show that the mud samples which includes MWCNTs in its formulation had higher values of plastic viscosity and yield point values than the base mud sample. In addition, as the concentration of nano-materials increased in the samples their plastic viscosity increased and yield point which the highest plastic viscosity and yield point value is observed for mud sample with 5 weight percent of MWCNTs. The comparison of gel strength 10 minute and 10 seconds between the muds samples are shown in figure 3. Figure 3 shows that as the concentration of MWCNTs increases in the samples both values of gel strength increases. This increase in gel strength value is due to the attractive force between nanoparticles which form a rigid structure by creating a linkage between nanoparticles and base fluid during 10 seconds and 10 minutes period (A.R Ismail, Tan. C Seong, N. A. Buang, & Sulaiman, 2014). By comparing the results of nanofluids and the base mud it can be proved that the nanoparticles can properly improve the rheological properties of drilling mud.

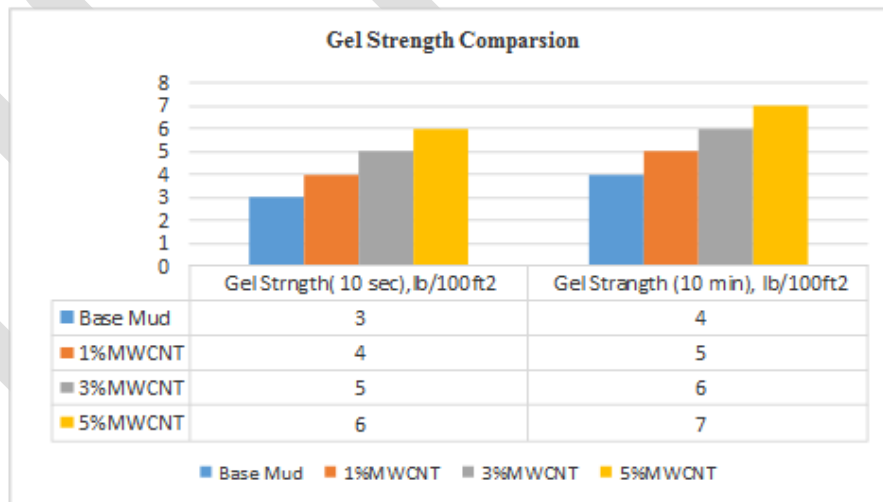


Figure 3- The comparison of Gel strength 10 min and 10 sec

3-3 Effects of Nanoparticles Concentration on the Mud Filtration Properties

The fluid loss of drilling mud should have the lowest value during the drilling operation to reduce the formation damage and prevent from the tight hole and differential pipe sticking. API LT-LP filtration tests were done on the mud samples to investigate the mud cake

thickness and quality and fluid loss volume loss for the mud sample under 100 psi pressure and room temperature condition. The volume fluid loss which was collected from the samples within thirty minutes filtration tests period is shown in table 4.

Time (min)	Filtrate volume (mL)			
	Base Mud	Mud 1	Mud 2	Mud 3
5	2.2	1.8	1.6	1.4
10	3	2.6	2.3	1.9
15	4.4	3.3	2.8	2.4
20	4.9	3.6	3.1	2.7
25	5.4	3.9	3.4	2.9
30	5.8	4.2	3.7	3.1

From the table 4, it can be noticed that generally, the addition of MWCNTs into mud sample formulation can significantly reduce the amount of collected filtrate volume during the test. The increase in nanoparticles concentration has a significant effect on filtrate volume which the smallest amount of filtrate volume observed for the sample by addition 5% MWCNTs in its mud formulation that is about 3.1 ml. there is a reduction of 46.55 %, 27.58% and 36.20% in passed filtrate volume from the mud cake during 30 minutes, respectively for the sample with 1%MWCNTs, 2% MWCNTs and 5% MWCNTs. The reduction of filtrate volume for Nanofluids is due to that the dispersed MWCNTs in the mud samples can act as plaster between the particles and seal the permeable formed mud cake to decrease the filtration loss (Park et al., 2012).The comparison of the thickness of filter cake of the samples is presented in figure 4.

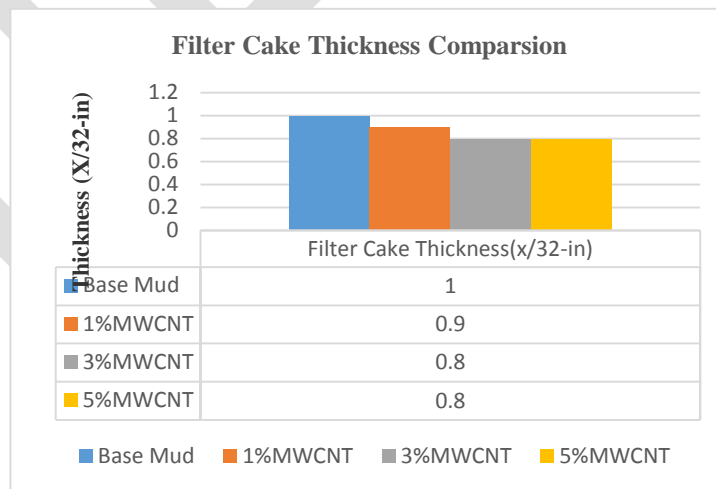


Figure 4 –The comparison of the thickness of filter cake for the

samples

From figure 4 it can be seen that the thickness of the formed mud cake from the nanofluids is thinner than the base mud filter cake thickness. In addition, the MWCNTs concentration increasing in the Nanofluids formulation does not dramatically change the filter cake thickness. The results of the rheology a filtration tests convinced that multi-walled carbon nanotube can substitute in mud formulation instead of polyanionic cellulose to improve the rheological properties and filtration properties of drilling fluid. Nanoparticles had a great effect on filtration properties which it observed the nanofluid had a smaller amount of fluid loss that can reduce the formation damage and the thinly formed filter cake of nanofluids can reduce the risk of differential sticking pipe. The most important aspect of this work is that the multi-walled carbon nanotube is applicable for using in the field mud formulation as it observed 1% MWCNTs had better filtration and rheology in compare to the base sample which had of 5 Wight percent PAC-LV as fluid loss control additive.

4- Conclusion

The multi-walled carbon nanotubes can use as fluid loss control additive in the mud formulation by 46 .5% reduction in the filtrate volume which was produced during the filtration test in compared to the base sample. An in an increase in MWCNTs concentration can properly increase the rheological properties such as of yield point, plastic viscosity and gel strength of the water base drilling fluid. The successful use of multi-walled carbon nanotube shows that MWCNT is more effective in improving the rheological properties and reducing the fluid loss than the commercial fluid loss control agent such low viscosity polyanionic cellulose, therefore, MWCNTs can be used as a substitution for PAC-LV in the mud formulation because of its a great capability to reduce the fluid loss and improve the rheology of the mud. According to that the selected water-based mud formulation for the work is an industrial (field applicable) formulation therefore the results of the tests proved that MWCNTs can utilize in the oilfield drilling operations to improve the performance of water-based drilling fluid.

REFERENCES:

1. A.R Ismail, Tan. C Seong, N. A. Buang, & Sulaiman, a. W. R. N. (2014). *Improve Performance of Water-based Drilling Fluids Using Nanoparticles*. Paper presented at the The 5th Sriwijaya International Seminar on Energy and Environmental Science & Technology, Indonesia.
2. Ahmad, S. N., Hakeem, S., Alvi, R. A., Farooq, K., Farooq, N., Yasmin, F., & Saeed, S. (2013). *Synthesis of multi-walled carbon nanotubes and their application in resin based nanocomposites*. Paper presented at the Journal of Physics: Conference Series.
3. Hareland, G., Wu, A., Lei, L., Husein, M. M., & Zakaria, M. F. (2012). *Innovative Nanoparticle Drilling Fluid and Its Benefits to Horizontal or Extended Reach Drilling*. Paper presented at the SPE Canadian Unconventional Resources Conference.
4. Krueger, R. F. (1963). Evaluation of drilling-fluid filter-loss additives under dynamic conditions. *Journal of Petroleum Technology*, 15(01), 90-98.
5. Nmegbu, C. G. J. (2014). Bacteria as a Filtration Loss Reducing Agent during Drilling. *international journal of engineering and research and application*, Vol. 4(Issue 6), 191-194.
6. Park, J., Kim, G., Yoon, D., Sin, C., Park, I., Bea, T., & Lee, M. (2012). The Effect of Dispersed MWCNTs Using SDBS Surfactant on Bacterial Growth. *World Academy of Science, Engineering and Technology*, 6, 697-700.
7. Quintero, L., Cardenas, A. E., & Clark, D. E. (2014). Nanofluids and methods of use for drilling and completion fluids: Google Patents.
8. Ragab, A. S., & Noah, A. (2014). Reduction of formation damage and fluid loss using nano-sized silica drilling fluids. *Petroleum Technology Development Journal*, 2, 75-88.
9. Wahid, N., Yusof, M. A. M., & Hanafi, N. H. (2015). *Optimum Nanosilica Concentration in Synthetic Based Mud (SBM) for High Temperature High Pressure Well*. Paper presented at the SPE/IATMI Asia Pacific Oil & Gas Conference and Exhibition.

Effect of Solar Illuminance (or Intensity) on Solar (Photovoltaic) cell's output and the use of Converging lenses and X or Gamma rays to enhance output performance

Joseph Amajama

Electronics and Computer Technology Unit – Physics Department – University of Calabar – Nigeria, joeamajama2014@yahoo.com
+234-7036357493

Abstract— The effect of solar illuminance (or intensity) on a photovoltaic panel has been examined. Illuminance is synonymous to light intensity. Illuminance is directly proportional to light intensity per square of the distance between the source of light and object. The solar illuminance (or intensity) within the weather parameters' ranges of 77 °F – 90 °F (air temperature), 30 inHg – 29.85 inHg (air pressure), 66 % and 89 % (relative humidity) and 5 mph – 10 mph (Wind speed), mainly in the WSW direction was measured and simultaneously the output current and voltage. The solar illuminance (or intensity) was measured with a Digital Illuminance Meter (DT-1309). The result spells that the current rises steadily with increase in solar illuminance or intensity. However, the rise rate reduces at a point with further increase in illuminance (or intensity), when the raining light excessively extract electrons (or holes), gradually resulting in collisions and a randomized flow, rather than the regular flow. The voltage output rises sharply with increasing illuminance (or intensity), but at a certain point attains the maximum level. Afterwards, the rate of change of the voltage with increasing illuminance (or intensity) becomes insignificant. The response curve at this point becomes steady. The current output of solar cells is polynomial while that of the voltage is logarithmic. The power output of the solar cell is directly proportional to the output current, regardless of that of the voltage under similar atmospheric conditions. The power output response curve takes the form of the current curve. Hence under similar weather conditions, provided that the capacity of a photovoltaic cell is not exceeded – $P = KIL^2$: where P is the power (Watt), I is the current (A), L is illuminance (Lux) and K is the loss or gain power factor depending on the photovoltaic cell. Also, since solar illuminance (or intensity) has a high positive effect on the solar cells, a good converging lens to focus solar radiations on the photovoltaic panel will enhance the efficiency of the output, most especially in regions of low sunlight. And, since the current is generated as a result of photoelectric effect: it is possible for higher energetic particles above the ultraviolet particles to extract and excite more electron or current than solar radiation (mainly visible light and ultraviolet particles) and improve output. This may be recommended for the Polar Regions. Gamma or X-ray particles may be incident on the photovoltaic panel.

Keywords— Effect, Solar illuminance, Solar intensity, Photovoltaic cell, Solar cell, Photovoltaic panel, Solar panel, Output, Performance, Converging lenses and X or Gamma rays.

INTRODUCTION

Luminosity is the rate of [emission](#) of [radiation](#), [visible](#) or otherwise [1]. Illuminance in short, is the amount of [luminous flux](#) incident on a surface per unit area [2]. It is a measure of how much the incident [light](#) illuminates the surface, wavelength-weighted by the [luminosity function](#) to correlate with human brightness perception. The SI unit of illuminance is Lux. Illuminance was formerly often called [brightness](#), but this leads to confusion with other uses of the word, such as to mean [luminance](#). "Brightness" should never be used for quantitative description, but only for non-quantitative references to physiological sensations and perceptions of light. [3].

As a surface that is illuminated by a light source moves away from the light source, the surface appears dimmer. In fact, it becomes dimmer much faster than it moves away from the source. The inverse square law, which quantifies this effect, relates illuminance (E) and intensity (I) as follows: $E = I/d^2$; Where d = the distance from the light source. For example, if the illuminance on a surface is 40 lux (lm/m²) at a distance of 0.5 meters from the light source, the illuminance decreases to 10 lux at a distance of 1 meter [4].

The sun radiates an overwhelming volume of energy onto the earth to meet the global energy demand for a whole year. Solar panels produce energy less than a tenth of one percent of the entire global energy demand. The panels are called photovoltaic cells which are found on things like spacecraft, rooftops, and calculators. The cells are made of semiconductor materials like those found in computer chips. When sunlight strikes the cells, it extracts and excites the electrons from their atoms. The electrons generate electricity as they flow through the cell [5].

Nearly every technological apparatus requires power for its optimal performance [6]. A solar panel can generate power with a four-piece battery system that can be filled with unfiltered water, and the battery can recycle water to generate battery or power. If three panels are put together, these can produce enough electrical energy to power a home with a family of four to eight people living within the structure it is powering [6]. It also allows a vehicle to run on solar power. In addition, a typical solar panel produces 200 watts of power or more. To power a building like a bank, for example, a five kilowatt-hour array, which is about 25 solar panels, is necessary [6]. The solar panels will absorb 1,000 watts of sunlight per square meter on the panels' surfaces. To power a high school building, a 6.25 megawatt capacity, equivalent to 24 solar panels, is needed [5].

Changing the light intensity incident on a solar cell changes all solar cell parameters, including the short-circuit current, the open-circuit voltage, the fill factor, the efficiency and the impact of series and shunt resistances [7] [8] [9]. The light intensity on a solar cell

is called the number of suns, where 1 sun corresponds to standard illumination at 1 kW/m^2 . Solar cells experience daily variations in light intensity, with the incident power from the sun varying between 0 and 1 kW/m^2 . At low light levels, the effect of the shunt resistance becomes increasingly important [7]. As the light intensity decreases, the bias point and current through the solar cell also decreases and the equivalent resistance of the solar cell may begin to approach the shunt resistance. When these two resistances are similar, the fraction of the total current flowing through the shunt resistance increases, thereby increasing the fractional power loss due to shunt resistance. Consequently, under cloudy conditions, a solar cell with a high shunt resistance retains a greater fraction of its original power than a solar cell with a low shunt resistance [7] [10].

This object of this paper is to find the relationship between solar illuminance (or intensity) and the output of solar panels and make recommendations on how the output can be enhanced through the science from this paper.

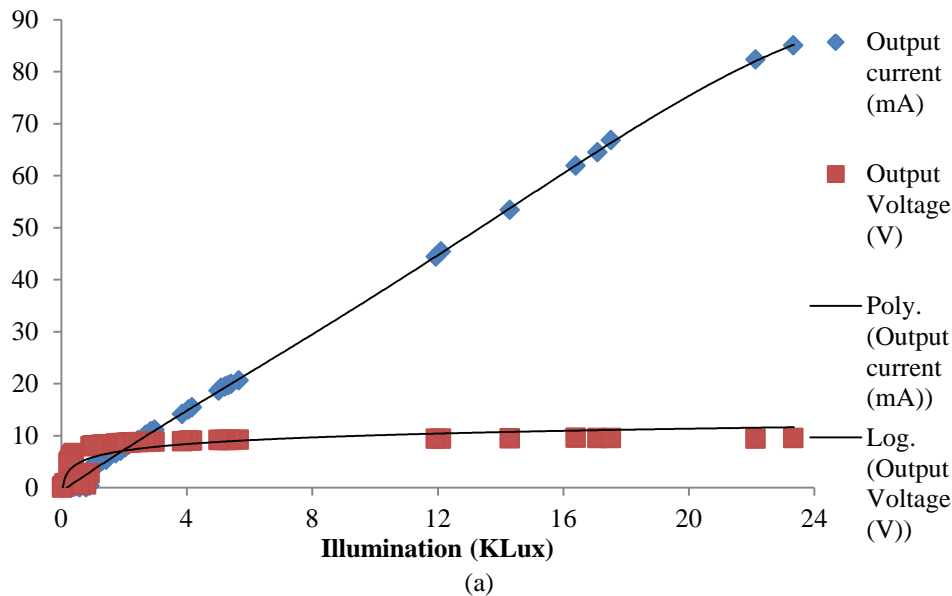
METHODOLOGY

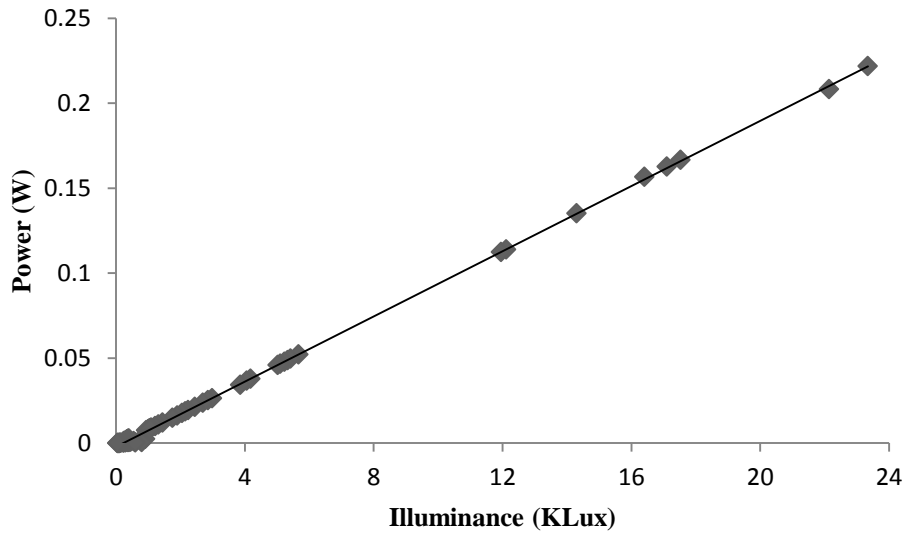
Weather parameters: air temperature, air pressure, relative humidity and wind speed and direction were measured intermittently and simultaneously with solar illuminance and output voltage (open circuit voltage) and output current (short circuit current) of the solar panel.

The solar panel is the mono-crystalline cell type with 1.5 W, 12 V rating. The dimensions of the solar cells' plate excluding the metallic frame of the panel is 45 cm by 14.5 cm. It was mounted on a platform of about 105 cm and exposed to direct sunlight. The outputs of the panel (current and voltage) were measured with the aid of a multimeter and the solar illuminance was measured with a Digital Illuminance Meter (model: DT-1309).

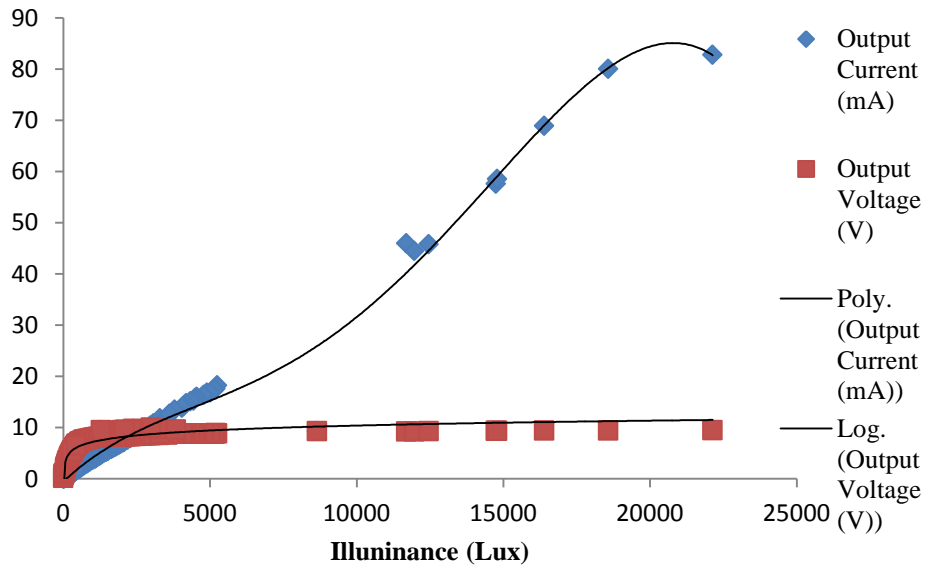
RESULT AND ANALYSIS

There are so many weather parameters. The major or basic ones are: air temperature, air pressure, relative humidity and wind [11] [12]. The following are the results from the comparison between solar illuminance (or intensity) and the outputs of the solar panel within the tropical weather parameters' ranges of $77^\circ\text{F} - 90^\circ\text{F}$ (air temperature), 30 inHg – 29.85 inHg (air pressure), 66 % and 89 % (relative humidity) and 5 mph – 10 mph (Wind speed). The wind was running mainly in the WSW direction. Measurements were taken in the time course of daylight, on three (3) different days to reach a rational decision. Fig. 1 shows solar illuminance (or intensity) against solar panel Outputs (Day 1). Fig. 2 shows solar illuminance (or intensity) against Solar panel Outputs (Day 2) and fig. 3 shows solar illuminance (or intensity) against solar panel Outputs (Day 3).

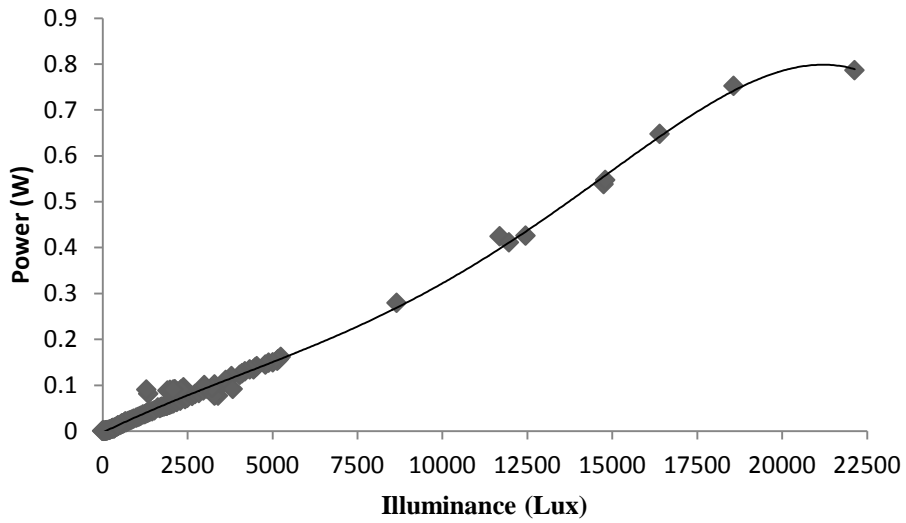




(b)
Fig. 1: Solar illuminance (or intensity) against Solar panel Outputs (Day 1)

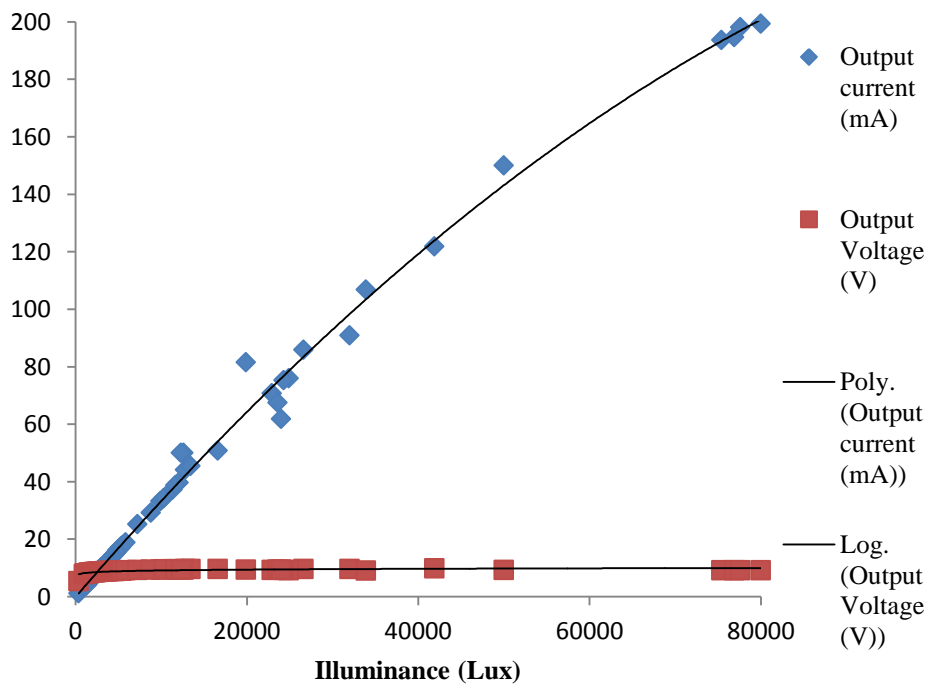


(a)



(b)

Fig. 2: Solar illuminance (or intensity) against Solar panel Outputs (Day 2)



(a)

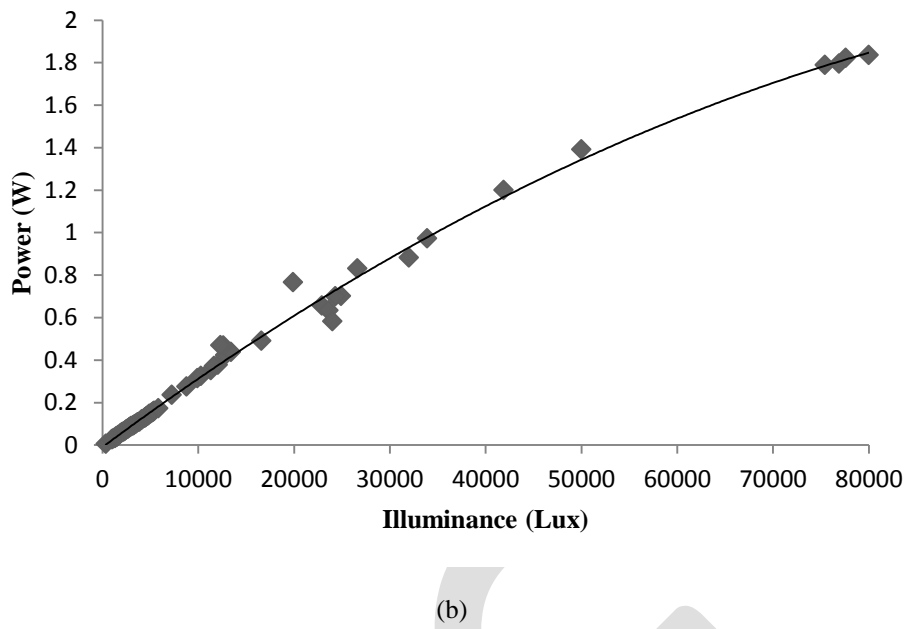


Fig. 3: Solar illuminance (or intensity) against Solar panel Outputs (Day 3)

In fig. 1 observe that the output voltage rises rapidly to a maximum value and remains steady throughout, despite increase in solar illuminance (or intensity). While the current rises steadily to a maximum against solar illuminance (or intensity). The voltage curve is logarithmic while the current curve is polynomial.

Also fig. 1, the power rises steadily to a maximum against solar illuminance (or intensity). The power output curve is a twin of that of the current in regard to form. In other words, with increasing solar illuminance (or intensity), the current output is directly proportional to the power output, regardless of the voltage output. The maximum solar illuminance in fig. 1 is 24 Klux and at this value, there was still room for increment of current output against increasing illuminance, since the curve at the tail end is still steep.

In fig. 2, the voltage output rises rapidly to a maximum value and ceases. Afterwards, it maintains a flat response curve, despite increase in solar illuminance (or intensity). However, the current output rises gradually, but retarding in steepness to a maximum value, thereafter, increment was nearly negligible and the output current begins to drop with further increment in solar illuminance (or intensity). The drop is as a result of random orientation and collision of the excess electrons extracted from the solar cell atoms, causing an opposition to free flow. This occurs at an illuminance (or intensity) of 25.5 Klux.

Also in fig. 2, the current output response is polynomial and that of the voltage is logarithmic like the latter fig. More so, the power output curve parallels the output current curve. Hence, the output current is positively proportional to the power output curve.

In fig. 3, there is a steady rise in the output current at the onset and gradual decay in the steepness towards the tail end. This is due to the approach of avalanche of extracted electrons from the solar cell atoms, resulting in a bit by bit disorientation of the electron flow. A point of fact is that current is a rhythmic but not randomize flow of electrons. In the event of an overwhelming rain of light particle, a flood of electrons is produced by the solar cells resulting in a disorientation and collision.

Also, in fig. 3, the power output response curve is an image of the current output curve in regard to form. This indicates that the current output is directly proportional to the power output. Similar to fig. 1 and fig. 2; the current output curve is polynomial and that of the voltage is logarithmic.

In the three (3) figs., the power output rating can be enhanced at high solar illuminance (or intensity), despite the solar panel rating (1.5 W, 12 V). This is as a result of increasing current due to higher level of illuminance (or intensity).

CONCLUSION AND RECOMMENDATIONS

This paper has shown that, solar cell output efficiency is highly enhanced by an increase in solar illuminance (or intensity). The current rises steadily with increase in solar illuminance or intensity. However, the rise rate reduces at a point with further increase in illuminance, when the raining light excessively extract and excite electrons (or holes), gradually resulting in a randomized flow, rather than the regular flow. The voltage output rises sharply with increasing illuminance or intensity, but at a certain point attains the maximum level. Afterwards, the rate of change of the voltage with increasing illuminance or intensity becomes insignificant. The response curve at this point becomes steady. The current output of solar cells is polynomial while that of the voltage is logarithmic. The power output of the solar cell is directly proportional to the output current with change in illuminance, regardless of that of the voltage under similar atmospheric conditions and within the limit of the photovoltaic cell rating. The power output response curve

takes the form of the current curve. Hence under similar weather conditions, provided that the capacity of a photovoltaic cell is not exceeded – $P = KIL^2$: where P is the power (Watt), I is the current (A), L is illuminance (Lux) and K is the loss or gain power factor depending on the photovoltaic cell.

Since solar illuminance (or intensity) has a high positive effect on the solar cells, a good converging lens to focus solar radiations on the photovoltaic panel will really enhance the efficiency of the output, most especially in regions of low sunlight.

Also, since the current is generated as a result of photoelectric effect. It is possible for higher energetic particles above the ultraviolet particles to extract and excite more electron or current than solar radiation (mainly ultraviolet particles) and improve output. This may be recommended for the Polar Regions. Gamma or X-ray particles may be incident on the photovoltaic panel.

REFERENCES:

- [1] Luminosity (2016.). Oxford Dictionaries. Oxford: Oxford University Press. Retrieved 30 May, 2016, From <http://www.oxforddictionaries.com/definition/english/luminosity>.
- [2] Illuminance (2016.). Oxford Dictionaries. Oxford: Oxford University Press. Retrieved 30 May, 2016, From <http://www.oxforddictionaries.com/definition/english/illuminance>.
- [3] Illuminance (2016). In Wikipedia: The Free Encyclopaedia. Retrieved 30 May, 2016, From <https://en.wikipedia.org/wiki/Illuminance>.
- [4] Taylor F. E. A. (N.D.). Illumination Fundamentals. Retrieved 30 May, 2016, From <https://optics.synopsys.com/lighttools/pdfs/illuminationfund.pdf>.
- [5] Gordo E., Khalaf N., Strangeowl T. (2015). Factors Affecting Solar Production Efficiency. New Mexico Supercomputing Challenge, Final Report By Team 88: Miyamura High School.
- [6] Amajama J. (2016). A Bizarre Design And Engineering Physics Of Small/Micro And Pico/Family Hydro-Electric Power Plants/Farms. *Journal Of Scientific And Engineering Research*. 3(2). In Press.
- [7] [Bunea G](#), [Wilson K](#), [Meydbray Y](#), [Campbell M](#), [Ceuster D](#). Low Light Performance of Mono-Crystalline Silicon Solar Cells. In: 4th World Conference on Photovoltaic Energy Conference. Waikoloa, Hi; 2006. Pp. 1312–1314. Available From: http://ieeexplore.ieee.org/xpls/abs_all.jsp?arnumber=4059885&tag=1.
- [8] Solar Cells: Solar Cell Model & What affects Solar Cell performance & Efficiency (2014). In Solar Love. Retrieved 10 May, 2016, from <http://solarlove.org/solar-cell-and-its-characteristics/>.
- [9] Science Buddies Staff (2016). How does Solar Cells output vary with incident light intensity?. Retrieved July 11, 2016 from http://www.sciencebuddies.org/science-fairprojects/project_ideas/energy_p014.shtml.
- [10] Narendra Kumar M., Saini H.S., Anjaneyulu K. S. R. & Singh K. (2014). Solar Power Analysis Based on Light Intensity. *The International Journal of Engineering and Science*, 2319 –1805.
- [11] Weather and Atmosphere (n.d.). In Fundamentals of Environmental Measurements. Retrieved 10 May, 2016 from http://www.fondriest.com/environmental_measurements/parameter/weather/.
- [12] Hocking W. K. (2000). *The Instruments Of Meteorology*. Retrieved 10 May, 2016, From <http://www.physics.uwo.ca/~whocking/P103/Instrum.html>.

Power Reduction in Row Address Circuitry of SRAM Design

Mariyamol.p.p, Aswathy.N

M.tech Student, ASIET kalady, mariyakunchi@gmail.com, 8086807807

Abstract— SRAM memories are used in high speed computers and embedded applications. They are used as register and cache memory of processor. SRAMs operating frequency is compatible with modern processor speed because they are fabricated in CMOS technology. So demand of SRAM memory will remain high in coming years. So there efficient design and fabrication has large scope in current and near future market. The sources of SRAM power are the sum of the power consumed by decoders, memory array, write drivers, Sense amplifiers, and I/O line drivers. This paper is mainly focuses on the development of power efficient SRAM structure. The paper describes the comparison of different decoder circuitries and optimized design of decoder with word line driver while driving large capacitive loads for minimizing power dissipation across load. The comparison has been designed and simulated using Cadence Virtuoso Spectre in 180 nm technology.

Keywords— SRAM, CMOS taper buffer, Decoders, Leakage power, Power dissipation, Tapering factor, SRAM Peripheral circuit

INTRODUCTION

In computers data (information) and program (sequence of commands) are store in some physical devices on permanent or temporary basis. This stored content is used in other computing or on time computing depends on the application. For large data which may need to access in future on permanent basis for that magnetic storage is used. Run time data is stored in semiconductor memories. Computer memories are mainly divided into two parts: Primary memory and Secondary Memory. Semiconductor memories come under primary storage. SRAM is random access memory that means its content can be access from anywhere of storage memory. Data are stored in cells and to access data randomly, fix address is assign to all locations of storage cell. SRAMs are volatile in nature that means their storage data will loss after power shutdown. Therefore they can be used to store run time data in computer systems. SRAM is used as register and cache memory to make faster program execution in computer system. SRAMs are made by using same sources as for process made therefore they are compatible with processor in all extent and their speed is matched with current processor speed. SRAM cell are made up with cross couple inverter latch having positive feedback loop therefore during write operation it store data rapidly.

CMOS technology scaling has been a primary driving force to increase the processor performance. A drawback of this trend lies in a continuing increase in leakage power dissipation .Recent results have shown that leakage in SRAM peripheral circuits, such as word line drivers as well as input and output drivers are now the main sources of leakage[1]. A CMOS Tapered buffer is used to increase the driving ability of the logic circuitry; it is connected with large capacitive load. These are used between logic gate and large capacitive load to increase its drain current strength. These circuits are required which can drive the load at high speed while not degrading the performance of previous stages in the chain of inverters [2].These buffers are used in the memory access path as word line drivers, which is place in the output stage of decoder section.

In brief, two main reasons explain this difference in leakage.

- Memory cells are designed with minimum-sized transistors mainly for area considerations. Unlike memory cells, periphery circuits use larger, faster and accordingly, more leaky transistors so as to satisfy timing requirements
- Memory cells use high threshold voltage transistors, which have a significantly lower leakage reduction compared with typical threshold voltage transistors used in peripheral circuits.

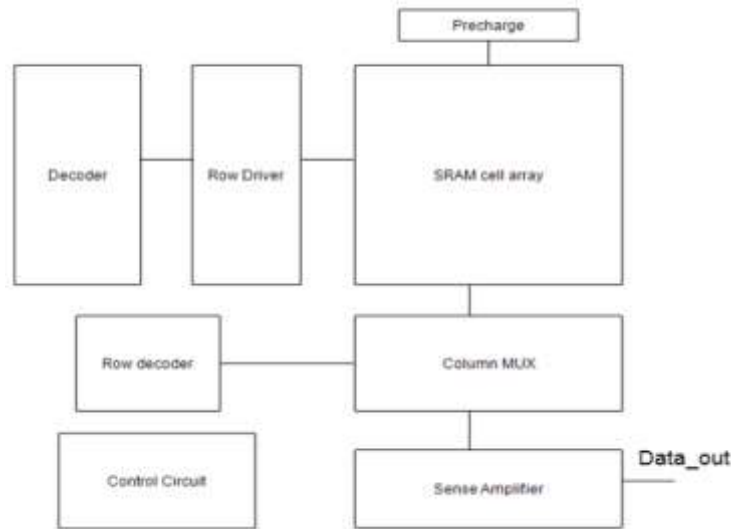


Fig 1: Block diagram of SRAM memory array

Address Decoder is an important digital block in SRAM which takes up to 50% of the total chip access time and notable amount of the total SRAM power in normal read/write cycle. Due to large amount of storage cells in memories it can be found various solutions of address decoder designs leading to power consumption reduction and performance improvement. The focus of this paper is, therefore, reduction of power dissipation across load of SRAM memory array. This paper explores the comparison of different decoder circuits. And also compares the combination of decoder section with word line driver which act as buffers while driving large capacitive load.

Results from the literature survey

TABLE 1: COMPARISON OF DECODER CIRCUITS

Type of decoder	Average power(μ W)
Conventional 2:4 decoder	39.22
Dynamic NAND 2:4 decoder	15.53






Topology's	Technology	Power dissipation(Watts)	Propagation delay
Conventional static CMOS inverter[3]	180-nm	14.44uw	-
Sleepy inverter chain[4]	180-nm	151.03nw	-
Sleepy inverter chain with state retention buffer[4]	180-nm	150.12nw	-
Zig zag sleep buffer[5]	180-nm	7.088 μ w	-
Two stage taper buffer with feedback network[6]	180-nm	15.97% 	4.703% 
Four stage Tapered Vth (constant) CMOS inverter buffer[7]	65-nm ,1.08V	39% 	4% 
1. Four stage Tapered Vth(varying) CMOS inverter buffer[8]	45-nm ,1-V	61% 	10% 
Four stage taper buffer with feedback network[6]	180-nm	13.11% 	7.213% 
Four stage Taper buffer with bypass [9]	65-nm	19.02% 	6.63% 

TABLE 2: COMPARISON OF EXISTING BUFFER TOPOLOGIES

From the survey we can see that, taper buffer with bypass circuits have low power and lower propagation delay compared to all other topologies. By combining best word line driver with power efficient decoder circuit which is dynamic NAND while driving large capacitive load.

DESIGN METHODOLOGY

TABLE 3: WORD LINE DRIVERS DESIGN REQUIREMENTS

Technology	180nm
V _{DD}	3.3V
Tapering factor	4.55
No: of stages	4
Capacitive load	295.8

CIRCUIT DIAGRAMS

Figure below shows the combination of dynamic NAND decoder with conventional taper buffer and the transient analysis

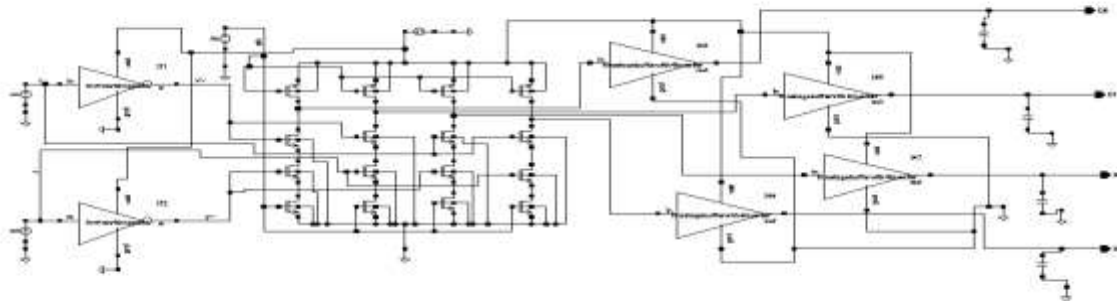


Fig 2: Integration of Dynamic NAND 2:4 decoder with conventional four stage taper buffer circuit

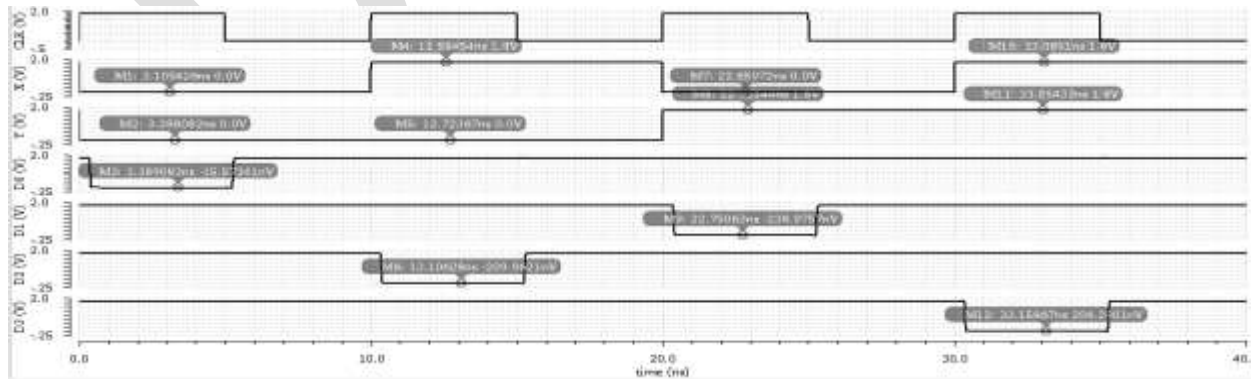


Fig 3: Transient analysis for dynamic NAND 2:4 decoder with conventional four stage taper buffer

Figure below shows the combination of dynamic NAND decoder with bypass buffer and the transient analysis

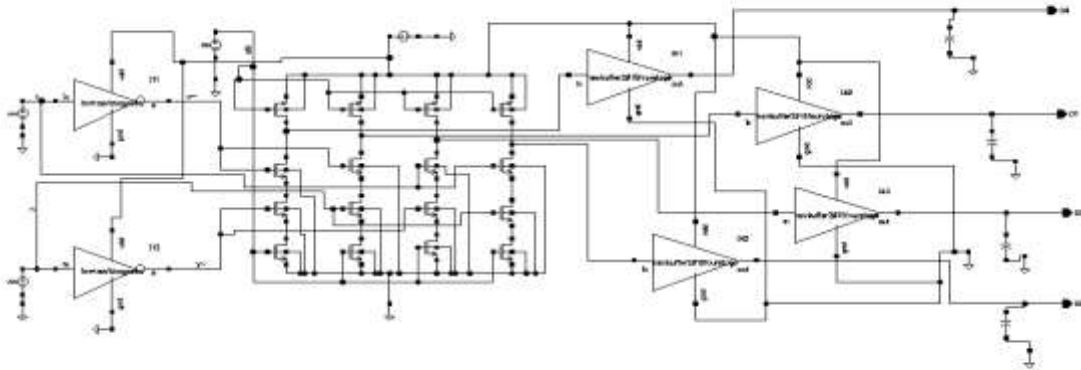


Fig 4: Integration of dynamic NAND 2:4 decoder with four stage CMOS taper with bypass buffer

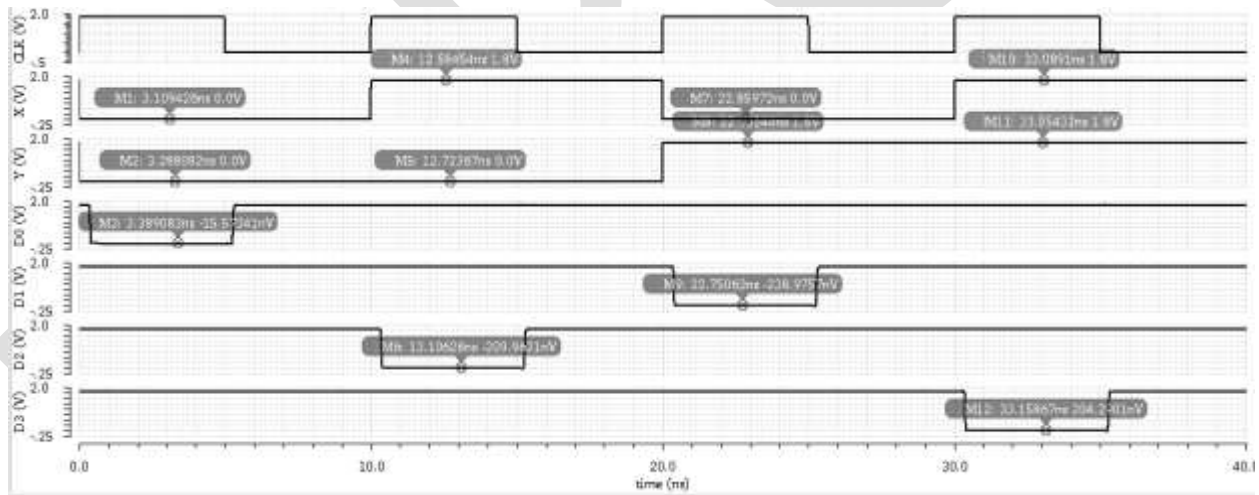


Fig 5: Transient analysis for dynamic NAND 2:4 decoder with four stage CMOS taper bypass buffer

EXPERIMENTAL RESULTS

TABLE 4: COMPARISON RESULTS

TOPOLOGYS	POWER DISSIPATION ACROSS LOAD (nW)			
	00	01	10	11
Dynamic NAND 2:4 decoder with conventional four stage buffer	C1=287.1	C2=224.1	C3=244.7	C4=179.2
Dynamic NAND 2:4 decoder with four stage CMOS tapper bypass buffer	C1=107.2	C2=139.4	C3=221.7	C4=124.5

From the experimental results it can be concluded that, the power dissipation across load while selecting the address of particular SRAM array location is reduced when using the combination of bypass circuit buffer and dynamic NAND decoder.

CONCLUSION

Periphery circuits are important components of SRAM memory and the performance of SRAM depends on these components. Leakage power dissipation of on-chip SRAM constitutes a significant amount of the total chip power consumption in microprocessors and System on chips. In this paper two types of decoders are designed and analyzed for optimum power dissipation across load during the design of SRAM memory architecture. The power dissipation across load can be reduced by combining dynamic decoder circuits with bypass buffer. The comparison has been designed and simulated using Cadence Virtuoso Spectre in 180 nm technology.

REFERENCES:

- [1] A. V. Houman Homayoun, Mohammad Makhzan, \Zz-hvs: Zig-zag horizon-tal and vertical sleep transistor sharing to reduce leakage power in on-chipsram peripheral circuits," IEEE, International Conference on Computer De-sign, pp. 699{706, Oct 2008.
- [2] J.B. Kim "Low-Power Digital Circuit Design with Triple-Threshold Voltage" September 2010, Volume 4, No.9 (Serial No.34) Journal of Energy and Power Engineering, ISSN 1934-8975, USA.
- [3] A. V. Houman Homayoun, Mohammad Makhzan, \Zz-hvs: Zig-zag horizon-tal and vertical sleep transistor sharing to reduce leakage power in on-chip sram peripheral circuits," IEEE, International Conference on Computer De-sign, pp. 699{706, Oct 2008.
- [4] Rajani H.P.1 and Srimannarayan Kulkarni Novel Sleep Transistor Techniques for low leakage power peripheral circuits International Journal of VLSI design & Communication Systems (VLSICS) Vol.3, No.4, August 2012
- [5] A. V. Houman Homayoun, Mohammad Makhzan, \Zz-hvs: Zig-zag horizon-tal and vertical sleep transistor sharing to reduce leakage power in on-chipsram peripheral circuits," IEEE, International Conference on Computer De-sign, pp. 699{706, Oct 2008.
- [6] Design of CMOS Tapered Buffer for High Speed and Low Power Applications using 65nm Technology International Journal of Science and Research (IJSR) ISSN (Online): 2319-7064 Index Copernicus Value (2013): 6.14 | Impact Factor (2013): 4.438

[7] A. V. Houman Homayoun, Mohammad Makhzan, "Zig-zag horizontal and vertical sleep transistor sharing to reduce leakage power in on-chip sram peripheral circuits," IEEE, International Conference on Computer Design, pp. 699-706, Oct 2008.

[8] F. Frustaci, P. Corsonello, and M. Alioto, "Tapered-CMOS buffer design for improved energy efficiency in deep nanometer technology," in *Proc. IEEE Int. Symp. Circuits Syst.*, May 2011, pp. 2075-2078.

[9] Mr. Ankur Saxena*, Mr. Sumit Khandelwal A Novel Design Approach for CMOS Tapered Buffer for Low Power and Low Delay Applications Volume 2 2015 Issue 4 JULY-AUG IJBRITISH

[10] B. S. Amrutur and M. A. Horowitz, "Fast low-power decoders for RAMs," *IEEE J. Solid-State Circuits*, vol. 36, no. 10, pp. 1506-1515, Oct. 2001.

[11] L. Wen Z. Li Y. Li, "High-performance dynamic circuit techniques with improved noise immunity for address decoders" Published in IET Circuits, Devices & Systems Received on 3rd January 2012.

[12] Behrad Razavi, *Design of Analog CMOS Integrated Circuits*, McGraw-Hill, New York, 2001.

Performance Evaluation of Solar Parabolic Trough for Cloths Laundry application

Shubham Gupta*, Prof. R. S. Mishra

Department of Mechanical Engineering Delhi Technological University,

Delhi-110042.

guptashubham@outlook.in , *Post Graduate Student

Abstract- Solar thermal technology installation has enabled to use a completely free and clean form of energy. Because of this diesel consumption in many industries can be saved and hence can positively affect the environment. In this paper particularly laundry of cloths application is evaluated as this process conventionally used diesel in large quantities and hence makes suitable for the use of solar thermal technology.

Key Words: Solar Thermal, Parabolic Trough, Collector, Laundry, Steam, Renewable energy, Solar Energy

Introduction

Thermal or heat energy from the sun can be utilized or converted in one form or another to meet the suitable requirement or application such as cooking, electricity generation, etc. there are two types of radiation that we deal in Solar Thermal Designing: DNI (Direct Normal Incidence) & GHI (Global Horizontal Incidence). Water Heating Parabolic-trough is a proficient technology of renewable energy for heating applications. In India Direct Normal Incidence is also high which makes this technology much more suitable. Hot water applications can be used at various places such as temples (Meal preparation), Hotels, Cloths laundry, etc. This technology has a good payback as compared to Solar PV technology. There are various types of Solar concentrating thermal technologies which includes Linear Fresnel, compound parabolic, paraboloid dish, solar tower, flat plate collector.

Solar Concentrator Parabolic Trough

Solar thermal collectors can be considered as a heat exchanger which transforms solar direct irradiation to enthalpy of the fluid medium in the tube. Following are the main components of Solar Thermal Collector

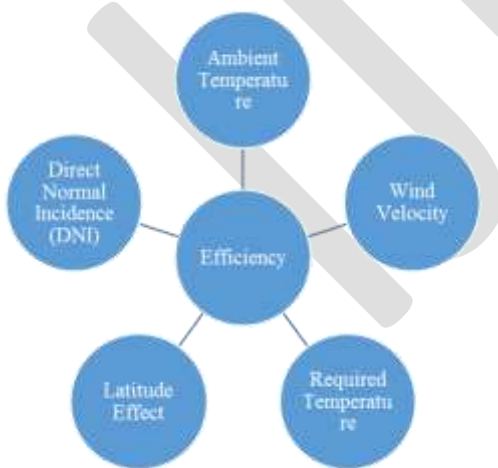


Fig 1: Factors effecting Efficiency of Solar Thermal Technology

- **Collector:** Receives or collects the sun radiation convert it to heat and directs or concentrates it to the receiver
- **Receiver:** It is a glass tube in working fluid which circulates and gains the heat from the collectors and transfers it to the desired equipment or heat storage tank
- **Fluid:** It can be organic fluids, water, heating oil, etc.
- **Tracking:** E-W tracking or N-S tracking or both can be done to increase the efficiency of parabolic trough
- **Storage tank:** In case of cloudy, rainy & non-sunshine conditions heat can be stored in a storage tank.

Literature Review

A. Valan Arsau et.al (2007) ^[1] designed the parabolic trough with rim angle 90° with the use of reinforced fibreglass and provide the manufacture techniques. This modal has very low drag coefficient in the acceptable range. Standard deviations of the of the parabolic surface error distribution was in the limit range of accuracy. Kalogirou et.al (2004) ^[2] Explains the importance of renewable energy considering environmental factors as a major issue. Author also discussed various solar thermal technologies such as flat plate collector, parabolic troughs, etc. and their applications. Krishnamurthy et.al (2012) ^[3] Focuses on economic evaluation of the solar thermal parabolic trough technology considering various factors such as rate of equity, discount rate, capital cost, generation cost, solar insolation and various models are compared. Omid karimi sadaghiyani et.al (2014) ^[4] Designed two solar collectors and evaluate and compared performance characteristics by using CFD and MATLAB. S. D.Odeh (1998) ^[5] Evaluate the performance characteristics of parabolic trough by considering absorber wall temperature instead of fluid bulk temperature to provide flexibility of use of any working fluid. Author used Syltherm 800 as a working fluid for experimental work. Vinay V Gadikar et.al (2016) ^[6] Assesses the Solar concentrator technology use in laundry purposes at Goa by detail specification discussion and also discussed about the problems and challenges faced and performance evaluation is also done. Richter et.al (1996) ^[7] provides the methods to improve the optical efficiency of parabolic trough which plays a great role in overall efficiency of the solar thermal technology. Price.H et.al (2002) ^[8] stated at low working temperature difference Concentrating solar thermal technology works with high efficiency. Many design considerations can also be improved to improve the efficiency.

Case study undertaken

Gandhinagar city is considered for the case study. It has good DNI. An industry of approximately load of 2000 cloths per day for dry cleaning is considered for the case study in this paper.

Methodology

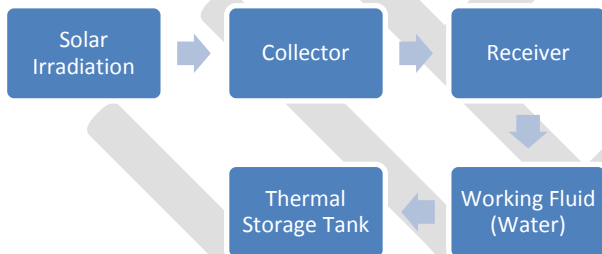


Fig 2: Methodology used in Solar Parabolic Trough

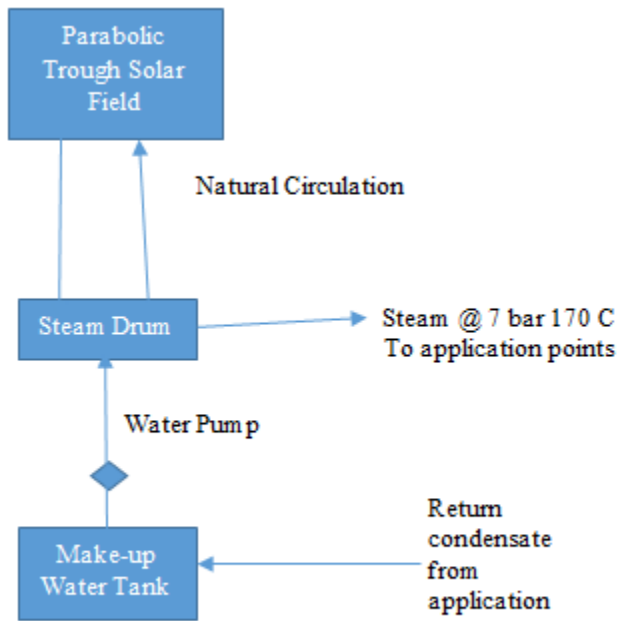


Fig 3: Schematic of Solar Parabolic Trough system

Design Considerations

Longitude: 23.2° N

Latitude: 72.6° E

No. of cloths: 2000-2500

Steam required: 2000 Kg/day

Shade free Area available for Solar Concentrator Technology installation: 80 square meters

No. of operational Hours in a year: 2700

Operating temperature: 170° C

Operating pressure: 7 bar

Table 2: Ambient Conditions Considered

Ambient Conditions		
Parameters	Units	
Wind Speed	m/s	3
Irradiation	W/m ²	1000
Tilt Factor		1.02

Table 3: Fluid Specifications Considered

Fluid Specifications		
Parameters	Units	Vapour
Mass Flow Rate	Kg/s	0.25
Density	Kg/m ³	5.147
Heat Capacity	KJ/Kg-K	2.5944

Thermal Conductivity	W/m-k	0.0364
Kinematic Viscosity	m ² /s	2.91948E-06
Dynamic Viscosity	Kg/m-s	1.50E-05

Table 4: Parabolic Trough Specifications Considered

Parabolic Trough Specifications		
Parameters	Units	
Outer Diameter	m	0.025
Inner Diameter	m	0.022
Outer Diameter Glass Cover	m	0.055
Inner Diameter Glass Cover	m	0.05
Aperture	m	2
Length	m	4
Aperture Area	m ²	7.9
Avg. Value transmissivity-Absorbivity product for beam radiation		0.9
Specular Reflectivity of the concentrator Surface		0.95
Intercept factor (The fraction of the reflected radiation intercepted by the absorber tube)		0.95
Temperature Outlet	Celsius	65
Temperature Inlet	Celsius	30

Computation of energy potential

Table 5: Monthly Thermal Output Generation

Parameter	Units	Jan	Feb	Mar	Apr	May	Jun	Jul	Aug	Sep	Oct	Nov	Dec
Incident Beam radiation	W/m ²	1000	1000	1000	1000	1000	1000	1000	1000	1000	1000	1000	1000
DNI	KWh/day	3.2353	4.9237	6.3184	5.7870	5.3760	4.1276	2.7863	3.4971	4.6744	4.2386	3.4537	3.1160
Overall Loss Coefficient	W/m ² -K	24.8	24.8	24.8	24.8	24.8	24.8	24.8	24.8	24.8	24.8	24.8	24.8
Useful Heat Gain	W	3907	3907	3907	3907	3907	3907	3907	3907	3907	3907	3907	3907
Thermal Units/Day	KWh	12.64	19.24	24.69	22.61	21.01	16.13	10.89	13.66	18.27	16.56	13.50	12.18
No. of Modules		8	8	8	8	8	8	8	8	8	8	8	8
Total Thermal Units	KWh/day	101	154	198	181	168	129	87	109	146	132	108	97

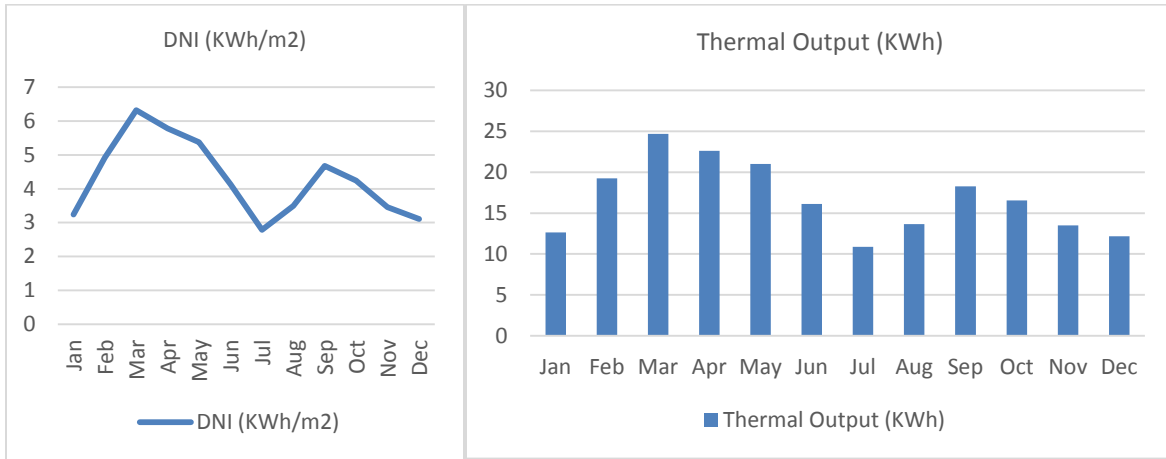


Fig 4: DNI variation with Month

Fig 5: Thermal Output with Month

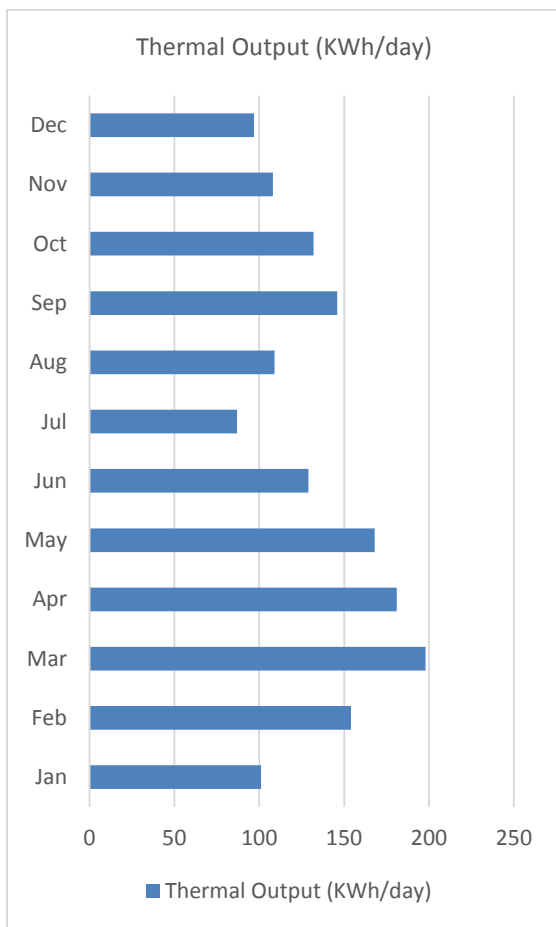


Fig 6: Thermal Output with Month

Results & discussion

15 KWh/day is produced from 8 parabolic troughs with 64 square meters of reflective area. Collector efficiency is 45 %. Concentration ratio is 27. This energy is enough to carry out laundry operation of around 2000 cloths per day. In overall 20 litres/day of Diesel is saved which provides of annual saving of 6000 Kg of LPG gas.

Conclusion

New concept of solar thermal technology has the potential to improve the efficiency of energy (i.e. the thermodynamically efficient use of fuel) supply systems, while at the same time integrate seamlessly with the use of renewable energy sources, for the delivery of the required energy in different forms in industries. Since because of various factors like clouds, dust, etc. Sun's rays reach the earth in a diffuse manner a less Direct rays is received. Solar PV technology works on GHI. While Solar thermal works on DNI. So if we use the Solar thermal output as a heat it will be more useful gain as in converting electricity much more losses occur in concentrating solar thermal technology. A fluid run through a pipe line continuously and gain heat from concentrated sun's rays by parabolic trough. Parabolic trough concentrator is such designed to achieve desire temperature difference. This fluid after gaining heat moves to storage tank where it can be utilized. After utilization again it moves to make up tank then to inlet of Parabolic Trough.

REFERENCES:

1. A. Valan Arsau, T. S. (2007). Design, manufacture and testing of fiberglass reinforced parabola trough for parabolic trough solar collectors. *Solar Energy*, 1273-1279.
2. Kalogirou, S. A. (2004). Solar thermal collectors and applications. *Progress in Energy and combustion science*, 231-295.
3. Krishnamurthy, P. M. (2012). An analysis of costs of parabolic trough technology in India. *Energy Policy*, 407-419.
4. Omid KARIMI SADAGHIYANI, M. B. (2014). Two new designs of Parabolic solar collectors. *Thermal Science*, 323-334.
5. S. D. ODEH, G. L. (1998). Modelling of parabolic trough through direct steam generation solar collectors. *Solar Energy*, 395-406.
6. Vinay V Gadikar, S. D. (2016, Jan-Mar). CST BEING USED IN LAUNDRY AT LAKAKI DRYCLEANERS, GOA . *Sun Focus*, pp. 15-17.
7. Richter, J. L. (1996), Optics of a Two-trough Solar Concentrator, *Solar Energy*, pp. 191-198
8. Price, H., et al. (2002), Advances in Parabolic Trough Solar Power Technology, *Journal of Solar Energy Engineering*, pp. 109-125

Developing 3D Finite element model of Head using Magnetic resonance imaging and algorithm developed in MATLAB

Dr Chandrashekhar Bendigeri¹, Sachin Patil²

¹ Associate Professor, Department of Mechanical Engineering UVCE, Bangalore

² ME, Department of Mechanical Engineering, UVCE, Bangalore

Abstract - Neurotrauma is the physical damage that results when the human skull and brain are suddenly or briefly subjected to intolerable levels of energy that is usually transmitted mechanically. Current trends suggest an increase in the number of survivors of neurotrauma throughout the world. This demands a new outlook giving high priority to establishing long-term goals in preventing, treating and rehabilitating people with an injury to the central nervous system. Multi-modal imaging has become increasingly important in medical research and clinical practices, particularly in skull fractures, therapeutic monitoring and brain functional imaging. The process of converting anatomical data from images to 3D models is called segmentation. In this research we would like to discuss various methods for developing 3D finite element model of human head from MRI scanned volumetric images. This information is then used to recreate a 3D model from the segmented structures.

Key words - Human head, MRI, Dicom, Medical imaging, Finite element model, MATLAB, Rapid prototype

1. INTRODUCTION

The initial step in developing 3 dimensional finite element model of the human head is to obtain some set of MRI scanned images of human head. After the Preprocessing of the image data, the set of images are imported to MATLAB and using suitable algorithm developed the 3Dimensional meshed finite element model can be obtained.

In the medical field, for any case of skull or head fractures, the custom implants are being developed from various materials. Reviewing of the implants developed can be made easy to the doctors efficiently by creating the rapid prototype model of the generated model from the MATLAB. The important parameters which affect the FEM model of the human head is mesh method and mesh quality. The difficulty in generation of model directly from grey scale Images can be eliminated through developed algorithms. Under segmentation there are three tools in the main tool bar: Thresholding, Region growing and Calculate 3D. Several operations need to be performed during model generation of MRI scanned human skull [2]. Some of those are noise reduction, filling holes in image, contrast modification and edge detection. After completion of Surface or volumetric geometry extraction from 3D voxel image, further the model need to be meshed properly. This paper presents methodology of developing 3Dimensional finite element model of human head from MRI scanned set of images. There are various steps involved in generation of the finite element model of human head which include, preprocessing of Dicom images, importing of images and finally surface mesh generation. Below methodologies discuss all the steps involved in developing the rapid prototype of the human head.

2. METHODOLOGY

The steps involved in generating 3D finite element modeling of human head are as follows,

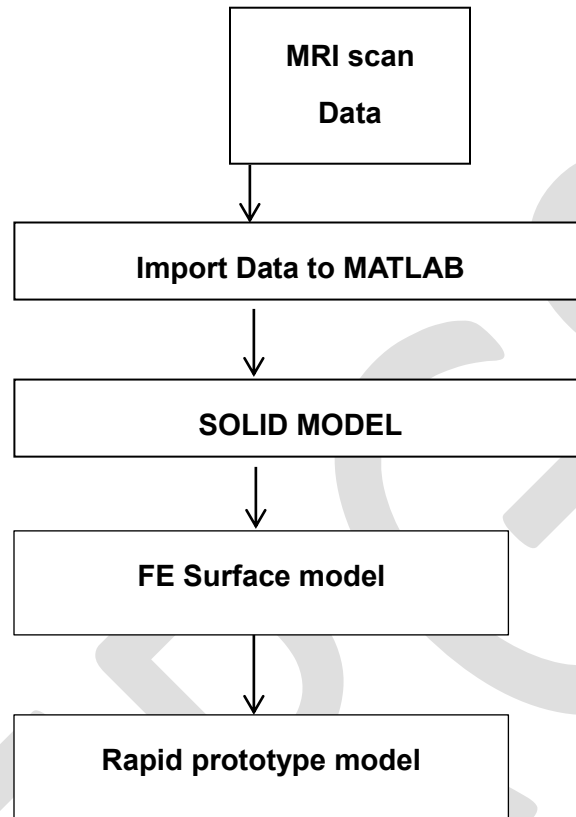


Figure 2.1: Steps of finite element modeling from MRI data in MATLAB

2.1 MAGNETIC RESONANCE IMAGING(MRI) METHOD

The image acquisition done in MRI (Magnetic resonance imaging) scan result in a series of 2D images displaying a density map of the sample, stacking these images creates a 3D representation of the scanned area. In this method the set of images obtained will be in Digital Imaging and Communications in Medicine (DICOM) format. Raw data from MRI Scanner were transferred to a computer and later processed. DICOM format images of the MRI Scan are effectively viewed in MATLAB if they are converted into specific image formats like JPEG, TIFF, and PNG and so on. So the DICOM format of Skull needs to be converted to these formats to as these can't be viewed in computer [3]. In order to convert DICOM images to desirable formats like tiff, software named DICOM converter can be used [4].

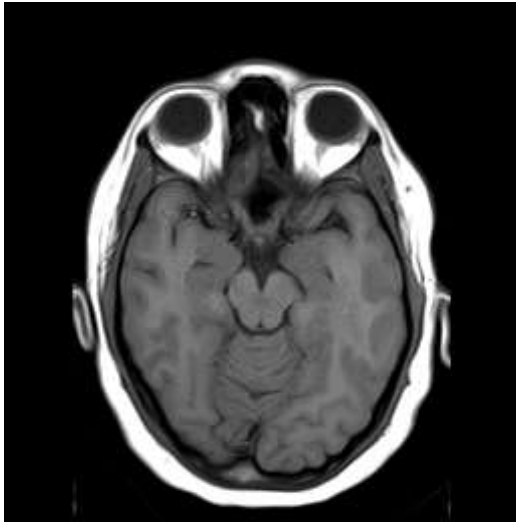


Fig 2.2 Axial sliced section of MRI scan data

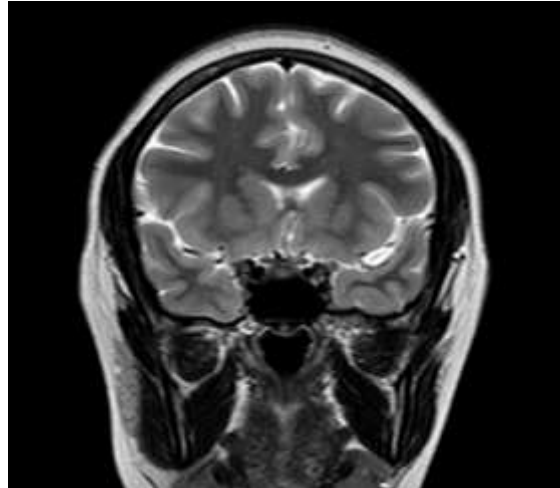


Fig 2.3 Coronal sectional view of MRI scan data

2.2 IMPORT MRI DATA TO MATLAB

In this process the set of MRI images converted into tiff format are imported to MATLAB in stack. After importing the images, several processes like repairing the images, cleaning of the images, noise filter reduction are being performed. 3D binary images of the MRI can be denoted by 0 or 1. These files can be used as input for the MATLAB [7].

2.3 GENERATION OF SURFACE MESH

Mesh generation is the practice of generating a polygonal or polyhedral mesh that approximates a geometric domain. The Delaunay triangulation mesh can be generated from a proper algorithm. One such algorithm for tetrahedral mesh generation using Delaunay refinement can be derived from cgal 4.8 3D mesh generation [11]. This tool box can be installed in MATLAB externally and it can provide the proper refined mesh structure on our application basis. The mesh generator is customized to output a mesh that fits as much as possible the user needs, for instance in terms of sizing field or with respect to some user customized quality criteria. The meshing engine used in this mesh generator is based on Delaunay refinement [7]. It uses the notion of restricted Delaunay triangulation to approximate 1-dimensional curve segments and surface patches. Before the refinement, a mechanism of protecting balls is set up on 1-dimensional features, if any, to ensure a fair representation of those features in the mesh, and also to guarantee the termination of the refinement process, whatever may be the input geometry, in particular whatever small angles the boundary and subdivision surface patches may form. The Delaunay refinement is followed by a mesh optimization phase to remove slivers and provide a good quality mesh.

By converting the generated file to specific file formats like inp, the generated meshed file can be viewed in any finite element solver softwares like Abaqus or Ansys.

2.4 RAPID PROTOTYPE GENERATION

For any implant generation for fractured head or skull, the main step after generation is to evaluate the implant specifically whether it fits for patients head. Hence for effective review and analyzing of the implants one need to develop the rapid prototype of the model. In order to obtain the rapid prototype of the model one needs to have model in stl file format. After generation of surface mesh from the model, for converting the file to stl file suitable algorithm needs to developed [10]. In development of algorithm in MATLAB, use of node, face, element matrices is mandatory. By defining the triangular coordinates from nodes, element and face matrices stl file can be obtained.

Effective rapid prototyping is being done by 3D printing technique. In 3d printing technique the model in stl file format can be printed out by suitable material. Acrylonitrile butadiene styrene (ABS) is one such thermoplastic material which can be used for 3d printing technique. The styrene in ABS gives the plastic a shiny, impervious surface. The polybutadiene, a rubbery substance, provides toughness even at low temperatures. The ability of strength and toughness property of ABS makes it to use as preferable material for 3D printing. Below is the 3D printed rapid prototyped model developed from the output of the MATLAB [2].

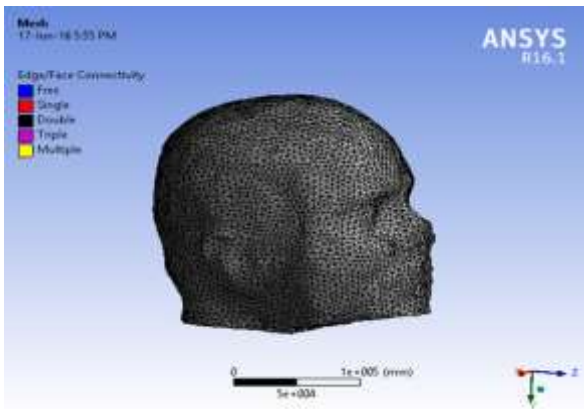


Fig 2.4 Tetrahedral meshed Finite element model



Fig 2.5 Rapid prototype model of human head

3. CONCLUSION

The following conclusions can be drawn with regard to the methods for developing 3D finite element model of human head:

In order to develop a 3D finite element model of human head from the set of MRI scanned images, a specific algorithm can be written in MATLAB which effectively generate the model with various cleaning operations such as, gap filling of holes, noise filter reduction. Further the tetrahedral meshed model can be used for finite element analysis of the head under various loading conditions. By assigning the material properties of human head surface like cortical and trabecular bone, one can carry out the finite element analysis. Using the above mentioned all the steps involved image processing technique for converting the binary grey scale volumetric images to the 3D finite element model we are able to get the effective result of the model.

REFERENCES:

- [1] N. Kishore Kumar, K. Ashok Kumar Raju, 2015. Modeling and analysis of human liver by finite Element method. International journal on science and research
- [2] Saeid Samiezadeh, Pouria Tavakkoli Avval, Zouheir Fawaz, Habiba Bougherara, 2015. Journal of biomedical Engineering
- [3] Pranita Balaji Kanade et al. "Brain Tumor Detection Using MRI Images". International Journal of Innovative Research In Electrical, Electronics, Instrumentation And Control Engineering Vol. 3, Issue, February 2015
- [4] Shaima Abd El-Kader et al. "Curvature Anisotropic Gaussian Filter for MRI brain Images enhancement and edge preserving", IJCSNS International Journal of Computer Science and Network Security, VOL.15 No.11, November 2015
- [5] Biplab Chatterjee, Prasanta Sahoo, 2013. "Finite element based parametric study of elastic-plastic contact of fractal surfaces". International Conference On Design And Manufacturing, IConDM 2013, p 552-561

[6] Chougule, V. N, Mulay, A. V, Ahuja, B.B.3,2013. Conversions of CT Scan Images into 3D Point Cloud Data for the Development of 3D Solid Model using B-Rep Scheme

[7] Qianqian Fang ,David A. Boas ,2009.” Tetrahedral mesh generation from volumetric binary and grayscale Images”. IEE 2009.

[8] Carolina Dopico-Gonzalez , Andrew M. New, Martin Browne, 2009. “Probabilistic finite element analysis of the uncemented hip replacement-effect of femur characteristics and implant design geometry”. Journal of bio mechanics

[9] F. S. Azar, X. Intes , 2008. Translational Multimodality Optical Imaging, Artech House, Norwood.

[10] O. Courchesne, F. Guibault, J. Dompierre and F. Cheriet, 2007."Adaptive Mesh Generation of MRI Images for 3D Reconstruction of Human Trunk", Springer Berlin / Heidelberg,.

[11] L. Rineau and M. Yvinec. 2008“3D Surface Mesh Generation,” In CGAL Editorial Board, editor, CGAL User and Reference Manual. 3.4 edition.

[12] Craig A. Simmons, Shaker A. Meguid, Robert M. Pilliar, 2000. “Mechanical regulation of Localized and appositional bone formation around bone-interfacing implants”. Journal of Biomedical materials research

[13] Mikhail Yakhnis and Robert Zhang. “Analysis of 2D Deformation and Creep Response of Articular Cartilage”.

Modeling and Simulation of a Manufacturing System by Using Time Petri Net

Chavan Vishwajit D^{a*}, Dr. Rajesh B. Buktar^b, Dr. Kiran Bhole^c

Mechanical Engineering Department, Sardar Patel College of Engineering, Mumbai, India^{a b c}

*Email: chavan.vishwajitd@gmail.com Tel.No. +91 8983706639

Abstract— The Petri Nets (PN) are being used for decision making in the manufacturing system using Petri Nets (PN). In this paper, PN has been applied successfully for modeling of discrete event dynamic systems such as manufacturing system that are characterized by conflicts, concurrency, and synchronization. An example of the manufacturing system of an XYZ industry consisting of four machines with operators has been taken into consideration and its PN model construction is explained. The model is then simulated in the MATLAB software using Petri Net toolbox. Furthermore, the modeled system is a Time Petri Net (TPN) model which is a well-known subclass of PNs for checking the coverability of the system. Analysis of the model using TPN depicts efficient performance evaluation and qualitative analysis.

Keywords— Petri Nets (PN), Manufacturing System, Time Petri Nets (TPN), Discrete Event Dynamic Systems (DEDS), Coverability, MATLAB, Petri Net Toolbox.

INTRODUCTION

Automated manufacturing systems belong to the domain of discrete event dynamical systems (DEDS) in which the evolution of the system in time depends on the complex interactions of the timing of different discrete events, such as the entry of raw workpiece, the exit of finished parts, failure of a machine etc. The state of DEDS changes only at these discrete instants of time, instead of continuously. Several classes of models have emerged in this context and the models are broadly classified as qualitative or quantitative. Qualitative models capture logical aspects of systems evolution such as controllability, stability, the existence of deadlocks in system operations etc. This paper mainly concentrates on Quantitative Models which is more specifically named as "Performance Modeling." The paper highlights the quantitative system performance in terms of the throughput and the lead time. Quantitative models include discrete event simulation, min-max algebra, Markov chains, Stochastic Petri nets, queues and queuing networks. [1] [6] [8]

The concept of the Petri net has originated by Carl Adam Petri's in 1962. [1] [6] [8]

The area or system which can be described graphically like flow charts and which needs some means of representing parallel or concurrent activities, PNs can be applied. Petri Net is also used to solve complex problems coupled with other tools such as Genetic Algorithms, Linear Programing, C++ etc. To apply PNs, it is necessary to add some special modifications and restrictions which suit the particular application.

PNs provide a graphical notation for the formal description of the dynamic behavior of systems. PNs are particularly well suited to systems which exhibit synchronization, concurrency, mutual exclusion, and conflict. [1] [6] [8]

PN consists of four types of components places, transitions, tokens and arcs (Refer Fig.1). Places denoted as circles, are used to represent conditions or local system states, e.g. place may relate to one phase in the behavior of a particular component or Places represent possible states of the system. Transitions denoted as bars, are events or actions which cause the change of state or transitions are used to describe the events that occur in the system; these will usually result in a modification to the system state. Arcs specify the relationships between local states or conditions (places) and events (transitions). An arc from place to transition is termed as input arc and from the transition to place is termed as output arc. Tokens denoted as a dark dot, are identity-less markers that reside in places. The token in a place represents the condition or local state holds. Each transition has some number of input and output places. These input and output places represent the pre and post conditions of an event (transition).



Fig.1. Components of Petri net

In section 2, transition enabling and the firing rule of PN is described along with an example of a simple manufacturing tool to show how transition enabling and firing rule executes. Section 3 gives an overview of the various properties of the PN of the modeled manufacturing system. In section 4, different analysis methods for the modeled PN are discussed by giving an example for the reachability analysis. Section 5 shows the actual creation of a model of a manufacturing system in PN toolbox in MATLAB environment following by doing a simulation of the modeled manufacturing system. Finally, section 6 concludes this paper.

ENABLING TRANSITION AND FIRING RULE FOR THE MANUFACTURING SYSTEM

A transition with the absence of any input place is called a *source transition*, and one with the absence of any output place is called a *sink transition*. The sink transition consumes tokens but doesn't produce any. The source transition is frequently used in a manufacturing system model, so as to represent the entry of raw material or semi-finished parts in the system, while sink transitions are frequently used to represent the exit of finished or semi-finished parts. The source transition is unconditionally enabled, and on the firing of a sink transition tokens get consumed but does not produce any.

If p is both an input and output place of t , then the pair of place p and a transition t is called a self-loop. A Petri net is said to be pure if it has no self-loops. A Petri net with self-loops can be converted into a pure PN by adding a place and transition to each self-loop in the original Petri net. [3] [7]

The formal definition of a Petri net is, the PN is a 5-tuple, $PN = (P, T, I, O, M_0)$; where,

$P = \{P_1, P_2, \dots, P_m\}$ is a finite set of places,

$T = \{t_1, t_2, \dots, t_n\}$ is a finite set of transitions,

$I = (P \times T) \rightarrow N$ is an input function that defines directed arcs from places to transitions,

$O = (T \times P) \rightarrow N$ is an output function which defines directed arcs from transitions to places,

$M_0 = P \rightarrow (0, 1, 2, \dots)$ is the initial marking.

Where, N is a set of non-negative integer i.e. $N = \{0, 1, 2, \dots\}$.

To simulate the dynamic behavior of a system, a marking or state in PN is changed according to the following firing rule; [1]

- A transition t is said to be enabled if each input place p of t is marked with at least one or more tokens or the weight of the directed arc from place p to transition t .
- An enabled transition may or may not fire, depending on whether or not the event actually takes place.
- On the firing of an enabled transition t , tokens get removed from the each input place p as the weight of the directed arc from place p to transition t and gets deposited equally to each output place.

Imposed by the transitions, tokens move between places according to the firing rules.

To fire a transition, each of the input places connected to it has at least one token; when transition fires, it removes a token from each of these input places and deposits a token in each of the output places connected. This is the firing rule. Sometimes a transition requires an input place which contains two or more tokens before it can fire. In this case, we denote the multiplicity of the arc by a small number written next to the arc instead of drawing a number of arcs between the place and the transition, similarly for output arcs. [1]

From an initial marking and followed by the firing rule, one can progress through the states of the model. Sometimes it is called playing the *token game*. On continuing we obtain all the possible states of the model, on recording all the states we see and stopping only when we can reach no states that we have not already seen. This is called the reachability set, which is the set of all possible markings that a net may exhibit, starting from the initial marking and following the firing rules. Various initial markings might lead to different reachability sets as we will see in the example below. That is why the initial marking is an important part of the model definition.

Example: For the simple Petri net shown in Fig. 2 the initial marking is (1, 0, 0) and the final marking is (0, 1, 1) on firing transition t_1 . These are the only possible markings as it has only one transition to be fired. If the initial marking of the example is changed to (3, 2, 1) the set of reachable markings will be: $\{(3, 2, 1), (2, 3, 2), (1, 4, 3), (0, 5, 4)\}$. Because, the input places connected to transition t_1 has more than one tokens in it, so when the t_1 will fire only one token will remove from the input place p_1 as the weight of the arc is a unity. But still there are two tokens in the input place p_1 , therefore the transition t_1 will remain enabled and it will fire again two times. Finally, all the tokens from input place removed and deposited to each output places and reached to a certain state of the system.

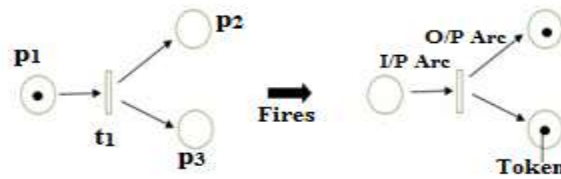


Fig. 2. Illustration Showing a Simple Petri Net Firing

EXAMINING PETRI NET PROPERTIES FOR MODELED MANUFACTURING SYSTEM

The Petri Net properties are the pre-requisite for validating the modeled system. On simulation, these properties get checked and if those gets satisfied then the modeled system meets the requirements.

Petri net is a mathematical tool which possesses a number of properties. These properties allow the system designer to identify under the design, the existence or absence of the application domain of specific functional properties of the system under. These properties can be distinguished as, behavioral and structural properties.

A. Reachability

In designing event-driven systems, an important issue is whether a system can reach a specific state, or exhibit a specific functional behavior. In general, the question arises is, whether the modeled system with Petri nets presents all prudent properties as specified in the requirement specification and no undesirable properties.

To find out the modeled system can reach a specific state as a result of a required functional behavior, it is important to find such a transition firing order which would transform a marking M_0 to M_i , where M_i is the specific state, and the firing order is the required functional behavior. The existence of additional sequences of transition firings in the Petri net model which transform M_0 to M_i shows that the Petri net model may not exactly reflect the structure and dynamics of the underlying system. A marking M_i is reachable from a marking M_0 if there exists an order of transitions firings which changes a marking M_0 to M_i . [4]

B. Safeness

In a Petri net, places are often used to depict product and tool storage areas in manufacturing systems. It is important to determine the proposed control strategies which prevent from the overflows of these storage areas.

The property, boundedness is the concept which helps to identify the existence of overflows in the modeled system in the Petri net [4].

A place p is k -bounded if the number of tokens in a place p is should be less than or equal to k for every marking M reachable from the initial marking M_0 where k is a non-negative integer number. It is safe if it is 1-bounded.

A Petri net $N = (P, T, I, O, M_0)$ is k -bounded (safe) if each place in p is k -bounded (safe).

C. Liveness

Liveness is the concept which is closely related to the deadlock situation.

A Petri net must be live which is modeled as a deadlock-free system. This indicates that for any reachable marking M , it is possible to fire any transition in the modeled net by progressing through some firing order. This requirement, however, might be too tough to represent some real systems that show a deadlock-free behavior. For some cases, the initialization of a system can be modeled by a set of transitions which fire a finite number of times. After initialization, the system may show a deadlock-free behavior, while the Petri net representing this system is no longer live as mentioned above. For this reason, various levels of liveness for transition t and marking M were defined. [4]

ANALYSIS OF MODELED TIME PETRI NET SYSTEM

It is important to analyse the modeled system. This analysis will lead to important insights into the behavior of the modeled system. There are three common approaches to Petri net analysis; reachability analysis, the matrix equation approach, and simulation. The first approach involves the computation of all reachable markings, but there is an issue of the state-space explosion. The matrix equations technique is strong but in many cases, it is applicable only to special situations or special subclasses of Petri nets. Discrete-event

simulation is an option to check the system properties for complex Petri net models. [4]

A. Reachability Analysis

Reachability analysis is done by construction of reachability tree and is also called a coverability tree. We can get the number of *new* markings as the number of the enabled transitions (firing transitions) from the initial marking M_0 in a given Petri net PN. From every new marking, we can reach more markings. On repeating the procedure over and over we will get the results in a tree representation of the markings. Markings generated from M_0 and its successors represent *nodes*, and every arc represents firing of transition, which will transform one marking to another. [4]

The tree will grow infinitely if the net is unbounded.

Example: Consider the Petri net shown in Fig. 3, all reachable markings are: $M_0 = (2, 0, 0, 0)$, $M_1 = (0, 2, 1, 0)$, $M_2 = (0, 1, 1, 1)$, $M_3 = (0, 2, 0, 1)$, $M_4 = (0, 0, 1, 2)$, $M_5 = (0, 1, 0, 2)$, and $M_6 = (0, 0, 0, 3)$.

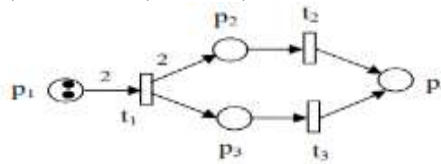


Fig. 3 Simple Petri Net

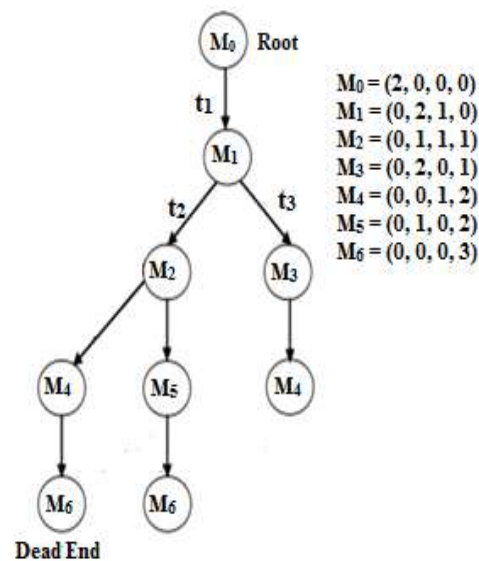


Fig. 4 Reachability Tree

B. Simulation

To check the system properties, simulation is another way for complex Petri net models. The idea of simulation is simple, that is, by using the execution algorithm to run the net. Simulation is time-consuming and an expensive technique. Simulation can show the presence of undesirable properties but it cannot prove the correctness of the modeled system in general case [4]. Regardless of this, Petri net simulation is truly a convenient and straightforward yet effective approach for engineers to prove the desired properties of a discrete event system. The algorithm is given as follows;

- Initialization: choose the initial marking and the set of all enabled transitions in the marking.
- If the number of predetermined simulation steps or certain stopping criteria is met, stop. Else, if there is no transition enabled, report a deadlock marking and either stop or go to Step (1).
- Randomly pick a transition to fire. Remove the same number of tokens from each of its input places as the number of arcs from that place to the transition and deposit the same number of tokens to each of its output places as the number of arcs from the transition to that place.
- Remove enabled transitions which are modified at the new marking by checking the output transitions of the input places used in Step (3). If the output transitions of the output places in Step (3) become enabled, add those enabled ones. Go to Step (2).

To simulate extended Petri nets such as timed ones, the above-given algorithm can be modified. The benefit of the simulation methods is to allow one to derive the temporal performance of a system under very realistic assumptions. A list of Petri net simulation tools along with their feature descriptions can be found in the Petri Nets world website [5].

MODELING AND SIMULATION OF A MANUFACTURING SYSTEM

The flow process of the manufacturing system consists of one Traub semi-automatic lathe machine (M_1), one Band Saw machine (M_2), one CNC lathe machine (M_3), one Thread Rolling machine (M_4) and two operators B_1 and B_2 as shown in figure 5.

The main objective of modeling this manufacturing system is to get the coverability question satisfied,

$$\text{If, } M_0 = \{P_1\} \text{ and } M = \{P_{13}\}, \text{ then } M' \geq M$$

The manufacturing system modeled by using PN modeling tool as Petri net toolbox in MATLAB environment as shown in Fig. 6. Initially, the author considered fifty parts to be processed from the store.

By doing so it is easy to understand the behavior of the system. To assess the system, various properties of Petri nets such as reachability, safeness, and liveness needs to be obtained. If these properties get satisfy after the simulation process then we can say that the modeled system meets the expectations.

By seeing the properties of the Petri nets, we can check the questions like is the net or system is bounded, is the net or system is repetitive, is the net or system is reachable, is the net or system is coverable, is the net or system is live, is it deadlock-free, using the Petri net toolbox in MATLAB environment. If we get these questions results in the software then we can say that the modeled system satisfies the pre-conditions. In Petri net toolbox in MATLAB environment, the author created a net of the considered manufacturing system as a *Time Petri Net* model as shown in the Fig.6.

Basically, there are two conditions one is clocks with *transitions* that is called Time Petri Nets (TPN) and clocks with *tokens* which are known as Timed Petri Nets (TDPN). Here, the author has used Time Petri Net. To use TPN, the modeled system must be a bounded network. After creating the net, to check the properties of the modeled system, need to run the simulation in Petri net toolbox in MATLAB environment, as the simulation is one of the analysis methods of the Petri net.

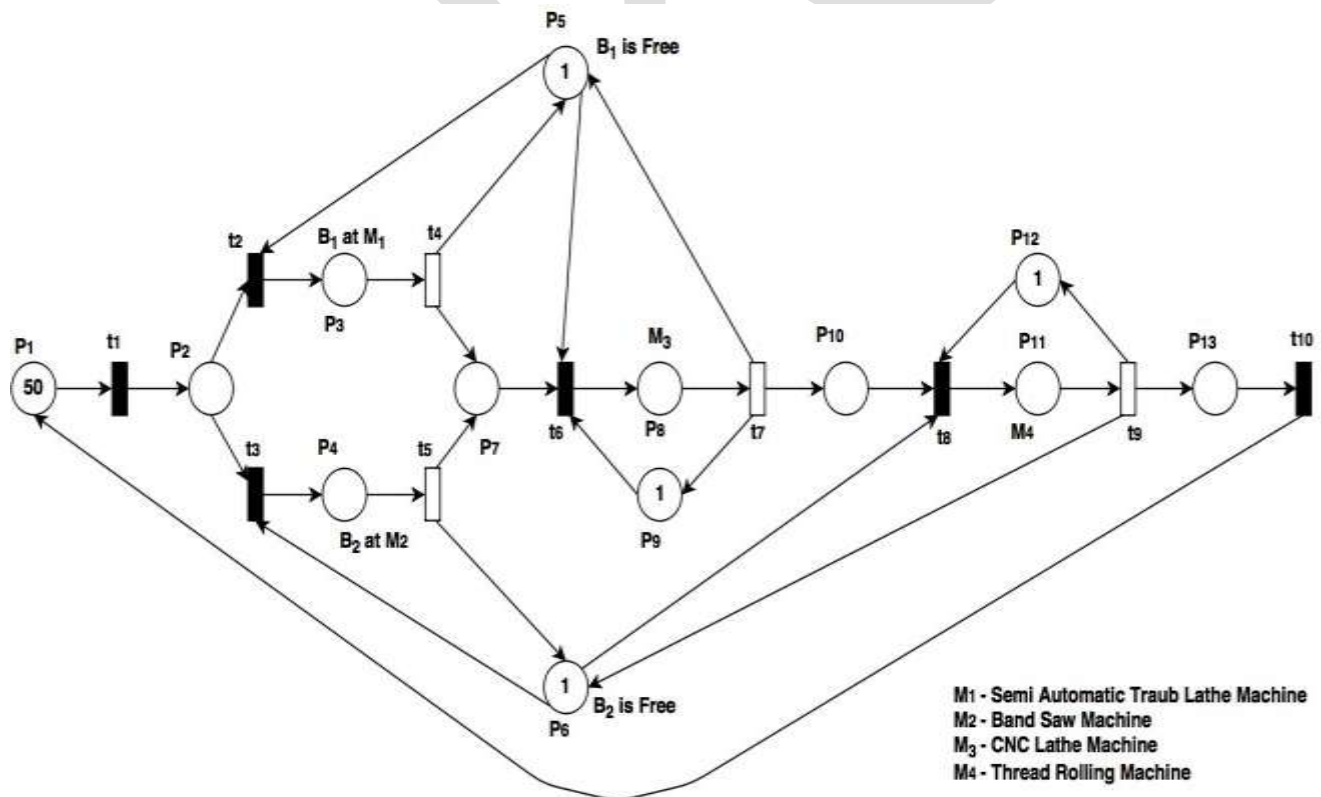


Fig. 6 Time Petri Net Model of a Manufacturing System

On doing simulation analysis author has got the results as shown in Table 1,

Properties	Result Status
Structural Boundedness	The Net is Bounded
Structural Repetitiveness	The Net is Repetitive
Liveness	The Net is Live
Reachability	The Net is Reachable

As the modeled manufacturing system is live so that the system is completely deadlock-free. If the initial marking is able to reach the final marking then we can say that the net is coverable too or if the net is reachable then it is coverable too.

CONCLUSION

In this study, author modeled the manufacturing system as a Time Petri Net (TPN) model with clocks with transitions a well-known subclass of PN. PN is a powerful tool and has been successfully employed to model manufacturing system as they capture various characteristics of manufacturing system such as concurrency, synchronization, and conflicts. A manufacturing system of an XYZ industry has been modeled using TPN approach and the construction has been explained in detail. From the reachability analysis and simulation analysis, it is evident that the Petri Net Model created for the Manufacturing System satisfies the pre-conditions for the Petri Net and which will assist the planner.

The concept has opened a new avenue for the diagnosis and performance measurement of complex manufacturing systems consists of the batch production system of a different variety of products.

REFERENCES:

- [1] N. Viswanadham and Y. Narahari. Performance Modeling of Automated Manufacturing System, Pearson Education, Inc., Prentice Hall.
- [2] Jain A., Jain P. K. & Singh I. P. Performance Modeling Of FMS With Flexible Process Plans A Petri Net Approach. International journal of simulation modeling 2006, vol. 5, no3, pp. 101-113.
- [3] Ozkan Basak, Y. Esra Albayrak (2015). Petri net based decision system modeling in real-time scheduling and control of flexible automotive manufacturing system, Computers & Industrial Engineering 86 (2015) 116—126.
- [4] J. Wang, Petri nets for dynamic event-driven system modeling, in Handbook of Dynamic System Modeling, Ed: Paul Fishwick, CRC Press, 2007.
- [5] <http://www.informatik.uni-hamburg.de/TGI/PetriNets/>
- [6] Viswanadham N., Narahari Y., & Johnson T. (1990). Deadlock prevention and deadlock-avoidance in flexible manufacturing systems using Petri net models. IEEE Transactions on Robotics and Automation, 6(6), 713-723.
- [7] Tavana M. (2008). Dynamic process modeling using Petri nets with applications to nuclear power plant emergency management. International Journal Simulation and Process Modeling, 4(2), 130-138.
- [8] Viswanadham N., Narahari Y., & Johnson T. L. (1992). Stochastic modeling of flexible manufacturing systems. Mathematical and Computer Modelling, 16(3), 15-34.
- [9] Rongming Zhu (2012). A Deadlock Prevention Approach for Flexible Manufacturing Systems with Uncontrollable Transitions In Their Petri Net Models.
- [10] Manuel Silva and Robert Valette (2005) Petri Nets and flexible Manufacturing. Advances in Petri nets 1989, 1990.
- [11] Abdulziz M., E.-T. S., H. Mian and M. H. Abidi, "Analysis of performance measures of the flexible manufacturing system," Journal of King Saud University - Engineering Sciences, pp. 115-129, 2012.
- [12] T. Aized, "Modeling and performance maximization of an integrated automated guided vehicle system using colored Petri net and response surface methods.," Computers & Industrial Engineering, vol. 57(3), pp. 822-831, 2009.

A Survey On Wireless Power Transfer Based Street Light Feeding System

Sanket Manik Kanchan, Prof. K. Sujatha.

Dept. Electronics & Tele-Communication Engineering,

Shree Ramchandra College of engineering Lonikand (Pune), India.

sankkanchan@gmail.com

Contact Number:- 8149329175

Abstract— This paper Represents Importance of Witricity in this Electricity Demanding era. In this paper an autonomous system based on Wireless power Transfer using Resonant Inductive Coupling is Discussed. WPT is based on Electromagnetic Effect produced in the Conductor when it is Carrying a Current Through it. Witricity Is Cost Effective and Very Efficient Power transmission Technology For Power transmission. It can be Used to Curb the losses and reduce Power theft which are Crucial Factors in Power Transmission.

Keywords— Witricity (Wireless Electricity) , Resonant Inductive Coupling , Electromagnetic Induction , WPT (Wireless Power Transfer) , Magnetic Brush Lines , Inductive Coupling Factor, EV (Electric Vehicle), DC (Direct Current) , AC (Alternating Current)

INTRODUCTION

Wireless power Transfer can be effective option to curb these losses as Wireless Power Transfer uses Wireless mode of transmission. Wireless Power Transfer and its application can be extremely useful in Electricity Generation and transmission. Wireless Power transfer is basically works on the principle of Transformers. We can say that transformer is a motive of Wireless Power Transfer. it is analogues to Wireless Data Transmission only power is transmitted instead of data. the concept can be used efficiently in Electricity to minimize Cost, losses and maximize the Efficiency. Concluding to this we can Develop a a system that could provide much higher Efficiency, low Transmission Cost and Secured to power theft. In proposed system we are Developing a Wireless Power transmission system in which Vehicles Battery power is used to feed a street light system. Generally any road have more than thousand vehicles running on it per day. If we collect energy from each vehicle without hampering its operation this energy can be used for feeding street lights on that road. Can be effective option to curb these losses.

METHODOLOGY

The Power From Electric Vehicle is a input to the System. this Power is DC in Nature So it is First Given to the DC to AC Converter as Wireless Power Transfer can only done with Alternating Current.

At Input Side A Controller is Used to Activate the Wireless Power transfer between Transmitting Coil and receiving Coil. To start the Power transfer a Switch is Provided at the Transmitter Side and when it is pressed the Controller will activate the Power Transfer and when it is again pressed the power Transfer will be Stopped.

A 16*2 LCD is Also Provided at the Transmitter section to Display the Wireless Power transfer activity i.e. Whether WPT is Ongoing or not. The Controller Will provide the Control Signal to Display the activity on LCD.

A DC to AC Converter is used to Convert the DC Current to AC Current and this AC Current is then Travels through transmitting Coil. The transmitting Coil is Copper Coil with 1000 turns. For greater Efficiency We Can Use Tesla Coil also. the Charge is Stored in the Coil based on the Principle Of Electromagnetic Induction. and this Charge is then transferred in wireless mode using Resonant Inductive Coupling.

At Receiver End The receiving Coil with 1000 turns and Made up of Copper will receive the Charge and Current Will Start Flowing through Coil. This Current Is Ac in Nature.

A Current Booster Circuit Using MOSFET and Capacitors is used to boost the Current as Efficiency is 70 %. it will boost the Current at Adequate Level.

To feed the Street Light (Specially Traffic lights) we need to Convert the AC power into DC power for that purpose DC to AC Converter is used. at Receiver Charge Storage Batteries are Used to Store the Charge. After Charging the Battery to its full level a circuit is broken using Circuit breaker Circuits.

HARDWARE UNITS REQUIRED :-

1.Power Supply Unit :

It Requires two Voltage 12 volt and 5 volt.

2. LCD Display :

it Required to Display the Power Transfer Activity. in this System we are using 16*2 LCD Display Unit.

3. Transmitting and Receiving Coils :

In this System we are Using Copper Coils with 1000 Turns For Higher Coupling Factor to increase Efficiency.Copper Coils have relatively high Coupling Factor and when the distance between the turns is reduced Coupling Factor increased and which inturns increases the Efficiency.

4. Microcontroller :

The Atmel AT89C51 microcontroller is used to control the overall operation of the LCD and Power Transfer using Switch. It is a 8-bit microcontroller. ATMEL 89C51 has 4KB of Flash programmable and erasable read only memory (PEROM) and 128 bytes of RAM. In 40 pin AT89C51, there are four ports designated as P1, P2, P3 and P0. All these ports are 8-bit bi-directional ports.

5. Current Booster Circuit :

This Circuit is used for boosting the Received Current. in this Circuit we are Using current booster Circuit implemented using N Channel MOSFET.

6. DC to AC and AC to DC Converter :

as Wireless Power Transfer Can Occur only in AC current Carrying Conductor the DC power is Converted in AC and Vice versa is done at the Receiver Side.

7. Relay :

It is a electromagnetic device. It will used to turn ON or OFF the device which is connected to relay. Here 12v relay is required

SOFTWARE REQUIREMENTS :

It requires Keil compiler μ Vision 3 Which is used For Converting the the Source Code into Hex code.

It Requires Proteus version 8 for Designing Power Supply and pcb. it is also used for Primary testing and Simulation of Circuits.

ADVANTAGES :

1. Wireless Power Transfer is Very Efficient Power Transfer Mode.
2. It reduces the Losses Occurred during Power Transmission.

3. As Medium Is Wireless It Does not Involve Cost of Wiring.
4. Extending the System can make Wireless Power transfer Secure.
5. As It uses Resonant Inductive Coupling technique it is not Harmful to Living Beings.

APPLICATIONS :

1. the System Can be Used as a Solution to the Solar powered Street lights in Extreme Weather Conditions.
2. Extended Applications of this System Can be Used in Trains and Aeroplanes.
3. Concept is also applicable in Consumer Electronics Solar Energy Harvesting.

FUTURE SCOPE :

1. This System Can be Used In Electric Vehicle Technology.
2. It Can also be used in Satellite Communication and other Transportation Facilities.

ACKNOWLEDGEMENT :

First of all I would like to thank my parents for their blessing and the trust they have shown for pursuing my M.E. degree. I wish to express my pleasure of acknowledging and thanks towards Prof. K.Sujatha, my Project Guide for providing the technical guidelines and constructive suggestions regarding the line of this work. He encourages me all the times for doing this quality research work in tune with the target puts before me. I have been very fortunate to have his appreciable guidance during my stay at the department.

I also wish to extend my sincere thanks our concerned teaching staff for their insightful comments and suggestions to improve my performance during my presentations at the department.

In addition, I would also like to thank Dr. A.D.Desai, Principal of SRE'S Shree Ramachandra College of Engineering for providing me necessary resources and support granted throughout my master's fellowship.

I also thank to my friends those have rendered their help during the course of this work.

CONCLUSION :

Wireless Power Transfer and Witricity can be used in Every Domain Which is Directly or Indirectly Related to Electricity. it can Curb the Losses arises due to Wired Power transmission. Transmission of power through Wireless Medium will Dominate this High Demand Electricity era. Systems like Proposed System are Solution to the Conventional Electricity Transmission Techniques.

REFERENCES :

- [1] Siqi Li and Chunting Chris Mi " Wireless Power Transfer For Electric vehicle applications" IEEE journal of Emerging and Selected Topics In Power Electronics, Vol. 3, No.1, March 2015

- [2] A. K. A. Kurs, R. Moffatt, J. D. Joannopoulos, P. Fisher, and M. Soljacic, "Wireless power transfer via strongly coupled magnetic resonances," *Science*, vol. 317, no. 5834, pp. 83–86, 2007.
- [3] A. P. Sample, D. A. Meyer, and J. R. Smith, "Analysis, experimental results, and range adaptation of magnetically coupled resonators for wireless power transfer," *IEEE Trans. Ind. Electron.*, vol. 58, no. 2, pp. 544–554, Feb. 2011.
- [4] B. L. Cannon, J. F. Hoburg, D. D. Stancil, and S. C. Goldstein, "Magnetic resonant. coupling as a potential means for wireless power transfer to multiple small receivers," *IEEE Trans. Power Electron.*, vol. 24, no. 7, pp. 1819–1825, Jul. 2009.
- [5] Askin Erdem Glindogdu and Dr. Erkan Afacan " Some Experiments Related to Wireless Power Transmission " Cross Strait Quad-Regional Radio Science and Wireless Technology Conference 2011
- [6] Yoon Do Chung , Chang Young Lee , Hyoung Ku Kang and Young Gun Park " Design Consideration and Efficiency Comparison of Wireless power Transfer with HTS and Cooled Copper Antennas. " *IEEE Transactions On Applied Superconductivity*, Vol. 25, No. 3, June 2015
- [7] S. J. Gerssen-Gondelach and A. P. C. Faaij, "Performance of batteries for electric vehicles on short and longer term," *J. Power Sour.*, vol. 212, pp. 111–129, Aug. 2012.
- [8] A. Kurs, R. Moffatt, and M. Soljacic, "Simultaneous mid-range power transfer to multiple devices," *Appl. Phys. Lett.*, vol. 96, no. 4, pp. 044102-1–044102-3, 2010.
- [9] C. Sanghoon, K. Yong-Hae, S.-Y. Kang, L. Myung-Lae, L. Jong-Moo, and T. Zyung, "Circuit-model-based analysis of a wireless energy transfer system via coupled magnetic resonances," *IEEE Trans. Ind. Electron.*, vol. 58, no. 7, pp. 2906–2914, Jul. 2011.
- [10] L. C. Kwan, W. X. Zhong, and S. Y. R. Hui, "Effects of magnetic coupling of nonadjacent resonators on wireless power domino-resonator systems," *IEEE Trans. Power Electron.*, vol. 27, no. 4, pp. 1905–1916, Apr. 2012.
- [12] Y. Nagatsuka, N. Ehara, Y. Kaneko, S. Abe, and T. Yasuda, "Compact contactless power transfer system for electric vehicles," in *Proc. IPEC*, Jun. 2010, pp. 807–813.
- [13] C. J. Chen, T. H. Chu, C. L. Lin, and Z. C. Jou, "A study of loosely coupled coils for wireless power transfer," *IEEE Trans. Circuits Syst.*, vol. 57, no. 71, pp. 536–540, Jul. 2010.
- [14] M. Budhia, G. A. Covic, and J. T. Boys, "Design and optimization of circular magnetic structures for lumped inductive power transfer systems," *IEEE Trans. Power Electron.*, vol. 26, no. 11, pp. 3096–3108, Nov. 2011.
- [15] C. Wang, O. H. Stielau, and G. A. Covic, "Design considerations for a contactless electric vehicle battery charger," *IEEE Trans. Ind. Electron.*, vol. 52, no. 5, pp. 1308–1314, Oct. 2005.
- [16] M. L. G. Kissin, G. A. Covic, and J. T. Boys, "Steady-state flat-pickup loading effects in polyphase inductive power transfer systems," *IEEE Trans. Ind. Electron.*, vol. 58, no. 6, pp. 2274–2282, Jun. 2011.

Role of Heat Treatments on Phase Decomposition and Microstructure Morphology Impact on Mechanical Properties of High Strength Steel

¹Enefolo S. Ameh, ²Basil O. Onyekpe

¹Mechanical Department, University of Benin, Nigeria

²Mechanical Department, University of Benin, Nigeria

Abstract—The research work studied the role of heat treatments on phase decomposition and microstructure morphology impact on fracture toughness, yield strength and hardness of high strength steel. Normalizing, austempering and quenching and tempering were performed after initial austenization of the as-received steel to 950°C at 90mins isothermal holding period and the respective microstructure characterized with light optical and scanning electron microscopes. J-integral, tensile and hardness tests were conducted in accordance with American standard test method E1820, E8 and E92 respectively. The results showed remarkable high fracture toughness, yield strength and hardness parameters sensitivity to microstructure morphology and quenched and tempered microstructure indicated the best mechanical properties combination trade off, followed by austempered, as-received and normalized microstructure.

Keywords— Fracture toughness, hardness, heat treatment, microstructure, yield strength.

1.0 INTRODUCTION

High strength steels are widely used in offshore environment such as platform leg tension, pressure vessel, pipelines and jacket structures owing to lower weight and lower manufacturing cost [1]. Fracture toughness, yield strength and hardness are fundamental mechanical properties considered in high strength steel design to overcome harsh offshore environment [2]. But the combination of these mechanical properties is usually difficult to attain because an increase in one of these properties leads to a decrease in the others [3]. High strength steel microstructures and its correlation to major mechanical properties remains complex and are being influenced by heat treatment process, homogeneousness and composition [4]. The impact of microstructure morphology on mechanical properties of high strength steel still have contradictory literatures because of complexity with microstructural phases, constituent formation mechanism including the fact that different microstructures offer different combination of toughness, strength and hardness for the same chemical composition [5].

2.0 LITERATURE SURVEY

Microstructural makeup and resultant mechanical properties depend on the heat treatment methods or cooling rates. Heat treatment has become an industrial process used to soften steel to change grain size, modify material structure and free induced-stress in a material [6]. It is a combination of heating usually to austenization temperature and then cooling in water, oil or air with a view to hardening or softening it [7]. The high temperature austenization phase in steel has the property to transform into mixture of two or more constituents like ferrite, pearlite, bainite, martensite and retained austenite depending on the cooling cycle [8]. The most widely used heat treatment processes include hardening, normalizing, annealing, quenching and tempering [9].

Microstructural constituents such as pro-eutectoid ferrite appearance at the grain boundaries which is usually formed at 520 – 720°C improves toughness properties of steel independent of heat treatment process [10]. Study has shown that impact fracture toughness of steel which had undergone normalization will probably yield tougher value than hardened and tempered steel [11]. While bainite microstructural constituent is believed to be formed during austempering heat treatment in the presence of Mo and Ni alloy elements which help to suppress pearlite reaction to allow austenite transformation to bainite. Lower bainite shape appeared more needle-like and formed within temperature range of 400 – 250°C while the upper bainite with feathery and broader plate appearance is usually formed with 500 – 400°C [12].

Mechanical properties and microstructures of mild steel subjected to annealed, normalized and hardened heat treatments at 850°C austenization temperature had been investigated and concluded that the hardness values of heat treated samples were all lower than the as-received which has ferrite-austenite duplex phase composition [13]. Similarly, examination of mechanical properties of medium carbon steel at the same initial austenization temperature for different heat treatment methods (normalizing, annealing, hardening and tempering) indicated annealed sample showed the lowest strength and hardness and highest ductility and toughness values but hardened samples indicated highest strength and hardness with lowest ductility and toughness values [14] and effect of heat treatment and mechanical properties of spring steel studied revealed decrease in hardness and strength but increased in ductility with increasing tempering temperature and time [15].

Several researches on heat treatments effect on microstructure and mechanical properties of carbon or spring steel have been carried out but rarely had work been done on high strength steel which has very complex microstructure owing to micro alloying elements. The present research work is aimed at examining the role of heat treatment on phase decomposition and impact of microstructure morphology on mechanical properties such as fracture toughness, strengths and hardness of high strength steel. The practical relevance of the work include further development of fundamental understanding of the complex high strength steel microstructure, improve mechanical properties trade off, material qualification and selection.

3.0 RESEARCH METHODOLOGY

3.1 Material Heat Treatment and Characterization

25mm thick plate of high strength steel was procured from Masteel Company in UK. The chemical composition of the steel are - 0.0017% boron, 0.076% aluminum, 0.026% niobium, 0.004% titanium, 0.062% chromium, 0.002% vanadium, 0.11% molybdenum, 0.051% nickel, 0.0006% sulphur, 0.0042% nitrogen, 0.011% phosphorus, 0.03% copper, 0.296% silicon, 1.3% manganese, 0.161% carbon and the remainder percentage for iron. Samples were cut from bulk material and heated initially to 950°C austenization temperature and 90minute isothermal holding time and processed through normalization, austempering and quenching and tempering heat treatments as prescribed by ASM [16]. The samples for austempering were quenched from 950°C to 350°C salt bath in electric resistance furnace with 2mole potassium chloride and 1mole barium chloride and held for 90minutes before cooling in air. But the samples for quenching and tempering were tempered at 550°C after initially being quenched in water and normalized samples cooled in air to ambient temperature. Samples extracted were sectioned and encapsulated prior to progressive grinding with 120, 220, 600 and 1200 emery paper. The samples were further polished with 6micron and 1micron. The shining mirror-like specimen surfaces etched in 2% nital and then viewed under both light optical and scanning electron microscopes fitted with digital camera and computer system at an accelerated 15KV.

3.2 J-integral Testing

Testing was carried out according to ASTM E1820. Specimens were machined to compact tension geometry (Fig 3.1) and dimensions as indicated Table 3.1. Each specimen was fatigue precracked to a/w of 0.5 and tested at room temperature using an Instron servo-hydraulic machine and automated computer controlled testing procedures. Load versus crack mouth opening displacement (v) was plotted online and a compliance technique was employed in crack increment measurement using the following mathematical expressions [17]:

$$a_i/w = 1.00196 - 4.06319U + 11.242U^2 - 106.043U^3 + 464.335U^4 - 650.677 \quad (3.1)$$

Where, $U = 1/\sqrt{BEC_i} + 1$, B = specimen thickness, C_i = compliance, E = Modulus of elasticity. But the crack mouth opening displacement (V) which is a function of crack length increment was computed with mathematical relationship:

$$V = P [65.351 - 298.06 a/W + 630.11(a/W)^2]/EB \quad (3.2)$$

Where, P = applied load and W = specimen width

J-integral versus crack extension curves was plotted online to for each crack length increment in order to determine critical fracture toughness using the following equation:

$$J = k^2(1 - v^2)/E \left[J_{pl(i-1)} + \left(\frac{\eta_{pl}}{B^{(i-1)}} \right) (A_{pl(i)} - A_{pl(i-1)}) (1 - \gamma_{pl}) \left(\frac{a_i - a_{(i-1)}}{B^{(i-1)}} \right) \right] \quad (3.3)$$

Where, k = stress intensity factor, $A_{pl(i)} - A_{pl(i-1)}$ = increment of plastic area under load versus CMOD, $J_{pl(i-1)}$ = initial plastic area under load versus CMOD and $a_i - a_{(i-1)}$ = incremental crack length.

Table 3.1: CT Specimen dimensions

Quantity	Measured value (mm)
Specimen height (H)	$1.2 * W = 30.50$
Specimen width (W)	25.40
Specimen thickness (B)	$0.5 * W = 12.70$
Crack length (notch + pre-cracked)	$0.45 \leq a_o / W \leq 0.55$.
Notch Length (n)	$0.25 * W = 6.35$
Pre-cracking length (L)	$0.05B = 0.64$
Notch height (N)	$0.1 * W = 2.54$
Span length (S)	$0.55 * W = 13.97$
Pin hole diameter (d)	$0.25 * W = 6.35$
Total specimen length (T)	$1.25 * W = 31.75$

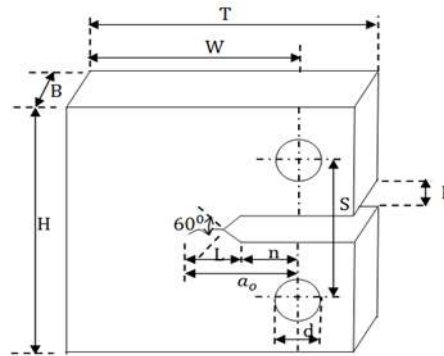


Figure 3.1: CT specimen geometry

3.3 Tensile Testing

Four specimens were extracted from bulk steel plate and machined to flat tensile specimen (Fig 3.2) and test conducted at ambient temperature according to ASTM E8 [18] at 1mm/s loading rate using automated controlled hydraulic testing machine and the elongation with corresponding loads recorded and stress – strain curves were automatically plotted on a computer controlled system.

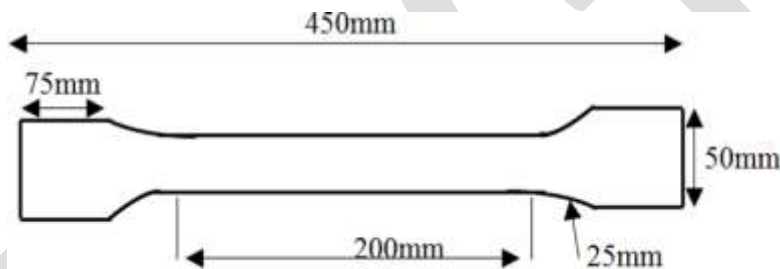


Figure 3.2: Flat tensile specimen geometry

3.4 Hardness Testing

Hardness test specimens were firstly cut from steel plate. Each specimen was encapsulated in a plastic for ease of handling and then polished on 1micron after grinding with several emery paper grades. The hardness test was performed using Vicker measuring technique with pyramidal diamond shaped tip indenter (Fig 3.3) which delivered load into the prepared surface of samples for a period of 14 seconds as prescribed by ASTM E92 [19]. 15kg load from the machine was applied to six different points on the test surface with indenter via weight lever and the vicker hardness value (Hv) calculated from the following mathematical expression:

$$HV = \frac{1.8544F}{d^2} \quad (3.4)$$

Where, F = applied load and d = diameter of indentation

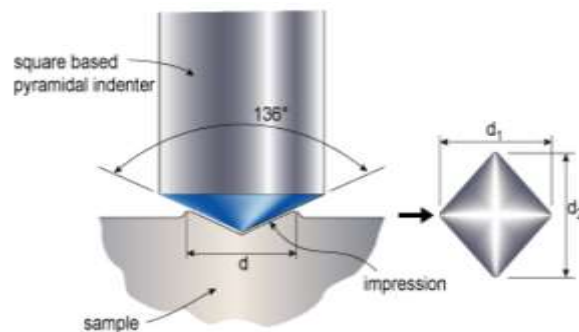


Figure 3.3: Vicker hardness test schematic [20]

4.0 RESULTS AND DISCUSSION

4.1 Role of Heat Treatments on Phase Decomposition

Microstructure (Fig 4.1) of the as-received exhibited complex arrangement of martensite with carbide precipitate distributed through the morphological structure and resemblance of the quenched and tempered microstructure indicating the as-received steel was probable produced through quenched and tempered heat treatment process. Normalization microstructure (Fig 4.2) had undergone complete recrystallization resulting in coarse ferrite/pearlite. The austenite partially transformed to pro-eutectoid ferrite, leaving the remaining carbon – enriched austenite transformed to pearlite during cooling. The microstructure micrograph revealed predominately pro-eutectoid ferrite matrix with interconnected and degenerated pearlite colonies at the grain boundaries. There was obvious coalescence and large interfacial between ferrite-pearlite structures but no evidence of ferrite/pearlite banding formation.

Resultant austempered microstructure after austenizing the as-received steel to 950⁰C and austempering to 350⁰C for 90minutes time consisted basically short bainite sheaves and traces of coarse ferrite/pearlite grains presence. The micrograph showed bainite sheaves started deforming but the sheaves shapes were still much visible. The amount of bainite formed was believed to be largely depended on austenization temperature and time which determine austenite quantity available to transform to bainite and it is formed during austempering heat treatment in the presence of Mo and Ni alloy elements which help to suppress pearlite reaction to allow austenite transform into bainite. The bainite structure revealed traces of upper bainite with feathery and broad plate appearance at 350⁰C austempering temperature in the lower bainite structure and was not in agreement with [12] the finding that upper bainite which is associated with feathering and broad appearance plate is usually formed within the temperature range of 500⁰C to 400⁰C. The lower bainite structure probably contained traces of upper bainite owing to the long austempering duration of 90minutes agreed with the [21] study that austempering duration extending beyond 15 to 25minutes lead to bainite structure coarsening phenomenon because of the austenite grain growth which consequently yielded thick and feathering bainite structure. The traces of ferrite/pearlite in the austempered microstructure may have resulted from incomplete transformation of austenite to bainite due to quenching and consequently resulted in some austenite transformation to ferrite/pearlite and the remaining untransformed austenite was trapped in the bainite matrix as retained austenite at room temperature. The volume fraction of ferrite depend largely on these transformation kinetics and it is known to increase and coarser with increasing austempering temperature.

The quenched and tempered microstructure (Fig 4.4) at 550⁰C for 90minutes austenization time clearly showed large packets and blocks of martensite structure with recrystallized ferrite grains as the white region. Microstructure of high strength steel consisted martensite/bainite matrix after austenization to 950⁰C and quenched. The matrix exhibited tempered martensite/bainite microstructure after tempering [22]. The tempered martensites contain ferrite with carbide precipitates within and at the boundaries of the laths. The tempered martensite structure produced coarse grain and well dispersed carbide precipitates in white ferrite region matrix [23] depending on the soaking time. Particle sizes increased due to long tempering time that permitted more precipitates, carbon diffused far and spacing of the of the carbon rich phase Fe₃C become larger.

But the as-received, austempered, quenched and tempered microstructures showed some light coloured regions probably representing retained austenite. Austenite is known to exist in normal phase at high temperature but retained austenite becomes unstable below the range of normal temperature and could be harmful to mechanical properties when the content is greater than 15%. Therefore the retained austenite will change to martensite if significant drop in temperature lower than the temperature to which it was quenched is allowed or if the room temperature austenite is allowed to undergo high level mechanical stress. This transformation is

usually accompanied with volume change or geometry within the internal structure that may induce internal stress and manifest itself as crack [24].

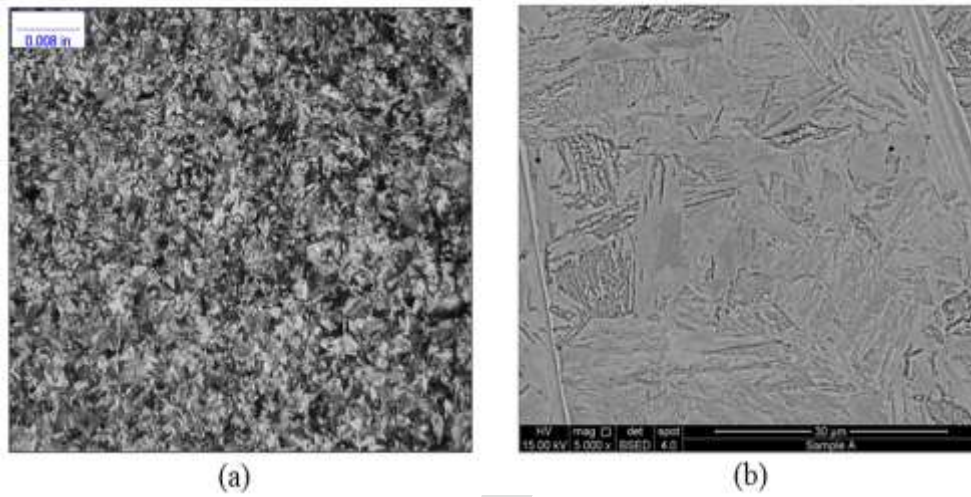


Figure 4.1: Microstructure of the as-received sample –a) LOM X200, b) SEM X5000

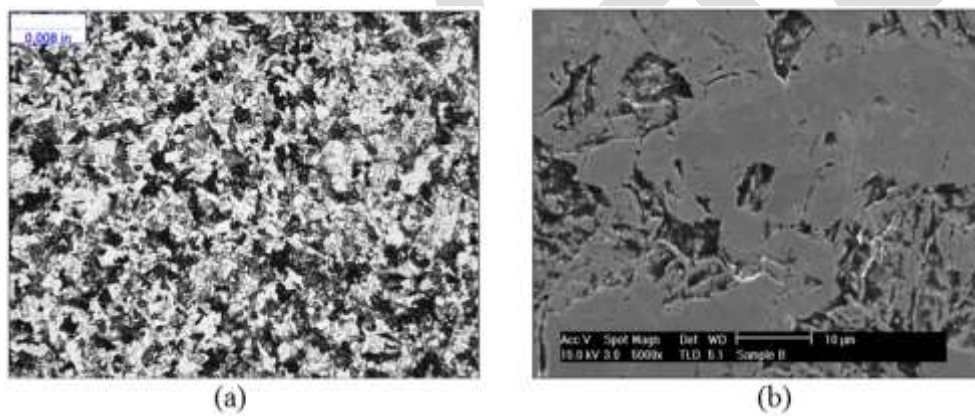


Figure 4.2: Microstructure of the normalized sample –a) LOM X200, b) SEM X5000

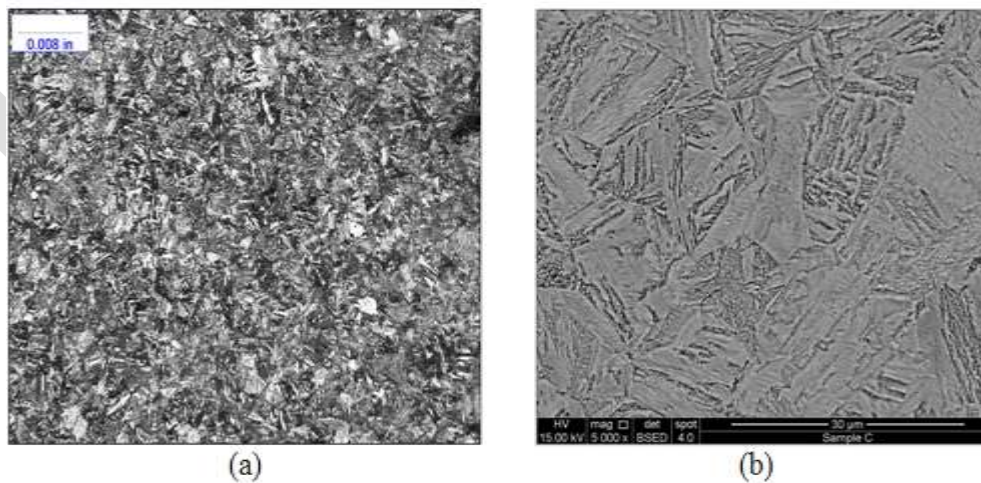


Figure 4.3: Microstructure of the austempered sample –a) LOM X200, b) SEM X5000

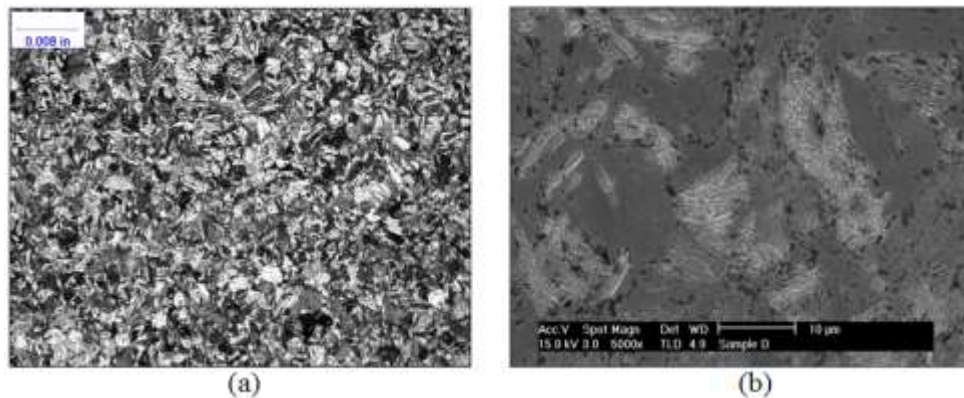


Figure 4.4: Microstructure of the quenched & tempered sample –a) LOM X200, b) SEM X5000

4.2 Microstructure Impact on Mechanical Properties

Microstructure impact on fracture toughness was evaluated using J-integral testing. Fig 4.5 shows normalized microstructure indicated highest remarkable critical fracture toughness of 373kJ/m^2 , trailed by quenched and tempered (202kJ/m^2), as-received (138kJ/m^2) and then austempered microstructure (109kJ/m^2). Soft pro-eutectoid ferrite matrix presence was responsible for the remarkable fracture toughness of normalization. The observation was in alignment with [11] the finding that steel impact toughness that had undergone normalization appeared tougher than austempered and quenched and tempered microstructure. But the austempered showed fracture toughness lower than the quenched and tempered due to presence of hard bainite matrix formation and possibly due to excessive retained austenite throughout the structure while the quenched and tempered exhibited higher level fracture toughness due to cementite precipitates, spheriodization and recrystallation ferrite matrix during tempering to 550°C . The toughness significant margin was not in alignment with [25] the recommendation to replace conventional quenching and tempering with austempering because of its better toughness owing to bainite-martensite or fully bainite structure composition.

Yield strengths were determined from stress-strain curves plotted on-line during tests. Comparative evaluation of the obtained yield strengths (Fig 4.6) indicated austempered microstructure has the highest yield strength of 940MPa, followed by quenched and tempered (780MPa), as-received (766MPa) and normalized microstructure (408MPa). The hardness results (Fig 4.7) showed marginal variation in the samples that had undergone different heat treatment methods in the same chronological order with yield strength which increased from austempered to normalization microstructure. The austempered microstructure showed highest average hardness value of 318Hv, closely followed by quenched and tempered with 251Hv, as-received (246Hv) and normalized microstructure (192Hv). The significant increase in the austempered yield strength and hardness values was attributed to hard constituent bainite sheaves and grain density formation in the structure which implied bainite appearance increases both yield strength and hardness of steel. But the quenched and tempered microstructure yield strength and hardness are slightly lower than the austempered despite tempering due to the presence of cementite formation in the martensite matrix which is a harder constituent than martensite. Contrastingly, the normalized sample indicated lowest yield strength and hardness values which suggested pro-eutectoid ferrite matrix and pearlite appearance in the microstructure were responsible for the obtained low values implying they are softer constituent compared with the bainite and martensite.

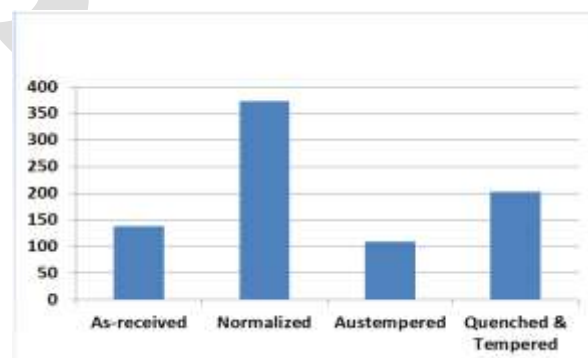


Figure 4.5: J-integral fracture toughness of microstructures chart

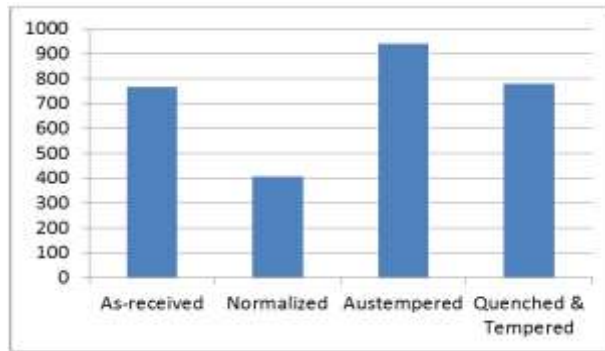


Figure 4.6: Yield strengths of microstructures chart

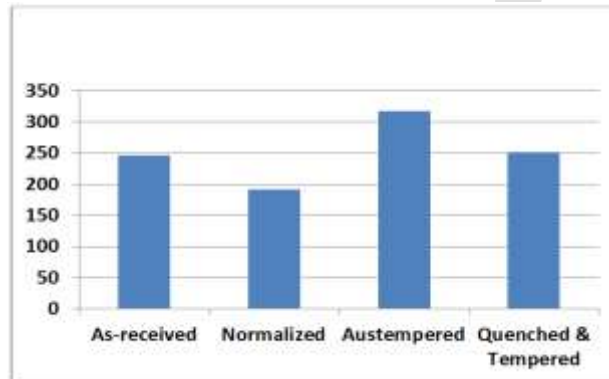


Figure 4.7: Vicker hardness of microstructures chart

5.0 CONCLUSION

The present study has shown that upper bainite structure with feathery and broad plate appearance could be formed at 350⁰C and not only within 500⁰C to 400⁰C depending on the isothermal holding period. Secondly, quenched and tempered microstructure indicated the best combination of fracture toughness, yield strength and hardness trade-off compared with normalization, austempered and as-received microstructures.

REFERENCES:

- [1] J. Billingham, J. Healy, and H. Bolt "High strength steel- the significance of yield ratio and work hardening for structural performance" *Marine Research Review* Pub MTD, 1997.
- [2] B.S. Motagi and R. Bhosle "Effect of Heat Treatment on Microstructure and Mechanical Properties of Carbon Medium Steel" *International Journal of Engineering Research and Development*, Vol. 2, Issue 1, 2012, Pp 07 – 13.
- [3] E. Gogou "Use of High Strength Steel Grades for Economic Bridges Design". *Master Thesis*, Delft University of technology, 2012.
- [4] L.W. Ma, X. Wu and X. Kenong "Microstructure and property of medium carbon steel processed by equal channel angular pressing" *Material forum* Vol. 32, 2008, Pub. Institute of materials engineering Australasia ltd.
- [5] S. Al-rubaiey, E. Anon and M.M. Hanoon "The influence of microstructure on the corrosion rate of carbon steel" *Engineering and Technological Journal*, vol.31, 2013, part (A) No 10.
- [6] T. P. Arasu, R. Dhanasekaran, S. P. Kumar and N. Srinivasan "Effect of Hardness and Microstructure on En 353 Steel by Heat Treatment" *International Journal of Engineering and Science*, vol 2, 2013, pp 01-05.
- [7] S. Danda "Effect of Induction Hardening on High Carbon Steel Forgings" *International Journal of Soft Computing and Engineering*, vol. 1, issue11, 2011, pp 01-05.
- [8] S. S. Sharma, K. Jagannath, C. Bhat, U. Achutha Kini, P.R. Prabhu, P.K. Jayashree and M.C Gowrishankar "3rd International Conference on Mechanical" *Automotive and Material Engineering*, 2013, Singapore

- [9] S.M.A Al-Qawabah, N. Alshabatat, and U.F. Al-Qawabeha “Effect of Annealing Temperature on the Microstructure, Microhardness, Mechanical Behavior and Impact Toughness of Low Carbon Steel Grade 45”. *International Journal of Engineering Research and Application*, vol 2, 2012, pp1550-1553.
- [10] M. M. Tash “Effect of Hot Forging Reduction Ratio and Heat Treatment on Hardness, Impact Toughness and Microstructure of Carbon and Low Alloy Steel” *International Journal of Advanced Technology in Engineering and Science*, Vol. 3, Issue 3, 2015.
- [11] C.A. Reddy “Effect of holding temperature and time for austempering on impact toughness of medium carbon and high alloy steel” *International Journal of Computer Network and Security*, vol 3, 2013.
- [12] X. Lian “The Complex Phase Transformation of Austenite in High Strength lineup steels and its influence on the mechanical properties” Doctoral thesis, University of Pittsburgh, 2012.
- [13] O. O. Joseph^{*1}, O. O. Joseph^{*2}, R. O. Leramo and O. S. Ojudun “Effect of Heat Treatment on Microstructure and Mechanical Properties of SAE 1025 Steel: Analysis by one – way ANOVA” *J. Mater. Environ. Sci*, Vol. 6, 2015, Pp 101 – 106.
- [14] D.A. Fadare, T.G. Fadara and O. Y. Akanbi “Effect of Heat Treatment on Mechanical Properties and Microstructure of NST 37-2 Steel” *Journal of Minerals and Materials Characterization & Engineering*, Vol. 10, Issue 3, 2011.
- [15] M.S. Htun, S.T. Kyaw and K.T. Lwin “Effect of Heat Treatment on Microstructure and Mechanical Properties of Spring” *Journal of Metals, Materials and Mineral*, vol 18, 2008, pp 191 – 197.
- [16] ASM International, ASM Handbook: Heat Treatment, Vol. 4, American Society for Metals, Ohio, 1999.
- [17] ASTM E1820 “Standard test method for measurement of fracture toughness” Pub. ASTM International USA, 2010.
- [18] ASTM E8 “Standard Test Method for Tension Testing of Metallic Materials” Pub. ASTM International USA, 2012.
- [19] ASTM E92 “Standard Test Method for Vicker Hardness and Knoop Hardness of Metallic Materials” Pub ASTM International, 2016.
- [20] G. Mathers, Hardness Testing Part 1, Article of TWI, 2005, Pp 4 – 5.
- [21] C. Chen, Fei-Yi, L. Truan-Sheng, and C. Li-Hui “Microstructure and Mechanical Properties of Austempering Cr-Mo alloy steel”. *Journal of Materials Transaction*, vol 5, 2013, pp 56 – 60.
- [22] J. D. Verhoeven “Fundamental of Physical Metallurgy” Pub. John Willey & Son, 1975.
- [23] W. Callister “Material Science and Engineering. An Integrated Approach” Second edition. Pub. John Wiley and sons, Inc, 2005.
- [24] D. H. Herring “Vacuum Heat Treatment: Principles, Practices and Application” Second Edition, Pub BNP Media, 2005.
- [25] J. Wen, Q. Li and Y. Long “Effect of Austempering and Mechanical Properties of GCr18Mo Steel” *Material Science Engineering A*, 2006, pp 251 – 253.

Nonlinear analysis of cortical bone using Finite Element Method and algorithms developed in MATLAB

Dr Chandrashekhar Bendigeri ¹, Rohith M ²

¹ Associate Professor, Department of Mechanical Engineering UVCE, Bangalore

² ME, Department of Mechanical Engineering, UVCE, Bangalore

csb.login@gmail.com

Abstract— The fabrication of patient-specific engineering Implant is highly appreciated which requires prior determination of porous and mechanical characteristics ^[1, 8]. This is because of, the increase in porosity decreases the mechanical properties and increases the damping factor which leads to subsequent bone loss upon healing or remodeling ^[2, 8]. The hypothesis is that the patient specific scaffold Implants should provide a biomimetic mechanical environment for initial function and appropriate remodeling of regenerating tissue while concurrently providing sufficient strength in compression and porosity for cell migration and cell delivery ^[6]. The reason behind this approach is to improve the host-implant response with a better Osseo-integration compared to classical approach ^[4]. This work primarily aims at study of Non-Linear ^[23, 24] behavior of patient specific hydroxyapatite (HAP-Cortical Bone) which can be fabricated as Implant using algorithms developed in MATLAB ^[3], a non-invasive polymer cranial fracture implant with biocompatible approach.

Keywords— Non-linear, Bio-mechanics, MATLAB, Mindlin-Reissner theory, Cranial Implants, Finite Element Method, Three-Point bending, Explicit loading, Cortical Bone.

INTRODUCTION

The ability to precisely design and manufacture biomaterial scaffold Implants is needed since traditional methods for scaffold design and fabrication cannot provide the control over scaffold Implants architecture design to achieve specified properties within fixed limits on porosity ^[1, 2, 8]. The theoretical formulation for polymeric implants approach provides a conducive environment with host compared to traditional implants in terms of non-carcinogenic, radio-opaque, Osseo-integration and non-toxic ^[2]. The study of this HAP implant is carried out by considering a rectangular plate of specified dimensions, which can be used for Implants using MATLAB ^[3], with the algorithms developed based on the theories matching to the behavior of the cadaveric cortical bone for non-linear analysis.

This work is focused mainly on study of the nonlinear behavior of cortical bone-HAP, as an alternative for the titanium Implants. This is because large dimensions of cranial bone defects and sometimes rather bad conditions of adjacent soft tissues, such as craniectomy defects do not only require reconstruction for the protection of the intracranial structures, but also requires creation of Bio-compatible environment with better Osseo-integration and less stress shielding effect, Host-Implant response and harmonic contours with long-term stability, reduction of patient complaints, easy handling of the implants, and the possibility of oncological follow-up with qualified imaging methods of cranial Implants ^[4].

This work is carried out by implementing the Mindlin-Reissner theory ^[25] for a rectangular plates of specified dimensions which can be used as an implant by considering the properties similar to that of a human bone and studying its behavior with human bone using the algorithms developed in MATLAB ^[3]. The analysis, specifically meshing of the rectangular plate with iso-p quadrilateral elements (plate elements), the boundary conditions and the explicit loading conditions were implemented using the algorithms developed in MATLAB ^[3] and the resulting displacement were studied.

Next, the real cadaveric bone specimen of HAP is prepared with proper dimensions. Also, the fixture for conducting the three-point bending test and tensile test is prepared. The prepared specimen is then subjected to three-point bending and tensile test. The obtained results from tensile test is used to determine the Young's modulus of cadaveric cortical bone, which is made used in the properties for the algorithms developed in MATLAB. Next, the displacements from the experimental data and finite element method in MATLAB are compared for best custom cranial implants and HAP for various parameters such as stress shielding, effective strength, stiffness, host-implant response, Osseo-Integration

METHODOLOGY

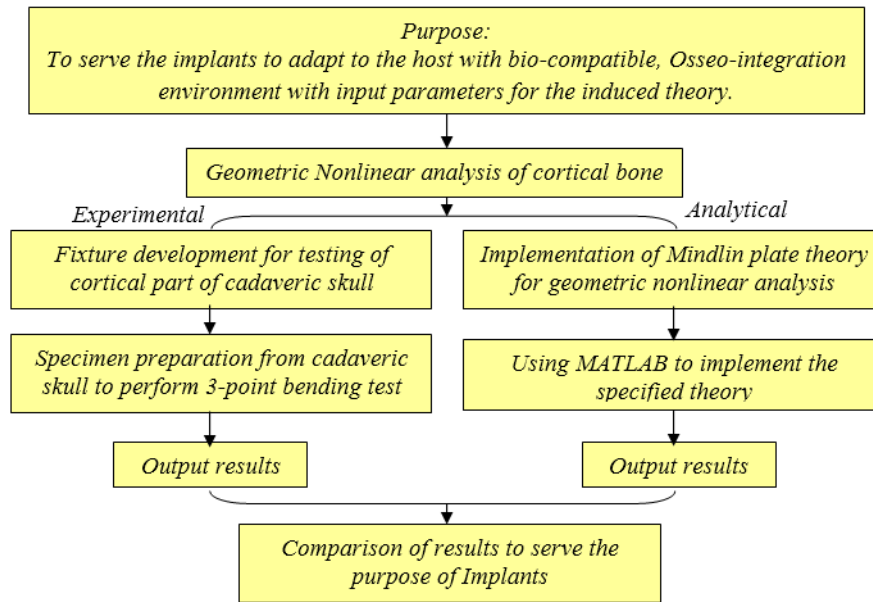


Figure 1: Overall procedure for the Non-linear analysis of cortical bone

Theoretical Formulations:

Geometric non linearity^[25] is considered because change in geometry as the structure deforms is taken into account in setting up the strain displacement and equilibrium equations. Strain-displacement equations $e=Du$. The operator D is nonlinear when finite strains are expressed in terms of displacements.

In all the geometric nonlinear problems we solve the following equation which is called the “force residual”.

$$r(u,\Lambda)=0$$

This vector includes all the discrete equilibrium equations encountered in nonlinear static analysis formulated by the displacement method. Here u is the state vector containing unrestrained degrees of freedom that characterize the configuration of the structure, r is the residual vector that contains out-of-balance forces conjugate to u, and Λ is an array of assignable control parameters. Now, varying the vector r with respect to the components of u while keeping Λ fixed yields the Jacobian matrix.

Mindlin Plate Theory

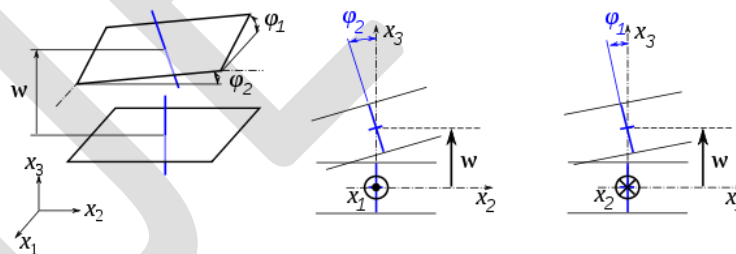


Figure 2: Out of plane deformation according to Mindlin plate theory.

The non-linear static analysis and only geometric non-linearity is considered where the material is considered to be homogeneous, isotropic and linear elastic. Dynamical effects are neglected and deformations are large to use finite deformation theory (Geometric non-linearity). This plate theory includes transverse shear deformations. Here we look at the elements with 5 degrees of freedom three translations (u, v, w) and three rotations ($\theta_x, \theta_y, \theta_z$) with $\theta_z = 0$, indicating zero stiffness.

$$\bar{u} = u - z\theta_x$$

$$\bar{v} = v - z\theta_y \text{ and } \bar{w} = w$$

Finite element discretization

For finite element analysis, we considered a rectangular plate of dimension from a real cadaveric skull specimen which was subjected to experimentation and used the same material properties determined experimentally being, Young’s modulus is 3020 MPa and Poisson ratio is 0.3. With these parameters the plate is divided into 80 mesh elements along length and 25 mesh elements

along the width to generate the mesh.

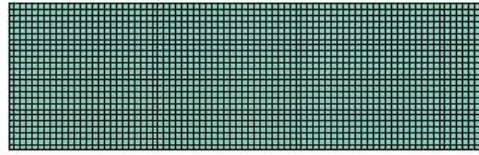


Figure 3: Rectangular plate with mesh elements

Quadrilateral iso-parametric shell element is used for discretization with five degree of freedom per node with $\theta_z = 0$.

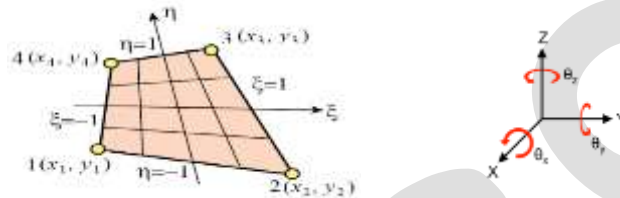


Figure 4: Figure representing Iso-parametric 4 noded Quadrilateral element and Five Degree of freedom at each node with $\theta_z = 0$.

The first variation of potential energy is written as

$$\delta\Pi = \delta U - \delta W = 0$$

$$\delta U = \delta W$$

The variation of strain energy of the plate is written as summation of in-plane bending strain energy and transverse shear strain energy.

$$\delta U = \int_A d\epsilon_{ib}^T \hat{\sigma}_{ib} dA + \int_A d\epsilon_s^T \hat{\sigma}_s dA$$

For non-linear system, the element equilibrium equation is

$$R = \int_A B_{ib}^T \hat{\sigma}_{ib} dA + \int_A B_s^T \hat{\sigma}_s dA - F = 0$$

where R is residual and F is a generalized forces comes from variation of external work done.

The solution algorithm for the assembled nonlinear equilibrium equations is based on Newton-Raphson method which need linearization of equations at equilibrium point. Here linearized equations are of the form

$$K_T d\alpha_{n+1}^i = R_{n+1}^i$$

where R is residual and i denotes iteration number. The residual can be written as

$$R = K_S \alpha - F_{n+1}$$

where F and $K_S \alpha$ are external and internal forces respectively.

The element In-plane, bending and the shear stiffness matrix are evaluated into global stiffness matrix. Implementing the Boundary condition and the explicit Loading condition, assemblage of element stiffness matrix and force vector into global level is carried out. The results obtained from these formulations and algorithms developed in MATLAB [3] are as shown below.

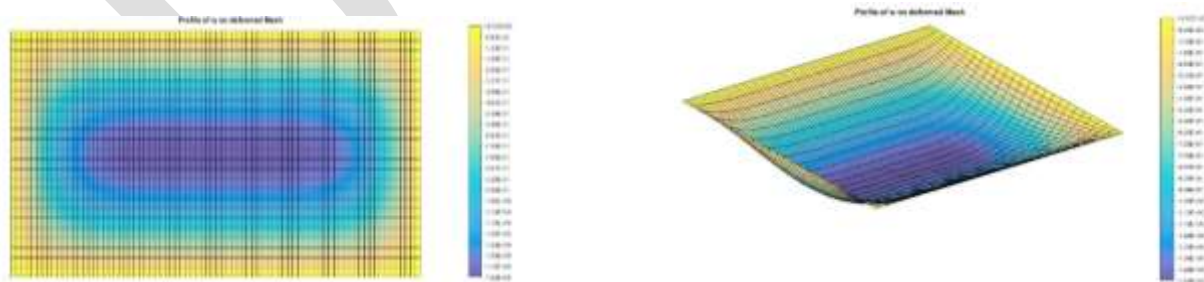


Figure 5: Output mesh of Transverse displacement of rectangular plate in MATLAB.

From the theoretical formulations and analysis in MATLAB [3] we have found that the transverse displacement of a rectangular plate according to Mindlin plate theory subjected to a transverse load of 360N has a transverse displacement of 1.524 mm which almost matches to the experimental results [14, 16, 22].

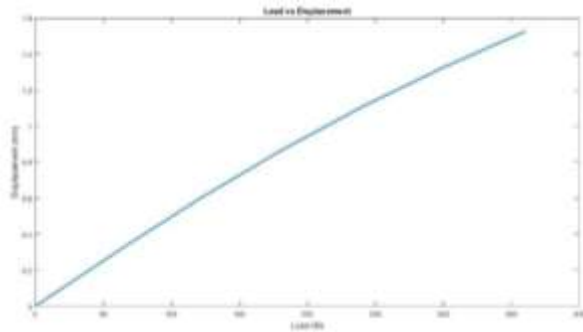


Figure 6: Theoretical plot of displacement vs. load in MATLAB.

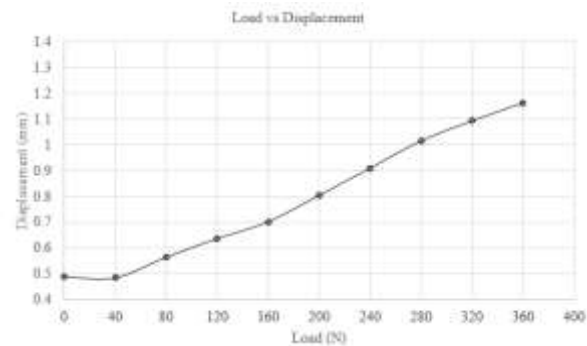


Figure 7: Experimental Plot of displacement vs. load

CONCLUSION

This study has focused on the development of improved non-linear theoretical and analytical methods for predicting the geometric nonlinear static response of cranial implants with human skull. The present report is limited to the study of non-linear static response of cortical bone and validation with experimental results. An extensive study on the material nonlinearity and dynamic response of these implants will be presented in a future work.

A new approach in describing the geometric nonlinearity of implants for cortical bone has been proposed. This approach consists of considering transverse loads including transverse shear deformations, this is because, an optimal fixation implant is one which maximizes the stability of the fracture by keeping the relative shear movement of the fragments to a minimum while allowing for sufficient compression across the fracture site, thereby promoting healing and reducing stress shielding effect [7].

The properties of these elements (Implants) can be derived from tensile test of cadaveric skull or from the journal references. The basic principles or refined finite element models including step loading and boundary condition have been simulated in MATLAB [3] for the geometric nonlinearity. Such a scheme was developed in this study within the framework of a special purpose analysis program for the nonlinear static analysis of cranial implants.

To establish the validity of the proposed models correlation studies of analytical predictions with experimental evidence of the load-displacement response of cadaveric skull specimen under static load reversals and three point bending test were conducted.

REFERENCES:

- [1] Cheng Yu Lin, Noboru Kikuchi, Scott J. Hollister, et al., "A novel method for biomaterial scaffold internal architecture design to match bone elastic properties with desired porosity", *Journal of Biomechanics* 37 (2004) 623–636.
- [2] Yong L. Chuan, Md. E. Hoque, and Ian Pashby, et al., "Prediction of Patient-Specific Tissue Engineering Scaffolds for Optimal Design", *International Journal of Modeling and Optimization*, Vol. 3, No. 5, October 2013 468-470.
- [3] MATLAB Release R2015a (8.5.0.197613), The MathWorks, Inc., Natick, Massachusetts, United States.
- [4] Buckwalter JA, Glimcher MJ, Cooper RR, Recker R; 1995. Bone Biology, Part I and Part II. *The Journal of Bone and Joint Surgery*, Vol. 77-A, No. 8, pp 1255-1290.
- [5] Hazelwood SJ, Martin RB, Rashid MM, Rodrigo JJ; 2001. A mechanistic model for internal bone remodeling exhibits different dynamic responses in disuse and overload. *Journal of Biomechanics*, Vol. 34, pp 299-308.
- [6] Hernandez CJ, Hazelwood SJ, Martin RB; 1999. The Relationship between Basic Multicellular Unit Activation and Origination in Cancellous Bone. *Bone*, Vol. 25, No. 5, pp 585-587.
- [7] Hernandez CJ; 2001. Simulation of bone remodeling during the development and treatment of osteoporosis. PhD Thesis, Stanford University.
- [8] Hernandez CJ, Beaupre GS, Keller TS, Carter DR; 2001a. The influence of Bone Volume Fraction and Ash Fraction on Bone Strength and Modulus. *Bone*, Vol. 29, No. 1, pp 74-78.
- [9] Martin RB; 1984. Porosity and specific surface of bone. Chapter 3 in: *Critical Reviews in Biomedical Engineering*, Vol. 10. CRC Press, pp 179-222.
- [10] Martin RB, Burr DR, Sharkey NA; 1998. *Skeletal Tissue Mechanics*. Springer, New York.
- [11] Martin RB; 2002. Is All Cortical Bone Remodeling Initiated by Microdamage? *Bone*, Vol. 30, No. 1, pp 8-13.
- [12] Ashman, R.B., Corin, J.D., Turner, C.H. Elastic properties of cancellous bone: measurement by an ultrasonic technique. *J. Biomechanics*. 1987;20:979–987.
- [13] Ashman, R.B., Cowin, S.C., van Buskirk, W.C., Rice, J.C. A continuous wave technique for the measurement of the elastic properties of cortical bone. *J. Biomechanics*. 1984;17:349–361.

- [15] Carter, D.R., Hayes, W.C. The compressive behavior of bone as a two-phase porous structure. *J. Bone Jt Surg.* 1977;59:954–962.
- [16] Choi, K., Kuhn, J.L., Ciarelli, M.J., Goldstein, S.A. The elastic modulus of trabecular, subchondral, and cortical bone tissue. *Trans 35th orthop. Res. Soc.* 1989;14:102.
- [17] Choi, K., Goldstein, S.A. The fatigue properties of bone tissues on a microstructural level. *Trans. 37th orthop. Res. Soc.* 1991;16:485.
- [18] Draper, N.R., Smith, H. in: *Applied Regression Analysis.* Wiley, New York; 1981.
- [19] Gong, J.K., Arnold, J.S., Cohn, S.H. Composition of trabecular and cortical bone. *Anat. Record.* 1964;149:325–332.
- [20] Jensen, K.S., Mosekilde, L., Mosekilde, L. A model of vertebral trabecular bone architecture and its mechanical properties. *Bone.* 1990;11:417–423.
- [21] MacGregor, C.W., Symonds, J., Vidosic, J.P., Hawkins, H.V., Thomson, W.T., Dodge, D.D. Strength of materials. in: T. Baumeister, E.A. Avallone, T. Baumeister III (Eds.) *Mark's Standard Handbook for Mechanical Engineers.* McGraw-Hill, New York; 1978:5.
- [22] Martin, R.B. Determinants of the mechanical properties of bones. *J. Biomechanics.* 1991;24:79–88.
- [23] P. J. Antunes, G. R. Dias, A.T. Coelho, F. Rebelo and T. Pereira, Non-Linear Finite Element Modelling of Anatomically Detailed 3D Foot Model, IPC – Institute for Polymers and Composites, University of Minho, Guimarães, Portugal.
- [24] Sivakumar V, Asish Ramesh U. N, NON-LINEAR 3D FINITE ELEMENT ANALYSIS OF THE FEMUR BONE, *International Journal of Research in Engineering and Technology.* Volume: 02 Issue: 03 | Mar-2013
- [25] FRANCO BREZZI, KLAUS-JURGEN RATBE, MICHEL FOKTIN, MIXED-INTERPOLATED ELEMENTS FOR REISSNER-MINDLIN PLATES, *INTERNATIONAL JOURNAL FOR NUMERICAL METHODS IN ENGINEERING*, VOL. 28, 1787 - 1801 (1989)

An Interlinked Methodology for Rapid and Better Production, Quality and Efficiency using Total Productive Maintenance, Kaizen and Lean Manufacturing

Ahsan Singh, Prakash Girwal

Scholar in Vikrant Institute of Technology and Management, Indore, singhahsan@gmail.com, cell: 9826252992

Abstract—In this project we are going to merge some important methodologies for the improving overall plant's efficiency, Production and Quality these methodologies are Kaizen, Lean Manufacturing and Total Productive Maintenance. Total Productive Maintenance belongs to system of maintaining and improving The Men, Machines, Equipment and process which is essential for the better production and quality we are applying Kaizen and Lean Manufacturing for the Continuous Improvements and Elimination of the Wastages respectively. We are also merging these three techniques and applying as a single process of working for the efficiency improvement, Better and Rapid Production, Quality Manufacturing. These three methodologies merging together Total Productive Maintenance belongs to The product, the process that allows the product to be produced, the companies that is giving the proper conditions which actually needed for the appropriate process to work, the leadership that guides the companies & confirming statement to being superior throughout the organization. Kaizen improvements are technically implemented in sequenced by using Plan Then Do Then Check and then Act (PDCA) and a popular misconception is that lean is suited only for manufacturing. The lean thinking can be applicable in every field Lean can be applicable to implementation in every business and every process. It is a tactic or a cost reduction program, by a way of thinking and acting for an entire organization.

Keywords— TPM, Kaizen, Lean, Rapid Production Rate, Quality for Efficiency, Interlinking of methodology,

INTRODUCTION

In this project we are going to merge some important methodologies for the improving overall plant's efficiency, Production and Quality these methodologies are Kaizen, Lean Manufacturing and Total Productive Maintenance. The nature of Kaizen helps to improve working method and practice continuously. It's a common knowing fact that in Japanese, Kaizen means continuous improvement. The word suggest improvement that embrace all levels of an organization from workers to higher level of management and entails relatively little expense. The Toyota has been known as the first company that has started Kaizen and also implement it in a success full way. The application that Toyota used was called "Toyota Production System", where all good implements are recompensed. Kaizen improvements- there are some concepts to understand kaizen. First of all, it should be known that 'Kaizen provides the tools to Management'. Basically, management has two sides: First one is maintenance side and second one is improvement side. Maintenance refers to maintain current technological facilities like machines, systems, working methods, managerial and operating standards through training, review, regular maintenance and discipline. Improvement refers to elevate current standard in all possible and available fields. The management should be classified all the subjects or mattes as in the maintenance or improvement side. Kaizen should be applicable in a little improvement side. kaizen signifies small improvements as a result of ongoing efforts, typically applied by using Plan-Do-Check-Act (PDCA). Lean is not only a technique but it is thinking "used to accelerate and minimize the cost of any methodology by removing the waste in either manufacturing or service." The wastes are all the things and working practically which is non-value added cost or unneeded wait time within the process may be caused by defects, excess production, and miss planning etc. Lean Manufacturing is also called Lean Production, is a philosophy that was originally developed in the Toyota Motor Company, and also known as the Toyota Production System or TPS. Basic goals of Lean are "better quality, low all kind of cost, short cycle times, flexibility, and relentless efforts to remove waste out from the organization, and make the product or provide the service as all value being defined by the customer." The result is reduced production cycle time, and greater efficiency. It also provides tools for reducing variability for the Continuous Improvements and Elimination of the Wastages respectively. A popular misconception about the lean is that it is suited only for manufacturing but it's not

true. The Lean can be applying in every business and every process. It is not only a tactic or a cost reduction program, but a way of thinking and acting for an entire organization. Total Productive Maintenance belongs to system of maintaining and improving your Men, Machines, Equipment and process. Total Productive Maintenance (TPM) is a tool that ensures timely and cost-effective equipment repair. It can be used in all businesses, including offices, but is particularly useful in the manufacturing sector which is essential for the better production and quality.

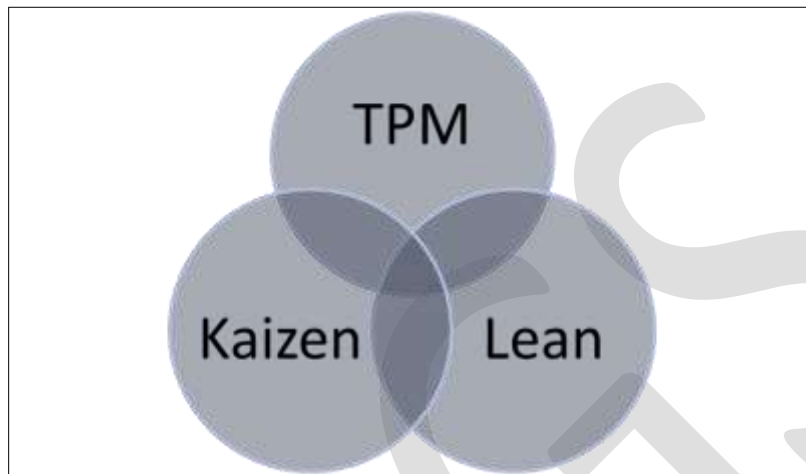


Figure 1- Methodologies Integration

By the combination of these three techniques and applying as a single process of working for the efficiency improvement better and Rapid Production, Quality Manufacturing. These three methodologies merging together Total Productive Maintenance belongs to The product, the process that allows the product to be produced, the companies that is giving the proper conditions which actually needed for the process to work, the leadership that guides the organization, and commitment to excellence throughout the organization.

Principle & Planning

This bonding of these three technologies are difficult to find in any organization. By this methodology I am looking forward for better results and planned improvements. It can be conquer the profitability and eliminate the losses by the mergence of these three techniques for the better results a sequenced planned implement can take place for the higher productivity and profitability and reduce/avoid to unwanted wastages. Kaizen involves all the employees of the firm, Kaizen improving the methodologies of work, Kaizen Improvements are easy to adopt, many people consider kaizen as a philosophy of ongoing improvement involving industries, it involves from top managers to the labor class. In Japan for competition& success in any industry and plant it is the most important element. It provides the result-oriented view of searching from the Wastes innovation-and method-oriented work practice. In general, kaizen is a system for regularly implementing new innovative idea as a tool, as per company levels; In this competitive market everyone is trying to seek out and exploit and new opportunities and institutional information from new researches.

The Kaizen Principle

The best thing about this basic idea is that it's probably pretty close to the truth. Yet there are a number of further presuppositions there that really open up the way for a whole new type of growth in any area where you wish to apply the Kaizen principle. I think the most suitable aspect of the Kaizen philosophy is the upfront presupposition that in whatever industry you apply it, and no matter how well you do it, it can never be best there is always scope for betterment & it can be achieved by kaizen system. Yet even from state of imperfection, there is no need to be dismayed, or afraid, if you follow the Kaizen principle. Here, we strive towards perfection - we do the best on each time we can to make things better, every way, and every day, to move towards perfection in an evolution of simple endeavors, all the time. Elimination of waste. Waste reduction is an effective way to increase the profitability of any organization. The managers should learn about the problems that happened in industry growth, from a report that reaches them several days or even weeks after the problem exist. In other words, industry is the place where value is added and problems are solved through processes such as taking temporary countermeasures on the spot, find out the root cause and standardize for prevention and recurrence. In short,

whenever there is progressive activity, it will involve team work and continues effort, it will make the clients to be more satisfy in view point of quality, cost, delivery and services.

The Kaizen in Practice

Kaizen appreciate for continuous improvement. It motivates the employer & employee both to think some innovative for better than before. Today Kaizen is being use in each MNC company worldwide as an important pillar of an organization's by this the company getting strong for long-term competitive strategy. Kaizen is continuous improvement that is based on certain guiding principles, Good processes bring good results., Go see for you to grasp the current situation., Speak with data, manage by facts., Take action to contain and correct root causes of problems., Work as a team., Kaizen is everybody's business and much more.

LEAN PRINCIPLE

Lean manufacturing or lean production is a very good approach; Core idea is to maximize customer value while minimizing waste. It's making a fair sense the lean means creating more value for customers with fewer resources. Certainly, lean is centrifugal force for making desired what adds value by reducing everything else. Lean manufacturing is a management philosophy derived mostly from the Toyota Production System (TPS) (hence the term Toyotism is also prevalent) and identified as "lean" only in the 1990s. TPS is regenerated for its focus on elimination of the original Toyota seven wastes to improve overall customer value, but there are varying opinion for implementation, how this is best achieved. It's a world knowing fact, the gradually growth of Toyota, from a very small scale company to the largest automaker company. Lean production is a technique to production and manufacturing developed in core Japan. Toyota, the Japanese car production department was that founded lean production. The overall aim of lean technology is to eliminate the excess using of resources used up in production. By implementing this, lean system uses less of -work place, raw

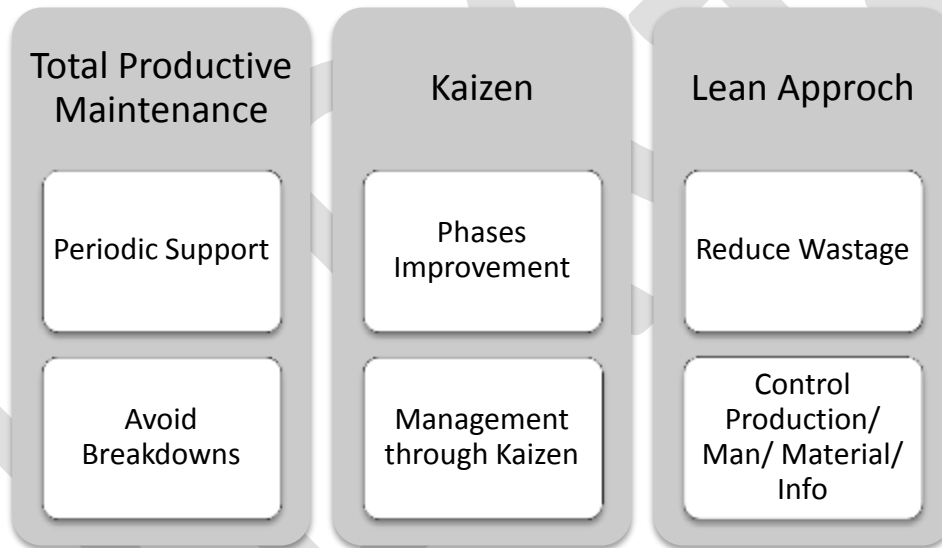


Figure 2- Phases of Methodology

inventory, stocks, labor, capital and time. Lean production reduces and tries to eliminate costs, increases productivity efficiency and output and productions reduces and try to eliminate costs, increases productivity efficiency and output and improves mental satisfaction & motivation. Lean production involves using a various practices designed to eliminate waste and increasing productivity and quality. Lean Production includes - Introduction "Lean" was first introduced in Japanese manufacturers. The Toyota production system is optimum admired as a very successful play on lean methodology. In another quote, lean methodology refers to production processes that improve upon mass production techniques to reduce cost, reduce time to produce, improve quality, and better respond to market demands. The benefits of lean production techniques have been documented in several studies, including a worldwide study of automotive industry.

PROPOSED METHODOLOGY

In this Methodology we have implemented three new and improved techniques of modern science which is kaizen, lean manufacturing and total productive maintenance. Industries are increasingly paying attention to maintenance efficiency optimizing the level in reliability and availability of assets. Many of the improvements could be obtained using new technologies and strategies to maximize service level and to reduce the maintenance costs, as long as it is possible to identify the business areas where a leap in technology could render and optimize the maintenance processes. Performance improvements in the maintenance and conservation activities of assets are measured by availability and operational reliability. They should be obtained preserving maximum quality and safety levels and minimizing the costs.

In the current scenario of competitiveness, improvement efforts are essential to reach high levels of effectiveness and efficiency in every company's production or operational department. The purpose is to achieve competitive advantage (in products or offered services) based on different hard-to-copy aspects, i.e. know-how.

- To obtain maximum performance, the organizations must be prepared for changes and there are three interconnected areas in the change concept:

- Processes, work fluxes to achieve the improvements (e.g. doing more preventive work instead of corrective work, etc.). Kaizen guide to implement the following points.

The workplace should have the environment including discipline support to work nature. Customer orientation at each single stage it should be came to about the choice and interact of customer this thinking guide for more value. Zero defect practically it is not possible to achieve the target of zero defect but it can be tending to achieve the target of zero defects, such attention leads the organization to reduce and eliminate defects

As we know that the defects are barrier for any industry defect cause, the work which is not profitable for company but result to be loss. The effect includes the following terms of losses.

- 1) Raw material loss used in product.
- 2) Machines parts and power consumption.
- 3) Labor work effort
- 4) Labor and machine time used to produce the particular product.
- 5) Labor & machine time and energy consumed to produce again a product unit similar specification confirming the quality of the place of defected place.

So it is conclusion that types of losses mentioned above can be encounter by view of Kaizen.

TPM Support:

As above entailed the defects are major causes and losses.

Basic defect resources:

- 1) Human Error
- 2) Material not confirming the required specification.
- 3) Machine errors

Above three mentioned root cause can be reducing or finished by the basic concept of TPM. Total Productive Maintenance matches all the dimensions regarding improvements of productivity and quality it reduces and elimination and defects. One of the most returning features of kaizen is that big results come from many small changes which are not even costly and may be accumulated over time, it doesn't require suddenly big expenditures. In general, this has been misunderstood to that kaizen means small changes. In fact, kaizen means everyone at every stage involved in making improvements. While the majority of changes may be small at number of stages. The greatest impact may be created by kaizen that are led by senior management as transformational projects, or by cross-functional and checking teams. In this Methodology it is suggested to implement three new and improved techniques of modern science which is kaizen, lean manufacturing and total productive maintenance. Industries must be paying attention to maintenance efficiency optimizing the level in reliability and availability of assets.

Implementation should in the way that reduces the maintenance costs, as long as it is possible to identify the business areas where a leap in technology could render and optimize the maintenance processes. Performance improvements in the maintenance and conservation activities of assets should be measured availability and operational reliability.

During the implementation of methodology following care should be taken-

- To obtain maximum performance, the organizations must be prepared for changes.
- Processes, work fluxes to achieve the improvements (e.g. doing more preventive work instead of corrective work, etc.).
- Technologies to facilitate or enable advanced and improved processes.

For implementation proper & regular implementation of proposed methodology following steps should be followed

- 1 Firstly, the problem occurring in implementation of methodology should be identify.
2. The identified problem should be analyzed appropriately.
3. After analysis the required solution or development can be found.
4. Implement new development. Evaluate the results coming from the implementation of new development.

5. If the results coming from evaluation are satisfactory then the process should be maintaining in correct format.

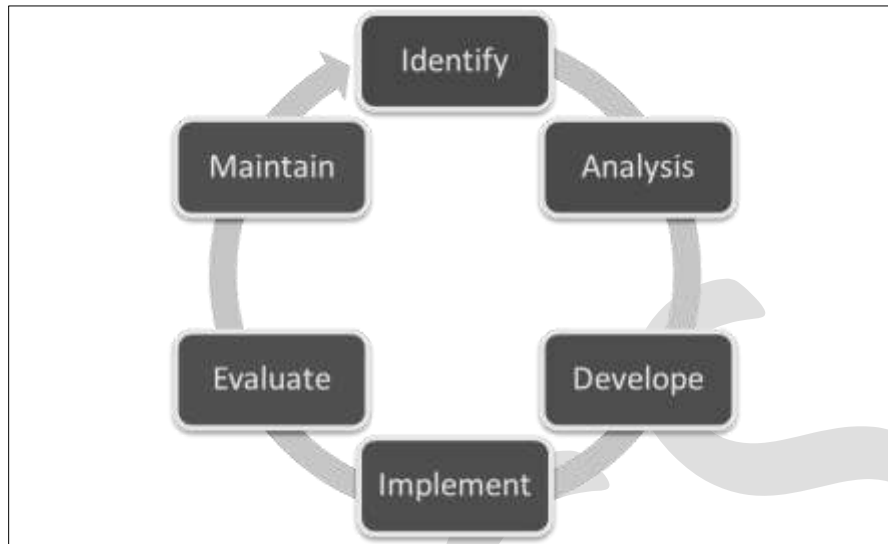


Figure 3- Process to Execute

RESULTS & DISCUSSIONS

As the proposed methodology is an interlinked methodology for rapid and better production, Quality and efficiency in various fields of plant improved by using TQM, Kaizen and lean manufacturing. Following are the points which can be improved by implementation of this methodology. No Breakdowns or comparatively lesser than before. No Small Stops or Slow Running. No Defects or reduction in percentage of defects. The interlinked system provides values to a safe working environment. No Accidents is target and can be achieved by a regular practice. Improvements in operational efficiency. The overall reliability of company enhances.

Regular improvements in qualities Become easy & possible. Better trained mechanics and higher levels of expertise. After practice Lower operating cost is possible. Provide better planning and preventative maintenance. Increased all machines, equipment and technical devices life span. Improved job satisfaction and job security. Help to sustain in competition. Increase departmental relation sheep like Maintenance partnership with production. Improve maintenance role in organization. Less capital tied up. Assures better quality performance in every sphere of activity. Helps in checking non-productive activities and waste. Improved service, delivering. Improvements in value per employ of organization. Lean help to reductions in defects and rework. Kaizen reduces waste in areas such as inventory. Reduced waiting times. Reduction in transportation. Efficient worker motion. Regular improving employee skills. Control over production. Remove use less quality operation from and in processes. Improved space utilization. Improved product quality. Efficient use of capital, communications, production capacity and employee retention.

ACKNOWLEDGMENT

First of all, I would like to thank my parents for all the continue support of them, without them it was not possible. I also would like to say thanks to my guide MrPrakash Girwal, for his outstanding motivation and support, I also want to say thanks to all my faculty and all the staff for them mesmerizing support and planning.

CONCLUSION

All of the above points have good effects on the related organization-financial impacts, business development, as well as helping to become a business that can better react, and meet exact customer's needs. The methodology is the combination of three very important system TPM, Kaizen and Lean so it covers a wide range of profitability of an industry or organization. As the interlinked working system ensure the efficient use of resources like as capital, Employees, machines and fix assets it all supports at last the organization financially.

The lower or zero break down enhance the system reliability in eternal organization as well in market. Improved maintenance system and active employees will be give regular growth to the quality of product indirectly which responsible for customer satisfaction.

The lean & kaizen based production system gives the higher efficiency of overall plant and reduce the product or service production cost which help to face the competition and also increase the profit. Regular thinking process system and awareness gives the new product development and improvement concepts which become stronger day by day when each employee is participating in this

methodology and working better at his or her level.

REFERENCES:

- [1] Womack, J., Jones, D. and Roos, D. (1990), *The Machine That Changed the World*, Rawson Associates, New York.
- [2] Hongyi Sun Richard Yam Ng Wai- Keung Thevimplementation and evaluation of TotalvProductive Maintenance (TPM)— an action case study in Hong Kong manufacturing company. *International Journal Advance in manufacturing Technology* (2003)Vol22: pp224- 228.
- [3] I.P.S. Ahuja and J.S. KhambaAn evaluation of TPM implementation initiatives in an Indian manufacturing enterprise. *Journal of Quality in Maintenance Engineering* (2007) Vol.13 No.4 pp338-352.
- [4] Marcelo Rodrigues, Kazuo Hatakeyama, Analysis of fall of TPM in companies, *Journal of Material Processing Technology* (2006) 276-279.
- [5] Alokumar A Uplap, Dr.R.S.Dalu, RavikantV.Paropate ,P.S.GhawadeS.R.Kewate, Implementation Strategy of Total productive Maintenance in Indian Industries
- [6] Womack, J. and Jones, D. (1996), *Lean Thinking: Banish Waste and Create Wealth in Your Corporation*, Simon & Schuster, NY.
- [7] Hines, P., Holweg, M. and Rich, N. (2004), Learning to evolve: A review of contemporary lean thinking, *Int. Journal of Operations & Production Management*, Vol. 24, No. 10, pp. 994-1011.
- [8] Holweg, M. (2007), "The genealogy of lean production", *Journal of Operations Management*, Vol. 25, No. 2, pp. 420-437.
- [9] Verma, A., Bao, H., Ghadmode, A. and Dhayagude, S. (2005), "Physical Simulations in Classroom as a Pedagogical Tool for Enhancing Manufacturing Instruction in Engineering Technology Programs" in *Proceedings of the 2005 American Society for Engineering Education Annual Conference & Exposition*, Paper No. 2005-220, 12pp.
- [10] MacDuffie, J. and Pil, F. (1997), "Changes in Auto Industry Employment Practices: An International Overview" in Kochan, T., Lansbury, R. and MacDuffie, J. (Eds.) *After Lean Production: Evolving Employment Practices in the World Auto Industry*, Cornell University Press, New York.
- [11] Ozelkan, E. and Galambosi, A. (2009), "Lampshade Game for lean manufacturing", *Production Planning &Control*,Vol. 20, No. 5, pp.385-402.
- [12] Okkola, T. and Kässi, T. (2012), "Designing an Industrial Management Curriculum, Overcoming Obstacles", *Int. Journal of Industrial Engineering and Management*, Vol. 3, No. 2, pp. 67-74.
- [13] Bonwell, C. and Eison, J. (1991), *Active Learning: Creating Excitement in the Classroom*, ASHE-ERIC Higher Education Reports, Washington.
- [14] Jorge L.Perez-Lafont, B.S.I.E., 'Installation of T.P.M. program in a Caribbean plant. International conference on Computers and Industrial Engineering' 33.1.2 315-318. (1997) .
- [15] F.T.S. Chan, H.C.W. LAU, R.W.L. Ip, H.K. Chan, S. Kong 'Implementation of Total Productive maintenance : A case study' *International journal of Production Economics* 95 .71-94. (2005)
- [16] F.-K. Wang, W. Lee 'Learning curve analysis in total productive maintenance' *International Journal of Management Science* 29 ,491–499, (2001)
- [17] Kathleen E. McKone a, Roger G. Schroeder b, Kristy O. Cuab 'The impact of total productive maintenance practices on manufacturing performance' *Journal of Operations Management* ,19, 39–58, (2001).
- [18] M.C. Eti a, S.O.T. Ogaji b, S.D. Probert b., 'Implementing total productive maintenance in Nigerian manu
- [19] Miles, M., Melton, D., Ridges, M. and Harrell, C. (2005), "The Benefits of Experiential Learning in Manufacturing Education", *Journal of Engineering Technology*, Vol. 22, No. 1, pp. 24-28.
- [20] Holweg, M. and Bicheno, J. (2002), "Supply chain simulation – a tool for education, enhancement and endeavour", *International Journal of Production Economics*, Vol. 78, No. 2, pp. 163-175.
- [21] Billington, P. (2004), "A Classroom Exercise to Illustrate Lean Manufacturing Pull Concepts", *Decision Sciences Journal of Innovative Education*, Vol. 2, No. 1, pp. 71-76.
- [22] Prusak, K. (2004), "Problem Definition and Problem Solving in Lean Manufacturing Environment", in *Proceedings of the 2004 American Society for Engineering Education Annual Conference & Exposition*, pp. 195-206.

Technique for the Risk Assessment of RMC Plants

Roshni Prabhakaran¹ , Nisha Babu ²

1 Scholar, SNGCE, Ernakulum, Kerala.

2 Asst. Professor, Civil Engineering Department, SNGCE, Ernakulum, Kerala

Abstract — The systematic identification and assessment of risk and effectively dealing with the results is significant to the success of any industries and projects. Unless other industries, RMC industries can be extremely complex and fraught with uncertainty. Due to the especial nature of the construction industries like RMC, and the growing need of having innovative and complex projects, the risk assessment process has become more and more complex. Still there is no efficient method for the effective assessment of various risks in these sector. In this work, an attempt is made to find out the most critical risk in RMC plants by developing a risk assessment model using Failure Mode and Effective Analysis (FMEA) technique. This was resulted in five risks with equal priority values and hence a risk prioritization was done using Analytical Network Process (ANP) with the help of Super decisions software. Finally remedial measures were suggested for the identified critical risk.

Keywords — Risk management, RMC plants, Risk assessment, FMEA, RPN, ANP, Super decisions software

INTRODUCTION

As per Indian Standard code of practice (IS 4926 - 2003) Ready Mixed Concrete (RMC) is defined as the concrete delivered in plastic condition and requiring no further treatment before being placed in position in which it is to set and harden. RMC is a specialized material in which the cement, aggregates and other ingredients are weigh-batched at a plant& mixed in a central mixer or truck mixer, before delivery to the construction site in a condition ready for placing. Thus, 'fresh' concrete is manufactured in a plant away from the construction site and transported within the estimated journey time. Today's high rise structures demands smaller column sizes, faster construction, prompting use of high grade Ready Mix concrete. Use of Ready Mixed concrete was expected to give better control on the quality of concrete as compared with the site mixed concrete. Like other industries, RMC industry is exposed to various risks. In European countries, there is an awareness and understanding about importance of risks and its management. Information gathered from RMC plants in India in places like Mumbai, Navi Mumbai, Pune, Bangalore, and Noida, established by different companies reveals that a systematic risk management approach is not practiced in Indian RMC Industry. Unless the risks are addressed properly, the RMC industry in India shall not gain credibility, confidence of customers and will also cause reduction in profit margins.

Managing of risk is an integral part of industrial management system, and fundamental to achieving efficient outputs. That is, systematic identification and assessment of risk and effectively dealing with the results is significant to the success of any industries and projects. The risk assessment process involves determining the likelihood of a dominant failure mode or modes and then evaluating the consequences of a failure. Unless other industries, RMC industries can be extremely complex and fraught with uncertainty. Although companies, project managers and risk engineers have defined many methodologies and application in order to assess project or system risk and to increase systems reliability and safety, it is very difficult to aver the existence of a complete tool or methodology that assure complete safety, reliability and riskless project or system. In addition, due to the especial nature of the construction industries like RMC, and the growing need of having innovative and complex projects, the risk assessment process has become more and more complex. Hence the need for a proper and most efficient technique for the risk assessment in RMC industry is very important.

In this work, a study is made with the traditional FMEA (Failure Mode Effective Analysis) in order to find out the most critical risk. The Failure Mode Effect Analysis (FMEA) technique is to identify risk factors for the potential failure mode in the production process of concrete and to take the appropriate corrective actions for improvement. For the prioritization of the identified risks, ANP technique is used. Analytical Network Process (ANP) is a multi-criteria decision making technique which is commonly used for the prioritization of critical risks. The ANP technique is implemented in this work with the help of the software Super decisions. Reputed RMC plants in Kerala were selected for the study and the results developed are analyzed to know the efficiency and effectiveness of the developed technique. Also remedial measures for the identified risks are suggested.

RELATED WORKS

Agnieszka Dziadosz et.al [1] conducted a study on Risk analysis in construction project - chosen methods. This article presents three different methods of the risk analysis as well as highlighting their disadvantages, advantages and primary areas of application (selection or pre-estimation). Oksana marinina et.al [2] were studied about analysis of the possibility of using modern risk assessment methods in mining industry. The article describes the components of the risk assessment process, the analysis and classification of modern approaches to the evaluation of risk events.

Dr. Chakradhar Iyanni et.al [3] were studied about the FMEA risk management technique for quality control of RMC production. In order to identify the major failure mode in production of Ready Mixed Concrete (RMC) of different grades (M20, M25, M30) FMEA is used. The risk priority number results indicated process failure in terms of irregular grading process, material testing prior use in mixing process which were the important factor to be monitored for quality control. Mehrzad et.al [4] were studied about assessment and risk management of potential hazards by Failure Modes and Effect Analysis (FMEA) method in Yazd Steel Complex. In this study, the risks in different parts of the complex were evaluated by using FMEA method and by using FMEA Worksheets (PFMEA) derived from the standard (MIL_STD-882). Gunjan Joshi et.al [5] were studied about the FMEA and Alternatives v/s Enhanced Risk Assessment Mechanism. In this work, the advantages of using Six Sigma in Risk Assessment are also pointed out and proposed a novel technique which would overcome the restrictions of existing Risk Management tools.

Goutam Dutta et.al [6] were conducted a study on design and application of Risk Adjusted Cumulative Sum (RACUSUM) for online strength monitoring of Ready Mixed Concrete. In this paper, an attempt is made to design and apply a new CUSUM procedure for RMC industry which takes care of the risks involved and associated with the production of RMC. This procedure is termed as Risk Adjusted CUSUM (RACUSUM). Ali Gorener [7] was studied about the application of strategic decision making in a manufacturing company. This paper mainly explains how to use the AHP and ANP methods for prioritize of SWOT factors. Strengths, Weaknesses, Opportunities and Threats (SWOT) analysis is a generally used tool which examines strengths and weaknesses of organization or industry together with opportunities and threats of the marketplace environment. SWOT framework provides the basic outline in which to perform analysis of decision situations. In this study, the SWOT analysis is enhanced with AHP and ANP (Analytical Network Process) in order to prioritize the identified factors.

RISK MANAGEMENT

Risk management is the identification, assessment, and prioritization of risks (defined in ISO 31000 as the effect of uncertainty on objectives) followed by coordinated and economical application of resources to minimize, monitor, and control the probability and/or impact of unfortunate events or to maximize the realization of opportunities. The management of any risks or uncertainties generally involves the following;

- Risk identification
- Risk assessment
- Risk prioritization

A. Risk Identification

Risk identification is one of the most important stages in risk management process. In this stage, all the potential risks that could affect the project objectives are identified. It is studying a situation to realize what could go wrong at any given point of time during the project. For risk identification, some of the methods used are Check list, Brainstorming, Tree Diagram, Cause – Effect Diagram, Interviewing, Questionnaire surveys etc. They are explained as following;

- Brainstorming – An idea generation group technique is divided in two phases. (i) Idea generation phase, in which participant generate as more ideas as possible (ii) idea selection phase, the ideas are filtered, remaining only those approved by the entire group.
- Delphi Technique – Delphi is a technique to obtain an opinion consensus about future events from a group of experts. It is supported by structured knowledge, experience and creativity from an expert panel.
- Interview/ Questionnaire surveys – Unstructured, semi structured or structured interviews individually or collectively conducted with a set of experienced project members, specialist or project stakeholder.
- Checklist – It consists of a list of item that are marked as yes or no, could be used by an individual project team members, a group or in an interview.

- Influence Diagram – It is a graphical representation containing nodes representing the decision variables of a problem. A traditional influence diagram is formed by three types of nodes: utility, decision and informational. The causal relationship occurs between utility and chance nodes and represents a probabilistic dependence.
- Flowchart – Graphical tool that shows the steps of a process. This technique is applied for a better comprehension of the risks or the elements interrelation.
- Cause-and-Effect Diagrams – These are also called Ishikawa diagrams or fishbone diagram, illustrate how various factor might be linked to potential problems or effects. The diagram is designed by listing the effect on the right sides and the causes on the left sides. There are categorized for each effect, and the main causes must be grouped according to these categories.

For this work, the method of questionnaire surveys are implemented to identify the types of risks that affect the RMC plants.

B. Risk Assessment

Risk assessment is merely a method of analyzing the seriousness of a risk. There are two approaches to analyzing identified risks, and they are the qualitative and quantitative methods.

Qualitative Risk Assessment

In the first method, viz. the Qualitative Analysis, all the identified risks are plotted on a matrix. Each is given a position on the matrix chart. The probability of the risk occurring can be plotted on the horizontal bar, while the impact of the risk can be noted along the vertical bar of the axis. The probability-impact value of a risk is a product of both the values assigned for the risk. Hence, it can be seen that a risk with a value of 9, where the probability and impact rate the highest, requires immediate attention. Those with a P-I rating of 1 or 2 requires the least attention and may even be ignored, if insignificant.

Quantitative risk assessment

At times, it is not easy to be precise when drawing up measures of risk resolution with just a generalized idea of a risk. In the process of making educated decisions, a quantitative analysis is necessary. Quantitative risk assessment assigns numbers to risks based on various risk reports and data generated. When compared to present criteria, a valid decision can be made. The different methods of quantitative risk assessment are as following;

- Fault tree analysis (FTA)
- Cost of exposure quality risk analysis
- Failure mode and effect analysis (FMEA)
- Cause-consequence analysis
- HAZOP technique
- Event tree analysis (ETA)

Failure Mode Effective Analysis (FMEA) Technique

Failure Mode and Effects Analysis (FMEA) is commonly defined as “a systematic process for identifying potential design and process failures before they occur, with the intent to eliminate them or minimize the risk associated with them”. It is a type of qualitative risk assessment. The FMEA technique was first reported in the 1920s but its use has only been significantly documented since the early 1960s. It was developed in the USA in the 1960s by National Aeronautics Space Agency (NASA) as a means of addressing a way to improve the reliability of military equipment. It has been used in the automotive industry since the early 1970s and its use has been accelerated in the 1990s to address the major quality and reliability challenges caused by the Far Eastern car manufacturers. In addition, the recent changes in the law on corporate responsibility have led to companies reviewing their product design safety through the use of the FMEA methodology. In doing the analysis, the system behavior is evaluated for every potential failure mode of every system component.

Where unacceptable failure effects occur, design changes are made to mitigate those effects. The criticality part of the analysis prioritizes the failures for corrective action based on the probability of the item's failure mode and the severity of its effects. It uses linguistic terms to rank the probability of the failure mode occurrence, the severity of its failure effect and the probability of the failure being detected on a numeric scale from 1 to 10. These rankings are then multiplied to give the Risk Priority Number. Failure modes having a high RPN are assumed to be more important and given a higher priority than those having a lower RPN. Among the different types of FMEAs, the process FMEA is applied for this study since the RMC industries deals with the manufacturing process of concrete. The procedure for all types of FMEA is similar and in this case the scale used for the FMEA is 1-5 rating scale for severity, occurrence and detection. The rating scale for these are as shown in the tables below.

	1	2	3	4	5
Severity	Remote	Low	moderate	High	Very high
Occurrence	None	Low	moderate	High	Extreme
Detection	Very high	high	moderate	low	Very low

Table 1 Rating scale of FMEA

After obtaining the ratings for severity, occurrence and detection, the Risk Priority Number (RPN) is calculated for each risks as per the equation;

$$\begin{aligned} \text{RPN} &= \text{Severity} \times \text{Occurrence} \times \text{Detection} \\ &= S \times O \times D \end{aligned}$$

The risk with maximum value of RPN is considered as the most critical risk and risk with minimum RPN is the least critical risk. Here the major consideration is given to the most critical risk, since it governs the overall performance of the plant. In case if it is difficult to identify the most critical risk, a prioritization can be carried out which is usually done with the help of ANP technique.

C. Risk Prioritization

In the risk prioritization step, the overall set of identified risk events, their impact assessments, and their probabilities of occurrences are "processed" to derive a most-to-least-critical rank-order of identified risks. The objective of Risk Prioritization is to prioritize the identified risks for mitigation. Both qualitative and quantitative methods can be used to categorize the risks as to their relative severity and potential impact on the project. To effectively compare identified risks, and to provide a proactive perspective, the risk prioritization method should consider the following factors:

- Probability of risk
- Consequence of risk
- Cost and resources required for the mitigation of risk

Risk Prioritization is a decision making tool to prioritize risks or prioritize alternatives under risky or uncertain situations. It combines decision making theory and risk analysis in making judgment, and use mathematics to quantify soft decisions. It generally involves the following steps;

- Establishing the problem criteria – Defining the problem with criteria and alternatives, formulating the decision hierarchy structure etc. involves in this stage.
- Assessing the alternatives – developing the pairwise comparisons between the alternatives to assess their importance
- Prioritizing the alternatives – involves the calculation of priority weights and formulating the priority matrix
- Validating and communicating the decision – involves discussing the decision with board, management team or with stakeholders.
- Monitoring the decision – involves periodic monitoring and reviewing of the decisions.

The most commonly used risk prioritization method is the Analytical Network Process (ANP).

Analytical Network Process (ANP)

The analytic network process (ANP) is a structured network technique for organizing and analysing complex decisions. Based on mathematics and psychology, it was developed by Thomas L. Saaty in the 1980s and has been extensively studied and refined since then. It has particular application in group decision making, and is used around the world in a wide variety of decision situations, in fields such as government, business, industry, healthcare, and education. Rather than prescribing a "correct" decision, the ANP helps decision makers find one that best suits their goals and their understanding of the problem. It provides a comprehensive and rational framework for structuring a decision problem, for representing and quantifying its elements, for relating those elements to overall goals, and for evaluating alternative solutions. ANP provides a general framework to deal with decisions without making

assumptions about the independence of higher-level elements from lower level elements and about the independence of the elements within a level. In fact ANP uses a network without the need to specify levels as in a hierarchy. Generally the ANP technique implements a decision scale made by Saaty, for the prioritization of the judgments. The rating scale for ANP is as shown below.

INTENSITY OF IMPORTANCE	DEFINITION	EXPLANATION
1	Equal importance	Two elements contribute equally to the objective
3	Moderate importance	Experience and judgment slightly favor one element over another
5	Strong importance	Experience and judgment strongly favor one element over another
7	Very strong importance	An activity is favored very strongly over another
9	Absolute importance	The evidence favoring one activity over another is of the highest possible order of affirmation
2,4,6,8	Used to express intermediate values	Nil

Table 2 Rating Scale of ANP

The procedure for using the ANP can be summarized as:

- Model the problem as a complete set of network clusters (components) and their elements that are relevant to each and every control criterion.
- Determine a complete set of network clusters (components) and their elements that are relevant to each and every control criterion.
- For each control criterion, construct the super matrix by laying out the clusters in the order they are numbered and all the elements in each cluster both vertically on the left and horizontally at the top. Enter in the appropriate position the priorities derived from the paired comparisons as sub columns of the corresponding column of the super matrix.
- Perform paired comparisons on the clusters and on the elements within the clusters themselves
- cluster and on those that it influences, with respect to that criterion
- Check the consistency of the judgments.
- Come to a final decision based on the results of this process.

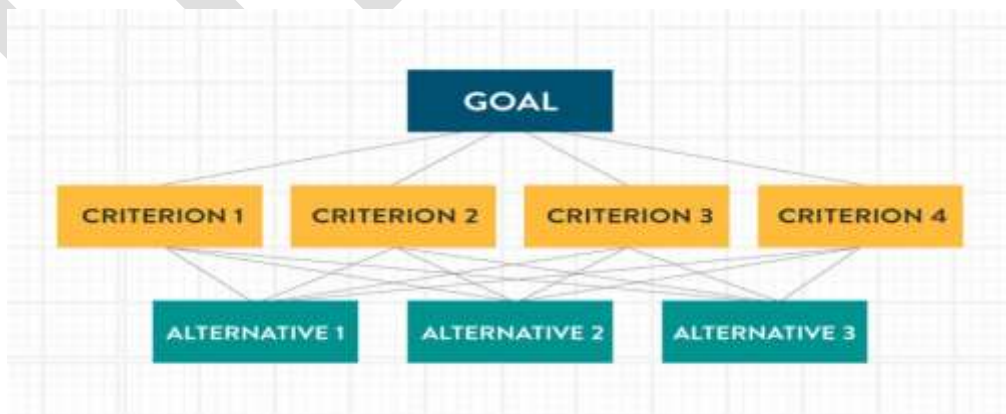


Figure 1: ANP Network structure

METHODOLOGY OF WORK

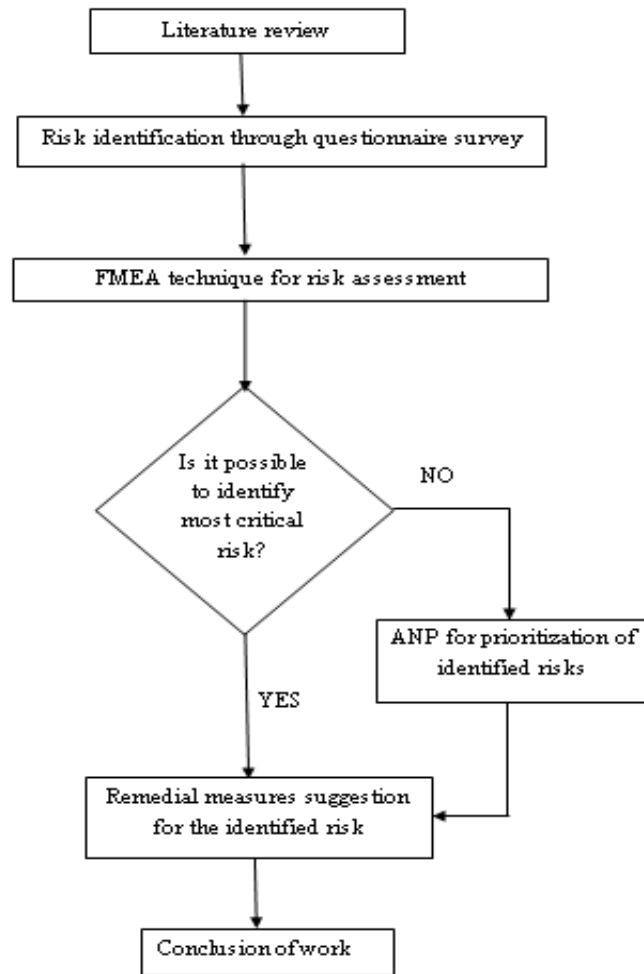


Figure 2: Frame work of the study

Data collection

The data collection for the work involves the identification of important risks that are occurring in the RMC plants. These are identified by carrying out a preliminary questionnaire survey. In this study 4 RMC plants are selected and the survey is carried out. The survey consisted of a pre-prepared risks factors with a 1- 4 scaling technique. The risk factors considered for the survey are categorized under 7 major risks, which are listed below.

- Financial risks
- Environmental risks
- Operational risks
- Political risks
- Safety risks
- Quality risks
- Procurement and storage risks

From the collected data, the RMC plant having risks with moderate and major effects on the working of plant are selected for the risk assessment technique. There was only one plant (Plant No: 4) under this, so the risk assessment method is implemented on that plant only.

FMEA Application

For the plant selected for the application of FMEA, the major risks with moderate and high rating, considered are as following;

- Operational risks
- Safety risks
- Quality risks

After obtaining the ratings for severity, occurrence and detection, the Risk Priority Number (RPN) is calculated for each risks as per the equation;

$$\begin{aligned} \text{RPN} &= \text{Severity} \times \text{Occurrence} \times \text{Detection} \\ &= \text{S} \times \text{O} \times \text{D} \end{aligned}$$

MAJOR RISK	FAILURE MODE	S	O	D	RPN
Operational risk	New technology adoption	3	2	3	18
	Lack of experts in plant	4	3	2	24
	Improper site access	4	4	2	32
	Delay due to traffic conditions	3	4	3	36
	Break down of machinery	4	4	2	32
	Wrongly designed plant layout	3	2	2	12
	Difficulty in pumping	2	3	2	12
Safety risks	Site injuries	4	3	3	36
	Slips, trips etc. during working	3	3	2	18
	Non-medical availability	3	2	2	12
	Mishandling of materials	2	2	2	6
	Accidents during transportation	4	3	2	24
	Improper working practices	3	3	4	36
	Improper maintenance of machinery	4	3	3	36
	Improper maintenance of hydraulic equipment	3	3	2	18
Quality risks	Varying moisture conditions	3	3	2	18
	No advanced testing facilities	3	4	2	24
	Poor maintenance of materials	2	3	2	12
	Inefficient mixers	3	4	3	36
	Not keeping proper check lists	3	4	2	24

Table 3. FMEA worksheet

The task of determining the most critical risk was carried out using the FMEA technique and it resulted with five risks with equal risk priority number (RPN = 36).

- Inefficient mixers
- Improper working practices
- Improper maintenance of machinery
- Site injuries
- Delay due to traffic conditions

Since it is difficult to choose the most critical risk from these, a prioritization was done using ANP technique with the help of Super decisions software.

Application of ANP

The Analytic Network Process (ANP) is a powerful and flexible decision making process to help people set priorities and make the best decision when both qualitative and quantitative aspects of a decision need to be considered. ANP is generally based on the decision network structure and pairwise comparisons.

In this study, the ANP analysis is performed using the software Super Decisions. It is used here for the prioritization of alternatives. The Super Decisions software implements the Analytic Hierarchy Process (AHP) and Analytic Network Process (ANP) for decision making with dependence and feedback, a mathematical theory for decision making developed by Thomas L. Saaty. The software for the decision making with dependence and feedback was developed by William Adams in 1999-2003. The Super Decisions software is a simple easy-to-use package for constructing decision models with dependence and feedback and computing results using the super matrices of the Analytic Network Process.

- **Decision Network structure**

This is the first stage in the Super decision software. In this case, a network structure is developed by breaking down the decision problem into a network of inter related decision elements. The network structure consists of clusters and nodes. Clusters are the main branches in the structure while nodes are the sub branches. Here the network structure consists of clusters as goal, criteria and alternatives. Figure below shows the decision network structure obtained from the software.

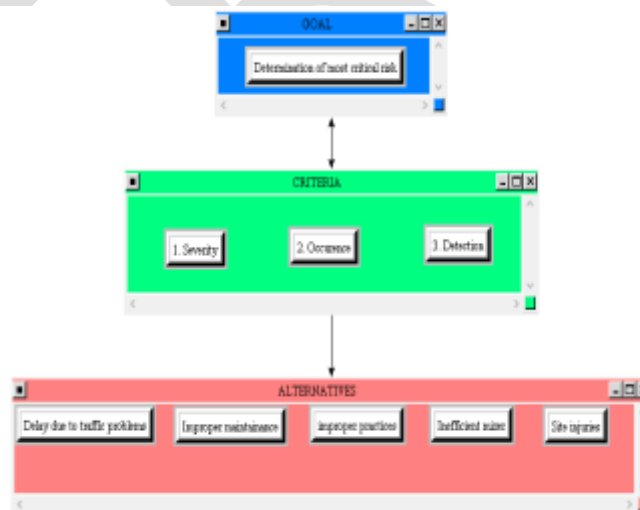


Figure 3. Decision network structure

- **Pairwise comparison**

Pairwise comparison generally is any process of comparing entities in pairs to judge which of each entity is preferred, or has a greater amount of some quantitative property, or whether or not the two entities are identical. In the ANP pairwise comparison, the significance/ importance of a risk over another is measured qualitatively. The ANP's pairwise comparison scale varies from 0 that indicates equal priority importance up to the score of 9, which reflect an extreme priority of an element/event over another. In this case the five risks with equal risk priority is compared with each other based on its severity, occurrence and detection of the risks. For performing the pairwise comparison, input is provided with the values obtained during the questionnaire survey. This is shown in the following figure from the software.

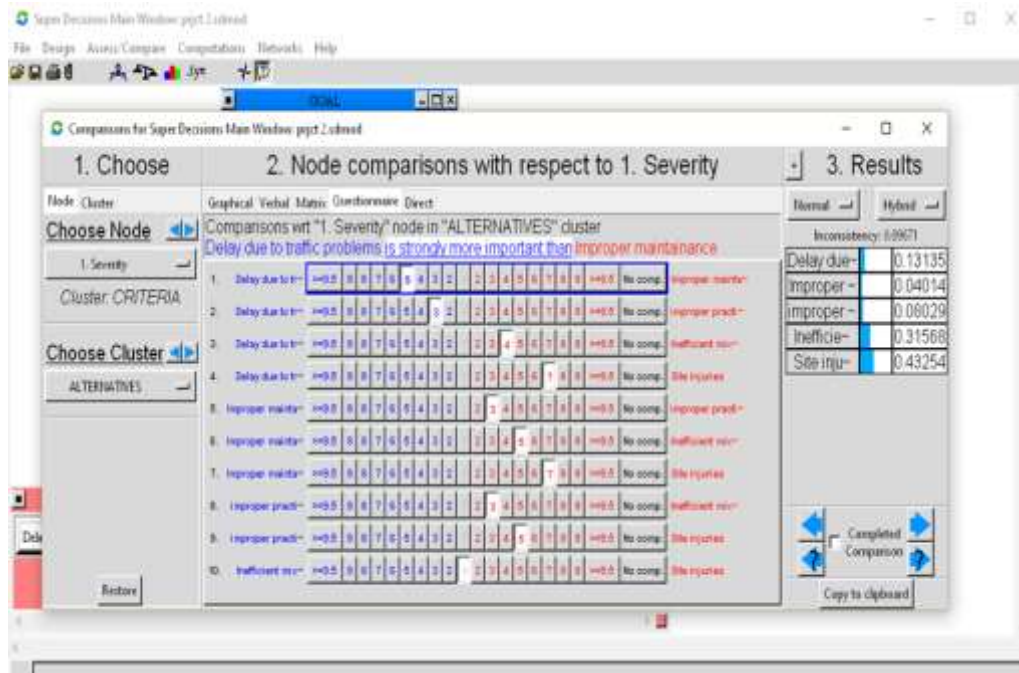


Figure 4. Pairwise comparison in software

• **Inconsistency analysis**

The final stage in the prioritization using the software is to calculate a Consistency Ratio (CR) to measure how consistent the judgments have been relative to large samples of purely random judgments. First of all, a comparison matrix of order (n × n) is formed. In this matrix, the diagonal members are always equal to one. The other members are filled based on the judgment values entered in the pairwise comparison. In order to evaluate the goodness of the judgment, consistency ratio (CR) should be defined as shown by (Saaty, 1990) as following:

$$CR = \frac{CI}{RI}$$

Where: CI = consistency index for an n × n matrix
RI = corresponding average random

$$CI = \frac{\lambda_{max} - n}{n - 1}$$

Where: λ max = maximum Eigen value of matrix
n = number of comparisons

The RI is defined by Saaty as below;

Number of comparisons (n)	1	2	3	4	5	6	7	8	9	10
RI	0.00	0.00	0.58	0.90	1.12	1.24	1.32	1.41	1.45	1.49

Table 4. Average Random values

Usually, the consistency ratio (CR) is used to check whether a criterion can be used for decision-making. If the CR is much in excess of 0.1 the judgments are untrustworthy because they are too close for comfort to randomness and the exercise is valueless or must be repeated. Consistency applies only to the pairwise comparison matrices. The consistency is desirable to be less than 0.10. In this study, for the all alternatives, the consistency is obtained as less than 0.10. Thus means that the pairwise comparison done is

acceptable. Since the inconsistency ratio obtained is less than 0.1, the prioritizations can be accepted. The comparison matrices (weighted priority matrices) for the criteria severity and consistency ratios (CR) obtained from the software is shown below.

Criteria	Consistency ratio (CR)
Severity	0.09671
Occurrence	0.09701
Detection	0.09017

Table 5. ANP Consistency ratio

SEVERITY					
	Delay due to traffic problems	Improper maintenance	improper practices	Inefficient mixer	Site injuries
Delay due to traffic problems	1	5	3	0.25	0.142
Improper maintenance	0.2	1	0.33	0.2	0.142
Improper practices	0.333	3.000	1	0.333	0.2
Inefficient mixer	4	5	3.00	1	1
Site injuries	7.0000	7.000	5	1	1

Table 6. Comparison matrix for severity

- **Final Priority ranking of the risks**

The final ranking of the alternatives was obtained after performing the inconsistency analysis. The priority ranking was done based on normalized and ideal weights of the alternatives. The priority ranking obtained is as shown below;

Alternatives	Normal weight	Ideal weight	Ranking
Site injuries	0.4789	1.0000	I
Inefficient mixer	0.1848	0.3859	II
Improper practices	0.1525	0.3184	III
Delay due to traffic problems	0.1306	0.2726	IV
Improper maintenance	0.0533	0.1113	V

Table 7. Final ranking of alternatives

From the priority ranking, it can be concluded that the most critical risk among the five alternatives is the site injuries with rank 1.

- **Graphical sensitivity analysis**

Sensitivity was performed using any element in the model. This is done as a check to confirm the final ranking of the alternative selected by the software is correct. There are different methods for the sensitivity analysis and in graphical sensitivity

analysis, the priority of criteria is changed and the corresponding changes in the graph are noted. If there is no significant changes in the graph, the ranking method can be taken as accurate. From the sensitivity analysis, it is clear that there is no change to the priority weight (0.5 or 50%) for all criteria. This means that the priority ranking was correct. The graphs obtained for the criteria severity is as following.

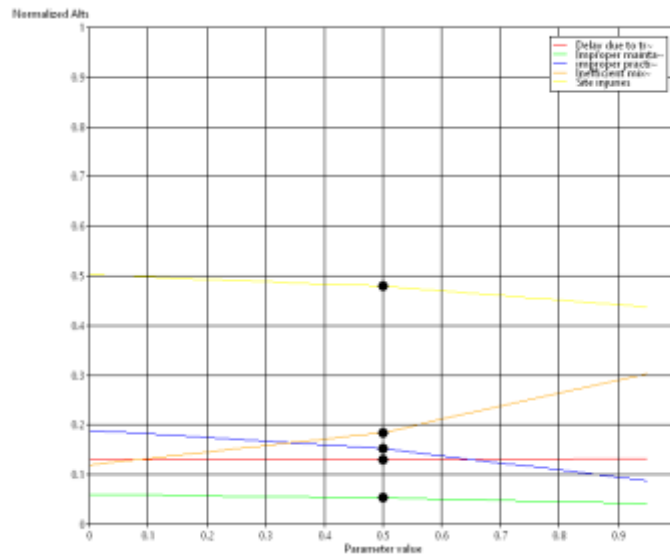


Figure 5. Sensitivity graph for severity

Hence from the overall results of the software the most critical risk in the plant 4 is identified as site injuries with the top rank under the three criteria: severity, occurrence and detection. This risk was prioritized with normalised weight of 0.4789 and with top ranking level.

RESULTS AND CONCLUSIONS

The systematic identification and assessment of risk and effectively dealing with the results is significant to the success of any industries and projects. Like other industries, RMC industry is also exposed to various risks and hence proper identification and assessment of these risks is very important for the effective working of the plant. Identification and assessment of the most critical risk is a difficult task due to the unavailability of an effective technique. This work proposed a technique for the proper and effective assessment of the critical risk in RMC plants and it includes FMEA technique with risk prioritization using ANP. Failure Mode Effective Analysis (FMEA) technique is a systematic process for identifying potential design and process failures before they occur and it is a risk rating technology based on the severity, occurrence and detection of risks. Risk prioritization involves the prioritization of risks based on a rating scale and Analytical Network Process (ANP) is a common technique for it.

In this work, the FMEA technique resulted in five critical risks with equal RPN of 36 (Site injuries, inefficient mixer, improper practices, Delay due to traffic problems and improper maintenance). Hence to find out the most critical risk, a prioritization was made with the help of Super decision software was used. Prioritization using pairwise comparison among the five alternatives resulted in identifying site injuries (normalized weight of 0.4789) with top ranking. According to the nature of the risk, some remedial measures were also suggested.

From this study, the most critical risk obtained is the site injuries. For this type of risk, the following remedial measures can be suggested.

- Provision of well awareness to each workers on the following facts;
 - ❖ Drivers Training
 - ❖ First –Aid Training
 - ❖ Fire Fighting Training
 - ❖ Lock–off and Machine Guarding
 - ❖ Concrete Pumping
 - ❖ Material Handling
 - ❖ Health Awareness

- Development of proper safety committee on the plant so that immediate actions can be taken on any site injuries or similar risks.
- Provision of proper personal protective equipment of very good quality
- Provision of engineering controls over the plant like;
 - ❖ Adequate machinery guarding
 - ❖ Proper guarding on transit mixers and on concrete pumps
 - ❖ Providing Fire Safety and Mock Drill (ERT) training programs at plant.
 - ❖ Proper up keeping of safety check lists in the plant.

In general, with proper safety management and safety measures, the critical risks in plants as well as in sites can be minimized.

REFERENCES:

- [1] Agnieszka Dziadosza, Mariusz Rejment. "Risk analysis in construction project - chosen methods" *Procedia Engineering* 122, 258 – 265. July 2015.
- [2] Oksana Marinina, Mariy Tochilo, "Analysis Of The Possibility of Using Modern Risk Assessment Methods In Mining Industry" *Zeszyty Naukowe Politechniki Śląskiej*, Volume 81, July 2012.
- [3] Dr. Chakradhar Iyanni, .Jyoti Trivedi, "FMEA risk management technique for quality control of RMC production" *International Journal of Advance Engineering and Research Development (IJAERD)*, e-ISSN: 2348 - 4470 , print-ISSN:2348-6406, May 2015.
- [4] Mehrzad Ebrahempzadiah, G. H. Halvani, Behzad Shahmoradi, Omid Giahil, " Assessment and Risk Management of Potential Hazards by Failure Modes and Effect Analysis (FMEA) Method in Yazd Steel Complex " *Open Journal of Safety Science and Technology*, 2014, 4, 127-135, September 2014.
- [5] Gunjan Joshi, Himanshu Joshi, "FMEA and Alternatives v/s Enhanced Risk Assessment Mechanism", *International Journal of Computer Applications* 0975 – 8887, Volume 93, No 14, May 2014.
- [6] Debasis Sarkar, Goutam Dutta, " Design and Application of Risk Adjusted Cumulative Sum (RACUSUM) for Online Strength Monitoring of Ready Mixed Concrete " *Indian institute of technology research and publications*, W.P. No.2008-08-01 August 2008.
- [7] Ali Gorener, "Comparing AHP and ANP: An Application of Strategic Decisions Making in a Manufacturing Company", *International Journal of Business and Social Science*, Vol. 3 No. 11 June 2012.
- [8] F.E. Mohamed Ghazali and H.C. Wong, "Risk Ranking for Tunneling Construction Projects in Malaysia", *KICEM Journal of Construction Engineering and Project Management*, September 24, 2013.
- [9] S. Baby, "AHP modeling for Multi criteria Decision-Making and to Optimize Strategies for Protecting Coastal Landscape Resource", *International Journal of Innovation, Management and Technology*, Volume 4, No. 2, April 2013.
- [10] Dr. R. K. Kansal, Manoj Sharma, " Risk Assessment Methods and Application in the Construction Projects", *International Journal of Modern Engineering Research (IJMER)*, Vol.2, Issue.3, 1081-1085. May-June 2012.

TEMPERATURE AND HUMIDITY MONITORING AND ALERT MANAGEMENT SYSTEM

Sophiya Kunjumon
Information Technology
Xavier Institute of Engineering
Mumbai

Kenneth Pinto
Electronics and Telecommunication
Xavier Institute of Engineering
Mumbai
Phone: 9619909318

Jude Saldanha
Electronics and Telecommunication
Xavier Institute of Engineering
Mumbai

Abstract— In the Temperature and Humidity Sensor Project, a solution is provided to monitor and get an alert of increase in temperature or humidity. This project is based on an Arduino and Ethernet Shield which communicates with DHT22 temperature sensor. The Data Center at an organization can receive information about temperature and humidity from anywhere in the world by using the Blynk application and an Internet connection on their phone. This creates a uniform interface which can be accessed locally or remotely using smart phones or laptops. The DHT22 sensor is calibrated according to the dimensions. If the temperature or humidity increases above a specified value, an alert via an email will be sent to the email ID specified in the program. The Arduino Ethernet Shield connects the Arduino to the internet in mere minutes. The Ethernet shield module is plugged onto the Arduino board, and it connects it to the network with an RJ45 cable.

Keywords — Temperature sensor, Humidity, Arduino, Ethernet Shield, DHT22 sensor, Blynk.

INTRODUCTION

The Temperature and Humidity Monitoring Project has been made to check the accuracy of temperature at a data center. The control and monitoring of the room temperature is done using a DHT22 sensor that is based on Arduino Uno. Thus, designed to make it easier to regulate and monitor the temperature and humidity of the data center. This smart project focuses on automation which relates to comfort instead of manual work.

Proposed System:

Interface:

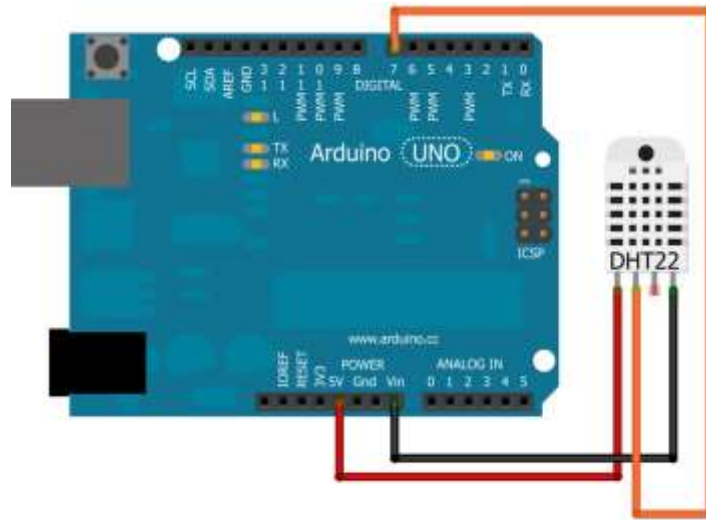
The Temperature and Humidity Sensor Project will be controlled using an application named Blynk (Available for Android or IOS) using Arduino, an Ethernet Shield and its libraries. User can securely login over Blynk to control and monitor the room temperature and humidity. The code involves:

The Arduino sketch.

The Arduino sketch handles the communications by setting up the network. The sketch runs the program and communicates one line at a time over the server. Users can login remotely on this web server.

Use of DHT22 Sensor:

DHT22 capacitive humidity sensing digital temperature and humidity module is one that contains the compound that has been calibrated digitally to signal output of the temperature and humidity sensors. The sensor includes a capacitive sensor, wet components and a high-precision temperature measurement devices, and connected with a high-performance 8-bit microcontroller. The product has excellent quality, fast response, strong anti-jamming capability, and high cost. It is definitely long-lasting and has great endurance.



Implemented Output:

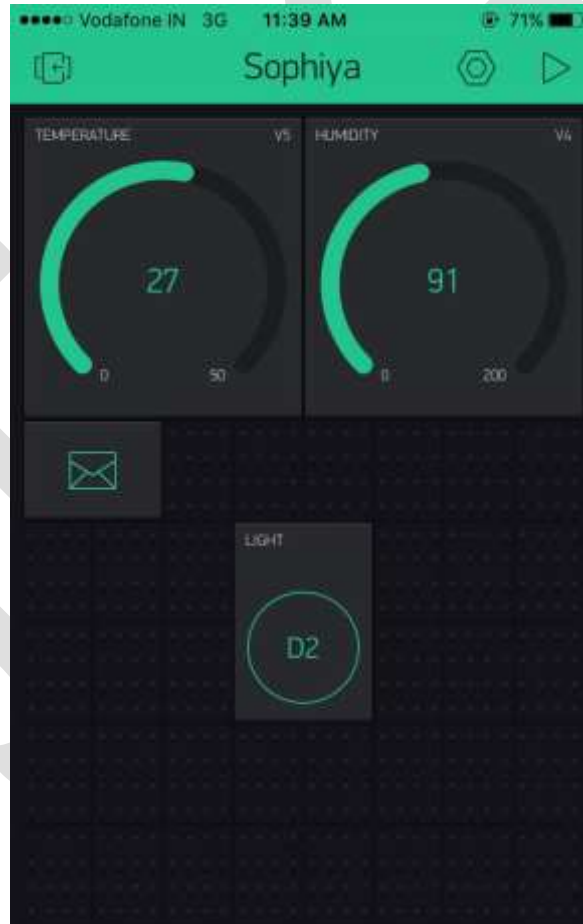


FIG 3. OUTPUT OF THE SYSTEM.

ACKNOWLEDGMENT

Our project “Temperature and Humidity Sensor Project” is a challenging and demanding project. This research was supported/partially supported by Bharat Petroleum Corporation Ltd. We thank our Project Guide from by Bharat Petroleum Corporation Ltd who provided insight and expertise that greatly assisted the research, although they may not agree with all of the

interpretations/conclusions of this paper. We thank Mr. Abhimanyu Waghmare for assistance, and thank Mr. Ravindra Patil -Sr. Software Engineer for comments that greatly improved the manuscript. We would also like to show our gratitude to Mr. Atul Patil for sharing his pearls of wisdom with us during the course of this research. We are also immensely grateful to the above for their comments on an earlier version of the manuscript, although any errors are our own and should not tarnish the reputations of these esteemed persons.

CONCLUSION

It is evident from this project work that Temperature and Humidity Sensor Project can be cheaply made from low-cost locally available components and be used to monitor and control the temperature and humidity at the data center. And better still, the components required are so small and few that they can be packaged into a small container. The designed project was tested a number of times and certified to achieve the aim of the project. This Temperature and Humidity Sensor Project can also be done using the esp8266 or various other sensors. Hence, this system is scalable and flexible.

REFERENCES:

- [1] Lopez, Jess Christopher B., and Harreez M. Villaruz. "Low-cost weather monitoring system with online logging and data visualization." *Humanoid, Nanotechnology, Information Technology, Communication and Control, Environment and Management (HNICEM), 2015 International Conference on. IEEE, 2015.*
- [2] Billies, Richard. "DIY Smart Home Sensors." (2016).
- [3] Matijevic, Milan, and Vladimir Cvjetkovic. "Overview of architectures with Arduino boards as building blocks for data acquisition and control systems." *2016 13th International Conference on Remote Engineering and Virtual Instrumentation (REV). IEEE, 2016.*
- [4] Cata, Marian. "Transmission and storage of data from a smart environment, in the context of Internet of Things." *Scientific Bulletin "Mircea cel Batran" Naval Academy 18.1 (2015): 304.*
- [5] Gertz, Emily, and Patrick Di Justo. *Environmental monitoring with Arduino: building simple devices to collect data about the world around us.* " O'Reilly Media, Inc.", 2012.
- [6] Arduino. [Online]. Available: <https://en.wikipedia.org/wiki/Arduino>
- [7] Arduino™ Sketches Tools and Techniques for Programming Wizardry, 2015

A STUDY TO UNDERSTAND ELLIOTT WAVE PRINCIPLE

Mr. Suresh A.S¹

Assistant Professor, MBA Department,

PES Institute of Technology, Bangalore South Campus,

1km Before Electronic city,

Hosur Road, Bangalore – 560100

Phone: 96861-95506

Email: sureshas7007@gmail.com, sureshas@pes.edu

Dr. S Naveen Prasath²

Assistant Professor, MBA Department,

PES Institute of Technology, Bangalore South Campus,

1km Before Electronic city,

Hosur Road, Bangalore – 560100

Email: naveenprasath@pes.edu

ABSTRACT- The Elliott Wave Principle states that markets move in natural patterns according to changing investor psychology and price momentum. Specifically, crowd psychology will move from optimism to pessimism, and back up again, making it possible to forecast the progression of certain market trends. "The Wave Principle" is Ralph Nelson Elliott's discovery that social, or crowd, behavior trends and reverses in recognizable patterns. The Wave Principle is not primarily a forecasting tool; it is a detailed description of how markets behave. Many areas of mass human activity follow the Wave Principle, but the stock market is where it is most popularly applied. Indeed, the stock market considered alone is far more important than it seems to casual observers.

According to the Elliott Wave theory, market move in the five distinct waves existing on the upside and the three distinct waves existing on the downside. The upwards waves that lie in the bull move are termed as Impulse waves and the other three waves that are against the trend direction are termed as Corrective waves. In the Financial market, major trend is determined by the major waves and the minor trend is determined by the minor waves.

Key words: Elliott wave principle, optimism, psychology, price momentum, stock market.

INTRODUCTION

The dilemma faced by the market participants in the secondary market as to predict the movement of stock prices is well managed with two approaches, Fundamental and Technical analysis. Due to high volatility in the stock markets it is considered as a very rigorous job to predict the future movement of the stock prices. Secondary market participants often use two forecasting techniques, Fundamental and Technical analysis. According to this distinction fundamentalists are market participants who predict movements of stock prices by analyzing the underlying economic conditions upon which they assume changes in the stock prices. Fundamental analysis believes that analyzing the economy, strategy, management, product, financial status and other related information will help choose shares that will outperform the market and provide consistent gains to the investor.

Technical analysts have developed tools and techniques to study past patterns and predict future price. Technical analysis is basically the study of markets only. Technical analysts study the technical characteristics which may be expected that may or market turning points and their objective assessment. The previous turning points are studied with a view to develop some characteristics that would help in identification of major market tops and bottoms. Human reactions are, by and large consistent in similar though not identical reaction; with the help of various tools, the technician attempts to correctly catch changes in trend and take advantage of them.

Thus, "Technical analysis is directed towards predicting the price of a security. The price at which a buyer and seller settle a deal is considered to be the one precise figure which synthesizes, weighs and finally expresses all factors, rational and irrational quantifiable and non-quantifiable and is the only figure that counts".

Stock market:

Stock market is a market where the trading of the company both listed and unlisted takes place. It is different from the stock exchange as stock markets include the stock exchanges of the country.

The stock market can be or the capital market can be divided into two segments

- **Primary market**
- **Secondary market**

Primary market:

Most of the companies are usually started privately by their promoters. However the promoter's capital and the borrowed capital from the banks or financial institution might not be sufficient for running the business over the long term. That is when the corporate and the government looks at the primary market to raise long term funds by issuing securities in the form of debt and majorly equity.

Secondary market:

The secondary market is the place which provides liquidity to the investors in the primary market. Today we would not invest in any instrument if there was no medium to liquidate our position. The secondary market provides an efficient for trading of those securities which are initially offered in the primary market.

Trading in the secondary market is done through the stock exchanges; the stock exchange is the place where the buyers and sellers meet to trade in shares in organized manner.

There are two leading stock exchanges in India which help us to trade in shares

- **Bombay Stock Exchange (BSE):**

BSE was set up in the year 1875 is the oldest stock exchange in Asia. It has evolved in to its present status as a premier stock exchange. At BSE you will find some scrip's not listed in NSE. Also BSE has the largest has the largest number of scrip's listed.

- **National Stock Exchange (NSE):**

NSE incorporated in the year 1992 provides trading in the equity and as well as the derivative market. Maximum volume takes place on NSE than compared to BSE and hence enjoys leadership in the cash segment. Not just the cash segment NSE holds a virtual monopoly in terms of derivative trading commanding more than 96% in the market.

Fundamental analysis

The basic purpose of buying a security is to earn dividends and ultimately sell it at a higher price. An investor therefore is interested in obtaining estimates of future prices of the share. These in turn will depend upon the performance of the industry to which the company belongs and the general economic situation of the country.

The multitude of factors affecting a company's profitability can be broadly classified as:

1. Economic wide factors: these include the factors like growth rate of the economy. The rate of inflation, foreign exchange rates etc which affects profitability of all companies.
2. Industry wide factors: these include factors which are specific to industry to which the company belongs. For instance the demand supply gap in the industry, the emergence of substitutes and changes in government policies towards industry affects the company belonging to an industry.
3. Companywide factor: these factors are specific to a firm. The firm specific factors like plant and machinery, the brand image of the product, and ability of the management to affect the profitability.

Fundamental analysis considers the financial and economic data that may influence the viability of a company. There are many flavors of fundamental analysts centered on such concepts as value, growth and turnarounds. Technical analysis is the study of the price chart. It assumes that by looking at the progress of that little squiggly line you can forecast the future trend of a stock. Fundamental analysis is essential to most investors, and a technical analyst is essential to most traders and speculators.

An investor with rational and scientific approach will therefore be interested in analyzing the influence of the expected performance of the company, industry and economy as a whole on share prices, even before taking the investment decision such analysis is called fundamental analysis.

Fundamental analysis is the method of evaluating securities by attempting to measure the intrinsic value of a particular stock. It is the study of everything from the overall economy and industry conditions, to the financial condition and management of specific companies (i.e... using real data to evaluate a stock's value) - The method utilizes items such as revenues, earnings, return on equity and profit margins to determine a company's underlying value and potential for future growth.

One of the major assumptions under fundamental analysis is that, even though things get mispriced in the market from time to time, the price of an asset will eventually gravitate toward its true value. This seems to be a reasonable bet considering the long upward march of quality stocks in general despite regular setbacks and periods of irrational exuberance. The key strategy for the fundamentalist is to buy when prices are at or below this intrinsic value and sell when they got overpriced.

Technical analysis:

Technical analysis takes a completely different approach; it doesn't care one bit about the "value" of a company or a commodity. Technicians (sometimes called chartists) are only interested in the price movements in the market.

Despite all the fancy and exotic tools it employs, technical analysis really just studies supply and demand in a market in an attempt to determine what direction, or trend, will continue in the future. In other words, technical analysis attempts to understand the emotions in the market by studying the market itself, as opposed to its components.

Elliott Wave Theory

Introduction

Elliott Wave Theory was developed by R.N. Elliott and popularized by Robert Prechter. This theory asserts that crowd behavior ebbs and flows in clear trends. Based on this ebb and flow, Elliott identified a certain structure to price movements in the financial markets. This article serves as a basic introduction to Elliott Wave Theory. A basic 5-wave impulse sequence and 3-wave corrective sequence are explained.

Wave Degrees

GrandSuper Cycle:	((I)) ((II)) ((III)) ((IV)) ((V)) ((a)) ((b)) ((c))
SuperCycle:	(I) (II) (III) (IV) (V) (a) (b) (c)
Cycle:	I II III IV V a b c
Primary:	((1)) ((2)) ((3)) ((4)) ((5)) ((A)) ((B)) ((C))
Intermediate:	(1) (2) (3) (4) (5) (A) (B) (C)
Minor:	1 2 3 4 5 A B C
Minute:	((i)) ((ii)) ((iii)) ((iv)) ((v)) ((a)) ((b)) ((c))
Minuette:	(i) (ii) (iii) (iv) (v) (a) (b) (c)
Subminuette:	i ii iii iv v a b c

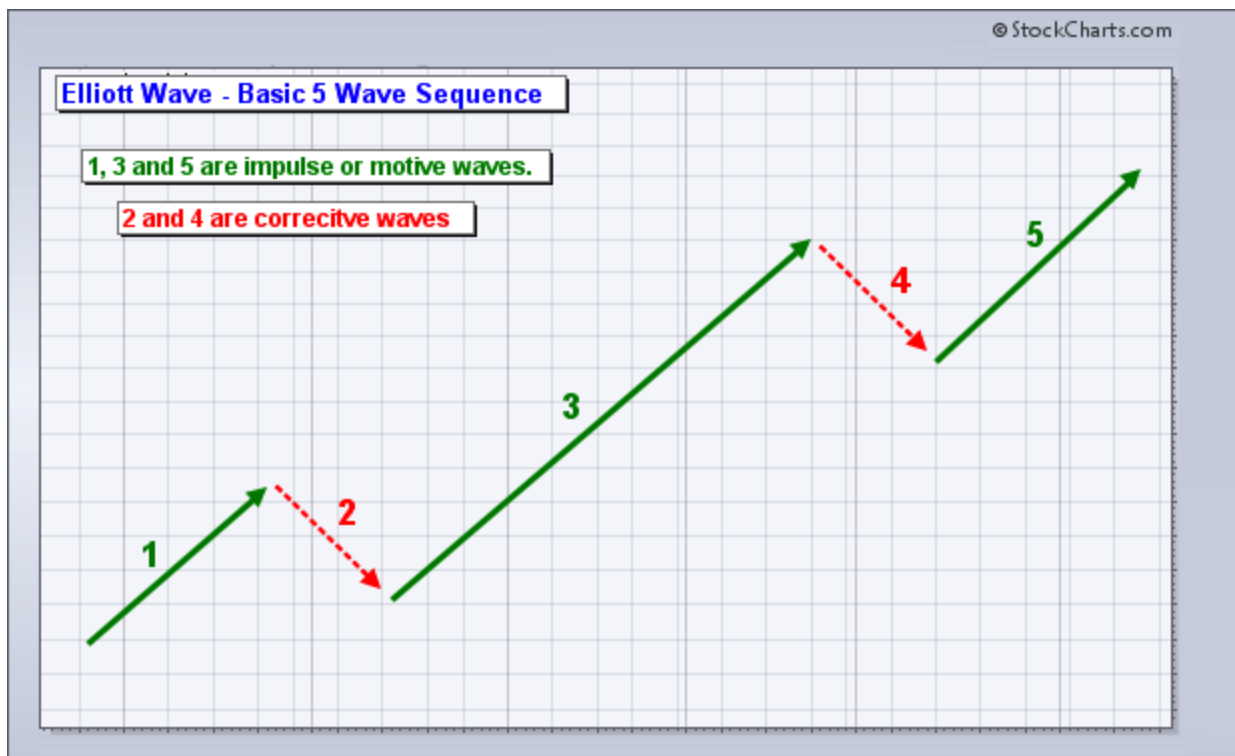
The labeling convention shown above is a hybrid between that is shown in the Elliott Wave book and the Elliott tools from Sharp Charts. In Elliott's book, this labeling convention is used to identify the degree or level of the wave, which represents the size of the underlying trend. The upper case Roman numerals represent the large degree waves, the simple numbers represent the medium degree waves and the small-case Roman numerals represent the small degree waves. The trends start with the largest degree (Grand Super cycle) and work their way down to waves of lesser degree.

For example, the Cycle wave is one larger degree than the Primary wave. Conversely, the Primary wave is one lesser degree than the Cycle wave. Wave 1 of (1) would indicate that Wave 1 is part of a larger degree Wave (1). Wave 1 is a lesser degree than Wave (1).

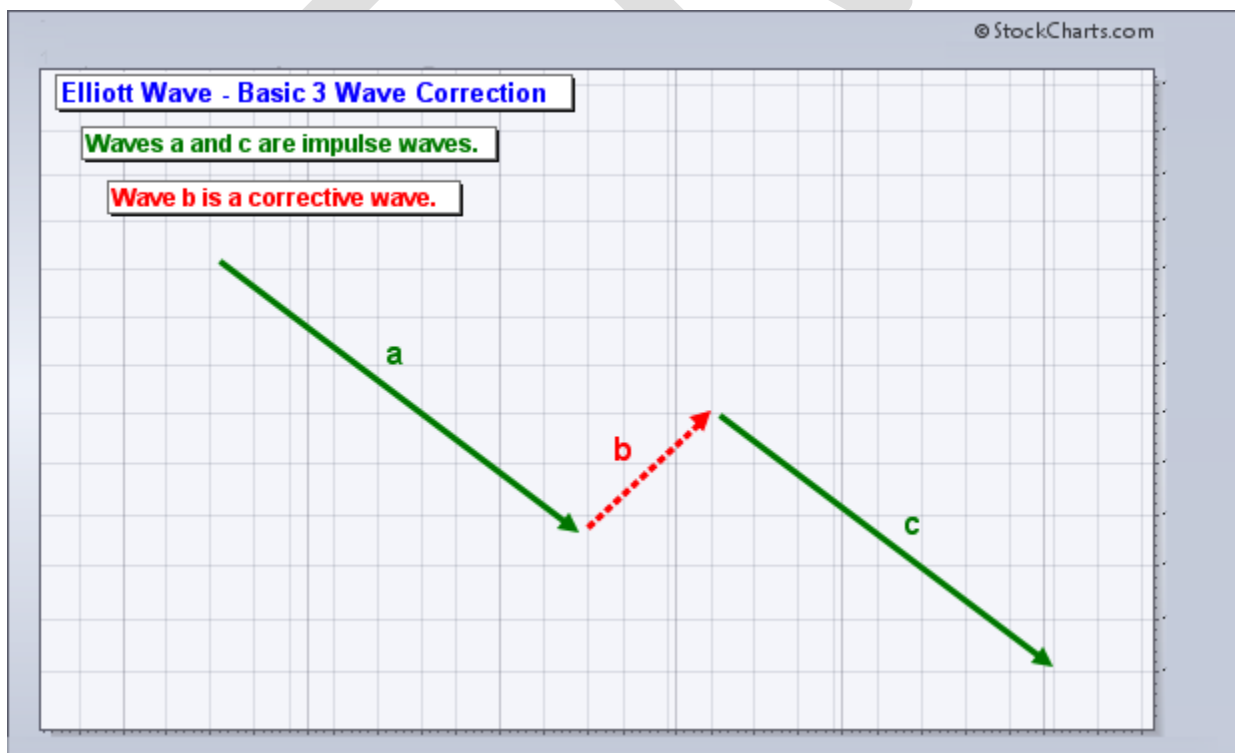
In reality, most chartists will only use 1 to 3 wave degrees on their charts. It can get quite complicated trying to apply nine Wave degrees or even just using the labeling convention in the order provided. Chartists using 1 to 3 wave degrees can simply label the highest degree waves with upper case Roman numerals (I, II, III, IV, V, a, b, c), the middle degree waves with numbers (1, 2, 3, 4, 5, A, B, C) and the lowest degree waves with lower case Roman numerals (i, ii, iii, iv, v, a, b, c). This provides three distinct groups for labeling various waves.

Basic Sequence

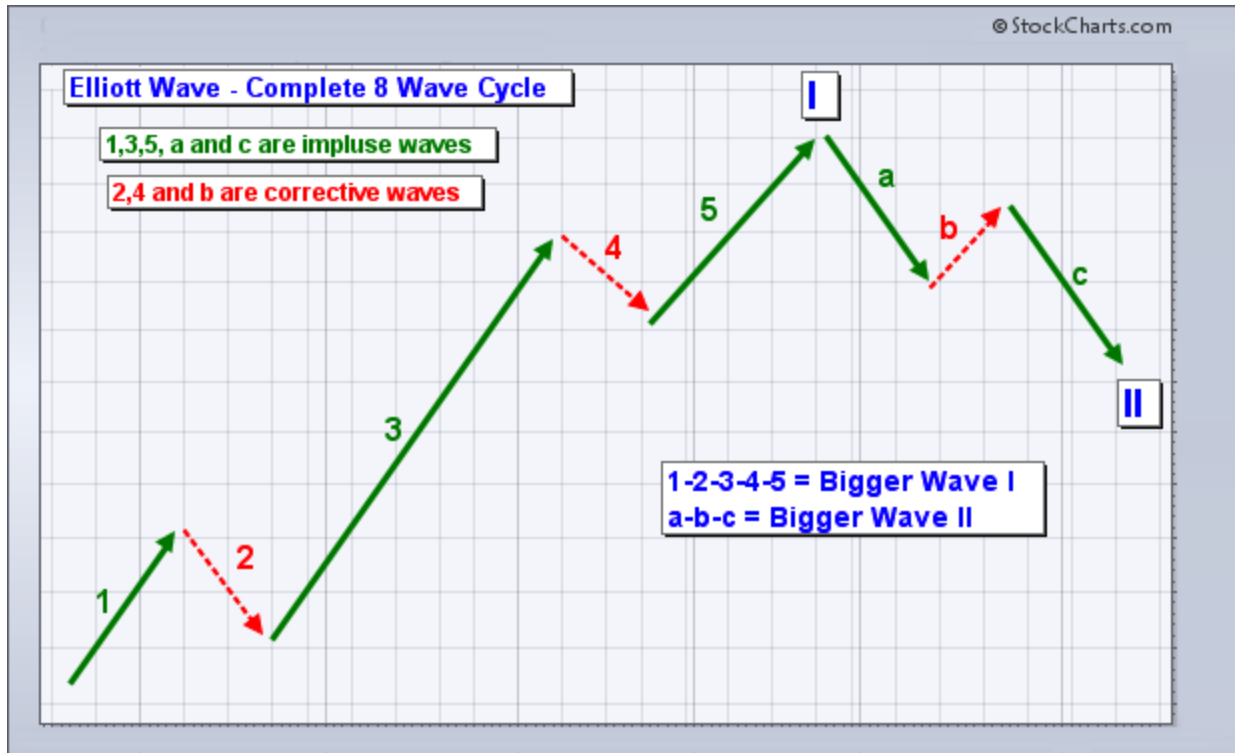
There are two types of waves: impulse and corrective. Impulse waves move in the direction of the larger degree wave. When the larger degree wave is up, advancing waves are impulsive and declining waves are corrective. When the larger degree wave is down, impulse waves are down and corrective waves are up. Impulse waves, also called motive waves, move with the bigger trend or larger degree wave. Corrective waves move against the larger degree wave.



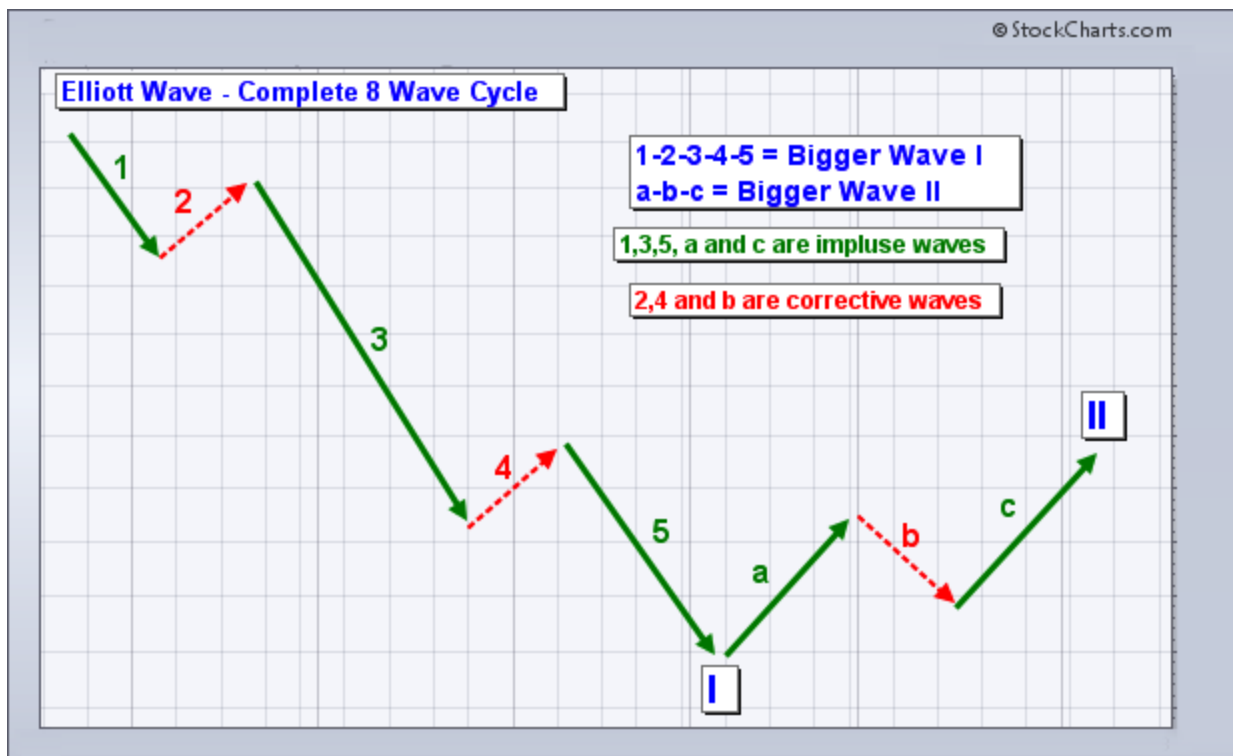
The chart above shows a rising 5-wave sequence. The entire wave is up as it moves from the lower left to the upper right of the chart. Waves 1, 3 and 5 are impulse waves because they move with the trend. Waves 2 and 4 are corrective waves because they move against this bigger trend. A basic impulse advance forms a 5-wave sequence.



A basic corrective wave forms with three waves, typically a, b and c. The chart below shows an abc corrective sequence. Notice that waves a and c are impulse waves (green). This is because they are in the direction of the larger degree wave. This entire move is clearly down, which represents the larger degree wave. Waves a and c move with the larger degree wave and are therefore impulse waves. Wave b, on the other hand, moves against the larger degree wave and is a corrective wave (red).



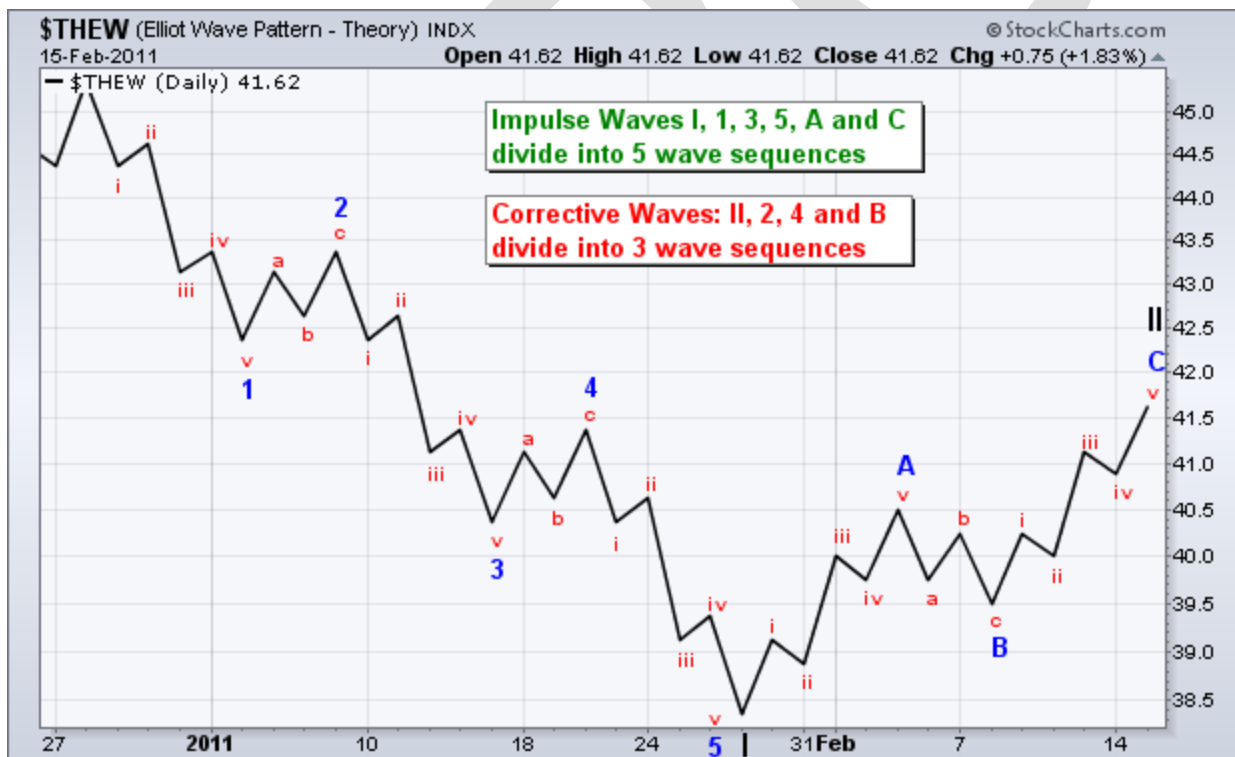
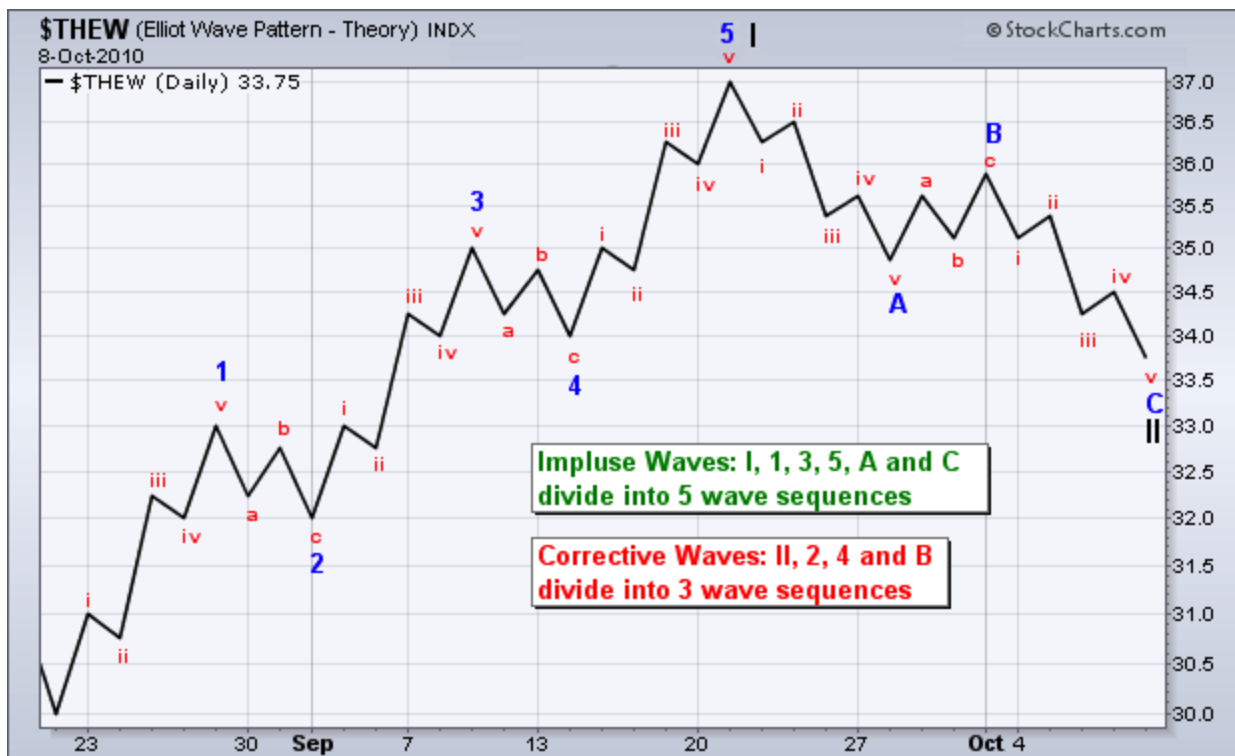
Combining a basic 5 wave impulse sequence with a basic 3 wave corrective sequence yields a complete Elliott Wave sequence, which is a total of 8 waves. According to Elliott, this complete sequence is divided into two distinct phases: the impulse phase and the corrective phase. The abc corrective phase represents a correction of the larger impulse phase.



These 8-wave charts show two larger degree waves (I and II) as well as the lesser degree waves within these larger degree waves. Waves 1-2-3-4-5 are one lesser degree than Wave I. By extension, Wave I is one larger degree than Waves 1-2-3-4-5. Waves a-b-c are one lesser degree than Wave II.

Fractal Nature

Elliott Wave is fractal. This means that wave structure for the Grand Super Cycle is the same as for the minuet. No matter how big or small the wave degree, impulse waves take on a 5-wave sequence and corrective waves take on a 3-wave sequence. Any impulse wave subdivides into 5 smaller waves. Any corrective wave subdivides into three smaller waves. The charts below show the fractal nature of Elliott Wave in action.



Three Rules

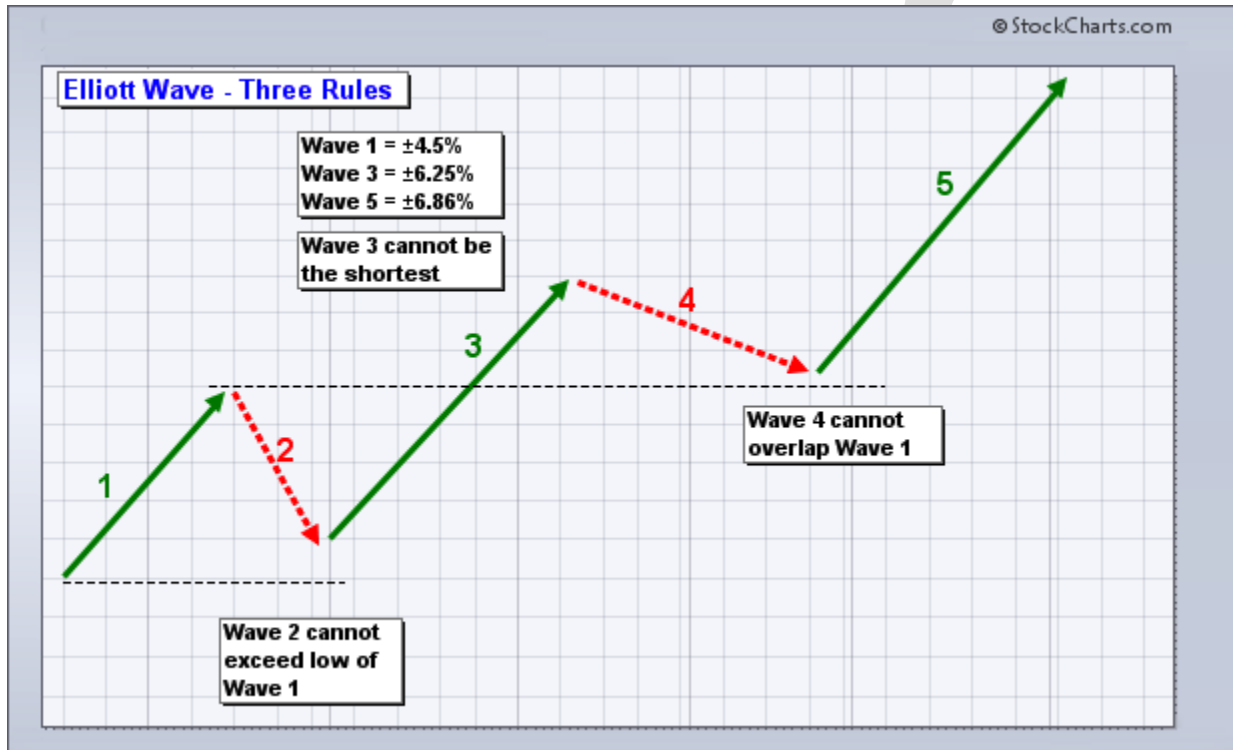
Believe it or not, there are only three rules when it comes to interpreting Elliott Wave. There are many guidelines, but only three HARD rules. These are unbreakable. Guidelines, on the other hand, are bendable and subject to interpretation. Furthermore, these

rules only apply to a 5-wave impulse sequence. Corrections, which are much more complicated, are given more leeway when it comes to interpretation.

Rule 1: Wave 2 cannot retrace more than 100% of Wave 1.

Rule 2: Wave 3 can never be the shortest of the three impulse waves.

Rule 3: Wave 4 can never overlap Wave 1.



Wave 2 cannot move below the low of Wave 1. A break below this low would call for a re-count. Even though Wave 3 is typically the longest of the three impulse waves, there is a specific rule that it cannot be the shortest. 1 or 5 can be longer than Wave 3, but both cannot be longer than Wave 3. It is probably best to use percentages or log scales when measuring Wave length. Elliott Wave indicates that Wave 3 must exceed the high of Wave 1. Failure to exceed this high would call for a re-count. Impulse moves are all about making progress. Failure to exceed the high of Wave 2 would not be making progress. The third, and final rule, is that Wave 4 cannot overlap Wave 1, which means the low of Wave 4 cannot exceed the high of Wave 1. Such a violation would call for a re-count.

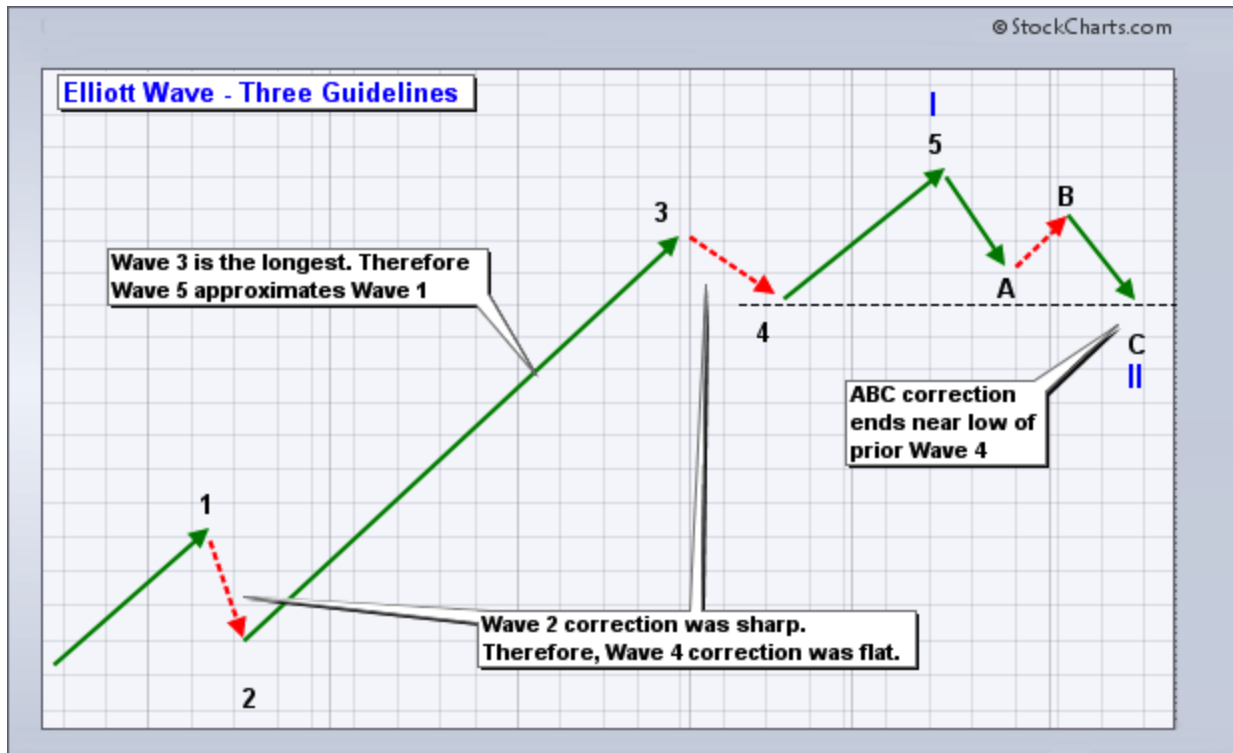
Three Guidelines

There are numerous guidelines, but this article will focus on three key guidelines. In contrast to rules, guidelines should hold true most of the time, not necessarily all of the time.

Guideline 1: When Wave 3 is the longest impulse wave, Wave 5 will approximately equal Wave 1.

Guideline 2: The forms for Wave 2 and Wave 4 will alternate. If Wave 2 is a sharp correction, Wave 4 will be a flat correction. If Wave 2 is flat, Wave 4 will be sharp.

Guideline 3: After a 5-wave impulse advance, corrections (abc) usually end in the area of prior Wave 4 low.



The first guideline is useful for targeting the end of Wave 5. Even though Wave 5 could be longer than Wave 3 and Wave 3 could still be longer than Wave 1, chartists can make initial Wave 5 projections once Wave 4 ends. In a larger uptrend, chartists simply apply the length of Wave 1 (percentage change) to the low of Wave 4 for an upside target. The opposite is true for a 5-wave decline. The percentage decline in Wave 1 would be applied to the high of Wave 4 for a Wave 5 estimate.

The guideline of alternation (2) is useful for determining the time of correction for Wave 4. After a sharp decline for Wave 2, chartists can expect a relatively flat correction for Wave 4. If Wave 2 is relatively flat, then chartists can expect a relatively sharp Wave 4. In practice, Wave 2 tends to be a rather sharp wave that retraces a large portion of Wave 1. Wave 4 comes after an extended Wave 3. This Wave 4 marks more of a consolidation that lays the groundwork for a Wave 5 trend resumption.

The third guideline is useful for estimating the end of a Wave II correction after a Wave I advance. Waves I and II are the larger degree waves. Waves 1-2-3-4-5 are lesser degree waves within Wave I. Once the Wave II correction unfolds, chartists can estimate its end by looking at the end of the prior wave 4 (lesser degree wave 4). In a larger degree uptrend, Wave II would be expected to bottom near the low of lesser degree Wave 4. In a larger degree downtrend, Wave II would be expected to peak near the high of lesser degree Wave 4.

Conclusions

Even though this article just scratches the surface of Elliott Wave Theory, chartists can greatly improve their counting by applying the three rules and three guidelines listed. Elliott Wave counts start with a process of elimination. Apply the rules for the first count attempt and then the guidelines on the second. Eliminating bogus counts paves the way to a more accurate count. Even with accurate counts, chartists will still need to re-evaluate and adjust counts as new price information emerges.

REFERENCES:

1. Investment Analysis and Portfolio Management – Prasanna Chandra
2. Security Analysis and Portfolio Management – V.A Avadhani
3. Suresh A S (2013), “A study on fundamental and technical analysis”, International Journal of Marketing, Financial Services & Management Research, Vol.2, No.5.
4. www.moneycontrol.com
5. www.stockchart.com

Secure Data Transmission Using Improved Diffie-Hellman Algorithm in VANET

¹Dr. T.Ramaprabha, ²V.Premalatha

¹Professor, Department of Computer Science and Applications,

²Full Time M.Phil Scholar, Department of Computer Science,

^{1,2}Vivekanandha College of Arts and Science for Women, Tiruchengode, Tamilnadu, India.

ramaradha1971@gmail.com , premkani11@gmail.com

Abstract- A Vehicular Ad-Hoc Network is a form of mobile ad hoc network, which provide communications among nearby vehicles and nearest fixed equipment, like traffic sensor. Vehicular network act as an infrastructure to transfer the data between vehicles. Road Side Unit acts as a base station to deliver the data about the path to the vehicles using Diffie-Hellman key exchange algorithm. It is one of the more popular and interesting methods of key distribution. It is a public-key cryptographic system whose sole purpose is for distributing secured keys and avoiding activities of attackers. It gives high level security and more energy efficient data transmission on the network. Diffie-Hellman key exchange is used to find out another route quickly in the case of false route. It also used to recover the failure nodes. In this paper, we discuss about the secure data transmission using Improved Diffie – Hellman algorithm in VANET.

Keywords- VANET, Security, Privacy, RSU, OBU

INTRODUCTION ON VANET

The Vehicular Ad-Hoc Network, or VANET, is a technology that uses moves cars as nodes in a network to create a mobile network. VANET turns every participating car into a wireless router or node, allowing cars approximately 100 to 300 metres of each other to connect and, in turn, create a network with a wide range. As cars fall out of the signal range and drop out of the network, other cars can join in, connecting vehicles to one another so that mobile internet is created. It is estimated that the first systems that will integrate this technology are police and fire vehicles to communicate with each other for safety purposes.

Vehicular network faces wide range of attacks and the most common attacks are: impersonation, bogus information injection, non integrity, non confidentiality, and Denial of Service (DOS). Two classes of attacks are like to occur in vehicular networks such as

1. external attacks, in which attackers not belonging to the network jam the communication or inject erroneous information.
2. Internal attacks, in which attackers are internal compromised nodes that are difficult to be detected.

Both types of attacks may be either passive intending to steal information and to eavesdrop on the communication within the network, or active modifying and injecting packets to the network. As a counter-measure against most of these attacks, the following security considerations should be satisfied providing a trusted infrastructure between communicating vehicles, mutual authentication between each communicating pair whether two vehicles or a vehicle and a fixed element of infrastructure, efficient access control mechanisms allowing not only the authorization to the network access but also the authorization to the services' access, confidential and secure data transfer.

Since ITS (Information Technology scheme) applications are mainly targeting the peoples' safety on roads, while passengers oriented Non-ITS applications are mostly concerned with commercial services provision on roads, thus Securing inter vehicular communication is different in both cases as shown in figure 1.1. As a consequence security requirements are different for each application type.

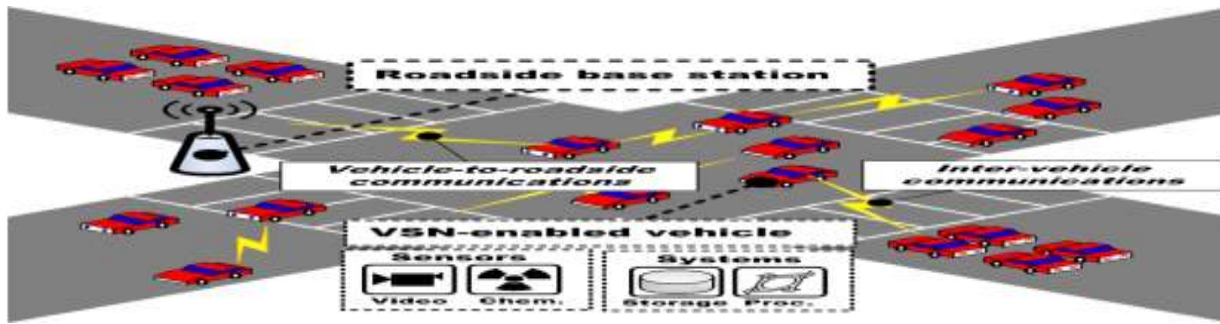


Figure 1.1: Communication Based on Vehicular Network by using the RSU

For both types of applications, we found that the non-repudiation, the integrity and the non-traceability is important security requirements for worth considerations. Thus a complex problem arises in this issue.

In fact, a tough requirement in vehicular networks environments is to manage traceability in terms of allowing this process for the concerned authorities and at the same time assuring the no traceability between mobile client's vehicles themselves. Nevertheless, the latter is difficult to be achieved and so far no promising solutions exist to resolve this issue in the vehicular networks dynamic and open environment. It is noticed that the word traceability can include:

1. Authentication, Authorization and Access Control.
2. Vehicular applications and Internet Implementations.
3. Routable addresses and position based addressing.

NEED OF SECURE DATA TRANSMISSION

Since the authentication scheme is susceptible to malicious attacks, the objective is to design a scheme that is robust to such attacks. Based on related studies. the following key security requirements for VANETs is defined.

1. **Efficiency:** In VANETs, the computational cost of vehicles must be as low as possible in order to have a real-time response.
2. **Anonymity:** The anonymous authentication procedure verifies that an OBU does not use its real identity to execute the authentication procedure.
3. **Location privacy:** An adversary collects the serial authentication messages of the OBU but it still failed to track the location of the vehicle.
4. **Mutual authentication:** A mutual authentication procedure is implemented whereby the LE must verify that the OBU is a legal user and the OBU must ensure that the LE is genuine.
5. **Integrity:** The message integrity means that data cannot be modified undetectably.

Vehicular networks permit [3] cars to communicate with each other and with a distinct infrastructure on the road. Infrastructures can be purely ad hoc between cars or facilitated by making use of an infrastructure. The organization typically consists of a set of so called roadside units that are connected to each other or even to the Internet [1].

VANET uses three systems:

1. Intelligent transportation systems
2. Vehicle-to-roadside communication and
3. Routing-based communication.

Intelligent Transportation Systems: The inter-vehicle communication conformation uses multi-hop multicast or programme to transmit traffic correlated information over multiple hops to a group of receivers. In intellectual transportation systems, vehicles need only be concerned with activity on the road forward and not behind.

Vehicle-to-Roadside Communication: The vehicle-to-roadside communication formation characterizes a single hop transmission where the roadside unit sends a broadcast message to all prepared vehicles in the vicinity. Vehicle-to-roadside communication formation provides a high bandwidth link between automobiles and roadside units. The roadside units may be placed every kilometre or less, succeeding high data rates to be continued in heavy traffic [2].

Routing-Based Communication: The routing based communication arrangement is a multi-hop unicast where a message is broadcasted in a multi Routing based announcement hop fashion until the vehicle carrying the anticipated data is reached. When the request is received by a vehicle preserving the desired piece of information, the application at that vehicle instantly sends a unicast message containing the information to the vehicle it established the request from, which is then exciting with the task of forwarding it towards the query source.

DIFFIE-HELLMAN KEY EXCHANGE ALGORITHM

It should be complemented with an authentication mechanism. In this approach for key distribution with security factors to solve attacking problem is very challenging and that the shared key is never itself transmitted over the channel. A distributed key management framework has advantage in revocation of malicious vehicles, system maintenance, and the implementation of heterogeneous security policies. The basic Structure of Diffie-Hellman Algorithm figure 3.1 as shown in below.

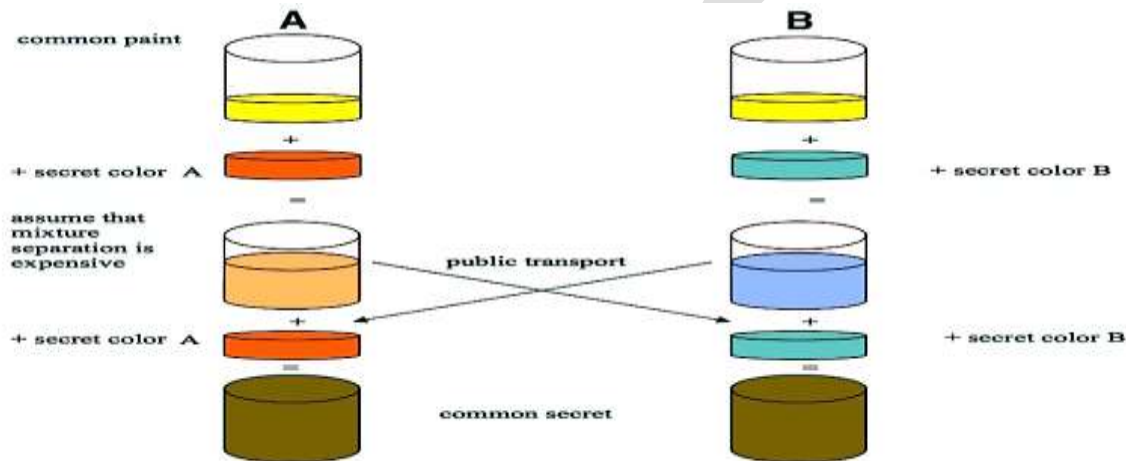


Figure 3.1 Structure of Diffie-Hellman Algorithm

A secure key distribution protocol is used with the capability of preventing from misbehaving. The protocol guarantees the traceability of compromised malicious vehicles. An efficient cooperative message authentication protocol is developed, by which cooperative verifiers are intelligently selected to significantly reduce the computation and communication overhead in the group signature based implementation.

A. Key Generating Node

Active attackers have the ability to send packets into wireless channels. Global attackers have an unlimited scope which means they can listen to any information in the network. Attackers May have strong transmission power to communicate over long distances. Adversarial parsimony means an attack involving a few malicious nodes is more likely to happen than an attack that requires collusion among a large number of nodes. The key generating node(KGN) will assume that the vehicles will report to authorities when they find that the other vehicle sends a false message. Wired network which connects authorities transmits data securely without packet loss. In the key distribution phase, our protocol is used to moderator whether a vehicle is a legitimate user or not.

B. Road Side Unit (RSU)

The RSU [4] Detection System using the Diffie Hellman key exchange method used to be one of the most interesting key distribution schemes in use today. However, one must be aware of the fact that although the algorithm is safe against passive dropping, it is not necessarily protected from active attacks distribution to allow malicious nodes to interact within the network for transferring data between sources to destination and hence complete security could not be achieved within the network due to the

presence of malicious nodes. In order to provide more secure communication between source and destination, DH uses risk as an input to determine how much source node can be trusted, so that only trusted nodes are allowed to communicate and hence high security can be achieved within VANET. They have to take a throughput, delay and delivery ratio are network performance on the network. It most efficient and security based data transmission.

Advantages

- Diffie-Hellman algorithm is used to find out another route easily.
- Each user have own time slot.
- Efficient data transformation.
- Data will be transferred without any packet loss.
- Network performance is increased effectively.

DIFFIE-HELLMAN ALGORITHM IMPLEMENTATION IN NS-2

Ns or the Network simulator (also popularly called ns-2) is a discrete event network simulator. It is popular in academia for its extensibility (due to its open source model) and plentiful online documentation. Ns are popularly used in the simulation of routing and multicast protocols among others and are heavily used in ad-hoc networking research. Ns supports an array of popular network protocols, offering simulation results for wired and wireless networks alike. It can be also used as limited –functionality network emulator. Ns are licensed for use under version 2 of the GNU General Public License.

A. Network Simulator 2.28 (NS-2)

Ns-2.28 is a packet-level simulator and essentially a centric discrete event scheduler to schedule the events such as packet and timer expiration. Centric event scheduler cannot accurately emulate “events handled at the same time” in real world, that is, events are handled one by one. This is not a serious problem in most network simulations, because the events here are often transitory. Beyond the event scheduler, ns-2 implements a variety of network components and protocols. Notably, the wireless extension, derived from CMU Monarch Project, has 2 assumptions simplifying the physical world. Nodes do not move significantly over the length of time they transmit or receive a packet. This assumption holds only for mobile nodes of high-rate and low-speed. Consider a node with the sending rate of 10Kbps and moving speed of 10m/s, during its receiving a packet of 1500B, the node moves 12m. Thus, the surrounding can change significantly and cause reception failure. Node velocity is insignificant compared to the speed of light.

B. Simulator Setup NS-2

NS-2 is an open-source simulation tool running on Unix-like operating systems. It is a discreet event simulator targeted at networking research and provides substantial support for simulation of routing, multicast protocols and IP protocols, such as UDP, TCP, RTP and SRM over wired, wireless and satellite networks. It has many advantages that make it a useful tool. LAN routing and broadcasts are part of routing algorithms. TCL script is used for configuring and parameterizing a simulation. Using Diffie-Hellman algorithm we implemented the NS-2 simulator to improve the performance of secure data transmission in VANET as shown in below figures.

This module figure 4.1 is developed to node creation and more than 10 nodes placed particular distance. wireless node placed intermediate area. Each node knows its location relative to the sink. The access point has to receive transmit packets then send acknowledge to transmitter.

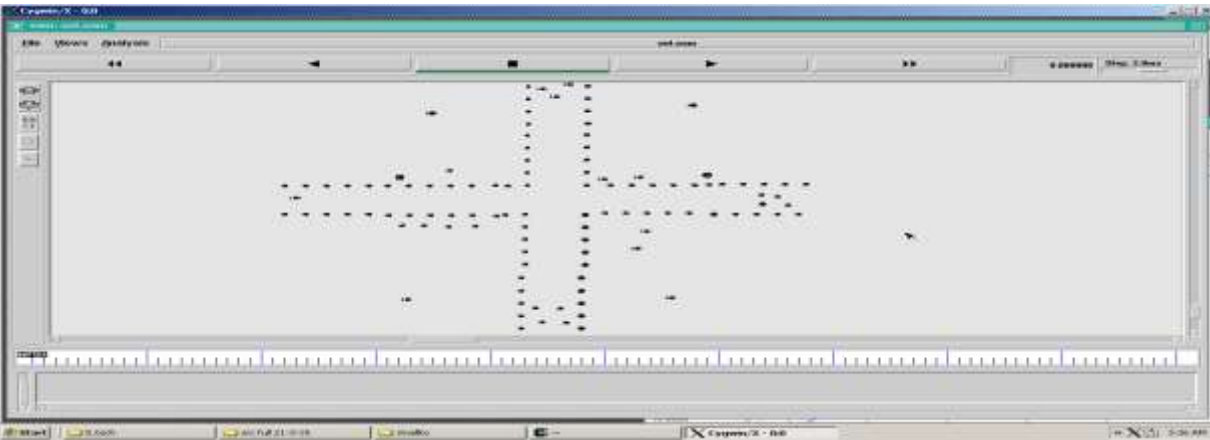


Figure 4.1: Multiple Number of Wireless Nodes Created

This module figure 4.2 is developed to Topology design all node place particular distance. Without using any cables then fully wireless sensor equipment based transmission and received packet data. Node and wireless between calculate sending and receiving packets. The cluster head is at the center of the circular sensing area. Intermediate the sender and receiver of this networking performance on this topology.

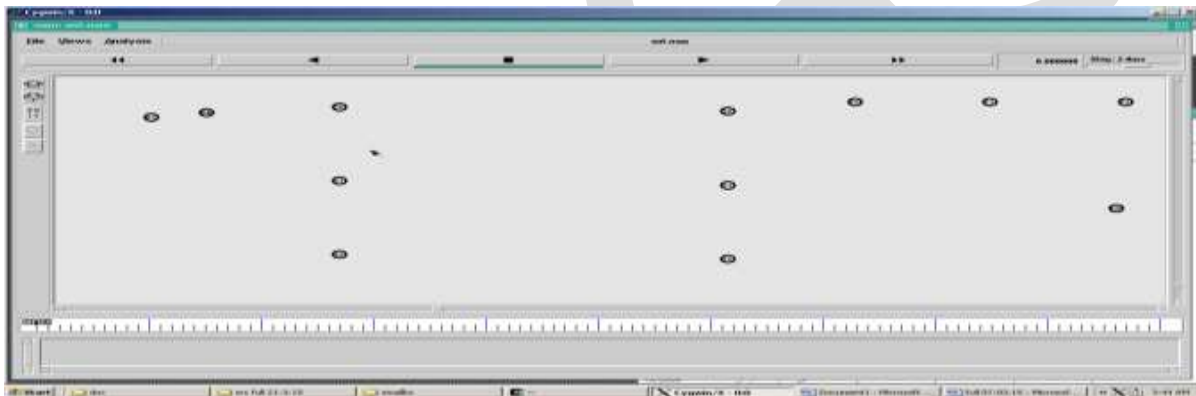


Figure 4.2: Wireless Nodes placed at Particular Distance

Figure 4.3 shows wireless networks to create the no of nodes. the packets to send and receiving through the source to destination. it's based the scheme of packets delivered for ack packet drop on the nodes. in this network to creating the source and destination node of the network and transmit the data to processing on their whole networking.

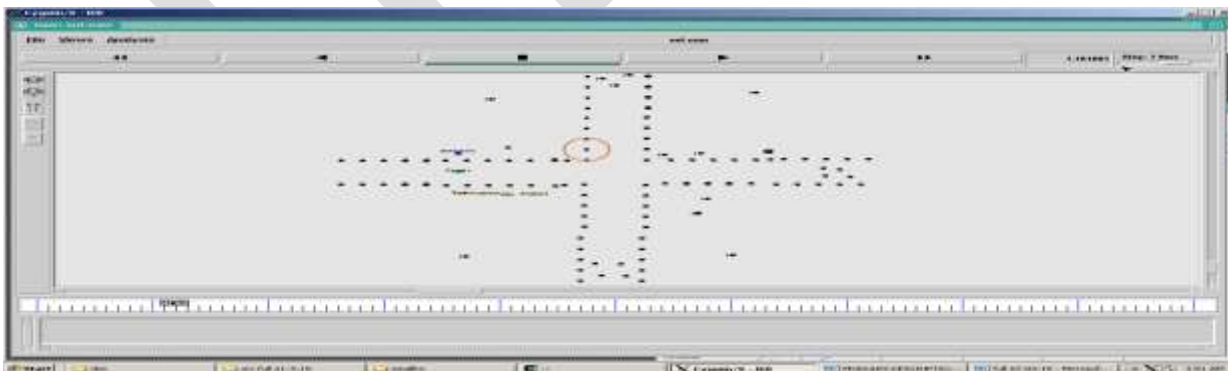


Figure 4.3: RSU can send Information about Transmitting Data

Figure 4.4 shows wireless networks use some sort of radio frequencies in air to transmit and receive data instead of using some physical cables. The most admiring fact in these networks is that it eliminates the need for laying out expensive cables and maintenance costs. Due to the dynamic nature of the clustering formation in the VANET the vehicle nodes are inter related with the

key generation node and thus lead to the security issue, as soon as collusion takes place the cluster head selects another KG node and keying process continues.

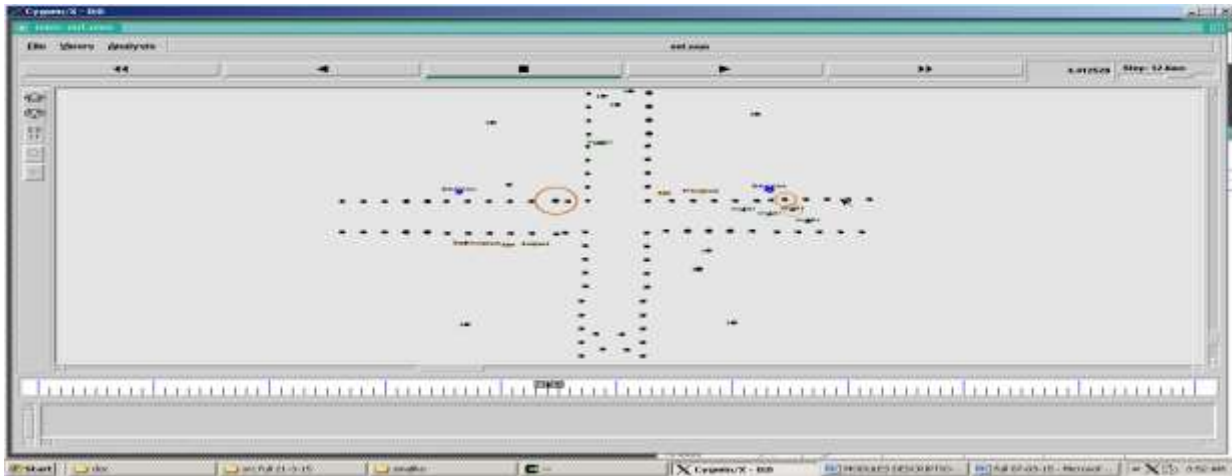


Figure 4.4: Vehicle Nodes are Inter-related with the Key Generation Nodes

This module figure 4.5 shows RSU consider into new way of communication. In this process to maintaining the separate time slot as well as key for every user.



Figure 4.5: Creating New Way Communication using RSU

Vehicular Ad-hoc networks enable vehicles that are not necessarily within the same radio transmission range to communicate with each other. It connects RSU than later connected to the internet, forming a fixed infrastructure that refers then the capability of communicating with each other with roaming vehicles.

This module figure 4.6 computing device located on the roadside that provides connectivity support to passing vehicles.



Figure 4.6: Creation of New Road Side Unit

In this module, figure 4.7 Based on Time Slots the Data can be delivered from Source to Destination. When used the communication networks, such as Ethernet or packet radio, throughput or network throughput is the rate of successful message delivery over a communication channel. The data these messages belong to may be delivered over a physical or logical link, or it can

pass through a certain network node. Throughput is usually measured in bits per second (bit/s or bps), and sometimes in data packets per second (p/s or pps) or data packets per time slot.

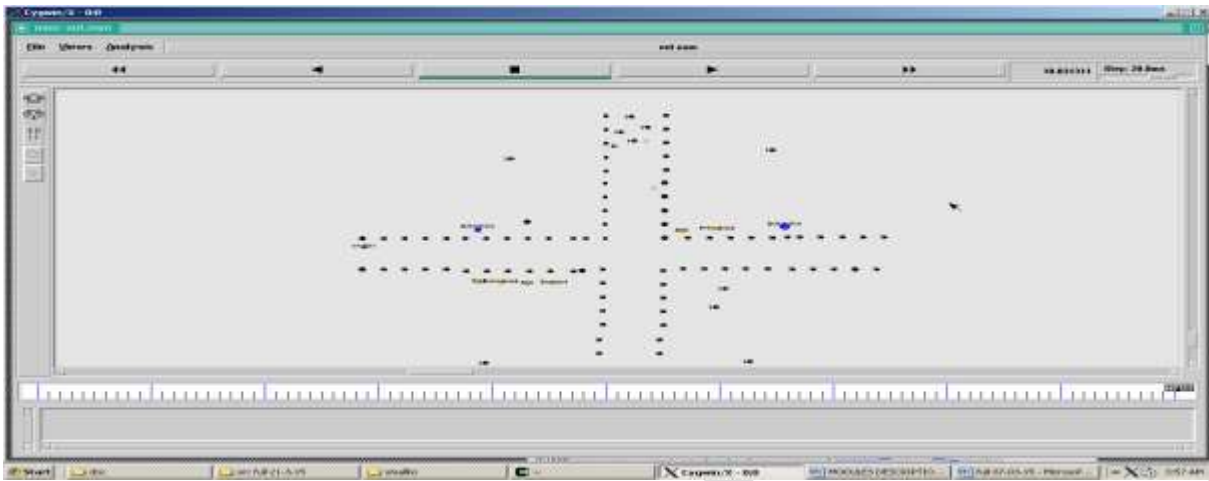


Figure 4.7: Based on Time Slots the Data can be delivered from Source to Destination

CONCLUSION

In this paper we have done , securely data transfer using Diffie-Hellman algorithm in VANET. To perform this algorithm, efficient data transformation. Data will be transferred without any packet loss. Each user have own time slot. In each time slot, all users that are predictable to connect to the RSU are specified. With the use of Diffie-Hellman key exchange it is easy to find out another route quickly in case of false route. To support data transfer in efficient manner high performance networks are required, which impose systematic design on the network to unleash the power of the VANET. Diffie-Hellman algorithm can be used to recover the failure nodes.

REFERENCES:

- [1] Balmahoon, R., and R. Pelpow. "Vehicular Ad- Hoc Networks: An Introduction to Privacy." Southern African Telecommunication Networks and Applications Conference (SATNAC) will be held from. Vol. 2.
- [2] De Castro, Cristina, Carla Raffaelli, and Oreste Andrisano. "A dynamic hierarchical VANET architecture for Named Data Networking applications." *Communications (ICC), 2015 IEEE International Conference on*. IEEE, 2015.
- [3] Liu, Kai, et al. "Cooperative Data Scheduling in Hybrid Vehicular Ad Hoc Networks: VANET as a Software Defined Network." (2015).
- [4] Z. Chen, H. Kung, and D. Vlah, "Ad Hoc Relay Wireless Networks over Moving Vehicles on Highways," Proc. ACM Mobihoc, pp. 247-250, 2001.
- [5] F. Bai, D.D. Stancil, and H. Krishnan, "Toward Understanding Characteristics of Dedicated Short Range Communications (DSRC) from a Perspective of Vehicular Network Engineers," Proc. ACM MobiCom, 2010.
- [6] Z. Li, Y. Liu, M. Li, J. Wang, and Z. Cao, "Exploiting Ubiquitous Data Collection for Mobile Users in Wireless Sensor Networks," IEEE Trans. Parallel and Distributed Systems, vol. 24, no. 2, pp. 312- 326, Feb. 2013.
- [7] M. Li and Y. Liu, "Traffic Management through Inter-Communication between Cars using VANET System," IEEE /ACM Trans. Networking, vol. 18, no. 1, pp. 320-332, Feb. 2010.
- [8] L. Chisalita and N. Shahmehri, "Distributed Key Management Techniques for Message Authentication in VANETs," Proc. Fifth IEEE Conf. Intelligent Transportation Systems, pp. 336-341, 2002.

- [9] Z. Li, Y. Zhu, H. Zhu, and M. Li, "Compressive Sensing Approach to Urban Traffic Sensing," Proc. IEEE 31st Int'l Conf. Distributed Computing Systems (ICDCS), 2011.
- [10] H. Zhu, Y. Zhu, M. Li, and L.M. Ni, "SEER: Metropolitan-Scale Traffic Perception Based on Lossy Sensory Data," Proc. IEEE INFOCOM, 2009.
- [11] J. Eriksson, L. Girod, B. Hull, R. Newton, S. Madden, and H. Balakrishnan, "The Pothole Patrol: Using a Mobile Sensor Network for Road Surface Monitoring," Proc. ACM Sixth Int'l Conf. Mobile Systems, Applications, and Services (MobiSys), 2008.
- [12] P. Gibbons, B. Karp, Y. Ke, S. Nath, and S. Seshan, "Privacy in Location-based Services: A System Architecture Perspective," IEEE Pervasive Computing, vol. 2, no. 4, pp. 22-33, Oct.-Dec. 2003.
- [13] U. Lee, B. Zhou, M. Gerla, E. Magistretti, P. Bellavista, and A. Corradi, "Mobeyes: Smart Mobs for Urban Monitoring with a Vehicular Sensor Network," IEEE Wireless Comm., vol. 13, no. 5, pp. 52-57, Oct. 2006.
- [14] I. Leontiadis and C. Mascolo, "GeOpps: Geographical Opportunistic Routing for Vehicular Networks," Proc. IEEE Int'l Symp. World of Wireless, Mobile and Multimedia Networks (WoWMoM), pp. 1-6, 2007.
- [15] G. Marfia, M. Rocchetti, C.E. Palazzi, and A. Amoroso, "Secure and Efficient Protocol for Vehicular Ad Hoc Network with Privacy Preservation," Proc. ACM MobiHoc Workshop Pervasive Wireless, 2011.
- [16] I. Leontiadis, P. Costa, and C. Mascolo, "Silent Cascade: Enhancing Location Privacy without Communication QoS Degradation," Proc. IEEE INFOCOM, 2010.
- [17] A. Balasubramanian, B. Levine, and A. Venkataramani, "A secure anonymous communication scheme in vehicular ad hoc networks from pairings," Proc. ACM SIGCOMM, 2007

Effect of Irradiation of the PEM of 1.531211SMJ29 Jeewanu with Clinical Mercury Lamp and Sunlight on the Morphological Features of the Silicon Molybdenum Jeewanu

Deepa Srivastava

Department of Chemistry, S.S.Khanna Girls' Degree College, Constituent College of Allahabad University, Allahabad, Uttar Pradesh, India

E- Mail – srivastava.deepa@gmail.com

Abstract— Sterilized aqueous mixture of ammonium molybdate, diammonium hydrogen phosphate, mineral solution and formaldehyde on exposure to sunlight results in the formation of self-sustaining coacervates which were coined as Jeewanu, the autopoietic eukaryote by Bahadur and Ranganayaki.

Jeewanu have been analyzed to contain a number of compounds of biological interest.

The presence of various enzyme like activities viz., phosphatase, ATP-ase, esterase, nitrogenase have been also been detected in Jeewanu mixture.

Gáinti (2003) discussed that Jeewanu possesses a promising configuration similar to protocell-like model.

Keywords— Autopoietic, eukaryote, Jeewanu, PEM, sunlight, mercury lamp, morphology, 1.531211SMJ29

INTRODUCTION

Sterilized aqueous mixture of ammonium molybdate, diammonium hydrogen phosphate, mineral solution and formaldehyde on exposure to sunlight results in the formation of self-sustaining coacervates which were coined as Jeewanu, the autopoietic eukaryote by Bahadur, K and Ranganayaki, S. in 1970. [1]

The photochemical, formation of protocell-like microstructures “Jeewanu” in a laboratory simulated prebiotic atmosphere capable of showing multiplication by budding, growth from within by actual synthesis of material and various metabolic activities has been reported by Bahadur *et al.* [1, 2, 3, 4, 5, 7, 8]

Jeewanu have been analyzed to contain a number of compounds of biological interest viz. amino acids in free as well as in peptide combination (Bahadur *et al.*; Briggs; Maurya;), [1,2,9,10,11,12], sugars as ribose as well as deoxyribose by Bahadur *et al.* [1,2,3,4,5], nucleic acid, bases as purines as well as pyrimidines by Bahadur *et al.*, [1,6] phospholipids by Bahadur *et al.* and Singh. [1, 13] and ferredoxin -like material in them by Rao *et al* and Bahadur *et al* [8, 14]. The presence of various enzyme like activities viz., phosphatase, ATP-ase, esterase (Briggs, 1965; Bahadur *et al.*, 1970; Singh, 1973; Gupta 1980) [1,11,13,15], nitrogenase (Smith *et al.*, 1965; Bahadur *et al.*, 1980) [8,16] have been also been detected in Jeewanu mixture.

Gáinti (2003) [17] discussed that Jeewanu possesses a promising configuration similar to protocell-like model.

Jeewanu is capable of spitting water molecule to hydrogen and oxygen in presence of sunlight and the proton set free, is utilized to fix nitrogen and carbon dioxide. (Bahadur, K, Ranganayaki, S, Smith and Folsome, 1980). [18]

Jeewanu under certain conditions showed characteristic movements at different periods of exposure. A very characteristic shivering movement, of Jeewanu which were prepared by the mixing of cerous sulphate solution to a mixture of potassium ferrocyanide solution and sucrose along with other constituents, was observed by Verma in 1970. (Verma, M, L, 1970). [19]

The movement which is observed in protoplasm is considered to be the movement of locomotion. As this movement of protoplasm is without the aid of external factors, it is considered to be due to some internal causes. Sometimes, certain chemical substances, light

and heat act as the external factors inducing the movement of protoplasm. These factors act as stimuli. Light also act as a stimulus as seen in algae which move towards the source of weak light but move away from the source of strong light. Protoplasm also responds to the stimulation of heat. When there are two different temperature areas, protoplasm moves towards the warmer area. However, if the tissue is gently warmed, the protoplasm shows more rapid rotation or circulation motion.

Effect of variation in the concentration of mineral solution in the PEM of 1.531211SMJ38 before and after exposure to sunlight, on morphology of 1.531211SMJ38 was studied by Srivastava, D. [20]

Effect of irradiation of 1.5312211SMJ29 Silicon Molybdenum Jeewanu PEM with clinical mercury lamp and sunlight on the blue colour intensity and the pH of the PEM of the silicon molybdenum Jeewanu was studied by Srivastava, D. [21]

In this paper, an attempt is made to investigate the effect of irradiation of 1.531211SMJ29 Silicon Molybdenum Jeewanu PEM with mercury lamp and sunlight on the formation and morphology of 1.531211SMJ29 Silicon Molybdenum Jeewanu has been carried out.

EXPERIMENTAL

The following solutions were prepared:

- a) 4% (w/v) ammonium molybdate
- b) 3% (w/v) diammonium hydrogen phosphate
- c) Mineral solution: It was prepared by mixing various minerals in appropriate proportions.
- d) 36% formaldehyde
- e) 3% (w/v) sodium chloride
- f) 5% (w/v) water soluble sodium silicate

PROCEDURE

Two clean, dry, sterilized corning conical flasks of 10 ml capacity were taken and labeled A and B. In each flask 15 ml of 4% ammonium molybdate, 30 ml of 3% diammonium hydrogen phosphate, 10 ml of mineral solution, 20 ml of formaldehyde, 10 ml of sodium chloride and 10 ml of soluble sodium silicate were added. The total volume of each flask was 95 ml separately.

Each flask was cotton plugged and shaken well. Flask A was exposed to sunlight and flask B was exposed to mercury lamp keeping the distance of flask B from mercury lamp 32 cms and the mercury bulb used was of 125 W. Both the flasks were exposed simultaneously for same exposure time each day giving half hour exposure daily for first two days, and then 2 hours exposure daily for fourteen days giving a total exposure of 29 hours. The intensity of the blue colour and the pH were noted both before and after each exposure for each flask A and B. the microscopic observations were also done simultaneously both before and after each exposure.

After total 29 hours of exposure, particles of each flask were filtered, dried in a desiccator and weighed. The yields of both flasks were noted.

The yields of the two flasks were as follows:

	Yield of 1.531211SMJ29 in g
a) Flask A exposed to sunlight	0.2984
b) Flask B exposed to mercury lamp	0.2430

TABLE – 1

Effect of exposure of 1.531211SMJ29 Jeewanu to sunlight and clinical mercury lamp on the number of the particles (SA/view)

Period of exposure in hours	Irradiation to sunlight		Irradiation to mercury lamp	
	Before exposure	After exposure	Before exposure	After exposure
½	No particle seen	8.0±0.71	No particle formation	
1	6.8±0.59	128.4±2.65		
3	142.±02.60	45.0±1.94		
5	118.0±0.94	114.0±4.30		
7	255.2±1.71	164.4±2.03		
9	285.0±1.84	197.0±1.78	164.6±1.93	125.0±1.84
11	605.6±1.96	165.0±1.84	205.0±1.94	154.6±1.88
13	277.8±2.13	205.0±1.72	234.8±1.79	129.6±1.86
15	339.8±3.07	255.6±1.80	305.0±1.84	204.6±1.93
17	213.8±2.76	154.8±1.77	202.4±1.63	60.6±1.91
19	37.2±1.06	28.4±1.06	93.8±2.20	56.4±2.01
21	353.8±1.41	301.2±1.25	249.0±1.81	199.4±2.10
23	602.0±1.14	367.4±1.77	367.4±1.77	303.2±1.14
25	156.1±1.88	396.8±1.98	203.2±1.39	100.8 ±1.59
27	599.8±1.39	419.4±0.67	301.2±1.15	203.2 ± 1.62
29	495.2±1.85	445.2±1.74	305.0±1.84	415.0 ±1.84

TABLE – 2

Effect of irradiation of 1.531211SMJ29 Jeewanu to sunlight and clinical mercury lamp on the size of the particles in μ (SA/view) with increasing exposure time.

Period of exposure in hours	Irradiation to sunlight		Irradiation to mercury lamp	
	Before exposure	After exposure	Before exposure	After exposure
½	No particle seen	0.80±0.120		
1	0.80±0.121	0.80±0.121		

3	1.00±0.001	0.50±0.006	No particle formation	
5	0.50±0.004	0.25±0.140		
7	0.50±0.020	0.50 ±0.201	0.50±0.008	0.50±0.006
9	0.75±0.006	0.50±0.008	0.50±0.014	0.25±0.001
11	0.50±0.018	0.50±0.043	0.25±0.006	0.25±0.015
13	0.50±0.013	0.25±0.001	0.25±0.218	0.25±0.026
15	0.25±0.104	0.25±0.006	0.12±0.143	0.25±0.018
17	0.25±0.001	0.25±0.044	0.12±0.014	0.12±0.006
19	0.25±0.005	0.12±0.068	0.25±0.061	0.25±0.004
21	0.25±0.063	0.12±0.014	0.25±0.043	0.25±0.048
23	0.25±0.041	0.25±0.005	0.25±0.140	0.12±0.064
25	0.25±0.002	0.25±0.084	0.12±0.008	0.12±0.001
27	0.12±0.043	0.25±0.134	0.12±0.002	0.25±0.084
29	0.25±0.061	0.25±0.206	0.25±0.006	0.25±0.091

CONCLUSION

The microscopic observations indicate that in the PEM exposed to sunlight, the particle formation was observed after half hour exposure but in the PEM exposed to clinical mercury lamp light, no particle formation took place up to 5 hours of exposure. Maximum particle formation was observed in the PEM exposed to sunlight and subsequently kept in shade. It was further observed that in both the cases, the number of particles was more when the PEM was kept in shade for overnight before exposure, and on exposure, in both the cases, the number of particles decreased. In PEM irradiated with sunlight, maximum particle size was observed before exposure after the night phase and after exposure the size decreased. In the PEM exposed to clinical mercury lamp radiation, smaller particles were formed and the maximum average size observed was 0.5μ . in later hours of exposure, in the PEM irradiated with sunlight, along with the spherical particles, oval particles were also observed. At certain stages of exposure, some crystals like structures were also recorded. It was further observed that the particles formed in the PEM which was exposed to sunlight were blue coloured whereas the particles which were formed in the PEM irradiated with clinical mercury lamp light were transparent.

Another salient feature observed was the oscillating motion of the particles which was observed after the night gap before 11 hours exposure in the PEM irradiation with sunlight. Similar motion was observed in the particles of the PEM exposed to clinical mercury lamp light after the night gap before 25 hours exposure. It was further observed that in both the PEM, the motion of the particle was more pronounced before exposure and after exposure it either became slow or vanished.

It has been observed that the motion of the Jeewanu was not due to the flow of the medium; it was not affected by the tapping of the stage of the microscope and was present even after 30 minutes. The motion of the particles was not zigzag but oscillatory and thus was not Brownian motion. Brownian motion is found only at certain temperatures and is not observed in electrolytes. But the PEM in which Jeewanu are formed contains many electrolytes viz. ammonium molybdate, diammonium hydrogen phosphate, biological minerals and 7% formaldehyde, so the motion observed in Jeewanu is one of the metabolic activity and not the Brownian motion. (Mathur, V, 1989). [22] According to Matsuno, k, 1986), [23] at an early stage of evolution, it might have been possible that the abiogenic microstructures or the model of protocell made of phospholipids like material showed photo biological motility due to

oxidative phosphorylation. He suggested that the origin of photo biological and biological motility is an evolutionary event that could have raised force equilibration proceeding at a definite velocity thus, the motion which was observed in Jeewanu, which has a number of phospholipids in them. (Singh, 1973), [13] materials with phosphate like activity (Briggs, 1964), [24] ATP-ase like activity (Bahadur, 1970) [1] and acid phosphatase like activity (Gupta, 1984), [25] could be considered to be a step forward in the process of evolution.

Comparing the yield of the particles produced it was observed that sunlight favoured greater formation of the particles.

REFERENCES:

1. Bahadur, K. and Ranganayaki, S., J. Brit. Interplanetary Soc., Vol. 23(12), pp 813-829, 1970.
2. Bahadur, K. (1963), Vijanana Parishad Anusandhan Patrika, 6, pp 94-117, 1963.
3. Bahadur, K. and Agarwal, K.M.L., Zbl. Bakt. 117, (2), pp585-602, 1964.
4. Bahadur, K., in "Synthesis of Jeewanu, the protocell", M/S Ram Narayan Lal Beni Prasad, Allahabad, India, 1966.
5. Bahadur, K., Zbl. Bakt. 121(2), pp291-319, 1967.
6. Bahadur, K. and Gupta, J.L., Zbl. Bakt. 127(11), pp 643-648, 1972.
7. Bahadur, K. and Ranganayaki, S., Singh, V.P. and Kumar, S., Ravista do. Institute de. Antibiotics Recife, vol. 15(No) (1/2), pp 33-36, 1975.
8. Bahadur K. and Ranganayaki S., "origin of life, a functional approach", M/S Ram Narain Lal and Beni Prasad, Allahabad, India, 1980.
9. Bahadur, K., "Photosynthesis of amino acids from paraformaldehyde and potassium nitrate", *Nature*, 173, pp1141, 1954.
10. Bahadur K., Pandey R.S., Perti O.N. and Pathak H.D., "Origin of living systems", *Agra Univ. J. Res. (Sci.)*, 13(II), pp197-224, 1965.
11. Briggs, M.H., *Space Flight*, 7(4), pp 129-131, 1965.
12. Maurya, H.K., "Studies in the Abiogenesis of Amino Acids", D.Phil. Thesis, Dept. of Chem. Univ. of Allahabad, Allahabad, India, 1977.
13. Singh, Y.P., "Studies in Abiogenesis of Phospholipids", D.Phil. Thesis, Dept. of Chemistry, Univ. of Allahabad, Allahabad, India, 1973.
14. Rao K.K., Morris P. and Hall D.O., presented at the workshop meeting on Hydrogenase, their catalytic activity, structures and functions, held at Gottingen, 1978.
15. Gupta, V.K., "Cytological investigation of photo chemically formed self-sustaining molecular associations" D.Phil. Thesis, Dept. of Chem. Univ. of Allahabad, Allahabad, India, 1980.
16. Smith, D.W. and Hanawatt, P.C., BioPhy. Soc. 9th Annual Meeting, San Francisco, 1965.
17. Ganti T., "The principles of life", Oxford University Press, Oxford, U.K., 2003.
18. Bahadur K., Ranganayaki S., Smith A. and Folsome C., Natl. Acad. Sci., India, Golden Jubilee Commemoration, Vol.I, pp 181-198, 1980.
19. Verma, M.L., "Studies in Abiogenesis of molecular Associations", D.Phil. Thesis, Dept. of Chemistry, Univ. of Allahabad, Allahabad, India, 1970.
20. Srivastava. D., "Study of the Effect of Variation in the Concentration of Mineral Solution in the PEM of 1.531211SMJ 38 before and after Exposure to Sunlight, on Morphology of 1.531211 SMJ 38". *Int J Recent Sci Res.* 7(4), pp. 10648-10651, 2016.
21. Srivastava, D., "Study of the kinetics of Jeewanu the Autopoetic Eukaryote", D.Phil. Thesis, Dept. of Chemistry, Univ. of Allahabad, Allahabad, India, 1991.
22. Mathur, V., "Studies in the origin of Life", D.Phil. Thesis, Dept. of Chem. Univ. of Allahabad, Allahabad, India, 1989.
23. Matsuno, K., Technological University of Nagaoka, Systems Laboratory, Nagaoka, Japan, pp 949-54, 1986.
24. Briggs, M.H., in 4th International Congress on Photobiology, Oxford, Aug. 1964, referred in Bahadur, K., "Synthesis of Jeewanu, The Protocell", Zbl. Bakt. II, Abt., 121, pp 312-315,(1967), 1964.
25. Gupta, V.K., (1984), 'Perspective in Cytology and Genetics', (Ed.Mauna, G.K. and Sinha, V.), 4, pp 205-208, 1984.

Design of EOG based Human Machine Interface system

Subash Khanal, Rajesh N., Prajwal Bhandari

Dept. of ECE, Nitte Meenakshi Institute of Technology, Bangalore, India

Email: subash.khanal33@gmail.com

Abstract— According to study on physically disabled individuals with severe paralysis, it is found that those patients still retain the ability of eyeball movements. Various systems are being developed to assist the mobility of such patients. Electroencephalogram (EEG) based Human Machine Interface (HMI) systems are being developed which not only require high computational complexity but also are not cost effective. In this paper we have discussed a cost effective and reliable approach towards Human Machine Interface using Electrooculography (EOG). EOG is a physiological signal which can be recorded from temple of eyes during eyeball movements. EOG being a voluntary biomedical signal, it can be used in HMI applications which make the desired control of a machine, a reality. In our work, we have designed a signal acquisition and conditioning unit which gives out the filtered and amplified signal used for the demonstration of HMI based on EOG. The designed system is found to showcase reliable performance in terms of obtaining EOG signal, its conditioning and its desired application.

Keywords— Electrooculography (EOG), paralysis, eye movements, electrodes, filters, signal conditioning, Human Machine Interface (HMI).

I. INTRODUCTION

According to world health organization 2-5% of people living in our society are suffering from motor disabilities, they cannot move their hand and/ or leg but they can think or they can move their eyes.[1]. In order to assist them for mobility various systems are being developed. Such systems should possess reliable interface between the disabled individual and the assisting machine. Electroencephalogram (EEG) based Brain Computer Interface (BCI) can be used to cater this need. However, the complexity involved, cost, number of electrodes required and discomfort experienced by the patient makes EEG based HMI rather an unsuitable approach. Then comes an easier and reliable approach, which exploits the fact that even severely paralyzed individuals retain their ability to move their eyes in the desired direction. Thus, in our work we have discussed about EOG based HMI targeted to individuals with motor disabilities. The signal acquisition and conditioning unit has been designed. EOG signal, filtered and amplified is fed to Arduino board. Finally, Light Emitting Diodes (LEDs) are used to demonstrate the interface with the help of movement of eyeballs by the subject.

II. Electrooculogram (EOG)

Various eye tracking methods like video-oculography with pupil and corneal reflection, video-oculography with pupil only and Electro-potential oculography are in practice [2], [3], [4]. The eye is known to have a resting potential and acts as a dipole in which the anterior pole (cornea) is positive and the posterior pole (retina) is negative. The magnitude of this cornea-retinal potential is in the range 0.4-1.0 mV. This difference in potential can be explained by the metabolic activities in the eye. The Electrooculogram (EOG) signal thus is derived from the polarization potential, also known as the Corneal-Retinal Potential (CRP), generated within the eyeball by the metabolically active retinal epithelium. The CRP is produced by means of hyper-polarizations and de-polarizations of the nervous cells in the retina [5]. Electrooculography (EOG) is a technique for measuring this resting potential. The resulting signal is called the "Electrooculogram"[6].

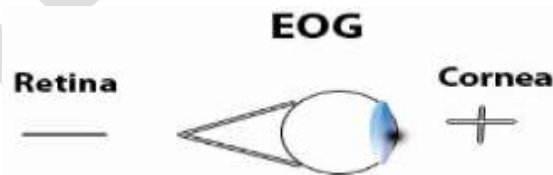


Fig 1. Polarity of Eye

The amplitude of the EOG signal is known to be in microvolt range (15 - 200 μ V) and most of the information is contained in 0 Hz to 38 Hz frequency range with dominant component in 0 to 25 Hz range [7], [8], [9]. Specially designed electrodes for EOG are placed

on the corners (lateral canthi) of both the eyes. When the eyes look left the positive end of the dipole (the eye) comes closer to the electrode on the left canthus and the negative end to the right canthus. The vice versa is observed for the eyes looking towards right. Ideally the difference in potential should be proportional to the sine of the angle the eye produces with respect to the central axis.

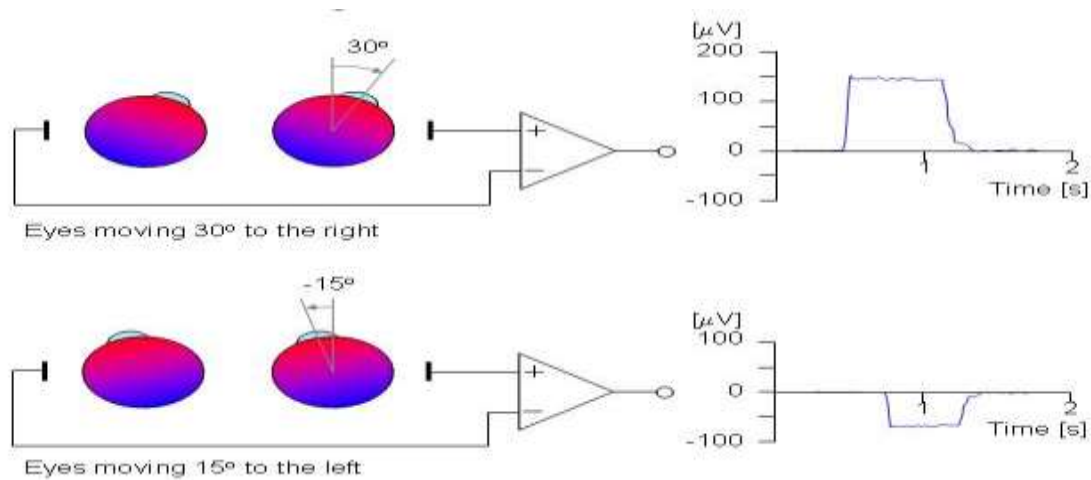


Fig 2. EOG signal based on eyeball movement

Silver/Silver Chloride (Ag/AgCl) Electrodes

These are specialized bio potential electrodes which are mainly used for bio signal acquisition. The signal from the eye is of low magnitude and is acquired through low impedance electrodes which minimizes signal attenuation. Non-invasive surface ECG Ag/AgCl electrodes were used for picking up EOG signals in our project. These electrodes are attached to the patients' skin and can be easily removed. The signal from the lateral canthi of the eyes is converted into voltage by electrodes. In our case, we have used only one pair of ECG surface electrode on the lateral canthi of the eyes. The system developed gives a single channel output to detect lateral eye movements. However, placing the same set of electrodes above and below the user's eye, vertical movement and blink of eyes can be detected.



Fig 3. Ag/AgCl electrodes

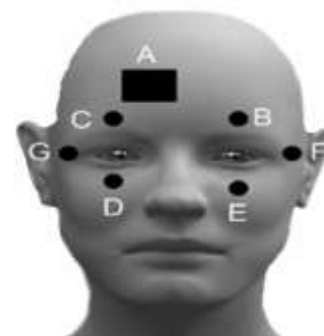


Fig 4. Placement of electrodes

III. Literature review

Satish Kumar et.al, 2015[1] have proposed a low-cost Electrooculogram (EOG) acquisition system that can be used efficiently in Human Machine Interface (HMI) systems. The proposed system consists of an Op-Amp based EEG/EOG amplifier circuit and ATmega8 microcontroller for analog to digital conversion and transferring of acquired data to PC. In this system five electrodes are used to acquire eye blinking, horizontal and vertical eye movements. In this system, the signals are first captured using EEG surface electrodes, amplified, filtered and then converted into digital form before stored into PC. The acquired EOG signal provides different eye related activities. Depending upon these eye related activities various systems can be developed to perform different tasks in real world, which provides a degree of independence to the user.

Kousik Srathy Sridharan, 2012[10] in his thesis work has built a portable system to acquire and analyse electro-oculographic (EOG) signals in real-time. The system contains two sub-systems; a hardware sub-system that consists of the filters, amplifiers, data acquisition card and isolation and the software sub-system that contains the program to acquire and analyse the signal and present the results to the observer. In his work, one paradigm records only normal blinks while the other records long blinks and the results showed differences in detection and error rates. The observations made from performance tests at various levels gave satisfactory results and proved the usefulness of the system for sleep state and drowsiness detection.

A Saravanan et. al, 2015[11] have designed a system which incorporates Texas embedded processor, wireless communication solutions and highly-customized analog front ends. As a demonstration of concept, this technology uses instrumentation amplifiers as analog front end and further single supply quad op-amp for analog signal processing in an effective manner.

W S Wijesoma et.al, 2005[12]. In this paper a complete system is presented that can be used by people with extremely limited peripheral mobility but having the ability for eye motor coordination. The Electrooculogram signals (EOG) that results from the eye displacement in the orbit of the subject are processed in real time to interpret the information and hence generate appropriate control signals to the assistive device. The effectiveness of the proposed methodology and the algorithms are demonstrated using a mobile robot for a limited vocabulary.

Ali Marjaninejad, Sabalan Daneshvar, 2014 [13]. In this paper an EOG based low-cost real-time wheelchair navigation system for severely disabled people is presented using signal processing techniques, bio-amplifiers and a microcontroller driven servomotor. All the digital signal processing and execution of commands were performed utilizing a microcontroller which drastically reduced the total cost of this project. The servomotor has been synchronized with the computed eye direction resulted from processing the horizontal EOG signal. The speed of the wheelchair was also regulated with the same EOG signal. Performed tests indicated that in 98.5% of trials, subjects could navigate to their targets in presence of simple obstacles in their first attempts which confirm the feasibility of the proposed system.

IV EOG acquisition and conditioning unit

EOG signal picked by the surface electrodes is in microvolts range and also contaminated by various noises eg. high frequency noise, junction potential noise between skin and the electrodes, etc. In order to extract essential features from the EOG signal proper signal conditioning is required. EOG acquisition and signal conditioning circuit has two main objectives: 1) To amplify the signal to necessary level and 2) Filter the signal to eliminate noise. Figure 5 depicts the components that were designed to achieve this purpose.

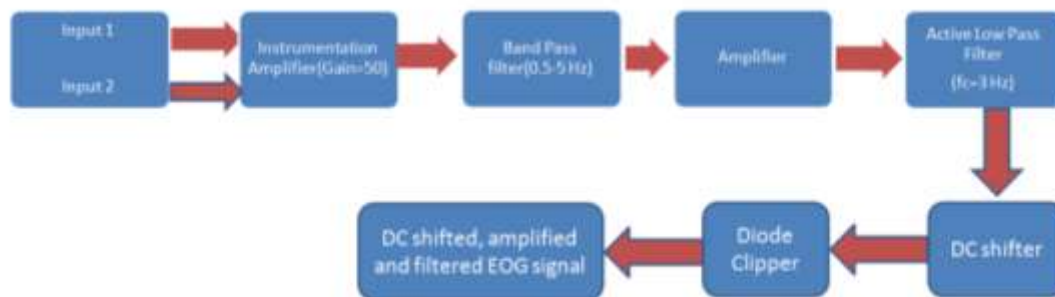


Fig 5. System block diagram of EOG acquisition and conditioning circuit

1. Instrumentation Amplifier Stage

An important stage of all bio-potential amplifiers is the input preamplifier which substantially contributes to the overall quality of the system. The main tasks of the preamplifier are to sense the voltage between two measuring electrodes while rejecting the common mode signal, and minimizing the effect of electrode polarization over potentials. Crucial to the performance of the preamplifier is the input impedance which should be as high as possible. Such a differential amplifier cannot be realized using a standard single operational amplifier design since this does not provide the necessary high input impedance. Hence, instrumentation amplifiers were used to meet the desired requirements.

$$\text{Design: } G = \frac{49.4K}{R_g} R_g + 1$$

For Gain=50, $R_g=1K$ ohm

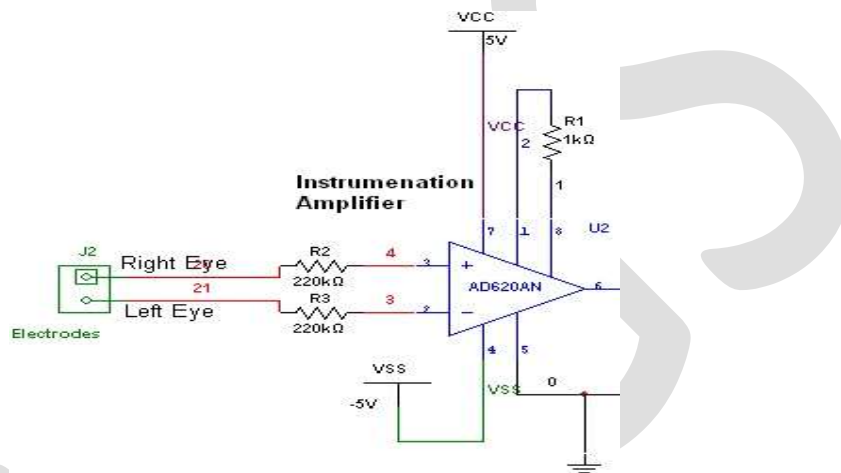


Fig1. Instrumentation amplifier designed

2. Active Band Pass filter:

The output obtained from first stage preamplifier has to pass through a band pass filter to remove the unwanted high and low frequencies from the desired EOG signal. Band pass filter used is the combination of a low pass filter (cut off frequency, $f_c=4.5$ Hz) and a high pass filter ($f_c=0.5$ Hz). Band Pass Filter used here is an active band pass filter. High pass filter removes any DC offset at the output of the preamplifier. It means necessary gain can be included in the pass band of the filter while attenuating out of band frequencies. A 100 K ohm potentiometer was used to adjust the gain required. (Filter Design equation: $RC = \frac{1}{2\pi f}$)

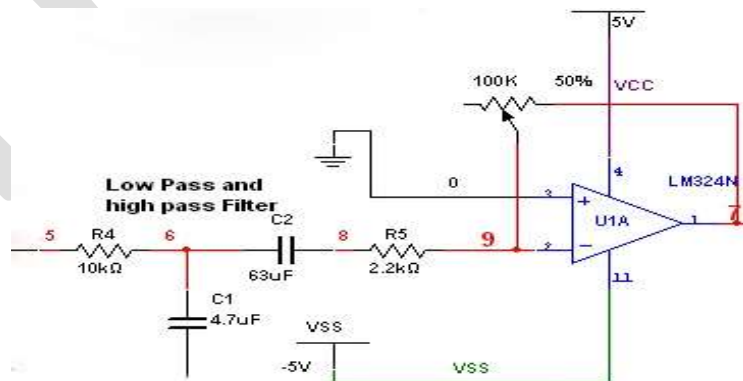


Figure 7. Band Pass Filter

3. Fixed Gain Amplifier

A fixed gain amplifier was used after the band pass filter amplifies the signal with the necessary gain. Inverting amplifier configuration in an op amp was used to achieve this fixed gain amplification.

$$\text{Gain} = \frac{R_2}{R_1}$$

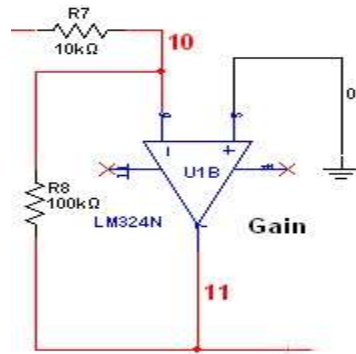


Fig 8. Fixed gain Amplifier

4. Active Low Pass Filter

While amplifying the signal using a fixed gain amplifier, there is a chance for unwanted high frequency noise getting amplified. Therefore, it became necessary to make use of an Active Low Pass filter which not only attenuates the high frequency components but also provides substantial gain to the signal within the required bandwidth. A variable gain can be implemented in the Low Pass Filter by making use of a potentiometer on the feedback path. A 100K potentiometer is used for adjusting required variable gain.

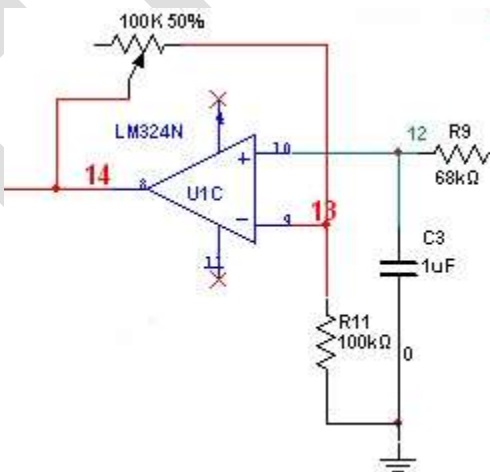


Figure 9. Active Low Pass Filter

5. DC Level Shifter

The EOG signal obtained after above signal conditioning steps is bipolar in nature, i.e. the signal has positive and negative peaks corresponding to the eyeball movements. However, in order to use the signal further into microcontroller we require to level shift the signal in such a way that no negative peaks are present in the signal. For this reason a DC level shifter was used followed by a negative voltage clipper (using a diode). This ensures the EOG signal have both the peaks above 0 V reference.

$$DC \text{ Offset} = VCC \cdot \frac{R2}{R1+R2}$$

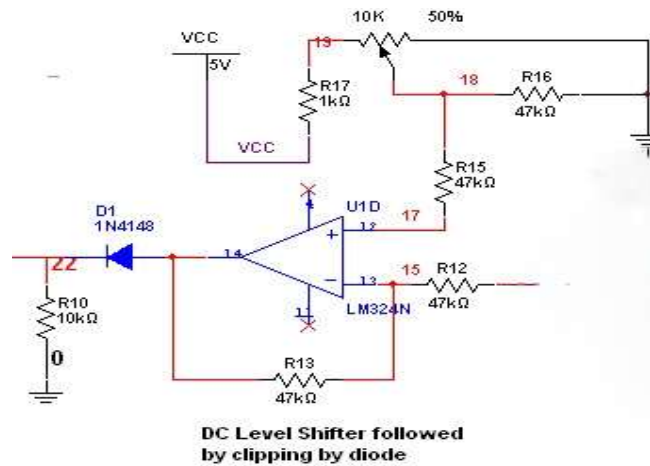


Fig 10. DC Level Shifter

To implement all the above circuit components after the pre amplification provided by an instrumentation amplifier, a Quad-Operational Amplifier (LM324) was used. The overall EOG conditioning circuit was designed and simulated to get the desired frequency response as shown in the figure 11.

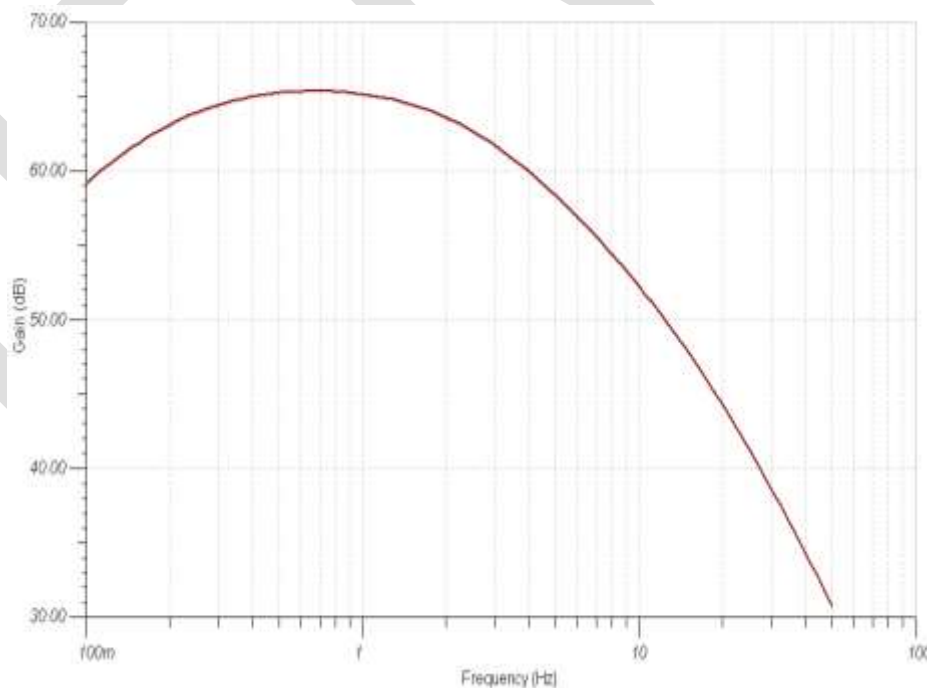


Fig 11. Frequency response of the EOG conditioning circuit

V Demonstration of EOG based HMI

The amplified and filtered EOG signal obtained from the designed signal conditioning circuit was sampled by using Analog to Digital Converter (ADC) which is already inbuilt in most of the available development boards. For the type of electrode placement used during our project, it was quite evident that the magnitude of the signal increases above the reference level as the subject moves his eye toward right direction. The signal reaches its positive peak when the eye is at the extreme right position. If the eye is not moving or at the center position the signal comes back to the reference level. Here the magnitude of reference level can be varied by making use of potentiometer available for the DC level shifter in the signal conditioning circuit. Similarly, if the eye ball moves towards the left direction, the signal drops below the reference level and reaches to minimum when the eye is at extreme left. The information about the magnitude of the EOG signal during the eyeball movement can be easily utilized to generate the necessary control signals. Thus, this demonstrates a cost effective, simple yet reliable solution for Human Machine Interface based on eye ball movement. The algorithm to extract the signal features for the eyeball location makes use of simple thresholds. Three thresholds are arbitrarily set for a center, extreme left and extreme right location of the eye. (Say th_1 , th , th_2 respectively).

- If $signal_sample > th_1$ this indicates eye movement towards right
- If $signal_sample < th_2$ this indicates eye movement toward left
- Else, this indicates eye ball is located at the center.

However during the implementation of the crude algorithm above, care should be taken that the decision of the generation of control signals is due to the real movements. There can be sudden momentary peaks occurring in the signals that cross the above mentioned thresholds, in such cases a concept of counter can be implemented in the algorithm, i.e. if the signal meets the threshold condition, counter for that particular case is increased. If both the conditions, the amplitude threshold and the counter number threshold, are met the decision is made and a control signal is generated according to that. In our case, for the idea demonstration we have used simple inexpensive LEDs (Light Emitting Diodes). Three LEDs are connected to output pin of the microcontroller used, one each for the three cases of the eye ball movement, LEFT, CENTER and RIGHT.

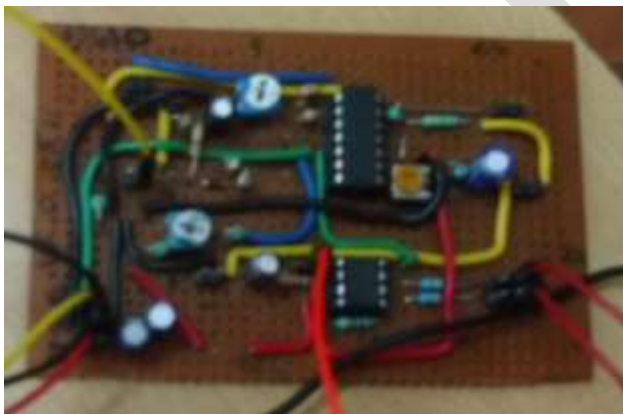


Fig 12. EOG conditioning unit designed



Fig 13. Demonstration of EOG based HMI

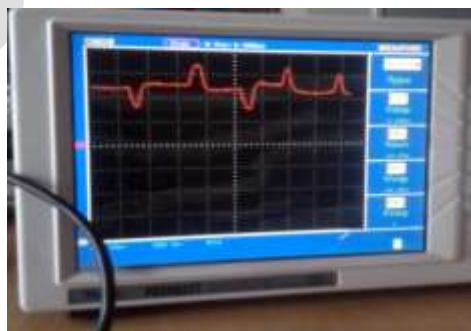


Fig 14. EOG signal displayed in DSO

ACKNOWLEDGMENT

We express our sincere thanks to every faculty member of the Department of Electronics and Communication Engineering, Nitte Meenakshi Institute of Technology, Bangalore for the support they have provided for successful completion of the project.

CONCLUSION

The frequency response of the designed EOG conditioning circuit clearly shows that there is a significant gain provided to signal within the desired frequency range (0.5 to 4 Hz) while attenuating the other high and low frequency components. The EOG signal acquired from eye using the designed conditioning circuit was found to be good enough, which was further used to generate control signals to demonstrate led blinks in accordance with eyeball movement. The approach was simple, inexpensive and yet so effective. This meets the objective of our project which aimed at utilizing a biomedical signal for Human Machine Interface targeted for physically disabled individuals. The performance of this approach was really promising in terms of its simplicity and reliability.

REFERENCES:

- [1] Satish Kumar, Adyasha Dash, Manoj Kumar Mukul "Design and Development of Low-Cost EOG Acquisition Circuit for HMI Application" 2015 2nd International Conference on Signal Processing and Integrated Networks (SPIN).
- [2] Young L. R. and Sheena D: "Survey of Eye Movement Recording Methods", Behavioural Research Methods and Instructions, Volume 7(5), 1975, pp.397-429.
- [3] Hansen D. W., Hansen, J. P., Nielsen, M., Johansen, A. S. and Stegmann M. B.: "Eye Typing using Markov and Active Appearance Models", IEEE Workshop on Applications on Computer Vision, Orlando, FL, USA, 2002, pp.32-136.
- [4] Gips J., DiMattia P., Curran F.X. and Olivieri P.: "Using EagleEyes: An Electrodes based Device for Controlling the Computer with Your Eyes to Help People with Special Needs", In Klaus, J. et al. (eds.) Interdisciplinary Aspects on Computers Helping People with Special Needs, Vienna, 1996.
- [5] S. Venkataramanan, Pranay Prabhat, Shubhdeep Roy Choudhury, Harshal B. Nemade, J.S. Sahambi "Biomedical Instrumentation based on Electrooculogram (EOG) Signal Processing and Application to a Hospital Alarm System" Proceedings of ICISIP – 2005
- [6] Jaakko Malmivuo, Robert Plonsey, "Bioelectromagnetism-Principles and Applications of Bioelectric and Biomagnetic Fields", Oxford University Press, 1995, Chapter 28, pp. 437-441.
- [7] Zhao Lv, Xiao-Pei Wu, Mi Li, De-Xiang Zhang, "Development of a human computer interface system," Health vol. 1, 2009.
- [8] Daud, W.M.B.W. Sudirman, R. ; Al Haddad, A., "Wavelet frequency energy distribution of electrooculogram potential towards vertical and horizontal movement," 2nd international conference on computational intelligence modelling and simulation, September 2010.
- [9] Daud, W.M.B.W., Sudirman, R., "A wavelet approach on energy distribution of eye movement potential towards direction", IEEE Symposium on Industrial Electronics & Applications (ISIEA), October 2010.
- [10] Kousik Sarathy Sridharan, "Real-time acquisition and analysis of Electro-oculography signals", Masters thesis, 2012
- [11] A Saravanan et al. , "Design and implementation of Low power, Cost effective Human Machine Interface by Left and Right Eye Movement Technique", 978-1-4673-7910-6/15 ©20 15 IEEE
- [12] W S Wijesoma et al., "EOG Based Control of Mobile Assistive Platforms for the Severely Disabled", 2005 IEEE International Conference on Robotics and Biomimetics.
- [13] Ali Marjaninejad, Sabalan Daneshvar "A Low-cost Real-time Wheelchair Navigation System Using Electrooculography", The 22nd Iranian Conference on Electrical Engineering (ICEE 2014), May 20-22, 2014

Consistency and Integrity as a Service in Auditing Cloud

Shwetha J, Prof. (Dr.) D. Nageswara Rao

¹KVM College of Engineering and IT,CUSAT University,
Cherthala-688583, Alappuzha, Kerala
Shwethajayachandran81@gmail.com

²KVM College of Engineering and IT,CUSAT University,
Cherthala-688583, Alappuzha, Kerala
dronamraju8@gmail.com

Abstract— For enabling ubiquitous, convenient, on-demand network access to a shared pool of configurable computing resources can be rapidly provisioned and released with very minimum effort, cloud computing is just a model for it. Cloud service provider maintains a multiple copies of each data in different geographical area, but this replication technique is highly expensive to achieve consistency and integrity on a worldwide. In this paper, we present a model which consist of data cloud and audit cloud. Cloud service provider maintains the data cloud and huge group of users constitute an audit cloud. Users are of two types, global and local users. The consistency is provided to the audit cloud using global auditing and local auditing algorithm. Integrity checking is allowed only for global users for checking whether the local users try to access any unauthorized data or not by using SHA algorithm.

Keywords— Data storage, Service model, local and global auditing algorithm, AES, SHA algorithm.

INTRODUCTION

Cloud computing is a term used to describe a new class of network based computing that takes place over the internet, basically a step on from utility Computing. The platform provides on demand services on rental basis that are always on, anywhere, anytime and anyplace. . e.g., Amazon is the best example for cloud storage; here all that we need is a Credit card. And also should be a registered member. Like every storage (laptops, mobile phone etc.) has a capacity, cloud used to provide a server according to the storage needs. Hardware and software services are available to general public, enterprises, corporations and business markets. Cloud service provider maintains a multiple replicas of each piece of data on geographically distributed servers. But it is very expensive to achieve consistency and integrity on a worldwide. For eliminating the limitation, we present a paper about a service model which consist of data cloud and audit cloud. Data cloud is maintained by cloud service provider and audit cloud contains a group of users, who can verify whether the data cloud provides a surety in consistency and integrity. To decrease the threat of data, integrity is a major issue. The purpose of data security protection cannot be adopted only due to the user's loss control of data under cloud computing. We need authentication of correct data storage in a cloud without explicit knowledge of whole data by considering various kinds of data for each user that are registered in the cloud. The verification of data in a cloud is a more challenging factor

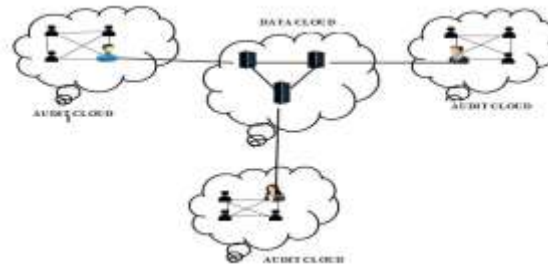


Figure 1: Service model in cloud

Fig.1. shows the service model in cloud, contains group of audit clouds and group of data clouds. Each server is maintained by an administrator by checking the integrity. Admin can create two types of account, global users and local users. Global user will get equal power like admin. Every user has a unique ID.

If suppose consider a company X have different branches in different places. Each group of users assigned a job. For the co-operation, they need to interact with different users and to access different data in other servers. Then in this cloud computing model, consistency and integrity is a key factor.

1. SERVICE MODELS IN CLOUD COMPUTING:

Cloud storage services become commercially popular due to its various advantages such as scalability, elasticity and high availability at low cost. The cloud service provider (CSP) offered various kinds of services and tools which are given below:

A. SOFTWARE AS A SERVICE:

By All users are geographically distributed by using cloud infrastructure and cloud platforms to the various customers with software applications.

B. INFRASTRUCTURE AS A SERVICE:

Registered member is allowed to access the physical computing hardware such as data storage, CPU, memory and network connectivity of the service provider etc. Server itself acts as virtual server. Any type of system i.e., Windows, Linux etc. should be compatible. The user gain greater flexibility in access to basic infrastructure.

C. PLATFORM AS A SERVICE:

It enables customers to use the cloud infrastructure as a service. Development of web application and others software can be controlled by users. Cloud SIM is a best example.

D. CONSISTENCY AS A SERVICE MODEL:

Distributed server maintains replicas of data of improve response time and avoid data loss in case of failures. The performance and the availability of data in the case of network partitioning are enabled by ensuring data consistency eventually but it won't work out all the times. Suppose for example, Alice, Bob and Clarks are global users working in different branches (different locations). If Alice updates a new version of a project and upload it to the cloud server. Then Alice calls the Bob and Clarks to download the latest version that she updated. But if the casual consistency is not there, then Bob and Clark try to download the project will get only the old version. Then the consistency is a major factor. Basically different applications need different consistency requirements. We are here to present model consisting of group of data cloud and audit cloud. In this virtualization technique, it is very hard for the user to find whether the data in a data cloud is latest one or not. For the solution, we need to trace the interaction among users. For the tracing operation, local auditing algorithm is used for local users and global auditing is used for the global users.

E. INTEGRITY AS SERVICE MODEL:

User interaction is a vital factor for an every organisation. For the completion of a particular work, sometimes employees need to send file or any project to other employee who is working in same company but different location in a cloud. Such a cases the company head need to check whether the user are sharing correct file or not. Otherwise it will affect the growth of the organisation. So admin need to trace the file the users are sharing. So we are providing a integrity checking with the help of SHA algorithm. Auditing cloud consist of two types of users, Global and Local users. Global users check the file that shared by local users.

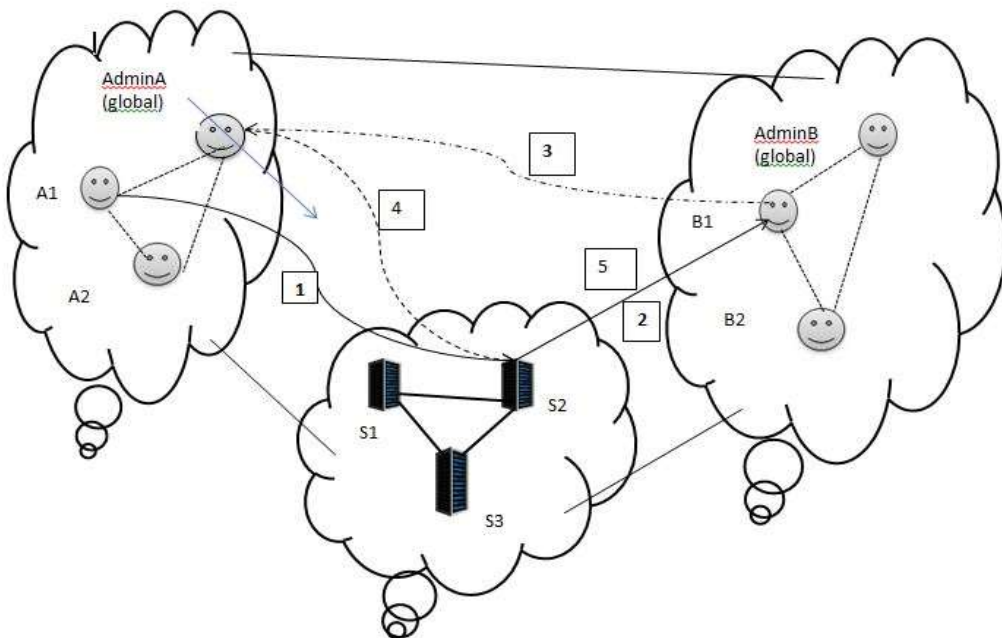


Fig2: Integrity Checking

Fig 2 shows the diagrammatic representation of integrity checking. The models contain group of audit cloud and data cloud. Admin A is a global user of one audit cloud and Admin B is the global user of other audit cloud. Each audit cloud contain local users (A1, A2, B1, B2). The expansion of above fig 2 as follows:

1. A1, local user of an audit cloud who located in S1 send file to the B1, local user of audit cloud located in S2.
2. B1 who located in S2 received the file.
3. AdminA, global user of sender side can view the confidential file sent to the B1
4. AdminA delete/ view/ update the same file.
5. B1 's file should be replaced by AdminA's action.

Algorithms used are:

1. AES - For Data Encryption and Decryption.
2. Sha1 - Secure Hash Algorithm
3. Local consistency auditing - For auditing local consistency - attackers while accessing file and checking read or write.

The Secure Hash Algorithm (SHA) developed by the National Institute of Standards and Technology (NIST) . This algorithm takes as input message with maximum length of less than 2^{128} bits and produces as output a 512-bit message digest. It is used for secure exchange of data and messages.

2. IMPLEMENTATION:

In this section, we first illustrate the consistency as a service model. Then, we describe the structure of the user operation table (UOT), with which each user records his operations. Then we apply auditing algorithms.

A. USER OPERATION TABLE:

User operation table is used to maintain a UOT for the operation to record all the local operation in a systematic manner. Each present record in UOT will be shown by three components. First is an operation which consists of sender and receiver id, next is the current logical vector means the number of message received by receiver's inbox and finally the current physical vector which means the total number of message received in a complete table. Consider 'op' be the operation, where $W(K,a)$ be the writing the value a to data which is identified by key K and $R(K,a)$ stands for reading data which is identified by K. Let us consider $W(K,a)$ as $R(K,a)$'s dictating write and $R(k,a)$ as $W(k,a)$'s detected read. Following are the properties:

- a. A read must have unique dictating write.
- b. A write must have either zero or more detected reads.

When an each operation happens each user will track logical and physical time to maintain logical vector and physical vector respectively. Suppose that there are N users in the audit cloud. A logical/physical vector is a vector of N logical/physical clocks, one clock per user, sorted in ascending order of user ID. For a user with ID_i where $1 \leq i \leq N$, his logical vector is $\langle L1, L2, \dots, LN \rangle$, where L_i is his logical clock, and L_j is the latest logical clock of user j and his physical vector is $\langle P1, P2, \dots, PN \rangle$, where P_i is his physical clock, and P_j is the latest physical clock of user j.

B. LOCAL AUDITING TECHNIQUE:

Local consistency auditing technique is an online algorithm. The operation in this module or unit, in which each user is going to record all his complete activities and store in his UOT. During the read operation, the authorized user is going to perform local consistency operation in an independent manner.

Algorithm:

Step 1: initially user operation table with null while issue an operation op do

Step 2: if op = w(a) then record w(a) in user operation table

Step 3: if op = r(a) then w(b) Belongs to user operation table is the last write

Step 4: if w(a) -> w(b) then read your write consistency is violated r(c) belongs to user operation table is the last read

Step 5: if $w(a) \rightarrow w(c)$ then monotonic consistency is violated

Step 6: record $r(a)$ in user operation table

C. GLOBAL AUDITING TECHNIQUE:

Global consistency auditing technique is going to be considered as an offline algorithm. Next to consider is that an auditor periodically will be selected from the audit cloud system to perform the special operation like global consistency auditing technique. Hence in this case the auditor is going to collect all users' UOTs for obtaining a special global trace of all activities. Then later executing global auditing technique, selected auditor is going to send results of auditing operation as well as its vectors values to all other authorized users. Now given the auditor's vector values, then each user will come to know other users' new clocks up to next global auditing.

Algorithm:

Step 1: for every operation in the global trace is represent by a vertex

Step 2: for operation $op1$ and $op2$ do

Step 3: if $op1 \rightarrow op2$ Then time edge is added between $op1$ and $op2$

Step 4: if $op1=w(a), op2=r(a)$ $op1$ and $op2$ comes from different user then data edge is inserted between $op1$ and $op2$

Step 5: if $op1=w(a)$ and $op2=r(b)$ and $op1$ and $op2$ comes from different users and $w(a) \rightarrow w(b) \rightarrow r(b)$ then causal edge is inserted between $op1$ and $op2$

Step 6: verify whether the graph is directed acyclic graph using topological sorting method .

D. INTEGRITY CHECKING:

The steps are:

Step 1: The sender first encrypts the data using encryption using shared key.

Step 2: Then the message digest is created using SHA-1 algorithm, $D=h(M')$.

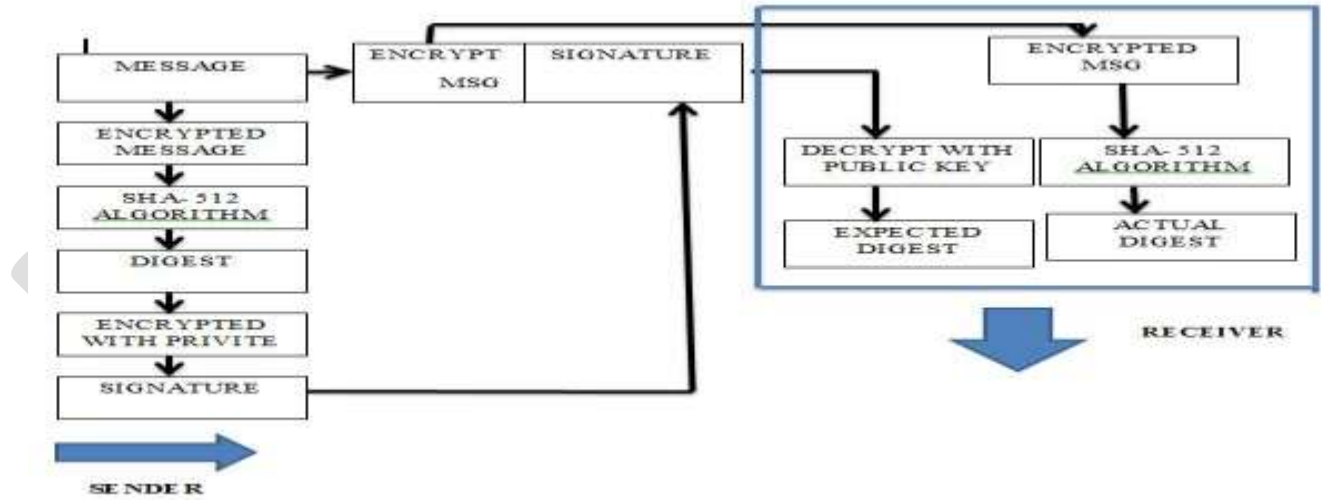
Step 3: Then the message is signed= $D^d \text{ mod } n$.

Step 4: Then the encrypted message and signature is sent to the cloud service provider.

Step 5: Then CSP uses the receiver's private key on the signature to retrieve the digest, $D'=S^e \text{ mod } n$.

Step 6: It applies the hash algorithm on the encrypted data to get the digest D .

Step 7: CSP now compares the two digests D and D' . If they are not equal, it posts the user that the data in the cloud is modified. Otherwise the message is accepted.



3. SAMPLE RESULTS:

STORAGE 1		
User Id	User	Privilege
1	Alice	Global
2	X	Local

Table1: User table of storage1

STORAGE 2		
User Id	User	Privilege
14	Bob	Global
15	Y	Local

Table2: User table of storage2

STORAGE 3		
User Id	User	Privilege
25	Clark	Global
26	Z	Local

Table3: User table of storage3

ALICE'S CONSISTENCY TABLE			
Sender	Receiver	Logical Vector	Physical Vector
1	14	5	10

Table4: Consistency table of Alice

BOB'S CONSISTENCY TABLE			
Sender	Receiver	Logical Vector	Physical Vector
14	25	6	9

Table4: Consistency table of Bob

CLARK'S CONSISTENCY TABLE			
Sender	Receiver	Logical Vector	Physical Vector
25	1	3	4

Table5: Consistency table of Clark

Above table1, table2, and table3 are the users table in three different storages. Table3 shows Consistency table of storage1 which means Alice be the sender and Bob be the receiver, and which contains corresponding logical vector and physical vector. Logical vector is the total number of message received for the receiver in his message table and total number of message received in message table of receiver's storage is its Physical vector. From table1 Alice sends message to Bob, Its logical vector is 5 and its physical vector is 10. Similarly table4 and table5 are defined.

CONCLUSION

The consistency is provided to the audit cloud using global auditing and local auditing algorithm. From this study we can conclude that the consistency service model is going to be maintained by the system, and also we have come across a two levels of auditing structure technique. This technique helps the user to check whether cloud service provider also called as CSP is going to provide a valid consistency operation or not. And in this system the user also can understand which Cloud Service Provider genuine service provider from the other different Cloud service provider. Integrity checking is allowed only for global users for checking whether the local users try to access any unauthorized data or not by using SHA algorithm.

REFERENCES:

- [1] E. Brewer, "Towards robust distributed systems," in Proc. 2000 ACM PODC.
- [2] Garima, "Ensuring data storage security in cloud using two way integrity check algorithm", International Journal of Advanced Research in Computer Science and Software Engineering, Volume 3, Issue 11, November-2013
- [3] Kapila Sharma, Kavita Kanwar, Chanderjeet Yadav, "Data Storage Security in Cloud Computing", International Journal of Computer Science and Management Research, Volume 2 Issue 1 January 2013
- [4] M. Ahamad, G. Neiger, J. Burns, P. Kohli, and P. Hutto, "Causal memory: definitions, implementation, and programming," Distributed Computing, vol. 9, no. 1, 1995
- [5] M. Armbrust, A. Fox, R. Griffith, A. Joseph, R. Katz, A. Konwinski, G. Lee, D. Patterson, A. Rabkin, I. Stoica, et al., "A view of cloud computing," Commun. ACM, vol. 53, no. 4, 2010.
- [6] P. Mell and T. Grance, "The NIST definition of cloud computing (draft)," NIST Special Publication 800-145 (Draft), 2011.
- [7] "Pushing the CAP: strategies for consistency and availability," Computer, vol. 45, no. 2, 2012.
- [8] Qin Liu, Guojun Wang, IEEE, Member, and Jie Wu, IEEE Fellow "Consistency as a Service: Auditing Cloud Consistency", IEEE TRANSACTIONS ON NETWORK AND SERVICE MANAGEMENT VOL:11 NO:1 YEAR 2014
- [9] Xuefeng Liu, Yuqing Zhang, Boyang Wang and Jingbo Yan, "Mona: secure multi-owner data sharing for dynamic groups in the cloud", IEEE transactions on parallel and distributed system, Volume 24, NO. 6, June- 2013

Response of Flare base Self supporting Steel stack

Under the static & dynamic wind loads with variable wind speed

Rinki^[1], Shashi Shekhar Singh^[2]

MVN University, Palwal, Haryana ^{[1][2]}

rinkitanguriya27@gmail.com

Abstract— This paper deals with the behaviour of Flare base steel stacks with variable Wind speed of 44m/s, 47m/s, and 50m/s respectively. The study aim is to find out the structural behaviour of Flare base steel stack under the Equivalent static and dynamic wind loads. The static & dynamic wind analysis is done by using the Staad. Pro Vi8 Ss5. software with assumptions as per IS 6533:1989(part1&part2). The study parameter of static and dynamic forces, maximum deflection due to static & dynamic wind forces for flare base steel stack for the three different wind speeds with constant height & shell thickness was compared.

Keywords— Steel stacks, static wind force, dynamic wind force, Maximum deflection.

INTRODUCTION

A steel stack is a vertical channel through which smoke and combustion gases pass out of a building. Steel stacks are used to emit and exhaust gases in atmosphere at higher elevation. Failure of steel stacks is prime issue in most of industries. The cause behind the failure is analyzed by the static & dynamic wind analysis of stacks. The steel stacks less than 80m are called short steel stacks. The first mode is sufficient for the analysis for the short circular steel stacks.

ANALYSIS OF STEEL STACKS:

Wind analysis include the effect of static and dynamic wind forces .Geometry of flare base is given in Table-1 as per accordance IS 6533 Part-1&2.

B. Geometry for flare base steel stacks:

Basic geometry of steel stacks is governed by top diameter (D_t), base diameter (D_b) and effective height (H_e). Following IS code are used for the analysis of steel stacks.

- d) IS 6533 (part-1):1989, “Indian standard code of practice for design and construction of steel chimney –code of practice-Mechanical aspects.”
- e) IS 6533 (part-2):1989, “Indian standard code of practice for design and construction of steel chimney –code of practice-Structural aspects.”
- f) IS 875:1987(part-3) used for the wind force analysis.

Minimum top diameter of unlined chimney should be one twentieth of effective Height of chimney/stacks and minimum outside diameter at base should be equal to 1.6 times the top diameter of stack. (As per IS 6533(part2):1989(reaffirmed in 2003) cl.7.2.4 (b) &(c).

Table: 1 Geometry of Flare base steel stacks

Steel stacks	Total Height of stack (Meters) (H)	Basic wind speed (m/s)	Effective Height (H_e) ($2/3 \times H$) (meter)	Top Diameter (constant) ($H_e/20$) (m)	Varying top to bottom diameters ratio (D_t/D_b) ratio (m)
					1.6
	H		H_e	D_t	D_b
1	30	44	20	1	1.6

2	30	47	20	1	1.6
3	30	50	30	1	1.6

PROBLEM -STATEMENT

Analyse the behaviour of self supporting Flare base Steel stack under the static and dynamic wind loads for variable wind speed as per Indian standard code of practice.

Detail of steel stack

- Type: self-supported unlined industrial circular steel stacks with constant shell thickness as IS 6533 Part-1.
- Total 3 steel stacks (Height constant with variable wind speed)
- Height of steel stack: 30m
- Top diameter for each stack is taken as minimum $h_c/20$ as per provision in IS 6533:1989.
- Variation in base diameter for each stack for fixed value of top diameter will be in following incremental ratio (ratio D_b/D_t) : 1.6
- Base condition : Rigid support at base
- Wind speed : 44m/s,47m/s,50m/s
- Shell thickness : 16mm(constant for all stacks)
- Materials for steel stack are conforming to IS2062:2006.

RESULTS:

A. Static & dynamic wind Responses for Flare base steel stack for (44m/s) wind speed:

Static and dynamic wind force increases with increment in wind speed. Static and dynamic wind force at wind speed 44m/s is given in table-2&table-3.

Table: 2 Static wind responses for Flare base steel stack for (44m/s)

FBC SC	Basic wind Speed (m/s)	Height (m)	Top Diameter (m)	Bottom Diameter (m)	Static Wind Pressure P_z (KN/m ²)	Static Wind Force (KN)	Max. Maximum deflection (mm)
30 m	44	10	1m	1.6 m	0.63	6.048	19.207
		20			0.78	7.488	
		30			0.86	8.256	

Table: 3 Dynamic wind responses for Flare base steel stack for (44m/s)

FBC SC	Basic wind Speed (m/s)	Height (m)	Top Diameter (m)	Bottom Diameter (m)	Dynamic Wind Force (KN)	Max. Maximum deflection (mm)
30 m	44	10	1	1.6	6.0782	181.145
		20			7.5327	

		30			8.3051	
--	--	----	--	--	--------	--

B. Static wind Response for Flare base steel stack for (47m/s) wind speed:

Static and dynamic wind force increases with increment in wind speed. Static and dynamic wind force at wind speed 47m/s is given in table-4&table-5.

Table: 4 Static wind responses for Flare base steel stack for (47m/s)

FBC SC	Basic wind Speed (m/s)	Height (m)	Top Diameter (m)	Bottom Diameter (m)	Static Wind Pressure P_z (KN/m ²)	Static Wind Force (KN)	Max. Maximum deflection (mm)
30 m	47	10	1	1.6	0.72	6.912	21.893
		20			0.89	8.544	
		30			0.98	9.408	

Table: 5 Dynamic wind responses for Flare base steel stack for (47m/s)

FBC SC	Basic wind Speed (m/s)	Height (m)	Top Diameter (m)	Bottom Diameter (m)	Dynamic Wind Force (KN)	Max. Maximum deflection (mm)
30 m	47	10	1	1.6	6.9486	208.271
		20			8.5984	
		30			9.4679	

C. Static wind Response for Flare base steel stack for (50m/s) wind speed:

Static and dynamic wind force increases with increment in wind speed. Static and dynamic wind force at wind speed 50m/s is given in table-6&table-7.

Table: 6 Static winds Response for Flare base steel stack for (50m/s)

FBC SC	Basic wind Speed (m/s)	Height (m)	Top Diameter (m)	Bottom Diameter (m)	Static Wind Pressure P_z (KN/m ²)	Static Wind Force (KN)	Max. Maximum deflection (mm)
30 m	50	10	1m	1.6	0.81	7.776	24.802
		20			1.01	9.696	
		30			1.11	10.656	

Table: 7 Dynamic wind responses for Flare base steel stack for (50m/s)

FBC SC	Basic wind Speed (m/s)	Height (m)	Top Diameter (m)	Bottom Diameter (m)	Dynamic Wind Force (KN)	Max. Maximum deflection
--------	------------------------	------------	------------------	---------------------	-------------------------	-------------------------

						(mm)
30 m	50	10	1	1.6	7.8195	234.158
		20			9.7614	
		30			10.7279	

D. Graphical representation of static and dynamic wind load:

Static and dynamic wind forces increase with increase in height of the steel stack and also increase with increment in wind speed. Fig-1 and Fig-2 shows the static and dynamic wind forces which is given below:

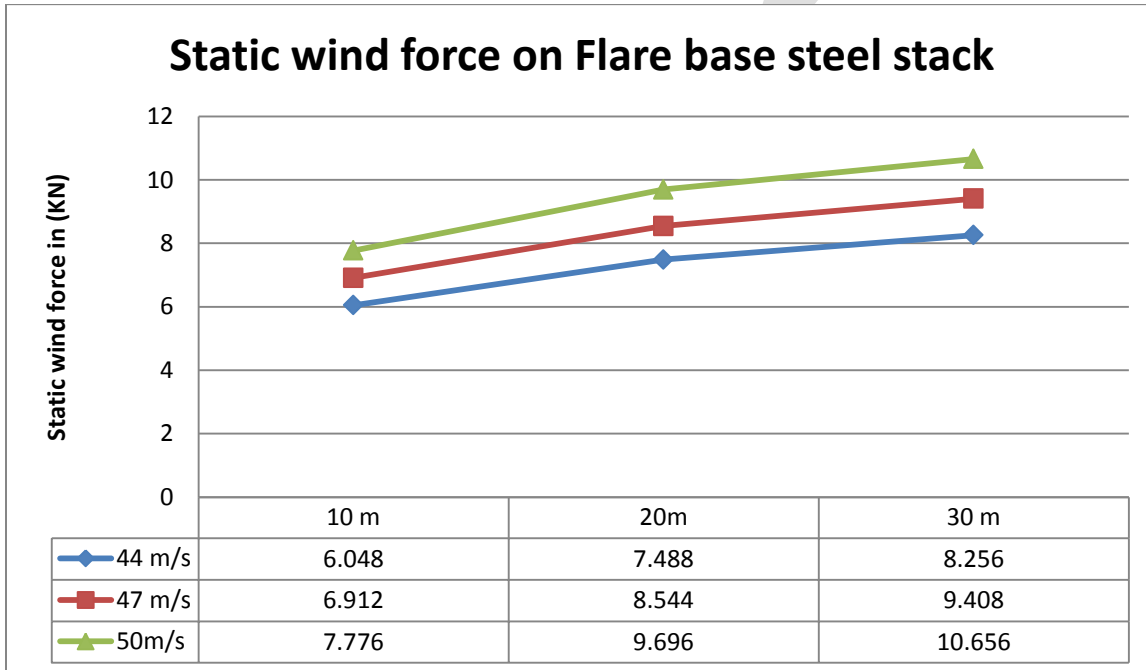


Fig-1 Static wind force on flare base steel stack of 30m with wind speed (44m/s, 47m/s, 50m/s)

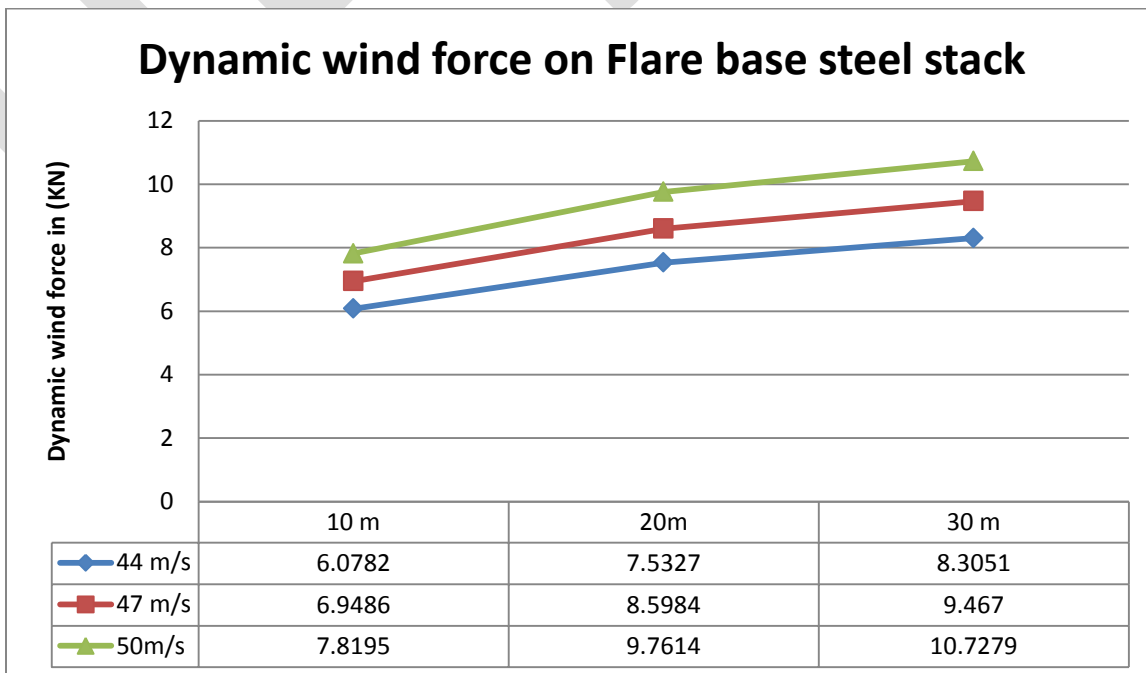


Fig-2 Dynamic wind force on flare base steel stack of 30m with wind speed (44m/s, 47m/s, 50m/s)

E. Maximum deflection due to static and dynamic wind responses:

Maximum deflection due to static and dynamic wind forces increases along the increment in wind speed. Maximum deflections at variable wind speed (44, 47 & 50m/s) are given in figure -3.

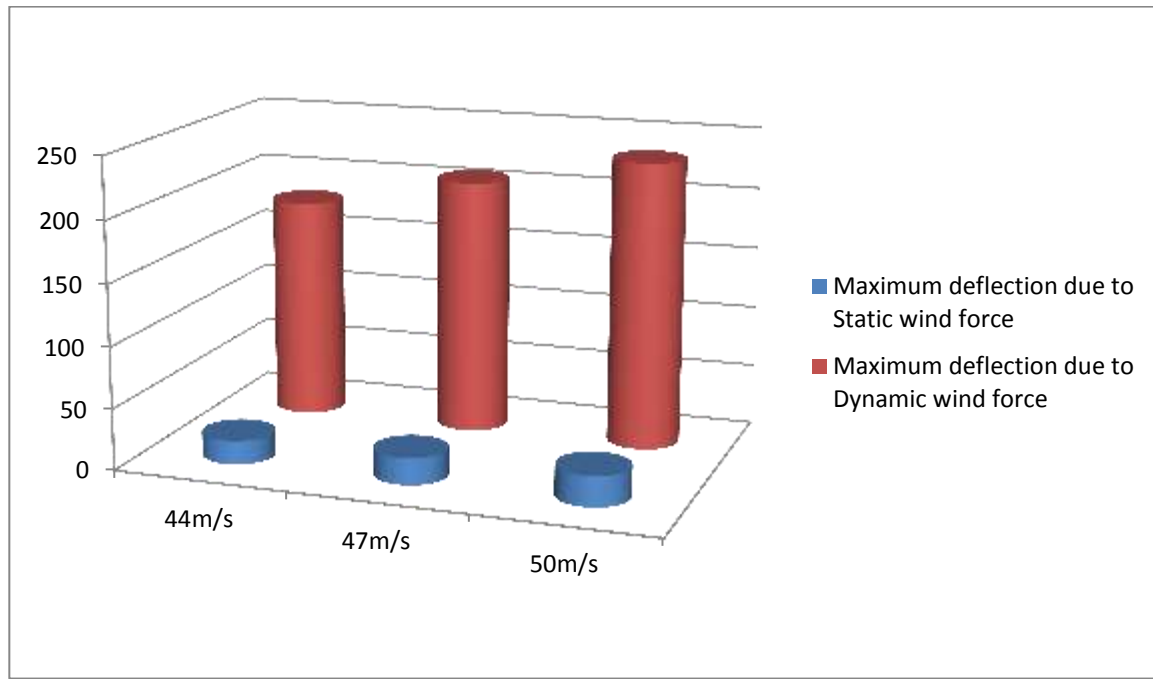


Fig-3 Maximum Deflection due to Static wind response with variable wind speed (for 1st mode)

CONCLUSION:

Following results are obtained from all above graphical representations:

1. Static & dynamic wind forces increases with the increment in wind speed (44, 47,50m/s).
2. Maximum deflection due to static wind force increases at 47m/s, 50m/s (14.45, 29.13%) as compare with wind speed 44m/s.
3. Maximum deflection due to dynamic wind force increases at 47m/s,50m/s (15.02, 29.32%) as compare with wind speed 44m/s.
4. Maximum deflections for wind speed (44,47 & 50m/s) due to static wind forces are (89.39, 89.49 ,89.41%) less as compare to maximum deflection due to dynamic wind force for (44,47,50 m/s) wind speed.

REFERENCES:

1. **IS 6533 (Part 2): 1989**, *Code of Practice for Design and Construction of Steel Chimney*, Bureau of Indian Standards, New Delhi.
2. **IS 6533 (Part 1): 1989**, *Design and Construction of Steel Chimney-Code of practice*, Bureau of Indian Standards, New Delhi.
3. **Harshal Deshpande, (2015)**, “*Correlation of Geometry and Dynamic Response of Self -Supported short Circular Steel stacks*”, Saraswati collage of Engineering, kharghar.
4. **G. Murali et al., (2012)**, “*Response of Mild Steel chimney Under Wind Loads*”, International Journal of Engineering Research and Applications, 2(2), pp. 490-498.
5. **Babita Devi, (2016)**, “*Analysis of se Analysis of Self supporting Steel Stacks with Variable Geometrical Configuration under the seismic loading for different shapes*”, International Journal of Engineering Research and general science.

Low Cost Controller Platform for Power Electronic Application

Aditya Porwal, Karan Varshney

IIT Delhi

aporwal25@gmail.com

Abstract— A DSP (Digital Signal Processor) is a basic controller platform which can be interfaced between a computer and a machine. It can be programmed to control the machines in a desired way for various power electronic applications. This project is based on an idea of replacing a typical DSP by a low cost alternative. As an alternative, it would consist of a micro-controller working as a processing unit. Other peripherals like Analog to Digital Converter (ADC) and Digital to Analog Converter (DAC) can be interfaced with the micro-controller depending upon the compatibility of the micro-controller. The report encapsulates the results of controlling a 3-phase induction motor using the Sinusoidal Pulse Width Modulation (SPWM) module developed, using a pre-programmed Voltage per Hertz (V/f) control method[1]. In the end comparison between a DSP and a micro-controller is included.

Keywords—digital signal processor, V/f control, controller platform, pulse width modulation, microcontroller, Arduino controller

INTRODUCTION

A DSP is a specialized micro-processing unit programmed according to the operational needs of digital signal processing. A basic DSP block is interfaced through its ADC and DAC. Analog signal is received by ADC which is sent to the processing unit of the DSP in digital domain. For power electronic applications, the goal of DSP is to follow the specific algorithms for controlling the machine parameters or the output signal[3]. DSP can either transmit the processed signal in digital format or in analog format with the help of DAC.

For most of the power electronic applications, a DSP can be replaced by a general purpose micro-processors like Arduino or Raspberry Pi. These micro-processors can be programmed as per the needs of application. Programming these devices is flexible as they can make use of third-party libraries and other modules on a higher machine level. This allows it to be used as a processing unit in several applications. Hence, the same micro-controller board can be interchangeably used for different kinds of power electronic applications by simply making use of different predefined programs. The merits of replacing a DSP with a generic micro-controller includes its low cost, compact size and high processing speed.

In the performed experiment, the feasibility and the extent of replacing a DSP with a micro-controller is established. The limitations of such a replacement and the fields where a DSP can be interchangeably used with a micro-controller is studied. As a part of the experiment, the micro-controller is used to run a 3-phase induction machine with an open loop control system. However, for implementing a closed loop control system a feedback to the micro-controller is required, this can be achieved by interfacing an ADC to the micro-controller. One of the key feature of the experiment is to introduce dead time through the control program rather than using hardware to introduce dead time. With a control on the dead time, the safety of the driving system and the overall control system can be ensured.

IMPLEMENTATION

Sinusoidal Pulse Width Modulation

In Sinusoidal Pulse Width Modulation, a sine wave of frequency f_s is sampled by a triangular wave of frequency f_t . During a period of the triangular wave, the sinusoidal signal is sampled and approximated by a constant DC signal of value V_{dc} . In this modulation scheme, the pulse width is varied in accordance with the sampled value of sinusoidal signal V_{dc} .

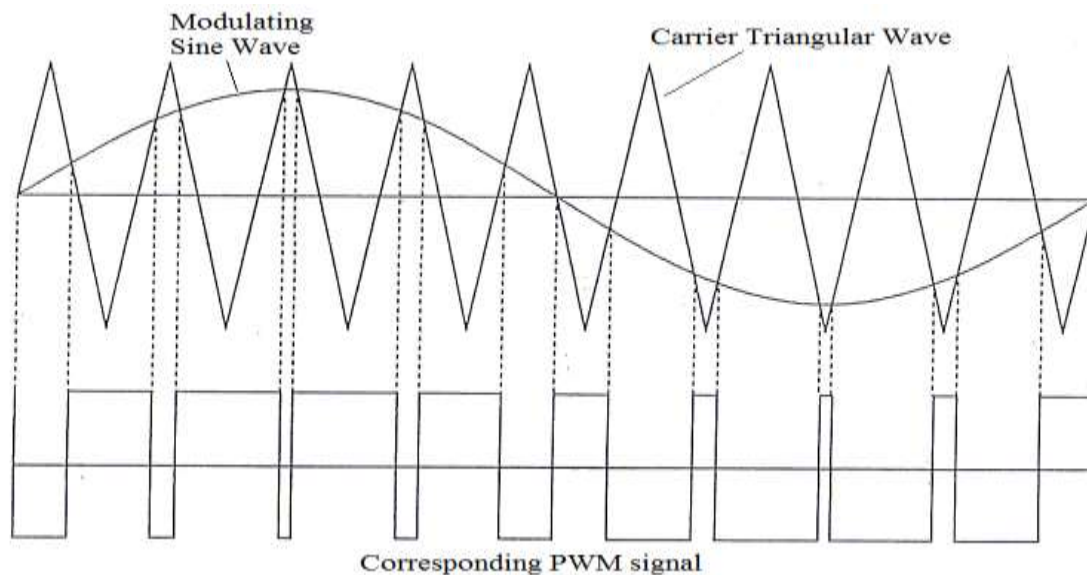


Figure 1. Sine PWM generation

Hardware and Software PWM

For implementing SPWM, the reference sinusoidal signal can be fed to the micro-controller through an ADC as a feedback for closed loop control or else the micro-controller can be pre-programmed to use tabulated samples of the sinusoidal wave. Many micro-controllers provide a hardware interface for PWM. Generally 8-bit or 16-bit counters are present, which are compared against a set of compare registers every clock cycle. Whenever the values in the counter and the compare register match, the output is changed according to the specified mode. Various kinds of modes provided by a micro-controller are phase correct mode, frequency correct mode and phase-frequency correct mode. For triangular wave, the counters need to be up-down counter which corresponds to phase correct mode. Thus by controlling the value in the compare register, corresponding to V_{dc} , desired pulse width can be achieved.

Another way to implement this would be to use any GPIO pin to toggle ON/OFF based on the control program written. In this method, known as software PWM, the output is generated by comparing the value of the V_{dc} against a counter which gets updated after every fixed number of clock cycles. Whenever the value matches the output is modified by the control program. To generate error free output, the counter must be updated very fast, i.e., almost every clock cycle. But in practice, when the program runs on the controller the counter gets updated after hundreds-thousands clock cycles, this happens because the processor needs to go through the overall control loop before updating the counter. Clearly software PWM requires large execution time and hence it is slow[2]. In generality, software PWM is good when the sampling frequency is low, as high frequencies cannot be achieved due to the inherent reasons[12].

Benefits of hardware PWM over software PWM includes the ability to generate more than one PWM channels simultaneously, processor is free to process other information without interrupting PWM channels, precise sampling frequencies can be generated.

Dead Time Incorporation

To drive a 3-phase 2-level inverter, the gate signals to the top and the bottom gates must be complementary. In case if both the top and the bottom gate signals are high then the power supply gets shorted, to avoid accidental shortening of the power supply, a dead time needs to be introduced in the two signals. This is like a safety margin to take care of the turn-on and turn-off time of the switches. In practice driving circuitry introduces rising delay and falling delay in the two driving signal which are supposed to be complementary of each other. Such delays can make the two signals high for a short interval of time. To introduce a dead time (dead band) in a signal either its rising edge is delayed or its falling edge is advanced by a fixed amount of time[6].

The need of having dead time between such signals is clear, especially when the power supply is in hundreds of volts. There are different ways to introduce dead time between such signals. One method employs the use of dedicated circuitry to introduce dead time. Although, in this experiment the dead time would be introduced with the help of the control program i.e., through software. Such method would allow a better control on the dead time to ensure the safety of the system. Apart from this, it will not require extra circuitry and hence reduce the size of the control circuitry.

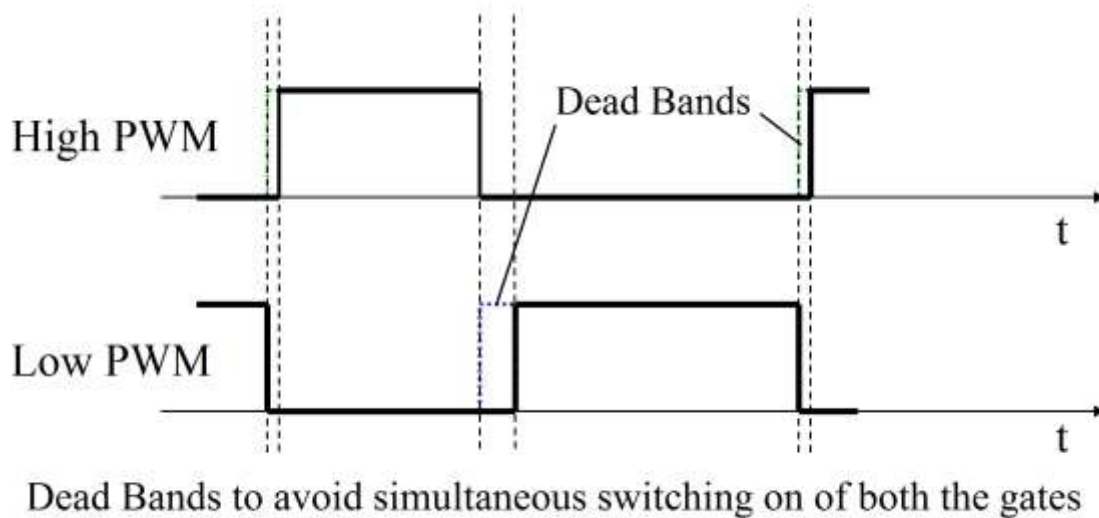


Figure 2. Complementary Signals with dead time in them

In this project, two low-cost microcontrollers are considered for the SPWM implementation, Arduino and Raspberry PI.

Working with Arduino

Arduino Mega2560 peripheral includes 12 PWM channels with programmable resolution from 2 to 16 bits along with four 16bit timer/counter with separate prescaler and compare mode. On varying the prescaler, the time to reach peak and fall down (or in turn frequency) can be varied and that's how hardware PWM can be modified according to the need[4]. The peripheral also provides 16 channels of 10bit ADC and no external interfacing is required for ADC in closed loop implementation. 86 programmable input/output lines (General Purpose Input Output) are available (including PWM and ADC channels) in peripheral and any GPIO pin of our choice could act as output.

PWM Implementation

In case of software PWM, the counter used for comparison against the sampled value of the sine wave, cannot be synchronized properly with the system clock. The code execution requires time for evaluation and it depends upon the availability of the processor. As long as the sampling frequency is small it would work but its performance would start deteriorating as the frequency is increased. Also software PWM is slow for the reasons discussed in the last section. On the other hand hardware completely devoted to PWM is

already in synchronization with the system clock and the sampling frequency can be controlled by setting the prescaler value and the top value in the PWM registers appropriately. Arduino provides 16-bit PWM channels along with 8-bit channels which provides better precision in terms of setting the sampling frequency.

PWM Registers

For using hardware PWM channels the registers associated with it must be initialized properly. A 16-bit timer in Arduino has three main control registers to control the channel operation, namely, *TCCRxA*, *TCCRxB* and *TCCRxC*.

Bit	7	6	5	4	3	2	1	0	
(0x80)	COM1A1 COM1A0 COM1B1 COM1B0 COM1C1 COM1C0 WGM11 WGM10								TCCR1A
Read/Write	R/W	R/W	R/W	R/W	R/W	R/W	R/W	R/W	
Initial Value	0	0	0	0	0	0	0	0	
Bit	7	6	5	4	3	2	1	0	
(0x81)	ICNC1 ICES1 - WGM13 WGM12 CS12 CS11 CS10								TCCR1B
Read/Write	R/W	R/W	R	R/W	R/W	R/W	R/W	R/W	
Initial Value	0	0	0	0	0	0	0	0	
Bit	7	6	5	4	3	2	1	0	
(0x82)	FOC1A FOC1B FOC1C - - - -								TCCR1C
Read/Write	W	W	W	R	R	R	R	R	
Initial Value	0	0	0	0	0	0	0	0	

Figure 3. *TCCRxA*, *TCCRxB* and *TCCRxC* registers format

Apart from them it has one 16-bit counter register, namely, *TCNTx* for keeping track of counter value and three output compare registers for setting the reference values, namely, *OCRxA*, *OCRxB* and *OCRxC* to provide three different kind of outputs per channel.

Bit	7	6	5	4	3	2	1	0	
(0x89)	OCR1A[15:8]								OCR1AH
(0x88)	OCR1A[7:0]								OCR1AL
Read/Write	R/W	R/W	R/W	R/W	R/W	R/W	R/W	R/W	
Initial Value	0	0	0	0	0	0	0	0	
Bit	7	6	5	4	3	2	1	0	
(0x85)	TCNT1[15:8]								TCNT1H
(0x84)	TCNT1[7:0]								TCNT1L
Read/Write	R/W	R/W	R/W	R/W	R/W	R/W	R/W	R/W	
Initial Value	0	0	0	0	0	0	0	0	

Figure 4. *OCRxX* and *TCNTx* registers format

A register Input Capture Register, *ICRx* for updating the counter value whenever an event occurs on input capture pin of the channel. Particularly useful in closed loop implementation.

Bit	7	6	5	4	3	2	1	0	
(0x87)	ICR1[15:8]								ICR1H
(0x86)	ICR1[7:0]								ICR1L
Read/Write	R/W	R/W	R/W	R/W	R/W	R/W	R/W	R/W	
Initial Value	0	0	0	0	0	0	0	0	

Figure 5. *ICRx* register format

For handling interrupts, two registers are provided: one *TIMSKx* for enabling which interrupt vectors are to be used and another *TIFRx* which gets updated as soon as interrupt is generated and handled.

Bit	7	6	5	4	3	2	1	0	
0x16 (0x36)	-	-	ICF1	-	OCF1C	OCF1B	OCF1A	TOV1	TIFR1
Read/Write	R	R	R/W	R	R/W	R/W	R/W	R/W	
Initial Value	0	0	0	0	0	0	0	0	

Bit	7	6	5	4	3	2	1	0	
(0x6F)	-	-	ICIE1	-	OCIE1C	OCIE1B	OCIE1A	TOIE1	TIMSK1
Read/Write	R	R	R/W	R	R/W	R/W	R/W	R/W	
Initial Value	0	0	0	0	0	0	0	0	

Figure 6. *TIMSKx* and *TIFRx* register format

Interrupts

Only single instruction set at a time can be executed by a processing unit, but instructions can be interrupted. Therefore, for multitasking, the events are prioritized for the processor to process in a queue. Hence in the given preference order the interrupts are handled by the interrupt handler (or ISR, Interrupt Service Routine)[7]. As soon as the interrupt is flagged for an instruction, current instruction is paused and is resumed once the flagged instruction is over.

Interrupts are required to set the new compare/reference value for each of the PWM channels based on the sine wave, every period of the triangular wave. To introduce dead time, it needs to be updated twice every period of triangular wave. This enables the processor to be free to process other data such as in the case of closed loop system, the feedback needs to be processed which in turn can be used in the next sampling cycle.

Memory

Arduino Mega2560 has only 256 KB of FLASH memory which can only be written at the time of flashing the micro-controller and SRAM is limited to 8 KB only. Hence in case of storing large data such as parameters, look-up tables cannot be stored in SRAM, one needs to use the FLASH memory. This limits the smooth operation of the system.

Clock speed

The system clock speed of the Arduino Mega2560 is 16 MHz and correspondingly the maximum MIPS it could achieve at 16 MHz is 16 MIPS. Whereas the clock speed for typical DSPs is 150-200 MHz which insures a much higher MIPS than Arduino. Hence, the amount of computation that can be done in each cycle of the sampling wave is limited to very few operations. In closed loop implementation, this plays an important role since the new reference value has to be calculated from the feedback which can involve complex arithmetic operations which needs to be finished before the next cycle of the sampling wave.

Working with Raspberry PI

PWM Implementation

Similar to Arduino, software PWM faces the same problem of synchronization when the sampling frequency is high. Raspberry PI provides only 2 hardware PWM channels with only a single output per channel. Incapability to generate 3 phase signals on the same micro-controller is the major reason which makes the use Raspberry PI in 3 phase power electronics application difficult.

PWM Registers

The hardware PWM channels of Raspberry PI provides very less flexibility. The counter available is down counter only in contrast to Arduino which has down counter, up counter and up-down counter modes. Up-down counters are required for triangular sampling

wave. The sampling frequency can only be controlled by changing the top value of the counter, which corresponds to the maximum value of the sampling wave but in Arduino even the width of the sampling wave can be controlled.

Absence of ADC on the micro-controller requires to interface an external ADC for closed loop implementation.

Interrupts

No predefined interrupt structure is available for the PWM hardware channels. Even user defined interrupts will not work at such high frequencies. The main reason being that Raspberry PI runs a Linux based operating system which is not a real time operating system. Thus program that runs on such a platform does not get updated in real time, this causes problem because when interrupt is fired it is not handled immediately. The same reason makes software PWM difficult because the parameters cannot be updated at fixed regular intervals.

Memory and Kernel Drivers

Raspberry PI provides 512 MB RAM significantly higher than a DSP and Arduino and extendable external storage. It allows to store a large amount of preprocessed data which can be used by the program as and when needed.

The problem of Linux being not a real time operating system can be bypassed by flashing a program developed for carrying out the only required function. This can be achieved by making use of kernel drivers and developing the code in assembly language making the use of the Raspberry PI's *SoC BCM2835* registers and then flashing the program on the micro-controller similarly as in the case of Arduino.

Clock Speed

Raspberry PI B+ was used for experimentation. It has significantly high clock speed (~700 MHz) as compared to a regular DSP (~200 MHz). Even the chip can be overclocked externally. Such high operating frequency allows it to do more computation with faster processing speed than a typical DSP. Big complex feedback algorithms can be implemented easily in case of closed loop implementation.

Experimentation

As per the points mentioned above, although Raspberry PI has two main features of large memory and high clock speed but lack of hardware PWM channels and inability to do software PWM at high sampling frequencies makes Raspberry PI less of a substitute for a DSP. Whereas Arduino has a wide flexibility in terms of PWM and the only problem is its low clock speed. Arduino's memory limitation can be avoided by using external memory modules which are readily available. Hence replacing a DSP with Arduino will work just as fine if open loop implementation of the system is carried out. In closed loop implementation, it is customary for the DSP to do several computations based on the feedback and then correspondingly update the system parameters. Owing to the low clock speed the amount of computation that can be done with Arduino is limited. Apart from that in terms of PWM generation Arduino can successfully replace a DSP.

For the current experimentation, Arduino is used rather than Raspberry PI. This experiment will illustrate the open-loop control of a three phase induction machine via Voltage per Hertz control method. The controlling unit will be Arduino which will generate the six gate driving signals based on the parameters provided which will drive the three phase inverter and hence the induction machine.

Interface Circuitry

(For Interface Circuitry refer Appendix)

The Arduino generates the 6 gate driving signals which are being fed to the 3 phase two level inverter. This requires an interfacing circuitry as Arduino cannot drive the inverter directly, due to the limited current carrying capability of Arduino, which is less than 10 μ A. Thus a buffer is introduced in between and an optocoupler to provide electrical isolation between the two circuits for safety.

Arduino Initialization

(For Codes refer Appendix)

The INO file to be flashed into Arduino is generated by a C++ program which takes the input for the operating conditions. First it calculates the appropriate parameter values and the needed sine look-up table. After this it generates the INO file which then can be flashed. This is required since the sine look-up is large and needs to be stored in the Program Memory, i.e., Flash memory of Arduino. Preprocessing the sine table reduces the time taken to compute the next reference value and thus leaves more time for other computation during the sampling period such as computation on feedback.

To setup the hardware channels of the Arduino the required 16-bit timer's control registers need to be updated. To get a triangular wave, i.e., an up-down counter the timer's mode needs to be set to *Phase Correct* PWM mode such that their top value can be controlled through code. This requires the $WGMx [3:0] = 1011$ in the control registers of the timer. For each of the three timers, three different kind of output can be generated, which can be controlled by the values of $COMxA [1:0]$, $COMxB [1:0]$ and $COMxC [1:0]$. It is required that one output gets clear when counter matches the reference value while up-counting and set while down-counting and the other output to do the vice versa and the last output is not required.

Hence, $TCCRxA = 00111011$ and $TCCRxB = 00010000$.

Also, to get the desired sampling frequency the top value of the counter and the timer's clock can be prescaled by a factor of powers of 2. The appropriate values of the prescaler and the top are found based on the desired frequency by a simple algorithm.

Hence, the value of the prescaler is set in the $TCCRxB$ and top value is stored in the $OCRxA$.

Now the reference values are to be set in the $OCRxB$ and $OCRxC$ registers which needs to update whenever the counter reaches top or bottom. This is required because the dead time is introduced by pre-processing the values. To achieve this interrupts from one of the timer are generated whenever such an event happens. To set this any one of the three timer's $TOIEx$ and $OCIExA$ bits in $TIMSKx$ are set to one and all the other timers to zero.

Hence, for any one timer $TIMSKx = 00000011$ and for other timers $TIMSKx = 00000000$.

Thus whenever the interrupt occurs the reference values, i.e., $OCRxB$ and $OCRxC$ updates based upon the next value in the look-up sine table which is generated beforehand the Arduino is flashed with the program. It is also needed in Voltage per Hertz control the frequency needs to be ramped from some starting value to the final value proportional to the sine amplitude. For this the reference values of that sine wave is processed and stored in memory.

Thus whenever the program runs in Arduino, the reference value gets updated by looking in the table corresponding to that frequency at that particular time of ramping. Therefore, the C++ program is required to generate a series of sine look-up table at different frequencies of ramping. The Arduino program also keep track of the ramping time and the ramping is stopped one the desired frequency is reached.

Execution Order:

Parameters → C++ Code → (If Possible) → INO File → Arduino Flash → Run → Observations

The parameters are passed to a C++ code and it checks if it is possible to implement the given configuration on Arduino. If it is possible this code generates a INO file which can be flashed on Arduino and then the Arduino can be used accordingly.

Results

The results are generated for sampling frequency of 5 KHz and fundamental frequency of 50 Hz with a 3 μ s dead time for a balanced 3 phase.

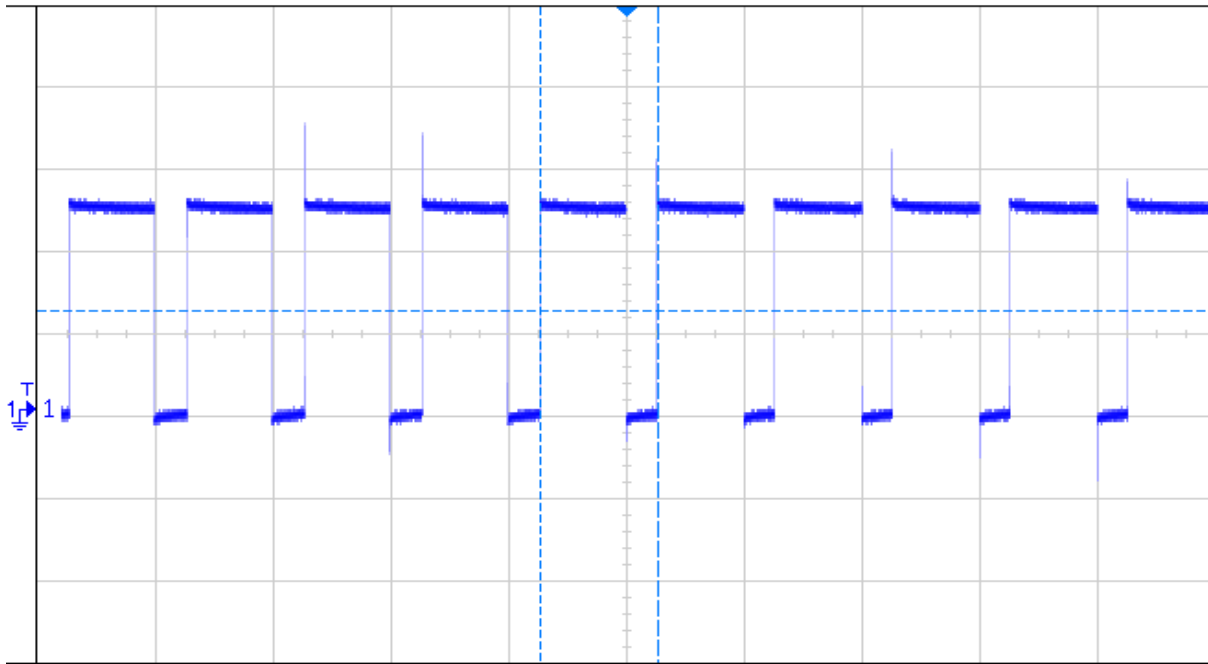


Figure 7. Sine PWM Output of a channel (Time Scale 200 μ s)

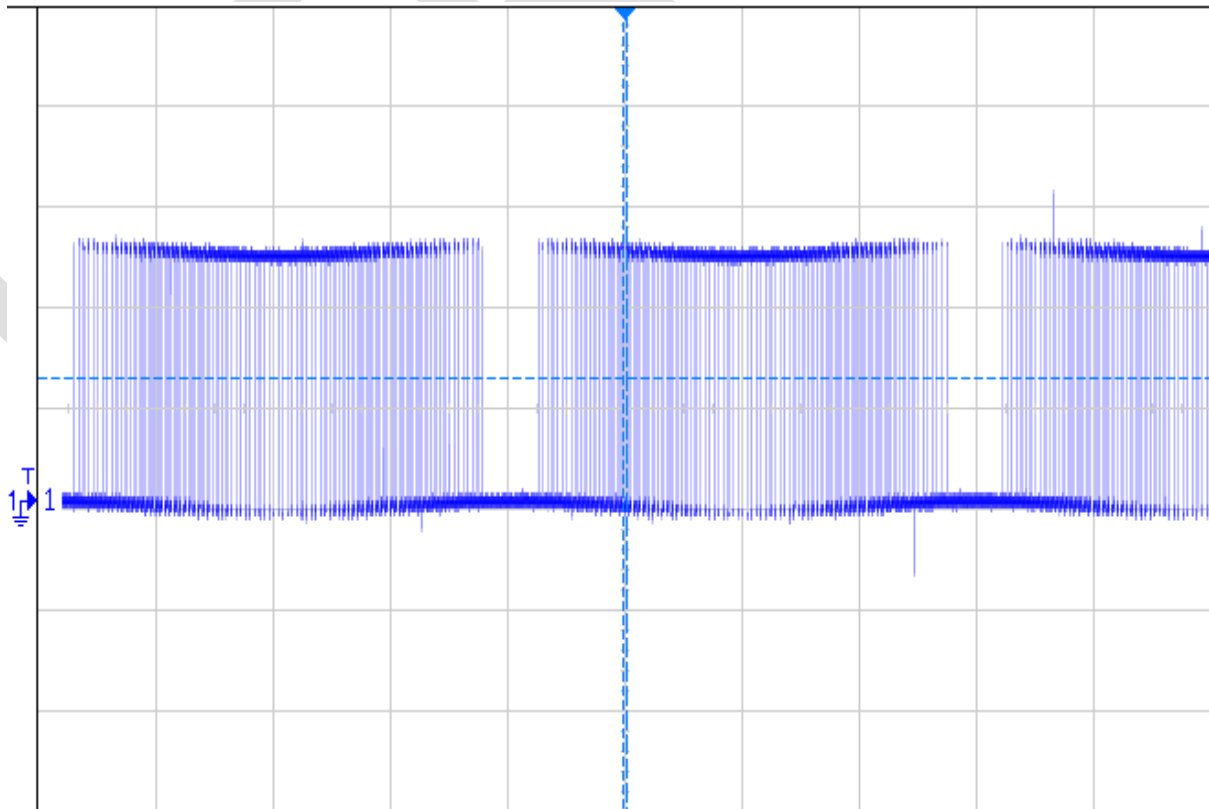


Figure 8. Sine PWM Output of a Channel (Time Scale 5 ms)

Figure 7 and 8 depict the output voltage of phase. The switching time of $200\ \mu\text{s}$ corresponding to the 5 KHz sampling frequency and at large time scale the fundamental period of about 20 ms can be observed corresponding to the fundamental frequency of 50 Hz.

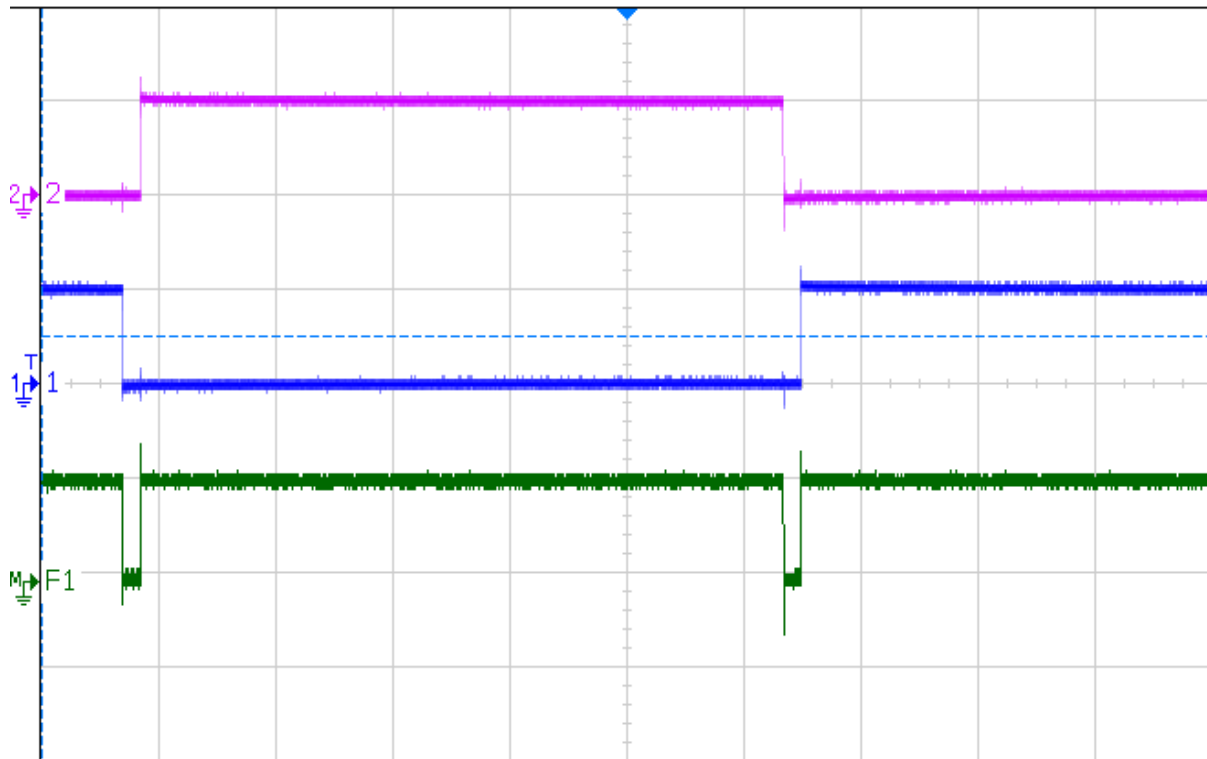


Figure 9. Dead Time (Channel M = Channel 1 + Channel 2) (Timescale $20\ \mu\text{s}$)

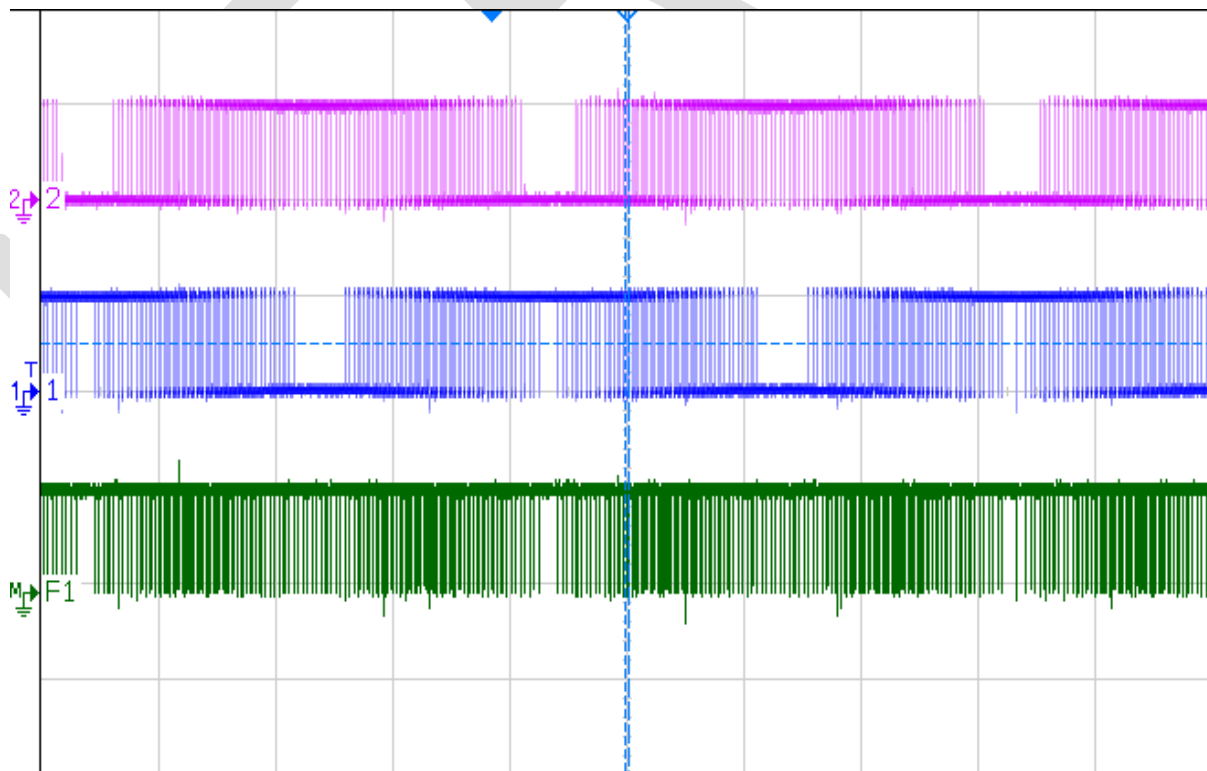


Figure 10. Dead Time (Channel M = Channel 1 + Channel 2) (Timescale 5 ms)

In figure 9 and 10, channel 1 and channel 2 are complementary signals which are fed to one of the 3 pairs of the top-bottom IGBTs. The signal M is the sum of channel 1 and channel 2 and all the three signals are scaled to 5 V/block, thus M represents the dead time of 3 μ s each, between the two channels. Channel M never goes beyond 5V implying that channels 1 and 2 are never high at the same time.

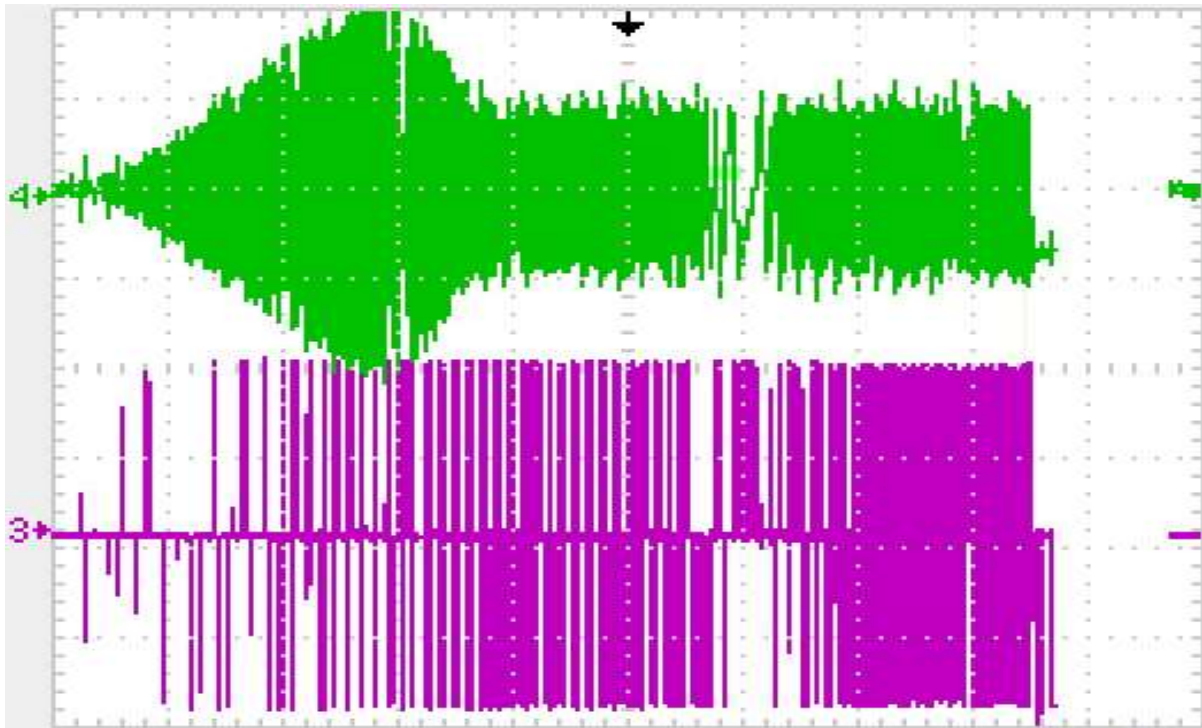


Figure 11. Channel 3 is voltage across one of the phase of 3 phase induction motor and Channel 4 is the current profile flowing in that phase during ramping (V/f control).

Figure 11, shows voltage and current across a phase when the V/f control is done. The machine is started at very low frequencies compared to the fundamental frequencies. At regular interval the frequency is increased in small steps keeping the flux almost same. Initially the voltage and the frequency is small and the motor is at standstill, slowly the current in the motor builds and the slip of the motor starts decreasing and as the motor goes into steady state operation the current amplitude becomes constant. During the transient the current rises sharply and overshoots the steady value due to the inertia of the motor which leads to high slip. This can be reduced by increasing the ramping time.

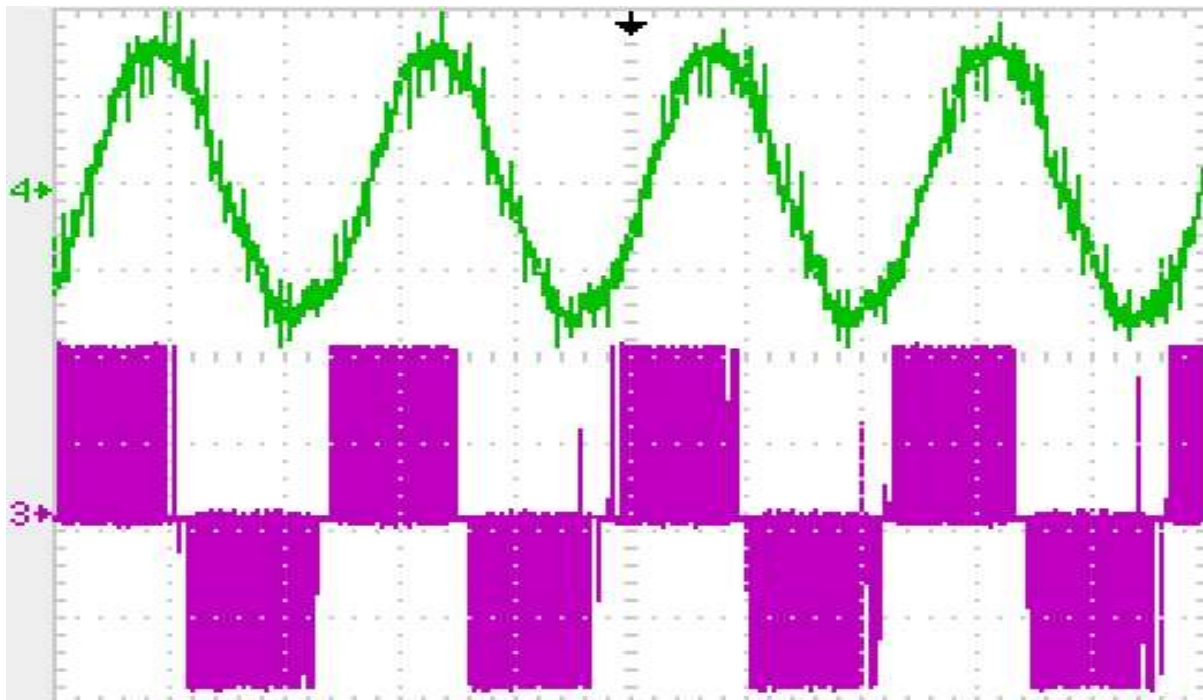


Figure 12. Channel 3 is voltage across one of the phase of 3 phase induction motor and Channel 4 is the current profile flowing in that phase.

Figure 12, shows the voltage across a phase of the 3 phase induction motor and current through that phase which is fairly a sinusoidal signal of 50 Hz. This voltage is simply the voltage available across one of the phase of the inverter which is nothing but the difference of the two signals generated by Arduino and amplified to the power supply level. Sinusoidal nature of the current is due to the large inductance of the motor allowing only smaller frequencies and filtering out higher harmonics which are present in the voltage waveform applied across it. Fourier analysis of this voltage signal reveals 50 Hz component and its harmonics are present in the signal.

CONCLUSION

Two methods of PWM, namely, software and hardware are available but software PWM is inefficient at high sampling frequencies, which is generally the case in power electronics application. Even at sampling frequencies as low as 1 khz, the software PWM output is not steady and accurate as it depends upon the availability of the processor. Thus hardware PWM is the only feasible option for PWM at such frequencies, where the processor is needed to only do the system parameters update and feedback computation.

Generally, dead time is introduced with the help of circuitry but in the experiment the dead time is generated as a part of the pulse width modulation scheme. This helps in getting rid of the circuitry needed to introduce the dead time in the signals.

Based on the results of the above experiment, Arduino can successfully replace a DSP for any pulse width modulation scheme. In open loop implementation Arduino can safely replace a DSP but in closed loop implementation the amount of computation on the feedback is limited. The inbuilt ADC of Arduino has a 10-bit precision which can be improved by interfacing a better ADC.

The Raspberry PI can prove to be a better substitute for a DSP because it has significantly high clock speed and large memory if only Raspberry PI have a better hardware PWM module. Even though making use of kernel drivers one can achieve software PWM but the performance is limited in terms of the sampling frequency. For now the current versions of Raspberry PI are incapable of replacing a DSP for a typical PWM application.

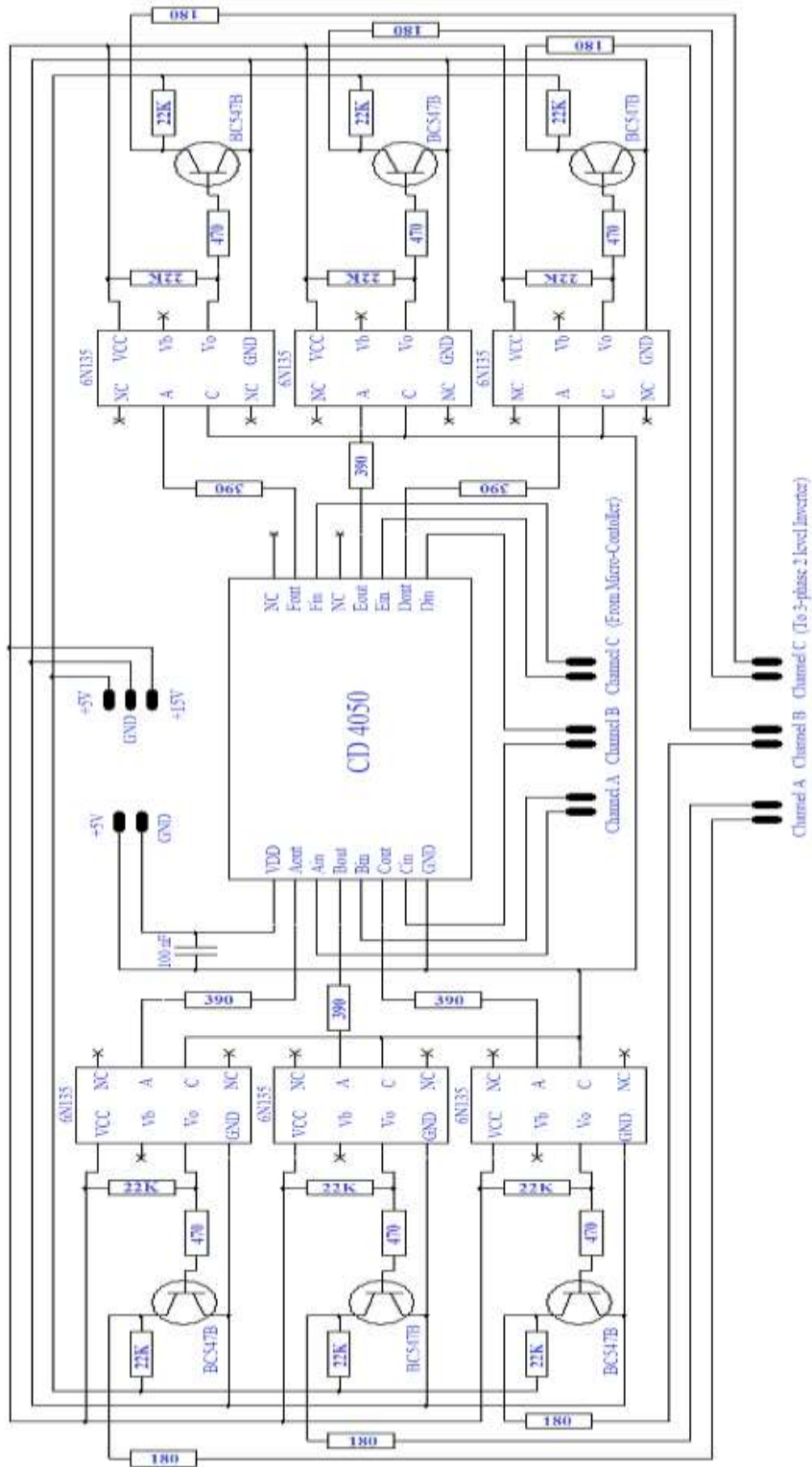
Such micro-controllers such as Arduino can easily substitute a DSP as a low cost alternative. This enables various individuals, firms, laboratories and students to use a micro-controller in place of a DSP for a variety of power electronic applications and experimentation purposes in schools and colleges.

REFERENCES:

- [1] A. Munoz-Garcia "A new induction motor V/f control method capable of high-performance regulation at low speeds" IEEE Transactions on Industry Applications, ISSN-number 0093-9994, Jul/Aug 1998
- [2] J. P. Agrawal , O. Farook ; C. R. Sekhar "Software controller for PWM converters" Applied Power Electronics Conference and Exposition, 1994. APEC '94. Conference Proceedings 1994., Ninth Annual, ISBN-number 0-7803-1456-5, 13-17 Feb 1994
- [3] A. H. M. Yatim; N. R. N. Idris "Implementation of direct torque control of induction machine utilising TMS320C31 digital signal processor" Signal Processing and its Applications, Sixth International, Symposium on. 2001, ISBN-number 0-7803-6703-0, 2001
- [4] Milan Matijevic; Vladimir Cvjetkovic "Overview of architectures with Arduino boards as building blocks for data acquisition and control systems" 2016 13th International Conference on Remote Engineering and Virtual Instrumentation (REV), ISBN-number 0-7803-6703-0, 24-26 Feb. 2016
- [5] Piotr Biczal; Andrzej Jasinski; Jacek Lachecki "Power Electronic Devices in Modern Power Systems" EUROCON, 2007. The International Conference on "Computer as a Tool", ISBN-number 978-1-4244-0813-9, 9-12 Sept. 2007
- [6] L. Schirone; M. Macellari "General purpose dynamic dead time generator" Clean Electrical Power (ICCEP), 2015 International Conference, ISBN-number 978-1-4244-0813-9, 16-18 June 2015
- [7] Yuting Zhang; Richard West "Process-Aware Interrupt Scheduling and Accounting" 2006 27th IEEE International Real-Time Systems Symposium (RTSS'06), ISBN-number 0-7695-2761-2, Dec. 2006
- [8] V. Miñambres-Marcos; I. Roasto; P. Szczepankowski; E. Romero-Cadaval; D. Vinnikov; F. Barrero-González "Code development of a DSP-FPGA based control platform for power electronics applications" 2015 IEEE International Conference on Industrial Technology (ICIT), 17-19 March 2015
- [9] M. F. Rahman; K. V. Baburaj; L. Zhong "A DSP laboratory platform for teaching power electronics and drives" 2006 27th IEEE International Real-Time Systems Symposium (RTSS'06), ISBN-number 0-7695-2761-2, Dec. 2006
- [10] A. Balestrino; G. de Maria; L. Sciavicco "Analysis of modulation processes in power convertors" Electrical Engineers, Proceedings of the Institution of, ISSN-number 0020-3270, May 1978
- [11] Babak Zamanlooy; Hamidreza Chamani Takaldani; Amir Moosavienia; Khalil Monfaredi; Reza Ebrahimi Atani "Design and implementation of a stable platform digital controller based on DSP" Signals and Electronic Systems, 2008. ICSES '08. International Conference on, ISBN-number 978-83-88309-47-2, 14-17 Sept. 2008
- [12] M. C. Trigg; H. Dehbonei; C. V. Nayar "Digital sinusoidal PWM generation using a low-cost micro-controller based single-phase inverter" 2005 IEEE Conference on Emerging Technologies and Factory Automation, ISBN-number 0-7803-9401-1, 19-22 Sept. 2005

APPENDIX

A. The schematic of the interface circuitry is as below:



The 3-phase from the micro-controller are fed to the buffer to prevent excessive current flowing into the microcontroller. These signals are passed through an optocoupler stage to provide an electrical insulation between the two stages. These 5V signals are then amplified to 15V through a transistor, which is needed to drive the gates of an inverter.

The three output channels are connected to the three legs of the inverter for driving the 3 phase induction machine by converting the input

AC or DC link voltage to the inverter.

B. C++ program code for generating the INO file can be found here:

https://docs.google.com/document/d/1HN1Oc3OyGnYVTc5W-0tXclh6qCX1ANrNDV6bf_xqyKc/edit?usp=sharing

C. Arduino program generated by the above code for 10 KHz sampling frequency, 50 Hz fundamental frequency, dead time of 3 μ s, ramping time of 60 seconds with a frequency step of 1 Hz starting from 5 Hz to produce a 3 phase balanced output can be found here:

<https://docs.google.com/document/d/1GgGYg2ZBTsnUOeruSHgLMpD3RzctSSuCKd75SLIOq0/edit?usp=sharing>

IJERGS

A Case Study of Plant Layout: To Compare Production Efficiency Of Manual Plant Layout And Computerized Plant Layout Using ARENA Software

Priyanka Yadav¹, Suman Sharma²

¹Student of Master of Engineering in Production Engineering and Engineering Design from Truba College of Engineering and Technology, Indore

²Prof. and Head of Mechanical Engineering Department in Truba College of Engineering and Technology, Indore

Abstract— Industries are working hard to set a benchmark in the present era, and they are working for increasing their potential in production and effectiveness to compete in markets. There are many ways to solve the problem relating to the production like Plant Layout, Line Balancing, Quality Control (QC), Total Quality Management (TQM), and Standard Time. Plant Layout helps in better utilization of man, material and machinery for effective utilization of all resources. And also by the help of simulation we can make a virtual model of Plant Layout of real world environment and also by inputting the data from real world environment. This study of plant layout is done in B. Shankara Sales Organization, Agra which is a piston and piston ring manufacturing company of two and three wheeler vehicle. Here the study of plant layout of company has been done by creating several virtual options of layout without disturbing the original one. And these studies gave a fantastic change in production rate, productivity & plant efficiency with efficient utilization.

Keywords—production, plant layout, line balancing, simulation software, production rate, productivity, plant efficiency.

INTRODUCTION

Plant layout defined as the physical arrangement of everything needed for the product or service (including machines, personnel, raw materials, and finished goods). Plant layout design is the fundamental basis of today's industrial plants which can influence parts of work efficiency.

In industry sectors, it is important to manufacture the products which have good quality products and meet customers' demand. This action could be conducted under existing resources such as employees, machines and other facilities. Plant layout improvement is one of the tools to increasing industrial productivities. Plant layout design has now become a fundamental basis of today's industrial plants which can influence parts of work efficiency. It is needed to appropriately plan and position employees, materials, machines equipments, and other manufacturing supports and facilities to create the most effective plant layout. [1]

Placement of the facilities in the plant area, often referred to as "facility layout problem", is known to have a significant impact upon manufacturing costs, work in process, lead times and productivity. A good placement of facilities contributes to the overall efficiency of operations and can reduce until 50% the total operating expenses. The design components of a plant layout consist of facility system, the layout, and the material handling system. Facility system consists of structural system the atmospheric system, life safety system and the sanitation system. The layout consists of all equipment and machinery system. Handling system consists of mechanism required to satisfy facility interactions [2]

CASE STUDY

This project study has been performed at "B. Shankra Sales Organization, Agra". B. Shankra Sales Organization is Piston and Piston Ring Manufacturer Company of two and three wheeler vehicles engine. It is established in 1985 by Mr. Rama Shankar Sharma and it exports pistons of two and three wheeler vehicles engine. Here in this company, pistons are manufactured by casing in casting cell then it goes to piston smoothening cell and after that they do fitting rings in pistons.

The Process Of Piston Making In A Piston Smoothening Cell:- The layout of piston making process with operations & cycle time assembly line is shown in fig 1 and which is related to table of sub production line machines with cycle time is shown in comparison table 1. Firstly we find the process of existing piston making data by arena approach in figure 2. In the present case of company we are using arena simulation, which results production of 307 piston/shift, in which 244 pistons are selected and 63 pistons are rejected. In this we get the efficiency of 69% of selected piston. This is the present layout of the company in which cycle time is 2 min/cycle.

In second case (Figure 3) we do modification in first case and increase 1 machine in the basic model M1 i.e. grinding machine. In this we get production rate of 307 shaft /shift in which selected pistons are 279 and rejected pistons are 28. In this we get efficiency of 69.75% of selected pistons.(7-days& 14-days).

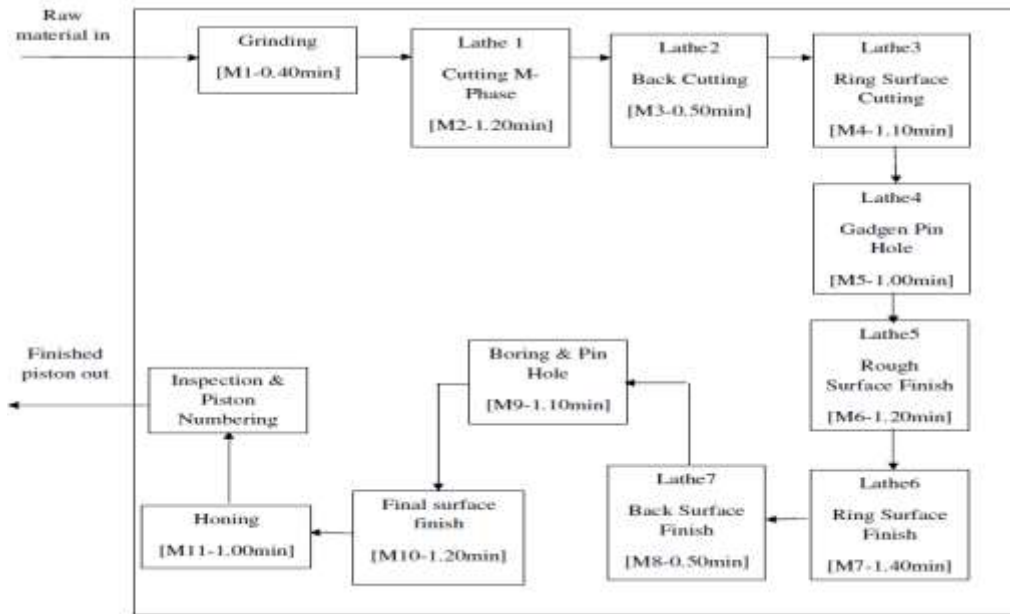


Figure 1: Flow chart of basic layout

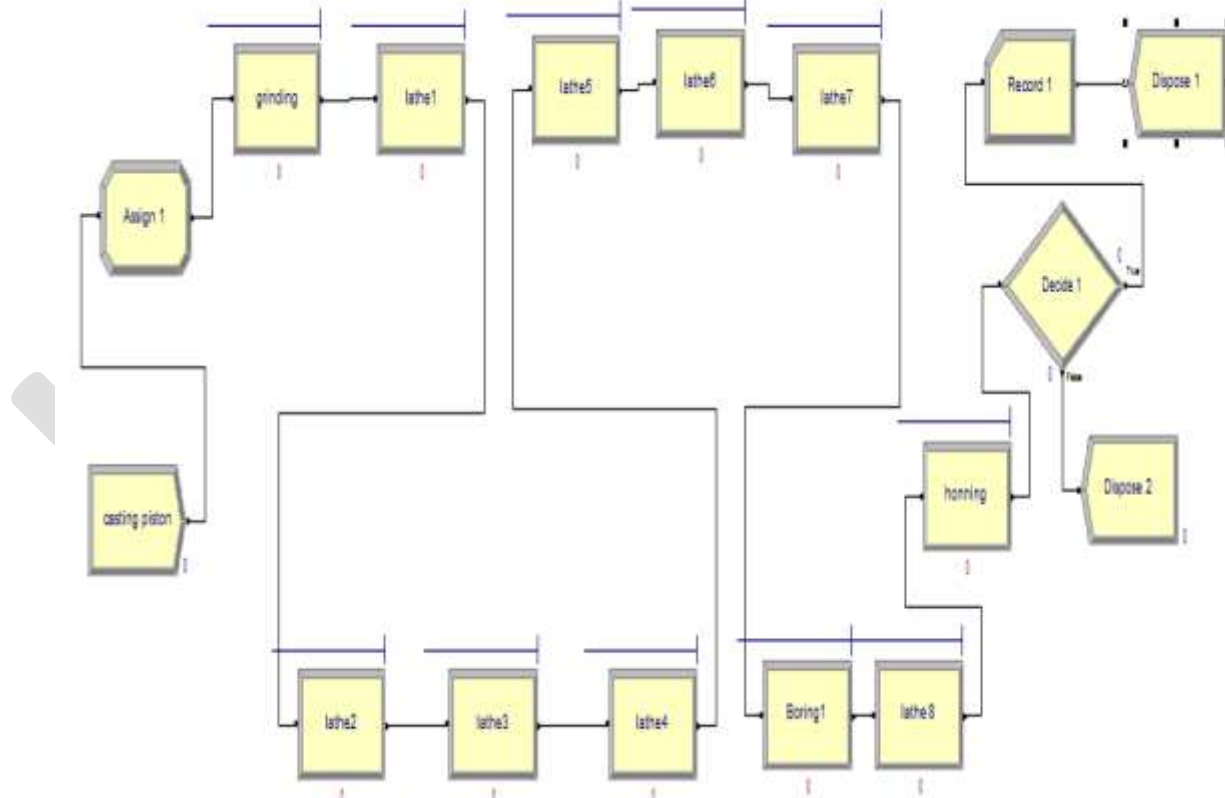


Figure 2: Flow chart of basic layout in ARENA

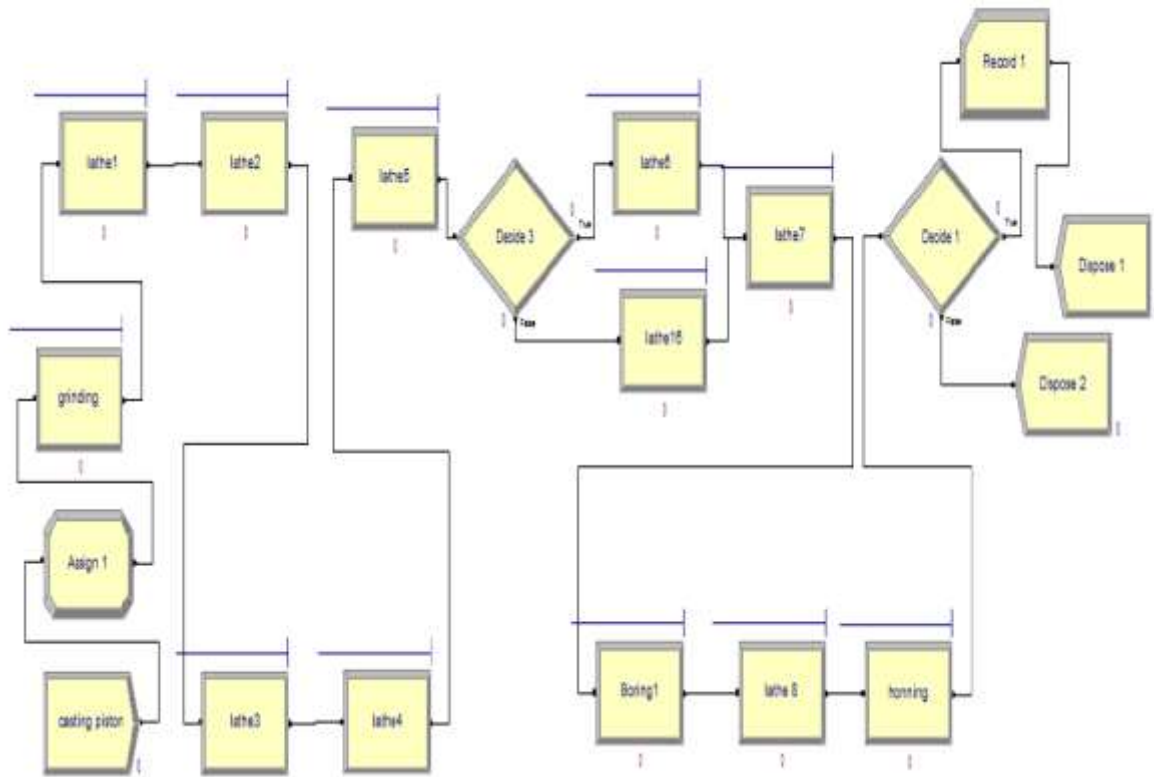


Figure 3: Flow chart of Proposed layout in ARENA

Figure 4 & figure 5 we just plot the graph for showing the utilization of all machines in 1 cycle. Figure 4 is for basic present layout of company & figure 5 is for simulated layout. We can compare the utilization here.

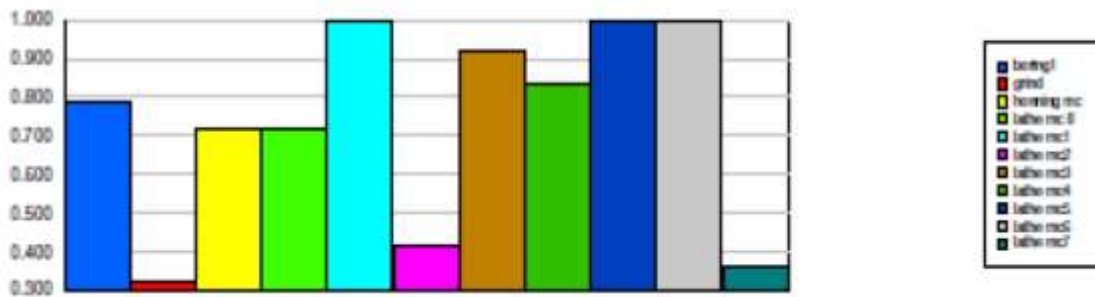


Figure 4: Scheduled Utilization of Machines in basic layout

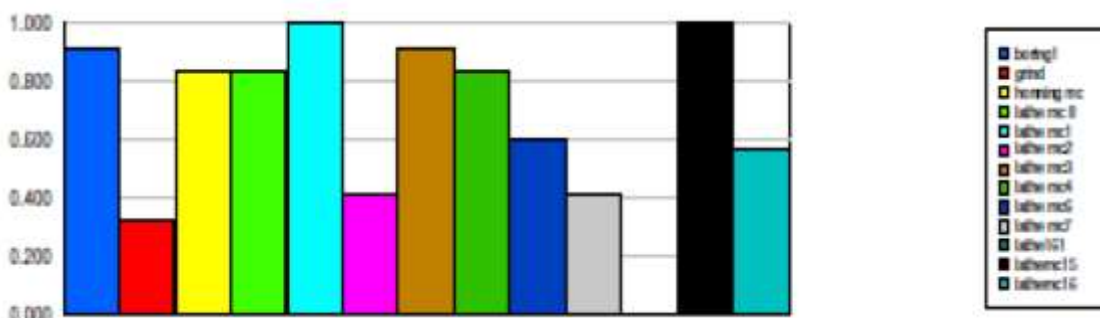


Figure 5: Scheduled Utilization of Machines simulated layout

RESULT

In the study we just got that the efficiency of 1 cycle is increased by 76.61 to 80.95%.and the rejection rate is decreased. In the current layout the total number of piston production in 1 shift is 307 piston/shift, in which 244 pistons are selected and 63 pistons are rejected while in simulated layout we get production rate of 307 shaft /shift in which selected pistons are 279 and rejected pistons are 28.here we are having the comparison table for both the layout in which we compare process time as well as efficiency of current layout & simulated layout. There are 2 areas where we found the results:

- Improvement in Productivity
- Line Balancing Efficiency
- Reduction in rejection Rate
- Increased production efficiency

TABLE – 1Table of % Scheduled Utilization of Machines in basic Layout & Simulated Layout

Sr. No.	M/C	Operations	Basic Layout results		Simulated Results	
			Prod Time (In min)	η	Prod Time (In min)	η
1	Grinding	Grinding	0.4	31.91	0.4	32.82
2	Lathe-1	Cutting M phase	1.2	100	1.2	100
3	Lathe-2	Back Cutting	0.5	41.65	0.5	41.65
4	Lathe-3	Ring Surface Cutting	1.1	91.65	1.1	91.65
5	Lathe-4	Gudgeon Pin Hole	1	83.35	1	83.35
6	Lathe-5	Rough Surface Finish	1.2	100	1.2	59.91
7	Lathe-6	Ring Surface Finish	1.4	100	1.4	41.72
8	Lathe-6a	Ring Surface Finish	-	-	-	-
9	Lathe-7	Back Surface Finish	0.5	35.70	0.5	100
10	Boring MC	Boring & Pin Hole	1.1	78.58	1.1	91.6
11	Lathe-8	Final Surface Finish	1.2	71.40	1.2	83.62
12	Honing	Rotor Surface Finish	1.0	31.91	1.0	83.23
Total Time and Efficiency			10.6 Min	76.61 %	10.6 Min	80.95%

CONCLUSIONS

The study has identified that production line is at under utilization. This is because of inefficiency on the line cause in work overload or idle time. One of the most powerful tools can use for improving productivity is that of “Line Balancing” which aims at examining the way an activity is being carried out and simplifying the method of operation to reduce unnecessary or excess work. And by proper line balancing and plant layout we reduce the power consumption of machine.

REFERENCES:

- [1] Watanapa, A., Kajondecha, P., Duangpitakwong P., and Wiyaratn W, 2011, “Analysis Plant Layout Design for Effective Production”, Proceedings of the Multi Conference of Engineers And Computer Scientists 2011 VOL-2, Hong Kong
- [2] Tompkins, J. A., White, J. A., Bozer, Y. A., Frazelle, E. H., and Tanchoco, J. M., 2010, “Facilities planning”, Fourth Edition, Published by John Wiley and Sons, NewYork.
- [3] Aryasri, A.R.,2006, “Economics, Accountancy and management”, Tata McGraw Hill (New Delhi)
- [4] Frazelle, E., 2002,” World-class warehousing and material handling”, Published by Tata McGraw-Hill, New York.
- [5] Abdul-Hamid, Y.T., Kochhar, A.K. and Khan, M.K., 1999, “An analytic hierarchy process approach to the choice of manufacturing plant layout”, Journal of Engineering Manufacture.
- [6] Agrawal, G.K., 2001, “Plant Layout and Material Handling”, Published By Jain Brothers(New Delhi).
- [7] Allen, T.T.,2011, “Introduction to Discrete Event Simulation and Agent-based Modeling”. Published by Springer New York.
- [8] Abdul-Hamid, Y.T., Kochhar, A.K. and Khan, M.K., 1999, “An analytic hierarchy process approach to the choice of manufacturing plant layout”, Journal of Engineering Manufacture.

DISCRETE FREQUENCY NOISE REDUCTION OF 100 kVA DIESEL ENGINE COOLING FAN

B. E. Okon., D. E. Bassey

Department of Physics,

University of Calabar, Calabar,

Cross River State, Nigeria.

benokon16@yahoo.com, basseyde1@yahoo.com

Abstract- This research work concentrates on measuring, analyzing and predicting the reduction of discrete frequency noise levels with focus on Perkins 100 kVA cooling fans. The measuring and fabricated materials used in carrying out the measurements were: digital sound level meter (SLM), frequency analyzer, AC electric motor, flange, basement and generating set cooling fan. The radiated sound levels were measured without contributions from other engine noise sources. These assisted in obtaining accurate sound pressure level (SPL) data on the fan noise. Discrete frequency tones of the cooling fans were measured within the audio and narrow band ranges using the calibrated TrueRTA spectrum analyzer. The sound power level (SWL) and sound intensity level (SIL) of the fans were calculated using values obtained from the measured SPL. Matrix Laboratory Application Software (MATLAB) was used for analysis of results. The background noise levels (BNL) were determined. It was observed that the un-banded fan used for 100 kVA generating set had SPL peak of 84 dB, at the fundamental blade passing frequency (BPF). In order to reduce the discrete tones at the blade passing frequency (BPF), the baseline fan were banded with a light flexible cylindrical plastic material. The band was found to effectively reduce the radiated sound levels (BPF tone) for the 100 kVA fan. Further observation showed that 10.89 dB SPL reduction was achieved by applying the flexible band on the fan used for the 100 kVA generating set. Almost all the blade rate tone levels were reduced which further increased the acoustical performance of the fan. However, a slight reduction in the aerodynamic performance of the system was observed. From the study, this effect can be mitigated by increasing the size of the radiator.

Keywords: Discrete Frequency Noise, Cooling Fan, Radiated Sound Level, Noise Reduction, Sound Level Meter, Sound Pressure Level.

1. INTRODUCTION

Generally, in industries, noise is referred to as an undesirable and unavoidable product of modern mechanized activities. To protect against the generation of these noise levels, noise limits have been recommended by control organizations and should be adhered to.

In developing countries, the main reason for high level of occupational noise is the absence of noise regulations [1].

In Nigeria for instance, frequent interruption of electricity supply have compelled many individuals, corporate bodies and industries to embark on massive purchase of large power generating plants for the generation of electricity. These generators in addition to generating electricity, generate noise.

Noise sources and vibration in most electrical machines are basically, aero-dynamic, electromagnetic and mechanical [2]. Hence the sources of noise from various components of these machines must be thoroughly investigated and properly understood.

Specifically, a good understanding of the dominant machine noise sources is very important and desirable, so that the required modifications can be carried-out. However, in machines that are complicated, it is sometimes difficult or cumbersome to acquire information; thereby making it hard to get relevant data on noise reduction [4]. In view of this hindrance, several attempts to reduce noise by researchers, innovators and industry regulators are often based on inadequate data. These in most cases, have led to very expensive, inefficient and uneconomical noise reduction procedures.

Noise sources identification methods depend on the specific problem, the duration, available resources, skilled personnel and required accuracy [4]. It is best practice to use more than one problem-solving methods in identifying issues relating to high noise levels.

2. LITERATURE REVIEW

The fundamental aerodynamic sound generation mechanisms of industrial fans are reviewed in this section. A great number of work has been done in the area of environmental acoustics. Most of the knowledge on fan noise reviewed was obtained for the high speed fans of aircraft engine, where contributions from monopole and quadrupole sources are significant.

It was however, shown by [5] that quadrupole radiation was very low for subsonic flow over thin blade sections. Monopole sources were generated by the volume displacements due to the finite thickness of the rotating fan blades. These volume displacements caused periodic changes in fluid mass and thus generated pressure fluctuations in the adjacent field. However, in the case of low to medium speed fans, the phase velocity of these pressure fluctuations was well below the speed of sound, this resulted to low acoustic radiation efficiency [6]. The primary mechanism for acoustic radiation from most subsonic industrial fans caused unsteady forces on the rotating blades due to blade interactions and unsteady incoming flow. The unsteady forces acting on the acoustic medium acted as dipole sources of sound.

The forces developed on the rotating fan blades can be either time periodic or random depending on the type of inflow that the blades encountered [7]. The periodic interaction generated discrete-frequency force spectrum on the blade. As the fan blades encountered these distortions, the generated unsteady force and radiated sound displayed broadband spectra [8].

Discrete-frequency noise radiation from a rotating steady force was first examined by [9]. His theory considered time-varying force-receiver positions that caused sound due to the Doppler Effect. Many authors including [10], [11], [12], [13] and [14], have derived expressions for the discrete-frequency sound radiation due to the fluctuating forces on rotor blades. Their derivations were based on the general solution of the inhomogeneous wave equation which was first formulated by [15]. Using Lighthill's inhomogeneous wave equation, [16], showed that stationary surfaces exposed to turbulent flow are equivalent to surface dipole distributions. [11], extended Curle's solution showing general features of noise radiation by arbitrary moving surface dipoles.

[17], identified the dominant noise sources of small subsonic electronic cooling fans and made modifications for discrete-frequency noise control. The influences of upstream obstructions to the tonal noise generation of a small cooling fan were also investigated experimentally by [18], [19].

[20], applied such discrete-frequency noise theory to the engine cooling fan noise problem. He measured the inlet flow field by a hot-wire probe fixed to the rotor and allowed it to rotate with the fan blades. The inlet velocity profile at only a single radial position was utilized though (a detailed flow measurement test set-up description was not published). [20], later investigated the influences of the radiator, cowl, and back-plate on automotive engine cooling fan noise.

Discrete-frequency fan noise can be reduced by either breaking up the periodic interactions of the fan blades with the incoming flow, or by adding a passive or active noise control device. An example is the skewed blade which is designed to mismatch the centers of lift of successive radial blade elements with the distorted incoming flow. It was noted that the skewed blade fan was advantageous to both the discrete-frequency noise and broadband noise. The skewed blade also reduced flow losses and dragged near the blade tip at transonic speed [21].

A fan with uneven blade spacing is another popular discrete-frequency fan noise control measure. The unevenly spaced blade fan disperses the harmonic tones of the blade-passing frequency (BPF). Therefore, it radiates less annoying noise than the regular evenly-spaced fan [22]; [23], although the sound power was not changed.

Passive noise control devices, such as resonators, can be used to reduce discrete-frequency tones, especially those generated by ducted fans. BPF tones that have frequencies below the first acoustic mode of the duct can be reduced by carefully tuned resonators. Successful applications of a quarter-wavelength tube to the reduction of the BPF noise of centrifugal blowers were reported by [24].

Active noise control techniques were also effective for the discrete-frequency fan noise reduction [25]; [26]. However, due to high cost, its application appears to be limited presently.

[27], investigated the noise sources of a half-stage automobile cooling fan. He showed that rotational and non-rotational noise sources dominate in high flow coefficient and low flow coefficient regions, respectively. [27] successfully reduced vortex shedding noise by the use of serrations located on the trailing edges of the blades. He also used rotating shrouds attached to the blade tips in order to prevent flow separation at the tips. Proper control and reduction of any recirculating flow was emphasized for successful noise control.

[28], reported an experimental investigation of the effects of clearance between the blade tips and a surrounding shroud on noise and aerodynamic performance of low pressure axial fans. They found that the broadband noise increased with increases in tip clearance. Likewise, the rotational tones increased with increases in fan eccentricity within the shroud.

[29], experimentally investigated the influence of tip vortices on the noise generation of turbo machines. Due mainly to the complicated nature of the vortex flow, no generalities regarding the tip noise mechanism was presented. However, most experimental works on tip clearance effects recommended that the tip clearance be kept as minimum as possible for very low noise generation and for better aerodynamic performance.

The fundamental theory of unsteady lift in noise level created on thin airfoils subjected to a transverse sinusoidal gust was investigated by [30]. This theory has subsequently been extended to include the influence of longitudinal gusts by [31], and angle of attack and camber effects by [32]. They derived closed-form solutions for a single airfoil exposed to two-dimensional flow. These theories have further been extended to include three-dimensional effects and the influence of adjacent blades and blade rows by other authors. However, the transverse velocity perturbations were the dominant sources of unsteady lift generation in many applications, particularly for low Mach number flow problems. Therefore, the Sears function was still the most widely used in practical applications.

[33], derived expressions for predicting the wideband noise of fans with axial-flow due to various mechanisms, and compared the predictions with empirical results. He observed a significant increase of the broadband noise when the blade encountered large-scale turbulence. He also noted that the noise spectra due to a stalled fan blade has a low-frequency hump centered roughly at a frequency associated with the frequency of vortex shedding from a bluff body in cross flow. Here, the size of the bluff body was analogous to the size of the stalled flow region.

[34], measured the spectrum of sound power radiated by a spoiler mounted inside a pipe at different angles of attack. He observed that the noise spectra due to the stalled spoiler agreed with the findings of Sharland.

Many efforts have been made by industries to utilize computational fluid dynamics (CFD) in fan noise analyses. [35], used a commercial CFD code to predict the discrete-frequency engine cooling fan noise of a passenger vehicle. The unsteady surface pressure statistics on the blade were calculated from the unsteady Reynolds Averaged Navier-Stokes Equations (RANS solutions), and the Hawkings and Ffowcs-Williams equation was utilized to predict sound pressure at field points. [36], utilized a boundary element solver to predict sound radiation by an HVAC radial blower. [37], utilized a three dimensional compressible unsteady CFD model to investigate the rotor-strut interaction of a computer cooling fan. [38], effectively utilized CFD, along with empirical equations, to predict the broadband noise of fans with axial-flow.

3.0 MATERIALS AND METHODS

This work was carried out using fabricated materials personally tailored and designed to suit the project. In addition, existing relevant tools necessary to aid measurements shall be used.

3.1 Materials

3.1.1 Measuring Tools

Measuring and analytical tools to be deployed in these investigations are listed below:

a. **Digital Sound Level Meter**

Mastech Precision Sound Level Meter was used to carry-out sound level measurements.

b. **Frequency Analyzer**

A spectrum analyzer was used for the measurement of the magnitude of the signal input against frequency taken within the maximum frequency range of the analyzer. This analyzer allows for the accurate measurement of the SPL against frequency, spurious phase noise and modulation analysis of communication signals without sacrificing dynamic range and speed.

c. **Electric Motor (AC)**

An electric motor was used to carry out this investigation. The motor used was a 1hp AC motor with frequency of 50/60 Hz and a voltage of 220/230V.

d. **Computer Application Software (MATLAB)**

A computer system with matrix laboratory (MATLAB) application software installed was used for statistical analysis.

1.1.2 Fabricated Tools

Fabricated tools to be deployed in these investigations are listed below:

a. Diesel Engine Cooling Fan

Diesel engine generator cooling fan used for 100 kVA generating set was fabricated and used to carry-out this research.

b. Flange

Flange was fabricated and was fitted properly to the Centre of the hub of each of the prototype fan. The flange was fastened suitably to the hub of the fan using metal springs. This was done to ensure proper alignment of the fan to the AC Electric motor's shaft as well as prevent wobbling of the fan.

3.2 Method

3.2.1 Meter Calibration

The meter was calibrated using an intelligent piston phone placed directly over the microphone. This was done to monitor the meter's performance.

3.2.2 Meter Response

The slow response characteristic was used in all measurements taken in this work, because the slow meter response helped average out the fluctuations of the meter.

3.2.3 Meter Positioning

The Sound Level Meter was held at 1m away from the source of noise and 1.2 m above the floor. To carry out these measurements, the microphone was placed away from interfering objects and surfaces in order to avoid unwanted influence on the measured sound levels.

3.2.4 Background Noise

The background noise level was determined by simply taking two readings of the levels of noise. The first reading was taken when the source of noise is turned "on" and the other reading was taken when the source of noise is turned "off". This method helped determine the extent to which the background noise is either affecting or not affecting the total noise level measured when the source of noise is "on".

3.2.5 Frequency Analyzer

The horizontal and vertical axes of the analyzer was calibrated in frequency and SPL respectively. The higher frequency was placed horizontally at the right hand side of the display while the SPL was placed vertically. Both logarithmic and linear scales was used in accordance with the range of frequency. For measurements taken within the audio range, the logarithmic scale was employed in order to allow a wide range of signal on the display, while for measurements taken within the narrowband range, the linear scale was used..

4.0 RESULT AND DISCUSSION

4.1 Results obtained for 100 kVA cooling fan

Radiated sound levels were measured for the 100 kVA cooling fan at a fixed speed of 1440 rpm and the results obtained are as shown in Tables 1, 2, 3 and 4 whereas the plots in FIGs. 1 and 2 display the comparison between the SPL of the un-banded and banded fan.

Broad band analysis was used to obtain noise spectra in the range 20 Hz – 20 kHz (known as audio band) while narrow band analysis was used to obtain noise spectra in the range 0 Hz - 2 kHz.

The audio spectrum for SPL of 100 kVA generator cooling fan un-banded and banded are tabulated in Tables 1 and 2. The ambient noise was also considered. In the same vein, Tables 3 and 4 depict data on SPL of 100 kVA un-banded and banded fan in the narrow band range. Considerations were also given that each noise level was taken at the various harmonic of the BPF.

FIG. 1 compare the noise levels (SPL) of the un-banded and banded fan used for the 100 kVA generating set in the audio range, while FIG. 2 present the noise levels in the narrow band range. The noise levels were plotted against the harmonics of the BPF.

The SWL and SIL displayed in Tables 1, 2, 3 and 4 were calculated using the equations below;

$$SWL (dB) = SPL + 20\log_{10}(r) + 11 \text{ dB} \quad (1)$$

The term r refers to the distance usually in meters away from the source of sound (Cory, 2010).

The sound intensity level was also calculated using the formula;

$$\text{SIL (dB)} = 10 \times \text{Log}_{10} (I/I_0) \quad (2)$$

Where I_0 is the reference intensity given as 10^{-12}W/m^2 and I , the intensity of sound given as $P^2/\rho c$, ρc is the characteristics impedance of sound in air given as 415 Rayls and P is the pressure of sound which can be obtained using the formula:

$$\text{SPL (dB)} = 20 \text{Log}_{10} \left(\frac{P_{rms}}{P_{ref}} \right), \quad (3)$$

where P_{rms} is the root mean square pressure and P_{ref} is the reference pressure.

TABLE 1

Result of sound level measurement obtained within the audio spectrum of an un-banded 100 kVA cooling fan

Un-banded Fan (100 kVA) Freq. (Hz)	Ambient Noise (dBA)	SPL (dBA)	SWL (dBA)	SIL (dBA)
15.6	31.79	52.24	63.24	32.08
31.2	34.67	60.77	71.77	40.59
62.5	38.55	74.53	85.53	54.35
125	32.90	83.64	94.64	63.46
250	26.98	80.11	91.11	59.93
500	23.23	78.82	89.82	58.64
1000	27.55	76.59	87.59	56.41
2000	12.16	72.51	83.51	52.33
4000	7.10	64.83	75.83	44.65
8000	4.48	52.16	63.16	31.98
16000	-11.66	21.68	32.68	1.52

TABLE 2

Result of sound level measurement obtained within the audio spectrum of a banded 100 kVA cooling fan

Banded Fan (100 kVA) Freq. (Hz)	Ambient Noise (dBA)	SPL (dBA)	SWL (dBA)	SIL (dBA)
15.6	31.79	49.64	60.64	29.46
31.2	34.67	60.81	71.81	40.63
62.5	38.55	68.62	77.62	48.44
125	32.90	72.81	83.81	52.63
250	26.98	70.82	81.82	50.64
500	23.23	68.09	79.09	47.91
1000	27.55	66.99	77.99	46.81
2000	12.16	61.41	72.41	41.23
4000	7.10	65.52	76.52	45.34
8000	4.48	56.66	64.66	36.48
16000	-11.66	21.42	32.42	1.24

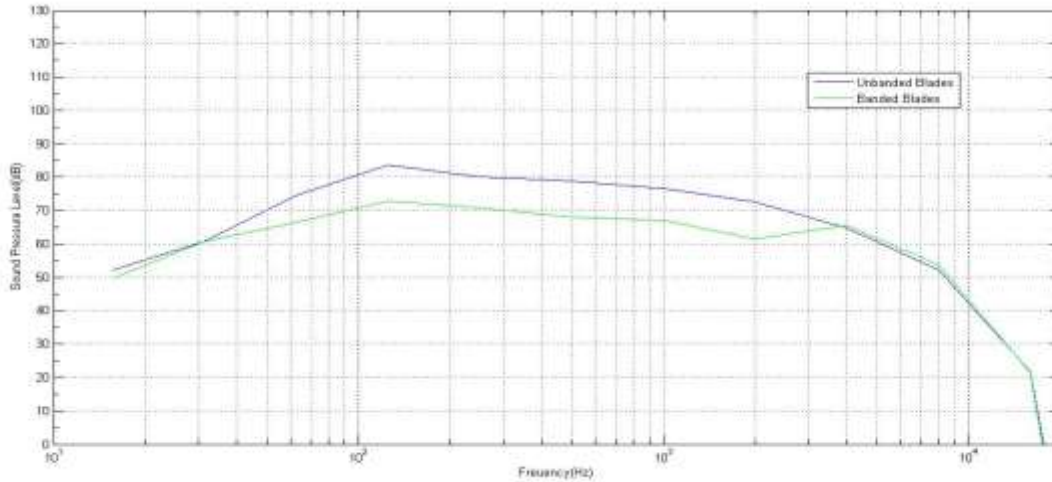


FIG 1: Comparison between SPL of un-banded and banded 100 kVA generator cooling fans within the audio spectrum.

TABLE 3

Result of sound level measurement obtained within the narrow band range of an un-banded 100 kVA cooling fan

F_p Un-banded Fan (100 kVA)	Ambient Noise (dBA)	SPL (dBA)	SWL (dBA)	SIL (dBA)
1 F_p	31.8	84	95	63.8
2 F_p	25.7	78	89	57.8
3 F_p	23.8	79	90	58.8
4 F_p	25.5	79	90	58.8
5 F_p	26.2	78	89	57.8
6 F_p	27.3	77	88	56.8
7 F_p	24.0	75	86	54.8
8 F_p	22.1	74	85	53.8
9 F_p	20.0	74	85	53.8
10 F_p	19.1	73	84	52.8

TABLE 4

Result of sound level measurement obtained within the narrow band range of a banded 100 kVA cooling fan

F_p Banded (100 kVA)	Ambient Noise (dBA)	SPL (dBA)	SWL (dBA)	SIL (dBA)
1 F_p	31.8	74.12	85.12	53.9
2 F_p	25.7	68.22	79.22	48.0
3 F_p	23.8	68.10	79.10	47.9
4 F_p	25.5	68.38	79.38	48.1
5 F_p	26.2	67.87	78.87	47.6
6 F_p	27.3	66.94	77.94	46.7
7 F_p	24.0	65.87	76.87	45.6
8 F_p	22.1	64.78	75.78	44.5
9 F_p	20.0	63.72	74.72	43.5
10 F_p	19.1	62.76	73.76	42.5

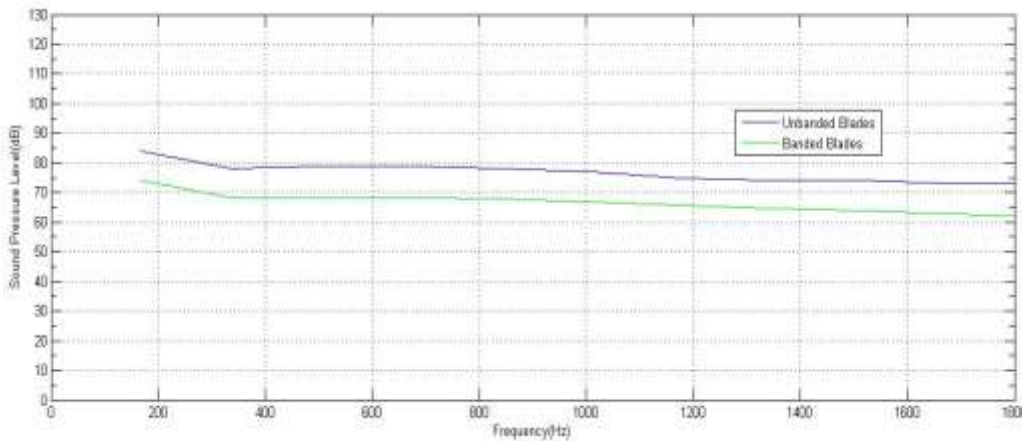


FIG. 2: Comparison between SPL of un-banded and banded 100 kVA generator cooling fans within the narrow band range.

4.2 Discussion of results

The results of measurement using fabricated 100 kVA fan blades are discussed here, after careful analysis of results obtained. These analysis were aided with the application software MATLAB.

4.2.1 100 kVA cooling fan evaluation

Results obtained showed that the ambient noise had no effect on the overall SPL. These results indicated that the fan blades were the major source of noise in the system.

Tables 1 and 3 show results obtained from sound level measurements taken within the audio spectrum and narrow band ranges respectively using an un-banded fan. From these results presented in Table 1, it was observed that SPL had a peak value of 83.64 dB at a frequency of 125 Hz, while from Table 3, SPL had a peak value of 84 dB at the fundamental BPF (168 Hz).

The SWL and SIL displayed in Tables 1 and 3 were calculated using Equations 1, 2 and 3. It was observed that the SWL and SIL taken within the audio and narrow band ranges also had their peaks at 125 Hz and fundamental BPF ($1F_p$) respectively.

From results tabulated in Tables 2 and 4, performed within the audio spectrum and narrow band range using a banded 100 kVA fan. It was observed that the SPL of the banded 100 kVA fan displayed in Table 2 had a maximum value of 72.81 dB at 125 Hz, while SWL had maximum value of 83.81 dB and SIL had maximum value of 52.63 dB at the same frequency. While for the banded 100 kVA fan in Table, a maximum SPL value of 74.13 dB was observed at the fundamental BPF ($1F_p$). It was further noted that this result influenced the SWL and SIL obtained.

From empirical results, it was also observed that the banded 100 kVA cooling fan reduced the radiated sound levels (BPF tones) by 10.89 dB. The maximum sound level reduction was observed at the third harmonic ($3F_p$) of the BPF, in line with several levels of reduction observed at other frequencies.

Investigations in this study, showed that the SWL of the system increased by 11 dB, while the SIL decreased by 20.2 dB, when viewed from the SPL. Based on this finding, the study generates a calibrated equation (Equation 23) in which the SIL can be obtained directly under similar conditions.

$$\text{SIL (dB)} = \text{SPL} + 20\log_{10}(r) - 20.2 \text{ dB} \quad (23)$$

This is a novel contribution to knowledge by this study.

5.0 CONCLUSION

The primary objective of this research was to measure, analyze and predict the reduction of discrete-frequency fan noise from a 100 kVA generator. This goal was achieved through comprehensive study and understanding of the characteristics of the fan noise and generator noise reduction methods. Key variables such as SPL, SWL and SIL spectra were measured and analyzed to determine the radiated sound levels. All sound measurements were taken in line with recommended measurement standards. From the study, the unsteady force and turbulence on the fan blades' tip were the dominant acoustic sources of the investigated fans.

The plastic fan blades designed with constant radii of curvature were examined. The feasibility of a banded fan was also examined. The banded fan was fabricated by mounting a cylindrical band to tips of the propeller fan. The analyses of this model successfully resulted in significant tonal noise reductions; though, careful observation noticed slight reduction in the aerodynamics performance of the fan.

Further empirical results, confirmed that banded 100 kVA cooling fan reduced the radiated sound levels (BPF tones) by 10.89 dB. The maximum reduction was observed at the third harmonic ($3F_p$) of the BPF, while several levels of reduction was also observed at other frequencies.

Investigations in this study, showed that the SWL of the system increased by 11 dB, while the SIL decreased by 20.2 dB, when viewed from the SPL. Based on this finding, the study generates a calibrated equation (Equation 23) in which the SIL can be obtained directly under similar conditions. This is a novel contribution to knowledge by this study.

These reductions are significant because they were achieved at minimal cost, using methods which could be adopted by any skilled maintenance trades person.

REFERENCES:

- [1] Okon, B. E & Umunnah, R. A (2015). Identification of Threats to Communication Security, Effects and Ways of Mitigation the Threats. *International Journal of Scientific and Engineering Research (IJSER)*, Vol.6, Issue 5 pp. 1219-1235.
- [2] Umunnah, R. A & Okon, B. E. (2015). A Survey of the Noise Generated by Timber Market Machines and its Health Implications on the Workers and their Environment, in Calabar, Cross River State. *International Journal of Scientific and Engineering Research (IJSER)*, Vol.6, Issue 5 pp.1713-1721.
- [3] Bassey, D. E., Okoro, R. C., Okon, B. E., & Eyime, E. E. (2016). Broadband – Infrastructural Deficit and ICT Growth Potentials in Cross River State, Nigeria. *International Journal of Innovative Research in Computer and Communication Engineering (IJRCCE)*, Vol. 4, Issue 5, pp. 8465-8476.
- [4] Bassey, D. E & Okon, B. E (2015). Comparative Studies between Reduction of Discrete Frequency Ranges and Radiated Sound Levels (A Case Study of 50 kVA Diesel Engine Cooling Fan). *International Journal of Engineering Research and Technology (IJERT)*, Vol. 4, Issue 9, pp. 429-437.
- [5] Bassey, D. E., Faith-Praise, F. O., Udoeno, E., & Eyime, E. E. (2016). Investigation of 2-Ghz Threshold Levels for Radio Waves in the Southern Region of Nigeria. *International Journal of Innovative Research in Computer and Communication Engineering (IJRCCE)*, Vol. 4, Issue 5, pp. 8477-8483.
- [6] Bassey, D. E., Okon, B. E., Faith-Praise, F. O., & Eyime, E. E. (2016). Characterization of Traffic Flow Consumption Pattern and Subscribers' Behaviour. *International Journal of Innovative Research in Computer and Communication Engineering (IJRCCE)*, Vol. 4, Issue 5, pp. 8484-8493.
- [7] Bassey, D. E., Okon, B. E. & Effiom, E. O. (2016). 'Broadband Network Penetration and Growth Pattern in North Eastern Part of Nigeria'. *International Journal of Scientific & Engineering Research (IJSER)*, Vol. 7, Issue 3, pp. 1156-1170.
- [8] Bassey, D. E., Okon, B. E. & Umunnah, R. (2016). 'The Security Implications of Virtual Local Area Network (VLAN), Niger Mills, Calabar, Nigeria'. *International Journal of Scientific & Engineering Research (IJSER)*, Vol. 7, Issue 3, pp. 1187-1194.
- [9] Gutin, L. (1936). *On the Sound Field of a Rotating Propeller*. NACA TM 1195, Heft 1 pp 67-71.
- [10] Bassey, D. E., Okon, B. E. & FaithPraise, F. O. (2016). Design and Construction of a GSM-Based Multipurpose Measuring Device for UHF Signal Strength Levels. *International Journal of Science, Engineering and Technology Research*, Vol. 5, Issue 3, pp. 841-846.
- [11] Ffowcs-Williams, J. E. & Hawkings, D. L. (1969). Theory Relating to the Noise of Rotating Machinery. *Journal of Sound and Vibration*, 10(1), 10-21.
- [12] Bassey, D. E., Ogbulezie, J. C. & R. Umunnah (2016). Empirical Review of Basic Concepts of Teletraffic Postulates. *International Journal of Scientific and Engineering Research*, Vol. 7, Issue 3, pp.1171-1186.
- [13] Goldstein, M. E. (1976). *Aeroacoustics*. New-York: McGraw-Hill., 233pp.
- [14] Blake, W. K. (2012). *Mechanics of Flow-Induced Sound and Vibration*. New York: Academic Press, 1-151.
- [15] Lighthill, M. J. (1952). On Sound Generated Aerodynamically. I. General Theory. *Proceedings of the Royal Society of London: Series A, Mathematical and Physical Science*, 211(1107), 564-587.
- [16] Curle, N. (1955). The Influence of Solid Boundaries upon Aerodynamic Sound. *Proceedings of the Royal Society of London: Series A, Mathematical and Physical Sciences*, 231(1187), 505-514.
- [17] Fitzgerald, J. M. & Lauchle, G. C. (1984). Reduction of Discrete Frequency Noise in Small, Subsonic Axial-flow Fans. *Journal of Acoustical Society of America*, 76(1), 158-166.
- [18] Washburn, K. B. & Lauchle, G. C. (1988). Inlet Flow Conditions and Tonal Sound Radiation from a Subsonic Fan. *Noise Control Engineering Journal*, 31(2), 101-110.

- [19] Chiu, W. S. & Lauchle, G. C. (1989). Subsonic Axial Flow Fan Noise and Unsteady Rotor Force. *Journal of Acoustical Society of America*, 85(2), 641-647.
- [20] Bassey, D. E., Okon, B. E. & Effiom, E. O. (2016). Pilot Case Study of GSM - Network Load Measurement in Ikeja - Nigeria. *International Journal of Science, Engineering and Technology Research*, Vol. 5, Issue 3, pp. 824-829.
- [21] Beiler, M. G. & Carolus, T. H. (1999). Computation and Measurement of the Flow in Axial Flow Fans with Skewed Blades. *Transactions of the American Society of Mechanical Engineering (ASME): Journal of Turbomachinery*, 121, 59-66.
- [22] Boltezar, M. & Mesaric, M. (1998). The Influence of Uneven Blade Spacing on the SPL and Noise Spectra Radiated From Radial Fans. *Journal of Sound and Vibration*, 216(4), 697-711.
- [23] Brungart, T. A. & Lauchle, G. C. (2001). Modification of a Handheld Vacuum Cleaner for Noise Control. *Noise Control Engineering Journal*, 49(2), 73-78.
- [24] Bassey, D. E., Ogbulezie, J. C. & Okon, B. E. (2016). Modeling a Low Latency IP Network in Nigeria. *International Journal of Science, Engineering and Technology Research*, Vol. 5, Issue 3, pp. 830-834.
- [25] Koopmann, G. H. & Fox, D. J. (1988). Active Source Cancellation of the Blade Tone Fundamental and Harmonics in Centrifugal Fans. *Journal of Sound and Vibration*, 126(2), 209-220.
- [26] Lauchle, G. C. & MacGillivray, J. R. (1997). Active Control of Axial-Flow Fan Noise. *Journal of Acoustical Society of America*, 101(1), 341-349.
- [27] Longhouse, R. E. (1977). Vortex Shedding Noise of Low Tip Speed, Axial Flow Fans. *Journal of Sound and Vibration*, 53(1), 25-46.
- [28] Fukano, T. & Takamatsu, Y. (1986). The Effect of Tip Clearance on the Noise of Low Pressure Axial and Mixed Flow Fans. *Journal of Sound and Vibration*, 105(2), 291-308.
- [29] Kameier, F. & Neise, W. (1997). Experimental Study of Tip Clearance Losses and Noise in Axial Turbomachines and Their Reduction. *Transaction of the American Society of Mechanical Engineering*, 119.
- [30] Bassey, D. E., Akpan, Aniefiok. O. & Udoeno, E. (2016). UHF Wave Propagation Losses Beyond 40 Percent Fresnel Zone Radius in South-South Nigeria. *International Journal of Science and Research*, Vol. 5, Issue 2, pp. 740-745.
- [31] Horlock, J. H. (1968). Fluctuating Lift Forces on Aerofoils Moving Through Transverse and Chord-wise Gusts. *Journal of Basic Engineering, Series D*, 90(4), 494-500.
- [32] Naumann, H. & Yeh, H. (1973). Lift and Pressure Fluctuations of a Cambered Airfoil under Periodic Gusts and Applications in Turbomachinery. *Journal of Engineering for Power*, 5, 1-10.
- [33] Sharland, I. J. (1964). Sources of Noise in Axial Flow Fans. *Journal of Sound and Vibration*, 1(3), 302-322.
- [34] Gordon, C. G. (1969). Spoiler-Generated Flow noise: II. Results. *Journal of Acoustical Society of America*, 45(1), 214-223.
- [35] Algermissen, G. & Siegert, R. (2001). Numerical Simulation of Aeroacoustic Sound Generalized by Fans under Installation Conditions. *7th AIAA/CEAS Aeroacoustics Conference, Maastricht, Netherlands, 1, 84.*
- [36] Bassey, D. E., Okoro, R. C., Okon, B. E. (2016). Modeling of Radio Waves Transmission of Building Located around Niger Delta Urban Microcell Environment Using "Ray Tracing Techniques". *International Journal of Science and Research*, Vol.5, Issue 2, pp. 337-346.
- [37] Bassey, D. E., Okoro, R. C., Okon, B. E. (2016). Issues of Variance of Extreme Values in a Heterogenous Teletraffic Environment. *International Journal of Science and Research*, Vol. 5, Issue 2, pp. 164-169.
- [38] Bassey, D. E., Okoro, R. C. & Okon, B. E. (2016). Issues Associated with Decimeter Waves Propagation at 0.6, 1.0 and 2.0 Peak Fresnel Zone Levels. *International Journal of Science and Research*, Vol. 5, Issue 2, pp. 159-163.

**D & R
I & A**



Publication

International Journal of Engineering Research and general science is an open access peer review publication which is established for publishing the latest trends in engineering and give priority to quality papers which emphasis on basic and important concept through which there would be remarkable contribution to the research arena and also publish the genuine research work in the field of science, engineering and technologies

**International Journal Of Engineering Research and
General Science**

ISSN 2091 - 2730